

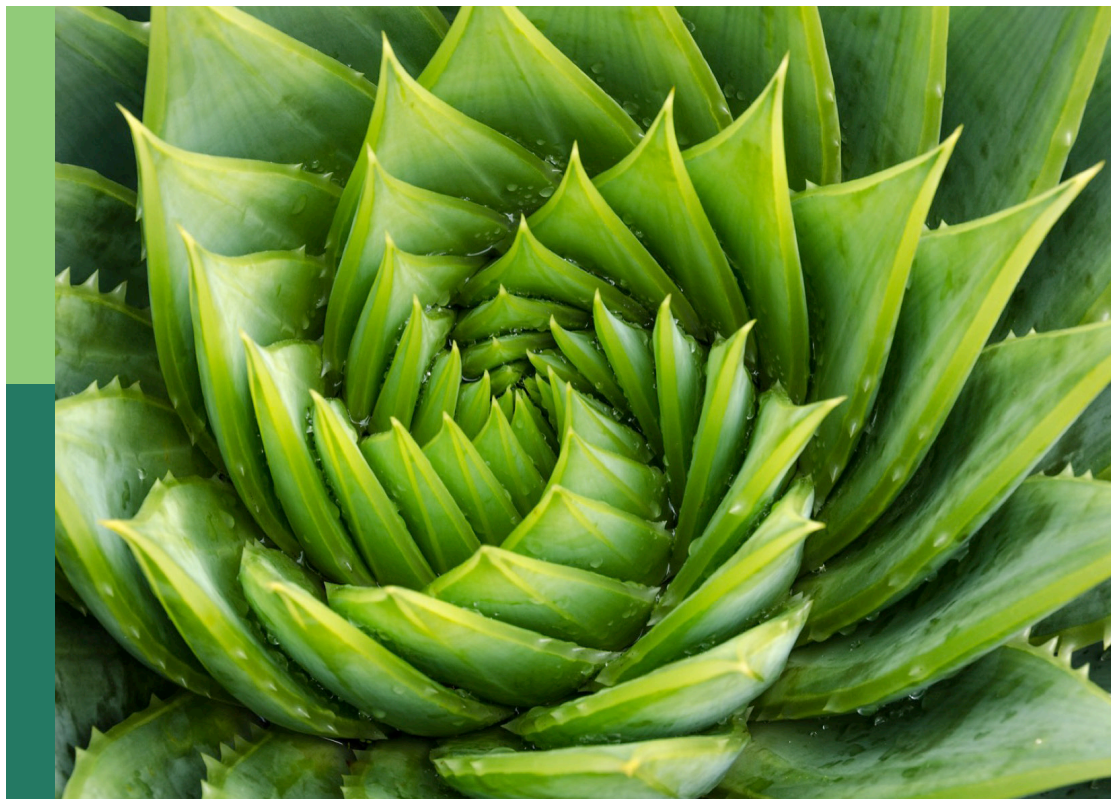
Secondary metabolites in grapevine stress response - women in plant science series

Edited by

Alessandra Ferrandino, Chiara Pagliarani
and Eva Pilar Pérez-Álvarez

Published in

Frontiers in Plant Science



FRONTIERS EBOOK COPYRIGHT STATEMENT

The copyright in the text of individual articles in this ebook is the property of their respective authors or their respective institutions or funders. The copyright in graphics and images within each article may be subject to copyright of other parties. In both cases this is subject to a license granted to Frontiers.

The compilation of articles constituting this ebook is the property of Frontiers.

Each article within this ebook, and the ebook itself, are published under the most recent version of the Creative Commons CC-BY licence. The version current at the date of publication of this ebook is CC-BY 4.0. If the CC-BY licence is updated, the licence granted by Frontiers is automatically updated to the new version.

When exercising any right under the CC-BY licence, Frontiers must be attributed as the original publisher of the article or ebook, as applicable.

Authors have the responsibility of ensuring that any graphics or other materials which are the property of others may be included in the CC-BY licence, but this should be checked before relying on the CC-BY licence to reproduce those materials. Any copyright notices relating to those materials must be complied with.

Copyright and source acknowledgement notices may not be removed and must be displayed in any copy, derivative work or partial copy which includes the elements in question.

All copyright, and all rights therein, are protected by national and international copyright laws. The above represents a summary only. For further information please read Frontiers' Conditions for Website Use and Copyright Statement, and the applicable CC-BY licence.

ISSN 1664-8714
ISBN 978-2-8325-3593-6
DOI 10.3389/978-2-8325-3593-6

About Frontiers

Frontiers is more than just an open access publisher of scholarly articles: it is a pioneering approach to the world of academia, radically improving the way scholarly research is managed. The grand vision of Frontiers is a world where all people have an equal opportunity to seek, share and generate knowledge. Frontiers provides immediate and permanent online open access to all its publications, but this alone is not enough to realize our grand goals.

Frontiers journal series

The Frontiers journal series is a multi-tier and interdisciplinary set of open-access, online journals, promising a paradigm shift from the current review, selection and dissemination processes in academic publishing. All Frontiers journals are driven by researchers for researchers; therefore, they constitute a service to the scholarly community. At the same time, the *Frontiers journal series* operates on a revolutionary invention, the tiered publishing system, initially addressing specific communities of scholars, and gradually climbing up to broader public understanding, thus serving the interests of the lay society, too.

Dedication to quality

Each Frontiers article is a landmark of the highest quality, thanks to genuinely collaborative interactions between authors and review editors, who include some of the world's best academicians. Research must be certified by peers before entering a stream of knowledge that may eventually reach the public - and shape society; therefore, Frontiers only applies the most rigorous and unbiased reviews. Frontiers revolutionizes research publishing by freely delivering the most outstanding research, evaluated with no bias from both the academic and social point of view. By applying the most advanced information technologies, Frontiers is catapulting scholarly publishing into a new generation.

What are Frontiers Research Topics?

Frontiers Research Topics are very popular trademarks of the *Frontiers journals series*: they are collections of at least ten articles, all centered on a particular subject. With their unique mix of varied contributions from Original Research to Review Articles, Frontiers Research Topics unify the most influential researchers, the latest key findings and historical advances in a hot research area.

Find out more on how to host your own Frontiers Research Topic or contribute to one as an author by contacting the Frontiers editorial office: frontiersin.org/about/contact

Secondary metabolites in grapevine stress response - women in plant science series

Topic editors

Alessandra Ferrandino — University of Turin, Italy

Chiara Pagliarani — Institute for Sustainable Plant Protection, National Research Council (CNR), Italy

Eva Pilar Pérez-Álvarez — Institute of Vine and Wine Sciences, Spanish National Research Council (CSIC), Spain

Citation

Ferrandino, A., Pagliarani, C., Pérez-Álvarez, E. P., eds. (2023). *Secondary metabolites in grapevine stress response - women in plant science series*. Lausanne: Frontiers Media SA. doi: 10.3389/978-2-8325-3593-6

Table of contents

- 05 **Editorial: Secondary metabolites in grapevine stress response - women in plant science series**
Alessandra Ferrandino and Chiara Pagliarani
- 07 **Temperature affects organic acid, terpene and stilbene metabolisms in wine grapes during postharvest dehydration**
Ron Shmulevitz, Alessandra Amato, Mauro Commisso, Erica D'Inca, Giovanni Luzzini, Maurizio Ugliano, Marianna Fasoli, Sara Zenoni and Giovanni Battista Torielli
- 22 **Secondary and primary metabolites reveal putative resistance-associated biomarkers against *Erysiphe necator* in resistant grapevine genotypes**
Ramona Mihaela Ciubotaru, Pietro Franceschi, Silvia Vezzulli, Luca Zulini, Marco Stefanini, Michael Oberhuber, Peter Robatscher, Giulia Chitarrini and Urska Vrhovsek
- 36 **Grapevine mono- and sesquiterpenes: Genetics, metabolism, and ecophysiology**
Robin Nicole Bosman and Justin Graham Lashbrooke
- 50 **Influence of late pruning practice on two red skin grapevine cultivars in a semi-desert climate**
Corrado Perin, Pankaj Kumar Verma, Gil Harari, Yedidya Suued, Matanya Harel, Danielle Ferman-Mintz, Elyashiv Drori, Yishai Netzer and Aaron Fait
- 63 **Holistic understanding of the response of grapevines to foliar application of seaweed extracts**
Iratxe Zarraonaindia, Enrico Cretazzo, Amaia Mena-Petite, Ana M. Díez-Navajas, Usue Pérez-López, Maite Lacuesta, Eva Pilar Pérez-Álvarez, Belén Puertas, Catalina Fernandez-Díaz, Nadia Bertazzon and Emma Cantos-Villar
- 80 **Grapevine genome analysis demonstrates the role of gene copy number variation in the formation of monoterpenes**
Robin Nicole Bosman, Jessica Anne-Marie Vervalle, Danielle Lisa November, Phyllis Burger and Justin Graham Lashbrooke
- 97 **Forcing vine regrowth under different irrigation strategies: effect on polyphenolic composition and chromatic characteristics of cv. Tempranillo wines grown in a semiarid climate**
Nieves Lavado Rodas, David Uriarte Hernández, Daniel Moreno Cardona, Luis A. Mancha Ramírez, María Henar Prieto Losada and María Esperanza Valdés Sánchez
- 116 **Impact of meteorological conditions, canopy shading and leaf removal on yield, must quality, and norisoprenoid compounds content in Franciacorta sparkling wine**
Isabella Ghiglieno, Silvia Carlin, Gabriele Cola, Urska Vrhovsek, Leonardo Valenti, Mar Garcia-Aloy and Fulvio Mattivi

- 131 **Secondary metabolites in grapevine: crosstalk of transcriptional, metabolic and hormonal signals controlling stress defence responses in berries and vegetative organs**
Alessandra Ferrandino, Chiara Pagliarani and Eva Pilar Pérez-Álvarez
- 149 **Aroma precursors of Grignolino grapes (*Vitis vinifera* L.) and their modulation by vintage in a climate change scenario**
Andriani Asproudi, Federica Bonello, Vasiliki Ragkousi, Silvia Gianotti and Maurizio Petrozziello



OPEN ACCESS

EDITED BY

Jian Chen,
Jiangsu Academy of Agricultural Sciences,
China

REVIEWED BY

Marcus Scotti,
Federal University of Paraíba, Brazil

*CORRESPONDENCE

Alessandra Ferrandino
✉ alessandra.ferrandino@unito.it

RECEIVED 04 August 2023

ACCEPTED 11 September 2023

PUBLISHED 15 September 2023

CITATION

Ferrandino A and Pagliarani C (2023)
Editorial: Secondary metabolites in
grapevine stress response - women in
plant science series.
Front. Plant Sci. 14:1272668.
doi: 10.3389/fpls.2023.1272668

COPYRIGHT

© 2023 Ferrandino and Pagliarani. This is an
open-access article distributed under the
terms of the [Creative Commons Attribution
License \(CC BY\)](#). The use, distribution or
reproduction in other forums is permitted,
provided the original author(s) and the
copyright owner(s) are credited and that
the original publication in this journal is
cited, in accordance with accepted
academic practice. No use, distribution or
reproduction is permitted which does not
comply with these terms.

Editorial: Secondary metabolites in grapevine stress response - women in plant science series

Alessandra Ferrandino^{1*} and Chiara Pagliarani²

¹Department of Agricultural, Forest and Food Sciences, University of Torino, Grugliasco, Italy,

²Institute for Sustainable Plant Protection, National Research Council (IPSP-CNR), Torino, Italy

KEYWORDS

grapevine biotic stress, abiotic stress, vineyard, berries, vegetative organs,
plant hormones

Editorial on the Research Topic

[Secondary metabolites in grapevine stress response - women in plant
science series](#)

The ten papers included in [this Research Topic](#) focus on two main subjects, one dealing with the effects of climate change-induced stress on the vine's secondary metabolism, and one concerning changes in secondary metabolites associated with the grapevine response to pathogens.

Half of the contributions falls in the framework of the first theme and describes either the impact of abiotic factors on the accumulation of secondary metabolites in berries or the application of innovative vineyard management strategies to mitigate the effects of climate alterations on the vine agronomic performance.

A second set of articles reports novel findings on the characterization of molecules involved in grapevine defence process and on the evaluation of natural compounds acting as resistance elicitors, alternative to the application of conventional chemical products.

[Schmulevitz et al.](#) evaluated the influence of environmental temperature on the berry metabolic composition of *Vitis vinifera* cv Corvina during postharvest dehydration. The trials were conducted within dedicated dehydration rooms mirroring the environmental conditions typical of two different sites of Northeastern Italy. They dissected the temperature effect from that of the dehydration rate, by excluding the influence of environmental relative humidity. Grape dehydration at higher temperatures (12 °C) promotes the accumulation of oligomeric stilbenes, in parallel with the upregulation of *PAL* and *STS* genes. Conversely, withering the grapes in a cooler environment (8 °C) favors the accumulation of organic acids, flavonols and aromatic compounds.

Variable vineyard microclimatic conditions largely influence berry qualitative traits: [Ghiglieno et al.](#) described the effects of strong defoliation on the concentration of some norisoprenoids in Pinot noir and Chardonnay berries, highlighting that high amounts of these compounds are detrimental in sparkling wines, particularly when associated to a drastic reduction of acid concentrations. [Asproudi et al.](#) found higher variability among vintages in the accumulation of aroma in berries collected from young Grignolino plants respect to the old ones, whose berries reached a higher concentration of terpenoids. Heat

waves with temperatures higher than 30°C, together with water scarcity, vary the berry aromatic profile by increasing the accumulation of benzene derivatives.

Late-pruning is a recent technique proposed to adapt viticulture to climate change: in semi-desert climatic conditions, [Perin et al.](#) tested three times of late pruning (1, 2 and 3 weeks after bud-break), highlighting that late pruning decouples the berry ripening dynamics of sugars and phenols, particularly in Syrah respect to Malbec (both grafted onto 110 Richter), resulting in a general increase of polyphenols at harvest. Late pruning in Syrah induced consistent increases in anthocyanins and flavonols, whereas in Malbec significant variation in hydroxycinnamic acid concentration occurred.

[Rodas et al.](#) applied a crop-forcing technique, consisting in hedging the growing shoots to seven nodes and removing all lateral leaves and clusters to force the bursting of the primary buds in cv Tempranillo, grown in semi-arid climatic conditions. Although a significant season effect was found for almost all the analyzed polyphenols, a general increase in polyphenol concentration was observed in the wines obtained from forced-vines.

An in-depth analysis of grapevine metabolic compounds acting as resistance trait-associated markers is the subject of the paper by [Ciubotaru et al.](#) The objective was to characterize the poorly explored metabolic signature of cultivars with one gene of resistance and with pyramided resistance in comparison with the susceptible variety Teroldego upon *Erysiphe necator* infection. Both timing and intensity of metabolite accumulation control the initiation and the establishment of defense responses, discriminating the resistant individuals from the susceptible ones. Ten metabolites, including pallidol and astringin, were exclusively up-accumulated in the resistant genotypes, suggesting their key biological role in the activation of resistance mechanisms.

Rugulopteryx okamurae (Ro) is a species of brown macroalgae belonging to the *Dictyotaceae* family and native to the north-western Pacific, detected at Gibraltar since 2015 and then found on the Andalusian coasts ([Zarraonaindia et al.](#)). Its use as a grapevine protection product in viticulture could represent a successful example of circular economy, acquired that some Ro extracts can effectively induce the transcription of defense genes, such as *PR10*, *PAL*, *STS48* and *GST1*, and the consequent accumulation of specific secondary metabolites.

The review article by [Ferrandino et al.](#) showcases subjects belonging to both the first and the second main themes addressed by this Research Topic, reaffirming how important is to deepen the knowledge on the biological processes that regulate grapevine stress resilience. The review first considers the impact of environmental cues on the berry secondary metabolism, focusing on the molecular and hormonal signalling cascades that control the accumulation of specific groups of quality- and/or defence-associated molecules. Then, the authors analyse recent findings concerning alterations in secondary metabolic compounds that could underlie tolerance/resistance to diseases.

A further and transversal sub-group outlines advances on the genetic regulation of specialized classes of secondary metabolites, namely monoterpenes and sesquiterpenes. The functional plasticity of the numerous terpene synthases and the significant duplication

of genes encoding structurally diverse terpene synthases ([Bosman et al.](#)) influence product and substrate specificity, impacting on cultivar-specific aroma profiles, a pivotal trait for defining grape quality. However, mono- and sesquiterpenes do play important ecophysiological roles: attraction of pollinators, agents of seed dispersal and herbivores, defense against fungi, promotion of mutualistic rhizobacteria interaction, and their concentration increases upon high light radiation ([Bosman and Lashbrooke](#)).

In this subgroup, as well as in all the papers, the paradigmatic nature of this Research Topic is evident: the secondary metabolites that the vine accumulates in its various organs characterize the different genotypes, the result of *millennia* of acclimation. During its evolution, the vine had to live by interacting with biotic and abiotic stresses present in the different areas where it developed and was progressively domesticated. The accumulated secondary metabolites have allowed grapevines to refine strategies of struggle and/or coexistence with the environment and with its microbiome, parasites and/or symbionts, giving to the existing genotypes an optimal level of growth/defense tradeoff. This compromise, the result of at least two *millennia* of attempts, is what we find in the secondary metabolites of the grapes and their derivatives in the wines, produced in different *terroirs*, and what allows the attentive taster to recognize the grape origin of the grapes and their history of adaptation to the environment, cultivation and winemaking.

Author contributions

AF: Conceptualization, Data curation, Funding acquisition, Writing – review & editing. CP: Conceptualization, Data curation, Funding acquisition, Writing – review & editing.

Acknowledgments

The authors would gratefully acknowledge all authors that have contributed to the present Research Topic as well as all committed editors and reviewers for the great work.

Conflict of interest

The authors declare that the research was conducted in the absence of any commercial or financial relationships that could be construed as a potential conflict of interest.

Publisher's note

All claims expressed in this article are solely those of the authors and do not necessarily represent those of their affiliated organizations, or those of the publisher, the editors and the reviewers. Any product that may be evaluated in this article, or claim that may be made by its manufacturer, is not guaranteed or endorsed by the publisher.



OPEN ACCESS

EDITED BY
Chiara Pagliarani,
National Research Council (CNR), Italy

REVIEWED BY
Stefania Savoi,
University of Turin, Italy
Fabio Mencarelli,
University of Pisa, Italy
Tiziana Nardi,
Council for Agricultural and Economics
Research (CREA), Italy

*CORRESPONDENCE
Giovanni Battista Tornielli
✉ giovannibattista.tornielli@univr.it
Sara Zenoni
✉ sara.zenoni@univr.it

SPECIALTY SECTION
This article was submitted to
Plant Abiotic Stress,
a section of the journal
Frontiers in Plant Science

RECEIVED 25 November 2022
ACCEPTED 09 January 2023
PUBLISHED 30 January 2023

CITATION
Shmulevitz R, Amato A, Commisso M,
D'Inca E, Luzzini G, Ugliano M, Fasoli M,
Zenoni S and Tornielli GB (2023)
Temperature affects organic acid, terpene
and stilbene metabolisms in wine grapes
during postharvest dehydration.
Front. Plant Sci. 14:1107954.
doi: 10.3389/fpls.2023.1107954

COPYRIGHT
© 2023 Shmulevitz, Amato, Commisso,
D'Inca, Luzzini, Ugliano, Fasoli, Zenoni and
Tornielli. This is an open-access article
distributed under the terms of the [Creative
Commons Attribution License \(CC BY\)](#). The
use, distribution or reproduction in other
forums is permitted, provided the original
author(s) and the copyright owner(s) are
credited and that the original publication in
this journal is cited, in accordance with
accepted academic practice. No use,
distribution or reproduction is permitted
which does not comply with these terms.

Temperature affects organic acid, terpene and stilbene metabolisms in wine grapes during postharvest dehydration

Ron Shmulevitz, Alessandra Amato, Mauro Commisso,
Erica D'Inca, Giovanni Luzzini, Maurizio Ugliano,
Marianna Fasoli, Sara Zenoni* and Giovanni Battista Tornielli*

Department of Biotechnology, University of Verona, Verona, Italy

The partial dehydration of grapes after harvest is a traditional practice in several winegrowing regions that leads to the production of high quality wines. Postharvest dehydration (also known as withering) has a significant impact on the overall metabolism and physiology of the berry, yielding a final product that is richer in sugars, solutes, and aroma compounds. These changes are, at least in part, the result of a stress response, which is controlled at transcriptional level, and are highly dependent on the grape water loss kinetics and the environmental parameters of the facility where grapes are stored to wither. However, it is difficult to separate the effects driven by each single environmental factor from those of the dehydration rate, especially discerning the effect of temperature that greatly affects the water loss kinetics. To define the temperature influence on grape physiology and composition during postharvest dehydration, the withering of the red-skin grape cultivar Corvina (*Vitis vinifera*) was studied in two conditioned rooms set at distinct temperatures and at varying relative humidity to maintain an equal grape water loss rate. The effect of temperature was also studied by withering the grapes in two unconditioned facilities located in geographic areas with divergent climates. Technological, LC-MS and GC-MS analyses revealed higher levels of organic acids, flavonols, terpenes and cis- and trans-resveratrol in the grapes withered at lower temperature conditions, whereas higher concentrations of oligomeric stilbenes were found in the grapes stored at higher temperatures. Lower expression of the malate dehydrogenase and laccase, while higher expression of the phenylalanine ammonia-lyase, stilbene synthase and terpene synthase genes were detected in the grapes withered at lower temperatures. Our findings provide insights into the importance of the temperature in postharvest withering and its effect on the metabolism of the grapes and on the quality of the derived wines.

KEYWORDS

postharvest dehydration, *vitis vinifera*, temperature, stilbene metabolism, terpene metabolism, grape

1 Introduction

Grapevine is one of the most important plant species especially due to the economic impact of its processing that leads to a wide range of wines largely traded and consumed worldwide. To meet certain wine styles, grape clusters can be left on the plant beyond ripening, or can be harvested and stored in dedicated dehydrating rooms prior to winemaking. In some wine regions such as the Verona province (Northeastern Italy), the latter process is followed to obtain Amarone, a premium wine largely commercialized all over the world. Grape postharvest dehydration (also known as withering) is a dynamic process that can last up to 90–100 days and features water loss and concentration of sugars and other metabolites, impacting both alcohol content and sensorially and technologically relevant wine constituents such as phenolics, aroma compounds and aroma precursors. Besides solutes concentration, metabolic processes already in play or specifically activated during withering may affect berry composition at the end of the process (Costantini et al., 2006; Mencarelli et al., 2010). The several physiological and biochemical changes described in postharvest berries were shown to be affected by factors like the environment and the genotype (Zenoni et al., 2016; Zenoni et al., 2020). In addition, structural modifications in the cell wall, likely influencing the extractability of solutes in the must during winemaking, were reported (Zoccatelli et al., 2013; Fasoli et al., 2019; Medina-Plaza et al., 2022). The transcriptional and metabolic reprogramming occurring during the process was also largely investigated at transcriptomic level in several works. These studies revealed that a massive gene modulation occurs in post-ripening berries and, at least in part, is responsible of the improved quality traits of withered grapes (Zamboni et al., 2008; Rizzini et al., 2009; Fasoli et al., 2012; Zenoni et al., 2016). For example, Zenoni et al. (2016) showed that an increase in sesquiterpenes and balsamic monoterpenes, contributing to the final aroma of Corvina wine (Slaghenaufl and Ugliano, 2018), occurs during postharvest dehydration of cv. Corvina grapes, in parallel to the upregulation of several members of the terpene synthase gene family. Similarly, it was observed that the accumulation of stilbene compounds followed the remarkable upregulation of genes encoding phenylalanine ammonia-lyases, stilbene synthases and laccases, in addition to cell wall remodeling expounded by the induction of pectin methylesterase encoding genes (Zoccatelli et al., 2013; Zenoni et al., 2016).

It is also known that the above-described changes largely depend on the environmental parameters (e.g., temperature, relative humidity, air flow and light) at the dehydration facilities that can have a profound impact on some grape characteristics such as skin force, polyphenolic composition, volatile organic compounds profile and on the final wine quality (Bellincontro et al., 2004; Rolle et al., 2013; Torchio et al., 2016; Tomasi et al., 2021). Grapes dehydrated under different environmental conditions generally differ in their dehydration kinetics and undergo increased water loss rate at higher temperatures and lower relative humidity (RH) (Barbanti et al., 2008). Noteworthy, Zenoni et al. (2020) recently investigated the specific effect of increasing dehydration rate with no temperature manipulation in grapes that exhibited – although mitigated – the typical postharvest transcriptomic program, indicating that the

dehydration rate itself can promote compositional changes in the berries and then contribute to the final wine characteristics. Thus, when grapes are dehydrated at different temperatures it is excessively complex to define the extent of the specific contribution of either the temperature regime or the dehydration rate or their interaction to the observed effects on the grapes.

Our experimental plan aimed at dissecting the effect of temperature from other variables during the postharvest dehydration of grapes. We compared the composition of berries and wines from cv. Corvina grapes dehydrated at two temperatures, while maintaining the same water loss kinetics by adjusting the relative humidity conditions of the dehydration chambers. The temperature effect was also evaluated by monitoring grape withering in two unconditioned dehydration rooms featuring the natural environmental conditions of two different geographical locations in the Valpolicella growing area (Verona, Italy). The metabolomic analysis of volatile and non-volatile compounds, together with the expression analysis of selected genes revealed that the temperature has a direct impact on organic acids, phenolics and volatile compounds metabolisms, affecting important wine quality traits.

2 Materials and Methods

2.1 Experimental setup

Grape bunches of cv. Corvina (*Vitis vinifera* L.) were manually harvested at commercial ripening in season 2018 from vines grown in the property of the Allegrini Estate, located in the Valpolicella wine district (45°53'N; 10°83'E, 305 m a.s.l., Verona, northeast Italy). One layer of intact clusters (about 5–6 kg) was laid on perforated three plastic trays (40 x 60 x 15 cm each). The trays were placed for dehydration in two thermo-hygrometrically controlled rooms (16 m³). One room was set to higher temperature and relative humidity (Controlled High Temperature room, C-HT; 12 ± 0.5°C and 70 ± 3%) while the other room to lower temperature and relative humidity (Controlled Low Temperature room; C-LT; 8 ± 0.5 °C and 60 ± 2%). In both dehydration rooms the relative humidity was adjusted daily to maintain the same grape water loss (WL) rate and infer exclusively the temperature effect on the dehydration process. The rooms were kept under constant ventilation (0.2 m/s).

In the same season, grape bunches of cv. Corvina grown in the area of Gazzo di Marano di Valpolicella (45°55'N; 10°90'E, 361 m a.s.l.) were harvested in trays as describe above and split between one withering facility located in a plain area and one rather hilly to evaluate the temperature effect on dehydration process under natural conditions. The hilly withering facility located in Gazzo di Marano di Valpolicella (45°55'N; 10°90'E, 382 m a.s.l.) registered the higher temperatures (Natural High Temperature room, N-HT), while the plain withering facility located in Valgatarà (45°54'N; 10°91'E, 191 m a.s.l.) registered the lower temperatures (Natural Low Temperature room, N-LT). Temperature and relative humidity were monitored every two hours employing data loggers (HOBO UX100-023, Onset®, USA) during the withering process at all conditions (C-HT, C-LT, N-HT and N-LT).

2.2 Grape sampling and berry quality assessment

During the withering period, weight loss was determined by periodically weighting three trays placed in each condition to account for the biological replicates until the end of the dehydration process that was stopped at ~25% and ~30% berry weight loss (WL) for withering under controlled and natural conditions, respectively. Berries were collected from bunches at three time points corresponding to harvest time (T0), to ~15% weight loss (T1) and at the end of withering (T2) (Table S1). For each sample, three replicates of 100 berries each were randomly collected. Only healthy undamaged bunches were considered for the analysis. The collected biological material was used for quality assessment of total soluble solids content (TSS; °Brix), titratable acidity (TA; g/L tartaric ac.), pH and molecular analysis (metabolomics and transcriptional analysis). The TSS, TA and pH were determined as previously described by Zenoni et al. (2016).

2.3 Metabolite extraction

Grape berry samples were differently managed depending on the dehydration stage as previously described (Brillante et al., 2018). For T0 samples, 300 mg of fresh frozen powders were weighed and extracted with 3 volumes (w/v) of methanol acidified with 1% (v/v) HCl. For T1 and T2 samples, 255 and 210 mg were respectively weighed and a volume of water equal to the measured mean weight loss occurred during withering was added. The extraction protocol was then applied like described for T0. The extraction was performed as previously described (Negri et al., 2021). Briefly, the extracts were vortexed for 30 s, sonicated at 40 kHz in an ultrasonic bath (SOLTEC, Milano, Italy) for 15 min in ice and centrifuged at 14,000× g at 4°C for 10 min. The supernatants were collected and eventually stored at -20°C. Prior the analysis, two quality controls were created by joining equal volumes from each sample belonging to a specific harvest year. Samples were diluted 1:10 with water LC-MS grade (Honeywell) and naringenin was used as internal standard at a final concentration of 100 pg/μL. The aqueous extracts were filtered through Minisart RC4 filters with 0.2 μm pores (Sartorius, Göttingen, Germany) and 2 μl were submitted to LC-MS analysis.

2.4 Untargeted metabolomics analysis

The instrument consisted of an ACQUITY UPLC I CLASS system (Waters, Milford, MA, USA) equipped with a reverse phase HSS T3 C18 column (2.1 mm × 100 mm, 1.8 μm), kept at 30°C. Water acidified with 0.1% (v/v) formic acid and pure acetonitrile were used as solvent A and B, respectively. The elution gradient started with 0% B; kept an isocratic condition at 0% B for 1 min; increased to 40% B at 10 min; reached to 70% B at 13.5 min; rose to 99% B at 14 min; kept an isocratic condition at 99% B for 2 min; decreased to 0% B at 16.10 min; kept an isocratic condition at 0% B (re-equilibrium to restore the initial condition) for 3.9 min. The method lasted 20 min. The flow rate was set at 0.350 mL/min. The instrument presented an autosampler Acquity FTN kept at 8°C, and an Acquity eLambda PDA

detector (Waters). The mass spectrometer was a Xevo G2-XS qTOF mass spectrometer (Waters) with an electrospray ionization (ESI) as ion source set up with parameters described in a previous report (Commisso et al., 2019). Metabolites were ionized in either positive or negative ionization and MS data was acquired in continuum and sensitivity modes. The scan range was set to 50–2000 m/z, with a scan time of 0.3 s. CID fragmentation was performed by using Argon with a fixed collision energy set at 35 V. Few samples were analyzed twice by using a higher (45V) and lower (20V) fragmentation energy in order to facilitate the identification process. Metabolites identification was performed as previously described (Negri et al., 2021). The accuracy of the mass spectrometer was monitored by infusing a solution of 100 pg/μl leucine-enkephalin (flow rate of 10 μl/min) and generating a signal of 556.2771 in positive mode and 554.2615 in negative mode. Masslynx v4.1 (Waters) was used to control the UPLC-MS functions and to manually check the peak area of specific metabolite of interests. The MS data files were processed by using Progenesis QI (Waters), using default parameters, to get a data matrix including m/z features and the relative metabolite abundances.

2.5 Grape maceration and micro-vinification

At the end of withering, berries from three trays that were withered under the same conditions were pooled together and manually destemmed to obtain two batches of 12.5 kg each, respectively for the C-HT and C-LT rooms. To analyze the berry volatile compounds profile 500 g of berries were taken from each batch, in three replicates. The berries were then hand crushed with 50 mg of MBK and placed for maceration into 1- glass vessel where 100 ml of 15% (w/w) ethanol and 60 mg of dimethyl dicarbonate were added. The vessels were hand stirred daily for 8 days then pressed, clarified by centrifugation at 4500 rpm for 15 minutes at 5° C (Avanti J-25, Beckman Coulter, California, USA) and bottled in 330 ml glass bottles with crown caps.

As for micro-vinification, 3.5 kg berries were taken from each batch in three replicates. The grapes were then hand crushed with 100 mg/kg of potassium metabisulphite (MBK) and put into 5 L glass vessel. Glucose + fructose, total acidity and tartaric acid were analyzed using a Biosystems Y15 multiparametric analyzer (SinaTech Srl, Fermo, Italy). For must inoculation, 100 g of *Saccharomyces cerevisiae* Zinfandel commercial starter (Vason, Verona, Italy) were rehydrated in 1-l water at 37° C for 15 min and 7.5 ml of the rehydrated culture was used to inoculate musts. Fermentations were carried out at 22 ± 1°C, with cap being broken twice a day by gently pressing it down skins with a steel plunger and density and temperature monitored daily. Upon completion of alcoholic fermentation (glucose + fructose < 2 g/l), wines were pressed, cold settled and then clarified by centrifugation at 4500 rpm for 15 minutes at 5° C (Avanti J-25, Beckman Coulter, California, USA). MBK was added up to a final free SO₂ concentration of 25 mg/l, after which the wines were bottled in 330 ml glass bottles with crown caps.

2.6 Analysis of volatile compounds

For free and glycolyzed volatile compounds (VOCs) profile, solid-phase extraction (SPE) followed by GC-MS analysis was used,

according to the procedure described by (Slaghenaufi et al., 2020). An amount of 100 μ l of internal standard 2-octanol (4.2 mg/l in ethanol) was added to samples prepared with 50 ml of wine and diluted with 50 ml of deionized water. Samples were loaded onto a BOND ELUT-ENV, SPE cartridge (Agilent Technologies, Santa Clara, CA, USA) previously activated with 20 ml of dichloromethane, 20 ml of methanol and equilibrated with 20 ml of water. After sample loading, the cartridges were washed with 15 ml of water. Free VOCs were eluted with 10 ml of dichloromethane, and then concentrated under gentle nitrogen stream to 200 μ l prior to GC injection. After SPE elution of free VOCs, glycosidic precursors were eluted with 20 ml of methanol and collected. Enzymatic hydrolysis was performed as described in Slaghenaufi et al. (2019). Glycosidic extracts were evaporated under vacuum thanks to Rotavapor (Buchi R-215 Rotavapor System), recovered with 5 ml of citrate buffer (pH 5), 100 mg of polyvinylpyrrolidone (PVPP) and 200 μ l of enzyme solution AR2000 (70 mg/ml in citrate buffer) were added. Samples were stored at 37°C overnight. Aglycones were extracted as free volatile compounds with the SPE protocol as described above.

GC-MS analysis, was carried out on an HP 7890A (Agilent Technologies) gas chromatograph coupled to a 5977B quadrupole mass spectrometer, equipped with a Gerstel MPS3 auto sampler (Müllheim/Ruhr, Germany). Separation was performed using a DB-WAX UI capillary column (30 m \times 0.25, 0.25 μ m film thickness, Agilent Technologies) and helium (6.0 grade) as carrier gas at 1.2 ml/min of constant flow rate. GC oven was programmed as follows: started at 40°C for 3 min, raised to 230°C at 4°C/min and maintained for 20 min. Mass spectrometer was operated in electron ionization (EI) at 70 eV with ion source temperature at 250°C and quadrupole temperature at 150°C. Mass spectra were acquired in synchronous Scan (m/z 40–200) and SIM mode. Samples were analysed in random order. The quantification was done by calibration curves as described in (Luzzini et al., 2021). Calibration curve was prepared for each analyte using seven concentration points and three replicate solutions per point in model wine (12% v/v ethanol, 3.5 g/l tartaric acid, pH 3.5) 100 μ l of internal standard 2-octanol (4.2 mg/l in ethanol) was added to each calibration solution, which was then submitted to SPE extraction and GC-MS analysis as described for the samples. Calibration curves were obtained using Chemstation software (Agilent Technologies, Inc.) by linear regression, plotting the response ratio (analyte peak area divided by internal standard peak area) against concentration ratio (added analyte concentration divided by internal standard concentration).

2.7 RNA extraction and reverse transcriptase quantitative PCR

Total RNA was extracted from ~200 mg of ground berry pericarp (pulp and skin) using the Spectrum Plant Total RNA kit (Sigma-Aldrich). Some modification to the protocol was performed according to Fasoli et al. (2012). RNA quality and quantity were determined using a Nanodrop 2000 spectrophotometer (Thermo Fisher Scientific) and DNA was removed with DNase I (Thermo Fisher Scientific). The cDNA synthesis and qRT-PCR analysis were carried out as previously described (Massonnet et al., 2017). Each expression value was measured in triplicate and normalized to the internal

control *VvUBIQUITIN1*. The primer sets are listed in Table S2. Amplification efficiency and standard error values were calculated as previously described (Zenoni et al., 2020).

2.8 Statistical analysis

For the metabolites analysis, peak area values presented in the data matrix were Pareto scaled and centered and then submitted to an unsupervised principal component analysis (PCA) through SIMCA 13.0 (Umetrics). Supervised multivariate statistical analysis were carried out by clustering the samples based on indications inferred by PCA or previous information, and by performing an Orthogonal Bidirectional Partial Least Square-Discriminant Analysis (O2PLS-DA). The models were validated by performing a CV-ANOVA and a permutation test (400 permutations). The stilbenes and flavonols metabolite families were further investigated applying hierarchical clustering analyses (HCA) and Heatmap presentations, using Pearson correlation coefficient and Ward as clustering algorithm employing R (version 4.0.3) within the RStudio (version 1.3.1093) platform. For specific metabolites of interests, a one-way ANOVA between groups was performed by using SPSS software and Tukey's test as post-Hoc ($p < 0.05$).

As for the VOCs detected, the compound concentrations were auto-scaled (mean centered and divided by the standard deviation of each variable) and analyzed applying unsupervised PCA. A *t*-test was additionally applied on the VOCs families concentrations in the different conditions ($p < 0.05$).

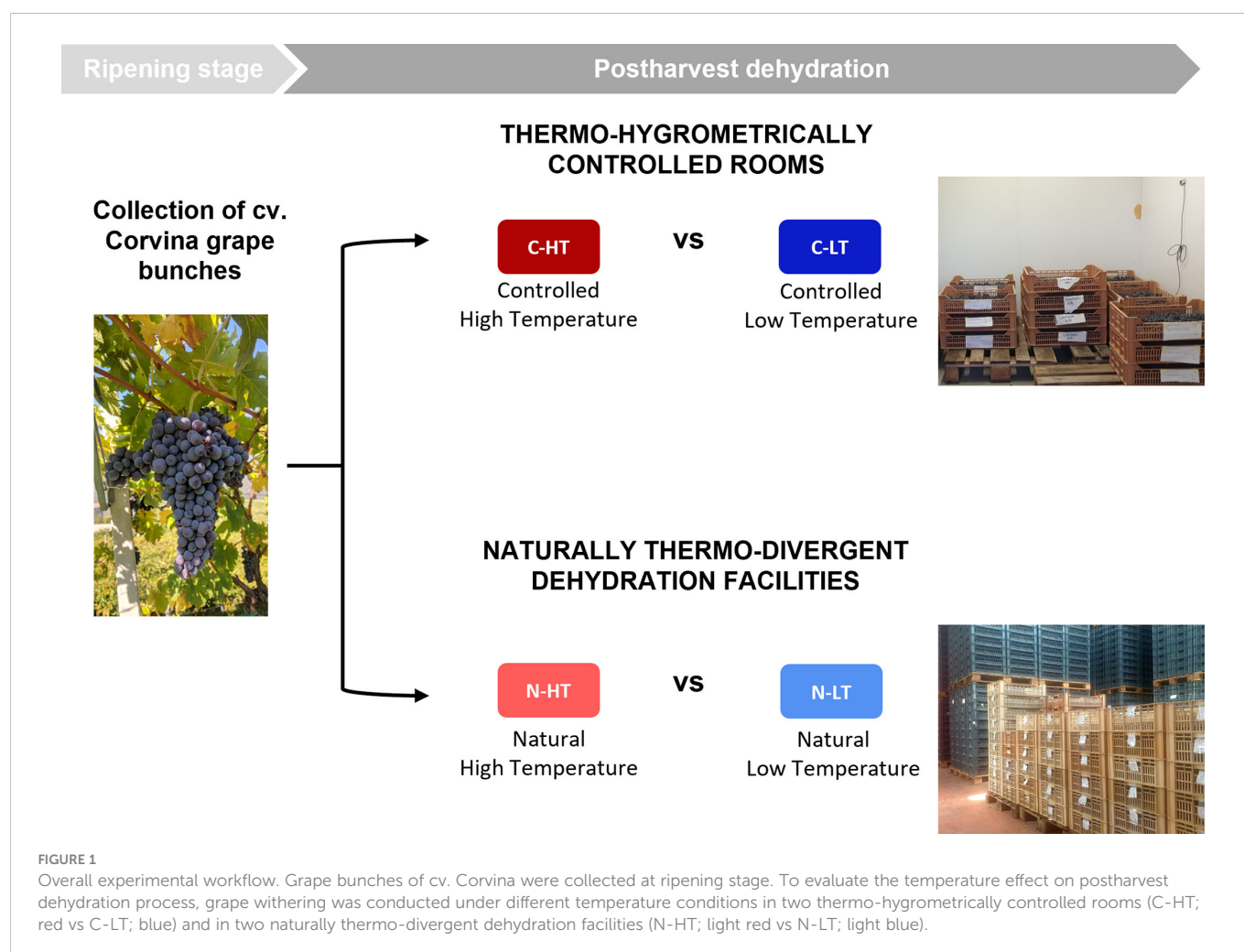
3 Results

3.1 Postharvest dehydration under different temperature conditions

In order to dissect the effect of the temperature from that of the dehydration rate on grapes during withering we propose the experimental workflow described in Figure 1. Grape bunches of cv. Corvina were harvested and placed in two dedicated rooms at different monitored thermo-hygrometric conditions. The two rooms were set at different temperatures (average delta = $3.6 \pm 0.5^\circ\text{C}$), while the relative humidity (RH) was adjusted to maintain the same grape water loss (WL) rate in both conditions. Thus, we defined a controlled high temperature ($12 \pm 0.5^\circ\text{C}$) and high RH ($70 \pm 3\%$) room (C-HT) and a controlled low temperature ($8 \pm 0.5^\circ\text{C}$) and low RH ($60 \pm 2\%$) room (C-LT; Figures 2A, B; Figure S1). RH adjustments allowed to obtain the 28% of WL in 87 days in both C-HT and C-LT rooms (Figure 2C). Berry samples were collected at harvest (T0), at ~15% weight loss (42 days after harvest, T1) and at ~25% weight loss (77 days after harvest, T2) and further characterized.

Despite the pH values increased under both settings, TSS and TA were higher in grapes withered in the C-LT room (Table 1). The higher TA likely reflected a higher level of malic acid because an equal concentration of tartaric acid was revealed (Table S3).

The temperature effect on cv. Corvina berries dehydration was also evaluated monitoring the process in two unconditioned dehydration rooms featuring the natural environmental conditions

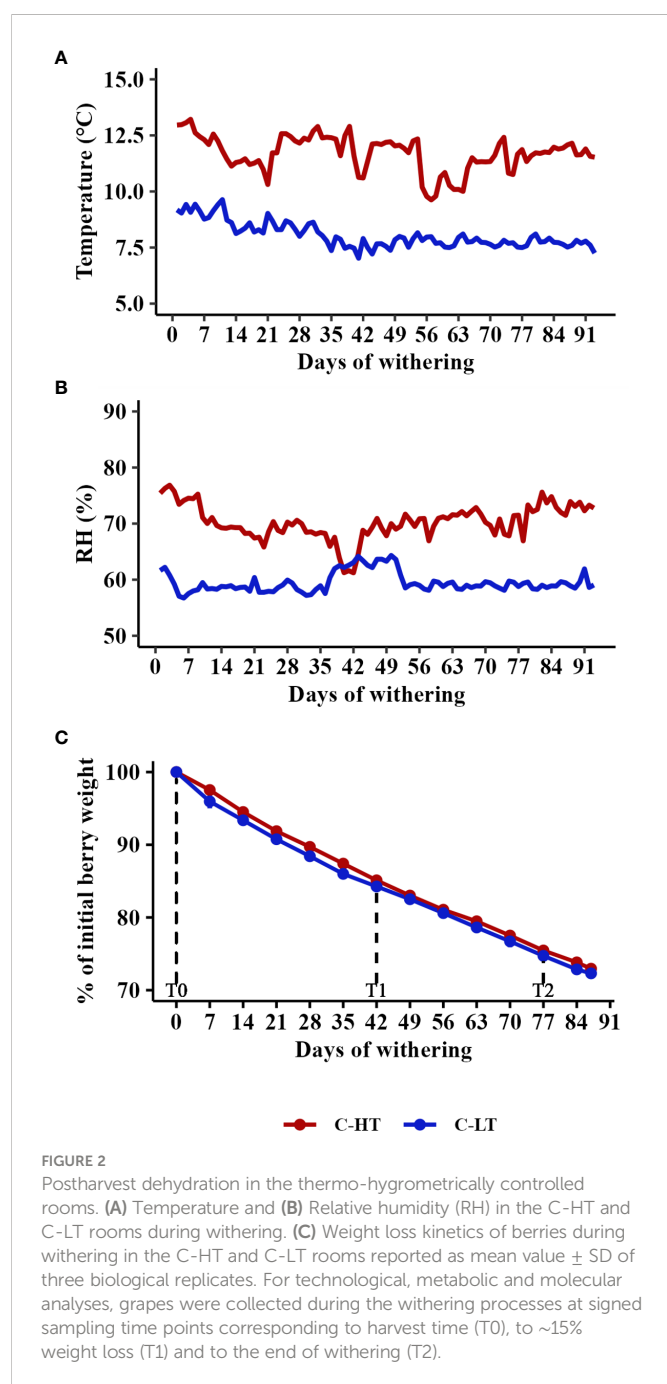


of two geographical locations, one located on a sunlight exposed hill side (N-HT) and the other located in a plain area typically characterized by the presence of fog (N-LT). Temperature and RH were monitored every two hours and daily average parameters were plotted (Figures 3A, B). Temperature trends of the two facilities were similar and varied within 10°C and 20°C during the first withering period (October–November). Only starting from the 45th day of withering the temperature gradually decreased and started to diverge between the two processes (Figure 3A). As expected, the lowest temperature was detected at the N-LT facility where we also recorded a greater temperature span (6 to 7°C) in comparison to the N-HT facility (2 to 3°C; Figure S2). Likewise, RH was quite comparable between the two conditions during the first two months and diverged throughout the rest of the process registering the lowest value at the N-HT facility (Figure 3B).

Differently from the controlled rooms, divergent withering kinetics were registered at the two facilities (Figure 3C). In fact, given that both withering processes were carried out for 96 days, final WL values ended up being 27% and 31% in N-LT and N-HT conditions, respectively. Similarly to the controlled conditions, pH values did not change during the N-LT and N-HT dehydration processes, while TSS and TA progressively increased. However, subtly higher TSS and TA values were registered at higher temperature at natural compared to controlled withering conditions (Table 2).

3.2 Non-volatile metabolite profile changes during postharvest dehydration under different temperatures

The impact of temperature in the C-HT and C-LT dehydration rooms on the metabolic profile of the berries collected at T0, T1 and T2 was investigated by an untargeted UPLC-HRMS approach. The data processing through Progenesis QI generated a data matrix of 1585 *rt*/*mz* features, 182 of which were putatively identified (Supplementary File 1). The detected metabolites belonged to the class of amino acids, anthocyanins, flavan-3-ols, flavanones, flavonols, hydroxybenzoic and hydroxycinnamic acids, organic acids, peptides, phenylethanoids, stilbenes and sugars. The data matrix was initially explored through an unsupervised PCA analysis (Figure 4A) that revealed a substantial distribution of the samples by withering time and C-HT/C-LT conditions along the PC1, explaining the 51% of the total variance. The PC2 explained the 20.6% of the total variance and appeared to discriminate samples mainly by the different withering condition. The PC1-PC2 plot showed that the samples of the two conditions were weakly separated at T1, whereas could be told apart at T2. In order to better highlight the effects of the withering condition, a O2PLS-DA supervised analysis was performed by superimposing the withering conditions as classes. The final model showed good sample clustering in the scatter plot (Figure 4B) and



allowed to visualize the metabolites characterizing the specific classes in the loading plot (Figure 4C). Anthocyanins and flavan-3-ols better correlated with the harvest stage (T0) that, on the contrary, was

poorly characterized by stilbenes. Interestingly, flavonols were associated with samples withered at low temperature (C-LT). Based on this information, an OPLS-DA was performed only on samples collected at T2 to emphasize any metabolic difference by withering condition at the end of the process (Figure 4D). The loading plot showed a strong correlation of stilbene oligomers, including dimers, trimers and tetramers with the C-HT condition, while several flavonols were highly associated with the C-LT condition. Due to their great correlation with the withering conditions, further investigations were carried out on the flavonol and stilbene classes of compounds (Figure 5). Hierarchical clustering analysis showed that flavonols were accumulated at T1 in both withering conditions and continued to increase at T2 in the berries exposed to low temperature, whereas a reduction was observed at T2 when exposed to high temperature (Figure 5A). This trend was well exemplified by the flavonols quercetin-3-O-glucoside and kaempferol-3-O-glucoside (Figures 5B, C). Concerning stilbenes, we observed the accumulation of these compounds to be a typical feature of the end of withering (T2) in both conditions. However, the polymerization degree diverged depending on the temperature conditions (Figure 5D) and higher stilbene complexity was found associated to HT-T2 grapes. Interestingly the stilbene monomers trans- and cis-resveratrol, representing the direct products of the key biosynthetic enzyme stilbene synthases, were found in greater amount in the LT-T2 grapes (Figures 5E, F).

3.3 Effect of withering temperature on the volatile profile in withered grapes and derived wines

At the end of the process, the grapes dried under both controlled conditions and the derived wines were analyzed in triplicate by SPE-GC-MS to determine their volatile profiles. In the grapes, 27 glycosidic precursors (8 benzenoids, 6 terpenes, 4 alcohols, 4 C6 alcohols, 3 fatty acids and 2 norisoprenoids) and 24 free volatile compounds (8 benzenoids, 5 terpenes, 4 C6 alcohols, 3 alcohols, 3 fatty acids and 1 norisoprenoid) were detected and quantified (Table S4). The samples were then analyzed applying an unsupervised PCA using the VOCs families as predictors (Figure 6A). The PC1 and 2 explained respectively the 60.3% and the 20.3% of the total variance and evidenced a clear separation of the withering conditions by the PC1 and replicate variability mainly by the PC2. Most of the identified VOC families were highly associated with grapes withered under low temperature (C-LT): free terpenes, C₆ alcohols, alcohol and their glycosidic precursors along with glycosidic norisoprenoids and free fatty acids. Interestingly, both free and

TABLE 1 Total soluble solids (TSS), total acidity (TA) and pH measured in grapes dehydrated in the C-HT and C-LT rooms at sampling time points (T0, T1 and T2).

Parameter	T0			T1						T2					
				C-HT			C-LT			C-HT			C-LT		
TSS (°Brix)	22.07	\pm	0.15	25.30	\pm	0.11	26.63	\pm	0.25	28.53	\pm	0.06	31.20	\pm	0.25
TA (g/L tartaric ac.)	5.67	\pm	0.14	5.83	\pm	0.07	6.00	\pm	0.12	6.00	\pm	0.00	6.33	\pm	0.12
pH	3.21	\pm	0.02	3.37	\pm	0.03	3.34	\pm	0.01	3.53	\pm	0.04	3.48	\pm	0.01

$n=3 \pm$ SD. SD, Standard Deviation.

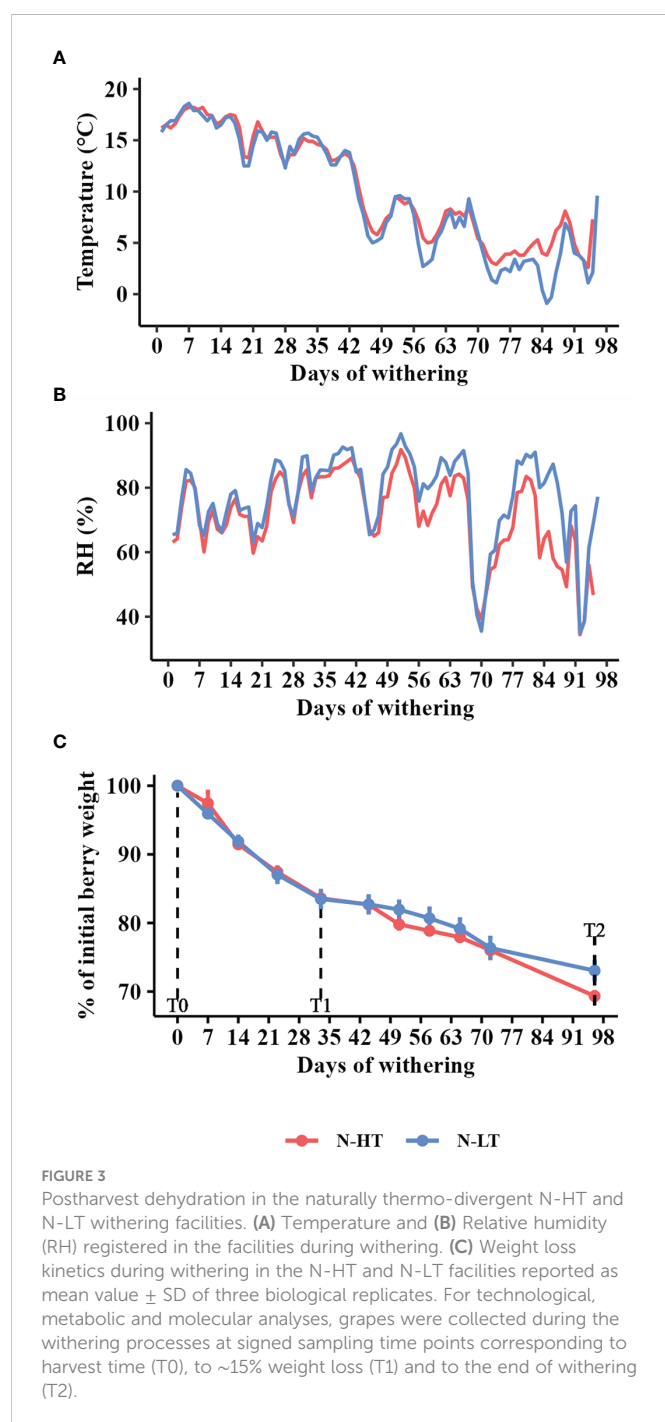


TABLE 2 Total soluble solids (TSS), total acidity (TA) and pH measured in grapes dehydrated in the N-HT and N-LT facilities at sampling time points T0, T1 and T2).

Parameter	T0			T1						T2					
				N-HT			N-LT			N-HT			N-LT		
TSS (°Brix)	20.83	\pm	0.15	24.13	\pm	0.21	23.93	\pm	0.12	28.70	\pm	0.20	27.77	\pm	0.29
TA (g/L tartaric ac.)	7.25	\pm	0.00	7.08	\pm	0.08	7.62	\pm	0.13	8.20	\pm	0.10	8.00	\pm	0.00
pH	2.73	\pm	0.02	2.83	\pm	0.01	2.80	\pm	0.01	2.89	\pm	0.02	2.84	\pm	0.01

$n=3 \pm$ SD. SD, Standard Deviation.

glycosidic benzenoids families were instead associated to samples withered under high temperature (C-HT).

The volatile profile of the wines analyzed by SPE-GC-MS revealed 42 identified free VOCs (8 terpenes, 8 benzenoids, 6 alcohols, 5 ethyl esters, 4 C₆ alcohols, 3 acetate esters, 3 fatty acids, 3 norisoprenoids and 2 branched-chain ethyl esters; [Table S5](#)) and was further investigated by unsupervised PCA. PC1 (explaining 44.5% variance) showed a better separation of the withering conditions compared to PC2 (explaining 27.9% variance) ([Figure 6B](#)). The C-LT wine samples were highly correlated with the terpenes, norisoprenoids and C₆ alcohols families and, to a minor extent, with ethyl and acetate esters. Conversely, benzenoids, fatty acids, alcohols and branched chain ethyl esters were more associated with the C-HT wines. A graphic presentation of the free VOCs concentration is available in [Figure S3A](#). To study the temperature effect on the compounds primarily deriving from the grape metabolism during withering, a further unsupervised PCA was performed using the single varietal VOCs as predictors ([Figure S3B](#)). Thus, only those compounds believed to be primarily of varietal origin and less affected by yeast activity during fermentation (i.e., terpenes, norisoprenoids, C₆ alcohols and benzenoids) were considered in this analysis. The PC1 and 2 of the PCA model explained 59.3% and 19.1% of the total variance, respectively, and the biplot projection showed a clear separation of the wine samples by PC1 according to the withering condition, with most of the varietal VOCs clustering with the C-LT wines. On the other hand, the C-HT wines showed strong correlation only with benzaldehyde. The relative concentration of terpene compounds is reported in [Figure 6C](#). Although the proportions among terpenes were analogous, the C-LT wines exhibited an overall higher content compared to the C-HT ones, suggesting that the effect exerted by temperature was comparable on each of the identified members of the terpene family.

These results suggest that different temperature conditions altered the wine VOC profile and that lower temperatures during grape withering could boost the overall terpenoid content in wines.

3.4 High temperature negatively affects the expression of quality-related genes during postharvest dehydration

To study the effect of the different postharvest conditions (C-HT versus C-LT) on dehydrating berries at transcriptional level, we

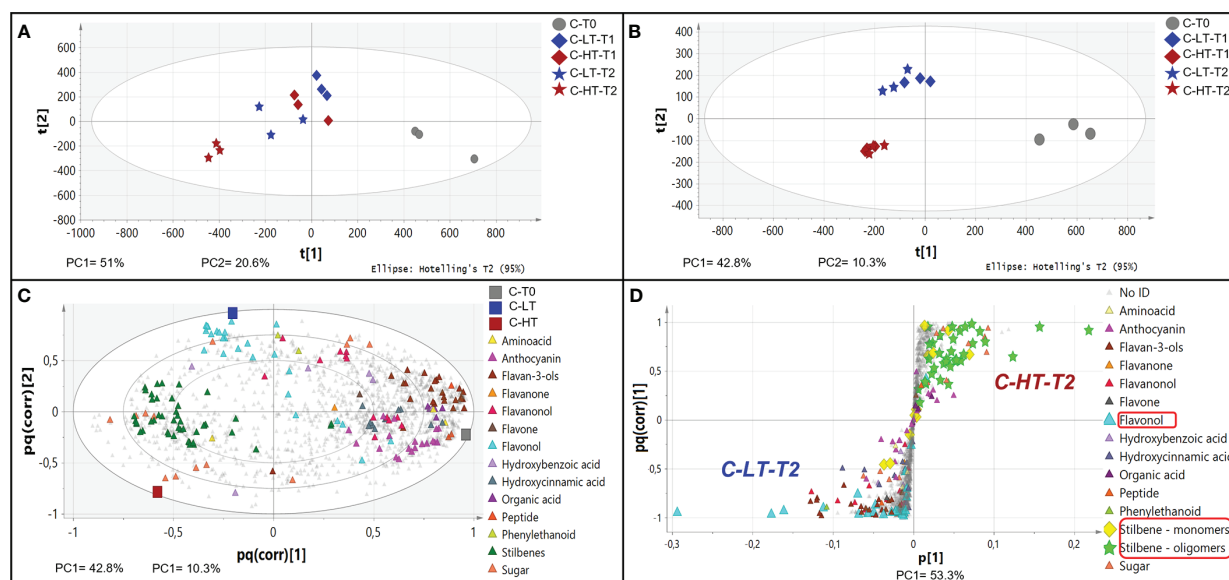


FIGURE 4

Non-volatile metabolite profile of grapes dehydrated in the C-HT and C-LT rooms. (A) PCA score scatter plot of non-volatile metabolites from berries collected during postharvest dehydration under C-HT and C-LT conditions. (B) O2PLS-DA score scatter plot highlighting a good sample clustering based on the withering conditions. (C) O2PLS-DA loading plot showing metabolites (triangles) featuring the mature phase (T0) and metabolites featuring drying berries collected in the C-HT and C-LT rooms. For this analysis, the T1 and T2 samples were grouped together. (D) OPLS-DA S-loading plot showing metabolites (triangles) correlating with the high or the low-temperature-condition at the end of the process (T2). Concerning stilbenes, monomeric forms are highlighted with yellow diamonds, whereas oligomers are shown as green stars.

profiled the expression of some candidate genes, previously identified as players in the molecular mechanisms controlling the development of quality traits (Zenoni et al., 2020), at three time points (T0, T1 and T2) over withering (Figure 7).

The analysis of the expression level of a *malate dehydrogenase* (*VvMDH*), involved in malic acid degradation, revealed a downward trend throughout the dehydration process in both conditions, with a lower expression at T1 in berries dehydrated in C-LT room (Figure 7A). This fits with the progressive increase of the total acidity observed in both processes but greater when grapes are withered at lower temperature (Table 1, Table S3). We also profiled the expression of a *phenylalanine ammonia-lyase* (*VvPAL*), enzyme in charge of channeling phenylalanine into the phenylpropanoid pathway. The *VvPAL* expression level progressively increased during withering with a higher expression level (greater than 3-fold) in grapes withered in the C-LT room in comparison to the grapes processed in the C-HT room (Figure 7B). As expected, an upward expression pattern during withering was also described for the *stilbene synthase 27* (*VvSTS27*) that was previously reported to be a molecular marker of a slow grape dehydration process (Zenoni et al., 2020) (Figure 7C). Moreover, the lower temperature of the C-LT room determined a stronger and earlier induction of the expression of this gene compared to the other condition. The opposite trend was found for a laccase gene (*VvLAC*), that was also reported to be a marker generally upregulated during withering (Zenoni et al., 2020). In fact, *VvLAC* showed a sharp induction at T1 in the C-HT room, followed by a drop in expression thereafter. The withering conditions of the C-LT room instead determined only a slight induction throughout the process (Figure 7D). Finally, we examined the expression of a terpene synthase gene (*VvTPS07*) whose response to

a lower temperature resembled that of *VvSTS27* at T1 that is significantly higher expression in the C-LT than in the C-HT room conditions (Figure 7E).

3.5 The temperature effect under natural conditions

In the N-HT and N-LT withering facilities, characterized by naturally divergent temperature conditions, dissimilar grape withering kinetics were determined (Figure 3C). In spite of that misalignment, the dehydrated berries at both conditions were compared for metabolomic changes at the end of the process and for the expression of *VvMDH*, *VvPAL*, *VvSTS27*, *VvLAC* and *VvTPS07*, at T0, T1 and T2 stages (Table S1).

By performing an untargeted UPLC-HRMS analysis we obtained a data matrix including 1584 *rt/mz* features, 181 of which were putatively identified (Supplementary File 1). The PCA analysis showed that the total explained variance was 81%, with the PC1 explaining the 55.9% and the PC2 the 25.1%, however, unlikely the PCA performed on C-HT and C-LT samples, it was not possible to clearly separate the berries withered at N-HT conditions from those at N-LT (Figure 8A). Nevertheless, focusing on flavonols and stilbenes families we found similarity to the trends observed for grapes withered under controlled conditions (Figures 8B–E). In details, the N-LT grapes presented an overall higher amount of flavonols, in comparison to the N-HT grapes. Besides, two distinct trends could be hypothesized: either higher accumulation in N-LT, as for quercetin and myricetin derivatives, or higher degradation in N-HT, as for kaempferol derivatives (Figures 8B, C). Moreover, the oligomeric form

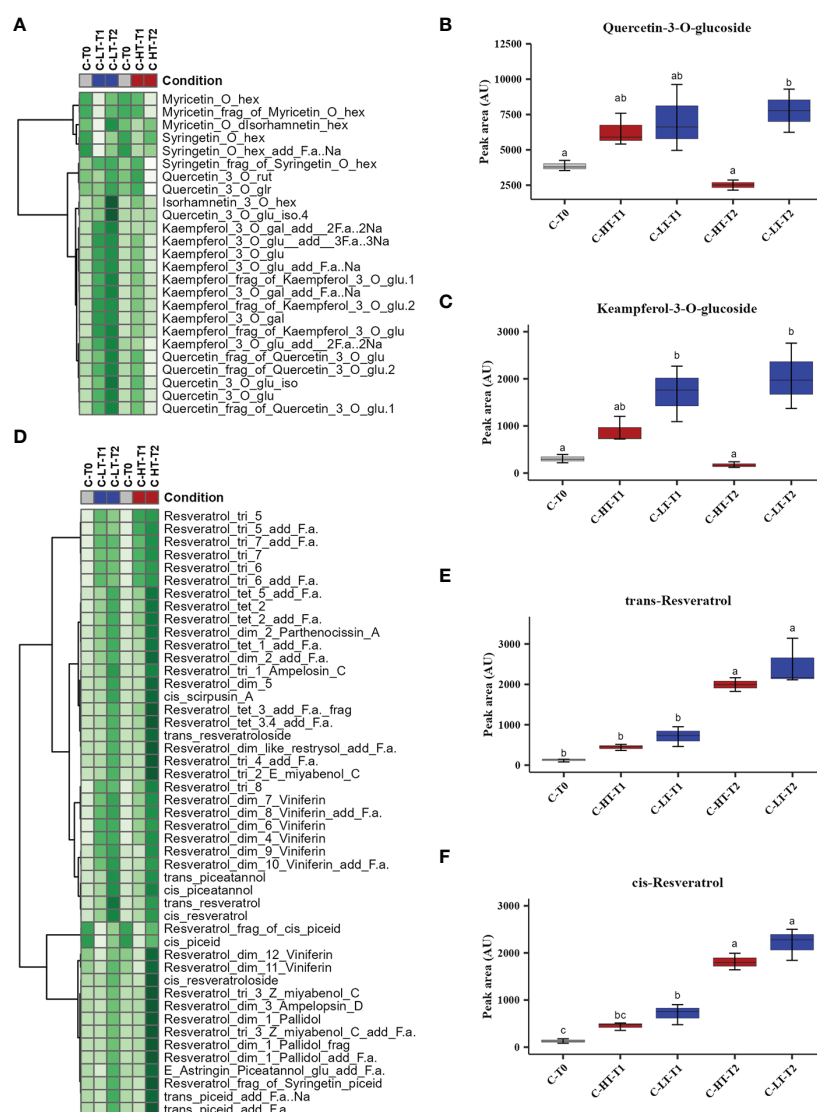


FIGURE 5

Variation of stilbenes and flavonols in grapes dehydrated in the C-HT and C-LT rooms. **(A)** Heatmap and Hierarchical Cluster Analyses performed on flavonols scaled peak areas (AU) measured at harvest (T0) and during withering (T1 and T2) under C-HT and C-LT conditions. Green and white colors represent high and low peak area values, respectively. Pearson correlation coefficient was employed to group the different metabolites, using average as clustering algorithm. Abbreviations: add=adduct; frag=fragment; f.a.=formic acid; gal=galactoside; glr=glucuronide; glu=glucose; hex=hexoside; iso=isotope; rut=rutinoside. **(B)** Quercetin-3-O-glucoside and **(C)** kaempferol-3-O-glucoside accumulation during withering in high and low temperature conditions. Lowercase letters represent statistically significant difference based on ANOVA and Tukey post-hoc test with $p \leq 0.05$. **(D)** Heatmap and Hierarchical Cluster Analyses performed on stilbenes. **(E)** Trans-resveratrol and **(F)** cis-resveratrol accumulation during withering in high and low temperature conditions. Lowercase letters represent statistically significant difference based on ANOVA and Tukey post-hoc test with $p \leq 0.05$. Abbreviations: add=adduct; dim=dimer; frag=fragment; f.a.=formic acid; gal=galactoside; glr=glucuronide; glu=glucose; hex=hexoside; iso=isotope; rut=rutinoside. tri=trimer; tet=tetramer. Gray colour indicates grapes at harvest (T0); blue colour indicates the C-LT condition; red colour indicates the C-HT condition.

of the stilbenes was generally more prevalent in the N-HT grapes, while the stilbenes monomers cis- and trans-resveratrol were more abundant in the grapes withered at the lower temperatures (N-LT) (Figures 8D, E).

The analysis of candidate genes revealed similar expression trends to the one observed in the samples withered under controlled conditions. We found that the *VvMDH* expression level at the end of the process was lower than that registered at harvest (Figure 9A). We also observed that *VvMDH* was less expressed at T1 and more expressed at T2 in grapes withered at N-LT compared to N-HT. The expression of *VvPAL*, *VvSTS27*, *VvLAC* and *VvTPS07* showed an

upward trend during withering under both natural conditions (Figures 9B–E). However, a differential expression level between the two different natural conditions was visible mainly at T2, likewise observed under controlled settings (Figure 7). This can be explained because major temperature differences between facilities were indeed observed only after the T1 sampling point. Notably, under natural conditions the higher induction of *VvSTS27* and *VvTPS07* at low temperature was maintained also at T2, while under controlled conditions, the temperature effect on the expression of the *VvSTS27* and *VvTPS07*, appeared strong at T1 and less effective at T2.

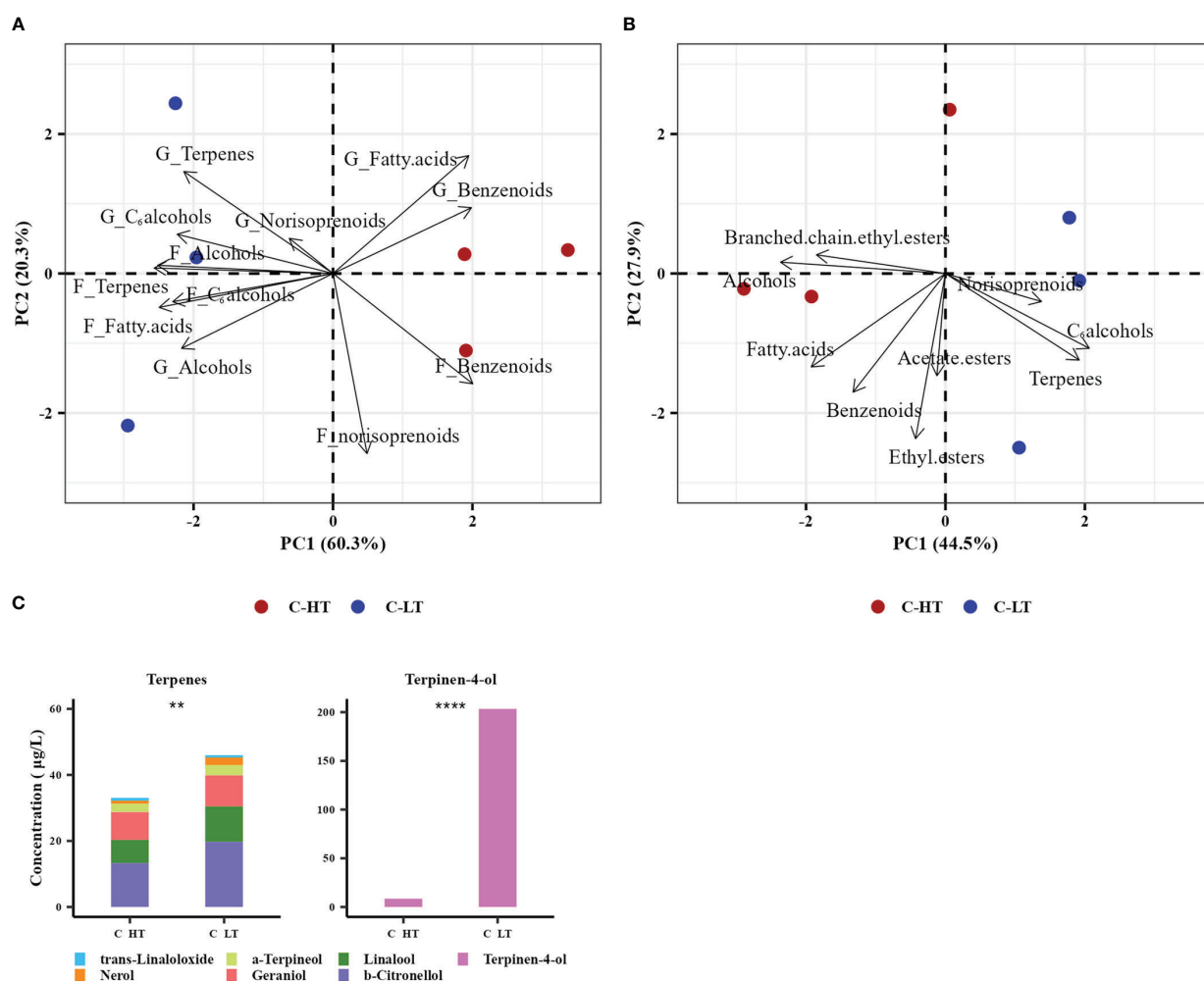


FIGURE 6

Aromatic profile of grapes dehydrated in the C-HT and C-LT rooms and in the derived wines. (A) PCA biplot of grape samples withered in the different rooms (circles) and the free VOCs (prefix F) and glycosidic precursors (prefix G) families identified in them (arrows). (B) PCA biplot of the derived wine samples (circles) and the free VOCs families identified in them (arrows). (C) Bar plot of the 7 free terpenes concentration in wines derived from grape berries dehydrated in the C-HT and C-LT rooms. Specific terpene accumulation is represented in different colors. Terpinen-4-ol was graphically separated due to its eminently higher concentration in both wines. Asterisks represent statistically significant difference based on t-test ($p \leq 0.01 = **$; $p \leq 0.0001 = ****$). Red color indicates the C-HT condition; blue color indicates the C-LT condition.

4 Discussion

4.1 A specific experimental design to dissect the temperature effect

The metabolic changes and the molecular events that characterize the grape postharvest dehydration process strictly depend on the genotype but also on the environmental parameters, in particular temperature and humidity, that typify the facilities where the grapes are placed to undergo withering (Costantini et al., 2006; Mencarelli et al., 2010; Zenoni et al., 2016). Despite the availability of many studies comparing processes conducted at different environmental conditions, including temperature variation, the effect of temperature on grapes placed in dehydrating room after harvest has not been conclusive. Besides the remarkable challenge of setting apart the temperature effect from other factors in experiments featuring a complexity of conditions (e.g., different grape varieties, environmental parameters, times, dehydration kinetics, etc.), the

complication consists in the influence of the temperature on the grape water loss rate that in turn affects the berry transcriptional and metabolic reprogramming occurring during the process (Zenoni et al., 2020). In this work, we analyzed the relationship between environmental conditions and chemical/molecular changes occurring in withering berries and took a step forward in exploring the effect of temperature excluding the puzzling effect of the dehydration rate. To do this we set up an experimental plan in which cv. Corvina grapes were dehydrated at two distinct temperatures while maintaining the same withering kinetics by daily adjustments of the relative humidity. Even though we could not completely rule out that such differences in relative humidity could have directly affected the berry metabolism, we assume that this is an unlikely scenario. Zhang and Keller (2017) postulated that increasing the relative humidity around bunches on the plant could impair the berry ripening metabolism as an effect of a reduced berry cuticular transpiration. Salvetti et al. (2016) showed that removing part of the humid air stacking around withering Corvina clusters

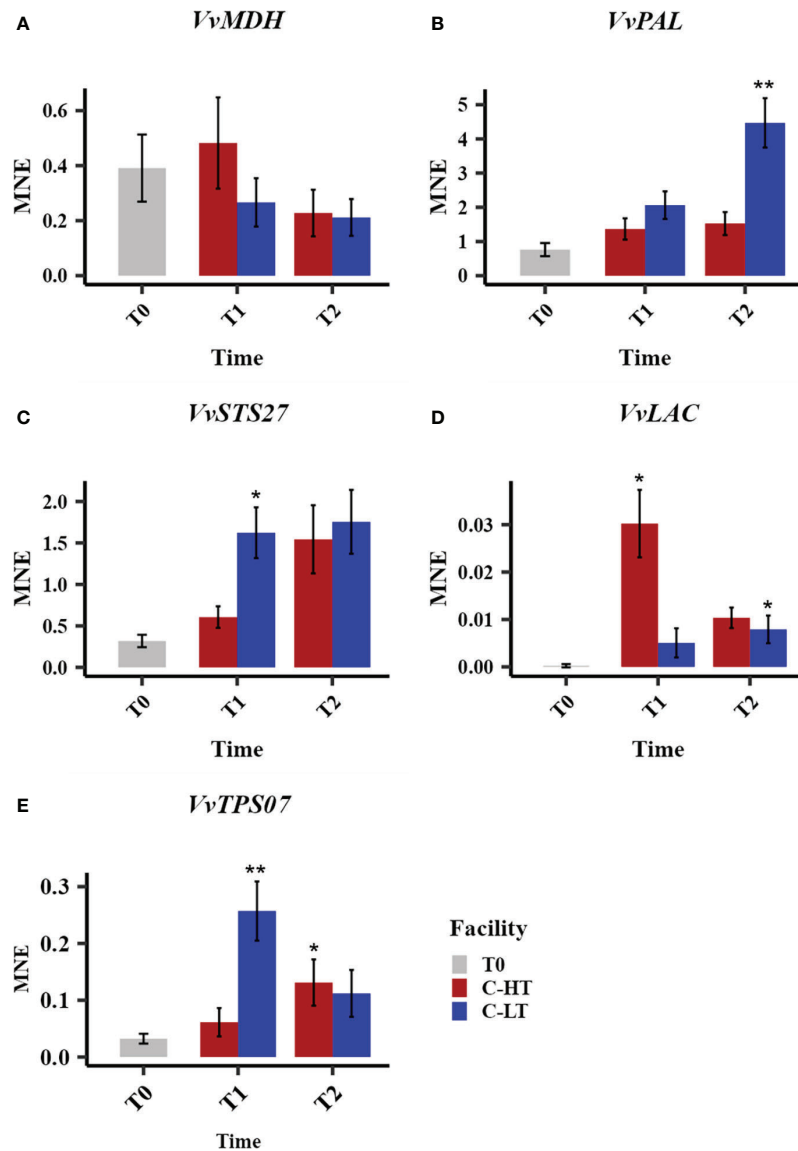


FIGURE 7

Relative expression of quality-related genes during withering in the C-HT and C-LT rooms. Expression profiles of *malate dehydrogenase* (*VvMDH*, A), *phenylalanine ammonia-lyases* (*VvPAL*, B), *stilbene synthase* (*VvSTS27*, C), *laccase* (*VvLAC*, D) and *terpene synthase* (*VvTPS07*, E) genes in grape sampled during withering in the C-HT and C-LT rooms. Error bars represent standard errors ($n = 3$). Blue colour indicates the C-LT condition; red colour the C-HT condition. Asterisks represent statistically significant difference between partially withered grapes (T1 and/or T2) and grapes at harvest (T0), based on t-test ($p \leq 0.05 = *$; $p \leq 0.01 = **$).

resulted in a diversification of the grape microbiota. We did not analyze the microbiota of the grapes withered in the two conditioned rooms that may indeed be different and may have influenced the berry composition. However, except for specific cases (e.g., the *Botrytis cinerea* infection), the relationships between berry metabolism and the microbial consortium associated to postharvest grapes is far to be elucidated.

The conditioned facilities housing the grapes could not ensure a strict control of temperature that fluctuated within a range of 2°C depending on the external climatic condition (fall season). Nonetheless, the temperature difference between the two rooms was maintained in the range of 4 ± 1.0 °C for the whole period. The daily adjustments of the relative humidity in the two rooms were based both on daily measurements of the grape weight loss and the

application of an empirical model. By this approach we obtained similar dehydration kinetics in the two rooms, allowing to attribute the observed grape compositional and molecular changes to the temperature difference. The grapes dehydrated at higher temperature featured slightly lower levels of sugars and titratable acidity (TA) which may be the result of the impact of the temperature on primary metabolism. The close relation between malic acid respiration and temperature is well known for ripening berries and few indications suggest that such relation may hold true also during the postharvest storage of the grapes (D'Onofrio et al., 2019). Tartaric acid was unaffected by temperature, strongly supporting that the differences in TA were entirely attributable to malic acid degradation. Interestingly, higher *MDH* gene expression level was detected in the grapes under C-HT conditions, indicating that an increased

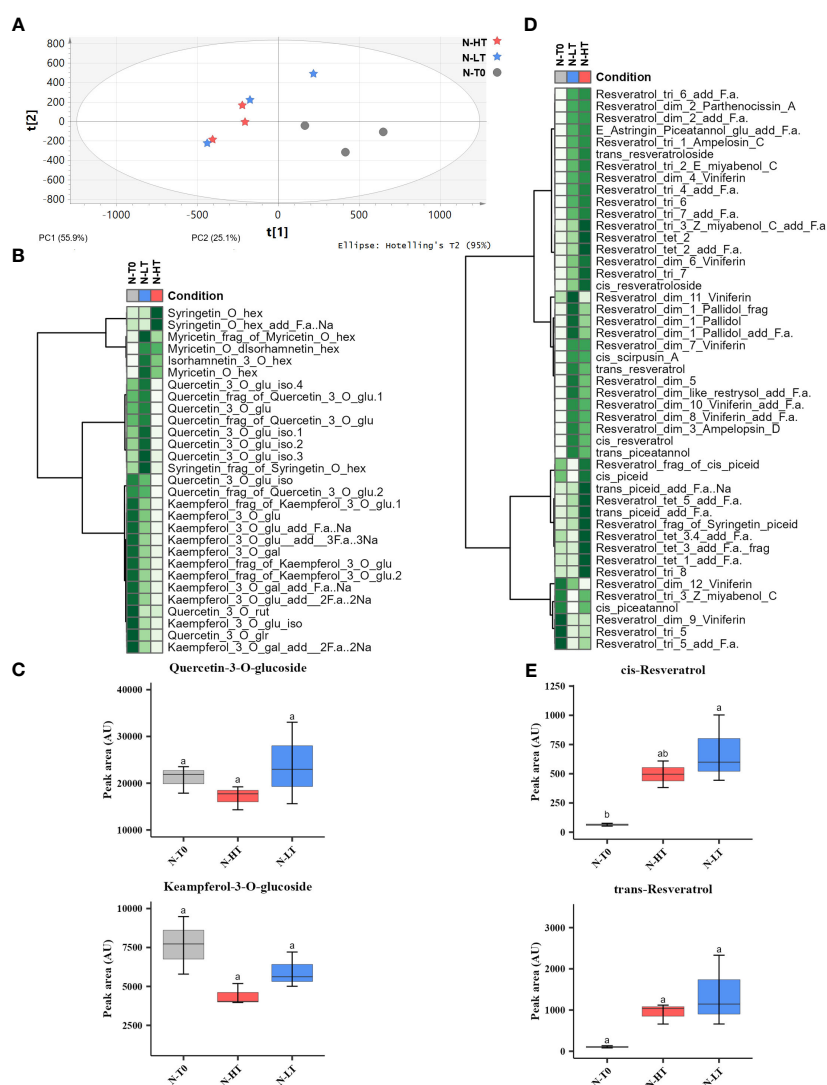


FIGURE 8

Metabolic profile and variation of stilbenes and flavonols in berries following dehydration in the N-HT and N-LT withering facilities. **(A)** PCA score scatter plot of non-volatile metabolites from berries collected at harvest (T0) and at the end of withering under N-HT and N-LT conditions. **(B)** Heatmap and Hierarchical Cluster Analyses performed on flavonols scaled peak areas (AU) measured at T0 and at the end of withering in the N-HT and N-LT conditions. Green and white colors represent high and low peak area values, respectively. Pearson correlation coefficient was employed to group the different metabolites, using average as clustering algorithm. Abbreviations: add=adduct; frag=fragment; f.a.=formic acid; gal=galactoside; glr=glucuronide; glu=glucose; hex=hexoside; iso=isotope; rut=rutinoside. **(C)** Quercetin-3-O-glucoside and kaempferol-3-O-glucoside accumulation during withering in high and low temperature conditions. Lowercase letters represent statistically significant difference based on ANOVA and Tukey post-hoc test with $p \leq 0.05$. **(D)** Heatmap and Hierarchical Cluster Analyses performed on the stilbenes. Abbreviations: add=adduct; dim=dimer; glu=glucose; hex=hexoside; iso=isotope; rut=rutinoside. tri=trimer; tet=tetramer. **(E)** Cis-resveratrol and trans-resveratrol accumulation during withering in high and low temperature conditions. Lowercase letters represent statistically significant difference based on ANOVA and Tukey post-hoc test with $p \leq 0.05$. Gray colour indicates grapes at harvest (T0); light blue colour indicates the N-LT condition; light red colour indicates the N-HT condition.

availability of malic acid degrading enzymes may account for its enhanced depletion.

Seeking to confirm the results obtained in the conditioned rooms, we set up a parallel trial placing the grapes in two unconditioned commercial facilities conjecturing they could hold different indoor temperatures in relation to their geographical locations. In the considered experimental year, the two commercial facilities showed very weak average daily temperature differences, that mainly occurred during the second half of the dehydration period. Despite this have certainly limited any differential response of berry metabolism, we could analytically highlight differences for few metabolite or molecular markers.

4.2 The influence of temperature on phenolic compounds

Several reports showed that changes in phenolic amounts and profile are part of the compositional rearrangement of the grapes when partially dehydrated after harvest and resulting from the simultaneous activity of biosynthetic and catabolic metabolic processes. Albeit highly dependent on the genotype and dehydration method, it was observed that most classes of compounds undergo a general decrease in absolute content possibly related to oxidation phenomena. Only in few cases, a clear induction

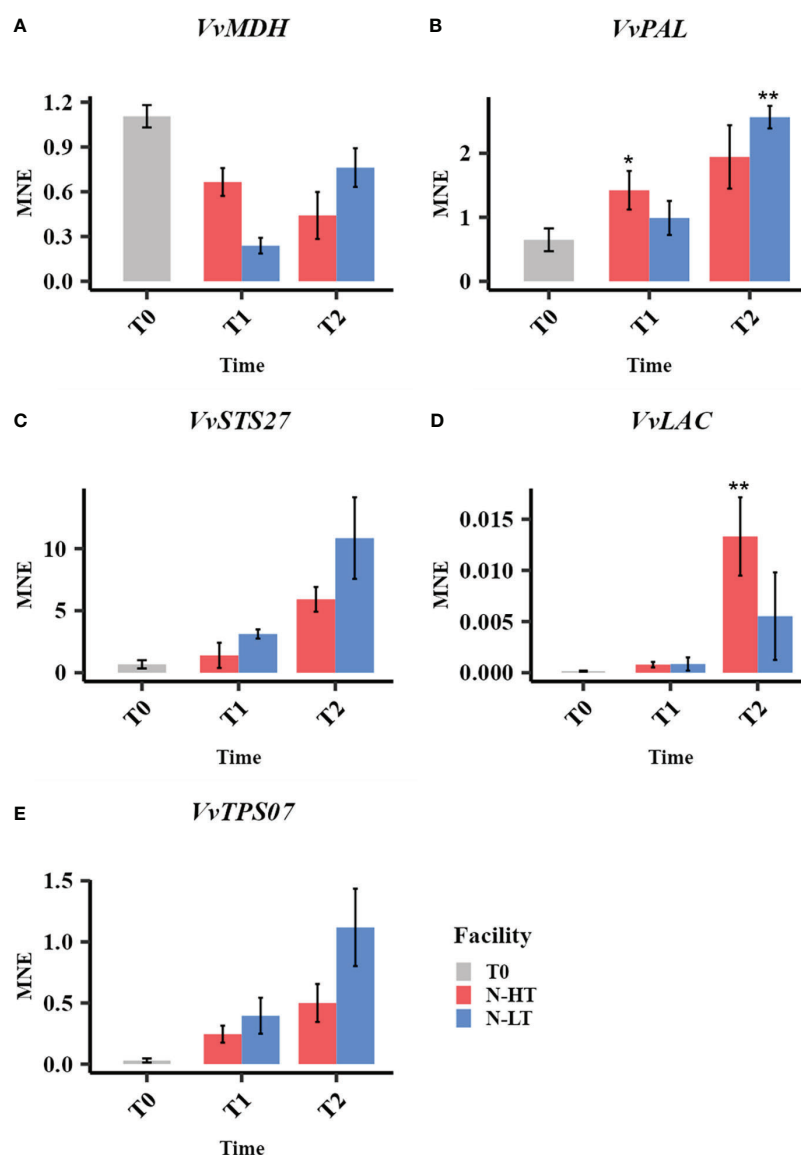


FIGURE 9
Expression profiles of malate dehydrogenase (*VvMDH*, A), phenylalanine ammonia-lyases (*VvPAL*, B), stilbene synthase (*VvSTS27*, C) laccase (*VvLAC*, D) and terpen synthase (*VvTPS07*, E) genes in grape sampled during withering in the N-HT and N-LT rooms. Error bars represent standard errors (n = 3). Light blue colour indicates the N-LT condition; light red colour the N-HT condition. Asterisks represent statistically significant difference between partially withered grapes (T1 and/or T2) and grapes at harvest (T0), based on t-test ($p \leq 0.05 = *$; $p \leq 0.01 = **$).

of specialized biosynthetic branches leads to the accumulation of a specific class of compounds. Consistently, we observed a reduction of the level of total anthocyanin together with a strong increase in monomeric and oligomeric stilbenes in berries dehydrated under both temperature regimes. However, while anthocyanins were not apparently different between C-HT and C-LT, lower temperatures promoted the accumulation of the two primary products of STS (i.e., the monomeric trans-resveratrol and cis-resveratrol) and higher temperatures stimulated the increase of stilbene oligomeric forms. This result is consistent with the expression analysis of *PAL* and *STS*, which were additionally induced by the lower temperature conditions. Moreover, considering the putative involvement of LACs in producing dimers or higher degree phenolic oligomers – including stilbenes (Zenoni et al., 2016; Vezzulli et al., 2019; Zenoni et al., 2020;

Pilati et al., 2021) – by oxidative polymerization, we speculate that the observed higher expression of a LAC gene at higher temperature conditions may denote the general higher stilbene complexity found in C-HT grapes containing greater amount of stilbene dimers, trimers and tetramers.

Among the phenolic compounds, the clear effect of the temperature on flavonols consisted in a general constant increase of kaempferol and quercetin derivatives throughout the whole C-LT process, and only a weak transient increase at C-HT conditions. Augmentation of flavonols, beyond the concentration effect, has been observed in grape berries undergoing postharvest dehydration. Bonghi et al. (2012) noted higher quercetin content in faster (by adjustments at higher temperature and lower RH) compared to slower dehydrating Raboso Piave berries, that however did not

match the expression of a flavonol synthase (FLS) that showed higher expression in slow dehydration rate conditions. Net increments in the content of quercetin and kaempferol were also reported for Cesanese grape berries subjected to the different rate of dehydration at either 10 or 20°C (Bellincontro et al., 2009), with a higher increase observed at 20°C corresponding to the faster dehydration rate. Contrary to our findings, these studies showed that the increase in flavonol content was associated to higher temperatures. Noteworthy, higher temperatures were associated with greater dehydration rates that may have limited the time for the oxidative catabolism of these compounds. By dissecting the effect of temperature from the dehydration rate we were able to highlight that the low temperature condition may act in favor of the accumulation of flavonols. However, because we did not measure the expression of *FLS*, we cannot establish whether this was the result of an increased biosynthesis or of a reduced degradation.

The additional recorded studies showing significant changes (either increase or decrease) in the level of flavonols (Sanmartin et al., 2021) deal with different genotypes and quite different applied dehydration conditions likely implying the presence of dissimilar processes acting on the flavonol composition and that make any comparison with our study rather inconclusive.

4.3 Effect of temperature on volatile organic compounds

Mencarelli and Bellincontro (2020) reported that the generation of volatile compounds from amino acid and fatty acid catabolism is a common feature in grape berries dehydrated at relatively high temperatures. Conversely, lower temperatures seem more effective in preserving the varietal aromatic compounds including terpenoids and aldehydes. In all the reported studies, the different temperature conditions impacted the grape dehydration rate, and it was recently demonstrated that higher dehydration rates, obtained without temperature manipulation, dampen the typical postharvest transcriptomic program and determine a weaker induction of the terpene synthase genes (Zenoni et al., 2020). Thus, it is impossible to establish at which extent the observed effect on the grape VOCs was due to the difference in temperature regimes or in dehydration rates. In our study we compared different temperature conditions while maintaining similar dehydration rates and were thus able to show the direct effect of the temperature on the berry VOCs. C-LT condition increased terpenes and C₆ alcohols content in grapes and wine, whereas C-HT favored esters and fatty acids content. Among the terpenes, the most significant change was recorded for terpinen-4-ol, a known marker of grape postharvest dehydration (Accordini, 2013; Negri et al., 2017) and, from our results, an indicator of grapes dehydrated at the lower temperature. Dehydration at low temperatures likely stimulated the terpene biosynthetic pathway directly as supported by the increased expression of in C-LT grapes.

Overall, our findings show that the temperature at which the grapes are dehydrated postharvest affects several berry metabolisms impacting the quality traits of the dehydrated grapes, hence of the resulting wines. We provided clear evidence of the positive effect of low temperatures in reducing the degradation of malic acid and favoring the accumulation of terpenes. Stilbenes metabolism was

aroused by low temperature conditions with increased synthesis of stilbene monomers, whereas higher temperatures likely favored the formation of complex oligomeric forms. This result showcases the great impact that the temperature has not only on growth and ripening of the grapes but also on physiology and metabolism of the berry during postharvest dehydration.

Given that in real-life commercial conditions, higher temperature regimes are always associated to higher dehydration rates and shorter dehydration processes, the general impact of temperature on the final product should be re-evaluated considering both the direct effect on grape metabolism and the indirect effect that takes place through the modulation of the dehydration rate.

Data availability statement

The original contributions presented in the study are included in the article/Supplementary Material. Further inquiries can be directed to the corresponding authors.

Author contributions

GT and SZ designed the research. RS set up the two-rooms withering comparisons, collected berry samples and performed technological analyses, performed the micro-vinifications. AA followed the grape withering in natural conditions. AA, ED'I and RS performed the molecular analyses. MC performed metabolomic analysis of non-volatile metabolites. GL and MU performed the metabolomic analysis of aroma compounds. RS, GT, AA, SZ and MF interpreted data and wrote the manuscript. All authors contributed to the article and approved the submitted version.

Funding

This work was supported by grant FSE_1695-11-11-2018_DIPBIO 2 “L'appassimento delle uve per il rafforzamento della tipicità delle produzioni locali e lo sviluppo di nuove tipologie di vino”. RS was supported by grant FSE-FESR POR 2014-2020 “Caratterizzazione di tratti migliorativi di interesse per la vitivinicoltura veronese, in popolazioni di vite ottenute da incrocio”

Acknowledgments

We wish to thank Franco Allegrini (to the memory of whom this work is dedicated) from Terre di Fumane s.r.l. and Allegrini winery, and Tenuta Santa Maria Valverde s.a. for kindly providing grapes, structures, and dehydration technologies.

Conflict of interest

The authors declare that the research was conducted in the absence of any commercial or financial relationships that could be construed as a potential conflict of interest.

The handling editor CP declared a past co-authorship with the authors AA & SZ.

Publisher's note

All claims expressed in this article are solely those of the authors and do not necessarily represent those of their affiliated organizations, or those of the publisher, the editors and the reviewers. Any product

that may be evaluated in this article, or claim that may be made by its manufacturer, is not guaranteed or endorsed by the publisher.

Supplementary material

The Supplementary Material for this article can be found online at: <https://www.frontiersin.org/articles/10.3389/fpls.2023.1107954/full#supplementary-material>

References

- Accordini, D. (2013). *Amarone, in Sweet, reinforced and fortified wines: Grape biochemistry, technology and vinification*. Eds. F. Mencarelli and P. Tonutti (Chichester: Wiley-Blackwell), 189–203.
- Barbanti, D., Mora, B., Ferrarini, R., Tornielli, G. B., and Cipriani, M. (2008). Effect of various thermo-hygrometric conditions on the withering kinetics of grapes used for the production of “Amarone” and “Recioto” wines. *J. Food Eng.* 85 (3), 350–358. doi: 10.1016/j.foodeng.2007.07.003
- Bellincontro, A., de Santis, D., Botondi, R., Villa, I., and Mencarelli, F. (2004). Different postharvest dehydration rates affect quality characteristics and volatile compounds of malvasia, trebbiano and sangiovese grapes for wine production. *J. Sci. Food Agric.* 84, 1791–1800. doi: 10.1002/jsfa.1889
- Bellincontro, A., Nicoletti, I., Valentini, M., Tomas, A., Santis, D., Corradini, D., et al. (2009). Integration of nondestructive techniques with destructive analyses to study postharvest water stress of winegrapes. *Am. J. Enol. Vitic.* 60 (1), 57–65. doi: 10.5344/ajev.2009.60.1.57
- Bonghi, C., Rizzini, F. M., Gambuti, A., Moio, L., Chkaiban, L., and Tonutti, P. (2012). Phenol compound metabolism and gene expression in the skin of wine grape (*Vitis vinifera* L.) berries subjected to partial postharvest dehydration. *Postharvest. Biol. Technol.* 67, 102–109. doi: 10.1016/j.postharvbio.2012.01.002
- Brillante, L., de Rosso, M., Dalla Vedova, A., Maoz, I., Flamini, R., and Tomasi, D. (2018). Insights on the stilbenes in raboso piave grape (*Vitis vinifera* L.) as a consequence of postharvest vs on-vine dehydration. *J. Sci. Food Agric.* 98, 1961–1967. doi: 10.1002/jsfa.8679
- Commisso, M., Negri, S., Bianconi, M., Gambini, S., Avesani, S., Ceoldo, S., et al. (2019). Untargeted and targeted metabolomics and tryptophan decarboxylase *in vivo* characterization provide novel insight on the development of kiwifruits (*Actinidia deliciosa*). *Int. J. Mol. Sci.* 19, 20(4):897. doi: 10.3390/ijms20040897
- Costantini, V., Bellincontro, A., de Santis, D., Botondi, R., and Mencarelli, F. (2006). Metabolic changes of malvasia grapes for wine production during postharvest drying. *J. Agric. Food Chem.* 54 (9), 3334–3340. doi: 10.1021/jf053117l
- D'Onofrio, C., Bellincontro, A., Accordini, D., and Mencarelli, F. (2019). Malic acid as a potential marker for the aroma compounds of amarone winegrape varieties in withering. *Am. J. Enol. Vitic.* 70, 259–266. doi: 10.5344/ajev.2019.18071
- Fasoli, M., Dal Santo, S., Zenoni, S., Tornielli, G. B., Farina, L., Zamboni, A., et al. (2012). The grapevine expression atlas reveals a deep transcriptome shift driving the entire plant into a maturation program. *Plant Cell* 24 (9), 3489–3505. doi: 10.1105/tpc.112.100230
- Fasoli, M., Dell'Anna, R., Amato, A., Balestrini, R., Santo, S. D., Monti, F., et al. (2019). Active rearrangements in the cell wall follow polymer concentration during postharvest withering in the berry skin of *Vitis vinifera* cv. corvina. *Plant Physiol. Biochem.* 135, 411–422.
- Luzzini, G., Slaghenau, D., and Ugliano, M. (2021). Volatile compounds in monovarietal wines of two amarone della valpolicella terroirs: Chemical and sensory impact of grape variety and origin, yeast strain and spontaneous fermentation. *Foods* 10 (10), 2474. doi: 10.3390/foods10102474
- Massonnet, M., Fasoli, M., Tornielli, G. B., Altieri, M., Sandri, M., Zuccolotto, P., et al. (2017). Ripening transcriptomic program in red and white grapevine varieties correlates with berry skin anthocyanin accumulation. *Plant Physiol.* 174 (4), 2376–2396. doi: 10.1104/pp.17.00311
- Medina-Plaza, C., Meade, H., Dokoozlian, N., Ponangi, R., Blair, T., Block, D. E., et al. (2022). Investigating the relation between skin cell wall composition and phenolic extractability in Cabernet sauvignon wines. *Fermentation* 8, 401. doi: 10.3390/fermentation8080401
- Mencarelli, F., and Bellincontro, A. (2020). Recent advances in postharvest technology of the wine grape to improve the wine aroma. *J. Sci. Food Agric.* 100 (14), 5046–5055. doi: 10.1002/jsfa.8910
- Mencarelli, F., Bellincontro, A., Nicoletti, I., Cirilli, M., Muleo, R., and Corradini, D. (2010). Chemical and biochemical change of healthy phenolic fractions in winegrape by means of postharvest dehydration. *J. Agric. Food Chem.* 58 (13), 7557–7564. doi: 10.1021/jf100331z
- Negri, S., Gambini, S., Ceoldo, S., Avesani, L., Commisso, M., and Guzzo, F. (2021). Undifferentiated *in vitro* cultured actinidia deliciosa as cell factory for the production of quercetin glycosides. *Plants* 10 (11), 2499. doi: 10.3390/plants10112499
- Negri, S., Lovato, A., Boscaini, F., Salvetti, E., Torriani, S., Commisso, M., et al. (2017). The induction of noble rot (*Botrytis cinerea*) infection during postharvest withering changes the metabolome of grapevine berries (*Vitis vinifera* L., cv. garganega). *Front. Plant Sci.* 8. doi: 10.3389/fpls.2017.01002
- Pilati, S., Malacarne, G., Navarro-Paya, D., Tomè, G., Riscica, L., Cavecchia, V., et al. (2021). *Vitis onegene*: A causality-based approach to generate gene networks in *Vitis vinifera* sheds light on the laccase and dirigent gene families. *Biomolecules* 11 (12), 1744. doi: 10.3390/biom11121744
- Rizzini, F. M., Bonghi, C., and Tonutti, P. (2009). Postharvest water loss induces marked changes in transcript profiling in skins of wine grape berries. *Postharvest. Biol. Technol.* 52, 247–253. doi: 10.1016/j.postharvbio.2008.12.004
- Rolle, L., Giacosa, S., Rio Segade, S., Ferrarini, R., Torchio, F., and Gerbi, V. (2013). Influence of different thermohygrometric conditions on changes in instrumental texture properties and phenolic composition during postharvest withering of “Corvina” winegrapes (*Vitis vinifera* L.). *Drying Technol.* 31, 549–564. doi: 10.1080/07373937.2012.745092
- Salvetti, E., Campanaro, S., Campedelli, I., Fracchetti, F., Gobbi, A., Tornielli, G. B., et al. (2016). Whole-Metagenome-Sequencing-Based community profiles of *Vitis vinifera* L. cv. corvina berries withered in two post-harvest conditions. *Front. Microbiol.* 7. doi: 10.3389/fmicb.2016.00937
- Sanmartin, C., Modesti, M., Venturi, F., Brizzolara, S., Mencarelli, F., and Bellincontro, A. (2021). Postharvest water loss of wine grape: When, what and why. *Metabolites* 11 (5), 318. doi: 10.3390/metabo11050318
- Slaghenau, D., Boscaini, A., Prandi, A., Dal Cin, A., Zandonà, V., Luzzini, G., et al. (2020). Influence of different modalities of grape withering on volatile compounds of young and aged corvina wines. *Molecules* 25 (9), 2141. doi: 10.3390/molecules25092141
- Slaghenau, D., Guardini, S., Tedeschi, R., and Ugliano, M. (2019). Volatile terpenoids, norisoprenoids and benzenoids as markers of fine scale vineyard segmentation for corvina grapes and wines. *Food Res. Int.* 125, 108507. doi: 10.1016/j.foodres.2019.108507
- Slaghenau, D., and Ugliano, M. (2018). Norisoprenoids, sesquiterpenes and terpenoids content of valpolicella wines during aging: Investigating aroma potential in relationship to evolution of tobacco and balsamic aroma in aged wine. *Front. Chem.* 6. doi: 10.3389/fchem.2018.00066
- Tomasi, D., Lonardi, A., Boscaro, D., Nardi, T., Marangon, C. M., de Rosso, M., et al. (2021). Effects of traditional and modern post-harvest withering processes on the composition of the *Vitis v. corvina* grape and the sensory profile of amarone wines. *Molecules* 26 (17), 5198. doi: 10.3390/molecules26175198
- Torchio, F., Urcan, D. E., Lin, L., Gerbi, V., Giacosa, S., Rio Segade, S., et al. (2016). Influence of different withering conditions on phenolic composition of avana, chatus and nebbiolo grapes for the production of “Reinforced” wines. *Food Chem.* 194, 247–256. doi: 10.1016/j.foodchem.2015.08.009
- Vezzulli, S., Malacarne, G., Masuero, D., Vecchione, A., Dolzani, C., Goremykin, V., et al. (2019). The Rpv3-3 haplotype and stilbenoid induction mediate downy mildew resistance in a grapevine interspecific population. *Front. Plant Sci.* 10. doi: 10.3389/fpls.2019.00234
- Zamboni, A., Minoia, L., Ferrarini, A., Tornielli, G. B., Zago, E., Delledonne, M., et al. (2008). Molecular analysis of post-harvest withering in grape by AFLP transcriptional profiling. *J. Exp. Bot.* 59 (15), 4145–4159. doi: 10.1093/jxb/ern256
- Zenoni, S., Amato, A., D'Inca, E., Guzzo, F., and Tornielli, G. B. (2020). Rapid dehydration of grape berries dampens the post-ripening transcriptomic program and the metabolite profile evolution. *Hortic. Res.* 7, 141. doi: 10.1093/hortres/rtz062-5
- Zenoni, S., Fasoli, M., Guzzo, F., Dal Santo, S., Amato, A., Anesi, A., et al. (2016). Disclosing the molecular basis of the postharvest life of berry in different grapevine genotypes. *Plant Physiol.* 172 (3), 1821–1843. doi: 10.1104/pp.16.00865
- Zhang, Y., and Keller, M. (2017). Discharge of surplus phloem water may be required for normal grape ripening. *J. Exp. Bot.* 68 (3), 585–595. doi: 10.1093/jxb/erv476
- Zoccatelli, G., Zenoni, S., Savoi, S., Dal Santo, S., Tononi, P., Zandonà, V., et al. (2013). Skin pectin metabolism during the postharvest dehydration of berries from three distinct grapevine cultivars. *Aust. J. Grape Wine Res.* 19 (2), 171–179. doi: 10.1111/ajgw.12014



OPEN ACCESS

EDITED BY

Chiara Pagliarani,
Institute for Sustainable Plant Protection
(CNR), Italy

REVIEWED BY

Arif Atak,
Bursa Uludağ University, Türkiye
Marta Sousa Silva,
University of Lisbon, Portugal
Yingqiang Wen,
Northwest A&F University, China
Andreia Figueiredo,
University of Lisbon, Portugal

*CORRESPONDENCE

Urska Vrhovsek
✉ urska.vrhovsek@fmach.it

SPECIALTY SECTION

This article was submitted to
Plant Metabolism and Chemodiversity,
a section of the journal
Frontiers in Plant Science

RECEIVED 30 November 2022

ACCEPTED 13 January 2023

PUBLISHED 31 January 2023

CITATION

Ciubotaru RM, Franceschi P, Vezzulli S,
Zulini L, Stefanini M, Oberhuber M,
Robatscher P, Chitarrini G and Vrhovsek U
(2023) Secondary and primary metabolites
reveal putative resistance-associated
biomarkers against *Erysiphe necator* in
resistant grapevine genotypes.
Front. Plant Sci. 14:1112157.
doi: 10.3389/fpls.2023.1112157

COPYRIGHT

© 2023 Ciubotaru, Franceschi, Vezzulli,
Zulini, Stefanini, Oberhuber, Robatscher,
Chitarrini and Vrhovsek. This is an open-
access article distributed under the terms of
the [Creative Commons Attribution License
\(CC BY\)](https://creativecommons.org/licenses/by/4.0/). The use, distribution or
reproduction in other forums is permitted,
provided the original author(s) and the
copyright owner(s) are credited and that
the original publication in this journal is
cited, in accordance with accepted
academic practice. No use, distribution or
reproduction is permitted which does not
comply with these terms.

Secondary and primary metabolites reveal putative resistance-associated biomarkers against *Erysiphe necator* in resistant grapevine genotypes

Ramona Mihaela Ciubotaru^{1,2}, Pietro Franceschi³, Silvia Vezzulli⁴,
Luca Zulini⁴, Marco Stefanini⁴, Michael Oberhuber⁵,
Peter Robatscher⁵, Giulia Chitarrini^{2,5} and Urska Vrhovsek^{2*}

¹Department of Agri-Food, Environmental and Animal Sciences, University of Udine, Udine, Italy,

²Food Quality and Nutrition Department, Research and Innovation Centre, Fondazione Edmund Mach,
San Michele all'Adige, Italy, ³Unit of Computational Biology, Research and Innovation Centre,
Fondazione Edmund Mach, San Michele All'Adige, Italy, ⁴Genomics and Biology of Fruit Crops
Department, Research and Innovation Centre, Fondazione Edmund Mach, San Michele All'Adige, Italy,

⁵Laboratory for Flavours and Metabolites, Laimburg Research Centre, Auer (Ora), Italy

Numerous fungicide applications are required to control *Erysiphe necator*, the causative agent of powdery mildew. This increased demand for cultivars with strong and long-lasting field resistance to diseases and pests. In comparison to the susceptible cultivar 'Teroldego', the current study provides information on some promising disease-resistant varieties (mono-locus) carrying one *E. necator*-resistant locus: BC4 and 'Kishmish vatkana', as well as resistant genotypes carrying several *E. necator* resistant loci (pyramided): 'Bianca', F26P92, F13P71, and NY42. A clear picture of the metabolites' alterations in response to the pathogen is shown by profiling the main and secondary metabolism: primary compounds and lipids; volatile organic compounds and phenolic compounds at 0, 12, and 48 hours after pathogen inoculation. We identified several compounds whose metabolic modulation indicated that resistant plants initiate defense upon pathogen inoculation, which, while similar to the susceptible genotype in some cases, did not imply that the plants were not resistant, but rather that their resistance was modulated at different percentages of metabolite accumulation and with different effect sizes. As a result, we discovered ten up-accumulated metabolites that distinguished resistant from susceptible varieties in response to powdery mildew inoculation, three of which have already been proposed as resistance biomarkers due to their role in activating the plant defense response.

KEYWORDS

powdery mildew, metabolomics, GC-MS, LC-MS, resistance, loci, biomarkers

1 Introduction

Vitis is a genus widely dispersed and with diverse taxonomy, yet practically most of the world's commercial grape production is focused on a single species, *Vitis vinifera* L., which is native to Europe and Asia Minor. *Vitis vinifera* is a species highly susceptible to various economically devastating pests and diseases, such as powdery mildew. This disease has several causal agents depending on the plant host. In grapevine, the causal agent of powdery mildew is the ascomycete *E. necator* [(syn. *Uncinula necator* (Schweinf.) Burrill)] (Gadoury et al., 2012; Dry and Thomas, 2015).

Originating from northern America, grapevine powdery mildew was recently discovered in extremely diverse climatic conditions, including temperate regions with high rainfall, especially during spring months (Pirrello et al., 2019). The causal pathogen is obligatorily parasitic on the genus *Vitis*, as well as on *Cissus*, *Parthenocissus*, and *Ampelopsis* within the Vitaceae family (Gadoury et al., 2012). *Erysiphe necator* can infect all green tissues of the host and cause significant losses in yield and reduction in berry quality (Pimentel et al., 2021). Due to the devastating effects of the disease, breeding studies have been initiated to develop varieties that are tolerant or resistant to this disease all over the world (Atak and Şen, 2021; Atak, 2022).

During the infection process, *E. necator* produces conidia that germinate and grow epiphytically on the plant tissue forming a germ tube and a lobed appressorium. This breaks the cell wall invading the underlying epidermal cells with haustoria, a feeding structure. Through it, the fungus retrieves nutrients and secretes effectors that suppress the plant's immunity, PAMP (pathogen-associated molecular pattern)-triggered immunity (PTI), allowing the colonization of plant tissue surfaces by the development of secondary hypha. The newly formed conidiophores sporulate to infect other host tissues and start a new infection cycle, which leads to an effector-triggered susceptibility (ETS) within the host (Gadoury et al., 2012). As an answer, the plants react using resistance (R) genes that are related to their evolutionary history (Feechan et al., 2011). These genes encode mainly for NBS-LRR (nucleotide-binding site – leucine-rich repeat) proteins that regularly express an interaction of the effector-triggered immunity (ETI) type in which the NB-LRR proteins act as receptors interacting with the strain-specific effectors of the pathogen released during infection. This is likewise true for the R genes that are transcribed into the Vitaceae plant family after *E. necator* infection (Qiu et al., 2015). The interaction generates a signaling cascade that leads to transcriptional re-programming in the host plant. The R genes activate several defense responses, including programmed cell death, the generation of reactive oxygen species, biosynthesis/signaling of plant stress/defense hormones, phytoalexin biosynthesis, and cell wall strengthening (Agurto et al., 2017; Welter et al., 2017).

Powdery mildew threatens many commercially important grapevine species and varieties, and thus, nowadays, the most used and efficient method of control is based on chemical treatments (Dry and Thomas, 2015). The most suitable fungicides against *E. necator* are benzimidazoles, ergosterol biosynthesis inhibitors, the quinone-oxidase inhibitor (QoI) compounds (strobilurins, quinolones), and the succinate dehydrogenase inhibitor (SDHI) group. Since the

majority of these fungicides are site-specific, their repeated use leads to fungicide-resistant isolates (Gadoury et al., 2012). Thus, the introduction of resistant cultivars represents the most promising strategy to reduce the use of fungicides in viticulture, avoiding the appearance of *E. necator* resistance isolates. Although all *V. vinifera* cultivars are highly susceptible to *E. necator*, several Vitaceae species belonging to various American and Asian genotypes have developed resistance mechanisms against this pathogen (Gadoury et al., 2012; Agurto et al., 2017; Schneider et al., 2019). The resistance quantitative trait loci (QTLs) in Vitaceae are clustered in tandem repeats of genomic areas that have been genetically mapped, revealing many loci that encode R gene sequences conferring resistance on *E. necator* and have been utilized to obtain resistant plants by pseudo-backcrossing (Agurto et al., 2017). The R genes identified in Vitaceae are named Ren (i.e. resistance to *E. necator*) and Run (i.e. resistance to *Uncinula necator*).

To date, 17 grapevine powdery mildew resistance loci have been identified and described (Sosa-Zuniga et al., 2022); a descriptive list of them is available online (www.vivc.de/loci). It is important to note, however, that the presence of only one gene or locus, even if it has a large effect, can favor the selection of fungus isolates capable of overcoming resistance (McDonald and Linde, 2002). In other words, if the resistance is based solely on the presence of a gene, the fungus may mutate and evade immune recognition through the emergence of new virulent isolates.

In this context, better and longer-lasting disease resistance would be beneficial (Merdinoglu et al., 2018) and a pyramiding technique that integrates multiple resistance loci in the same genotype has been proposed (Mundt, 2018) as a potential solution. To guarantee the longevity of this type of resistance, it is required that loci with different mechanisms of action, spectrums of target isolates and contributions (minor and major) to the resistance be combined. This approach should bring in a more improved, durable and secure implementation strategy, given that, if any mutation or virulence factor occurs, the pathogen will be still recognized by at least one R gene (Peressotti et al., 2010; Cadle-Davidson et al., 2011; Feechan et al., 2015; Pap et al., 2016; Agurto et al., 2017).

Understanding disease resistance or tolerance mechanisms against *E. necator* in grapevine cultivars with different resistant loci at various time points post-inoculation may provide a holistic interpretation of the incompatible interactions between *Vitis* and *E. necator* and provide valuable information for breeding programs. In this respect, characterizing the metabolic profiles associated with disease resistance and susceptibility represents a key step for the identification of trait-related biomarkers. As we have seen in our previous study (Ciubotaru et al., 2021), metabolomics provided novel insights into the resistance mechanisms underlying the hybrid-pathogen interaction by identifying 22 putative biomarkers of grapevine resistance to *Plasmopara viticola*. Thus, the aim of our study is to provide important metabolomics evidence by monitoring changes in the concentration of a large set of metabolites belonging to four chemical classes in grapevine leaves subjected to artificial infection with *E. necator*. The significance of these findings is important for experiments studying the different behavior of resistant (totally or partially) varieties and susceptible ones in terms of the biochemical mechanisms involved in disease resistance. A

better understanding of resistance biochemistry may lead to an improved selection of resistant plants promoting the reduction of fungicide treatments.

In this sense, metabolomics provides a comprehensive and quantitative investigation of metabolites belonging to both primary and secondary classes, including metabolites that play an important role in fighting pathogens. Moreover, metabolomics studies can help in the identification of key metabolites in plant adaptation to biotic stress. Despite the broad interest in more sustainable agriculture, metabolomics studies performed so far have focused on understanding the mechanism of grapevine defense against downy mildew, while only a limited number of investigations focused on *E. necator* (Pimentel et al., 2021). Recent studies have shown the mechanisms underlying the synergy between metabolomics and various omics approaches (Maia et al., 2020; Pimentel et al., 2021; Sosa-Zuniga et al., 2022; Yin et al., 2022), the metabolic differences in the composition of the berries and leaves in several grapevine cultivars (Atak et al., 2021; Rienth et al., 2021) as well as control of the pathogen (Gur et al., 2022).

In this work, we focused on two mono-locus resistant genotypes ('VRH 3082-1-42' - commonly named BC4 - and 'Kishmish vatkana') and four pyramided resistant genotypes ('Bianca', F29P92, F13P71, and NY42) comparing them with the susceptible cultivar (cv) 'Teroldego'. To date, our current work is the first study that addresses the way *E. necator* induces metabolic changes in grapevine genotypes harboring one or more R loci.

2 Material and methods

2.1 Genetic material

Six different resistant grapevine genotypes and the *V. vinifera* cv 'Teroldego' which is highly susceptible to powdery mildew were used in this study. BC4 and 'Kishmish vatkana' had a mono-locus resistance to powdery mildew, whereas 'Bianca', F26P92, F13P71, and NY42 had a pyramided resistance. The grapevine varieties, their pedigree, and their resistance-related loci are listed in Table 1.

TABLE 1 Grapevine varieties used in this study together with their origin [¹ North American *Vitis*; ² Asian *Vitis*; ³ Interspecific hybrids of *V. vinifera* with North American *Vitis* species; ⁴ pure *V. vinifera*], host response [PCD (programmed cell death), ROSs (reactive oxygen species)] and their powdery mildew associated resistance related loci (*Ren/Run*).

Genotypes		Resistance related powdery mildew loci (<i>Ren/Run</i>)	Resistance mechanism within the hosts			Preliminary leaf resistance level	Source of resistance	References
			PCD	ROS	Callose			
mono-locus resistance	BC4	<i>Run1</i>	yes	yes	yes	total resistance	<i>M. rotundifolia</i> ¹	Feechan et al., 2013; Agurto et al., 2017;
	'Kishmish vatkana'	<i>Ren1</i>	yes	yes	yes	partial resistance	<i>V. vinifera</i> ⁴	Hoffmann et al., 2008;
pyramided resistance	'Bianca'	<i>Ren3</i>	yes	yes	yes	partial resistance	<i>V. rupestris</i> ³	Welter et al., 2007; Zendler et al., 2020;
		<i>Ren9</i>	yes	n.d	n.d	partial resistance	<i>V. rupestris</i> ³	Zendler et al., 2017; Zendler et al., 2020;
	F26P92	<i>Ren3</i>	yes	yes	yes	partial resistance	<i>V. rupestris</i> ³	Welter et al., 2007; Zendler et al., 2020;
		<i>Ren9</i>	yes	n.d	n.d	partial resistance	<i>V. rupestris</i> ³	Zendler et al., 2017; Zendler et al., 2020;
	F13P71	<i>Run1</i>	yes	yes	yes	total resistance	<i>M. rotundifolia</i> ¹	Feechan et al., 2013; Agurto et al., 2017;
		<i>Ren1</i>	yes	yes	yes	partial resistance	<i>V. vinifera</i> ²	Hoffmann et al., 2008;
	NY42	<i>Run1</i>	yes	yes	yes	total resistance	<i>M. rotundifolia</i> ¹	Feechan et al., 2013; Agurto et al., 2017;
		<i>Ren2</i>	yes	n.d	n.d	partial resistance	<i>V. cinerea</i> ²	Feechan et al., 2015;
		<i>Ren3</i>	yes	yes	yes	partial resistance	<i>V. rupestris</i> ³	Welter et al., 2007; Zendler et al., 2020;
		<i>Ren9</i>	yes	n.d	n.d	partial resistance	<i>V. rupestris</i> ³	Zendler et al., 2017; Zendler et al., 2020;
control	'Teroldego'	-	-	-	-	susceptible	-	

The levels of resistance described in the table: Total = greatly suppressed symptoms or the absence of visible symptoms; Partial = in cases where the symptomatology decreases without disappearing completely (Sosa-Zuniga et al., 2022; Julius Kühn-Institut, 2022).

The so-called BC4 hybrid was created in France and was derived from the intergeneric cross between *Muscadinia rotundifolia* and *V. vinifera* (Volynkin et al., 2021). It is resistant to the pathogen *E. necator* through the locus *Run1*, which is the earliest *E. necator* resistance loci to be identified in grapevine and one of the very few well characterized from the causal gene viewpoint (Agurto et al., 2017). The genotype ‘Kishmish vatkana’ is a cultivated grape from Central Asia obtained from the cross of ‘Vasarga chernaya’ with ‘Sultanina’ and resistant through *Ren1* locus (Hoffmann et al., 2008).

‘Bianca’ is a hybrid between ‘Bouvier’ and ‘Villard Blanc’ created in 1963 at the Kölyuktető - viticulture research facility in Hungary. Its resistance is conferred by the *Ren3* locus that was discovered on chromosome 15 of the hybrid ‘Regent’ (Welter et al., 2007) and the *Ren9* locus.

F29P92 and F13P71 are two pyramided hybrids created at Fondazione Edmund Mach (Italy). F26P92 is a mid-resistant genotype derived from ‘Bianca’ and ‘Nosiola’ with two resistance loci, *Ren3* and *Ren9*, while F13P71 is a cross between BC4 and ‘Kishmish vatkana’ having resistance through *Run1* and *Ren1* loci. The pyramided genotype NY42 is derived from a cross performed at USDA-Geneva (NY-USA) between NY95 and Eger99 and its resistance is given by the loci *Run1*, *Ren2*, *Ren3*, and *Ren9*. All three pyramided genotypes are considered breeding selections as they are still under the evaluation process. As a result, our paper is the first to report them in the literature.

The genotypes were grafted on Kober 5BB rootstock and grown in potted soil in controlled greenhouse conditions at the Fondazione Edmund Mach located in San Michele all’Adige (Trento), Italy (46° 12′ 0″ N, 11° 8′ 0″ E). Fourteen days prior to the experiment, all plants were treated with sulfur to make sure they were uniformly healthy. The sulfur treatment was repeated at the beginning of the experiment for all non-inoculated plants, which represented the control.

2.2 Pathogen inoculation

The inoculation of *E. necator* onto grapevine-potted plants in the greenhouse was done using conidia from the greenhouse and field; thus, the inoculum actually represented a mixture of *E. necator* strains.

The pathogen requires strict and stable climatic conditions for proper development, which is why in this study we tested two inoculation methods by following three different protocols. Three to four infected leaves were used as a source of inoculum for each round of inoculation depending on the spore quantity present on the leaves.

2.2.1 Dry inoculation

The first inoculation method was a dry dispersion of spores. For this method, we tested a combination of Deliere et al. (2010) modified protocol: the upper surfaces of healthy leaves were inoculated by dispersing spores with an air pump from infected leaves, and a cellophane funnel as per Valdés-Gómez et al. (2011) was placed around the inoculated shoots. Funnels were stapled, to allow air circulation, and were left in place for 24 h instead of 12 h as per the original inoculation method of Deliere et al. (2010) (Figure 1A-left).

2.2.2 Wet inoculation

The second method of pathogen inoculation was based on a conidial suspension. We tested the protocol described by Atak (2017). We collected conidia of *E. necator* by washing three severely infected grapevine leaves in 15 ml of sterile distilled water with one drop of Tween-20 (2μl). The conidial suspension obtained had a concentration of 8.4×10^5 conidia mL⁻¹. Leaves were inoculated by spraying the conidia suspension using a spraying bottle of 10 mL, using roughly 0.5 mL of suspension per leaf (4 times spray per leaf). Inoculated leaves were immediately covered with thin plastic for 24 hours to obtain high humidity (Figure 1B-middle). For the same

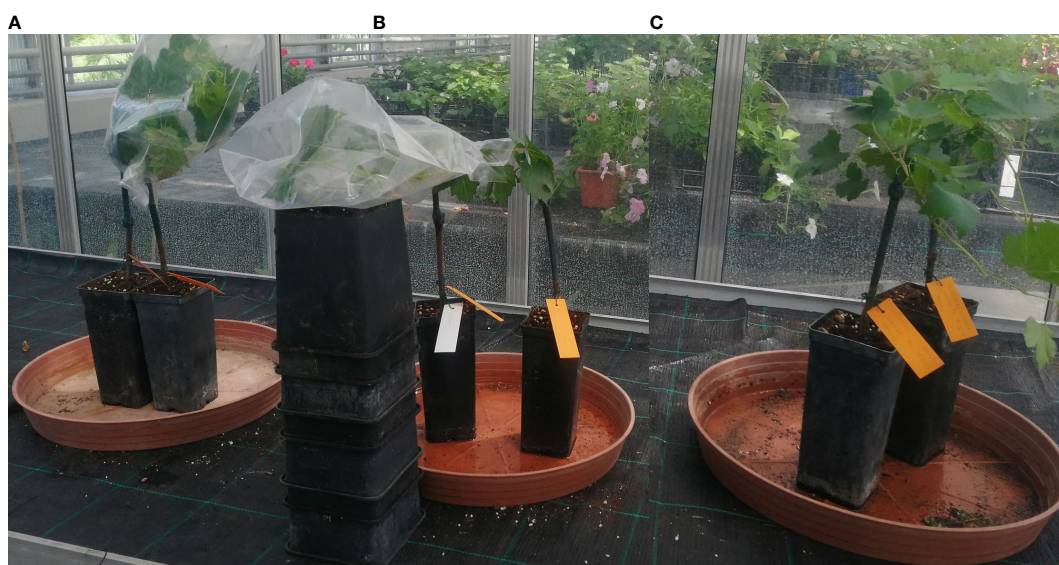


FIGURE 1

The artificial inoculation of *E. necator* conidia onto a susceptible genotype using three different methods: (A) - dry dispersion of spores covered by a stapled funnel (left); (B) - spray of a conidial suspension covered with plastic (middle); (C) - spray of a conidial suspension air-dried (right).

method (conidial suspension), we also tested the protocol described by Miclot et al. (2012) in which the above-prepared suspension was used to spray the upper surface of the leaves. The plants were subsequently air-dried using a ventilator and left uncovered (Figure 1C-right).

We carried out our experiment using the dry inoculation method. For each individual plant, the second, third and fourth fully expanded leaves from below the apex were inoculated by dusting the spores with an air pump for aquariums Nawa Wind (Nawa Tecno Industria, IT) that had attached a Pasteur glass. The spores were dusted directly into the adaxial surface of the leaves. The climatic conditions in the greenhouse were set at min 20°C – max of 22°C for temperature and 80% for relative humidity (Pertot and Gessler, 2006).

To evaluate the success of the experiments and of the inoculation with *E.necator*, we measured a parameter related to the pathogen performance: the OIV - 455 descriptor at 3, 7, and 11 dpi according to Miclot et al. (2012) (Supplementary Table 1). Briefly, we monitored the disease progression on a daily basis and quantified it based on observations of the plants' reactions.

2.3 Experimental design

Around the twelve-leaf shoot stage, the plants (n=15 plants/genotype) were randomly sorted into two homogenous groups: control and inoculated. The two groups were kept in the same greenhouse (under same conditions) separated by a physical barrier to create two separate compartments in order to prevent any possible transmission of the pathogen. The plant material (three leaves below the shoot apex) was collected at 0, 24, and 48 h post-inoculation (hpi), starting from the morning (8:00 am, which is time zero), and immediately stored at -80°C until use. Three biological replicates were performed per time-point (Figure 2). The experiment was conducted for a 2-year period, in 2019 and 2021.

2.4 Metabolomics analysis

Extraction procedure and analysis of compounds:

Primary compounds were extracted following the method published by Chitarrini et al. (2017a). They were then subjected to derivatization using methoxamine hydrochloride in pyridine and later N-methyl-N-trimethylsilyl-trifluoroacetamide with 1% trimethylchlorosilane for trimethylsilylation. One μ L of the derivative extract was then injected for GC/MS analysis using a Trace GC Ultra combined with a TSQ Quantum GC mass spectrometer and a Triplus autosampler (Thermo Electron Corporation, Waltham, MA). A RXI-5-Sil MS w/Integra-Guard[®] (fused silica) (30 m x 0.25 mm x 0.25 μ m) column was used for compound separation. Data acquisition was performed using the software "Xcalibur" (version 4.0) in full scan mode from 50 to 700 m/z. Compounds were identified using their reference standards, retention time, quantifier and qualifier ion, and quantified using their standard calibration curves as mg/kg of fresh leaves.

Lipidic compounds were extracted according to the method of Folch et al. (1957) with some modifications. In the first phase, 0.3 mL of methanol; 0.6 mL of chloroform containing butylated hydroxyl toluene (500 mg/L), and 10 μ L of internal standard (stearic acid 100

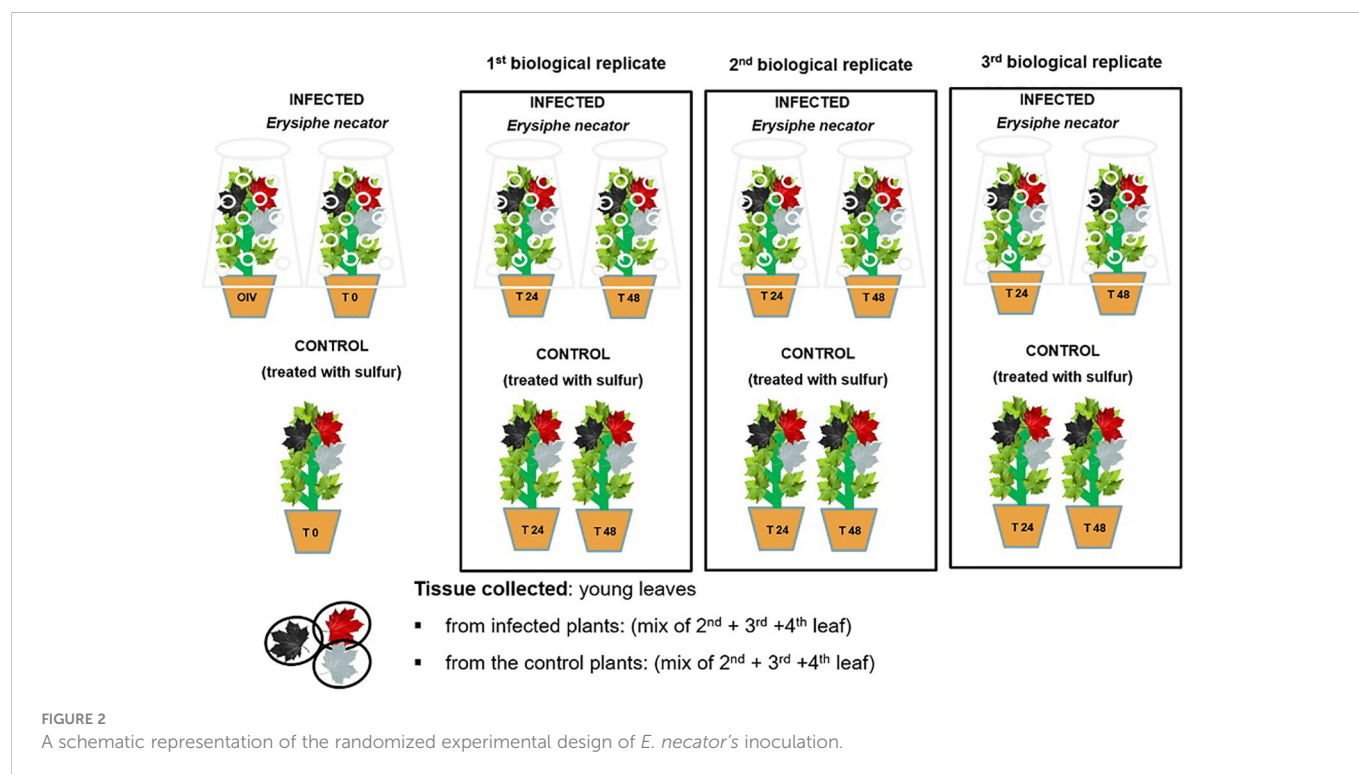
μ g/mL) were used. In a second phase, 0.4 mL of chloroform containing butylated hydroxyl toluene (500 mg/L)/methanol/water 86:14:1 v/v/v was used for the extraction. The combined lower lipid-rich layer of the two extracted phases was finally evaporated to dryness under N₂ and the samples were re-suspended in 300 μ L of acetonitrile/isopropanol/water (65:30:5 v/v/v) containing cholesterol as the internal standard at a concentration of one μ m/mL. Samples were injected into UHPLC Dionex 3000 (Thermo Fischer Scientific Germany) with a RP Ascentis Express column (15 cm x 2.1 mm; 2.7 μ m C18), following a 30 min multistep linear gradient as described in Della Corte et al. (2015). The UHPLC system was coupled to an API 5500 triplequadrupole mass spectrometer (Applied Biosystems/MDS Sciex). Compounds were identified based on their reference standard, retention time, and qualifier and quantifier ion, and were quantified (expressed as mg/kg) from linear calibration curves built with standard solutions using Analyst 1.7 software.

Volatile compounds were extracted and injected following the method of Chitarrini et al. (2017a) by using a solid phase micro-extraction. A Trace GC Ultra gas chromatograph coupled to a Quantum XLS mass spectrometer (Thermo Scientific, Electron Corporation, Waltham, MA) was used with a fused silica Stabilwax[®]-DA column (30 m x 0.25 mm i.d. x 0.25 μ m) (Restek Corporation, Bellefonte, USA). The headspace was sampled using 2-cm DVB/CAR/PDMS 50/30 μ m fiber from Supelco (Bellefonte, PA). Data processing was performed using the software "Xcalibur" (version 4.0). The identification of volatile compounds was done by reference to standards or by comparing retention index and mass spectra using the NIST MS Search 2.3 mass spectral database. Results were semi-quantified as the equivalent of the internal standard (1-heptanol) and expressed as μ g/kg of fresh leaves.

Phenolic compounds were extracted according to Vrhovsek et al. (2012) with some modifications made by Chitarrini et al. (2017a). Briefly, the phenolic compounds were extracted from 100 mg of fresh leaves using 0.4 mL of chloroform and 0.6 mL of methanol: water (2:1 v/v); the extraction was repeated by adding 0.6 mL of methanol and water (2:1 v/v) and 0.2 mL of chloroform. The aqueous-methanolic phase of two extractions was collected, combined, and evaporated to dryness under N₂. Samples were re-suspended in 500 μ L of methanol: water (1:1 v/v) and injected into a Waters Acquity UPLC system (Milford) with a Waters Acquity HSS T3 column (100 mm x 2.1 mm; 1.8 μ m). Mass spectrometry detection was performed on a Waters Xevo triple-quadrupole mass spectrometer detector (Milford) with an electrospray ionization (ESI) source (Vrhovsek et al., 2012). Compounds were identified based on their reference standard, retention time, and qualifier and quantifier ion, were quantified using their standard calibration curves and expressed as mg/kg of fresh leaves. Data processing was performed using Waters MassLynx V4.1 software.

2.5 Data analysis

A customized R script was used for statistical analysis and data visualization (R Core Team, 2020). To perform multivariate analysis, the metabolomics dataset's missing values were filled in using median imputation. To account for the anticipated year-to-year fluctuation in the overall metabolic response, the average effect of each year was subtracted for each metabolite/genotype. The base 10 logarithm was



used to transform the metabolite concentrations in order to compensate for the heteroscedasticity of the data (van den Berg et al., 2006). Thereafter, metabolic principal component analysis (PCA) was carried out on the resulting multidimensional dataset after UV scaling.

The differential response of the individual metabolites at 24 and 48 hpi was characterized by applying a series of univariate non-parametric tests to the data corrected for the effect of the year. To focus on widely present metabolites, only the compounds detected in eight samples were considered for the univariate analysis. Cohen's *d*-effect size was calculated to identify the metabolites that were strongly altered following infection. Statistical significance and effect size were combined in a set of "volcano plots". Uncorrected $p < 0.05$ and a $d > 1$ were used as arbitrary thresholds to identify strongly responding metabolites. The "*d*" values can range from a very small effect ($d = 0.01$) to a huge one ($d = 2.0$), as per the study of Sawilowsky (2009). Supplementary Table 6 displays the "*d*" values of the identified up-accumulated metabolites, as well as their related effect size and *p* values. No statistical analysis was conducted on the qualitative assessments of leaf health status.

3 Results

The results of *E. necator*'s inoculation were phenotypically observed and the best infections (highest sporulation observed on the leaves) were obtained with the modified dry methods of Deliere et al. (2010) and Valdés-Gómez et al. (2011). The dry inoculation method provided more effective infections than the wet inoculation, most likely due to conidia germination being inhibited or reduced in

the presence of water, which was reported to have a detrimental influence on the viability and infectivity of powdery mildew conidia (Miclot et al., 2012). Furthermore, high humidity has been demonstrated to have a severe negative influence on grapevine powdery mildew conidia germination (Carroll and Wilcox, 2003). The reduced efficacy of the wet inoculation is most likely due to residual water remaining in the leaves during or after the drying step. Pictures of the inoculated genotypes taken during the OIV-455 score evaluated at 3, 7 and 11 dpi are available as Supplementary Figures (2–22).

Over a two-year period, we were able to identify and quantify/semi-quantify 177 metabolites from four chemical classes. These include 60 primary compounds, 56 volatile organic compounds, 43 phenolic compounds and 17 lipids. In the class of primary compounds, we quantified (26) acids, (13) amino acids, (3) amines, one gamma-butyrolactone, and (17) sugars. Within the lipids, we quantified: (2) glycerophospholipids, one sphingolipid, one glycerolipid, one prenol, and (12) fatty acids. We semi-quantified: (4) acids, (9) alcohols, (8) aldehydes, (6) benzenoids, one ester, (2) other volatile organic compounds, (3) fatty acids, (3) fatty acids esters, one fatty alcohol, one benzofuran, (8) terpenoids, (2) terpenes, (3) ketones, one secondary alcohol, and (4) unknowns for the organic volatile compounds. For phenols, we quantified: (3) benzoic acid derivatives, one coumarin, one dihydrochalcone, (12) flavan-3-ols, one flavanone, (12) flavonols, (3) phenylpropanoids, (8) stilbenes and stilbenoids and two other compounds.

The obtained concentrations of all investigated metabolites for each genotype in both years are presented in Supplementary Table 2 for primary compounds, in Supplementary Table 3 for lipids, in Supplementary Table 4 for VOC(s), and in Supplementary Table 5 for phenolic compounds.

3.1 Resistant and susceptible genotypes reveal different kinetics upon pathogen inoculation

After the removal of the effect of the year, PCA was used to depict the global metabolite changes of the 177 identified metabolites in response to pathogen inoculation in all seven genotypes for both years (Figure 3). The six biological replicates of each genotype (three per year) are represented in the plots as small colored dots (the red color corresponds to the inoculated samples and the blue color to the non-inoculated samples). Samples collected at 24 and 48 hpi were analyzed separately to account for possible differences in response among the different genotypes.

The PCA revealed different timescales for the onset of the metabolic response. In fact, in 'Bianca' and 'Teroldego', the separation of infected and non-infected samples began at 24 hpi along the first dimension and became very evident at 48 hpi (Figure 3). Oddly, 'Kishmish vatkana' and F13P71 did not show any separation, neither at 24 hpi nor at 48 hpi (Figure 3). BC4, F26P92, and NY42 showed instead a partial separation through the second dimension at 24 hpi, which was no longer observable by 48 hpi (Figure 3).

3.2 The modulation of classes of compounds upon pathogen inoculation

To determine to which classes of compounds the metabolites that were responsible for the various sorts of separations between genotypes belong, we analyzed the percentages of compounds per class that had a significant effect after infection (Figure 4). The graph represents the percentage of metabolites per each class of compounds that were highly modulated in the plants of each genotype out of the total number of identified and quantified/semi-quantified metabolites per class in both years, as a response to the infection (i.e., 61 primary

compounds, 56 volatile organic compounds, 43 phenolic compounds, and 17 lipids).

The class of compounds that were highly modulated due to the infection consisted in lipids. This class showed higher levels compared to the control (non-infected plants), due to the biotic stress in five out of the seven studied genotypes (i.e., BC4, F13P71, F26P92, NY42, and 'Teroldego'). The estimated percentage of lipids affected in BC4 was around 80%; in F13P71 and in 'Teroldego', the percentage of affected lipids decreased to 60% and continued to decrease in F26P92 and NY42 down to 40% reaching 20% in 'Bianca' and less than 20% in 'Kishmish vatkana'.

Within the class of phenols, the genotype BC4 had the topmost modulated metabolites with a percentage of around 40%. 'Bianca', F26P92, and NY42 reached an approximate value of 20%, whereas the modulation of the metabolites in 'Kishmish vatkana' and 'Teroldego' remained below 20%. An exception was the genotype F13P71, which showed a very low percentage of modulation, not reported in the figure.

The primary compounds exhibited a similar trend of approximately 20% modulated metabolites within the genotypes BC4 and 'Bianca', with a slow decrease in F13P71 and 'Teroldego'. A much lesser percentage was observed in NY42 and F26P92.

The modulation of metabolites in the class of volatile compounds was estimated below 40% for the genotype F26P92, 20% for BC4, 'Kishmish vatkana', and 'Teroldego'; below 20% for NY42, and lower in F13P71.

3.3 Modulated metabolites induced by *Erysiphe necator*

We set out to identify specific metabolites that varied during the infection consistently in both years based on the results of the classes of compounds shown above. As discussed in materials and methods, the most relevant metabolites were identified by combining statistical

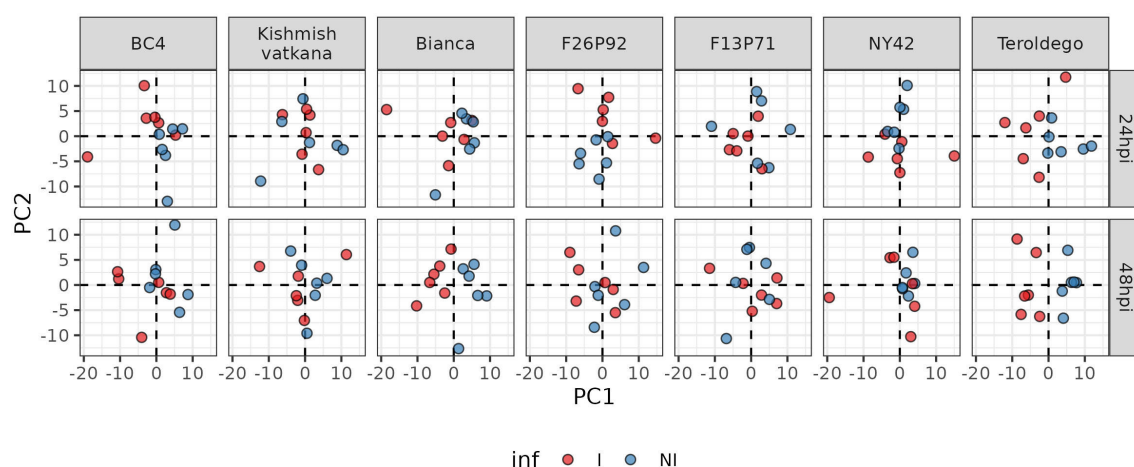


FIGURE 3

Principal component analysis performed on the log₁₀-transformed metabolite concentration of 24 and 48hpi samples. Each genotype has three biological replicates (small dots) for each year (2019 and 2021). The red color is for inoculated samples (I, inoculated samples) and the blue is for non-inoculated samples (NI, not inoculated samples).

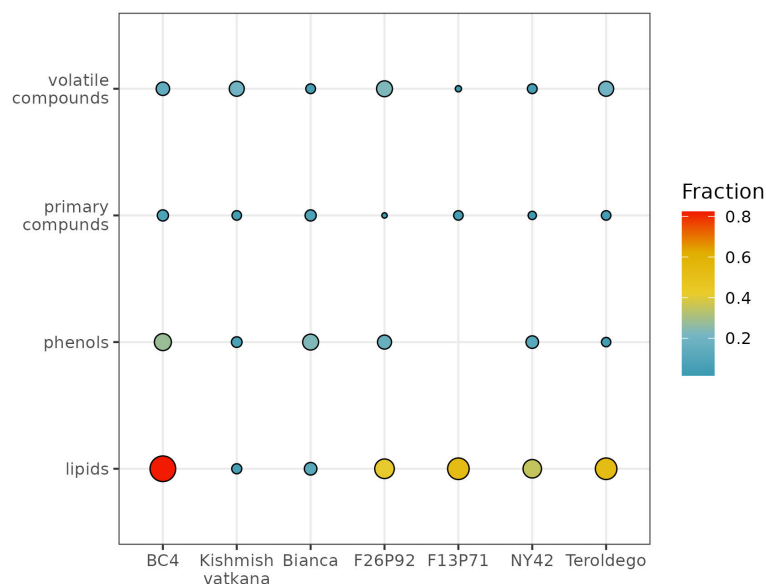


FIGURE 4

Global visualization of highly modulated metabolites by chemical class (in percentage) in response to *E. necator* inoculation. The size and color intensity of the dots are proportional to the estimated percentage of metabolites modulated in each genotype in both years, based on the total number of identified and quantified/semi-quantified metabolites per class.

significance (assessed by a univariate test) and strength of the effect (estimated by calculating the effect size). We then presented this information in a series of volcano plots (Figure 5 and 6) that highlight the modulation of the distinct classes for each genotype. Positive impact magnitude suggests abundant production (up-accumulation) of the metabolite in infected plants. As a result, a high

tail in the volcano's right arm indicates a favorable metabolic response to infection. The lowered (down-accumulation) quantity of metabolites as a reaction to infection, on the other hand, has a negative effect size. It can be seen graphically as the high tail in the volcano's left arm.

Overall, Figure 5 and 6 confirm the trends observed in the initial PCA results, but the plots can be used to get an insight into the classes

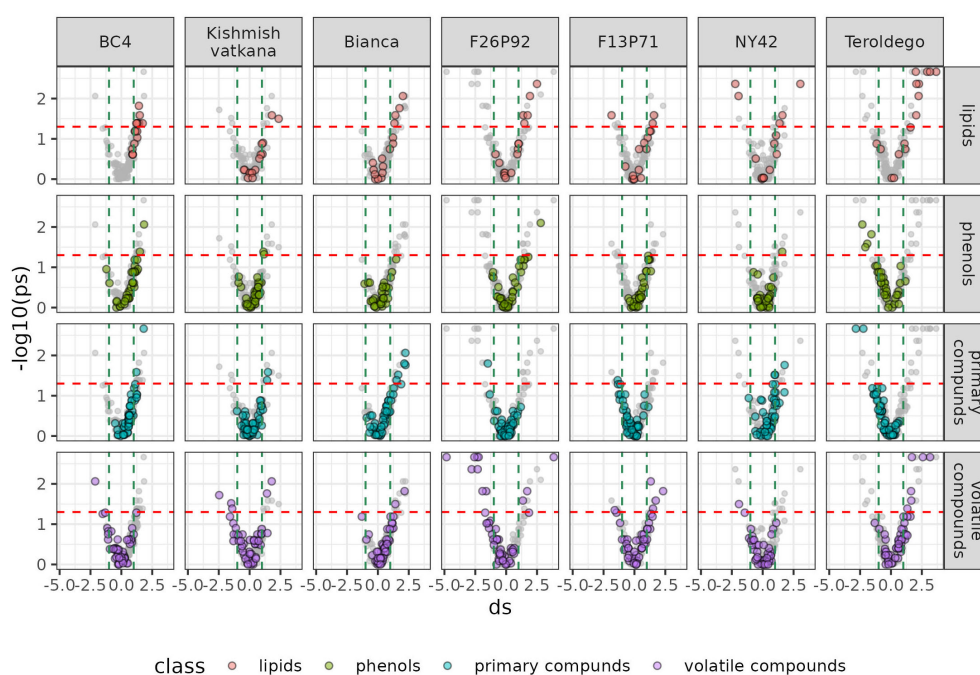


FIGURE 5

Metabolites significantly modulated by the infection (up- and down-accumulated) by class of compounds in all seven genotypes at 24 hpi in the two years of data analysis (2019–2021). The colors identify the different chemical classes (red for lipids, green for phenols, blue for primary compounds, and violet for volatile organic compounds) and "ds" represents the calculated Cohen's d values.

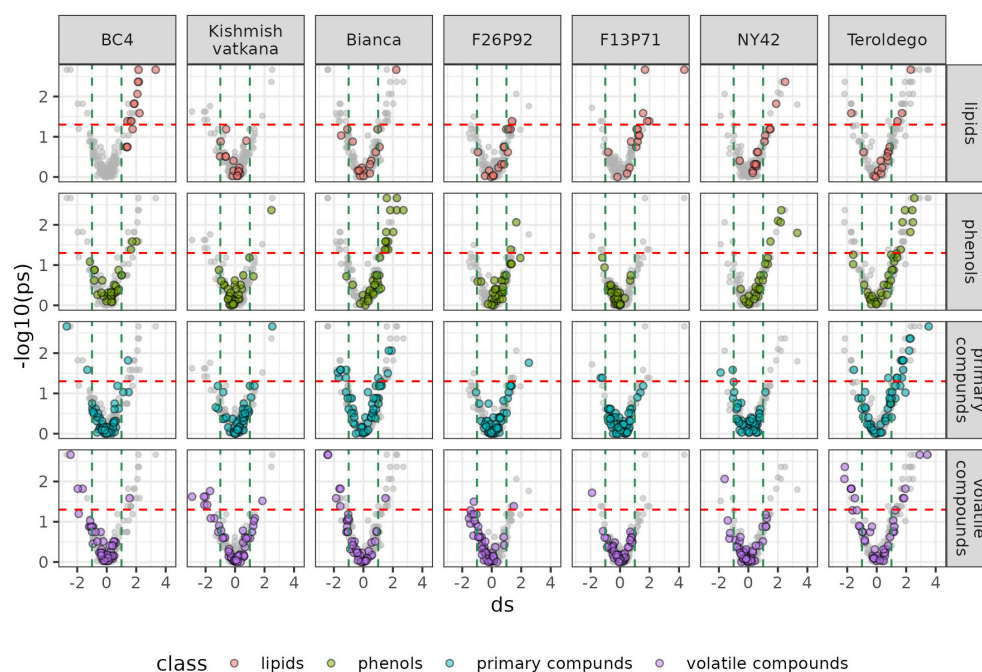


FIGURE 6

Metabolites significantly modulated by the infection (up- and down- accumulated) by class of compounds in all seven genotypes at 48 hpi in the two years of data analysis (2019–2021). The colors identify the different chemical classes (red for lipids, green for phenols, blue for primary compounds, and violet for volatile organic compounds) and “ds” represents the calculated Cohen’s d values.

of metabolites, which are more involved in the response. Generally, it can be noticed that the genotypes ‘Bianca’ and ‘Teroldego’ begin to react at 24 hpi (Figure 5) and that the effect becomes much larger at 48 hpi (Figure 6), reaching in some cases an effect size value of 2 and even 3 (e.g. phenols in ‘Bianca’ and ‘Teroldego’). In fact, ‘Bianca’ exhibits the onset of an infection response in all four classes of compounds at 24 hpi, which becomes stronger at 48 hpi by producing a large number of up-accumulated phenols, followed by primary compounds and lipids, and several down-accumulation of volatile compounds. ‘Teroldego’ produces primarily up-accumulated chemicals such as lipids and volatiles at 24 hpi, whereas, at 48 hpi, there is a large production of up-accumulated phenols, primary and volatile compounds.

The genotypes F13P71 and ‘Kishmish vatkana’, which appeared not to show major changes in the PCA analysis, showed an up-accumulation in a limited number of lipids and volatiles at 24hpi. At 48hpi, however, ‘Kishmish vatkana’ reestablished an equilibrium that modulated the levels of up-accumulated lipids and volatiles to levels comparable to the non-infected plants of the same genotype. In the case of F13P71, the levels of lipids increased by 48 hpi, while volatiles appeared not to be modulated anymore.

As for genotypes BC4, F26P92 and NY42, they showed the third type of trend in the PCA where a partial separation between infected and non-infected plants was observed at 24 hpi, BC4 up-accumulated lipids and phenolic compounds at 24 hpi and an increase in that up-accumulation at 48 hpi. It also showed an increase in down-accumulation of volatiles from 24 hpi to 48 hpi. F26P92 showed an active reaction in the synthesis of up-accumulated lipids and down-accumulation of volatile compounds only at 24hpi. NY42 showed a rise in lipids and primary compounds at 24hpi only, while phenols highly increased from 24hpi to 48hpi.

A list of modulated metabolites with the highest reaction in terms of effect size and *p-values* is synthesized in [Supplementary Table 6](#). Among them, we noticed ten up-accumulated metabolites that might potentially distinguish resistant (partial/total) genotypes from the susceptible genotype at 48hpi, when we know that the pathogen’s infection structures had already interfered with the plant’s metabolome. These metabolites were 2-pyrrolidinone, oleanolic acid, behenic acid, palmitoleic acid, arachidic acid, oleic acid +*cis*-vaccenic acid, pallidol, isorhapontin, quercetin-3-glucuronide, and astringin. Their presence and/or absence in the genotypes is outlined in the [Figure 7](#). The changes of the discriminative compounds at 0hpi, 24hpi and 48hpi for all genotypes based on the corrected concentration values as described in materials and methods are displayed in [Supplementary Figure 1](#).

4 Discussion

In nature, plants protect themselves mostly through mechanical means (spines, trichomes, thick cuticles, and hard or sticky surfaces) and the emission of a variety of poisonous, repellent or unattractive compounds. Plants produce a wide range of metabolites through the latter protection strategy, including fundamental metabolites such as primary compounds and lipids, as well as secondary metabolites like phenolic and volatile organic compounds (Mazid et al., 2011). Secondary metabolism is known to play a defensive role against predators, parasites and diseases (Ali et al., 2010), and primary metabolism, in addition to controlling plant growth, development and reproduction, contributes to plant defense as a source of energy

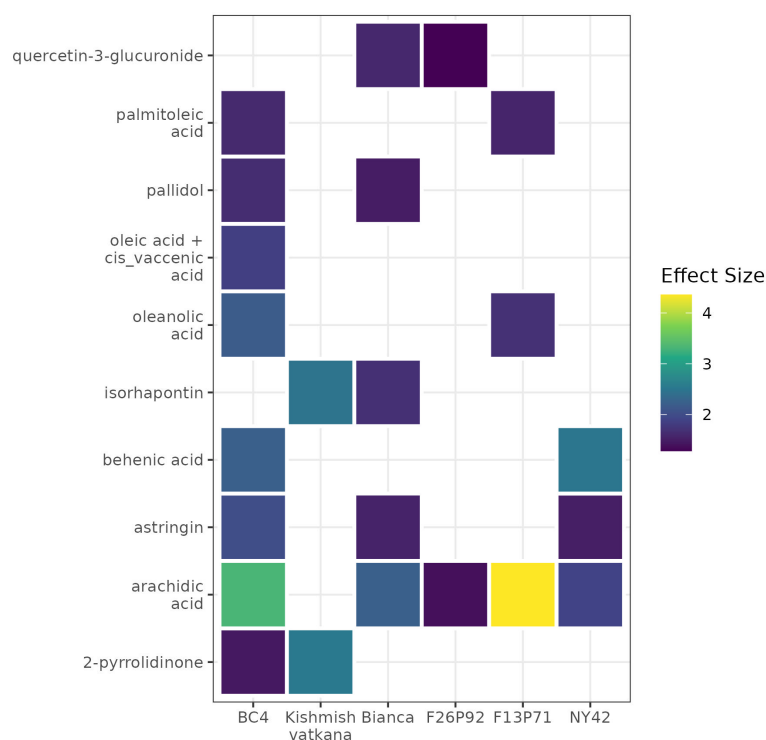


FIGURE 7

A heat map using color-encoded effect size of the discriminative compounds identified as present in the resistant genotypes and absent in the susceptible genotype at 48 hpi. The colors and their intensities mark the modulation of the metabolites in the resistant genotypes according to the calculated effect size (Cohen's *d* test).

and by signaling molecules that directly or indirectly trigger defense responses (Wolfender et al., 2013).

In this study, we examined the contribution of secondary and primary metabolic components in mediating plant defense responses in resistant grapevine genotypes inoculated by *E. necator*. To the best of our knowledge, this is the first study to look at the responsiveness of multiple classes of metabolites in varieties with one gene of resistance versus varieties with multiple barriers of resistance against powdery mildew.

Our findings indicated that diverse grapevine genotypes react with different time scales to infection. Interestingly, metabolic response (primary and secondary) was more active in the partial and total resistant varieties (i.e., 'Bianca', F26P92, NY42, and BC4) and in the susceptible cultivar 'Teroldego' compared to the partially resistant mono-locus ('Kishmish vatkhana') and the totally resistant pyramided variety (F13P71) (Table 1). 'Bianca', as well as 'Teroldego', showed metabolic variability caused by pathogen inoculation at both time points, while F26P92 and NY42 showed metabolic variability only at 24 hpi. This could be explained by the studies of Feechan et al. (2015) and Pap et al. (2016), which indicated that the existence of several resistance genes or loci does not result in a stronger resistance response for all genotypes, thereby suggesting that combinations of loci such as *Ren3Ren9* do not always have additive effects (Zendler et al., 2020) when compared to the *Run1Ren1* combination that produces an additive effect (Agurto et al., 2017). The method of activating a gene is complicated since just having the gene is not enough; instead, transcription factors are required (Agurto et al., 2017).

Such responses have been observed in some genotypes carrying the combination of *Ren3* and *Ren9*, which did not generate an immune response that has an advantage in terms of the intensity or speed of the response compared to *Ren3* alone (Zini et al., 2019; Zendler et al., 2020). The presence of these loci (*Ren3* and *Ren9*) in all three of the pyramided genotypes, 'Bianca', F26P92, and NY42 (Table 1), could explain our PCA results, which revealed that 'Bianca' had a metabolic variability caused by pathogen inoculation at both time points similar to 'Teroldego', followed by F26P92 and NY42, which showed metabolic variability only at 24 hpi (Figure 3).

On the other hand, studies showed that combinations of *Run1Ren1* and *Run1Ren2* have an additive effect as the combination of both genes/loci generated a stronger immune response than the one triggered by each one individually, however, this effect has been proven to be genotype dependent (Agurto et al., 2017). In fact, in our study, the genotypes F13P71 and NY42 showed little to partial metabolic variability despite possessing the loci *Run1Ren1* and *Run1Ren2*, respectively. Moreover, other studies showed that by powdery mildew isolates could overcome, in some cases, *Run1* resistance (Cadde-Davidson et al., 2011; Schneider et al., 2019). This could explain the observed metabolic variability in F13P71. Furthermore, the additive effect of *Run1Ren2* can be race-specific (Feechan et al., 2015) and in addition, the existence of the other two extra loci in the genotype NY42, might interfere with the metabolomics response to the pathogen. All these factors contribute to the complexity of the effects of resistance genes in the metabolic variability of infected grapevine genotypes, requiring additional research.

Considering all these aspects, it seems that the level of resistance (partial or total) of the loci is more important than their numbers. The level of resistance is referred to as “total” when there are greatly suppressed symptoms or no observable symptoms of infection at all and “partial” when there is a decrease in symptoms but not a complete disappearance (Julius Kühn-Institut, 2022; Sosa-Zuniga et al., 2022). This is corroborated in our study by the assessment of the OIV-455 descriptor at 7 days after the artificial infection (Supplementary Table 1).

We found for ‘Kishmish vatkana’, a genotype with partial resistance, a high level of resistance (OIV-455 = 7) and for F13P71, a genotype with total resistance, a very high level of resistance (OIV-455 = 9). Indeed, an 84% decrease in the number of cells the fungus invaded has been observed among the responses brought on by *Ren1* (‘Kishmish vatkana’). Other reactions include the induction of PCD (programmed cell death), the development of callose deposits at 48 hpi, and the promotion of ROS (reactive oxygen species) at 96 hpi (Agurto et al., 2017). A more intense defense response was likewise observed in genotypes carrying *Run1Ren1*, such as F13P71, in terms of ROS production, callose accumulation and PCD (Agurto et al., 2017).

NY42 and F26P92, genotypes with partial resistance, scored a high level of resistance (OIV-455 = 7) and BC4, a genotype with total resistance, was assessed as having a very high level of resistance (OIV-455 = 9). Possamai et al. (2021) observed in genotypes carrying *Run1Ren2* loci such as NY42 a significant decrease in colony formation, and Feechan et al. (2015) showed that *Ren2* confers partial resistance on plants by inducing an efficient immune response that prevents fungal sporulation. Rapid programmed cell death, which hinders the growth of secondary hyphae and sporulation, is one of the immunological responses inflicted by *Run1* (BC4) on resistant plants. A quick HR is seen at 48 hpi in cells where the fungus developed secondary hyphae as evidenced by the rise in ROS and the appearance of PCD. The buildup of callose deposits at the *E. necator* infection site is another reaction caused by *Run1* (Agurto et al., 2017). *Ren3Ren9* (F26P92) elicits similarly high resistance responses (Zendler et al., 2020), with a high level of resistance score (OIV-455 = 8) assigned to ‘Bianca’, a partial resistant genotype carrying the exact same loci (*Ren3Ren9*). As expected, the susceptible genotype ‘Teroldego’ was assessed as having a very low level of resistance (OIV-455 = 1). As far as primary metabolites are concerned, powdery mildew induced changes mainly in the class of lipids (Figure 4). Lipids are recognized to be important components of plant cell membranes that provide energy for metabolic activities. In recent years, there has been increasing evidence that lipids play a role in combating biotic stress, such as powdery mildew. Lim et al. (2017) showed that lipids regulate the PCD response during pathogen defense, as well as membrane fluidity, stability, and permeability during plant responses to microbial pathogens. The accumulation of C16:0 might be used to produce C18 fatty acids. Also higher DBI may account for an increase in chloroplasts’ membrane fluidity that may be crucial to avoid any damage in the photosynthetic machinery with inevitable effects on the energy transduction pathways and primary productivity (Laureano et al., 2018; Laureano et al., 2021). Moreover, lipids play important signaling roles also in plant defense and ROS regulating levels. Because of the various functions of lipids, Della Corte et al. (2015) observed that their abundance in plants is influenced by genotype and phenotype. Thus, the fluctuating lipid levels observed in the various

resistant genotypes tested may be attributed in part to this aspect as a result of *E. necator* inoculation.

The role of primary metabolic pathways in the regulation of plant defense responses is not very well known. Mainly, all primary compounds function as signaling molecules that trigger defense responses through signal transduction and pathogen recognition processes (Madiha et al., 2019). The accumulation of the primary compounds in our study, which was comparable to the susceptible genotype, made us lend support to the idea that susceptible plants initiate a basal defense similar to the response in resistant plants, but insufficient in timing and/or intensity to limit disease progression, as observed by Marsh et al. (2010). Similarly, there is a clear alteration of primary compounds in the defense against powdery mildew in resistant genotypes, but the amount raises the question of whether this modulation is a result of resistance or a normal plant reaction.

One of the most important functions of phenolic compounds as secondary metabolites is an antibacterial activity in plants, which acts as a barrier against pathogens like *E. necator*. Their accumulation in plants is associated with host resistance (Atak, 2017). However, it is noteworthy that Keller (2015) found that despite some *Vitis* species (such as *V. cinerea* and *V. champinii*) exhibiting pathogen resistance, the buildup of stilbenes, the most well-known class of phenolic defense chemicals, did not occur in these plants. This finding could support the hypothesis that metabolite accumulation is not totally linked to the number of loci present in the resistance genotypes. Such was the case in our study where the pyramided genotype F13P71 accumulated very low levels of phenolic compounds. The same genotype displayed low levels of volatile organic compounds (VOCs). Thus, similar assumptions could be made also about VOCs, but further research is needed to confirm it.

Although some chemical classes in some of our resistant varieties showed similar reactions to the susceptible genotype, it should be noted that the resistant genotypes nonetheless produce a number of up-accumulated metabolites that were not found in the susceptible ‘Teroldego’, with the exception of a few whose calculated effect sizes were smaller than in the resistant genotypes. The study of Viret et al. (2018) showed that the induction and accumulation of defensive metabolites increase only during the pathogen’s infectious structure development, which takes around 24 hours (Boddy, 2016). This was noticed in the pyramided genotypes in which the metabolite overaccumulation had a significantly larger impact size at 24 hpi than at 48hpi, when their modulation appeared to subside, except for ‘Bianca’. In our earlier research, we provided evidence that *P. viticola* caused an early modulation in pyramided genotypes, which began earlier, between 0 and 12 hpi, and peaked at 48hpi. Even though the current work studies *E. necator* and genotypes that carry different loci than the prior study, we can presume that a similar but somewhat different reaction happened for this study as well. On the other hand, the up-accumulation of metabolites in mono-locus genotypes was shown to be established at 24 hpi and to become stronger at 48hpi. The same finding was obtained in the work of Chitarrini et al. (2017a), in which the plant defense systems were activated 48 hours after inoculation.

Investigating the biological relevance of the ten compounds found as discriminative between resistant and susceptible genotype (Figure 7), we found out that pallidol, oleic acid+*cis* vaccenic acid and astringin were already discussed as potential biomarkers of resistance in our previous study (Ciubotaru et al., 2021) due to their role in activating plant defense

response. Moreover, pallidol has been in some cases linked to the grapevine's response to fungal attack (Pezet et al., 2004; Jean-Denis et al., 2006). We have also found that the remaining seven- up-accumulated metabolites contribute to plant defense. Isorhapontin, like pallidol and astringin, belongs to the class of stilbenes and stilbenoids, and it has been demonstrated that this class accumulates in larger concentrations in disease-resistant cultivars than in susceptible cultivars, due to its role in plants that inhibits fungal growth (Chitarrini et al., 2017b; Vezzulli et al., 2019). Similarly, the increased accumulation of fatty acids in the plant metabolome, specifically behenic acid, palmitoleic acid, arachidic acid and oleic acid+*cis* vaccenic suggests that these fatty acids are involved in intracellular signaling processes as well as desaturases-mediated membrane fluidity adjustment (He and Ding, 2020; Ciubotaru et al., 2021). The fatty acid desaturase 7 (FAD7) and fatty acid desaturase 8 (FAD8) genes, which play a key role in the synthesis of fatty acids, have also been linked to protective mechanisms (Rojas et al., 2014; Cavaco et al., 2021). Last but not least, oleanolic acid is known to play a role in plants' defense mechanisms against pathogens and water loss (Gudoityte et al., 2021), whereas quercetin is a powerful antioxidant that effectively protects plants from a variety of biotic and abiotic challenges (Singh et al., 2021). Our findings confirm previous research about the importance of these compounds in disease resistance because of their different roles in plant defense.

5 Conclusions

Many metabolomics studies have been conducted on understanding the mechanism of grapevine defense, mainly on downy mildew, but few on powdery mildew. Thus, we designed this study as a promising endeavor in order to contribute to a better understanding of plant defense mechanisms. To our knowledge, this is the first time that metabolic investigations of the most important classes of compounds with a role in plant defense were carried out in artificially inoculated genotypes with mono-locus and pyramided resistance in order to characterize the host's response to the infection of *E. necator*.

Overall, the results of this study indicate that how cultivars behaved to pathogen attack can be linked to genotype and/or resistant loci differences; however, resistance is not exclusively related to *Run/Ren* loci. Additionally, although it cannot be strictly classified as a connection, we saw similar metabolomic responses in our experiment between the mono-locus and pyramided genotypes that share the exact *Run/Ren* loci. Therefore, additional transcriptome studies are required to fully comprehend the unfavorable interaction between these resistant loci and *E. necator*. Further research is needed also to validate the molecules identified as biologically relevant compounds produced during the pathogen-host interaction and recommended as possible biomarkers for resistance to *E. necator*. In terms of plant resistance strength against powdery mildew, our findings show no direct relationship between the number of resistance loci present in plants and the production of metabolites recommended as resistance biomarkers.

The findings of this study add to our understanding of plant defense mechanisms and call for more metabolomics research, as well as additional complementary omics research to clarify which genes are responsible for powdery mildew resistance and how they function in the majority of *Run* and *Ren* loci, as only one study in this area has been conducted. The integration of transcriptomics and metabolomics data can be exploited to uncover commonalities and

differences between diverse R-gene-mediated resistances to *E. necator*. This approach will enable breeders to choose more reliable genotypes for marker-assisted breeding by using genetic and biochemical markers.

Data availability statement

The original contributions presented in the study are included in the article/Supplementary Material. Further inquiries can be directed to the corresponding author.

Author contributions

RMC, GC, LZ, MS, and UV designed the experiment. MS and SV provided the plant material. RMC, SV and LZ performed the experiment. RMC did the extractions and analytical analysis. PF, RMC, and UV conducted the data treatment, statistical analysis and data visualization. RMC wrote the original draft preparation of the manuscript. UV, SV, PF, MO, PR and GC did the review and editing. UV, MO, and PR supervised the project. All authors discussed the results and implications and commented on the manuscript at all stages. All authors contributed to the article and approved the submitted version.

Funding

This research was supported by Centro di Sperimentazione Agraria e Forestale Laimburg Research Centre (Bolzano Autonomous Province of Bolzano/South Tyrol) and Fondazione Edmund Mach (San Michele all'Adige), Italy in collaboration with Università degli studi di Udine.

Acknowledgments

RMC acknowledges the assistance, support, and guidance in GC-MS by Cesare Lotti, and LC-MS analysis by Domenico Masuero and Andrea Angeli.

Conflict of interest

The authors declare that the research was conducted in the absence of any commercial or financial relationships that could be construed as a potential conflict of interest.

Publisher's note

All claims expressed in this article are solely those of the authors and do not necessarily represent those of their affiliated organizations, or those of the publisher, the editors and the reviewers. Any product that may be evaluated in this article, or claim that may be made by its manufacturer, is not guaranteed or endorsed by the publisher.

Supplementary material

The Supplementary Material for this article can be found online at: <https://www.frontiersin.org/articles/10.3389/fpls.2023.1112157/full#supplementary-material>

References

- Agurto, M., Schlechter, R. O., Armijo, G., Solano, E., Serrano, C., Contreras, et al. (2017). *RUN1* and *REN1* pyramiding in grapevine (*Vitis vinifera* cv. crimson seedless) displays an improved defense response leading to enhanced resistance to powdery mildew (*Erysiphe necator*). *Front. Plant Sci.* 8. doi: 10.3389/fpls.2017.00758
- Ali, K., Maltese, F., Choi, Y. H., and Verpoorte, R. (2010). Metabolic constituents of grapevine and grape-derived products. *Phytochem. Rev.* 9, 357–378. doi: 10.1007/s11101-009-9158-0
- Atak, A. (2017). Determination of downy mildew and powdery mildew resistance of some grape cultivars. *South Afr. J. Enology Viticulture* 38 (1), 11–17. doi: 10.21548/38-1-671
- Atak, A. (2022). “New perspectives in grapevine breeding,” in *Plant breeding - new perspectives*. Ed. H. Wang (Rijeka, Croatia: IntechOpen). doi: 10.5772/intechopen.105194
- Atak, A., Göksel, Z., and Yilmaz, Y. (2021). Changes in major phenolic compounds of seeds, skins, and pulps from various vitis spp. and the effect of powdery and downy mildew diseases on their levels in grape leaves. *Plants* 10, 2554. doi: 10.3390/plants10122554
- Atak, A., and Şen, A. (2021). A grape breeding programme using different vitis species. *Plant Breed.* 140 (6), 1136–1149. doi: 10.1111/pbr.12970
- Boddy, L. (2016). “Pathogens of autotrophs,” in *The fungi* (Oxford, UK: Academic Press), 245–292.
- Cadle-Davidson, L., Mahanil, S., Gadoury, D. M., Kozma, P., and Reisch, B. I. (2011). Natural infection of *Run1*-positive vines by naïve genotypes of *Erysiphe necator*. *Vitis* 50 85, 173–175.
- Carroll, J. E., and Wilcox, W. F. (2003). Effects of humidity on the development of grapevine powdery mildew. *Phytopathology* 93, 1137–1144. doi: 10.1094/PHYTO.2003.93.9.1137
- Cavaco, A. R., Laureano, G., Cunha, J., Eiras-Dias, J., Matos, A. R., and Figueiredo, A. (2021). Fatty acid modulation and desaturase gene expression are differentially triggered in grapevine incompatible interaction with biotrophs and necrotrophs. *Plant Physiol. Biochem.* 163, 230–238. doi: 10.1016/j.plaphy.2021.04.001
- Chitarrini, G., Soini, E., Riccadonna, S., Franceschi, P., Zulini, L., Masuero, D., et al. (2017a). Identification of biomarkers for defense response to *Plasmopara viticola* in a resistant grape variety. *Front. Plant Sci.* 8. doi: 10.3389/fpls.2017.01524
- Chitarrini, G., Zulini, L., Masuero, D., and Vrhovsek, U. (2017b). Lipid, phenol and carotenoid changes in ‘Bianca’ grapevine leaves after mechanical wounding: a case study. *Protoplasma* 254 (6), 2095–2106. doi: 10.1007/s00709-017-1100-5
- Ciubotaru, R. M., Franceschi, P., Zulini, L., Stefanini, M., Škrab, D., Rossarolla, M. D., et al. (2021). Mono-locus and pyramided resistant grapevine cultivars reveal early putative biomarkers upon artificial inoculation with *Plasmopara viticola*. *front. Plant Sci.* 12. doi: 10.3389/fpls.2021.693887
- Deliere, L., Miclot, A. S., Sauris, P., Rey, P., and Calonnec, A. (2010). Efficacy of fungicides with various modes of action in controlling the early stages of an *Erysiphe necator*-induced epidemic. *Pest Manag. Sci.* 66 (12), 1367–1373. doi: 10.1002/ps.2029
- Della Corte, A., Chitarrini, G., Di Gangi, I. M., Masuero, D., Soini, E., Mattivi, F., et al. (2015). A rapid LC-MS/MS method for quantitative profiling of fatty acids, sterols, glycerolipids, glycerophospholipids and sphingolipids in grapes. *Talanta* 140, 52–61. doi: 10.1016/j.talanta.2015.03.003
- Dry, I. B., and Thomas, M. R. (2015). Fast-tracking grape breeding for disease resistance. *Wine Vitic. J.* 5, 52–55.
- Feechan, A., Anderson, C., Torregrosa, L., Jermakow, A., Mestre, P., Wiedemann-Merdinoglu, S., et al. (2013). Genetic dissection of a TIR-NB-LRR locus from the wild north American grapevine species *Muscadinia rotundifolia* identifies paralogous genes conferring resistance to major fungal and oomycete pathogens in cultivated grapevine. *Plant J.* 76, 661–674. doi: 10.1111/tpj.12327
- Feechan, A., Kabbara, S., and Dry, I. B. (2011). Mechanisms of powdery mildew resistance in the Vitaceae family. *Mol. Plant Pathol.* 12, 263–274. doi: 10.1111/j.1364-3703.2010.00668.x
- Feechan, A., Kocsis, M., Riaz, S., Zhang, W., Gadoury, D. M., Walker, M. A., et al. (2015). Strategies for *RUN1* deployment using *RUN2* and *REN2* to manage grapevine powdery mildew informed by studies of race specificity. *Phytopathology* 105, 1104–1113. doi: 10.1094/PHYTO-09-14-0244-R
- Folch, J., Lees, M., and Sloane Stanley, G. H. (1957). A simple method for the isolation and purification of total lipids from animal tissues. *J. Biol. Chem.* 226, 497–509. doi: 10.1016/S0021-9258(18)64849-5
- Gadoury, D. M., Cadle-Davidson, L., Wilcox, W. F., Dry, I. B., Seem, R. C., and Milgroom, M. G. (2012). Grapevine powdery mildew (*Erysiphe necator*): A fascinating system for the study of the biology, ecology and epidemiology of an obligate biotroph: Grapevine powdery mildew. *Mol. Plant Pathol.* 13, 1–16. doi: 10.1111/j.1364-3703.2011.00728.x
- Gudoityte, E., Arandarcikaite, O., Mazeikiene, I., Bendokas, V., and Liobikas, J. (2021). Ursolic and oleanolic acids: Plant metabolites with neuroprotective potential. *Int. J. Mol. Sci.* 22, 4599. doi: 10.3390/ijms22094599
- Gur, L., Cohen, Y., Frenkel, O., Schweitzer, R., Shlissel, M., and Reuveni, M. (2022). Mixtures of macro and micronutrients control grape powdery mildew and alter berry metabolites. *Plants* 11, 978. doi: 10.3390/plants11070978
- He, M., and Ding, N. Z. (2020). Plant unsaturated fatty acids: Multiple roles in stress response. *Front. Plant Sci.* 11. doi: 10.3389/fpls.2020.562785
- Hoffmann, S., Di Gaspero, G., Kovács, L., Howard, S., Kiss, E., Galbács, Z., et al. (2008). Resistance to *Erysiphe necator* in the grapevine ‘Kishmish vatkana’ is controlled by a single locus through restriction of hyphal growth. *Theor. Appl. Genet.* 116, 427–438. doi: 10.1007/s00122-007-0680-4
- Jean-Denis, J. B., Pezet, R., and Tabacchi, R. (2006). Rapid analysis of stilbenes and derivatives from downy mildew-infected grapevine leaves by liquid chromatography-atmospheric pressure photoionisation mass spectrometry. *J. Chromatogr.* 1112 (1–2), 263–268. doi: 10.1016/j.chroma.2006.01.060
- Julius Kühn-Institut. (2022). *Federal research centre for cultivated plants (JKI), institute for grapevine breeding* (Geilweilerhof (ZR)). Available at: www.vivc.de/loci (Accessed October 22nd, 2022).
- Keller, M. (2015). *The science of grapevines: Anatomy and physiology* (London, UK: Academic Press).
- Laureano, G., Cavaco, A. R., Matos, A. R., and Figueiredo, A. (2021). Fatty acid desaturases: Uncovering their involvement in grapevine defence against downy mildew. *Int. J. Mol. Sci.* 22 (11), 5473. doi: 10.3390/ijms22115473
- Laureano, G., Figueiredo, J., Cavaco, A. R., Duarte, B., Caçador, I., Malhó, R., et al. (2018). The interplay between membrane lipids and phospholipase a family members in grapevine resistance against *plasmopara viticola*. *Sci. Rep.* 8 (1), 14538. doi: 10.1038/s41598-018-32559-z
- Lim, G. H., Singhal, R., Kachroo, A., and Kachroo, P. (2017). Fatty acid-and lipid-mediated signaling in plant defense. *Annu. Rev. Phytopathol.* 4, 55, 505–536. doi: 10.1146/annurev-phyto-080516-035406
- Madiha, Z., Mahpara, F., Yasir, S., Muhammad, H., Zafar, H. A., and Khalid, A. K. (2019). Role of primary metabolites in plant defense against pathogens. *Microbial Pathogenesis* 137:103728. doi: 10.1016/j.micpath.2019.103728
- Maia, M., Ferreira, A. E. N., Nascimento, R., Monteiro, F., Traquete, F., Marques, A. P., et al. (2020). Integrating metabolomics and targeted gene expression to uncover potential biomarkers of fungal/oomycetes-associated disease susceptibility in grapevine. *Sci. Rep.* 10, 15688. doi: 10.1038/s41598-020-72781-2
- Marsh, E., Alvarez, S., Hicks, L. M., Barbazuk, W. B., Qiu, W., Kovacs, L., et al. (2010). Changes in protein abundance during powdery mildew infection of leaf tissues of Cabernet sauvignon grapevine (*Vitis vinifera* L.). *Proteomics* 10, 2057–2064. doi: 10.1002/pmic.200900712
- Mazid, M. A., Khan, T. A., and Mohammad, F. (2011). Role of secondary metabolites in defense mechanisms of plants. *Biol. Med.* 3, 232–249.
- McDonald, B. A., and Linde, C. (2002). Pathogen population genetics, evolutionary potential, and durable resistance. *Annu. Rev. Phytopathol.* 40, 349–379. doi: 10.1146/annurev-phyto.40.120501.101443
- Merdinoglu, D., Schneider, C., Prado, E., Wiedemann-Merdinoglu, S., and Mestre, P. (2018). Breeding for durable resistance to downy and powdery mildew in grapevine. *Oeno One* 52, 189–195. doi: 10.20870/oeno-one.2018.52.3.2116
- Miclot, A. S., Wiedemann-Merdinoglu, S., Duchêne, E., Merdinoglu, D., and Mestre, P. (2012). A standardized method for the quantitative analysis of resistance to grapevine powdery mildew. *Eur. J. Plant Pathol.* 133, 483–495. doi: 10.1007/s10658-011-9922-z
- Mundt, C. C. (2018). Pyramiding for resistance durability: Theory and practice. *Phytopathology* 108, 792–802. doi: 10.1094/PHYTO-12-17-0426-RVW
- Pap, D., Riaz, S., Dry, I. B., Jermakow, A., Tenschler, A. C., Cantu, D., et al. (2016). Identification of two novel powdery mildew resistance loci, *Ren6* and *Ren7*, from the wild Chinese grape species *Vitis piasezkii*. *BMC Plant Biol.* 16, 170. doi: 10.1186/s12870-016-0855-8
- Peressotti, E., Wiedemann-Merdinoglu, S., Delmotte, F., Bellin, D., Di Gaspero, G., Testolin, R., et al. (2010). Breakdown of resistance to grapevine downy mildew upon limited deployment of a resistant variety. *BMC Plant Biol.* 10, 147. doi: 10.1186/1471-2229-10-147
- Pertot, I., and Gessler, C. (2006). “Potential use and major constraints in grapevine powdery and downy mildew biocontrol. efficacy of KBV 99-01 against *Erysiphe necator* and *Plasmopara viticola*,” in *Proceedings of the 5th international workshop on grapevine downy and powdery mildew* (San Michele all’Adige, Italy: SafeCrop Centre Istituto Agrario di San Michele all’Adige), 18–23.
- Pezet, R., Gindro, K., Viret, O., and Richter, H. (2004). Effects of resveratrol, viniferins and pterostilbene on *Plasmopara viticola* zoospore motility and disease development. *Vitis* 43, 145–148. doi: 10.5073/vitis.2004.43.145-148
- Pimentel, D., Amaro, R., Erban, A., Mauri, N., Soares, F., Rego, C., et al. (2021). Transcriptional, hormonal, and metabolic changes in susceptible grape berries under powdery mildew infection. *J. Exp. Bot.* 72, 6544–6569. doi: 10.1093/jxb/erab258
- Pirrello, C., Mizzotti, C., Tomazetti, T. C., Colombo, M., Bettinelli, P., Prodanutti, D., et al. (2019). Emergent ascomycetes in viticulture: An interdisciplinary overview. *Front. Plant Sci.* 22:10. doi: 10.3389/fpls.2019.01394
- Possamai, T., Wiedemann-Merdinoglu, S., Merdinoglu, D., Migliaro, D., De Mori, G., Cipriani, G., et al. (2021). Construction of a high-density genetic map and detection of a major QTL of resistance to powdery mildew (*Erysiphe necator* sch.) in Caucasian grapes (*Vitis vinifera* L.). *BMC Plant Biol.* 21, 528. doi: 10.1186/s12870-021-03174-4

- Qiu, W., Feechan, A., and Dry, I. (2015). Current understanding of grapevine defense mechanisms against the biotrophic fungus (*Erysiphe necator*), the causal agent of powdery mildew disease. *Hortic. Res.* 2, 15020. doi: 10.1038/hortres.2015.20
- R Core Team (2020). *A language and environment for statistical computing* (Vienna: R Foundation for Statistical Computing). Available at: <https://www.R-project.org/>.
- Rienth, M., Vigneron, N., Walker, R. P., Castellarin, S. D., Sweetman, C., Burbidge, C. A., et al. (2021). Modifications of grapevine berry composition induced by main viral and fungal pathogens in a climate change scenario. *Front. Plant Sci.* 12. doi: 10.3389/fpls.2021.717223
- Rojas, C. M., Senthil-Kumar, M., Tzin, V., and Mysore, K. S. (2014). Regulation of primary plant metabolism during plant-pathogen interactions and its contribution to plant defense. *Front. Plant Sci.* 10:5. doi: 10.3389/fpls.2014.00017
- Sawilowsky, S. S. (2009). New effect size rules of thumb. *J. Modern Appl. Stat. Methods* 8:26, 597–599. doi: 10.22237/jmasm/1257035100
- Schneider, C., Onimus, C., Prado, E., Dumas, V., Wiedemann-Merdinoglu, S., Dorne, M. A., et al. (2019). INRA-ResDur: the French grapevine-breeding programme for durable resistance to downy and powdery mildew. *Acta Hort.* 1248, 207–214. doi: 10.17660/ActaHortic.2019.1248.30
- Singh, P., Arif, Y., Bajguz, A., and Hayat, S. (2021). The role of quercetin in plants. *Plant Physiol. Biochem.* 166, 10–19. doi: 10.1016/j.plaphy.2021.05.023
- Sosa-Zuniga, V., Vidal Valenzuela, A., Barba, P., Espinoza Cancino, C., Romero-Romero, J. L., and Arce-Johnson, P. (2022). Powdery mildew resistance genes in vines: An opportunity to achieve a more sustainable viticulture. *Pathogens* 11, 703. doi: 10.3390/pathogens11060703
- Valdés-Gómez, H., Gary, C., Cartolaro, P., Lolas-Caneo, M., and Calonnec, A. (2011). Powdery mildew development is positively influenced by grapevine vegetative growth induced by different soil management strategies. *Crop Prot.* 30–9, 1168–1177. doi: 10.1016/j.cropro.2011.05.014
- van den Berg, R. A., Hoefsloot, H. C., Westerhuis, J. A., Smilde, A. J. K., and van der Werf, M. J. (2006). Centering, scaling, and transformations: improving the biological information content of metabolomics data. *BMC Genomics* 7, 142. doi: 10.1186/1471-2164-7-142
- Vezzulli, S., Malacarne, G., Masuero, D., Vecchione, A., Dolzani, C., Goremykin, V., et al. (2019). The Rpv3-3 haplotype and stilbenoid induction mediate downy mildew resistance in a grapevine interspecific population. *Front. Plant Sci.* 10. doi: 10.3389/fpls.2019.00234
- Viret, O., Spring, J. L., and Gindro, K. (2018). Stilbenes: biomarkers of grapevine resistance to fungal diseases. *Oeno One* 52, 235–240. doi: 10.1186/1471-2164-7-142
- Volynkin, V., Vasylyk, I., Volodin, V., Grigoreva, E., Karzhaev, D., Lushchay, E., et al. (2021). The assessment of agrobiological and disease resistance traits of grapevine hybrid populations (*Vitis vinifera* L. × *Muscadinia rotundifolia* Michx.) in the climatic conditions of Crimea. *Plants* 10 (6), 1215. doi: 10.3390/plants10061215
- Vrhovsek, U., Masuero, D., Gasperotti, M., Franceschi, P., Caputi, L., Viola, R., et al. (2012). A versatile targeted metabolomics method for the rapid quantification of multiple classes of phenolics in fruits and beverages. *J. Agric. Food Chem.* 60, 8831–8840. doi: 10.1021/jf2051569
- Welter, L. J., Göktürk-Baydar, N., Akkurt, M., Maul, E., Eibach, R., Töpfer, R., et al. (2007). Genetic mapping and localization of quantitative trait loci affecting fungal disease resistance and leaf morphology in grapevine (*Vitis vinifera* L.). *Mol. Breed.* 20, 359–374. doi: 10.1007/s11032-007-9097-7
- Welter, L. J., Tisch, C., Kortekamp, A., Topper, R., and Zyprian, E. (2017). Powdery mildew responsive genes of resistant grapevine cultivar 'Regent'. *Vitis* 56, 181–188. doi: 10.5073/vitis.2017.56.181-188
- Wolfender, J. L., Rudaz, S., Choi, Y. H., and Kim, H. K. (2013). Plant metabolomics: from holistic data to relevant biomarkers. *Curr. Med. Chem.* 20 (8), 1056–1090. doi: 10.2174/0929867311320080009
- Yin, W., Wang, X., Liu, H., Wang, Y., van Nocker, S., Tu, M., et al. (2022). Overexpression of *VqWRKY31* enhances powdery mildew resistance in grapevine by promoting salicylic acid signaling and specific metabolite synthesis. *Horticulture Res.* 9, 64. doi: 10.1093/hr/uhab064
- Zendler, D., Schneider, P., Töpfer, R., and Zyprian, E. (2017). Fine mapping of *Ren3* reveals two loci mediating hypersensitive response against *Erysiphe necator* in grapevine. *Euphytica* 213, 68. doi: 10.1007/s10681-017-1857-9
- Zendler, D., Töpfer, R., and Zyprian, E. (2020). Confirmation and fine mapping of the resistance locus *Ren9* from the grapevine cultivar 'Regent'. *Plants* 10, 24. doi: 10.3390/plants10010024
- Zini, E., Dolzani, C., Stefanini, M., Gratl, V., Bettinelli, P., Nicolini, D., et al. (2019). R-loci arrangement versus downy and powdery mildew resistance level: A *Vitis* hybrid survey. *Int. J. Mol. Sci.* 18:20 (14), 3526. doi: 10.3390/ijms20143526



OPEN ACCESS

EDITED BY
Alessandra Ferrandino,
University of Turin, Italy

REVIEWED BY
Yifan Jiang,
Nanjing Agricultural University, China
Joseph Lynch,
West Virginia University, United States

*CORRESPONDENCE
Justin Graham Lashbrooke
✉ jglash@sun.ac.za

SPECIALTY SECTION
This article was submitted to
Plant Metabolism and Chemodiversity,
a section of the journal
Frontiers in Plant Science

RECEIVED 29 November 2022
ACCEPTED 24 January 2023
PUBLISHED 03 February 2023

CITATION
Bosman RN and Lashbrooke JG (2023)
Grapevine mono- and sesquiterpenes:
Genetics, metabolism, and ecophysiology.
Front. Plant Sci. 14:1111392.
doi: 10.3389/fpls.2023.1111392

COPYRIGHT
© 2023 Bosman and Lashbrooke. This is an
open-access article distributed under the
terms of the [Creative Commons Attribution
License \(CC BY\)](#). The use, distribution or
reproduction in other forums is permitted,
provided the original author(s) and the
copyright owner(s) are credited and that
the original publication in this journal is
cited, in accordance with accepted
academic practice. No use, distribution or
reproduction is permitted which does not
comply with these terms.

Grapevine mono- and sesquiterpenes: Genetics, metabolism, and ecophysiology

Robin Nicole Bosman and Justin Graham Lashbrooke*

South African Grape and Wine Research Institute, Stellenbosch University, Stellenbosch, South Africa

Mono- and sesquiterpenes are volatile organic compounds which play crucial roles in human perception of table grape and wine flavour and aroma, and as such their biosynthesis has received significant attention. Here, the biosynthesis of mono- and sesquiterpenes in grapevine is reviewed, with a specific focus on the metabolic pathways which lead to formation of these compounds, and the characterised genetic variation underlying modulation of this metabolism. The bottlenecks for terpene precursor formation in the cytosol and plastid are understood to be the HMG-CoA reductase (HMGR) and 1-deoxy-D-xylylose-5-phosphate synthase (DXS) enzymes, respectively, and lead to the formation of prenyldiphosphate precursors. The functional plasticity of the terpene synthase enzymes which act on the prenyldiphosphate precursors allows for the massive variation in observed terpene product accumulation. This diversity is further enhanced in grapevine by significant duplication of genes coding for structurally diverse terpene synthases. Relatively minor nucleotide variations are sufficient to influence both product and substrate specificity of terpene synthase genes, with these variations impacting cultivar-specific aroma profiles. While the importance of these compounds in terms of grape quality is well documented, they also play several interesting roles in the grapevine's ecophysiological interaction with its environment. Mono- and sesquiterpenes are involved in attraction of pollinators, agents of seed dispersal and herbivores, defence against fungal infection, promotion of mutualistic rhizobacteria interaction, and are elevated in conditions of high light radiation. The ever-increasing grapevine genome sequence data will potentially allow for future breeders and biotechnologists to tailor the aroma profiles of novel grapevine cultivars through exploitation of the significant genetic variation observed in terpene synthase genes.

KEYWORDS

grapevine, terpenes, genes, metabolism, flavour, genomics, ecophysiology

1 Introduction

Terpenes, or terpenoids, are one of the most diverse classes of natural compounds with more than 80 000 identified compounds in insects, micro-organisms, and plants (Christianson, 2017). The majority of these terpenes are produced by plants where they serve various primary and secondary (or specialised) functions. Terpenes that serve vital roles

in primary metabolic processes such as plant growth and development, photosynthesis, and respiration are conserved throughout the plant kingdom. These terpenes include sterols, quinones, photosynthetic pigments (chlorophylls, carotenoids), and plant hormones (brassinosteroids, abscisic acid, and gibberellins). However, in addition to these, plants produce a tremendous variety of terpenes involved in specialised metabolism, typically increasing plant fitness through their role in plant-environment interactions. So called specialised terpenes such as monoterpenes and sesquiterpenes are involved in plant-pathogen interactions, protection of plants against herbivores, and also attract pollinators and seed-dispersing animals (Dudareva et al., 2013; Vranová et al., 2013). These mono- and sesquiterpenes are characterised by their immense structural diversity which is largely due to terpene synthase (TPS) enzymes which catalyse the formation of diverse terpenes from a small pool of substrates (Degenhardt et al., 2009).

For grapevine and indeed viticulture, specialised terpenes such as, mono- and sesquiterpenes play a particularly important role in both table grape and wine aromas and are largely responsible for the distinctive flavour/aroma profile of specific cultivars. For instance, grape cultivars can be classified based on their berry monoterpene levels into three groups: muscat varieties (up to 6 mg.L⁻¹ of free monoterpenes), non-muscat aromatic varieties (between 1–4 mg.L⁻¹) and neutral varieties (less than 1 mg.L⁻¹) (Mateo and Jiménez, 2000). While the sesquiterpene, rotundone, imparts the typical peppery aroma of Shiraz wine (Mattivi, 2016), and the monoterpene derived wine lactone leads to the sweet woody aroma of Gewürztraminer wines (Guth, 1997). Furthermore, non-volatile mono- and sesquiterpene glucosides can be enzymatically hydrolysed and released as volatiles during wine fermentation, contributing a “hidden” aromatic potential to wine (Dunlevy et al., 2009).

In grapevine, as in other plants, the first step in the biosynthesis of mono- and sesquiterpenes is the formation of prenyldiphosphate precursors, in either the cytosol (sesquiterpenes) or plastid (monoterpenes). The availability of these precursors directly regulates the capacity of the plant to synthesise volatile terpenes thereby influencing the flux of terpene metabolism. The activity of structurally diverse terpene synthases (TPSs) on the prenyldiphosphate precursors results in the diversity of terpenes produced by the plant. Additionally, these terpenes can undergo further secondary modifications, such as glycosylation and oxidation (Nagegowda & Gupta, 2020). While it has been observed that plants typically contain large *TPS* gene families, this is particularly true in grapevine, with reports of between 192–203 *TPS* genes identified in various grapevine genomes (Smit et al., 2020). While this duplication is likely due to the domestication and human selection for flavour and aroma of grapes, the eco-physiological roles of terpenes in *Vitis vinifera* are significant. Specific combinations of terpenes either attract or repel the European grapevine moth, a known grapevine pest (Salvagnin et al., 2018), while volatile terpenes induced during fungal infection and have been found to inhibit fungal growth (Simas et al., 2017; Brilli et al., 2019).

This review provides an overview of grapevine specialised terpene metabolism, focusing on monoterpene and sesquiterpene biosynthesis. The genetic and biochemical contribution of prenyldiphosphate metabolism as a regulatory point for terpene biosynthesis is highlighted, while the contribution of grapevine

terpene synthases to the structural diversity of terpene compounds is discussed. Lastly, an overview of the eco-physiological functions of mono- and sesquiterpenes in grapevine is summarised.

2 Terpene diversity – spatial and temporal variation

Terpene profiles can vary greatly between different grapevine cultivars, as demonstrated in several studies which have characterised the terpene profile of a wide range of cultivars (Díaz-Fernández et al., 2022; D’Onofrio et al., 2017; Ji et al., 2021; Liu S. et al., 2022; Liu X. et al., 2022; Luo et al., 2019; Šikuten et al., 2022; Wu et al., 2016). However direct comparison between these studies is challenging due to differences in the methods used to quantify terpene content. Additionally, several factors influence terpene accumulation such as abiotic and biotic stress (reviewed in Rienth et al., 2021; Lazazzara et al., 2022), genetics (discussed in this review), and spatial and temporal variation (outlined here).

In grapevine, as in other plants, volatile emissions are both spatially and developmentally regulated (Abbas et al., 2017; Dudareva et al., 2013). However, unlike several other plants, grapevine does not accumulate terpenes and other volatiles in specialised organs. Generally, monoterpenes are most abundant in the berry skin, with some monoterpenes being present in the berry pulp (Wu et al., 2016; Lin et al., 2019). Sesquiterpenes are most abundant in grapevine flowers and in early fruit development (Martin et al., 2009; Matarese et al., 2014; Smit et al., 2019). A study by Matarese et al. (2014) analysed the VOCs present in various grapevine organs and found a clear distinction between the terpene profiles present in different organs with roots having the most distinctive volatile profile and grapevine flowers found to have the highest volatile terpene content. These results indicate the specialisation of terpenes in different grapevine organs, which is likely due to evolved ecophysiological roles of specialised terpenes and human selection. In grapevine, the accumulation of terpenes over development has been mostly limited to grape berries and specifically focused on monoterpenes. Generally, monoterpene content is found to increase over the course of berry development (Ji et al., 2021; Liu X. et al., 2022; Luo et al., 2019; Martin et al., 2012). Research on the evolution of sesquiterpenes over development is limited due to their low levels of accumulation in grape berries (Dunlevy et al., 2009; Lin et al., 2019).

3 Biosynthesis of the prenyldiphosphate precursors of terpenes

3.1 Key enzymes of the MVA and MEP pathways

Monoterpenes and sesquiterpenes, like all other terpenes, are derived from the C₅ isoprene precursors isopentenyl diphosphate (IPP) and dimethyl allyl diphosphate (DMAPP) (Tholl, 2015). Plants employ two independent pathways to produce these precursors, namely the mevalonate pathway (MVA) and the methylerythritol phosphate

(MEP) pathway which are compartmentalised into the cytoplasm and plastids, respectively (Figure 1). Compartmentalisation of MVA and MEP intermediates is not strict, and it has been shown that intermediates can be exchanged across the plastidial membrane in a process termed “metabolic crosstalk” (Gutensohn et al., 2013; Schwab and Wüst, 2015). Metabolites which are exchanged between these pathways include IPP itself, as well as the prenyldiphosphate precursors of terpene biosynthesis, geranyl diphosphate (GPP), farnesyl diphosphate (FPP) and geranylgeranyl diphosphate (GGPP) (reviewed in Hemmerlin et al., 2012; Gutensohn et al., 2013; Liao et al., 2016). Table 1 shows enzymes of the MVA and MEP pathway which have been characterised in grapevine.

The first step in the MEP pathway is catalysed by 1-deoxy-D-xylulose-5-phosphate synthase (DXS), an enzyme which plays a major contribution to metabolic flux control in plastidial terpene biosynthesis (Tholl, 2015). Grapevine DXS (*VvDXS1*) has been established as an important contributor to the aroma of Muscat cultivars (Doligez et al., 2006; Battilana et al., 2009). Battilana et al. (2009) reported that *VvDXS1* co-localizes with a major QTL on linkage group 5 which associates with three monoterpenes: linalool, nerol, and geraniol, which are responsible for the distinct floral and citrus aromas of Muscat cultivars. Further studies of *VvDXS1* found a single nucleotide polymorphism (SNP) at position 1822 (G substituting a T) that was hypothesised to be a “gain of function” mutation (Emanuelli et al., 2010). *VvDXS1* genes that were heterozygous (GT) at position 1822 caused a non-synonymous substitution of a lysine (K) with an asparagine (N) at position 284

of the *VvDXS1* protein. Functional characterisation of *VvDXS1* showed that the non-synonymous amino acid substitution influences enzyme kinetics by increasing the catalytic efficiency of *VvDXS1*, thereby increasing the total monoterpene content of cultivars carrying this SNP (Battilana et al., 2011). This was further supported by transgenic tobacco lines overexpressing the K284N SNP allele of *VvDXS1* showing up to 20 times higher levels of glycosylated monoterpenes than lines expressing the neutral allele (Battilana et al., 2011). Additionally, microvine lines overexpressing the neutral and muscat allele of *VvDXS1* had a 1.7- and 4.4-fold increase in total monoterpene content compared to the wild type, respectively (Dalla Costa et al., 2018). The K284N SNP of *VvDXS1* appears to be a reliable marker for muscat-aroma in grapevine cultivars. A recent study looking at the association between *VvDXS1* and aromatic substance content in different flavour types (muscat-like, aromatic and neutral aroma) of grapevine varieties also associated the K284N SNP with increased monoterpene content in grapevine (Yang et al., 2017b).

Dalla Costa et al. (2018) investigated the effect of the K284N SNP on terpene content in 90 grapevine germplasms. Predictably, cultivars that were homozygous (TT) or heterozygous (GT) for the Muscat-allele had a significantly higher level of monoterpenes than cultivars homozygous (GG) for the neutral allele. Interestingly, the authors also reported a similar trend, albeit to a lesser extent, in sesquiterpene content. Furthermore, overexpression of *VvDXS1* in combination with *VvLinNer* (see Table 1), a linalool/nerolidol synthase, led to a significant increase in linalool (a monoterpene) and nerolidol (a

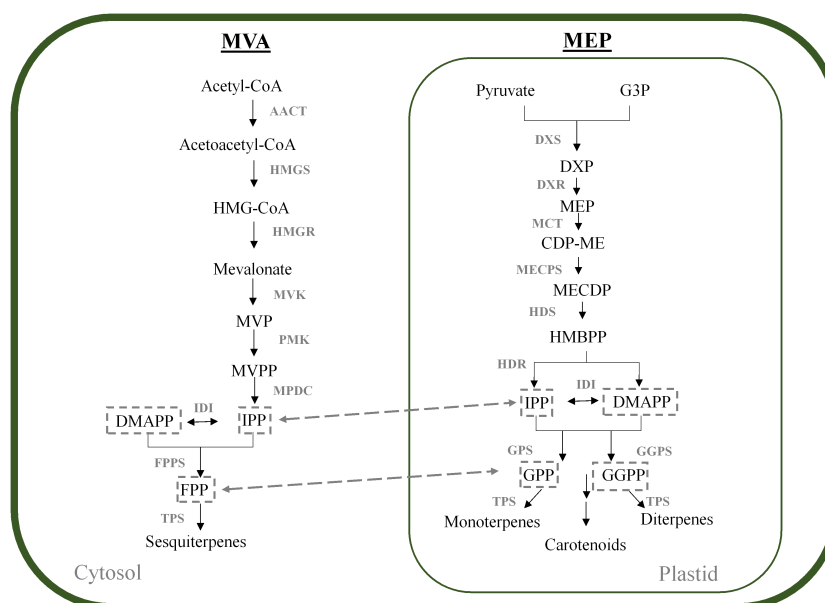


FIGURE 1

MVA and MEP pathways in plants. The MVA and MEP pathways forming the prenyldiphosphate precursor molecules for terpene synthesis are shown in the cytosol and plastid, respectively. Downstream metabolites are indicated. AACT, acetyl-CoA acetyltransferase; CDP-ME, 4-diphosphocytidyl-2-C-methyl-D-erythritol; CDP-MEP, CDPME 2-phosphate; CMK, 4-(cytidine 5'-diphospho)-2-C-methyl-D-erythritol kinase; DMAPP, dimethyl allyl diphosphate; DXP, 1-deoxy-D-xylulose 5-phosphate; DXS, DXP synthase; DXR, 1-deoxy-D-xylulose 5-phosphate reductoisomerase; FPP, farnesyl diphosphate; FPPS, FPP synthase; G3P, glyceraldehyde 3-phosphate; GGPP, geranylgeranyl diphosphate; GGPPS, GGPP synthase; GPP, geranyl diphosphate; GPPS, GPP synthase; HDR, hydroxymethylbutenyl diphosphate reductase; HDS, 4-hydroxy-3-methylbut-2-en-1-yl diphosphate synthase; HMBPP, (E)-4-hydroxy-3-methylbut-2-en-1-yl diphosphate; HMG-CoA, hydroxymethylglutaryl-CoA; HMGR, HMG-CoA reductase; HMGS, HMG-CoA synthase; IDI, isopentenyl pyrophosphate isomerase; IPP, isopentenyl diphosphate; MCT, 2-C-methyl-D-erythritol 4-phosphate cytidyltransferase; MECPD, 2-C-methyl-D-erythritol 2,4-cyclodiphosphate; MECPS, MECPD synthase; MVP, mevalonate kinase; MPDC, mevalonate diphosphate decarboxylase; MVPP, mevalonate 5-phosphate; MVPP, mevalonate 5-pyrophosphate; PMK, phosphomevalonate kinase; TPS, terpene synthase.

TABLE 1 Functionally characterised grapevine genes involved in terpene biosynthesis.

Gene name	Closest PN40024 v3 gene model	Major product(s)	Substrate(s)	Cultivar	Type of characterisation study (eg. <i>in vitro</i> , <i>in planta</i>)	Reference
MVA and MEP pathway enzymes						
VvDXS1	N/A	1-deoxy-D-xylulose 5-phosphate	Pyruvate and glyceraldehyde 3-phosphate	Moscato Bianco	Enzyme assay and heterologous <i>in planta</i> expression	(Battilana et al., 2011)
VvHMG3	N/A	Mevalonate	HMG-CoA	Kyoho	Transient heterologous <i>in planta</i> expression	(Zheng et al., 2020)
TPS-a subfamily						
VvGwECar1	TPS03	(E)-caryophyllene	FPP	Gewürztraminer	<i>In vitro</i> enzyme assay	(Martin et al., 2010)
VvGwECar2	TPS27	(E)-caryophyllene	FPP	Gewürztraminer	<i>In vitro</i> enzyme assay	
VvGwECar3	TPS02	(E)-caryophyllene	FPP	Gewürztraminer	<i>In vitro</i> enzyme assay	
VvPNECar1	TPS02	(E)-caryophyllene	FPP	Pinot Noir	<i>In vivo</i> enzyme assay	
VvPNECar2	TPS13	(E)-caryophyllene	FPP	Pinot Noir	<i>In vivo</i> enzyme assay	
VvGwGerA	TPS03	Germacrene A	FPP	Gewürztraminer	<i>In vitro</i> enzyme assay	
VvGwaBer	TPS10	(E)- α -bergamotene	FPP	Gewürztraminer	<i>In vitro</i> enzyme assay	
VvGwGerD	TPS07	germacrene D	FPP	Gewürztraminer	<i>In vitro</i> enzyme assay	
VvPNGerD	TPS15	germacrene D	FPP	Pinot Noir	<i>In vitro</i> enzyme assay	
VvCSaFar	TPS20	(E,E)- α -Farnesene	FPP	Cabernet Sauvignon	<i>In vitro</i> enzyme assay	
VvGwgCad	TPS08	γ -Cadinene	FPP	Gewürztraminer	<i>In vitro</i> enzyme assay	
VvPNbCur	TPS30	β -curcumene	FPP	Pinot Noir	<i>In vitro</i> enzyme assay	
VvPNSesq	TPS12	sesquithujene	FPP	Pinot Noir	<i>In vivo</i> enzyme assay	
VvPNaZin	TPS14	α -zingiberene	FPP	Pinot Noir	<i>In vivo</i> enzyme assay	
VvPNSelInt	TPS24	selina-4,11-diene	FPP	Pinot Noir	<i>In vivo</i> enzyme assay	
VvPNCuCad	TPS26	Cubebol δ -Cadinene	FPP	Pinot Noir	<i>In vivo</i> enzyme assay	
VvPNaHum	TPS11	α -humulene	FPP	Pinot Noir	<i>In vivo</i> enzyme assay	
VvPNEb2epi Car	TPS21	(E)- β -caryophyllene 2-epi-(E)- β -Caryophyllene	FPP	Pinot Noir	<i>In vivo</i> enzyme assay	
VvGuaS	TPS24	α -guaiane	FPP	Shiraz	Heterologous <i>in planta</i> expression	(Drew et al., 2016)
VvGerD	TPS28	Germacrene D	FPP	Gewürztraminer	<i>In vitro</i> enzyme assay	(Lücker et al., 2004)
VvVal	TPS15	(+)-valencene	FPP	Gewürztraminer	<i>In vitro</i> enzyme assay	
VvSBTPS01	TPS01	α -Selinene		Sauvignon Blanc	<i>In vivo</i> enzyme assay	(Smit et al., 2019)
VvMATPS01	TPS01	α -Selinene		Muscat of Alexandria	<i>In vivo</i> enzyme assay	
VvSBTPS02	TPS02	(E)- β -Caryophyllene		Sauvignon Blanc	<i>In vivo</i> enzyme assay	
VvMATPS10	TPS10	(E)- β -Farnesene		Muscat of Alexandria	<i>In vivo</i> enzyme assay and Heterologous <i>in planta</i> expression	
VvSHTPS27	TPS27	(E)- β -Caryophyllene		Shiraz	<i>In vivo</i> enzyme assay	
VvMATPS27	TPS27				<i>In vivo</i> enzyme assay	

(Continued)

TABLE 1 Continued

Gene name	Closest PN40024 v3 gene model	Major product(s)	Substrate(s)	Cultivar	Type of characterisation study (eg. <i>in vitro</i> , <i>in planta</i>)	Reference
		(<i>E</i>)- β -Caryophyllene		Muscat of Alexandria		
<i>VvShirazTPS07</i>	TPS07	Ylangene Germacrene D		Shiraz	Heterologous <i>in planta</i> expression	(Dueholm et al., 2019)
<i>VvShirazTPS26</i>	TPS26	α -Cubebene α -Copaene δ -Cadinene		Shiraz	Heterologous <i>in planta</i> expression	
<i>VvShirazTPS27</i>	TPS27	Isocaryophyllene		Shiraz	Heterologous <i>in planta</i> expression	
<i>VvShirazTPS-Y1</i>	TPS28	δ -Cadinene		Shiraz	Heterologous <i>in planta</i> expression	
<i>VvShirazTPS-Y2</i>	TPS29	Isocaryophyllene β -cadinene		Shiraz	Heterologous <i>in planta</i> expression	
TPS-b subfamily						
<i>VvTer</i>	TPS39	α -terpineol	GPP	Gewürztraminer	<i>In vitro</i> enzyme assay	(Martin & Bohlmann, 2004)
<i>VvGwaPhe</i>	TPS45	(+)- α -phellandrene	GPP	Gewürztraminer	<i>In vitro</i> enzyme assay	(Martin et al., 2010)
<i>VvPNaPin1</i>	TPS44	(+)- α -pinene	GPP	Pinot Noir		
<i>VvPNaPin2</i>	TPS44	(+)- α -pinene	GPP	Pinot Noir		
<i>VvGwbOci</i>	TPS34	(<i>E</i>)- β -ocimene	GPP	Gewürztraminer		
<i>VvCSbOci</i>	TPS35	(<i>E</i>)- β -ocimene	GPP	Cabernet Sauvignon		
<i>VvCSbOciM</i>	TPS39	(<i>E</i>)- β -Ocimene/ Myrcene	GPP	Cabernet Sauvignon		
<i>VvGwbOciF</i>	TPS46	(<i>E</i>)- β -Ocimene (<i>E,E</i>)- α -Farnesene	GPP FPP	Gewürztraminer		
<i>VvPNRLin</i>	TPS31	(3 <i>R</i>)-Linalool	GPP	Pinot Noir		
TPS-g subfamily						
<i>VvGwGer</i>	TPS52	Geraniol	GPP	Gewürztraminer	<i>In vitro</i> enzyme assay	(Martin et al., 2010)
<i>VvCSGer</i>	TPS51	Geraniol	GPP	Cabernet Sauvignon		
<i>VvPNGer</i>	TPS52	Geraniol	GPP	Pinot Noir		
<i>VvPNLinNer1</i>	TPS59	(3 <i>S</i>)-Linalool (<i>E</i>)- Nerolidol	GPP FPP	Pinot Noir		
<i>VvPNLinNer2</i>	TPS56			Pinot Noir		
<i>VvCSLinNer</i>	TPS56			Cabernet Sauvignon		
<i>VvPNLNGL1</i>	TPS57			Linalool (<i>E</i>)- Nerolidol (<i>E,E</i>)-Geranyl-linalool		
<i>VvPNLNGL2</i>	TPS63	Pinot Noir				
<i>VvPNLNGL3</i>	TPS53	Pinot Noir				
<i>VvPNLNGL4</i>	TPS53	Pinot Noir				
Terpene modifying enzymes						
<i>VvSTO2</i>	N/A	Rotundone	α -guaiene	Syrah	<i>In vitro</i> enzyme assay	(Takase et al., 2016a)

(Continued)

TABLE 1 Continued

Gene name	Closest PN40024 v3 gene model	Major product(s)	Substrate(s)	Cultivar	Type of characterisation study (eg. <i>in vitro</i> , <i>in planta</i>)	Reference
VvCYP76F14	N/A	(E)-8-carboxylinalool	Linalool	Gewurztraminer	<i>In vitro</i> enzyme assay and Transient heterologous <i>in planta</i> expression	(Ilc et al., 2017)
VvGT7	N/A	geranyl and neryl glucoside	geraniol, nerol, and citronellol	Gewurztraminer and White Riesling	<i>In vitro</i> enzyme assay	(Bönisch et al., 2014a)
VvGT14	N/A	geranyl and neryl glucoside	geraniol, nerol, citronellol and linalool	Gewurztraminer and White Riesling	<i>In vitro</i> enzyme assay	(Bönisch et al., 2014b)
VvGT15	N/A	geranyl and neryl glucoside	geraniol, nerol, and citronellol	Gewurztraminer and White Riesling	<i>In vitro</i> enzyme assay	(Bönisch et al., 2014b)

sesquiterpene) content (Wang et al., 2021). The increase in sesquiterpene content associated with *VvDXS1* overexpression may be explained by the phenomenon of “metabolic cross-talk” between the MEP and MVA pathways. The increased flux towards plastid-bound MEP pathway precursors, due to overexpression of *VvDXS1*, potentially leads to an increase in transport of these precursors to the cytosol where they are incorporated in the MVA pathway resulting in an increase in sesquiterpene biosynthesis.

While *VvDXS1* is an effective marker for muscat-aroma, it is not the sole determinant of monoterpene biosynthesis. Emanuelli et al. (2010) found that several cultivars which are characterised as aromatic show no presence of the K284N SNP. Indeed, out of 20 aromatic cultivars, it was reported that 75% are homozygous for the neutral allele (Emanuelli et al., 2010). Therefore, the monoterpene content of aromatic cultivars is likely influenced by enzymes other than *VvDXS1*. Furthermore, three cultivars with muscat-like aroma but no Muscat parentage were also shown to be homozygous for the neutral allele. However, these three cultivars (Gewürztraminer, Chardonnay musqué clone 44-60 Dijon, and Chasselas musqué) each had unique heterozygous SNPs in *VvDXS1* located close to the K284N SNP. Further investigation of these SNPs is necessary to determine whether they are associated with increased monoterpene accumulation in Muscat-like aromatic cultivars.

While apparently predominantly controlled by DXS, the metabolic flux through the MEP pathway in plants is further regulated by other enzymes which include hydroxymethylbutenyl diphosphate reductase, HDR (Vranová et al., 2013). In grapevine, the expression of *VvHDR* has been shown to correlate with the veraison-initiated accumulation of monoterpenes in certain cultivars (Martin et al., 2012; Wen et al., 2015; Costantini et al., 2017; Yue et al., 2020), indicating the potentially regulatory role of *VvHDR* in grapevine monoterpene biosynthesis.

A major contributor to metabolic flux control of the MVA pathway is HMG-CoA reductase (HMGR) (Rodríguez-Concepción, 2006). Three HMGRs have been identified in grapevine, *VvHMGR1-3* (Zheng et al., 2020; Zheng et al., 2021). The three genes are differentially expressed in grapevine organs and during berry development. Interestingly, it was found that *VvHMGR3* plays a role in fruit colour formation. Heterologous suppression of *VvHMGR3* in strawberry increased the rate of colour formation and increased anthocyanin formation and inversely, overexpression of *VvHMGR3* suppressed colour (Zheng et al., 2020). Furthermore, the authors found that brassinosteroids (BRs) (which are produced

via the MVA pathway) inhibit *VvHMGR* expression. A BR-HMGR model is proposed whereby *VvHMGR* expression leads to an increase in BR accumulation and in turn BRs have negative feedback on HMGR activity. Additionally, BRs increases anthocyanin content.

3.2 GGP, FPP and GGPP

The final products of the MEP and MVA pathways, IPP and DMAPP, are fused through consecutive head-to tail condensation reactions, catalysed by short chain prenyltransferases, to form prenyl diphosphates which serve as the precursor backbones for terpenoids (Vranová et al., 2013; Tholl, 2015).

C₁₀ Geranyl diphosphate (GPP) is the precursor for monoterpene biosynthesis and is formed through the activity of GPP synthases (GPPS). Plant GPPSs exist as either hetero- or homodimeric enzymes (Nagegowda & Gupta, 2020). Heterodimeric GPPS consists of a large subunit (LSU) and a catalytically inactive small subunit (SSU-I). GPPS-LSU shares high homology with geranylgeranyl diphosphate synthase (GGPPS) and in some instances has been shown to possess GGPPS activity as a homodimer (Tholl, 2015). GGPP is the precursor molecule to many other primary and specialised terpenes such as carotenoids, abscisic acid, chlorophylls, phytol tocopherols, gibberellins, plastoquinones, polyprenols, and diterpenoids.

To date, very little research has been done on grapevine GPPSs (VvGPPSs). Early reports indicate that VvGPPSs are localised to the plastids, as is the case with plant GPPSs in general (Feron et al., 1990; Soler et al., 1992). More recently, gene expression and transcriptomic studies investigated the expression of *VvGPPS* with respect to terpene accumulation. Transcript abundance levels of the *VvGPPS* gene were shown to parallel the veraison-initiated accumulation of monoterpenes and is potentially contributes to flux control in monoterpene biosynthesis (Martin et al., 2012; Wang et al., 2021). However, these studies do not differentiate between GPPS-LSU and GPPS-SSU. An integrated transcriptomic and metabolomic study of ripening Moscato Bianco berries showed no correlation between *VvGPPS-LSU* and terpene accumulation (Costantini et al., 2017).

C₁₅ farnesyl diphosphate (FPP), produced by FPP synthase (FPPS) is the precursor for sesquiterpenes, triterpenes and primary metabolites such as phytosterols, brassinosteroids, dolichols and ubiquinones (Tholl, 2015). Plant FPPSs are homodimeric enzymes and have been reported to localise to cytosol, mitochondria, or peroxisomes in different plant species (Tholl, 2015). As with

VvGPPSs, the molecular functional characterisation of grapevine FPPSs (VvFPPSs) is limited. The importance of VvFPPS in grapevine sesquiterpene biosynthesis is highlighted in a study analysing the transcription of genes related to the biosynthesis of rotundone, the sesquiterpene responsible for the peppery aroma of Syrah cultivars. This work indicated that VvFPPS potentially plays a vital role in the accumulation level of rotundone in Syrah cultivars by increasing the substrate pool available for rotundone precursor synthesis (Takase et al., 2016a).

3.3 Alternative routes for terpene biosynthesis

Plant GPPSs and FPPSs were generally accepted to be *trans* prenyltransferases, i.e., they synthesise the *trans* (*E*) conformation of GPP and FPP, respectively, however, short-chain *cis* prenyltransferases have been identified in several plants (Akhtar et al., 2013; Demissie et al., 2013). For example, a *cis* FPPS (zFPPS) was demonstrated to produce Z,Z-FPP in the glandular trichomes of tomatoes (Sallaud et al., 2009). zFPPS is localised to the plastids, unlike cytosolic *trans* FPPS, and is therefore theorised to use precursors from the MEP pathway. Furthermore, Z,Z-FPP was shown to be used as a substrate for sesquiterpene synthase. To date, tomato is the only species where *cis* prenyldiphosphates have been reported as terpene synthase (TPS) substrates.

Another non “traditional” route for terpene biosynthesis was shown through the function of isopentenyl phosphate kinases (IPKs). IPK catalyses the conversion of isopentenyl phosphate (IP) and possibly dimethylallyl phosphate (DMAP) to IPP and DMAPP, respectively (Henry et al., 2018). The presence of genes encoding IPKs in all sequenced plant genomes indicate a possible regulatory role for terpene biosynthesis *via* IPK *via* IPP/IP and DMAPP/DMAP ratio modulation (Nagegowda & Gupta, 2020). IP and DMAP was shown to be produced through dephosphorylation of IPP (and DMAPP) by members of the Nudix hydrolase super family (AtNudx1 and AtNudx3) (Henry et al., 2018). Nudix hydrolases in rose has also recently been reported to provide a TPS-independent path for monoterpene production (Magnard et al., 2015). Rose Nudix hydrolase (RhNudx1) catalyses the formation of geranyl monophosphate (GP) from GPP; GP is then further converted to geraniol by an unidentified phosphatase. With regards to grapevine, a nudix hydrolase (VIT_10s0003g00880), whose expression increased along berry development and correlated with linalool content in Moscato Bianco was proposed as a candidate gene for an alternative route of monoterpene production in grapevine (Costantini et al., 2017).

4 Terpene synthases

The major contributor to the diversity of terpenes are terpene synthases (TPSs) which catalyse the formation of terpenes from prenyldiphosphate precursors, e.g. GPP, FPP and GGPP. The ability of TPSs to produce this wide variety is due to various structural features of the enzyme, as well as rapid evolutionary diversification. The following sections explore the contribution of TPSs to grapevine terpene diversity.

4.1 Plant terpene synthase gene family

The plant TPS gene family is mid-sized with TPS genes typically ranging from 30-170 per plant species. The gene family has been divided into seven subfamilies (TPS-a, -b, -c, -d, -e/f, -g and -h) based on their sequence similarity and proposed function (Bohlmann et al., 1998; Chen et al., 2011). The TPS-c and TPS-e/f subfamilies are involved in primary metabolism, encoding copalyl diphosphate synthases (CPSs) and kaurene synthase (KSs) which are involved in gibberellin biosynthesis (Chen et al., 2011). The TPS-d family produce gymnosperm-specific terpene synthases, while TPS-h genes encode putative bifunctional diterpene synthases in the lycophyte *Selaginella moellendorffii* (Chen et al., 2011). TPS-a, b, and g families are angiosperm-specific and produce mono-, sesqui-, and diterpenes involved predominantly in specialised metabolism (Chen et al., 2011). TPS-a subfamily members typically produce sesquiterpenes and diterpenes, while members of the TPS-b and TPS-g subfamilies produce monoterpenes, although the TPSs from the TPS-g subfamily exclusively produce acyclic terpene alcohols. Grapevine TPSs (*VvTPSs*) fall within every subfamily except TPS-d and TPS-h (Martin et al., 2010; Smit et al., 2020). More than half of the specialised *VvTPSs* are sesquiterpene synthases (TPS-a), with the rest making up the TPS-b and -g subfamilies. Several *VvTPSs* from a number of cultivars have been functionally characterised and are summarised in Table 1. Additionally, Figure 2 shows a phylogenetic tree of functionally characterised *VvTPSs*.

The expansion of the TPS gene family within plants is thought to occur primarily through tandem or segmental gene duplication. The highly inbred and homozygous Pinot Noir genome has served as the reference genome (PN40024) for grapevine for the last decade (Jaillon et al., 2007). In a keystone study for grapevine TPSs by (Martin et al., 2010), using the reference genome, the grapevine TPS gene family was functionally annotated which revealed that this gene family is

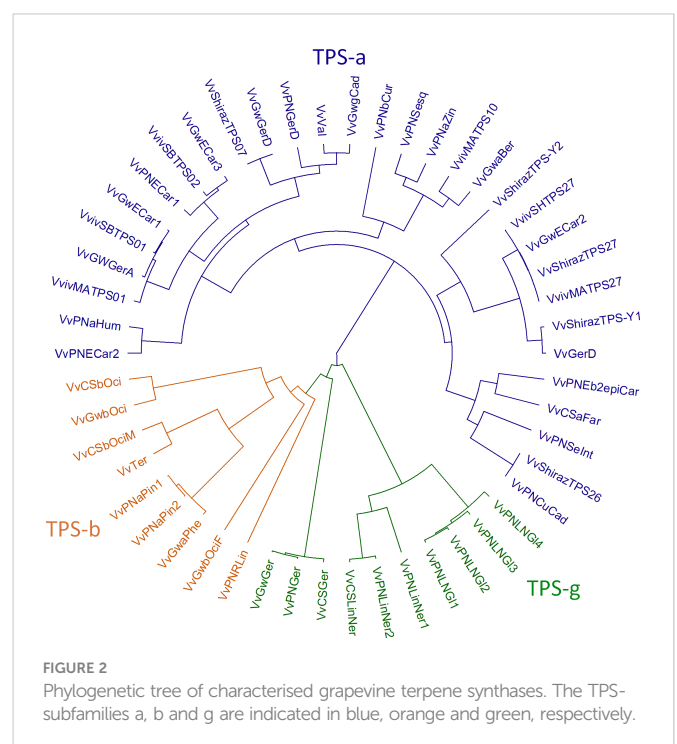


FIGURE 2
Phylogenetic tree of characterised grapevine terpene synthases. The TPS-subfamilies a, b and q are indicated in blue, orange and green, respectively.

substantial with 69 putatively functional TPSs. The increasing number of available genome sequences for different grapevine cultivars shows that due to its homozygosity PN40024 is limiting to our understanding of *VvTPSs*. Indeed, a comparison of the draft diploid genomes of Cabernet Sauvignon, Carménère, and Chardonnay to PN40024 revealed that there is a larger number of *VvTPSs* in these cultivars than the canonically accepted 69 (Smit et al., 2020). Furthermore, the number of *VvTPSs* varies significantly between cultivars, ranging from approximately 80 to 200. Grapevine genomes show extensive duplication events, which led to the expansion of the *VvTPS* family and the fact that 69–90% of *VvTPSs* in grapevine are related to gene duplication events (Jiang et al., 2019; Smit et al., 2020). Additionally, annotation of *VvTPSs* revealed that the majority of sesquiterpene synthases cluster on chromosome 18, while monoterpene synthases cluster on chromosome 13 (Martin et al., 2010; Smit et al., 2020). Another interesting feature of *VvTPSs* revealed by the sequencing of diploid genomes is that approximately 30% of *VvTPSs* are hemizygous, which can play a vital role in understanding the inheritance of these genes for molecular breeding. Taken together, these factors including the large gene family size, cultivar variation, extensive duplication, and hemizygosity of *VvTPSs* goes a long way in explaining the large variation in terpene composition observed in different grapevine cultivars and highlights the immense potential of grapevines to produce novel and diverse terpenes.

Extensive gene duplication of TPSs has also been associated with the variation in plant terpene composition in different organs and at different developmental stages. Duplicated TPS genes serve the same enzymatic function, but often show divergent temporal and spatial expression patterns resulting in tissue or time specific terpene profiles. These sub-functionalisation events have also been demonstrated in grapevine. Expression analysis of gene paralogs of (*E*)- β -caryophyllene synthases, β -ocimene synthases, and linalool synthases showed that all gene paralogs were differentially expressed during Moscato Bianco grape berry development (Matarese et al., 2013). Beyond the grape berry, these gene paralogs were also differentially expressed in different grapevine organs (Matarese et al., 2013; Matarese et al., 2014). Differential gene expression patterns for paralogs of β -ocimene synthases and linalool synthases were also shown in Sauvignon Blanc, Riesling, and Hamburg Muscat berry development (Yue et al., 2020). Moreover, the expression pattern of gene paralogs differed between cultivars, further showcasing the high level of variation of *VvTPSs* and terpene accumulation between grapevine cultivars.

4.2 Terpene synthases: enzyme structure and function

Terpene synthase enzymes can be divided into two classes (type I TPSs or type II TPSs) based on their mechanism of catalysis. Class II TPSs catalyse the ionisation of GGPP *via* protonation. More common are the class I TPSs which contain all mono- and sesquiterpenes. Class I TPSs catalyse the ionisation of the phosphate group on the prenyldiphosphate substrate (GPP, FPP, or GGPP), forming a highly reactive carbocation intermediate which can undergo various reactions such as cyclisations or hydride shifts until the reaction ends

with proton loss or the addition of a nucleophile (Degenhardt et al., 2009).

TPSs have various protein motifs that play an important role in their enzyme function. Class I TPSs contains two aspartate-rich motifs, DDxxD and NSE/DTE in the C-terminal domain which flank the active site. DDxxD and NSE/DTE both bind a trinuclear magnesium cluster which is involved in the positioning of the substrate (Degenhardt et al., 2009). Unlike the DDxxD motif, which is highly conserved through all plant TPSs, the NSE/DTE motif is less conserved with a consensus sequence of (L,V)(V,L,A)-(N,D)D(L,I,V)x(S,T)xxxE (Degenhardt et al., 2009). Upstream of the DDxxD motif is a highly conserved RxR motif which prevents nucleophilic attack on any of the carbocationic intermediates (Degenhardt et al., 2009). An altered RxQ motif appears in sesquiterpene synthases which produce nerolidol, an acyclic terpene. This altered motif may be less effective at preventing nucleophilic attack of the carbocationic intermediate leading to the termination of the enzyme reaction before cyclisation can occur (Durairaj et al., 2019). On the N-terminal end, TPSs contain an RRx₈W motif which has been predicted to play a role in terpene cyclization. Mono- and diterpene synthases contain an N-terminal plastid transit peptide upstream of the RRx₈W motif resulting in their localization to plasmids.

In the grapevine TPS-g subfamily the RRx₈W motif is not well conserved (Martin et al., 2010) which supports the proposed involvement of the RRx₈W motif in cyclisation as TPSs from the TPS-g subfamily primarily produce acyclic monoterpene alcohols. Interestingly, the NSE/DTE motif of the TPS-g subfamily in grapevine has a modified and highly conserved sequence LWDDLx(S,T)xxxE (Martin et al., 2010). The NSE/DTE motif may thus play a role in determining the cyclisation function in grapevine TPSs.

4.3 Substrate and product specificity of TPSs

In the plant kingdom, several multi-substrate TPSs which can use GPP, FPP, and GGPP *in vitro* to produce monoterpenes, sesquiterpenes, and diterpenes respectively, have been identified (reviewed in (Pazouki and Niinemetst, 2016)). Three multi-substrate TPSs have been characterized in grapevine, namely, *VvPNLinNer1*, *VvPNLinNer2*, and *VvCSLinNer*, capable of producing linalool (a monoterpene) and nerolidol (a sesquiterpene) from GPP and FPP, respectively (Table 1) (Martin et al., 2010). Additionally, four TPSs, *VvPNLNG1-4*, also accepted GGPP to produce (*E,E*)-geranyl linalool (Martin et al., 2010). *VvGwbOciF* and *VvCSbOciF* could also accept both GPP and FPP to produce (*E*)- β -ocimene or (*E,E*)- α -farnesene, respectively. Lastly, *VvCSEnerGl* and *VvPNEnerGl* accepted either FPP or GGPP to produce *E*-nerolidol or (*E,E*)-geranyl linalool, respectively (Martin et al., 2010). These enzymes were characterised *in vivo* using metabolically engineered *E. coli*. Subcellular localisation of Riesling *VvLinNer* (*VvRiLinNer*) showed that the enzyme is localized to the chloroplasts and the authors proposed that due to its localisation, *VvRiLinNer* could only produce linalool *in planta* (Zhu et al., 2014). This inference is supported by a previous study that demonstrated grape derived monoterpenes are almost exclusively synthesised *via* the plastid-localised MEP pathway (Luan, 2002), while cytosolic localised sesquiterpenes are produced from both the cytosolic MVA and plastidial MEP pathway intermediates (May et al.,

2013). Contrarily, a recent study reported that *N. benthamiana* leaves transiently overexpressing *VvLinNer* (isolated from the cultivar Shine Muscat) had elevated levels of both linalool and nerolidol, with linalool being predominant (Wang et al., 2021). Seeing as *VvLinNer* is localised to the plastids, this recent finding potentially demonstrates that the substrate pool in plastids may be derived from both the MEP and MVA pathways in grapevine. However, the authors do not state whether the overexpressed *VvLinNer* was efficiently taken up by the plastids therefore it is unclear whether the increased nerolidol is due to FPP production within the plastids or that the heterologously expressed *VvLinNer* may be acting within the cytosol. Studies in other plants have indicated the potential for FPP presence in plastids. For example, targeting of FaNES1, a cytosolically localised linalool/nerolidol synthase from strawberry, to plastids in *Arabidopsis* resulted in an increase in nerolidol abundance, albeit at lower levels than linalool (Aharoni et al., 2004).

Terpene synthases are also able to produce multiple products from a single substrate, a trait that greatly increases terpenoid diversity. Nearly half of the identified mono- and sesquiterpene synthases generate more than one product (Vattekkatte et al., 2018). The ability of TPSs to generate such a wide variety of products is not yet fully understood. One contribution may be the highly reactive carbocationic intermediate that can undergo various reactions to be stabilised. However, single product TPSs do exist, therefore it's likely that a structural feature of the enzyme contributes to its ability to produce multiple products. No common feature has been identified in TPSs that contribute to their ability to produce multiple products; however, several studies suggest that the conformation of the active site influences this ability (reviewed by Degenhardt et al., 2009; Vattekkatte et al., 2018). For example, the ability of γ -humulene from *A. grandis* to produce 52 different sesquiterpenes was associated with the presence of two DDxxD motifs flanking the active site (Steele et al., 1998; Little & Croteau, 2002). Furthermore, through modelling studies it was shown that TPS4 from *Zea mays* can produce multiple products due to two pockets in the active site which control the conformational change of the carbocationic intermediate (Kollner et al., 2004).

It is important to note that several characterisation studies infer the function of the gene through *in vitro* analysis and heterologous gene expression. A recent study by Salvagnin et al. (2016) highlighted the importance of studying TPS function within its native plant. The authors analysed grapevine *E*-(β)-caryophyllene synthase (*VvGwECar2*) under three conditions: *in vitro*, in a heterologous plant system (*Arabidopsis*) and in a homologous plant system (*Vitis vinifera*). While the enzyme still produced *E*-(β)-caryophyllene and α -humulene as its major products in all systems, the ratio of these compounds was different in each system. Furthermore, the composition and abundance of secondary products were different in each system. For instance, in the *Arabidopsis* system thujopsene was also produced, but this was not detected in grapevine.

4.4 Functional plasticity of terpene synthases

Another major contribution to terpene diversity is the functional plasticity of TPS active sites, i.e., a single nucleotide substitution can

lead to a change in the enzyme function. While TPSs share conserved motifs (e.g., DDxxD and NSE/DTE) that are vital to enzyme function, several structure-function studies have demonstrated that small amino acid substitutions can lead to TPSs producing entirely new products.

Various examples of functional plasticity have been reported for grapevine TPSs. Recent studies into the sesquiterpene rotundone revealed genotypic variation in the cultivars that have high levels of this terpene. Rotundone is responsible for the peppery aroma associated with cultivars such as Shiraz, Cagnulari, Schioppettino, Vespolina, Graciano, and Gruene Veltliner (Mattivi, 2016). A novel allele of the *VvTPS24* gene model, *VvGuaS*, a sesquiterpene synthase whose main product is the rotundone precursor α -guaiene, was identified in Shiraz berries (Drew et al., 2016). Previously, *TPS24* was shown to encode for *VvPnSeInt*, which produces selina-4,11-diene as its main product (Martin et al., 2010). Drew et al. (2016) also identified two polymorphisms in the *TPS24* gene of Shiraz which is responsible for two non-synonymous amino acid substitutions in the active site of the enzyme resulting in functional conversion of the enzyme from *VvPnSeInt* to *VvGuaS*. This is an example of how small genetic variations (single nucleotides) in TPS genes can lead to a complete functional change of the enzymes for which they encode, further increasing the diversity of terpene profiles observed across grapevine cultivars. Additionally, an association study between *VvTer*, an α -terpineol synthase gene, and α -terpineol content in the grape berries derived from 61 cultivars identified two SNPs that associated with higher α -terpineol content. However further study is necessary to ascertain the functional effects of these polymorphisms (Yang et al., 2017a). Another example of the cultivar specific nature of grape TPSs is the recently characterised (*E*)- β -farnesene synthase (*VvMATPS10*) from Muscat of Alexandria flowers (Smit et al., 2019). This gene had been previously characterised to code for a bergamotene synthase (*VvGwBer*) in Gewürztraminer (Martin et al., 2010), however when isolated from Muscat of Alexandria it showed a unique sequence and function, producing (*E*)- β -farnesene, as opposed to bergamotene, as a single product. These studies highlight the high functional plasticity of *VvTPSs* and how this plasticity results in the cultivar-specific functions of *VvTPSs*.

5 Secondary modifications of mono- and sesquiterpenes

The carbon scaffold of terpenes produced by terpene synthases can be additionally enzymatically modified, further contributing to the diverse terpene profiles of plants. Most terpene modifications are catalysed by cytochrome P450 monooxygenases (CYPs). Regarding grapevine studies, only two CYPs that are involved in terpene modification have been characterised. The first is *VvSTO2*, which forms the sesquiterpene rotundone by oxygenating its precursor, α -guaiene (Takase et al., 2016b). Secondly, CYP76F14 is a CYP involved in the formation of wine lactone. Wine lactone is a monoterpene which largely contributes to the aroma of Gewürztraminer wines. It is formed during fermentation and aging of wine through a slow, nonenzymatic, acid-catalysed cyclisation from an odourless precursor, (*E*)-8-carboxylinalool. (*E*)-8-carboxylinalool is a grape-derived monoterpene and is synthesised in the berries through the action of CYP76F14 catalysed oxygenation of linalool (Ilc et al., 2017).

Congruently, the authors also show that *CYP76F14* maps to a QTL associated with (E)-8-carboxylinalool content in grape berries. Figure 3 is a phylogenetic analysis comparing functionally characterised CYP genes which act on sesquiterpenes or monoterpenes from other plant species. VvSTO2 (alpha-guaiene oxidase) shows similarity with another CYP which has a bicyclic sesquiterpene substrate from tobacco, 5-epi aristolochene 1,3-hydroxylase. Furthermore, *CYP76F14* ((E)-8-carboxylinalool synthase) clusters closely with geraniol 8-hydroxylases from *C. roseus* and *S. musotii* and linalool and geraniol are both acyclic monoterpene alcohols.

Monoterpenes, and other volatiles, are often present in grapevine as non-volatile glucosides, which are formed through the action of glucosyltransferases. These compounds can either occur as monosaccharides bound to a β -d-glucose moiety or disaccharides with the addition of rhamnose, apiose, or arabinose to the glucose moiety (Hjelmeland & Ebeler, 2015). The formation glucosides are catalysed by glucosyltransferases (GTs). Three GTs, namely VvGT7, VvGT14, and VvGT15, have been functionally characterised in grapevine. All three enzymes accept geraniol, nerol, and citronellol as substrates, with VvGT14 also accepting linalool (Bönisch et al., 2014a; Bönisch et al., 2014b). Additionally, correlation analysis of transcriptomic and metabolic data indicated that UDP-glucosyltransferase 89B2 (LOC100264439) and UDP-glucosyltransferase 83A1 (LOC100248406) potentially contribute to the glycosylation of linalool, hotrienol, α -terpineol, geraniol, and *cis*-rose oxide (Wang et al., 2021).

6 Ecophysiological roles of specialised terpenes

The structural diversity of specialised terpenes allows them to fulfil multiple ecological functions related to plant-environment

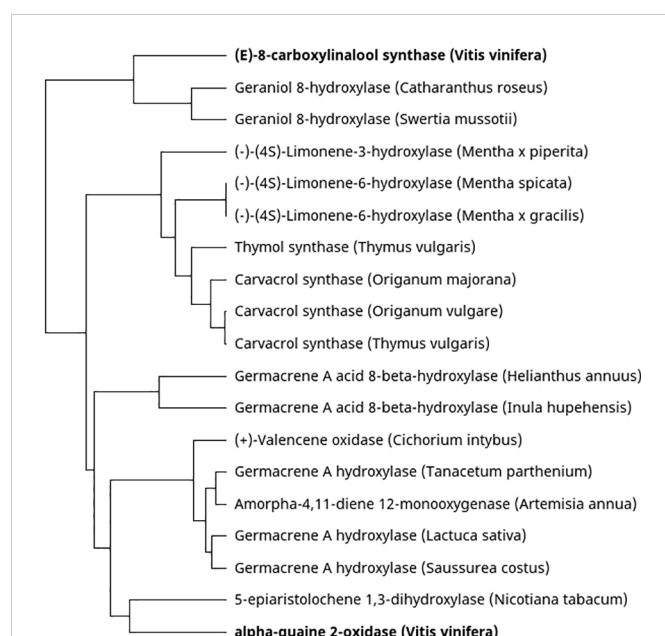


FIGURE 3
Phylogenetic tree of characterised cytochrome P450 monooxygenases which use mono- or sesquiterpenes as a substrate. The characterised *V. vinifera* CYPs are shown in boldface.

interactions. The following section summarises some of the ecophysiological roles of mono- and sesquiterpenes, particularly as they relate to grapevine (Figure 4).

Volatile terpenes attract plant pollinators and seed dispersers (Dudareva et al., 2013). Pollinator attraction has not been associated with an individual compound, but instead a blend of different specialised volatile organic compounds which include terpenes. Furthermore, these compounds may also play a defensive role, protecting the important reproductive organs of the plant against pathogens. Sesquiterpenes are the most abundant specialised terpene in grapevine buds and flowers with sesquiterpene synthase genes showing peak expression in buds and flowers (Matarese et al., 2013; Smit et al., 2019). The precise role of grapevine floral sesquiterpenes in pollinator-attraction or defence is yet to be elucidated. However, domesticated grapevine (*Vitis vinifera*) is hermaphroditic; and self-pollination plays a more dominant role than insect-mediated pollination (Zou et al., 2021). It can therefore be inferred that the role of grapevine flower sesquiterpenes may predominantly be in defence. Alternatively, it is highly likely that human selection for berry and wine aroma is the driving force behind diverse sesquiterpene profiles in domesticated grapevine. This has already been shown for increased monoterpene content associated with *VvDXS1* which underwent a strong selection in Muscats due to human selection during grapevine domestication (Emanuelli et al., 2010).

Individual terpenes or terpene blends that increase its herbivore defence have been identified in different plants (Tholl, 2015; Boncan et al., 2020). The blend and ratio of volatiles emitted as defence is species and herbivore specific. This underlies the role of diverse terpene structure in increasing the overall fitness of individual species for their unique environments. Furthermore, research has shown that some plants release herbivore-induced volatiles which attract the natural predators of herbivores (Tholl, 2015). Regarding grapevine, it has been shown that the European grapevine moth (*Lobesia botrana*) is attracted to a specific blend of (E)- β -caryophyllene, (E)-4,8-dimethyl-1,3,7-nonatriene (DMNT), and (E)- β -farnesene emitted by green grape berries (Tasin et al., 2006). Furthermore, transgenic grapevine lines with modified (E)- β -caryophyllene and (E)- β -farnesene emissions (three times higher or less than half compared to the wild-type) were shown to effectively interrupt the host-finding ability of grapevine moths (Salvagnin et al., 2018). *Lobesia botrana* is a major pest of vineyards and understanding its host-finding mechanism may lead to the development of sustainable pest treatment strategies aimed at interrupting these mechanisms.

Volatile terpenes are also induced during pathogen infection and have been shown to inhibit pathogen growth (Brilli et al., 2019). *Botrytis cinerea*, a necrotrophic fungus which causes bunchrot in grapevine, has been shown to be inhibited by the monoterpene limonene (Simas et al., 2017). α -pinene, β -pinene, citral, and γ -terpinene were also shown to inhibit *B. cinerea* albeit to a lesser extent. Another major grapevine pathogen, *Plasmopara viticola*, responsible for grapevine downy mildew, could also be inhibited by certain specialised terpenes (Ricciardi et al., 2021). *In vitro* analysis of antifungal activity demonstrated that farnesene, ocimene, nerolidol, and valencene are able to reduce disease severity. The sesquiterpene nerolidol also showed antifungal activity in grapevine, inhibiting the growth of *Phaeoacremonium parasiticum* (Escoriaza et al., 2019).

Plant roots show similar defence responses to the aboveground plant organs. Grapevine roots have been shown to have a distinctive

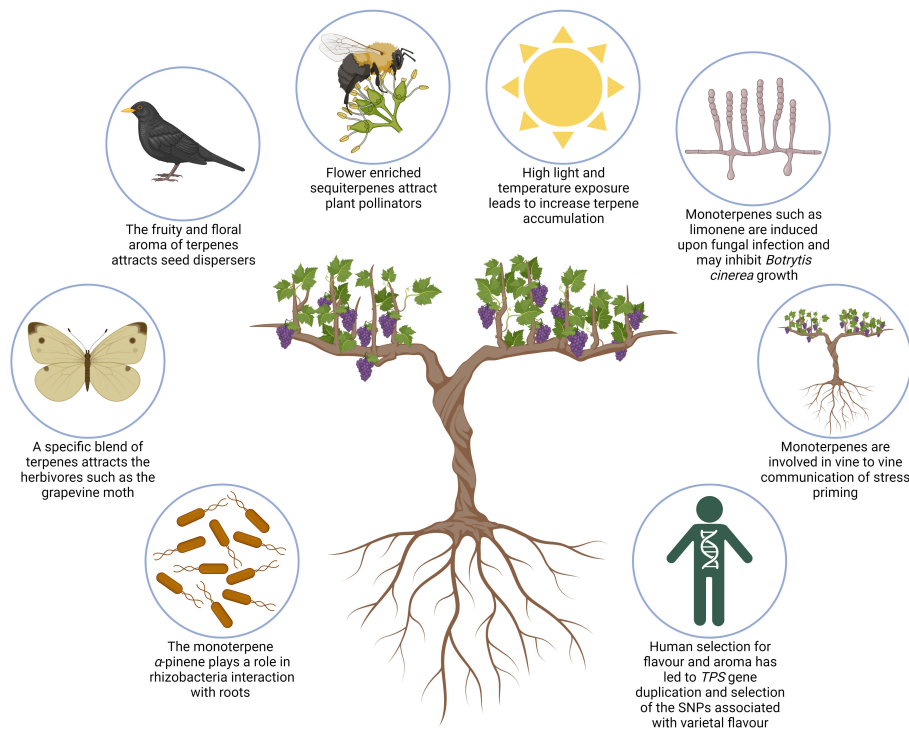


FIGURE 4

Schematic illustrating ecophysiological roles of mono- and sesquiterpenes in Grapevine. Clockwise, from bottom left, images illustrate the following: monoterpenes have been shown to play a unique function in grapevine roots and their interaction with mutualistic rhizobacteria; the European grapevine moth pest is attracted by a mix of VOCs containing sesquiterpenes; a blend of terpenes is involved in attraction of agents of seed dispersal; sesquiterpenes are the most abundant specialised terpene in grapevine buds and flowers and are involved in attraction of pollinators; light exposure, high temperatures, and UV-B radiation can all increase terpene accumulation in grape berries; several monoterpenes have been found to inhibit fungal growth of *Botrytis cinerea* and *Plasmopara viticola*; monoterpenes such as α -pinene are suggested to play a role in vine-to-vine communication and priming of stress; human selection of cultivars has led to gene duplication of *TPS*s and the selection of SNPs associated with varietal flavour.

volatile profile when compared with other grapevine vegetative organs in Moscato bianco (Matarese et al., 2014). Myrtenol, borneol, and pinocarveol were more abundant in roots than other organs and are thought to be derived from α -pinene. Furthermore, expression analysis indicated that α -pinene synthase, *VvPNaPin1*, was expressed highest in roots and flower buds. Additionally, α -pinene content increased in grapevine tissues that were inoculated with plant growth promoting rhizobacteria (PGPR), which was isolated from grapevine roots (Salomon et al., 2014; Salomon et al., 2016). These findings may indicate a unique function for α -pinene in grapevine roots and their interaction with mutualistic rhizobacteria.

Additionally, it was previously found that grapevine was able to take up monoterpenes emitted from other plants, such as 1,8-cineole emitted by eucalyptus (*Eucalyptus globulus*) trees (Capone et al., 2012; Pardo-Garcia et al., 2015). This may form part of a plant-to-plant communication systems observed in several species (Rosenkranz et al., 2021). Recent results suggest such communication may occur within and between grapevine plants experience abiotic stress (Midzi et al., 2021). Vines exposed to drought stress appear to be able to prime neighbouring vines through the emission of VOCs such as the monoterpene α -pinene.

Agronomic practices such as leaf removal, training systems and irrigation have traditionally been used to modulate terpene and other volatiles in grapevine to improve the final aroma of the grape berries or wine (Alem et al., 2019). These practices alter the climate around the grapevine and the effect of abiotic factors such as sunlight, water deficit

and UV radiation on VOC accumulation, and by extension terpene accumulation, in grapevine has been studied extensively. Furthermore, the influence of climate change on agriculture has also necessitated the understanding of the effect of changing environmental conditions on grapevine quality (Rienth et al., 2021). Lazazzara et al. (2022) provides a comprehensive review of grapevine biogenic VOCs and how they are influenced by various biotic and abiotic factors. Generally, these studies show that light exposure, high temperatures, UV-B radiation and moderate water deficit can all increase terpene accumulation in grape berries indicating that these compounds play a role in the abiotic stress response of plants. In addition to acting as signalling molecules, terpenes, particularly isoprene, are thought to play a role in ROS modulation and membrane stabilisation, however the mechanism of these roles are still poorly understood (Lazazzara et al., 2022).

6 Conclusion and future prospects

Grapevine genomic research has made significant contributions to our understanding of specialised terpene metabolism and several key enzymes involved in grapevine monoterpene and sesquiterpene biosynthesis have been identified. The increasing availability of grapevine cultivar genomes have displayed the variation of the *VvTPS* gene family between cultivars and gives insight into *VvTPS* evolution and gene expansion. Furthermore, these studies highlight the limitations of the reference genome with regards to specialised terpene research, as it does not display the cultivar-specific

variation of the grapevine TPS family. The availability of more grapevine cultivar genomes and the use of a multi-omics approach may in future provide a more efficient means of identifying and characterising novel *VvTPSs*. Moreover, increased knowledge of grapevine terpene metabolism is agriculturally significant as it can lead to the development of grapevine crops with improved or altered flavour and aroma profiles, while potentially increasing disease resistance.

Author contributions

RB and JL conceptualised the review and cowrote the manuscript. All authors contributed to the article and approved the submitted version.

Funding

This work is based on the research supported by grants from the South African Table Grape Industry (SATI), Winetech and The

National Research Foundation of South Africa. Grant numbers: S005411, S006681 and 129344, respectively.

Conflict of interest

The authors declare that the research was conducted in the absence of any commercial or financial relationships that could be construed as a potential conflict of interest.

Publisher's note

All claims expressed in this article are solely those of the authors and do not necessarily represent those of their affiliated organizations, or those of the publisher, the editors and the reviewers. Any product that may be evaluated in this article, or claim that may be made by its manufacturer, is not guaranteed or endorsed by the publisher.

References

- Abbas, F., Ke, Y., Yu, R., Yue, Y., Amanullah, S., Jahangir, M. M., et al. (2017). Volatile terpenoids: multiple functions, biosynthesis, modulation and manipulation by genetic engineering. *Planta* 246 (5), 803–816. doi: 10.1007/s00425-017-2749-x
- Aharoni, A., Giri, A. P., Verstappen, F. W. A., Bertea, C. M., Sevenier, R., Sun, Z., et al. (2004). Gain and loss of fruit flavor compounds produced by wild and cultivated strawberry species. *Plant Cell* 16 (11), 3110–3131. doi: 10.1105/tpc.104.023895
- Akhtar, T. A., Matsuba, Y., Schavuinhold, I., Yu, G., Lees, H. A., Klein, S. E., et al. (2013). The tomato cis-prenyltransferase gene family. *Plant J.* 73 (4), 640–652. doi: 10.1111/tj.12063
- Alem, H., Rigou, P., Schneider, R., Ojeda, H., and Torregrosa, L. (2019). Impact of agronomic practices on grape aroma composition: A review. *J. Sci. Food Agric.* 99 (3), 975–985. doi: 10.1002/jsfa.9327
- Battilana, J., Costantini, L., Emanuelli, F., Sevini, F., Segala, C., Moser, S., et al. (2009). The 1-deoxy-d-xylulose 5-phosphate synthase gene co-localizes with a major QTL affecting monoterpene content in grapevine. *Theor. Appl. Genet.* 118 (4), 653–669. doi: 10.1007/s00122-008-0927-8
- Battilana, J., Emanuelli, F., Gambino, G., Griboaud, I., Gasperi, F., Boss, P. K., et al. (2011). Functional effect of grapevine 1-deoxy-D-xylulose 5-phosphate synthase substitution K284N on Muscat flavour formation. *J. Exp. Bot.* 62 (15), 5497–5508. doi: 10.1093/jxb/err231
- Bohlmann, J., Meyer-Gauen, G., and Croteau, R. (1998). Plant terpenoid synthases: Molecular biology and phylogenetic analysis. *Proc. Natl. Acad. Sci. United States America* 95 (8), 4126–4133. doi: 10.1073/pnas.95.8.4126
- Boncan, D. A. T., Tsang, S. S. K., Li, C., Lee, I. H. T., Lam, H. M., Chan, T. F., et al. (2020). Terpenes and terpenoids in plants: Interactions with environment and insects. *Int. J. Mol. Sci.* 21 (19), 1–19. doi: 10.3390/ijms21197382
- Bönisch, F., Frotscher, J., Stanitzek, S., Rühl, E., Wüst, M., Bitz, O., et al. (2014a). A UDP-glucose: Monoterpenol glucosyltransferase adds to the chemical diversity of the grapevine metabolome. *Plant Physiol.* 165 (2), 561–581. doi: 10.1104/pp.113.232470
- Bönisch, F., Frotscher, J., Stanitzek, S., Rühl, E., Wüst, M., Bitz, O., et al. (2014b). Activity-based profiling of a physiologic aglycone library reveals sugar acceptor promiscuity of family 1 UDP-glucosyltransferases from grape. *Plant Physiol.* 166 (1), 23–39. doi: 10.1104/pp.114.242578
- Brilli, F., Loreto, F., and Baccelli, I. (2019). Exploiting plant volatile organic compounds (VOCs) in agriculture to improve sustainable defense strategies and productivity of crops. *Front. Plant Sci.* 10 (March). doi: 10.3389/fpls.2019.00264
- Capone, D. L., Jeffery, D. W., and Sefton, M. A. (2012). Vineyard and fermentation studies to elucidate the origin of 1,8-cineole in Australian red wine. *J. Agric. Food Chem.* 60 (9), 2281–2287. doi: 10.1021/jf204499h
- Chen, F., Tholl, D., Bohlmann, J., and Pichersky, E. (2011). The family of terpene synthases in plants: A mid-size family of genes for specialized metabolism that is highly diversified throughout the kingdom. *Plant J.* 66 (1), 212–229. doi: 10.1111/j.1365-3113.2011.04520.x
- Christianson, D. W. (2017). Structural and chemical biology of terpenoid cyclases. *Chem. Rev.* 117 (17), 11570–11648. doi: 10.1021/acs.chemrev.7b00287
- Costantini, L., Kappel, C. D., Trenti, M., Battilana, J., Emanuelli, F., Sordo, M., et al. (2017). Drawing links from transcriptome to metabolites: The evolution of aroma in the ripening berry of moscato bianco (*Vitis vinifera* L.). *Front. Plant Sci.* 8 (May). doi: 10.3389/fpls.2017.00780
- Dalla Costa, L., Emanuelli, F., Trenti, M., Moreno-Sanz, P., Lorenzi, S., Coller, E., et al. (2018). Induction of terpene biosynthesis in berries of microvine transformed with *VvDXS1* alleles. *Front. Plant Sci.* 8 (January). doi: 10.3389/fpls.2017.02244
- Degenhardt, J., Köllner, T. G., and Gershenzon, J. (2009). Monoterpene and sesquiterpene synthases and the origin of terpene skeletal diversity in plants. *Phytochemistry* 70 (15–16), 1621–1637. doi: 10.1016/j.phytochem.2009.07.030
- Demissie, Z. A., Erland, L. A. E., Rheault, M. R., and Mahmoud, S. S. (2013). The biosynthetic origin of irregular monoterpenes in lavender. *J. Biol. Chem.* 288 (9), 6333–6341. doi: 10.1074/jbc.M112.431171
- Díaz-Fernández, Á., Díaz-Losada, E., and Cortés-Diéguez, S. (2022). Diversity among traditional minority red grape varieties according to their aromatic profile. *Agronomy* 12 (8), 1799. doi: 10.3390/agronomy12081799
- Doligez, A., Audiot, E., Baumes, R., and This, P. (2006). QTLs for muscat flavor and monoterpene odorant content in grapevine (*Vitis vinifera* L.). *Mol. Breed.* 18 (2), 109–125. doi: 10.1007/s11032-006-9016-3
- D'Onofrio, C., Matarese, F., and Cuzzola, A. (2017). Study of the terpene profile at harvest and during berry development of *Vitis vinifera* L. aromatic varieties aleatico, brachetto, malvasia di candia aromatica and moscato bianco. *J. Sci. Food Agric.* 97 (9), 2898–2907. doi: 10.1002/jsfa.8126
- Drew, D. P., Andersen, T. B., Sweetman, C., Möller, B. L., Ford, C., and Simonsen, H. T. (2016). Two key polymorphisms in a newly discovered allele of the *vitis vinifera* TPS24 gene are responsible for the production of the rotundone precursor α -guaiene. *J. Exp. Bot.* 67 (3), 799–808. doi: 10.1093/jxb/erv491
- Dudareva, N., Klempien, A., Muhlemann, J. K., and Kaplan, I. (2013). Biosynthesis, function and metabolic engineering of plant volatile organic compounds. *New Phytol.* 198 (1), 16–32. doi: 10.1111/nph.12145
- Dunlevy, J. D., Kalua, C. M., Keyzers, R. A., and Boss, P. K. (2009). *Grapevine molecular physiology and biotechnology: Second edition. 2nd ed.* Ed. K. A. Roubelakis-Angelakis (Netherlands: Springer). doi: 10.1007/978-90-481-2305-6
- Durairaj, J., Di Girolamo, A., Bouwmeester, H. J., de Ridder, D., Beekwilder, J., and van Dijk, A. D. (2019). An analysis of characterized plant sesquiterpene synthases. *Phytochemistry* 158 (June 2018), 157–165. doi: 10.1016/j.phytochem.2018.10.020
- Emanuelli, F., Battilana, J., Costantini, L., le Cunff, L., Boursiquot, J.-M. M., This, P., et al. (2010). A candidate gene association study on muscat flavor in grapevine (*Vitis vinifera* L.). *BMC Plant Biol.* 10 (1), 1–17. doi: 10.1186/1471-2229-10-241
- Escoriaza, G., García Lampasona, S., Gomez Talquenca, S., and Piccoli, P. (2019). *In vitro* plants of *vitis vinifera* respond to infection with the fungus *phaeoacremonium parasiticum* by synthesizing the phytoalexin nerolidol. *Plant Cell Tissue Organ Cult (PCTOC)* 138 (3), 459–466. doi: 10.1007/s11240-019-01641-3
- Feron, G., Clastre, M., and Ambid, C. (1990). Prenyltransferase compartmentation in cells of *vitis vinifera* cultivated *in vitro*. *FEBS Lett.* 271 (1–2), 236–238. doi: 10.1016/0014-5793(90)80414-E
- Gutensohn, M., Nagegowda, D. A., Dudareva, N., Bach, T. J., and Rohmer, M. (2013). Isoprenoid Synthesis in Plants and Microorganisms. In T. J. Bach and M. Rohmer Eds.

Isoprenoid Synthesis in Plants and Microorganisms: New Concepts and Experimental Approaches. New York: Springer. doi: 10.1007/978-1-4614-4063-5

Guth, H. (1997). Quantitation and sensory studies of character impact odorants of different white wine varieties. *J. Agric. Food Chem.* 45 (8), 3027–3032. doi: 10.1021/jf970280a

Hemmerlin, A., Harwood, J. L., and Bach, T. J. (2012). A raison d'être for two distinct pathways in the early steps of plant isoprenoid biosynthesis? *Prog. Lipid Res.* 51 (2), 95–148. doi: 10.1016/j.plipres.2011.12.001

Henry, L. K., Thomas, S. T., Widhalm, J. R., Lynch, J. H., Davis, T. C., Kessler, S. A., et al. (2018). Contribution of isopentenyl phosphate to plant terpenoid metabolism. *Nat. Plants* 4 (9), 721–729. doi: 10.1038/s41477-018-0220-z

Hjelmeland, A. K., and Ebeler, S. E. (2015). Glycosidically bound volatile aroma compounds in grapes and wine: A review. *Am. J. Enol Viticult* 66 (1), 1–11. doi: 10.5344/ajev.2014.14104

Ilc, T., Halter, D., Miesch, L., Lauvoisard, F., Kriegshauser, L., Ilg, A., et al. (2017). A grapevine cytochrome P450 generates the precursor of wine lactone, a key odorant in wine. *New Phytol.* 213 (1), 264–274. doi: 10.1111/nph.14139

Jaillon, O., Aury, J. M., Noel, B., Policriti, A., Clepet, C., Casagrande, A., et al. (2007). The grapevine genome sequence suggests ancestral hexaploidization in major angiosperm phyla. *Nature* 449 (7161), 463–467. doi: 10.1038/nature06148

Ji, X., Wang, B., Wang, X., Wang, X., Liu, F., and Wang, H. (2021). Differences of aroma development and metabolic pathway gene expression between kyoho and 87-1 grapes. *J. Integr. Agric.* 20 (6), 1525–1539. doi: 10.1016/S2095-3119(20)63481-5

Jiang, S.-Y., Jin, J., Sarojam, R., and Ramachandran, S. (2019). A comprehensive survey on the terpene synthase gene family provides new insight into its evolutionary patterns. *Genome Biol. Evol.* 11 (8), 2078–2098. doi: 10.1093/gbe/evz142

Kollner, T. G., Schnee, C., Gershenzon, J., and Degenhardt, J. (2004). The variability of sesquiterpenes emitted from two zea mays cultivars is controlled by allelic variation of two terpene synthase genes encoding stereoselective multiple product enzymes. *Plant Cell* 16 (May), 1115–1131. doi: 10.1105/tpc.019877.tive

Lazazzara, V., Avesani, S., Robatscher, P., Oberhuber, M., Pertot, I., Schuhmacher, R., et al. (2022). Biogenic volatile organic compounds in the grapevine response to pathogens, beneficial microorganisms, resistance inducers, and abiotic factors. *J. Exp. Bot.* 73 (2), 529–554. doi: 10.1093/jxb/erab367

Liao, P., Hemmerlin, A., Bach, T. J., and Chye, M.-L. (2016). The potential of the mevalonate pathway for enhanced isoprenoid production. *Biotechnol. Adv.* 34 (5), 697–713. doi: 10.1016/j.biotechadv.2016.03.005

Lin, J., Massonnet, M., and Cantu, D. (2019). The genetic basis of grape and wine aroma. *Horticulture Res.* 6 (1), 81. doi: 10.1038/s41438-019-0163-1

Little, D. B., and Croteau, R. B. (2002). Alteration of product formation by directed mutagenesis and truncation of the multiple-product sesquiterpene synthases δ -selenene synthase and γ -humulene synthase. *Arch. Biochem. Biophys.* 402 (1), 120–135. doi: 10.1016/S0003-9861(02)00068-1

Liu, X., Fan, P., Jiang, J., Gao, Y., Liu, C., Li, S., et al. (2022). Evolution of volatile compounds composition during grape berry development at the germplasm level. *Scientia Hort.* 293, 110669. doi: 10.1016/j.scienta.2021.110669

Liu, S., Shan, B., Zhou, X., Gao, W., Liu, Y., Zhu, B., et al. (2022). Transcriptome and metabolomics integrated analysis reveals terpene synthesis genes controlling linalool synthesis in grape berries. *J. Agric. Food Chem.* 70 (29), 9084–9094. doi: 10.1021/acs.jafc.2c00368

Luan, F. (2002). Differential incorporation of 1-deoxy- γ -xylulose into (3S)-linalool and geraniol in grape berry exocarp and mesocarp. *Phytochemistry* 60 (5), 451–459. doi: 10.1016/S0031-9422(02)00147-4

Lücker, J., Bowen, P., and Bohlmann, J. (2004). Vitis vinifera terpenoid cyclases: functional identification of two sesquiterpene synthase cDNAs encoding (+)-valencene synthase and (–)-germacrene d synthase and expression of mono- and sesquiterpene synthases in grapevine flowers and berries. *Phytochemistry* 65 (19), 2649–2659. doi: 10.1016/j.phytochem.2004.08.017

Luo, J., Brothie, J., Pang, M., Marriott, P. J., Howell, K., and Zhang, P. (2019). Free terpene evolution during the berry maturation of five vitis vinifera l. cultivars. *Food Chem.* 299, 125101. doi: 10.1016/j.foodchem.2019.125101

Magnard, J.-L., Rocca, A., Caissard, J.-C., Vergne, P., Sun, P., Hecquet, R., et al. (2015). Biosynthesis of monoterpene scent compounds in roses. *Science* 349 (6243), 81–83. doi: 10.1126/science.aab0696

Martin, D. M., Aubourg, S., Schouwey, M. B., Daviet, L., Schalk, M., Toub, O., et al. (2010). Functional annotation, genome organization and phylogeny of the grapevine (*Vitis vinifera*) terpene synthase gene family based on genome assembly, FLcDNA cloning, and enzyme assays. *BMC Plant Biol.* 10 (1), 226. doi: 10.1186/1471-2229-10-226

Martin, D. M., and Bohlmann, J. (2004). Identification of vitis vinifera (–)- α -terpineol synthase by in silico screening of full-length cDNA ESTs and functional characterization of recombinant terpene synthase. *Phytochemistry* 65 (9), 1223–1229. doi: 10.1016/j.phytochem.2004.03.018

Martin, D. M., Chiang, A., Lund, S. T., and Bohlmann, J. (2012). Biosynthesis of wine aroma: Transcript profiles of hydroxymethylbutenyl diphosphate reductase, geranyl diphosphate synthase, and linalool/nerolidol synthase parallel monoterpene glycoside accumulation in gewürztraminer grapes. *Planta* 236 (3), 919–929. doi: 10.1007/s00425-012-1704-0

Martin, D. M., Toub, O., Chiang, A., Lo, B. C., Ohse, S., Lund, S. T., et al. (2009). The bouquet of grapevine (*Vitis vinifera* l. cv. cabernet sauvignon) flowers arises from the

biosynthesis of sesquiterpene volatiles in pollen grains. *Proc. Natl. Acad. Sci.* 106 (17), 7245–7250. doi: 10.1073/pnas.0901387106

Matarese, F., Cuzzola, A., Scalabrelli, G., and D'Onofrio, C. (2014). Expression of terpene synthase genes associated with the formation of volatiles in different organs of vitis vinifera. *Phytochemistry* 105, 12–24. doi: 10.1016/j.phytochem.2014.06.007

Matarese, F., Scalabrelli, G., and D'Onofrio, C. (2013). Analysis of the expression of terpene synthase genes in relation to aroma content in two aromatic vitis vinifera varieties. *Funct. Plant Biol.* 40 (6), 552–565. doi: 10.1071/FP12326

Mateo, J. J., and Jiménez, M. (2000). Monoterpenes in grape juice and wines. *J. Chromatogr. A* 881 (1–2), 557–567. doi: 10.1016/S0021-9673(99)01342-4

Mattivi, F. (2016). Key enzymes behind black pepper aroma in wines. *J. Exp. Bot.* 67 (3), 555–557. doi: 10.1093/jxb/erw008

May, B., Lange, B. M., and Wüst, M. (2013). Biosynthesis of sesquiterpenes in grape berry exocarp of vitis vinifera l.: Evidence for a transport of farnesyl diphosphate precursors from plastids to the cytosol. *Phytochemistry* 95, 135–144. doi: 10.1016/j.phytochem.2013.07.021

Midzi, J., Baumanna, U., Jeffery, D., Rogiers, S., Tyerman, S., and Pagaya, V. (2021). “Abiotic stress-induced inter-vine signalling via plant volatiles,” in *11th International Symposium on Grapevine Physiology and Biotechnology*. Stellenbosch, South Africa: International Society for Horticultural Science.

Nagegowda, D. A., and Gupta, P. (2020). Advances in biosynthesis, regulation, and metabolic engineering of plant specialized terpenoids. *Plant Sci.* 294 (February), 110457. doi: 10.1016/j.plantsci.2020.110457

Pardo-García, A. I., Wilkinson, K. L., Culbert, J. A., Lloyd, N. D. R., Alonso, G. L., and Salinas, M. R. (2015). Accumulation of glycoconjugates of 3-Methyl-4-hydroxyoctanoic acid in fruits, leaves, and shoots of vitis vinifera cv. monastrell following foliar applications of oak extract or oak lactone. *J. Agric. Food Chem.* 63 (18), 4533–4538. doi: 10.1021/acs.jafc.5b01043

Pazouki, L., and Niinemetst, U. (2016). Multi-substrate terpene synthases: Their occurrence and physiological significance. *Front. Plant Sci.* 7 (JULY2016). doi: 10.3389/fpls.2016.01019

Ricciardi, V., Marciánò, D., Sargolzaei, M., Maddalena, G., Maghradze, D., Tirelli, A., et al. (2021). From plant resistance response to the discovery of antimicrobial compounds: The role of volatile organic compounds (VOCs) in grapevine downy mildew infection. *Plant Physiol. Biochem.* 160 (January), 294–305. doi: 10.1016/j.plaphy.2021.01.035

Rienth, M., Vigneron, N., Darriet, P., Sweetman, C., Burbidge, C., Bonghi, C., et al. (2021). Grape berry secondary metabolites and their modulation by abiotic factors in a climate change scenario—a review. *Front. Plant Sci.* 12. doi: 10.3389/fpls.2021.643258

Rodríguez-Concepción, M. (2006). Early steps in isoprenoid biosynthesis: Multilevel regulation of the supply of common precursors in plant cells. *Phytochem. Rev.* 5 (1), 1–15. doi: 10.1007/s11101-005-3130-4

Rosenkranz, M., Chen, Y., Zhu, P., and Vlot, A. C. (2021). Volatile terpenes – mediators of plant-to-plant communication. *Plant J.* 108 (3), 617–631. doi: 10.1111/tpj.15453

Sallaud, C., Rontein, D., Onillon, S., Jabès, F., Duffé, P., Giacalone, C., et al. (2009). A novel pathway for sesquiterpene biosynthesis from Z,Z'-farnesyl pyrophosphate in the wild tomato solanum habrochaites. *Plant Cell* 21 (1), 301–317. doi: 10.1105/tpc.107.057885

Salomon, M. V., Bottini, R., de Souza Filho, G. A., Cohen, A. C., Moreno, D., Gil, M., et al. (2014). Bacteria isolated from roots and rhizosphere of vitis vinifera retard water losses, induce abscisic acid accumulation and synthesis of defense-related terpenes in *in vitro* cultured grapevine. *Physiol. Plantarum* 151 (4), 359–374. doi: 10.1111/ppl.12117

Salomon, M. V., Purpora, R., Bottini, R., and Piccoli, P. (2016). Rhizosphere associated bacteria trigger accumulation of terpenes in leaves of vitis vinifera l. cv. Malbec that protect cells against reactive oxygen species. *Plant Physiol. Biochem.* 106, 295–304. doi: 10.1016/j.plaphy.2016.05.007

Salvagnin, U., Carlini, S., Angeli, S., Vrhovsek, U., Anfora, G., Malnoy, M., et al. (2016). Homologous and heterologous expression of grapevine e-(β)-caryophyllene synthase (VvGwECar2). *Phytochemistry* 131, 76–83. doi: 10.1016/j.phytochem.2016.08.002

Salvagnin, U., Malnoy, M., Thöming, G., Tasin, M., Carlini, S., Martens, S., et al. (2018). Adjusting the scent ratio: Using genetically modified vitis vinifera plants to manipulate European grapevine moth behaviour. *Plant Biotechnol. J.* 16 (1), 264–271. doi: 10.1111/pbi.12767

Schwab, W., and Wüst, M. (2015). Understanding the constitutive and induced biosynthesis of mono- and sesquiterpenes in grapes (*Vitis vinifera*): A key to unlocking the biochemical secrets of unique grape aroma profiles. *J. Agric. Food Chem.* 63 (49), 10591–10603. doi: 10.1021/acs.jafc.5b04398

Šikuten, I., Štambuk, P., Tomaz, I., Marchal, C., Kontić, J. K., Lacombe, T., et al. (2022). Discrimination of genetic and geographical groups of grape varieties (*Vitis vinifera* l.) based on their volatile organic compounds. *Front. Plant Sci.* 13. doi: 10.3389/fpls.2022.942148

Simas, D. L. R., de Amorim, S. H. B. M., Goulart, F. R. V., Alviano, C. S., Alviano, D. S., and da Silva, A. J. R. (2017). Citrus species essential oils and their components can inhibit or stimulate fungal growth in fruit. *Ind. Crops Prod* 98, 108–115. doi: 10.1016/j.indcrop.2017.01.026

Smit, S. J., Vivier, M. A., and Young, P. R. (2019). Linking terpene synthases to sesquiterpene metabolism in grapevine flowers. *Front. Plant Sci.* 10 (February). doi: 10.3389/fpls.2019.00177

Smit, S. J., Vivier, M. A., and Young, P. R. (2020). Comparative (Within species) genomics of the vitis vinifera l. terpene synthase family to explore the impact of genotypic

variation using phased diploid genomes. *Front. Genet.* 11 (May). doi: 10.3389/fgene.2020.00421

Soler, E., Feron, G., Clastre, M., Dargent, R., Gleizes, M., and Ambid, C. (1992). Evidence for a geranyl-diphosphate synthase located within the plastids of *Vitis vinifera* L. cultivated *in vitro*. *Planta* 187 (2), 171–175. doi: 10.1007/BF00201934

Steele, C. L., Crock, J., Bohlmann, J., and Croteau, R. (1998). Sesquiterpene synthases from grand fir (*Abies grandis*). *J. Biol. Chem.* 273 (4), 2078–2089. doi: 10.1074/jbc.273.4.2078

Takase, H., Sasaki, K., Ikoma, G., Kobayashi, H., Matsuo, H., Suzuki, S., et al. (2016a). Farnesyl diphosphate synthase may determine the accumulation level of (–)-rotundone in “Syrah” grapes. *Vitis J. Grapevine Res.* 55 (3), 99–106. doi: 10.5073/vitis.2016.55.99-106

Takase, H., Sasaki, K., Shinmori, H., Shinohara, A., Mochizuki, C., Kobayashi, H., et al. (2016b). Cytochrome P450 CYP71BE5 in grapevine (*Vitis vinifera*) catalyzes the formation of the spicy aroma compound (–)-rotundone. *J. Exp. Bot.* 67 (3), 787–798. doi: 10.1093/jxb/erv496

Tasin, M., Bäckman, A.-C., Bengtsson, M., Ioriatti, C., and Witzgall, P. (2006). Essential host plant cues in the grapevine moth. *Naturwissenschaften* 93 (3), 141–144. doi: 10.1007/s00114-005-0077-7

Tholl, D. (2015). “Biosynthesis and biological functions of terpenoids in plants,” in *Advances in biochemical Engineering/Biotechnology*. Switzerland: Springer International Publishing, 48, 63–106. doi: 10.1007/10_2014_295

Vattekatte, A., Garms, S., Brandt, W., and Boland, W. (2018). Enhanced structural diversity in terpenoid biosynthesis: Enzymes, substrates and cofactors. *Org. Biomol. Chem.* 16 (3), 348–362. doi: 10.1039/C7OB02040F

Vranová, E., Coman, D., and Gruijssem, W. (2013). Network analysis of the MVA and MEP pathways for isoprenoid synthesis. *Annu. Rev. Plant Biol.* 64 (1), 665–700. doi: 10.1146/annurev-arplant-050312-120116

Wang, W., Feng, J., Wei, L., Khalil-Ur-Rehman, M., Nieuwenhuizen, N. J., Yang, L., et al. (2021). Transcriptomics integrated with free and bound terpenoid aroma profiling during “Shine muscat” (*Vitis labrusca* × *V. vinifera*) grape berry development reveals coordinate regulation of MEP pathway and terpene synthase gene expression. *J. Agric. Food Chem.* 69 (4), 1413–1429. doi: 10.1021/acs.jafc.0c06591

Wen, Y.-Q., Zhong, G.-Y., Gao, Y., Lan, Y.-B., Duan, C.-Q., and Pan, Q.-H. (2015). Using the combined analysis of transcripts and metabolites to propose key genes for differential terpene accumulation across two regions. *BMC Plant Biol.* 15 (1), 240. doi: 10.1186/s12870-015-0631-1

Wu, Y., Duan, S., Zhao, L., Gao, Z., Luo, M., Song, S., et al. (2016). Aroma characterization based on aromatic series analysis in table grapes. *Sci. Rep.* 6 (1), 31116. doi: 10.1038/srep31116

Yang, X., Guo, Y., Zhu, J., Ma, N., Sun, T., Liu, Z., et al. (2017a). Associations between the α -terpineol synthase gene and α -terpineol content in different grapevine varieties. *Biotechnol. Biotechnol. Equip.* 31 (6), 1100–1105. doi: 10.1080/13102818.2017.1364978

Yang, X., Guo, Y., Zhu, J., Shi, G., Niu, Z., Liu, Z., et al. (2017b). Associations between the 1-deoxy-D-xylulose-5-phosphate synthase gene and aroma in different grapevine varieties. *Genes Genomics* 39 (10), 1059–1067. doi: 10.1007/s13258-017-0574-z

Yue, X., Ren, R., Ma, X., Fang, Y., Zhang, Z., and Ju, Y. (2020). Dynamic changes in monoterpene accumulation and biosynthesis during grape ripening in three *Vitis vinifera* L. cultivars. *Food Res. Int.* 137 (September), 109736. doi: 10.1016/j.foodres.2020.109736

Zheng, T., Dong, T., Haider, M. S., Jin, H., Jia, H., and Fang, J. (2020). Brassinosteroid regulates 3-Hydroxy-3-methylglutaryl CoA reductase to promote grape fruit development. *J. Agric. Food Chem.* 68 (43), 11987–11996. doi: 10.1021/acs.jafc.0c04466

Zheng, T., Guan, L., Yu, K., Haider, M. S., Nasim, M., Liu, Z., et al. (2021). Expressional diversity of grapevine 3-Hydroxy-3-methylglutaryl-CoA reductase (VvHMGCR) in different grapes genotypes. *BMC Plant Biol.* 21 (1), 279. doi: 10.1186/s12870-021-03073-8

Zhu, B.-Q., Cai, J., Wang, Z.-Q., Xu, X.-Q., Duan, C.-Q., and Pan, Q.-H. (2014). Identification of a plastid-localized bifunctional Nerolidol/Linalool synthase in relation to linalool biosynthesis in young grape berries. *Int. J. Mol. Sci.* 15 (12), 21992–22010. doi: 10.3390/ijms151221992

Zou, C., Massonnet, M., Minio, A., Patel, S., Llaca, V., Karn, A., et al. (2021). Multiple independent recombinations led to hermaphroditism in grapevine. *Proc. Natl. Acad. Sci.* 118 (15), e2023548118. doi: 10.1073/pnas.2023548118



OPEN ACCESS

EDITED BY

Alessandra Ferrandino,
University of Turin, Italy

REVIEWED BY

Darko Preiner,
University of Zagreb, Croatia
Davide Neri,
Marche Polytechnic University, Italy

*CORRESPONDENCE

Yishai Netzer

✉ ynetzer@gmail.com

Aaron Fait

✉ fait@bgu.ac.il

[†]These authors have contributed
equally to this work and share
first authorship

SPECIALTY SECTION

This article was submitted to
Plant Metabolism and Chemodiversity,
a section of the journal
Frontiers in Plant Science

RECEIVED 02 December 2022

ACCEPTED 25 January 2023

PUBLISHED 08 February 2023

CITATION

Perin C, Verma PK, Harari G, Suued Y,
Harel M, Ferman-Mintz D, Drori E, Netzer Y
and Fait A (2023) Influence of late pruning
practice on two red skin grapevine cultivars
in a semi-desert climate.
Front. Plant Sci. 14:1114696.
doi: 10.3389/fpls.2023.1114696

COPYRIGHT

© 2023 Perin, Verma, Harari, Suued, Harel,
Ferman-Mintz, Drori, Netzer and Fait. This is
an open-access article distributed under the
terms of the [Creative Commons Attribution
License \(CC BY\)](#). The use, distribution or
reproduction in other forums is permitted,
provided the original author(s) and the
copyright owner(s) are credited and that
the original publication in this journal is
cited, in accordance with accepted
academic practice. No use, distribution or
reproduction is permitted which does not
comply with these terms.

Influence of late pruning practice on two red skin grapevine cultivars in a semi-desert climate

Corrado Perin^{1†}, Pankaj Kumar Verma^{2†}, Gil Harari³,
Yedidya Suued⁴, Matanya Harel⁴, Danielle Ferman-Mintz⁴,
Elyashiv Drori^{4,5}, Yishai Netzer^{4,5*} and Aaron Fait^{2,6*}

¹Dipartimento di Agronomia Animali Alimenti Risorse Naturali e Ambiente, University of Padova, Padova, Italy, ²Albert Katz International School for Desert Studies, Jacob Blaustein Institutes for Desert Research, Ben-Gurion University of the Negev, Midreshet Ben-Gurion, Israel, ³Carmel Winery, Soham, Israel, ⁴Eastern Regional R&D Center, Ariel, Israel, ⁵Chemical engineering Department, Ariel University, Ariel, Israel, ⁶Albert Katz Department of Dryland Biotechnologies, French Associates Institute for Agriculture and Biotechnology of Drylands, Jacob Blaustein Institutes for Desert Research, Ben-Gurion University of the Negev, Midreshet Ben-Gurion, Israel

Continually increasing global temperature could severely affect grape berry metabolite accumulation and ultimately wine polyphenol concentration and color intensity. To explore the effect of late shoot pruning on grape berry and wine metabolite composition, field trials were carried out on *Vitis vinifera* cv. Malbec and cv. Syrah grafted on 110 Richter rootstock. Fifty-one metabolites were detected and unequivocally annotated employing UPLC-MS based metabolite profiling. Integrating the data using hierarchical clustering showed a significant effect of late pruning treatments on must and wine metabolites. Syrah metabolite profiles were characterized by a general trend of higher metabolite content in the late shoot pruning treatments, while Malbec profiles did not show a consistent trend. In summary, late shoot pruning exerts a significant effect, though varietal specific, on must and wine quality-related metabolites, possibly related to enhanced photosynthetic efficiency, which should be taken into consideration when planning mitigating strategies in warm climates.

KEYWORDS

grape must, wine, UPLC-MS, late shoot pruning, secondary metabolites, anthocyanin, stilbene

1 Introduction

Grape berry metabolite composition is crucial for producing premium-quality wine with regional characteristics, as the grape berry metabolic status is intimately associated with environmental and seasonal variation (Bokulich et al., 2016). Climate change forecasts predict significant thermal increases for Mediterranean climate zones, which will intensify the effects on vine phenology and berry composition. Elevated ambient temperature is one of the most prominent adverse environmental factors affecting wine quality (Gutiérrez-Gamboa et al., 2021). Elevated temperature causes the compression of the harvest period (Rienth et al.,

2021), or varietal shifts in phenology of certain developmental phases (Gashu et al., 2020). These phenological changes can directly impact grape metabolism entailing significant composition changes (Abeyasinghe et al., 2019; Venios et al., 2020), e.g., increased content of total soluble solids (TSS), increased pH, alteration in the amino acid profile as well as a negative effect on the accumulation of phenolic compounds (Kliewer, 1971; Kliewer, 1977; Baeza et al., 2019). Taken together, the impact on the wine quality and regional characteristics can be severe (Rienth et al., 2016), thus, to produce grapes with the desired metabolic balance and mitigate the climate challenges, optimizing proper viticulture practices will be fundamental.

A possibility for adapting viticulture to impending climate changes is to improve photosynthetic efficiency during grape ripening processes, e.g., by postponing winter pruning from dormancy to post-dormancy. Other field practices capable of modifying vine phenology include post-veraison leaf removal, post-bud-break pruning, and severe trimming or forcing vine regrowth (Allegro et al., 2019; Buesa et al., 2019). Late shoot pruning, also referred to as delayed winter pruning, is a pruning technique practised in the spring after the bud break occurs to tune growth and yield. Recently, its application has been proposed as a significant tool for optimizing vine growth in warm regions, containing crop yield, and improving wine quality (Netzer et al., 2022). It was shown that late shoot pruning was also associated with improved photosynthetic efficiency and lower crop load. However, the effect of the practice seems not to be consistent between varieties, e.g., increased yield of Merlot in New Zealand (Friend and Trought, 2007), while the decreased yield of cv. Sangiovese in Italy (Frioni et al., 2016). More importantly, slight or no information exists from different varieties on the response of berry and wine chemistry following late pruning treatments from within the same experimental setup.

The goal of this work was to investigate the effect of incremental late shoot pruning on the chemical composition of must and wine from Syrah and Malbec varieties. Earlier works showed phenological syncing between the treatments, but lower yield and higher quality in the late shoot pruned vines (Netzer et al., 2022). Using a liquid chromatography-mass spectrometry-based approach we compared the varietal profiles of must and wine from late shoot pruning (LSP1, LSP2, LSP3), standard winter pruning (WP), and winter pruning and cluster thinning (WP+T) pruning treatments.

2 Materials and methods

2.1 Experimental site and plant material

The study was performed in 2017 and 2018 on an experimental vineyard planted in 2010 in Ayalon Valley, Israel (31°86'N; 35°01'E), 186 m above sea level. The experimental layout was a randomized complete block design with five treatments, and it was replicated four times. Row orientation was east/west, with a slight tendency to the south and vine and row spacing 1.5 and 3 m, respectively (4.5 m²/vine) (Figure S1). Pest management, irrigation and fertilization in the vineyard were applied according to standard local agricultural practices. Must and wine samples from the 2017 and 2018 seasons were collected and analyzed by LC-MS.

2.2 Winter pruning and late shoot pruning

The winter pruning and late shoot pruning treatments were performed exactly as described by (Netzer et al., 2022) on the vines of *Vitis vinifera* cv. Syrah, and *Vitis vinifera* cv. Malbec was grafted on 110 Richter rootstock. Briefly, five pruning treatments including LSP1 (pruning after 1 week of bud break), LSP2 (pruning after 2 weeks of bud break), LSP3 (pruning after 3 weeks of bud break), WP+T (standard winter pruning and cluster thinning as control), and WP (standard winter pruning as control). These pruning treatments were randomly assigned to blocks, so there were 11*4 vines for each treatment and treatments were applied to the same vines in both years.

2.3 Berry sampling and metabolite analysis in must and wine

Each year, berries from all the treatments were harvested at a more or less, similar TSS (°Brix) value. Must samples were collected from bulk unfermented juice after settling for an hour and then decanting the liquid. The wine samples were obtained from the micro vinification process of the corresponding treatments (Drori et al., 2017). Must and wine from both the 2017 and 2018 seasons were then analyzed by LC-MS as described below.

2.3.1 Metabolite extraction

For the metabolite analysis, must samples were pulverized by mortar and pestle while keeping the material frozen by pouring liquid nitrogen. Approximately 200 mg of must powder was weighed and lyophilized in ScanVac CoolSafe™ (Labogene, Denmark, <https://www.labogene.com>). While wine samples were directly lyophilized in polypropylene tubes without pulverization. Metabolites were then extracted by adding 1ml pre-chilled methanol: chloroform: water extraction solution (2.5:1:1 v/v), following the protocol described by (Hochberg et al., 2013; Degu et al., 2014). After that, internal standards (300µl of 1mg/ml ampicillin in water and 380µl of 1mg/ml corticosterone in methanol) were subsequently added as described (Degu et al., 2016). The mixture was then briefly vortexed, 100µl of methanol was added and then placed on a horizontal shaker for 10min at 1000rpm. The samples were sonicated for 10min in an Elmasonic S30 ultrasonicator (Elma Singen, Germany, <http://www.elma-ultrasonic.com/>) and centrifuged at 14000rpm for 10 min (Centrifuge 5417R, Eppendorf SE, Hamburg, Germany, <https://www.eppendorf.com>). The supernatant was then decanted into new tubes, mixed with 300µl of chloroform and 300µl of MiliQ water (Millipore, MA, USA, <https://www.merckmillipore.com>), vortexed for 10s and then centrifuged again for 5min at 14000rpm. The water/methanol phase, obtained from the extraction protocol (around 1ml), was collected, and filtered using 0.22 µm (Millipore, MA, USA, <https://www.merckmillipore.com>) and stored in vials for UPLC analysis.

2.3.2 UPLC analysis

Each sample was analyzed twice in an Ultra Performance Liquid Chromatography coupled with a Quadrupole Time-of-Flight Mass-

Spectrometer (UPLC-QTOF MS, Waters, MA, USA, <https://www.waters.com/>) system operating in both positive and negative ion modes, alternatively (Table S6). The MassLynxTM software (Waters, MA, USA, <https://www.waters.com/>) version 4.1 was used for UPLC system control and data acquisition. The acquired raw data were processed using the MarkerLynx application manager (Waters, MA, USA, <https://www.waters.com/>) as described by Hochberg et al., 2013. Metabolite's annotation was based on the mass fragment (mass/charge; m/z), their retention time (RT), and the comparison with the internal library as well as the current scientific literature (Degu et al., 2014). In addition, metabolites were also annotated based on fragmentation patterns crossed with the ChemSpider metabolite database (www.chemspider.com).

2.3.3 Data normalization and statistical analysis

The chemical feature's peak area detected by the instrument was normalized by internal reference for UPLC analysis (i.e., ampicillin and corticosterone in the negative and positive ion mode, respectively). We used two different internal standard references as analytes have different ionizing efficiency in positive and negative ion modes, e.g., some analytes are not ionized in negative mode, but very well ionized in positive mode. We annotated metabolites uniquely in both negative and positive ion modes. We used corticosterone as an internal standard reference to normalize data of metabolites annotated in positive ion mode, and due to poor ionization of corticosterone in negative mode, we use another internal standard ampicillin as a reference to normalize data of metabolites annotated in negative mode to minimize the variability in sample preparation as well as variability generated by the instrument such as injection volume. Further accuracy was acquired by normalizing samples' values to the relative dry weight (post-lyophilization). Therefore, data refer to the relative metabolite abundance based on ion counts. For hierarchical clustering representation, mean values were used, and metabolite values were $\ln(x+1)$ transformed. In addition, unit variant scaling was applied for this analysis.

The two datasets (wine and must) were utilized for statistical analysis based on i) hierarchical clustering as a multivariate approach to the study; ii) analysis of variance for each detected metabolite (multifactorial ANOVA) considering the effect of three factors (pruning, cultivar, and year), the effect of their interactions (pruning \times cultivar, pruning \times year, cultivar \times year, pruning \times cultivar \times year); iii) Pearson correlation analysis for investigating on the putative relationships among metabolites both as must and wine autocorrelations and must-to-wine bipartite correlation. Statistical analysis and data visualizations were performed in the R environment (R Core Team, 2022a) using R studio IDE (R Studio Team, 2022b).

3 Results

3.1 Pruning exerts a significant effect on must and wine metabolite status

Standard winter pruning was conducted according to common agricultural practice in mid-February. In examining the seasonal patterns of phenological development throughout the three seasons,

previous findings showed that late pruning treatments re-started the phenological process at a similar pace (Netzer et al., 2022). A one-week difference between dates of late pruning, conducted per the relevant treatments, was evident in the phenological pattern until mid-May. Nonetheless, a significant increase in the pace of development in the later winter pruning treatments was apparent from mid-May until the end of June, bringing all treatments to sync at veraison (stage 35).

To test if the phenological syncing was reflected in the must and wine chemistry, we analysed samples of must and wine using LC-MS-based protocol across the entire experimental setup, i.e., a total of 160 samples. Fifty metabolites were consistently identified and unequivocally annotated. Metabolites primarily belong to polyphenols, including anthocyanins, flavonoids, phenolic acids, and stilbenes (Figure 1; Tables S1, S2). Hierarchical clustering was performed using the metabolic data of must and wine. The dendrogram obtained after the cluster analysis sharply divided the samples based on their origin (wine vs must) (Figure 1). Next, the samples were clustered by 'cultivar' (Malbec vs Syrah), and then by 'year' (2017 vs 2018). The opposite pattern was shown for the wine samples, i.e., first by 'year', then by 'cultivar'. Within each sub-cluster (pruning-cultivar-year combination), samples from the most extreme late shoot pruning treatments (LSP3 and LSP2) and samples from the no-late pruning treatments (WP+T and WP) formed two separate groups (Figure 1). When repeating the analysis for must and wine samples separately, clustering was observed primarily by 'cultivar' (Malbec vs Syrah), then by year in the must (Figures 2A, B). In the wine, clustering was observed primarily by treatment (Figures 3A, B). In both datasets, five main groups of metabolites were identified based on their pattern of change i) amino acids, (ii) anthocyanins (iii) flavonoids (flavanols, flavanones, flavanone and flavonols) (iv) hydroxycinnamic acids and (v) stilbenes. The analysis of variance revealed that different pruning treatments had a significant effect on most of the detected metabolites (Tables S1, S2), but all metabolic groups were differentially affected, with the most influenced metabolic classes being anthocyanins (Figures S2A–D) and stilbenes (Figures S3A–D). The highest relative content of anthocyanins and stilbenes were detected in the most extreme late pruning treatment in must, i.e., vines pruned three weeks after bud-break (LSP3). For instance, a general trend in Syrah must sample was observed from the "late shoot pruning" treatments (i.e., LSP3, LSP2, and LSP1) which measured higher anthocyanin and stilbene content in comparison with the standard pruning treatments, i.e., WP+T and WP. Among the anthocyanins, Pet-3-glu, Cyan-3-glu, Peo-3-glu, Delph-3-acet, Pet-3-acet, Cyan-3-acet, Peo-3-acet, Peo-3-coum showed higher content in the LSP3 Syrah must (Figure S2A), while Delph-3-glu, Delph-3-acet, Peo-3-acet, accumulated in LSP3 wine samples (Figure S2B). On the other hand, in Malbec, the LSP3 late-pruning treatments reported higher anthocyanin abundance as compared with the "no-late-pruning" with higher accumulation in LSP3 in must and LSP2 treatment in wine samples, but it significantly depends on the season (Figures S2C, D). Among the stilbenes trans-piceid, cis-piceid, trans-resv, cis-resv and delta-viniferin showed higher content in Syrah must and wine samples which were also affected by seasonal variations (Figures S3A, B), on the other hand, Malbec showed higher content of trans-piceid and cis-piceid in both must and wine in 2017's most extreme late pruning treatment, i.e., LSP3

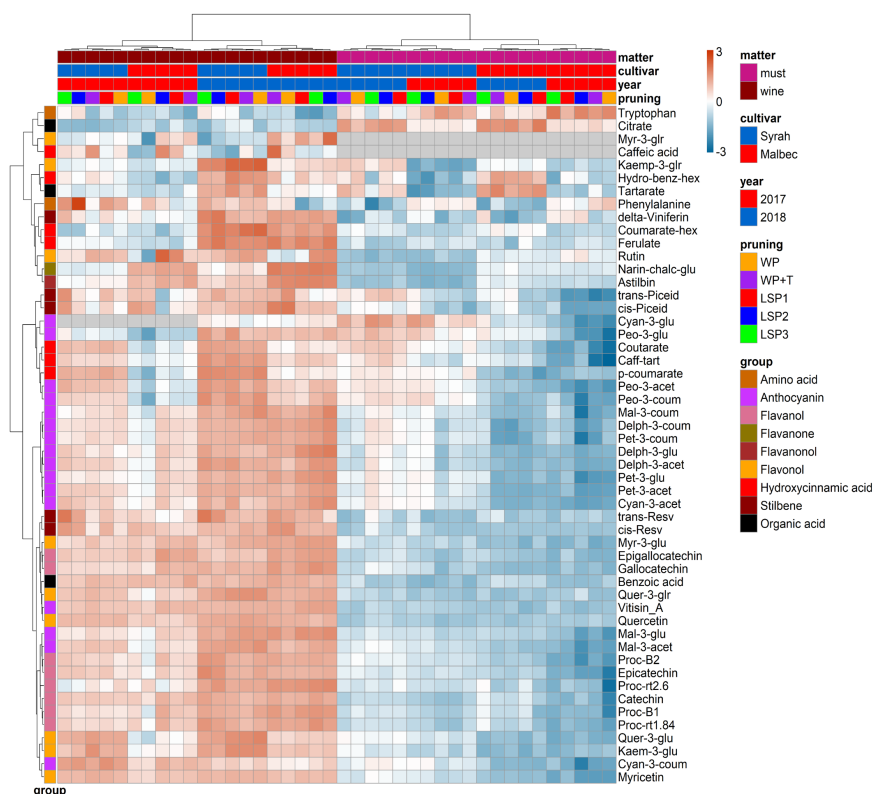


FIGURE 1

Hierarchical clustering heatmap obtained from cluster analysis. Cluster sharply divided the samples based on the kind of sample (wine vs must) then *cultivar*, year and pruning treatments. Samples from the most extreme late shoot pruning treatments ("LSP3" and "LSP2") and samples from the no-late pruning treatments ("WP+T" and "WP") seemed to form two different groups. The late shoot pruning treatment "LSP1" alternatively clustered with one of the two groups.

(Figures S3C, D). Flavanols such as Proc-B2 and epicatechin followed the same trend as anthocyanins in the Syrah wine sample (Figure 3A). Flavanols like Proc-B1, Proc-rt1.84, Proc-B2, catechin, epicatechin, epigallocatechin and galocatechin followed a general trend with the highest accumulation in LSP3 2018 in Malbec must (Figure 2A) and Proc-rt1.84, epigallocatechin in wine samples (Figure 3A). Among flavonols, quercetin and myricetin were higher in the late pruning treatments, in Syrah must samples (Figure 2A). Notably, naringenin-chalcone and astilbin were not affected by the pruning treatments. The statistical analysis using *post hoc* Tukey's test revealed a significant difference between cultivars (Malbec vs Syrah) and between vintages (2017 vs 2018) (Tables S1, S2).

3.2 Factor interaction affected metabolite accumulation

Cultivar \times treatment interaction mainly concerned the group of anthocyanins and stilbenes (Tables S1, S2). A general trend of higher metabolite content in the late pruning treatments was evident in must samples. All other metabolites either did not follow a common trend or were not significantly affected. Must flavanols, flavonols, and hydroxycinnamic acids were affected by cultivar and year interaction, while wine anthocyanins and flavonols were affected by

cultivar and year interaction (Table S1). No effect from the interaction between pruning and year factors was detected except for the flavanol (Proc-rt1.84), the flavonol (myricetin-3-glucoside), and stilbene (cis-piceid). The triple interaction effect (treatment \times cultivar \times year) denotes a high sensitivity of secondary metabolites to external conditions. The triple interaction effect involved some classes of flavanols (Proc-B1, Proc-rt1.84, Proc-rt2.6, epigallocatechin) and hydroxycinnamic acids (p-coumarate, coumarate, ferulate, caff-tart), stilbene (trans-piceid, trans-resv) as well as flavanone (astilbin) and the flavonol (myr-3-glu) in the must (Figure 2; Table S1). While in wine samples, flavanols (Proc-B1, Proc-rt1.84, Proc-B2) flavonols (quer-3-glu), and stilbene (delta-viniferin) were affected by the interaction between (treatment \times cultivar \times year) (Figure 3; Table S2). When repeating the ANOVA separating the two cultivars, Syrah reported more significant and consistent metabolite changes than Malbec in the anthocyanin and flavonol classes, whereas Malbec showed more significant variations in the hydroxycinnamic acids (Figures 2, 3; Table S2). The number of metabolites affected by the cultivar-to-pruning interaction (cultivar \times pruning) was higher in wine than in must. Besides stilbenes, cultivar-to-pruning interactions also concerned flavanols, flavonols, and more anthocyanins than in the must samples. Other interactions also regarded the combined effect of treatment and cultivar with vintage; they were generally noticed for some metabolites from every class except for hydroxycinnamic acids and flavanols.

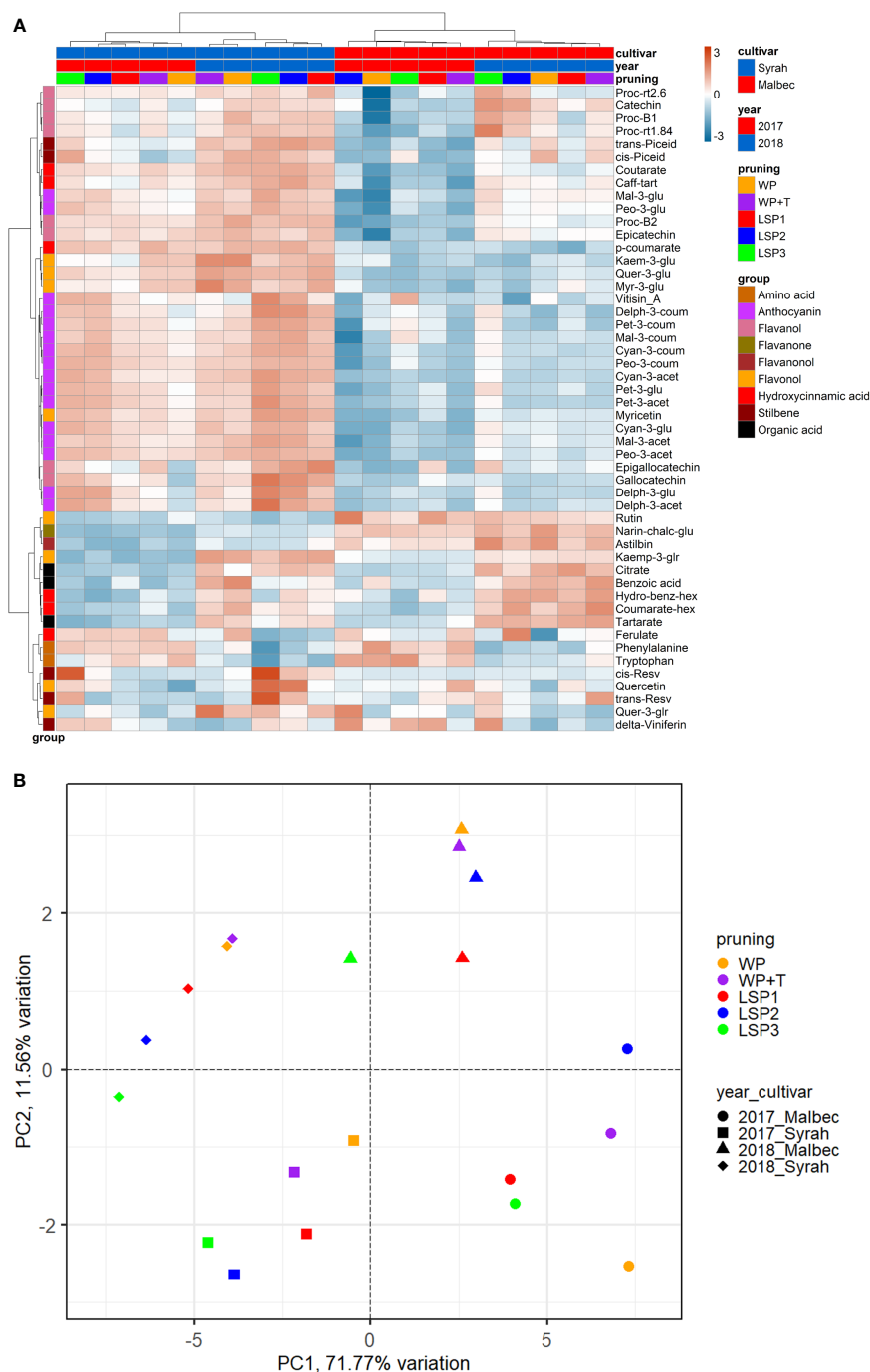


FIGURE 2

Heatmap and 2D PCA score plot of annotated LC-MS based metabolites in must Samples. **(A)** Hierarchical clustering heatmap obtained from the cluster analysis sharply divided the samples into cultivar and year and pruning. **(B)** PCA score plot from metabolite data including cultivar and year and pruning treatments. Samples from the most extreme late shoot pruning treatments ("LSP3" and "LSP2") and samples from the no-late shoot pruning treatments ("WP+T" and "WP") seemed to form two different groups. The late shoot pruning treatment "LSP2" alternatively clustered with one of the two groups.

3.3 Correlation analysis showed a positive correlation between anthocyanin and flavanols

To study the coordination of metabolic processes concerning the pruning treatments, a correlation analysis using Pearson correlation was performed. The correlation analysis of must samples revealed high positive correlations among anthocyanins

and flavanols. Vitisin_A showed a negative correlation with most of the metabolite classes except anthocyanins and stilbenes in must samples of Syrah and Malbec. Cultivar differences included a high number of positive correlations of gallocatechin and quercetin with anthocyanins in Syrah (Figure 4A; Table S3 Sheet1), and strong positive correlations among flavanols in Malbec (Figure 4B; Table S3 Sheet2) as well as strong positive correlations of astilbin, coumarate, caff-tart, and trans-piceid with

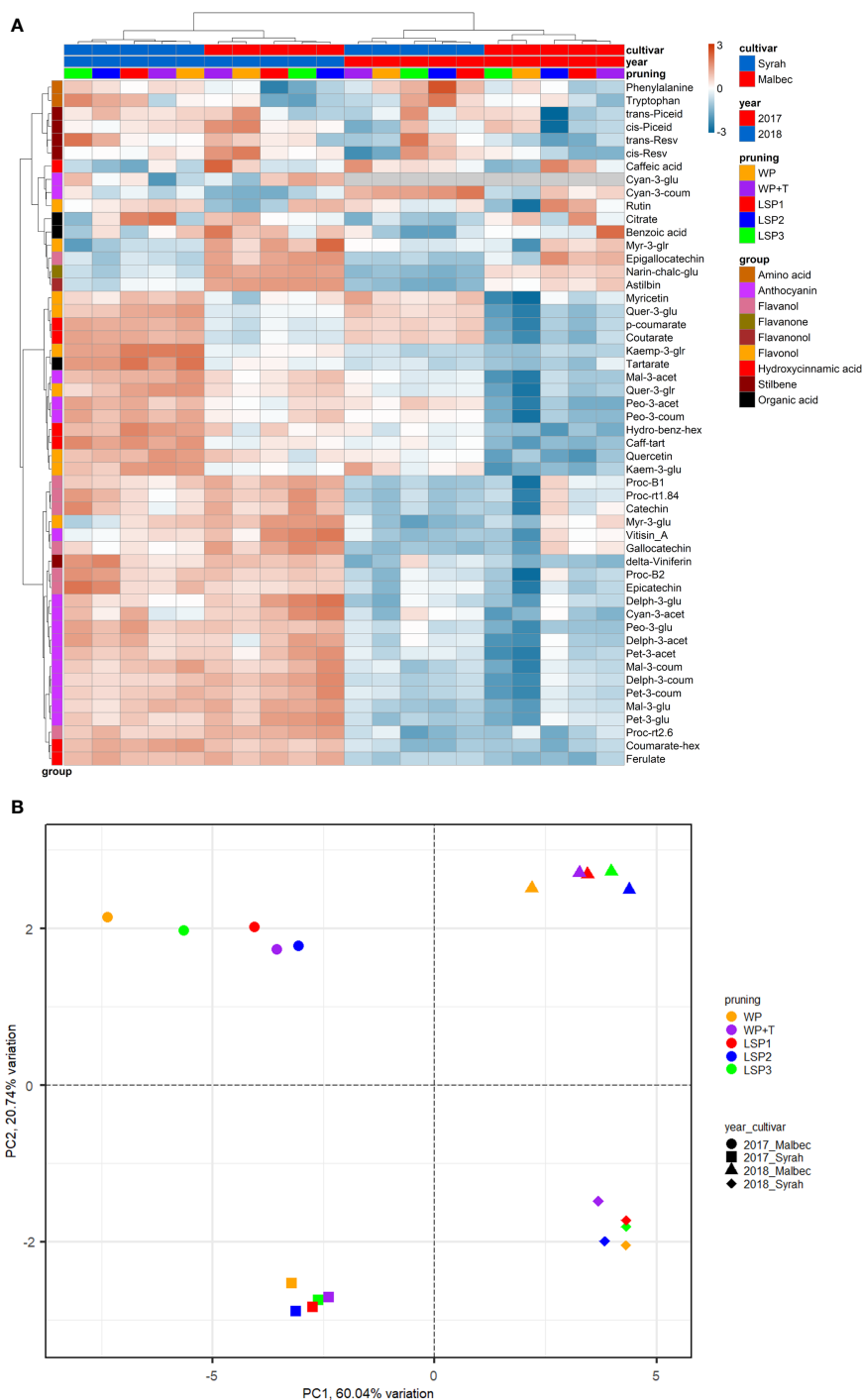


FIGURE 3

Heatmap and 2D PCA score plot of annotated LC-MS-based metabolites in wine samples. **(A)** Hierarchical clustering heatmap obtained from the cluster analysis sharply divided the samples by year and then cultivar and pruning. **(B)** PCA analysis suggests that the wine samples were clustered by 'year' (2017 vs 2018) and then by 'cultivar' (Malbec vs Syrah).

the group of flavanol. Similar relations were also observed in the wine samples. When comparing the two cultivars separately, the Malbec correlation matrix reported higher indices in the number of correlations and their strength (Figures 5A, B; Table S4 Sheet1 and Sheet2). On the contrary, must and wine anthocyanins did not correlate well except for the wine delph-3-glu, delph-3-acet and peo-3-acet with all the must anthocyanins (Figure 6; Table S5 Sheet1 and Sheet2).

4 Discussion

The wine quality is reflected by the amount and composition of a large number of primary and secondary metabolites that shape its sensorial experience. Considering this view, it is likely that optimizing the environmental conditions during the grape ripening period will be required to produce good quality wine. These conditions can be achieved by modifying the viticulture practices in which late shoot

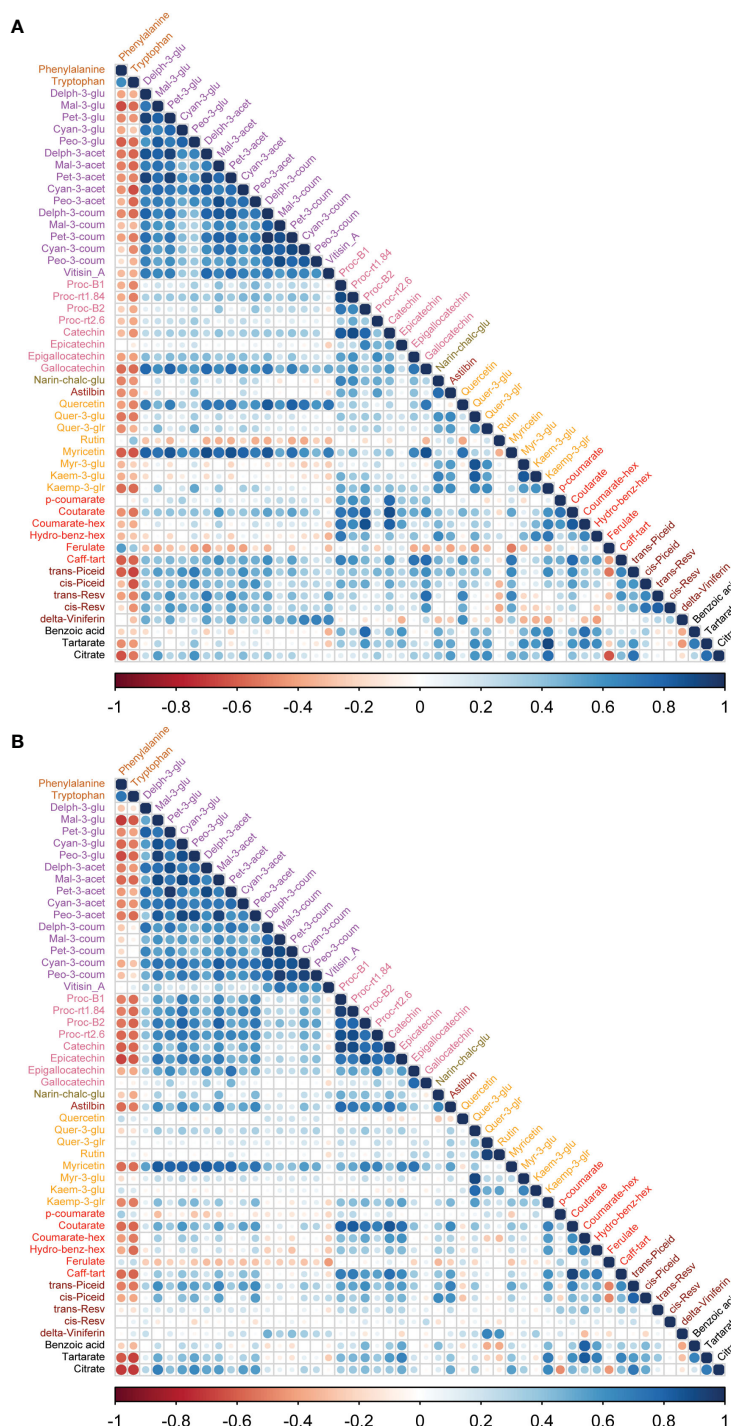


FIGURE 4

Correlation analyses between metabolites of two cultivars (A) Syrah must, most of the metabolites were positively correlated except rutin, myr-3-glu, kaem-3-glu, hydro-benz-hex, ferulate and benzoic acid which were negatively correlated. (B) Malbec must, most of the metabolites were positively correlated except p-coumarate, ferulate and cis-resv were negatively correlated with other metabolites. Amino acids were negatively correlated with most of the metabolites except rutin, ferulate in Syrah must, while quercetin, kaem-3-glu, p-coumarate and ferulate showed a positive correlation with amino acids. Vitisin_A was negatively correlated with most other metabolite groups.

pruning is the most important and economical way. Late shoot pruning can delay the phenology towards a cooler environment, thus able to minimize the effect of elevated temperature. The current study aimed to dissect the effect of late shoot pruning on differential metabolite accumulation in two red grapevine varieties, Malbec and Syrah.

In the LC-MS based metabolite profiles, amino acids did not follow a general trend, but their concentration decreased in late pruning, likely because these aromatic amino acids are precursors to the biosynthesis of secondary metabolites (Wang et al., 2017), and play a role in fruit and wine chemical quality. Among secondary metabolites, anthocyanins, flavanols, flavonols and stilbenes were the

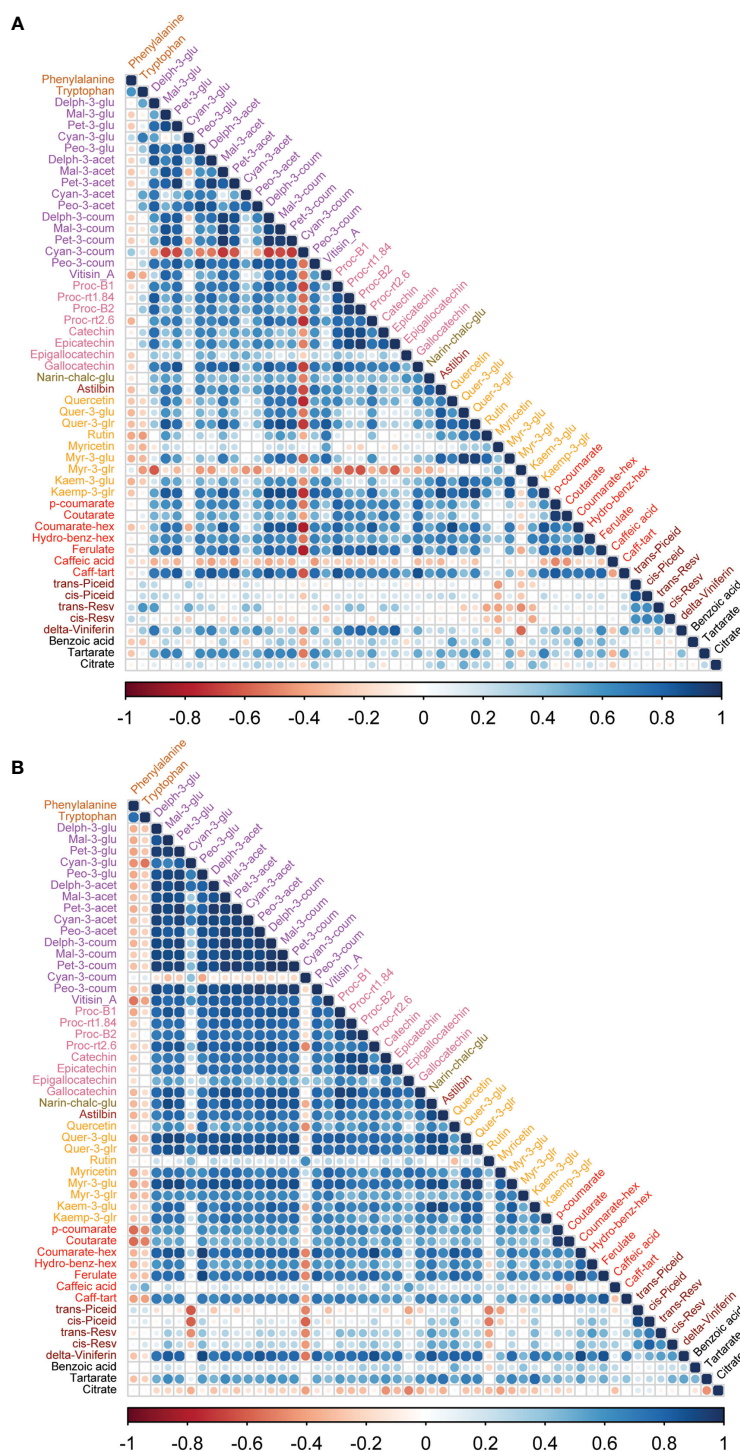


FIGURE 5

Correlation analyses between metabolites of wine samples from two cultivars. (A) In Syrah wine, most of the metabolites were positively correlated except cyan-3-coum, myr-3-glu and caffeic acid, which were negatively correlated. (B) In Malbec wine, most of the metabolites were positively correlated except cyan-3-coum, and citrate which were negatively correlated while rutin, caffeic acid, trans-piceid, cis-piceid, and benzoic acid had a weak correlation with other metabolites. Amino acids, phenylalanine and tryptophan were negatively correlated with most of the metabolites except trans-resv, cis-resv in Syrah wine, while caffeic acid, trans-piceid, and cis-piceid in Malbec wine showed a positive correlation with amino acids.

most affected groups by pruning treatments. Our findings suggest that flavanol accumulation is linked to the time of pruning in addition to environmental factors reported, e.g., light (Cortell and Kennedy, 2006; Reshef et al., 2017), soil conditions (Perin et al., 2020) temperature (Del-Castillo-Alonso et al., 2016b), UV-B radiation

(Del-Castillo-Alonso et al., 2016a), and biotic stresses (Kuhn et al., 2013).

Among stilbenes, our study showed that resveratrol and viniferin were significantly modulated by the pruning treatments, with Syrah showing higher resveratrol content and Malbec in viniferin content.

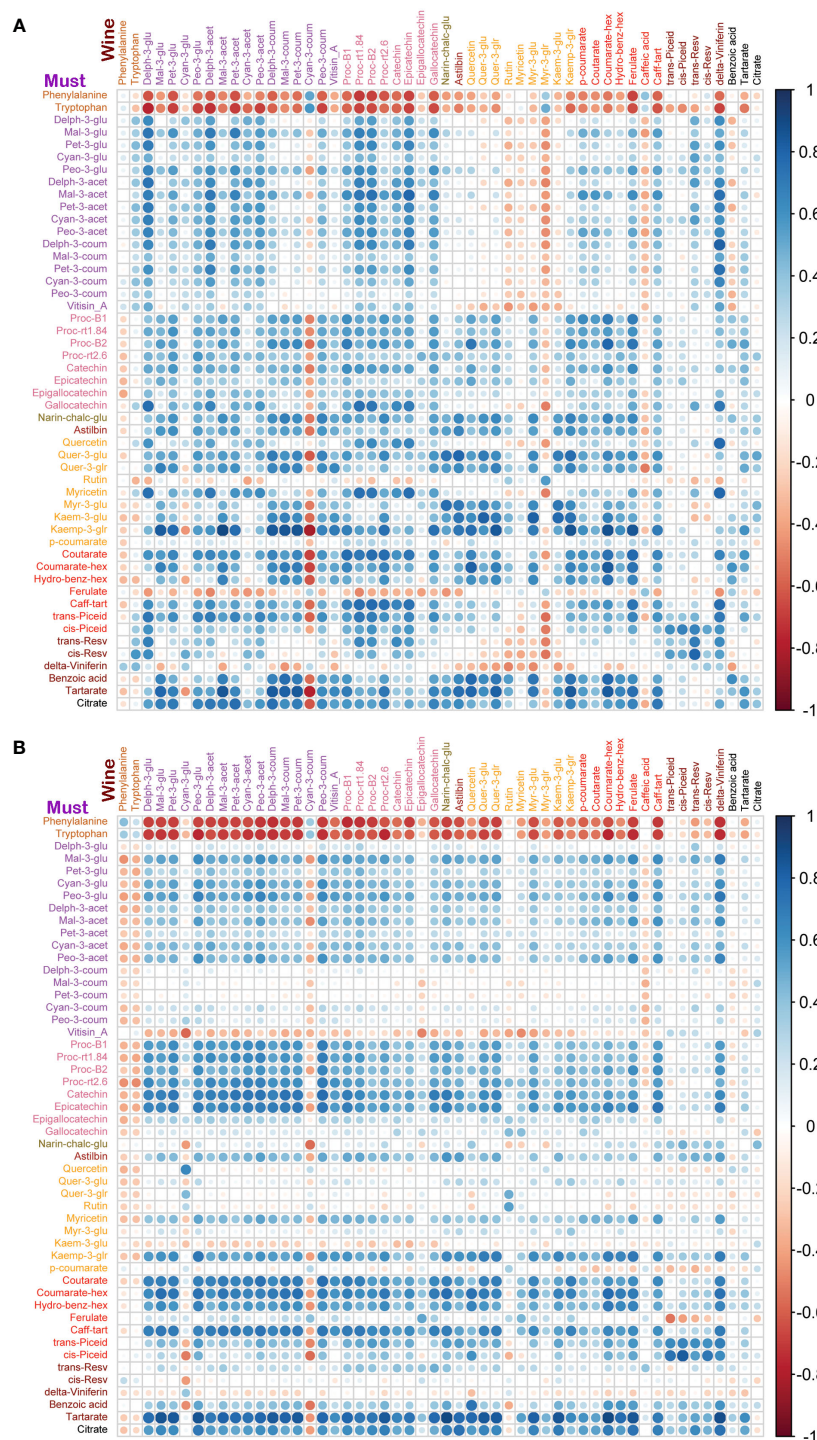


FIGURE 6

Correlation analyses between metabolites of must and wine samples from two cultivars. (A) In Syrah must and wine samples, must amino acids were negatively correlated with wine metabolites except for phenylalanine, cyan-3-coum, myr-3-glr and caffeic acid which were negatively correlated with most of the must metabolites. Must delta-viniferin was negatively correlated with most of the wine metabolites. (B) In Malbec must and wine samples, must amino acids were negatively correlated with wine metabolites except for amino acids and cyan-3-coum which were negatively correlated with most of the must metabolites. Must vitisin_A, kaem-3-glu and delta-viniferin were negatively correlated with most of the wine metabolites.

These results are consistent with previous studies showing the high plasticity of these phytoalexins (Anesi et al., 2015) and their relation to climate conditions (Dal Santo et al., 2016; Guerrero et al., 2020).

Our study shows a clear varietal specificity with respect to the effect of pruning treatments on the metabolite profile. For example, the role of the genotype is evident in anthocyanin's pattern of change

across the experimental setup, which follows a general trend of accumulation towards the later pruning treatments in Syrah. These results are supported by the findings that anthocyanin content changes in relation to climate conditions (Shah et al., 2021), and the effect of pruning on their accumulation (Zheng et al., 2017). However, many anthocyanins in Malbec did not follow a similar

trend, suggesting that different varieties have specific mechanisms regulating anthocyanin metabolism.

The effectiveness of the time-dependent late pruning technique for improving grape composition was confirmed in both Syrah and Malbec. Grapes from the late shoot pruning treatments had a higher concentration of polyphenols in the must, which is in line with earlier observations of late pruning to decouple the ripening dynamics of sugars and phenolic substances (Sadras and Moran, 2012; Frioni et al., 2016; Silvestroni et al., 2018; Moran et al., 2021).

Wine metabolite profiling also confirmed the ameliorating effect of pruning, which is consistent with previous findings (Moran et al., 2018; Moran et al., 2019). Statistical analysis on a dataset of 51 detected metabolites revealed significant differences for all the metabolite classes except hydroxycinnamic acids. Differences between treatments were augmented in Syrah and slightly attenuated in Malbec wine, but in both cultivars, the higher color intensity and phenolic substances found in response to late shoot pruning are desirable attributes, as described also by Moran et al. (2019) for Syrah wine. Notably, in wine, the extreme late shoot pruning treatment (three weeks after bud break) was not characterized by the highest values of anthocyanin content as reported for the must samples. This suggests the existence of a non-linear relation between wine and must metabolites mediated by practices in the field. The year of production (vintage) and cultivar were major factors in the separation of wine samples on a PCA, while the treatment factor was more apparent in Malbec than in Syrah, which is not consistent with the must data. When considering the interaction between cultivar and treatments, Syrah positively modulates its metabolites in response to pruning treatments compared to Malbec. The results of this study also suggest a strong effect of late shoot pruning on both must and wine, consistent throughout the years.

Late shoot pruning can be effective when environmental conditions may limit the achievement of the desired grape ripeness, which is supported by earlier studies performed by (Mori et al., 2007; Sadras and Moran, 2012) as well as observations by Moran et al. (2018). Moran et al. (2018) found an interaction between the timing of pruning and temperature, whereby late pruning enhanced grape phenolic substances-to-sugars ratio in high-temperature vines but not in unheated control vines. Thus, the present study suggests that late shoot pruning by forcing the plant (1) to produce leaves later in the season, which will be considerably more efficient for photosynthesis and (2) having less sink load, improves carbon utilization by secondary metabolite biosynthetic pathways, including increased synthesis of phenolic substances.

5 Conclusion

The late shoot pruning shifted grapevine phenology and perturbed its metabolism. Nonetheless, a combination of a highly

regulated berry phenological syncing, renewed leaf development with improved carbon assimilation capacity and a lower cluster load, led to improved metabolic features such as more stilbenes and flavonoids. Having that said, varietal-specific qualitative and quantitative metabolic alterations of the berry metabolism should be considered, and similar studies should be conducted before upscaling conclusions.

Data availability statement

The original contributions presented in the study are included in the article/Supplementary Material. Further inquiries can be directed to the corresponding authors.

Author contributions

CP: Conceptualization, Data curation, Methodology, Investigation. PV: Data curation, Methodology, Investigation, Writing – original draft, Writing – review & editing. GH: Formal analysis, Methodology, Investigation. YS: Formal analysis, Methodology, Investigation. MH: Formal analysis, Methodology, Investigation. DF-M: Formal analysis, Methodology, Investigation. ED: Conceptualization, Investigation, Methodology, Resources. YN: Conceptualization, Investigation, Methodology, Supervision, Resources, Project administration, Writing – original draft, Writing – review & editing. AF: Conceptualization, Investigation, Methodology, Supervision, Resources, Project administration, Writing – original draft, Writing – review & editing. All authors contributed to the article and approved the submitted version.

Funding

The current work was funded by the Israeli Ministry of Agriculture, Grant number: 31-01-0017.

Acknowledgments

The authors wish to thank Oren Shleif for the support and drive of this experiment. We thank Avner Yonatcha and Meir Aqua for their help in the vineyard, and Maria Stanevsky and Nir Chen for preparing the wine and quality analysis. We also want to thank all the field technicians: Guy Aharon, Tom Dotan, Alon Katz, Yael Sewid, Roni Michaelovsky, Matan Golomb, Shachak Nesharim, Yossi Shteren, Itamar Netzer, and Shilo Netzer. Pankaj Kumar Verma thanks 'The Jacob Blaustein Center for Scientific Cooperation, the Ben-Gurion University of the Negev' for the BCSC postdoctoral fellowship.

Conflict of interest

The authors declare that the research was conducted in the absence of any commercial or financial relationships that could be construed as a potential conflict of interest.

Publisher's note

All claims expressed in this article are solely those of the authors and do not necessarily represent those of their affiliated

organizations, or those of the publisher, the editors and the reviewers. Any product that may be evaluated in this article, or claim that may be made by its manufacturer, is not guaranteed or endorsed by the publisher.

Supplementary material

The Supplementary Material for this article can be found online at: <https://www.frontiersin.org/articles/10.3389/fpls.2023.1114696/full#supplementary-material>

References

- Abeysinghe, S., Greer, D., and Rogiers, S. (2019). The effect of light intensity and temperature on berry growth and sugar accumulation in *Vitis vinifera* 'Shiraz' under vineyard conditions. *Vitis* 58, 7–16. doi: 10.5073/vitis.2019.58.7-16
- Allegro, G., Pastore, C., Valentini, G., and Filippetti, I. (2019). Effects of delayed winter pruning on vine performance and grape composition in cv. merlot, BIO web of conferences. *EDP Sci.* 13, Article 04003. doi: 10.1051/bioconf/20191304003
- Anesi, A., Stocchero, M., Dal Santo, S., Commisso, M., Zenoni, S., Ceoldo, S., et al. (2015). Towards a scientific interpretation of the terroir concept: Plasticity of the grape berry metabolome. *BMC Plant Biol.* 15, 191. doi: 10.1186/s12870-015-0584-4
- Baeza, P., Junquera, P., Peiro, E., Lissarrague, J. R., Uriarte, D., and Vilanova, M. (2019). "Effects of vine water status on yield components, vegetative response and must and wine composition," in *Advances in grape and wine biotechnology*. Eds. A. Morata and I. Loira (London: IntechOpen), 1–23. doi: 10.5772/intechopen.87042
- Bokulich, N. A., Collins, T. S., Masarweh, C., Allen, G., Heymann, H., Ebeler, S. E., et al. (2016). Associations among wine grape microbiome, metabolome, and fermentation behavior suggest microbial contribution to regional wine characteristics. *MBio* 7, e00631–e00616. doi: 10.1128/mBio.00631-16
- Buesa, I., Caccavello, G., Basile, B., Merli, M. C., Poni, S., Chirivella, C., et al. (2019). Delaying berry ripening of bobal and tempranillo grapevines by late leaf removal in a semi-arid and temperate-warm climate under different water regimes. *Aust. J. Grape Wine Res.* 25, 70–82. doi: 10.1111/ajgw.12368
- Cortell, J. M., and Kennedy, J. A. (2006). Effect of shading on accumulation of flavonoid compounds in (*Vitis vinifera* L.) pinot noir fruit and extraction in a model system. *J. Agric. Food Chem.* 54, 8510–8520. doi: 10.1021/jf0616560
- Dal Santo, S., Fasoli, M., Negri, S., D'Inca, E., Vicenzi, N., Guzzo, F., et al. (2016). Plasticity of the berry ripening program in a white grape variety. *Front. Plant Sci.* 7. doi: 10.3389/fpls.2016.00970
- Degu, A., Ayenew, B., Cramer, G. R., and Fait, A. (2016). Polyphenolic responses of grapevine berries to light, temperature, oxidative stress, abscisic acid and jasmonic acid show specific developmental-dependent degrees of metabolic resilience to perturbation. *Food Chem.* 212, 828–836. doi: 10.1016/j.foodchem.2016.05.164
- Degu, A., Hochberg, U., Sikron, N., Venturini, L., Buson, G., Ghan, R., et al. (2014). Metabolite and transcript profiling of berry skin during fruit development elucidates differential regulation between Cabernet sauvignon and Shiraz cultivars at branching points in the polyphenol pathway. *BMC Plant Biol.* 14, 188. doi: 10.1186/s12870-014-0188-4
- Del-Castillo-Alonso, M. Á., Castagna, A., Csepregi, K., Hideg, E., Jakab, G., Jansen, M. A., et al. (2016b). Environmental factors correlated with the metabolite profile of vitis vinifera cv. pinot noir berry skins along a European latitudinal gradient. *J. Agric. Food Chem.* 64, 8722–8734. doi: 10.1021/acs.jafc.6b03272
- Del-Castillo-Alonso, M. Á., Diago, M. P., Tomás-Las-Heras, R., Monforte, L., Soriano, G., Martínez-Abaigar, J., et al. (2016a). Effects of ambient solar UV radiation on grapevine leaf physiology and berry phenolic composition along one entire season under Mediterranean field conditions. *Plant Physiol. Biochem.* 109, 374–386. doi: 10.1016/j.plaphy.2016.10.018
- Drori, E., Rahimi, O., Marrano, A., Henig, Y., Brauner, H., Salmon-Divon, M., et al. (2017). Collection and characterization of grapevine genetic resources (*Vitis vinifera*) in the holy land, towards the renewal of ancient winemaking practices. *Sci. Rep.* 7, 44463. doi: 10.1038/srep44463
- Friend, A. P., and Trought, M. C. (2007). Delayed winter spur-pruning in new Zealand can alter yield components of merlot grapevines. *Aust. J. Grape Wine Res.* 13, 157–164. doi: 10.1111/j.1755-0238.2007.tb00246.x
- Frióni, T., Tombesi, S., Silvestroni, O., Lanari, V., Bellincontro, A., Sabbatini, P., et al. (2016). Postbudburst spur pruning reduces yield and delays fruit sugar accumulation in sangiovese in central Italy. *Am. J. Enol Viticulture* 67, 419–425. doi: 10.5344/ajev.2016.15120
- Gashu, K., Sikron Persi, N., Drori, E., Harcavi, E., Agam, N., Bustan, A., et al. (2020). Temperature shift between vineyards modulates berry phenology and primary metabolism in a varietal collection of wine grapevine. *Front. Plant Sci.* 11. doi: 10.3389/fpls.2020.588739
- Guerrero, R. F., Valls-Fonayet, J., Richard, T., and Cantos-Villar, E. (2020). A rapid quantification of stilbene content in wine by ultra-high pressure liquid chromatography-mass spectrometry. *Food Control* 108, 106821. doi: 10.1016/j.foodcont.2019.106821
- Gutiérrez-Gamboa, G., Zheng, W., and de Toda, F. M. (2021). Current viticultural techniques to mitigate the effects of global warming on grape and wine quality: A comprehensive review. *Food Res. Int.* 139, 109946. doi: 10.1016/j.foodres.2020.109946
- Hochberg, U., Degu, A., Toubiana, D., Gendler, T., Nikoloski, Z., Rachmilevitch, S., et al. (2013). Metabolite profiling and network analysis reveal coordinated changes in grapevine water stress response. *BMC Plant Biol.* 13, Article 184. doi: 10.1186/1471-2229-13-184
- Kliewer, W. (1971). Effect of day temperature and light intensity on concentration of malic and tartaric acids in *Vitis vinifera* L. grapes. *J. Am. Soc. Hortic. Sci.* 96, 372–377. doi: 10.21273/JASHS.96.3.372
- Kliewer, W. M. (1977). Influence of temperature, solar radiation and nitrogen on coloration and composition of emperor grapes. *Am. J. Enol Viticulture* 28, 96–103. doi: 10.5344/ajev.1974.28.2.96
- Kuhn, N., Guan, L., Dai, Z. W., Wu, B.-H., Lauvergeat, V., Gomès, E., et al. (2013). Berry ripening: recently heard through the grapevine. *J. Exp. Bot.* 65, 4543–4559. doi: 10.1093/jxb/ert395
- Moran, M. A., Bastian, S., Petrie, P. R., and Sadras, V. O. (2018). Late pruning impacts on chemical and sensory attributes of Shiraz wine. *Aust. J. Grape Wine Res.* 24, 469–477. doi: 10.1111/ajgw.12350
- Moran, M., Bastian, S., Petrie, P., and Sadras, V. (2021). Impact of late pruning and elevated ambient temperature on Shiraz wine chemical and sensory attributes. *Aust. J. Grape Wine Res.* 27, 42–51. doi: 10.1111/ajgw.12470
- Moran, M., Petrie, P., and Sadras, V. (2019). Effects of late pruning and elevated temperature on phenology, yield components, and berry traits in Shiraz. *Am. J. Enol Viticulture* 70, 9–18. doi: 10.5344/ajev.2018.18031
- Mori, K., Goto-Yamamoto, N., Kitayama, M., and Hashizume, K. (2007). Loss of anthocyanins in red-wine grape under high temperature. *J. Exp. Bot.* 58, 1935–1945. doi: 10.1093/jxb/erm055
- Netzer, Y., Suwed, Y., Harel, M., Ferman-Mintz, D., Drori, E., Munitz, S., et al. (2022). Forever young? late shoot pruning affects phenological development, physiology, yield and wine quality of *Vitis vinifera* cv. Malbec. *Agriculture* 12, 605. doi: 10.3390/agriculture12050605
- Perin, C., Fait, A., Palumbo, F., Lucchin, M., and Vannozzi, A. (2020). The effect of soil on the biochemical plasticity of berry skin in two Italian grapevine (*V. vinifera* L.) cultivars. *Front. Plant Sci.* 11. doi: 10.3389/fpls.2020.00822
- R Core Team (2022a). *R: A language and environment for statistical computing* (Vienna, Austria: R Foundation for Statistical Computing). Available at: <https://www.R-project.org/>.
- Reshef, N., Walbaum, N., Agam, N., and Fait, A. (2017). Sunlight modulates fruit metabolic profile and shapes the spatial pattern of compound accumulation within the grape cluster. *Front. Plant Sci.* 8. doi: 10.3389/fpls.2017.00070
- Rienth, M., Torregrosa, L., Sarah, G., Ardisson, M., Brillouet, J.-M., and Romieu, C. (2016). Temperature desynchronizes sugar and organic acid metabolism in ripening grapevine fruits and remodels their transcriptome. *BMC Plant Biol.* 16, 164. doi: 10.1186/s12870-016-0850-0
- Rienth, M., Vigneron, N., Darriet, P., Sweetman, C., Burbidge, C., Bonghi, C., et al. (2021). Grape berry secondary metabolites and their modulation by abiotic factors in a climate change scenario—a review. *Front. Plant Sci.* 12. doi: 10.3389/fpls.2021.643258
- R Studio Team (2022b). *RStudio: Integrated development environment for R* (Boston, MA: RStudio, PBC). Available at: <http://www.rstudio.com/>.

Sadras, V. O., and Moran, M. A. (2012). Elevated temperature decouples anthocyanins and sugars in berries of Shiraz and Cabernet franc. *Aust. J. Grape Wine Res.* 18, 115–122. doi: 10.1111/j.1755-0238.2012.00180.x

Shah, M. H., Rafique, R., Rafique, T., Naseer, M., Khalil, U., and Rafique, R. (2021). “Effect of climate change on polyphenols accumulation in grapevine,” in *Phenolic compounds-chemistry, synthesis, diversity, non-conventional industrial, pharmaceutical and therapeutic applications* (London, SW7 2QJ, UNITED KINGDOM: IntechOpen) 1, 243–258. doi: 10.5772/intechopen.99779

Silvestroni, O., Lanari, V., Lattanzi, T., and Palliotti, A. (2018). Delaying winter pruning, after pre-pruning, alters budburst, leaf area, photosynthesis, yield and berry composition in sangiovese (*Vitis vinifera* L.). *Aust. J. Grape Wine Res.* 24, 478–486. doi: 10.1111/ajgw.12361

Venios, X., Korkas, E., Nisiotou, A., and Banilas, G. (2020). Grapevine responses to heat stress and global warming. *Plants* 9, 1754. doi: 10.3390/plants9121754

Wang, L., Sun, X., Weizmann, J., and Weckwerth, W. (2017). System-level and granger network analysis of integrated proteomic and metabolomic dynamics identifies key points of grape berry development at the interface of primary and secondary metabolism. *Front. Plant Sci.* 8. doi: 10.3389/fpls.2017.01066

Zheng, W., del Galdo, V., García, J., Balda, P., and de Toda, F. M. (2017). Use of minimal pruning to delay fruit maturity and improve berry composition under climate change. *Am. J. Enol Viticulture* 68, 136–140. doi: 10.5344/ajev.2016.16038

Glossary

LSP3	Late shoot pruning 3 (three weeks after bud-break)
LSP2	Late shoot pruning 2 (two weeks after bud-break)
LSP1	Late shoot pruning 1 (one week after bud-break)
WP+T	Standard winter pruning and cluster thinning
WP	Standard winter pruning
Delph-3-glu	Delphinidin-3-O-glucoside
Mal-3-glu	Malvidin-3-O-glucoside
Pet-3-glu	Petunidin-3-O-glucoside
Cyan-3-glu	Cyanidin-3-O-glucoside
Peo-3-glu	Peonidin-3-O-glucoside
Delph-3-acet	Delphinidin-3-O-(6''-acetylglucoside)
Mal-3-acet	Malvidin-3-O-(6''-acetylglucoside)
Pet-3-acet	Petundin-3-O-(6''-acetylglucoside)
Cyan-3-acet	Cyanidin-3-O-(6''-acetylglucoside)
Peo-3-acet	Peonidin-3-O-(6''-acetylglucoside)
Delph-3-coum	Delphinidin-3-O-(6''-p-coumaroylglucoside)
Mal-3-coum	Malvidin-3-O-(6''-p-coumaroylglucoside)
Pet-3-coum	Petunidin-3-O-(6''-p-coumaroylglucoside)
Cyan-3-coum	Cyanidin-3-O-(6''-p-coumaroylglucoside)
Peo-3-coum	Peonidin-3-O-(6''-p-coumaroylglucoside)
Proc-B1	Procyanidin B1
Proc-rt1.84	unknown (similar to Procyanidin retention time 1.84 minute)
Proc-B2	Procyanidin B2
Proc-rt2.6	unknown (similar to Procyanidin retention time 2.6 minute)
Narin-chalc-glu	Naringenin-chalcone-4-O-glucoside
Quer-3-glu	Quercetin-3-O-glucoside
Quer-3-glr	Quercetin-3-O-glucuronide
Rutin	Quercetin-3-O-rutinoside
Myr- 3-glu	Myricetin-3-O-glucoside
Myr-3-glr	Myricetin-3-O-glucuronide
Kaem-3-glu	Kaempferol-3-O-glucoside
Kaemp-3-glr	Kaempferol-3-O-glucuronide
Coumarate-hex	Coumarate-hexoside (p-Coumaric acid glucoside)
Hydro-benz-hex	Hydroxybenzoate hexoside (Hydroxybenzoic acid 4-O-glucoside)
Caff-tart	caffeoyl-tartaric acid
Resv	Resveratrol



OPEN ACCESS

EDITED BY

Rakesh Kumar Shukla,
Central Institute of Medicinal and Aromatic
Plants, Council of Scientific and Industrial
Research (CSIR), India

REVIEWED BY

Alok Pandey,
Chhatrapati Shahu Ji Maharaj University,
India
Rajiv Kumar Yadav,
University of Allahabad, India
Vikas Dwivedi,
Agricultural Research Organization (ARO),
Israel

*CORRESPONDENCE

Iratxe Zarraonaindia
✉ iratxe.zarraonaindia@ehu.eus
Emma Cantos-Villar
✉ emma.cantos@juntadeandalucia.es

SPECIALTY SECTION

This article was submitted to
Plant Metabolism and Chemodiversity,
a section of the journal
Frontiers in Plant Science

RECEIVED 09 December 2022

ACCEPTED 06 February 2023

PUBLISHED 24 February 2023

CITATION

Zarraonaindia I, Cretazzo E, Mena-Petite A,
Díez-Navajas AM, Pérez-López U,
Lacuesta M, Pérez-Álvarez EP, Puertas B,
Fernandez-Díaz C, Bertazzon N and
Cantos-Villar E (2023) Holistic
understanding of the response of
grapevines to foliar application of
seaweed extracts.
Front. Plant Sci. 14:1119854.
doi: 10.3389/fpls.2023.1119854

COPYRIGHT

© 2023 Zarraonaindia, Cretazzo,
Mena-Petite, Díez-Navajas, Pérez-López,
Lacuesta, Pérez-Álvarez, Puertas,
Fernandez-Díaz, Bertazzon and
Cantos-Villar. This is an open-access article
distributed under the terms of the [Creative
Commons Attribution License \(CC BY\)](#). The
use, distribution or reproduction in other
forums is permitted, provided the original
author(s) and the copyright owner(s) are
credited and that the original publication in
this journal is cited, in accordance with
accepted academic practice. No use,
distribution or reproduction is permitted
which does not comply with these terms.

Holistic understanding of the response of grapevines to foliar application of seaweed extracts

Iratxe Zarraonaindia^{1,2*}, Enrico Cretazzo³, Amaia Mena-Petite⁴,
Ana M. Díez-Navajas⁵, Usue Pérez-López⁶, Maite Lacuesta⁴,
Eva Pilar Pérez-Álvarez⁷, Belén Puertas³,
Catalina Fernandez-Díaz⁸, Nadia Bertazzon⁹
and Emma Cantos-Villar^{3*}

¹Department of Genetics, Physical Anthropology and Animal Physiology, Faculty of Science and Technology, University of the Basque Country Universidad del País Vasco/Euskal Herriko Unibertsitatea (UPV/EHU), Leioa (Bizkaia), Spain, ²IKERBASQUE, Basque Foundation for Science, Bilbao, Spain, ³Instituto de Investigación y Formación Agraria y Pesquera (IFAPA) Rancho de la Merced, Consejería de Agricultura, Pesca, Agua y Desarrollo Rural, Junta de Andalucía, Cádiz, Spain,

⁴Department of Plant Biology and Ecology, Faculty of Pharmacy, University of the Basque Country Universidad del País Vasco/Euskal Herriko Unibertsitatea (UPV/EHU), Vitoria-Gasteiz (Araba), Spain,

⁵Department of Plant Production and Protection, Instituto Vasco de Investigación y Desarrollo (NEIKER)-Basque Institute of Agricultural Research and Development, Basque Research and Technology Alliance (BRTA), Arkaute (Araba), Spain, ⁶Department of Plant Biology and Ecology, Faculty of Science and Technology, University of the Basque Country Universidad del País Vasco/Euskal Herriko Unibertsitatea (UPV/EHU), Leioa (Bizkaia), Spain, ⁷VIENAP Group, Instituto Vasco de Investigación y Desarrollo (ICVV), Carretera de Burgos, Logroño, Spain, ⁸Instituto de Investigación y Formación Agraria y Pesquera (IFAPA) El Toruño, Consejería de Agricultura, Pesca, Agua y Desarrollo Rural, Junta de Andalucía, Cádiz, Spain, ⁹The Council for Agricultural Research and Economics (CREA), Research Centre for Viticulture and Enology, Conegliano, Italy

Viticulture is highly dependent on phytochemicals to maintain good vineyard health. However, to reduce their accumulation in the environment, green regulations are driving the development of eco-friendly strategies. In this respect, seaweeds have proven to be one of the marine resources with the highest potential as plant protective agents, representing an environmentally-friendly alternative approach for sustainable wine production. The current work follows an interdisciplinary framework to evaluate the capacity of *Ulva ohnoi* and *Rugulopteryx okamurae* seaweeds to induce defense mechanisms in grapevine plants. To our knowledge, this is the first study to evaluate *Rugulopteryx okamurae* as a biostimulator. This macroalgae is relevant since it is an invasive species on the Atlantic and Mediterranean coast causing incalculable economic and environmental burdens. Four extracts (UL1, UL2, RU1 and RU2 developed from *Ulva* and *Rugulopteryx*, respectively) were foliar applied to Tempranillo plants cultivated under greenhouse conditions. UL1 and RU2 stood out for their capacity to induce defense genes, such as a *PR10*, *PAL*, *STS48* and *GST1*, mainly 24 hours after the first application. The increased expression level of these genes agreed with i) an increase in *trans*-piceid and *trans*-resveratrol content, mainly in the RU2 treated leaves, and, ii) an increase in jasmonic acid and decrease in salicylic acid. Moreover, an induction of the activity of the antioxidant enzymes was observed at the end of the experiment, with an increase in superoxide dismutase and catalase in the RU2-treated leaves in particular. Interestingly, while foliar fungal diversity was not influenced by the treatments, alga extract amendment modified fungal composition, RU2 application enriching the

content of various groups known for their biocontrol activity. Overall, the results evidenced the capacity of *Rugulopteryx okamurae* for grapevine biostimulation, inducing the activation of several secondary metabolite pathways and promoting the abundance of beneficial microbiota involved in grapevine protection. While further studies are needed to unravel the bioactive compound(s) involved, including conducting field experiments etc., the current findings are the first steps towards the inclusion of *Rugulopteryx okamurae* in a circular scheme that would reduce its accumulation on the coast and benefit the viticulture sector at the same time.

KEYWORDS

Ulva ohnoi, *Rugulopteryx okamurae*, biostimulation, PR protein genes, stilbenes, jasmonic acid, superoxide dismutase, microbiota

Introduction

Seaweeds are macroalgae with high nutritional, nutraceutical and medicinal properties. Their use as fertilizers in agriculture has evolved recently as they are beneficial to crops in several ways. They stimulate seed germination, enhance plant health and growth through shoot and root elongation, improve water and nutrient uptake by the plant, promote frost and saline resistance, and remediate pollutants from contaminated soils (Beckers and Spoel, 2006). In addition, polysaccharides (e.g. ulvan, laminarin) or lipids (e.g. terpenes, fucoxanthines) extracted from seaweed have proven to induce resistance towards phytopathogenic organisms by stimulating the natural defenses of plants (Nabti et al., 2017). Plant biostimulants are “fertilizing products able to stimulate plant nutrition processes independently of the products’ nutrient content” according to the recent European Union regulation (<https://eur-lex.europa.eu/legal-content/EN/TXT/PDF/?uri=CELEX:32019R1009&from=EN>). Based on the European Commission report, seaweed extracts, including both macroalgae and microalgae, make up to 40% of the total biostimulant market (European Commission 2009) (https://eur-lex.europa.eu/resource.html?uri=cellar:5aa49d31-ec29-11e5-8a81-01aa75ed71a1.0001.02/DOC_3&format=PDF). The exposure of plants to seaweed-derived products induces the transduction of various plant signaling pathways, which leads to the synthesis and synchronized accumulation of defensive molecules, some of which play a structural role, while others exert a direct antimicrobial function (Stadnik and de Freitas, 2014; Bouissil et al., 2019). Therefore, seaweed application is considered one of the most

promising and sustainable alternative strategies for protecting crops against biotic and abiotic stressors.

The edible green seaweed of the genus *Ulva* belongs to the Ulvaceae family of green macroalgae and is one of the most common shallow-water seaweeds found around the world. *Ulva* species have been shown to contain several direct antifungal compounds, such as proteins, fatty acids and aromatic compounds, many of which are suggested to have direct antifungal properties (Shomron et al., 2022). Ulvan is the main water-soluble, sulfur-containing polysaccharide in *Ulva*. Ulvan extract has been shown to activate plants’ jasmonic acid signaling pathway, involved in the induction of defense mechanisms (Beckers and Spoel, 2006). Moreover, ulvan protected grapevines from powdery mildew disease and *Botrytis cinerea* pathogen (Jaulneau et al., 2011; Shomron et al., 2022). In fact, this polysaccharide capacity to elicit plant immune responses has been shown to be a promising way to reduce agricultural reliance on traditional pesticide treatments (Kidgell et al., 2019).

Rugulopteryx okamurae is a brown alga belonging to the Dictyotaceae family, originally from the coasts of the warm and temperate northwestern Pacific Ocean. It was introduced to the Mediterranean through the Strait of Gibraltar, where it has found a highly favorable environment. From 2015 to 2020, it exhibited extensive northerly and southerly geographical expansion, along both the Atlantic and the Mediterranean coasts, causing a considerable negative environmental impact. In 2020 it was ranked among the most invasive non-indigenous species in the Mediterranean Sea and included in the Spanish Catalog of Invasive Exotic Species, since it represents one of the main threats to the biodiversity in the Mediterranean (García-Gómez et al., 2020; Santana et al., 2022). Five thousand tons of this Asian alga were removed from the beaches of Ceuta (North of Africa, Spain) in 2015, and 400 tons from the beaches of Tarifa (Andalucía, Spain) in July 2020 alone (Personal communication Dr. Hachero-Cruzado). Thus, the valorization of the biomass of this macroalgae can provide an incentive for its withdrawal and control. Regarding its biochemical composition and bioactivity, little is yet known. Recently, Cuevas et al. (2021) reported the anti-inflammatory

Abbreviations: *t*-caftaric, *trans*-caffeoyltartaric acid; *t*-coumaric, *trans*-coumaroyltartaric acid; *c*-coumaric, *cis*-coumaroyltartaric acid; DW, dry weight; FW, fresh weight; CK, Cytokinins; *t*-Z, *trans*-zeatin; iP, isopentenyl adenine; ZR, zeatin riboside; IAA, indole-3-acetic acid; ABA, abscisic acid; JA, jasmonic acid (JA); SA, salicylic acid; SOD, superoxide dismutase; APX, ascorbate peroxidase; CAT, catalase; GR, glutathione reductase; ROS, reactive oxygen species.

capacity of several terpenoids derived from this alga. Similar to other species classified within brown seaweeds, alginates and fucoidans are expected to be present in *Rugulopteryx okamurae*. Both polysaccharides, extracted from the most widely studied brown algae, *Ascophyllum nodosum* and *Laminaria digitata*, have already proven their biostimulant activity (Bittkau et al., 2020; Samuels et al., 2022). However, to our knowledge, no studies have analysed *Rugulopteryx okamurae* fertilizer or its biostimulant properties in agriculture.

Viticulture is a sector with great socioeconomic importance worldwide, Europe having the largest cultivated area, the top wine producing countries being Italy, France and Spain (<https://www.oiv.int/what-we-do/statistics>). However, grapevine functioning, development and production face growing pressures associated with abiotic (drought, salt, mineral nutrition disturbances, light and temperature) and biotic (wounding, pathogens, and herbivores) stressors, all of which contribute to the overuse of chemical fertilizers and synthetic pesticides (Samuels et al., 2022). The use of biostimulants derived from algae applied as foliar sprays onto grapevines could be a suitable strategy to promote sustainability in viticulture. These substances have been shown to affect vine growth parameters (Salvi et al., 2019; Monteiro et al., 2022; Samuels et al., 2022), secondary metabolites such as polyphenolic compounds (Krzyzaniak et al., 2018), antioxidant enzymes and hormones (Salvi et al., 2019; Monteiro et al., 2022; Samuels et al., 2022), and increase the abundance of particularly beneficial microbial groups (Perazzolli et al., 2020). All in all, this could enhance the protection of grapevines against stressors and thereby reduce the accumulation of chemical compounds in soil and vines.

Seaweed extracts, or purified molecules from them, are able to induce defense reactions through a cascade of signaling events previously described (Delaunois et al., 2014; Bodin et al., 2020). However, despite the great interest in developing and testing new seaweed extracts as biostimulants, few well-characterized products with reliable performance are available on the market, with those that are deriving mainly from *Ascophyllum nodosum* (Jindo et al., 2022). Therefore, the objective of the current work is to provide an comprehensive overview of the vine response to seaweed application by studying the biostimulant efficiency of *Ulva ohnoi* and *Rugulopteryx okamurae* extracts through different layers (genetics, plant physiology, secondary metabolites and microbiology) to provide insights into their activity. With this aim in mind, four crude extracts (two per macroalgae) were developed and biochemically characterized. Then, the four crude seaweed extracts were foliar applied to vines of a Tempranillo (*Vitis vinifera* L.) cultivar under greenhouse-controlled conditions. The immune and physiological response of the vines after one or two foliar applications was addressed by targeting the expression of immune-related genes, phenolic compounds, phytohormone levels and oxidative-related enzymes. The implications for vine development were also addressed (e.g. plant growth and photosynthetic capacity). In addition, the impact of seaweed on leaf fungal diversity and structure was evaluated through Next Generation Sequencing. Reducing the dependence of the

viticultural sector on chemical inputs while contributing to the blue bioeconomy will help in achieving the objectives of the European Green Deal, which seeks to transition to a green, circular and carbon neutral EU.

Material and methods

Algae extracts elaboration and biochemical composition

The green macroalgae *Ulva ohnoi* was provided by “La Huerta Marina” (Huelva, Spain, 7° 09′ 41.8″ W, 37° 15′ 20.9″ N). The brown *Rugulopteryx okamurae* macroalgae was collected in the area near Algeciras (Cadiz, Spain, 5° 25′ 34.75″ W, 36° 4′ 37.56″ N). After harvesting, the seaweed biomass was rinsed with tap water, freeze-dried (Cryodos, Telstar, Spain) and milled to a fine powder and kept in dry conditions until the preparation of the extracts.

Two different extracts were generated with each alga, hereafter UL1 and UL2 for *Ulva ohnoi*, and RU1 and RU2 for *Rugulopteryx okamurae*. UL1 was provided by “La Huerta Marina” (ECOALGA[®], Huelva, Spain) and was formulated without the addition of conserving agents to prevent any possible interference. UL2 extract was generated following the protocol of Coste et al. (2015) with modifications. Briefly, 50 g of freeze-dried algae were combined with 500 mL of milliQ water (70 °C, 2 hours, and shaking) twice. The aqueous solution was frozen and freeze-dried. RU1 extraction started from 50 g of algae with 500 mL of milliQ water (70 °C, 2 hours, and shaking). The residue was re-extracted with a water:ethanol (20:80) solution. The two liquid phases were combined, and after lyophilization, a crude extract of *Rugulopteryx* was obtained. RU2 was created following the same protocol as for UL2.

The composition of each algae extract was characterized. Their ash content was measured by heating the sample overnight in a furnace at 525 °C, and the content was determined gravimetrically. CNHS content was determined by the Institute of Marine Sciences of Andalusia (ICMAN-CSIC) using a CHNS elemental analyzer (Thermo Fisher Scientific, USA). The soluble proteins present in the extracts were calculated from the nitrogen content. Lipids were measured using methods described in (Folch et al., 1957). The total carbohydrate content was determined using the phenol-sulfuric acid method (DuBois et al., 1956). In addition, L-fucose was determined following a method developed by Dische and Shettles (1948) and modified according to January et al. (2019) for microplates. Uronic acid was evaluated by a method first developed by Dische (1947) and later optimized by Cesaretti (2003) using glucuronic acid as a standard. The content of sulfates in the different algae extracts was determined following the protocol described in Torres et al. (2021).


























Macroelements (Ca, K, Mg, P, Na), microelements (Fe, Mn, Cr, Mo, Cu, Zn, and Se) and heavy metals (Cd, Hg, Pb, and As) were simultaneously analyzed at the ICMAN-CSIC by Inductively Coupled Plasma Optical Emission spectrometry (ICP-OES) using a Perkin-Elmer Optima 4300 DV spectrometer (Shelton, CT, USA).

Plant material, greenhouse treatments and sampling

Grapevine plants (*Vitis vinifera* L. cv. Tempranillo grafted on R-110 rootstock) provided by a commercial nursery (Vitis Navarra, Navarra, Spain) were grown in a level 2 biosafety greenhouse. The grapevines were placed in 5 L pots in an enriched nutrient substrate containing organic matter 90 %, Sphagnum peat (160 g/L), calcium carbonate (7 g/L), NPK fertilizer (1.5 g/L) and trace elements (PotgrondH, Klasmann-Deilmann GmbH, Germany). The plants were grown for 2 months with a 16h day/8h night photoperiod, at an average room temperature of 18 °C, and were irrigated to field capacity when necessary.

Plants with 10-12 leaves were used for the experiment (75 plants). An initial foliar treatment of water (CT), UL1, UL2, RU1 or RU2 was applied to the grapevines (Figure 1) at a concentration of 6 g/L. All the treatments contained 0.1 % of

retenol® (Daymsa, Zaragoza, Spain) as an adjuvant. A batch of the plants received a second application six days after the first one at the same dose (6 g/L). The plants that received either one or two applications per treatment (N= 5 plants, per treatment and application) were used to evaluate gene expression and polyphenols 24 and 48 hours after each application (referred as TTO_1, 24h and TTO_2, 48h, Figure 1). The evaluation of hormones was performed at TTO_1, 24h. The 4th and 5th leaf starting from the apex was collected at each time point, respectively. Additional plants receiving two applications per treatment were evaluated at the end of the experiment (12 days after first application, TTO_2, 144h) for oxidative enzyme determination (5th leaf), microbiota analysis (4th-8th leaves) and physiological parameters including plant height, root weight and photosynthetic pigments. The leaf samples collected were frozen in liquid nitrogen and stored at -80 °C until analysis.

N Plants	FOLIAR TREATMENT DAY 0	TTO_1		FOLIAR TREATMENT DAY 5	TTO_2		
		Analysis			Analysis		
		24h	48h		24h	48h	144h
 X5	Water 	○●□	○●				
		N=5					
 X5	UL1 	○●□	○●				
		N=5					
 X5	UL2 	○●□	○●				
		N=5					
 X5	RU1 	○●□	○●				
		N=5					
 X5	RU2 	○●□	○●				
		N=5					
 X10	Water 			Water 	○●	○●	▽▲◎X
				N=5		N=5	
 X10	UL1 			UL1 	○●	○●	▽▲◎X
				N=5		N=5	
 X10	UL2 			UL2 	○●	○●	▽▲◎X
				N=5		N=5	
 X10	RU1 			RU1 	○●	○●	▽▲◎X
				N=5		N=5	
 X10	RU2 			RU2 	○●	○●	▽▲◎X
				N=5		N=5	

Water: plants treated with water (Control), UL1: plants treated with UL1, UL2: plants treated with UL2, RU1: plants treated with RU1, RU2: plants treated with RU2. Symbols: ○, Defense genes; ●, Polyphenols; □, Hormones; ▽, photosynthetic pigments; ▲, Antioxidant enzymes; ◎, Plant physiology; X, Fungal community.

FIGURE 1
Experimental design.

Gene expression analysis

Expression changes of fifteen defense and stress-related genes (Table 1) were quantitatively determined by real-time PCR assay (RT-qPCR). More specifically, this evaluated the following: the expression of six genes encoding pathogenesis-related-proteins (PR) (Beta-1,3-glucanase (PR2), Chitin binding Chitinases type I, II (PR4), Thaumatin-like/Osmotin (PR5), Proteinase inhibitor (PR6), Chitinase type III (PR8), Ribonuclease-like (PR10)); four genes from the phenylpropanoid pathway (phenylalanine ammonia lyase (PAL), and stilbene synthase group A (STS1), B (STS16) and C (STS48); three genes involved in flavonol and anthocyanin biosynthesis (chalcone synthase1 (CHS1), dihydroflavonol reductase (DFR), leucoanthocyanidin dioxygenase (LDOX); a gene involved in redox status regulation (glutathione-S-transferase (GST1); and a transcription factor gene (WRKY1). Reactions were carried out in a CFX Connect Real-Time PCR system (Bio-Rad Laboratories, Hercules, CA, USA). Each assay was done in a final volume of 10 μ L, consisting of 5 μ L SsoAdvanced Universal SYBR Green Supermix (Bio-Rad Laboratories, Hercules, CA, USA), 2 μ L diluted cDNA template, 400 nM of each primer and nuclease free water. The thermal cycling conditions were as follows: an initial denaturation phase at 95 °C for 3 mins, followed by 39 cycles at 95 °C for 15 s and 60 °C for 30 s. According to the melting temperature, for some primer pairs the 30 s annealing-extension step was split into two sub-steps at 55 °C (10 s) and 60 °C (25 s), respectively. At the end of each RT-qPCR run, the specificity of the primer annealing was confirmed by melting curves.

Two technical replicates were run for each of the independent biological replicates, and the geometric mean of the expression ratios of three reference genes (Table 1) was used to normalize transcript expression levels. The comparative Ct ($2^{-\Delta\Delta Ct}$) method was used to calculate the transcript expression levels, as all the genes showed similar amplification efficiencies (between 90 and 100 %). The expression profile of defense marker genes was determined by comparing treated and untreated plants at each time point. A heatmap to visualize under- and overexpression of genes was generated using the Heatmapper web server (<http://www.heatmapper.ca/>).

Phenolic compounds

Polyphenols were extracted from the leaves following the method described by Krzyzaniak et al. (2018). Briefly, 50 mg of freeze-dried powdered leaves was extracted with 1 mL of methanol for 15 min at 22 °C in an ultrasonic bath. The supernatant was recovered and the process was repeated four times. The supernatants were evaporated, redissolved in methanol:water (1:5), and then filtered through a 0.22 μ m filter (PTFE Teknokroma, Barcelona, Spain). The samples (20 μ L) were analyzed using a Waters HPLC system (Milford, MA, USA) equipped with a model 1525 pump, W2707 injector, and Waters 2996 photodiode detector and a Mediterranean Sea C18 column (Tecknokroma, Barcelona, Spain) (RP-18, 25 \times 0.46 cm; 5 μ m particle size) with a precolumn of the same material.

TABLE 1 Defense and stress-related genes studied.

Pathway	Gene name	Code	Primers from
PR protein	PR2 (Beta-1,3-glucanase)	PR2	Dufour et al., 2016
	PR4 (Chitin binding Chitinases type I, II)	PR4	Dufour et al., 2016
	PR5 (Thaumatin-like/Osmotin)	PR5	Dufour et al., 2016
	PR6 (Proteinase inhibitor)	PR6	Bertazzon et al., 2019
	PR8 (Chitinase type III)	PR8	Dufour et al., 2016
	PR10 (Ribonuclease-like)	PR10	Dufour et al., 2016
Phenylpropanoid metabolism	phenylalanine ammonia lyase	PAL	Repetto et al., 2012
	stilbene synthase (group A)	STS1	Sparvoli et al., 1994
	stilbene synthase (group B)	STS16	Vannozzi et al., 2012
	stilbene synthase (group C)	STS48	Vannozzi et al., 2012
Flavonols and anthocyanins biosynthesis	chalcone synthase1	CHS1	Gutha et al., 2010
	dihydroflavonol reductase	DFR	Gutha et al., 2010
	leucoanthocyanidin dioxygenase	LDOX	Gutha et al., 2010
Redox status regulation	glutathione-S-transferase	GST1	Dufour et al., 2016
	WRKY1 transcription factor	WRKY1	Repetto et al., 2012
Reference	cytochrome oxidase	COX	Bertazzon et al., 2012
	pyruvate decarboxylase	PDC	Bertazzon et al., 2012
	glyceraldehyde-3-phosphate dehydrogenase	GAPDH	Bertazzon et al., 2012

Hydroxycinnamic acids were quantified at 320 nm as caffeic acid, while stilbenes were quantified at 306 nm as resveratrol. Concentrations were expressed in mg/L. A one-way analysis of variance (ANOVA) of the mean values was used to test for differences between time points and treatments. Significant results ($p \leq 0.05$) were then evaluated with Tukey's test using Statistix version 9.0 (Analytical Software, Tallahassee, FL, USA).

Endogenous plant hormones

The main classes of plant hormones, namely cytokinins [*trans*-zeatin (t-Z), zeatin riboside (ZR) and isopentenyladenine (iP)], indole acetic acid (IAA), abscisic acid (ABA), jasmonic acid (JA) and salicylic acid (SA), were extracted and analyzed at the first sampling point (TTO_1, 24h, [Figure 1](#)) as described previously in [Albacete et al. \(2008\)](#) with some modifications. Lyophilized plant material (50 mg) was homogenized in liquid nitrogen and incubated in 1 mL of cold (-20 °C) extraction mixture of methanol:water (80:20) for 30 min at 4 °C. Solids were separated by centrifugation (20,000 g, 15 min at 4 °C) and re-extracted for another 30 min at 4 °C with 1 mL of extraction solution. Pooled supernatants were passed through Sep-Pak Plus C₁₈ cartridges (previously conditioned with 3 mL of extraction buffer) to remove interfering lipids and some plant pigments. The supernatant was collected and evaporated under vacuum at 40 °C. The residue was dissolved in 1 mL methanol:water (20:80) solution using an ultrasonic bath. The dissolved samples were filtered through 13 mm diameter Millex filters with a 0.22 µm pore size nylon membrane (Millipore, Bedford, MA) and placed into opaque microcentrifuge tubes. Ten microliters of filtered extract were injected into an ultra-high performance liquid chromatography (UHPLC) system coupled with mass spectrometry (MS) consisting of an Accela Series U-HPLC (ThermoFisher Scientific, Waltham, MA) coupled to an Exactive mass spectrometer (ThermoFisher Scientific, Waltham, MA) using a heated electrospray ionization (HESI) interface. Mass spectra were obtained using the Xcalibur software version 2.2 (ThermoFisher Scientific, Waltham, MA). To quantify plant hormones, calibration curves were constructed for each analyzed component (0, 1, 10, 50 and 100 µg/L).

SPSS 28.0 (IBM Corp. Armonk, NY: IBM Corp, USA) was used for the statistical analysis. A one-way analysis of variance (ANOVA) of mean values was used to test for differences between treatments. Tukey's test was used to compare all the samples tested when significant differences were observed by ANOVA ($p \leq 0.05$).

Antioxidant enzymes

The activity of enzymes including superoxide dismutase (SOD, EC 1.15.1.1), ascorbate peroxidase (APX, EC 1.11.1.11), catalase (CAT, EC 1.11.1.6) and glutathione reductase (GR, EC 1.6.4.2) was determined as described in [Pérez-López et al. \(2009\)](#). Briefly, grinded leaf tissue (0.15 g fresh weight) was extracted in a specific buffer (3 mL) for each enzyme extraction. The homogenates were

centrifuged at 16,100 g for 25 min. SOD activity was assayed by the ferricytochrome-c reduction spectrophotometric test, using xanthine/xanthine oxidase as the source of superoxide radicals. One unit of SOD was defined as the amount of enzyme that inhibited the rate of ferricytochrome-c reduction by 50 %. CAT activity was measured spectrophotometrically, by monitoring the disappearance of H₂O₂ at 240 nm. To measure GR activity, the GSSG (oxidized glutathione) dependent oxidation of NADPH was monitored by the decrease in absorbance at 340 nm at 25 °C. APX activity was assayed by measuring the oxidation of ASA (ascorbate) at 290 nm.

SPSS 28.0 (IBM Corp. Armonk, NY: IBM Corp, USA) was used for the statistical analysis. A one-way analysis of variance (ANOVA) of mean values was used to test for differences between treatments. Tukey's test was used to compare all the samples tested when significant differences were observed by ANOVA ($p \leq 0.05$).

Vine development and photosynthetic pigments

Plant growth parameters were evaluated, determining the number of leaves per plant and the stem height (cm) at the end of the experiment (TTO_2, 144h, [Figure 1](#)). In addition, the root system was weighed (fresh weight, FW) and then oven dried at 65 °C for at least 72 hours (dry weight, DW) to calculate the FW/DW ratio.

Measurements of the photochemical efficiency of photosystem II (ϕ_{PSII}) and the leaf chlorophyll level (SPAD index) were performed *in situ* by a FluorPen FP 100 fluorometer (Photon Systems Instruments, Brno, Czech Republic) and a Konica-Minolta SPAD-502 Plus, respectively, in accordance with the authors [Pérez-López et al. \(2012\)](#) and [Yuan et al. \(2016\)](#).

Chlorophyll a, chlorophyll b, and carotenoids were determined according to [Pérez-López et al. \(2015\)](#). Briefly, 25 to 50 mg of ground powder were extracted with 1.5 mL dimethyl sulfoxide for 2 hours at 80 °C. Absorbances were determined at 750, 665, 649, and 480 nm.

Statistix version 9.0 (Analytical Software, Tallahassee, FL, USA) and SPSS 28.0, IBM Corp.) was used for the statistical analysis. Tukey's test was used to compare all the samples tested when significant differences were observed by ANOVA ($p \leq 0.05$).

Fungal community diversity and structure

A total of 180 mg of the ground homogenized leaf material collected at the end of the experiment (TTO_2, 144h, [Figure 1](#)) was used for total microbial DNA extraction with the innuPREP Plant DNA Kit (Analytik Jena, GmbH, Germany). Cell lysis was performed with the SDS-based OPT lysis buffer (provided in the kit) and a chemical disruption was included by beating samples in a Precellys (6500 rpm 3 x 30 s), before continuing the extraction following the manufacturer's instructions. DNA was quantified using a NanoDrop and the internal transcribed spacer 2 region (ITS2) was amplified with fITS7/ITS4 primers (GTGARTCATCGAATCTTTG/

TCCTCCGCTTATTGATATGC) (Ihrmark et al., 2012). The dual indexing of amplicons was performed using Nextera XT index kit v2 and libraries were purified using the CleanNGS kit (CleanNA, Waddinxveen, Netherlands). Cleaned products were mixed in equal molar proportions and sequencing was conducted in a MiSeq Illumina sequencer at the Genotyping Service of the University of the Basque Country (SGIKER) using MiSeq Reagent Kit v2 (PE 2 x 250 bp, 500 cycles). In addition, 50 mL of each treatment (UL1, UL2, RU1 and RU2), stored at -80 °C the day they were applied, were thawed and centrifuged at 4000 rpm for 20 min. The pellets were used for DNA extraction, ITS2 library preparation and MiSeq sequencing following the aforementioned procedure.

Sequences were quality trimmed and demultiplexed in QIIME 2 (Bolyen et al., 2019). DADA2 was used for denoising, merging, chimera removing and amplicon sequence variant (ASV) determination. The leaves and algae extracts were taxonomically classified against the UNITE database (v8 04.02.2020). The alpha diversity of the leaves was determined based on Faith's Phylogenetic Diversity index, while the Kruskal-Wallis test was used to test for significant differences in richness between treatments. Community composition differences based on Bray-Curtis index were visualized by principal coordinate analysis (PCOA) plots and significance was tested using the PERMANOVA test. The taxonomic composition of the leaf samples and algae extracts were inspected using bar plots. The taxa significantly differing in abundance between samples receiving algae extract and water treated samples were determined by linear discriminant analysis of effect size (Lefse) (<https://huttenhower.sph.harvard.edu/galaxy/>) setting the significance at a Kruskal-Wallis Bonferroni p value < 0.05, Wilcoxon test p < 0.01 and LDA > 2. In addition, differences between the mean relative abundance of particular beneficial groups known for their biocontrol activity were evaluated by the Mann-Whitney U test (significance threshold p < 0.05) using SPSS 28.0 (IBM Corp.).

Results & discussion

Characterization and biochemical composition of the extracts

The *Ulva ohnoi* extracts (UL1 and UL2) elaborated for this study contained lower total carbohydrate values (14–24 %) and a

higher protein content in the case of UL1 (Table 2) than the data previously described for this species (Kidgell et al., 2019). These discrepancies are not surprising, as protein and carbohydrate are highly dependent on external conditions such as temperature, light intensity and nutrient concentration in water, and therefore vary with the season and habitat of collection (Hentati et al., 2020; Lafarga et al., 2020). Comparing both *Ulva* extracts showed that UL1 had a higher concentration of uronic acid and sulfate than UL2 (Table 2). This may suggest a higher bioactivity of UL1 regarding antimicrobial activity (Ibrahim et al., 2022) as uronic acid and sulfate groups of ulvan, the main polysaccharide found in *Ulva* spp, have previously been described to be bioactive (Guidara et al., 2021).

In contrast to *Ulva*, the composition of *Rugulopteryx okamuræ* has been scarcely described. A recently published work by Cuevas et al. (2021) found 18.47 ± 0.35 % ashes, 9.76 ± 0.16 % proteins, and 11.63 ± 0.22 % lipids in lyophilized algae collected from the Cádiz coast (close to the studied area in the present work). In contrast, the RU1 and RU2 extracts studied here ranged between 26–32 % for ashes, 2–11 % for proteins, 4–9 % for lipids, and 12–15 % for carbohydrates. Sulfate and uronic acid content were higher in RU1 (59.07 % and 7.66 % respectively) than in RU2 (23.76 % and 4.39 % respectively), while fucose content was similar in both RU extracts. Importantly, RU2 exhibited a particularly high C/N ratio due to its low nitrogen content.

Macroelements, microelements, and heavy metals in the extracts were analyzed (Supplementary Table 1). Some data have previously been reported regarding the mineral composition in fresh algae (Maehre et al., 2014), but as far as we know, no data on the mineral composition of extracts have been published. UL1 was rich in Fe, Cr and Cu, while RU2 showed a high concentration of Na and As. Besides, the composition of the extracts complied with the legal requirements imposed by the EU to be used as fertilizers (<https://eur-lex.europa.eu/legal-content/EN/TXT/?uri=CELEX%3A52016PC0157>).

Gene expression

Most seaweed extracts are able to elicit specific responses from the innate immunity of plants. The activation of signaling pathways leads to an increased expression of gene encoding: (i) pathogenesis-

TABLE 2 Biochemical composition of *Ulva ohnoi* and *Rugulopteryx okamuræ* extracts.

	Ash (%)	Carbohydrates (%)	Proteins (%)	Lipids (%)	Sulfate (%)	Uronic (%)	Fucose (%)	C (%)	H (%)	N (%)	S (%)	C/N
UL1	26.16 (0.74)	23.79 (0.04)	24.09 (1.38)	5.81 (0.41)	55.18 (0.14)	19.78 (1.52)	7.75 (0.50)	31.58	5.97	4.38	0.81	7.21
UL2	49.03 (0.84)	13.87 (0.01)	5.01 (1.49)	5.43 (0.33)	43.49 (0.03)	12.30 (1.09)	7.74 (0.28)	15.28	4.52	0.91	4.62	16.79
RU1	26.36 (1.43)	14.40 (0.04)	10.23 (1.55)	4.21 (0.26)	59.07 (0.11)	7.66 (2.85)	1.07 (0.20)	37.50	6.12	1.86	0.15	20.16
RU2	32.00 (0.64)	12.79 (0.02)	2.31 (0.21)	8.29 (0.79)	23.76 (0.07)	4.39 (1.00)	1.01 (0.08)	27.98	5.25	0.42	0.04	66.62

Results are referenced to extract dry weight and expressed in % as the means of samples analyzed in triplicate (n=3) except for CHNS. Standard deviation between brackets.

related (PR) proteins with antifungal and antibacterial activities; (ii) defense enzymes such as phenylalanine ammonia lyase (PAL) and lipoxygenase (LOX), which determine the accumulation of phenylpropanoid compounds and oxylipins with antiviral, antifungal and antibacterial activities; and (iii) enzymes involved in the synthesis of terpenes, terpenoids and/or alkaloids (Vera et al., 2011; Bodin et al., 2020).

The analysis of the Tempranillo greenhouse plants showed that the pool of PR proteins behaved differently according to the treatment and sampling point. The most induced protein was the Ribonuclease-like PR10, which has been shown to be induced by pathogen attack in a wide variety of plant species (Hashimoto et al., 2004), suggesting that grapevines could recognize the algae extract compounds as an elicitor of plant defense (Delaunoy et al., 2014). PR10 was upregulated by RU2 and UL1 24h and 48h after the first application (TTO_1), and only 24h after a second application (TTO_2) (Figures 2A, D). Previous studies performed in grapevine showed a long-lasting overexpression of PR10 protein after treatment with *Ascophyllum nodosum*-derived extract, where PR10 was still induced up to two weeks post application (Bodin et al., 2020). Other PR proteins were either induced at 24h or at 48h after the application of the seaweed extracts. For instance, PR6, the main function of which is to inhibit proteolytic enzymes of fungal origin (Sels et al., 2008), was slightly upregulated 24h after the second application (TTO_2, 24h) by UL1 and UL2 (Figures 2A, B), while in RU2 its induction was detected 24h after first application

(TTO_1, 24h) (Figure 2D). PR4 and PR2, on the other hand, showed a later response. PR4 proteins, classified as endochitinases able to bind chitin (Brunner et al., 1998), were upregulated at 48h TTO_1 by UL1, UL2 and RU2 (Figures 2A, B, D). Similarly, PR2, involved in the degradation of the cell wall of invading fungal pathogens (Leubner-Metzger and Meins, 1999), was highly upregulated by RU2 at 48h TTO_2 with a fold induction as high as 5.29 (Figure 2D). In addition, it was upregulated to a lesser extent by UL1 at 48h TTO_1 (Figure 2A). In accordance with our results, PR2 has been shown to be induced by a sulfated laminarin elicitor in grapevine (Gauthier et al., 2014).

Expression of PR protein families is linked to hormonal signaling, being PR10, PR4 and PR6 induction mainly related to JA signaling, in contrast to PR2 regulation that is known to be more related to SA signaling (van Loon et al., 2006; Guerreiro et al., 2016; Dermastia et al., 2021).

The WRKY1 transcription factor was upregulated by UL1 24h after the second application (TTO_2, 24h, Figure 2A), and after 48h by RU1 (TTO_2, 48h, Figure 2C). This factor can correlate with PR10 expression and participates in the oxidative burst induction and in H₂O₂ cellular accumulation (Guo et al., 2014).

Overall, the remaining pathways studied, including anthocyanins and flavonols accumulation, and biosynthetic pathways of phenylpropanoids and stilbene synthesis, were mostly induced 24h after the algae applications. For instance, UL2 treatment generated a 6.87-, 4.63- and 5.46-fold inductions

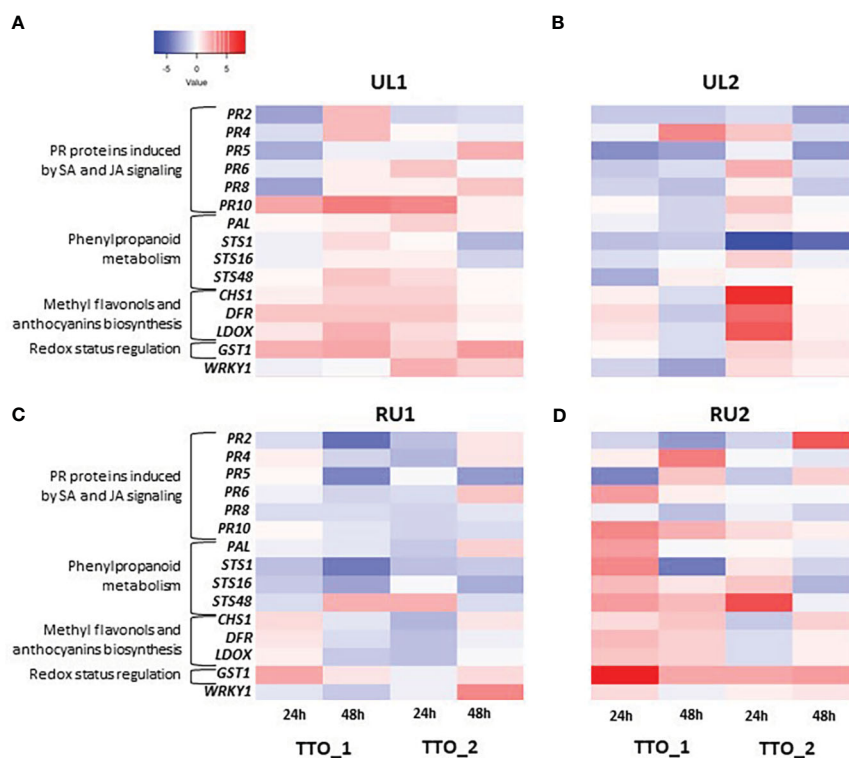


FIGURE 2

Transcript levels of defense-related genes in leaves induced by algae extract applications on grapevine plants (A) UL1; (B) UL2; (C) RU1; (D) RU2. Each column represents the sampling time, and each row represents one gene. A tree color scale was used to show fold induction of each gene (log transformed). The fold induction values were normalized to the reference genes PDC, GAPDH and COX and to water-treated leaves as the control samples.

for *CHS1*, *DFR* and *LDOX*, respectively (TTO_2, 24h, [Figure 2B](#)). Similar results were reported by [Bodin et al. \(2020\)](#), who found that two days after *A. nodosum* extract application *DFR* and *LDOX* genes were also up-regulated. The genes involved in the biosynthetic pathways of phenylpropanoids and stilbene synthesis were especially induced by RU2. *STS48* was particularly induced after two applications (TTO_2, 24h, [Figure 2D](#)), while *PAL* and *STS* proteins were mostly induced after the first treatment. *PAL* and *STS* overexpression correlated with *GST1* induction after *A. nodosum* extract treatment ([Bodin et al., 2020](#)). Similarly, *GST1* was highly upregulated at all sampling points by RU2 and to a lesser extent by UL1 ([Figures 2A, D](#)). GST proteins are involved in the detoxification of reactive molecules such as membrane lipid peroxides by conjugation to glutathione ([Conn et al., 2008](#)), in glutathione peroxidation to detoxify reactive oxygen species ([Bartling et al., 1993](#)), and in the transport and accumulation of phenylpropanoid compounds into the vacuole ([Tavares et al., 2013](#)). Importantly, both *PAL* and *STS* were reported to be major genes in the resistance against fungus of *Vitis vinifera* L. ([Kortekamp, 2006](#)). Similarly, the upregulation of *GST1* has been shown to correlate with stilbene-related genes in response to fungal infection ([Gruau et al., 2015](#); [De Bona et al., 2019](#)). Therefore, the results from the present study suggest the potential in particular of the *Rugulopteryx okamurae*-derived extract RU2 as a biostimulant, triggering grapevine defenses at early stages.

Phenolic compounds

In grapevine, polyphenols are present as constitutive compounds of the lignified organs (roots, canes, seeds, stems, ripe cluster stems) and/or as induced substances in leaves and berries. Among the phenolic families of compounds, the stilbenes are well-known phytoalexins counteracting oxidative stress and activating defense pathways ([Gabaston et al., 2017](#); [Šamec et al., 2021](#)).

Up to 132 phenolic compounds, including 40 stilbenes, have been described in grapevine leaves ([Goufo et al., 2020](#)). Flavonols (mainly quercetins) are usually found in leaves. However, their detection depends on both the grapevine variety and extraction method ([Fernandes et al., 2013](#)). In the present work, flavonols were only detected in a few samples and were under the limit of quantification. Two flavonols (quercetin-3-O-glucuronide and an unknown flavonol) were detected in the UL2 leaf samples 24h after the second treatment (TTO_2, 24h), coinciding with the strong induction of *CHS1*, *DFR* and *LDOX* genes observed at this sampling point for the leaves treated with this extract ([Figure 2B](#)).

The main polyphenols detected here in grapevine leaves were those belonging to hydroxycinnamic acids, such as *trans*-caffeoyltartaric acid (*t*-caftaric), *trans*-coumaroyltartaric acid (*t*-coumaric), and *cis*-coumaroyltartaric acid (*c*-coumaric) ([Table 3](#)). *t*-Caftaric acid was predominant among this family of compounds, ranging from 676 mg/kg DW (RU2, TTO_1, 48h) to 2889 mg/kg DW (Water, TTO_2, 24h). These compounds are known to play a role in epidermal UV-screening, and therefore reflect light conditions, but they are not commonly found to be involved in stress response ([Latouche et al., 2013](#)). Overall, the

measurements obtained in the present study were highly variable and dependent on the sampling date and treatment.

Regarding stilbenes, significant differences in the concentration of *t*-piceid and *t*-resveratrol were observed between treatments, especially after the first application (TTO_1, 24h). At this sample point, the leaf samples treated with RU2 extract showed the highest stilbene values among the treatments (8.65 and 40.57 mg/kg DW leaf of *t*-piceid and *t*-resveratrol, respectively), which coincides with the observed activation of the defense mechanisms associated with phenylpropanoid genes for this extract (*PAL*, *STS1* and *STS48*; [Figure 2D](#)). Similar results have been described for a commercial algae extract applied at 5 g/L dosage tested as an elicitor on Marselan plants ([Krzyzaniak et al., 2018](#)), where *t*-piceid reached 10 mg/kg DW after 24 hours of the treatment. However, 48h after the first treatment (TTO_1, 48h), the concentrations of stilbenes in the RU2 samples decreased to values similar to those found in the control plants ([Table 3](#)). While these data agree with what was described for *t*-resveratrol elicitation after a plant extract application in [Krzyzaniak et al. \(2018\)](#), conversely these authors described that *t*-piceid concentration was maintained 48h after the treatment. Unfortunately, the authors did not describe the composition of the product applied, and therefore it is not possible to make further comparisons. When studying the plants receiving two applications, the increase in stilbenes was again evident mainly after 24h (TTO_2, 24h, [Table 3](#)), especially in the UL1 leaf samples. *t*-Piceid was strongly induced in UL1, while *t*-resveratrol increased in UL1, RU1 and RU2, but was significant only for UL1 with regard to the control (water). After 48h (TTO_2, 48h) only UL1 maintained a high *t*-piceid concentration ([Table 3](#)).

Therefore, the results suggest that RU2 and UL1 were the extracts with highest capacity for phytoalexin production, inducing stilbene biosynthesis, and therefore showing promising results as biostimulant products.

Endogenous plant hormones

Phytohormones are key molecules involved in several processes throughout plant growth and development ([Ross et al., 2011](#); [De Diego et al., 2012](#)). They play an essential role in the ability of plants to respond to different stress situations, either abiotic (e.g. drought) or biotic (e.g. pathogen attack), by mediating a wide range of adaptive responses ([Santner and Estelle, 2009](#)). The complexity of plants' response includes hormone synthesis, transport and signaling pathways, and many interactions between them. In addition, hormone signaling and gene expression form a network in which relevant genes regulate hormone activities and *vice versa* ([Liu et al., 2017](#)). Gene expression results (Section 3.2) pointed to an early response of grapevine to algae amendment, and therefore in the present work the levels of the main phytohormones involved in plant growth regulation and plant defense mechanisms were studied in the samples from 24 hours after the first treatment (TTO_1, 24h).

The results show that the extracts significantly reduced the total content of hormones, this reduction ranging between 40 % in UL1 and RU2, and 50 % in UL2 and in RU1 treated plants, in comparison with the water-treated samples ([Figure 3](#)). SA was the

TABLE 3 Polyphenol content (mg/kg DW) in treated leaves at different sampling times.

TTO_1, 24h						
	Water	UL1	UL2	RU1	RU2	L.S
<i>t</i> -Caftaric acid	1905.6 (493.4) a	1154.2 (596.2) b	2245.2 (567.7) a	1901.2 (197.8) a	2204.4 (383.1) a	***
<i>t</i> -Coutaric Isom	65.97 (25.30)	49.66 (31.97)	53.87 (41.14)	58.75 (22.63)	82.43 (11.16)	n.s
<i>c</i> -Coutaric acid	176.37 (34.22) ab	134.22 (48.15) ab	114.66 (88.55) b	151.75 (13.09) ab	198.27 (29.04) a	**
<i>t</i> -Piceid	0.07 (0.00) b	1.16 (0.94) b	0.07 (0.00) b	0.07 (0.00) b	8.65 (6.52) a	***
<i>t</i> -Resveratrol	0.07 (0.00) b	21.18 (10.38) abc	7.42 (2.53) bc	28.32 (22.68) ab	40.57 (27.00) a	***
TTO_1, 48h						
	Water	UL1	UL2	RU1	RU2	L.S
<i>t</i> -Caftaric acid	1707.8 (337.5) a	938.8 (391.5) bc	1639.8 (869.5) ab	1067.5 (152.6) abc	676.4 (309.3) c	***
<i>t</i> -Coutaric Isom	82.45 (14.47) ab	67.53 (16.68) ab	87.29 (25.74) a	72.94 (13.45) ab	57.19 (19.39) b	*
<i>c</i> -Coutaric acid	169.06 (20.24) a	127.85 (31.87) ab	133.19 (41.14) ab	122.41 (18.98) ab	99.74 (36.57) b	**
<i>t</i> -Piceid	4.77 (1.24)	8.25 (7.12)	4.98 (2.15)	5.36 (4.76)	5.60 (4.49)	n.s
<i>t</i> -Resveratrol	16.58 (12.11)	12.05 (11.73)	10.77 (8.65)	25.04 (23.21)	10.03 (4.54)	n.s.
TTO_2, 24h						
	Water	UL1	UL2	RU1	RU2	L.S
<i>t</i> -Caftaric acid	2889.1 (447.2) a	1861.8 (1165.0) b	2107.2 (919.5) b	1838.8 (282.6) b	1726.6 (341.6) b	*
<i>t</i> -Coutaric Isom	84.08 (12.05)	73.64 (18.66)	71.54 (9.65)	70.63 (7.58)	67.88 (5.69)	n.s.
<i>c</i> -Coutaric acid	221.55 (31.61) a	151.36 (46.63) b	162.78 (45.10) b	152.07 (16.18) b	147.96 (7.15) b	***
<i>t</i> -Piceid	0.07 (0.00) c	10.42 (1.47) a	0.07 (0.00) c	0.07 (0.00) c	3.05 (0.65) b	***
<i>t</i> -Resveratrol	19.06 (13.11) ab	35.26 (24.97) a	10.02 (7.37) b	29.44 (7.91) ab	27.42 (10.25) ab	*
TTO_2, 48h						
	Water	UL1	UL2	RU1	RU2	L.S
<i>t</i> -Caftaric acid	1542.9 (645.5)	2416.0 (1082.0)	1921.1 (744.3)	1387.2 (192.4)	1587.4 (126.6)	ns
<i>t</i> -Coutaric Isom	63.11 (9.82) b	88.42 (17.10) a	80.91 (14.63) ab	70.97 (11.66) ab	73.93 (7.57) ab	*
<i>c</i> -Coutaric acid	141.83 (38.00) b	207.12 (56.25) a	180.77 (42.63) ab	141.54 (13.47) b	124.88 (50.78) b	**
<i>t</i> -Piceid	0.07 (0.00) b	11.62 (5.41) a	1.93 (1.44) b	2.47 (1.48) b	3.01 (1.65) b	***
<i>t</i> -Resveratrol	14.14 (7.77)	18.52 (12.65)	19.00 (16.39)	28.47 (15.42)	19.99 (12.55)	ns

Water: leaves treated with water (Control), UL1: leaves treated with UL1, UL2: leaves treated with UL2, RU1: leaves treated with RU1, RU2: leaves treated with RU2. Results are the means of three independent samples analyzed in triplicate. Standard deviations are indicated between brackets. Different letters for the same parameter denote significant differences ($p < 0.05$). Analysis of variance. Level of significance (LS): * $p < 0.05$, ** $p < 0.01$, *** $p < 0.001$; ns: not significant.

most abundant hormone, constituting 67 % of total hormone content found in the control plants and being the one that showed the highest decrease (by 50 % in the treated plants). The *t*-Z, which is considered one of the most active CK forms (Lacuesta et al., 2018), was the only CK detected in the Tempranillo leaf samples, iP and ZR being under the detection limit. Neither the *t*-Z levels nor the auxin IAA were significantly affected by the algae extract treatments (Figure 3).

JA was the only hormone to increase its content with the algae treatments when compared to water, especially in the UL1 and RU2 leaves. These plants were also the ones that showed the greatest decrease in ABA (Figure 3). These results reinforce the previously reported findings that ABA is an important signal in the activation

of plant defenses by a possible enhancement of JA synthesis (Adie et al., 2007; Trotel-Aziz et al., 2019).

JA has been reported to enhance the tolerance of grapevine foliar cuttings and vineyards to the pathogen *Erysiphe necator* in cv. Cabernet Sauvignon and has been associated with an increase in transcript levels of PR proteins, phytoalexin biosynthesis, and with the accumulation of stilbenes (Belhadi et al., 2006). Similar to the mentioned studied, JA induction corresponded with the up-regulation of *PR10* (in RU2 and UL1) and *PR6* (in RU2) (Figure 2D) 24 hours after the first application (TTO_1, 24h), as well as with the significant accumulation of stilbenes in the UL1 and RU2 samples (Table 3). In the same line, Cruz et al. (2019) evidenced that external applications of JA and methyl jasmonate (a derivative

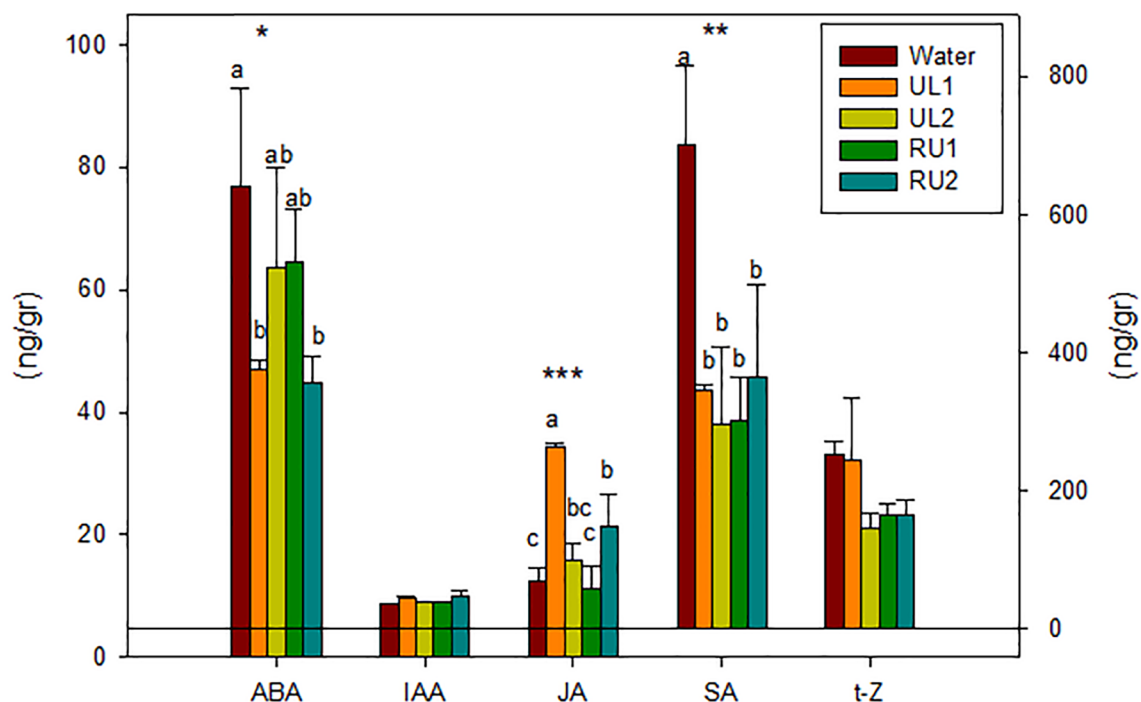


FIGURE 3

Leaves phytohormones content 24 hours after first treatment (TTO_1, 24h) (ng/g DW). ABA, Absciscic acid; IAA, Indolacetic acid; JA, Jasmonic acid; SA, Salicylic acid; t-Z, trans-zeatine. Analyses of variance. levels of significance (LS): * $p < 0.05$, ** $p < 0.01$, *** $p < 0.001$.

of JA) are potent elicitors that act as signaling molecules upon biotic stress and are involved in plant defense mechanisms leading to an amplified endogenous jasmonate response (Paolacci et al., 2017) as can also be seen in Figure 3, or triggering the synthesis of secondary compounds such as stilbenes (Table 3).

In contrast to the JA induction, SA content after the first application (TTO_1, 24h) decreased for all the algae treated samples compared to water. The studied Tempranillo plants seemed to be activating the SA-dependent defense response later in the experiment, as the SA induced gene *PR2* was found to be overexpressed at (TTO_1, 48h). Thus our results suggest that the JA signaling is negatively regulating the expression of SA-mediated defenses. The antagonistic activity of JA and SA signaling found in the present study after algae extract amendment has been previously evidenced by other authors after elicitors in grapevine and other species (Gupta et al., 2000; Kunkel and Brooks, 2002; Paolacci et al., 2017; Trotel-Aziz et al., 2019).

Overall, our results suggest that the seaweed extracts are mainly activating the defense mechanisms of grapevines through JA synthesis, RU2 and UL1 being the extracts that showed a higher hormonal response.

Enzymes related to plant defense

Increasing the activity of enzymes within the antioxidant defense system of the plant is considered to be an effective mechanism to combat the oxidative stress induced by various

stresses (e.g. drought, chilling, UV irradiation, exposure to intense light, wounding and pathogens) (Sharma et al., 2012). In the present work, the main antioxidant enzymes were measured, including GR, SOD, CAT and APX enzymes. These enzymes are known to be involved in scavenging the toxic ROS (reactive oxygen species). ROS drastically increase in plants in response to environmental stresses, being a main player in plant growth and the improvement of plant tolerance to stress (Das and Roychoudhury, 2014).

GR activity was not significantly modified by the treatments, but the lowest amounts were found in the CT samples (water) (Figure 4). A significant increase in SOD ($p < 0.001$) and CAT ($p < 0.05$) was observed in UL1, RU1 and RU2. However, APX significantly decreased in RU1 and RU2 ($p < 0.05$) (Figure 4). As it is known, SOD catalyzes the dismutation of the superoxide radical, generating H_2O_2 which is then eliminated by both APX and CAT, among other enzymes. The contrasting values observed in both RU1 and RU2 between SOD (increasing) and APX (decreasing) might suggest that they are promoting the accumulation of H_2O_2 . Importantly, H_2O_2 has been shown to inhibit pathogens directly or by generating other free radicals with antimicrobial activity that could also be toxic for fungi (Raj et al., 2018). Liu et al. (2015) demonstrated that *Vitis vinifera* genotypes resistant to *Plasmopara viticola* accumulated H_2O_2 , while the susceptible *Vitis vinifera* Pinot noir did not. Other authors have described an induction of SOD in grapevine leaves after infection with this fungus (Wang et al., 2022). A potential accumulation of H_2O_2 seems contradictory with the increase of CAT, since catalase

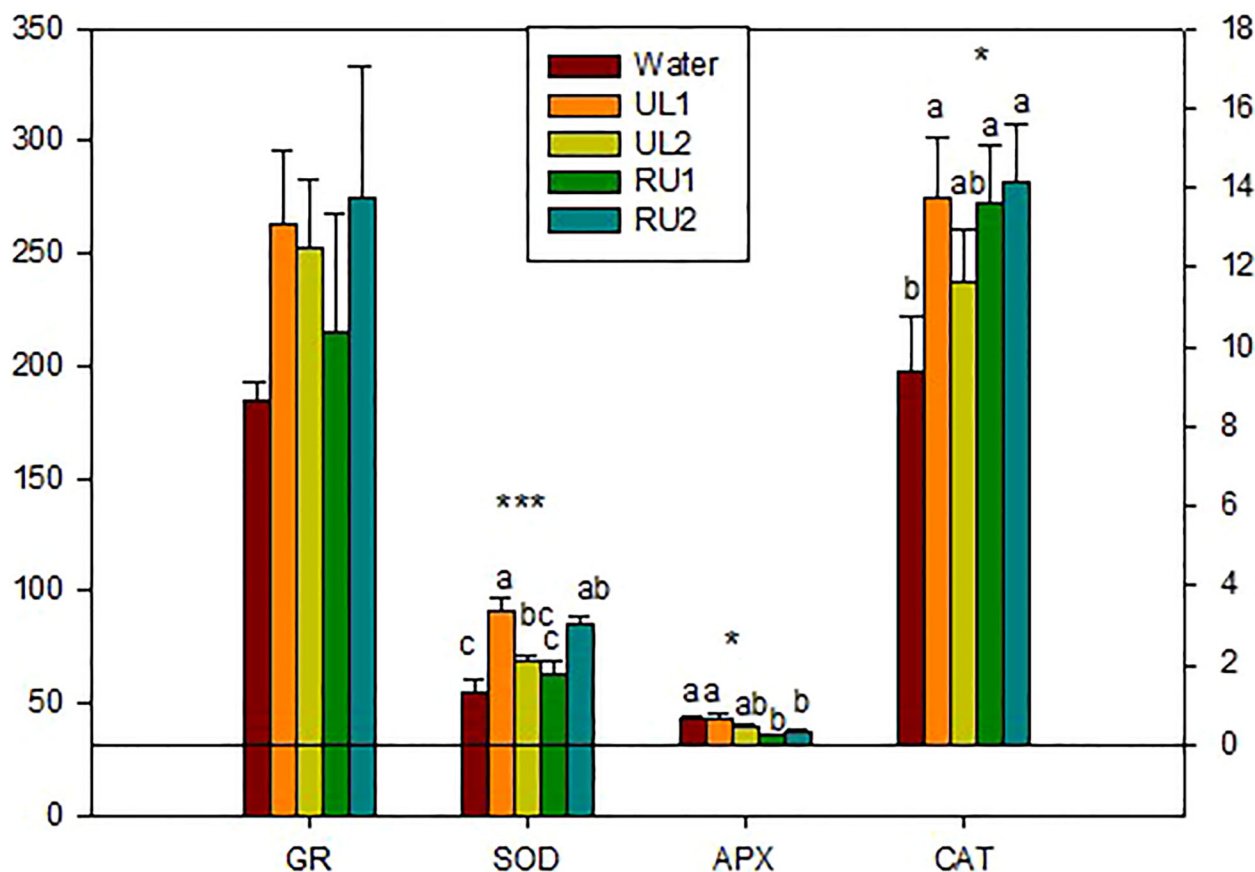


FIGURE 4

Enzymes related to plant defense at the end of the experiment. SOD, superoxide dismutase (U/mg protein); APX, ascorbate peroxidase (mmol Ascorbate/min mg protein); CAT, catalase (nmol H₂O₂/min mg protein); GR, glutathione reductase (nmol NADPH/min mg protein). Analyses of variance. levels of significance (LS): **p* < 0.05, ****p* < 0.001.

detoxifies H₂O₂. However, the reason for this discrepancy could be that CAT levels increase to eliminate the H₂O₂ produced due to higher photorespiration. At this point we cannot elucidate which are the specific molecules (polysaccharides, lipids, metals, among others) detected by the receptors of the host plant to induce the observed response. A direct measurement of the potential H₂O₂ accumulation in RU2 by chemiluminescence assay would be necessary to confirm the explanations raised.

Vine development and photosynthetic pigments

Many biostimulants are thought to enhance nutrition efficiency, biotic stress tolerance, crop yield, plant physiology (Sabir et al., 2014; Salvi et al., 2019) and plant growth (du Jardin, 2015; Yakhin et al., 2017). The analysis of the content of photosynthetic pigments is a direct indicator of the plant's ability to respond adequately to biotic stress since they are essential to synthesize the carbohydrates necessary for both plant growth and to serve as carbon skeletons for the different pathways of secondary metabolism.

The seaweed extracts applied in the present study, however, did not show a significant effect on i) growth parameters (the leaf

number/plant, stem height and root system biomass), ii) the composition of photosynthetic pigments (chlorophylls and carotenoids), or iii) the maximum photochemical efficiency in the light of photosystem II (ϕ_{PSII}), at the end of the experiment (TTO_2, 144h, [Supplementary Table 2](#)). These data suggest that the treatments performed were not efficient as biofertilizers, in agreement with the CK hormone data ([Figure 3](#)). Treating for longer periods or performing more intensive treatments might be necessary to observe changes in the morphophysiological characteristics of grapevines.

Leaf fungal community diversity and composition

Leaf-associated microorganisms are involved in the diffusion of xenobiotics and represent a barrier against pathogens by activating plant defenses and competing with pathogenic organisms (Bulgarelli et al., 2013; Trouvelot et al., 2014). The stimulation of the beneficial microbiota of the grapevine phyllosphere by protein-derived products, carbohydrate-based treatments and commercial elicitors has been previously evidenced in grapevines cultivated in greenhouses (Cappelletti et al., 2016) and field experiments

(Perazzolli et al., 2014; Nerva et al., 2019). This contributes to plant health by enhancing biocontrol activities against phytopathogens (Perazzolli et al., 2020). Seaweed extracts are therefore expected to alter the abundance of particular taxa in grapevine leaves, which could play an indirect role in their protection.

The results from the present study evidenced that the foliar treatments with algae extracts did not significantly alter the fungal phylogenetic diversity of grapevine leaves (Kruskal-Wallis $H=4.710$, $p\text{-value}=0.318$), although the RU1 samples showed the highest variability (Figure 5A). However, the fungal composition of the leaves (based on Bray-Curtis index) differed significantly between treatments (PERMANOVA pseudo- $F=3.927$, $p\text{-value}=0.001$). The samples associated with each of the treatments were grouped into separated clusters in the PCOA plot (Figure 5B). UL1 mycobiota composition differed the most from the water-treated samples. In agreement with this, LefSe analysis, comparing the relative abundances of fungal groups of the samples receiving the algae treatments with leaf samples receiving water (Supplementary Table 3), identified the highest number of biomarkers for UL1, which showed a significantly higher abundance of Sporidiobolaceae (genera *Apiotrichum* and *Rhodotorula*), an anti-phytopathogenic microorganism known to be common in grapes and leaves (Pinto et al., 2014), as well as members of Filobasidiaceae (*Filobasidium magnum* and *Naganishia albida*) and Rhynchogastremaceae (*Papiliotrema albida*) (Supplementary Table 3). However, the source of these groups is likely the algae phylloplane, as these were the most abundant families encountered when sequencing this algae extract (Supplementary Figure 1). The study of microbial consortia in seaweed has attracted considerable attention lately as a result of the capacity of seaweed endosymbiotic microorganisms to generate antimicrobial and antioxidant compounds, as well as other molecules with biotechnological applications (Ren et al., 2022). Although the characterization of *Ulva ohnoi* and *Rugulopteryx okamurae* macroalgae microbial consortia was beyond the scope of this study, the sequencing of the extracts was performed. Aside from the above-mentioned genera present in UL1, Saccharomycetes were abundant in the extracts (particularly in UL2, Supplementary

Figure 1). Importantly, the UL2 and RU2 Tempranillo leaf samples had an enrichment of *S. cerevisiae* compared to the control samples (Supplementary Table 2), with mean relative abundances of 18 % in UL2, 13 % in RU2 and 2 % in the water-treated samples (Table 4). Saccharomyces are part of the native microflora of grapevine leaves (Pinto et al., 2014). Therefore, aside from the accumulation of putative cells coming from the algae extract, the enrichment of *S. cerevisiae* in the leaf samples could in part be due to the response of the indigenous microbiota of the leaves to the treatments. While we cannot confirm *S. cerevisiae* activity, as amplicon sequencing method does not allow dead and active organisms to be discerned, studies conducted by (Mishko and Lutsky, 2020) evidenced that a pre-treatment of grape leaves with *S. cerevisiae* enhanced the immune response of a *Plasmopara viticola* resistant vine cultivar, while it induced phytoalexin synthesis (stilbenes) in a susceptible variety prior to the disease infection.

The seaweed treatments did not result in a clear shift in the abundance of various known biocontrol agents, such as *Trichoderma* (Pollard-Flamand et al., 2022), *Aureobasidium pullulans* (Harm et al., 2011), *Candida* (Sipiczki, 2006), among others (Table 4). These organisms were found in general at low abundances in the analyzed samples and showed a high variability within treatment plant replicates. However, other groups such as *Sporobolomyces*, known for their antifungal activity (Sipiczki, 2006), were particularly abundant in the RU2 samples compared with the water-treated leaves (Table 4). It was also noteworthy that *Debaryomyces hansenii* was significantly enriched in UL2 (0.68 % relative abundance), and particularly in RU2 leaves (2 %), while it was almost absent in the remaining treatments. Several strains within this genus exhibit antagonistic activity against fungal phytopathogens through diverse mechanisms, such as competition for nutrients and space, mycoparasitism, the secretion of antifungal substances (e.g. volatile organic compounds, glucanases, and killer toxins) or the induction of plants' immune response to pathogens (Fernandez-San Millan et al., 2020).

Further analysis is needed to confirm the functional activity and strain classification of the microbial changes induced by the

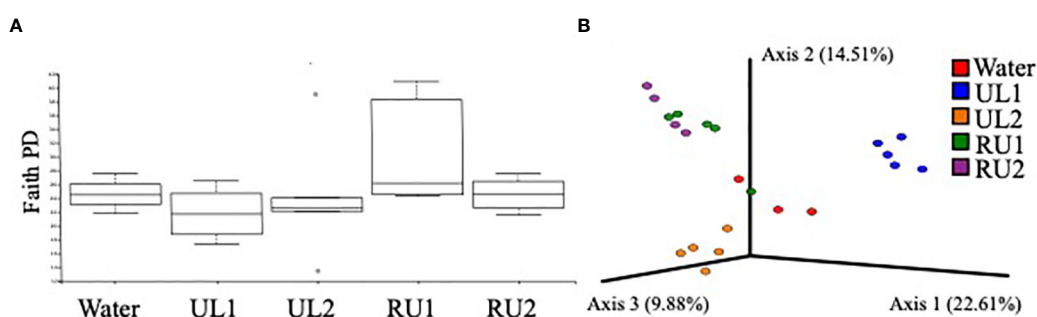


FIGURE 5

(A) Alpha diversity plot showing the mean fungal phylogenetic diversity by treatment. No significant differences in Faith PD index were observed between treatments (Kruskal-Wallis $H=4.710$, $p=0.318$). (B) PCOA plot showing fungal community composition dissimilarity between treatments (based on Bray-Curtis distance) at the end of the experiment (144h after the second application). Fungi composition significantly differed between treatments (PERMANOVA Pseudo- $F=3.927$, $p=0.001$). ASV tables were rarified to 20000 sequences per sample, so samples that did not reach that sequencing depth were excluded from the analysis.

TABLE 4 Mean relative abundance (%) and standard deviation of beneficial genera known to have antifungal or antagonistic activity.

	<i>Trichoderma</i>	<i>Aspergillus</i>	<i>Penicillium</i>	<i>Fusarium</i>	<i>Aureobasidium</i>	<i>Candida</i>	<i>Rhodotorula</i>	<i>Debaryomyces</i>	<i>Sporobolomyces</i>	<i>Saccharomyces</i>
Water	0.04 (0.06)	0.12 (0.04)	0.56 (0.46)	0.14 (0.24)	0.84 (0.96)	1.11 (1.93)	0.09 (0.16)	0.00 (0.00)	0.62 (1.07)	2.26 (1.97)
UL1	0.00 (0.00)	0.11 (0.11)	0.19 (0.07)	0.00 (0.00)	0.24 (0.41)	0.52 (1.02)	8.09 (1.07)	0.00 (0.00)	0.62 (0.47)	0.35 (0.45)
UL2	0.02 (0.05)	0.12 (0.13)	0.70 (0.33)	0.00 (0.00)	0.18 (0.34)	1.72 (1.81)	0.97 (0.82)	0.68 (0.69)	0.82 (0.78)	18.71 (4.72)
RU1	0.00 (0.00)	0.13 (0.15)	0.52 (0.39)	0.06 (0.08)	0.40 (0.30)	0.60 (0.58)	0.60 (0.43)	0.00 (0.00)	1.03 (0.59)	6.21 (5.51)
RU2	0.03 (0.05)	0.05 (0.04)	0.37 (0.14)	0.00 (0.00)	0.75 (0.87)	0.87 (0.96)	0.26 (0.30)	2.32 (2.28)	2.80 (1.29)	13.03 (6.61)

The different letters indicate the between treatments significance according to Mann-Whitney U 2-sided test.

treatments and their role in grapevine protection, but the results highlight that fungal composition is partially altered with the enrichment of particular beneficial species, predominantly after RU2 foliar applications.

Conclusion

In the current work, two crude extracts each from *Ulva ohnoi* and *Rugulopteryx okamurae* have been developed and biochemically characterized. The sulfate, uronic acid, fucose and metal content of *Rugulopteryx okamurae* have been described for the first time. However, a deeper characterization of the extracts' carbohydrates (laminarin, fucoidan, alginates) and lipids (fucoxanthine, fucosterol, glucolipids, terpenes and lipids from betaine) is required to establish a relationship between the seaweed composition and extract bioactivity.

The greenhouse assay conducted here on the Tempranillo variety suggests that the aqueous *Rugulopteryx okamurae* extract (RU2) induces grapevine defense and immunity genes, as well as secondary metabolites such as stilbenes, phytohormones and antioxidant enzymes involved in the protection and resistance to biotic/abiotic stress. In addition, RU2 enriched the abundance of fungal antagonists in the leaves. Further studies are needed to confirm the enhanced protection of the plants receiving RU2 extract, by evaluating the changes induced under pathogen inoculation. In addition, while the development of the vines was not altered by the algae extracts, further understanding of dosage and application spans, as well as the possible risks or benefits of RU2 for grapevine yield and grape quality would be necessary for its consideration as an alternative product with advantages for viticulture.

Evidencing *Rugulopteryx okamurae* efficacy as a biostimulator is a major finding as it would be a first step towards its inclusion in a circular scheme, reducing its accumulation in the coast and at the same time benefiting the viticulture sector.

Data availability statement

The data (raw sequences) presented in the study are deposited in Qiita database repository under study ID-1024 (<https://qiita.ucsd.edu/study/description/1024>) and in ENA database with accession number ERP143695 (<https://www.ebi.ac.uk/ena/browser/view/PRJEB58628>).

Author contributions

IZ, AD-N, AM-P, UP-L, ML and EP-A performed experiments (plants culture, development monitoring and sampling). CF-D and EC-V harvested/pick up the seaweed, performed the extracts and analyzed them. EC and NB performed analysis of gene expression. BP and EC-V developed the analysis of polyphenols. ML performed the analysis of hormones. UP-L performed the analysis of antioxidant enzymes. AM-P performed the vine development and photosynthetic pigments measurement. IZ performed the fungal community study.

EC-V, IZ, AD-N, EC, AM-P, UP-L, ML and EP-A contributed to the experimental design. EC-V, IZ, EC, AM-P, UP-L and ML contributed to data interpretation. IZ and EC-V contributed to draft the manuscript and drafted led the project. All authors contributed to the article and approved the submitted version.

Funding

This research has been supported by the Project SEAWINES PID2020-112644RR-C21 and -C22 financed by MCIN/AEI/10.13039/501100011033.

Acknowledgments

The authors thank Dr. Ismael Hachero-Cruzado for his support in the harvest of *Rugulopteryx okamurae* and David Gonzalez from “La Huerta Marina” for providing *Ulva ohnoi*. We are also grateful to the Sequencing and Genotyping Unit—SGIker from UPV/EHU for their technical support. Authors ML, AM-P and UP-L are part of the consolidated research group IT1682-22 and IZ belongs to IT1571-22 of the Basque University System.

References

- Adie, B. A. T., Pérez-Pérez, J., Pérez-Pérez, M. M., Godoy, M., Sánchez-Serrano, J.-J., Schmelz, E. A., et al. (2007). ABA is an essential signal for plant resistance to pathogens affecting JA biosynthesis and the activation of defenses in *Arabidopsis*. *Plant Cell* 19, 1665–1681. doi: 10.1105/tpc.106.048041
- Albacete, A., Ghanem, M. E., Martínez-Andujar, C., Acosta, M., Sanchez-Bravo, J., Martínez, V., et al. (2008). Hormonal changes in relation to biomass partitioning and shoot growth impairment in salinized tomato (*Solanum lycopersicum* L.) plants. *J. Exp. Bot.* 59, 4119–4131. doi: 10.1093/jxb/ern251
- Bartling, D., Radzio, R., Steiner, U., and Weiler, E. W. (1993). A glutathione S-transferase with glutathione-peroxidase activity from *Arabidopsis thaliana*. molecular cloning and functional characterization. *Eur. J. Biochem.* 216, 579–586. doi: 10.1111/j.1432-1033.1993.tb18177.x
- Beckers, G. J. M., and Spoel, S. H. (2006). Fine-tuning plant defence signalling: Salicylate versus jasmonate. *Plant Biol.* 8, 1–10. doi: 10.1055/s-2005-872705
- Belhad, A., Saigne, C., Telef, N., Cluzet, S., Bouscaut, J., Corio-Costet, M.-F., et al. (2006). Methyl jasmonate induces defense responses in grapevine and triggers protection against *Erysiphe necator*. *J. Agric. Food Chem.* 54, 9119–9125. doi: 10.1021/jf0618022
- Bertazzon, N., Bagnaresi, P., Forte, V., Mazzucotelli, E., Filippin, L., Guerra, D., et al. (2019). Grapevine comparative early transcriptomic profiling suggests that flavescence dorée phytoplasma represses plant responses induced by vector feeding in susceptible varieties. *BMC Genomics* 20, 526. doi: 10.1186/s12864-019-5908-6
- Bertazzon, N., Raiola, A., Castiglioni, C., Gardiman, M., Angelini, E., Borgo, M., et al. (2012). Transient silencing of the grapevine gene VvPGIP1 by agroinfiltration with a construct for RNA interference. *Plant Cell Rep.* 31, 133–143. doi: 10.1007/s00299-011-1147-2
- Bitkau, K. S., Neupane, S., and Alban, S. (2020). Initial evaluation of six different brown algae species as source for crude bioactive fucoidans. *Algal Res.* 45, 101759. doi: 10.1016/j.algal.2019.101759
- Bodin, E., Bellée, A., Dufour, M.-C., André, O., and Corio-Costet, M.-F. (2020). Grapevine stimulation: A multidisciplinary approach to investigate the effects of biostimulants and a plant defense stimulator. *J. Agric. Food Chem.* 68, 15085–15096. doi: 10.1021/acs.jafc.0c05849
- Bolyen, E., Rideout, J. R., Dillon, M. R., Bokulich, N. A., Abnet, C. C., Al-Ghalith, G. A., et al. (2019). Reproducible, interactive, scalable and extensible microbiome data science using QIIME 2. *Nat. Biotechnol.* 37, 852–857. doi: 10.1038/s41587-019-0209-9
- Bouissil, S., Pierre, G., Alaoui-Talibi, Z. E., Michaud, P., El Modafar, C., and Delattre, C. (2019). Applications of algal polysaccharides and derivatives in therapeutic and agricultural fields. *CPD* 25, 1187–1199. doi: 10.2174/1381612825666190425162729
- Brunner, F., Stintzi, A., Fritig, B., and Legrand, M. (1998). Substrate specificities of tobacco chitinases. *Plant J.* 14, 225–234. doi: 10.1046/j.1365-3113.1998.00116.x
- Bulgarelli, D., Schlaeppi, K., Spaepen, S., Ver Loren van Themaat, E., and Schulze-Lefert, P. (2013). Structure and functions of the bacterial microbiota of plants. *Annu. Rev. Plant Biol.* 64, 807–838. doi: 10.1146/annurev-arplant-050312-120106
- Cappelletti, M., Perazzolli, M., Antonielli, L., Nesler, A., Torboli, E., Bianchedi, P. L., et al. (2016). Leaf treatments with a protein-based resistance inducer partially modify phyllosphere microbial communities of grapevine. *Front. Plant Sci.* 7. doi: 10.3389/fpls.2016.01053
- Cesaretti, M. (2003). A 96-well assay for uronic acid carbazole reaction. *Carbohydr. Polymers* 54, 59–61. doi: 10.1016/S0144-8617(03)00144-9
- Conn, S., Curtin, C., Bézier, A., Franco, C., and Zhang, W. (2008). Purification, molecular cloning, and characterization of glutathione S-transferases (GSTs) from pigmented vitis vinifera L. cell suspension cultures as putative anthocyanin transport proteins. *J. Exp. Bot.* 59, 3621–3634. doi: 10.1093/jxb/ern217
- Coste, O., Malta, E., López, J. C., and Fernández-Díaz, C. (2015). Production of sulfated oligosaccharides from the seaweed *Ulva* sp. using a new ulvan-degrading enzymatic bacterial crude extract. *Algal Res.* 10, 224–231. doi: 10.1016/j.algal.2015.05.014
- Cruz, S., Guerrero, R. F., Puertas, B., Fernández-Marín, M. I., and Cantos-Villar, E. (2019). “Preharvest methyl jasmonate and postharvest UVC treatments: Increasing stilbenes in wine,” in *Co-Evolution of secondary metabolites reference series in phytochemistry*. Eds. J.-M. Merillon and K. G. Ramawat (Cham: Springer International Publishing), 1–18. doi: 10.1007/978-3-319-76887-8_20-1
- Cuevas, B., Arroba, A. I., de los Reyes, C., Gómez-Jaramillo, L., González-Montelongo, M. C., and Zubía, E. (2021). Diterpenoids from the brown alga *Rugulopteryx okamurae* and their anti-inflammatory activity. *Mar. Drugs* 19, 677. doi: 10.3390/md19120677
- Das, K., and Roychoudhury, A. (2014). Reactive oxygen species (ROS) and response of antioxidants as ROS-scavengers during environmental stress in plants. *Front. Environ. Sci.* 2. doi: 10.3389/fenvs.2014.00053
- De Bona, G. S., Adrian, M., Negrel, J., Chiltz, A., Klinguer, A., Poinsot, B., et al. (2019). Dual mode of action of grape cane extracts against *Botrytis cinerea*. *J. Agric. Food Chem.* 67, 5512–5520. doi: 10.1021/acs.jafc.8b07098
- De Diego, N., Perez-Alfocea, F., Cantero, E., Lacuesta, M., and Moncalean, P. (2012). Physiological response to drought in radiata pine: phytohormone implication at leaf level. *Tree Physiol.* 32, 435–449. doi: 10.1093/treephys/tps029
- Delaunoy, B., Farace, G., Jeandet, P., Clément, C., Baillieu, F., Dorey, S., et al. (2014). Elicitors as alternative strategy to pesticides in grapevine? current knowledge on their

Conflict of interest

The authors declare that the research was conducted in the absence of any commercial or financial relationships that could be construed as a potential conflict of interest.

Publisher's note

All claims expressed in this article are solely those of the authors and do not necessarily represent those of their affiliated organizations, or those of the publisher, the editors and the reviewers. Any product that may be evaluated in this article, or claim that may be made by its manufacturer, is not guaranteed or endorsed by the publisher.

Supplementary material

The Supplementary Material for this article can be found online at: <https://www.frontiersin.org/articles/10.3389/fpls.2023.1119854/full#supplementary-material>

- mode of action from controlled conditions to vineyard. *Environ. Sci. Pollut. Res.* 21, 4837–4846. doi: 10.1007/s11356-013-1841-4
- Dermastia, M., Škrlić, B., Strah, R., Anžič, B., Tomaž, Š., Križnik, M., et al. (2021). Differential response of grapevine to infection with ‘*Candidatus* phytoplasma solani’ in early and late growing season through complex regulation of mRNA and small RNA transcriptomes. *Int. J. Mol. Sci.* 22, 3531. doi: 10.3390/ijms22073531
- Dische, Z. (1947). A new specific color reaction of hexuronic acids. *J. Biol. Chem.* 167, 189–198. doi: 10.1016/S0021-9258(18)35155-4
- Dische, Z., and Shettles, L. B. (1948). A specific color reaction of methylpentoses and a spectrophotometric micromethod for their determination. *J. Biol. Chem.* 175, 595–603. doi: 10.1016/S0021-9258(18)57178-7
- DuBois, M., Gilles, K. A., Hamilton, J. K., Rebers, P. A., and Smith, F. (1956). Colorimetric method for determination of sugars and related substances. *Anal. Chem.* 28, 350–356. doi: 10.1021/ac60111a017
- Dufour, M.-C., Magnin, N., Dumas, B., Vergnes, S., and Corio-Costet, M.-F. (2016). High-throughput gene-expression quantification of grapevine defense responses in the field using microfluidic dynamic arrays. *BMC Genomics* 17, 957. doi: 10.1186/s12864-016-3304-z
- du Jardin, P. (2015). Plant biostimulants: Definition, concept, main categories and regulation. *Scientia Hort.* 196, 3–14. doi: 10.1016/j.scienta.2015.09.021
- Fernandes, F., Ramalhosa, E., Pires, P., Verdial, J., Valentão, P., Andrade, P., et al. (2013). Vitis vinifera leaves towards bioactivity. *Ind. Crops Products* 43, 434–440. doi: 10.1016/j.indcrop.2012.07.031
- Fernandez-San Millan, A., Farran, I., Larraya, L., Ancin, M., Arregui, L. M., and Veramendi, J. (2020). Plant growth-promoting traits of yeasts isolated from Spanish vineyards: benefits for seedling development. *Microbiological Res.* 237, 126480. doi: 10.1016/j.micres.2020.126480
- Folch, J., Lees, M., and Stanley, G. H. S. (1957). A simple method for the isolation and purification of total lipides from animal tissues. *J. Biol. Chem.* 226, 497–509. doi: 10.1016/S0021-9258(18)64849-5
- Gabaston, J., Cantos-Villar, E., Biais, B., Waffo-Teguo, P., Renouf, E., Corio-Costet, M.-F., et al. (2017). Stilbenes from *Vitis vinifera* L. waste: A sustainable tool for controlling *Plasmopara viticola*. *J. Agric. Food Chem.* 65, 2711–2718. doi: 10.1021/acs.jafc.7b00241
- García-Gómez, J. C., Sempere-Valverde, J., González, A. R., Martínez-Chacón, M., Olaya-Ponzzone, L., Sánchez-Moyano, E., et al. (2020). From exotic to invasive in record time: The extreme impact of rugulopterix okamurae (Dictyotales, ochrophyta) in the strait of Gibraltar. *Sci. Total Environ.* 704, 135408. doi: 10.1016/j.scitotenv.2019.135408
- Gauthier, A., Trouvelot, S., Kelloniemi, J., Frettinger, P., Wendeheime, D., Daire, X., et al. (2014). The sulfated laminarin triggers a stress transcriptome before priming the SA- and ROS-dependent defenses during grapevine's induced resistance against plasmopara viticola. *PLoS One* 9, e88145. doi: 10.1371/journal.pone.0088145
- Goufo, P., Singh, R. K., and Cortez, I. (2020). A reference list of phenolic compounds (Including stilbenes) in grapevine (*Vitis vinifera* L.) roots, woods, canes, stems, and leaves. *Antioxidants* 9, 398. doi: 10.3390/antiox9050398
- Gruau, C., Trotel-Aziz, P., Villaume, S., Rabenoelina, F., Clément, C., Baillieu, F., et al. (2015). *Pseudomonas fluorescens* PTA-CT2 triggers local and systemic immune response against *Botrytis cinerea* in grapevine. *MPMI* 28, 1117–1129. doi: 10.1094/MPMI-04-15-0092-R
- Guerreiro, A., Figueiredo, J., Sousa Silva, M., and Figueiredo, A. (2016). Linking jasmonic acid to grapevine resistance against the biotrophic oomycete plasmopara viticola. *Front. Plant Sci.* 28 (7). doi: 10.3389/fpls.2016.00565
- Gutha, L. R., Casassa, L. F., Harbertson, J. F., and Naidu, R. A. (2010). Modulation of flavonoid biosynthetic pathway genes and anthocyanins due to virus infection in grapevine (*Vitis vinifera* L.) leaves. *BMC Plant Biol.* 10, 187. doi: 10.1186/1471-2229-10-187
- Guidara, M., Yaich, H., Amor, I. B., Fakhfakh, J., Gargouri, J., Lassoued, S., et al. (2021). Effect of extraction procedures on the chemical structure, antitumor and anticoagulant properties of ulvan from ulva lactuca of Tunisia coast. *Carbohydr. Polymers* 253, 117283. doi: 10.1016/j.carbpol.2020.117283
- Guo, C., Guo, R., Xu, X., Gao, M., Li, X., Song, J., et al. (2014). Evolution and expression analysis of the grape (*Vitis vinifera* L.) WRKY gene family. *J. Exp. Bot.* 65, 1513–1528. doi: 10.1093/jxb/eru007
- Gupta, V., Willits, M. G., and Glazebrook, J. (2000). *Arabidopsis thaliana* EDS4 contributes to salicylic acid (SA)-dependent expression of defense responses: Evidence for inhibition of jasmonic acid signaling by SA. *MPMI* 13, 503–511. doi: 10.1094/MPMI.2000.13.5.503
- Harm, A., Kassemeyer, H.-H., Seibicke, T., and Regner, F. (2011). Evaluation of chemical and natural resistance inducers against downy mildew (*Plasmopara viticola*) in grapevine. *Am. J. Enology Viticulture* 62, 184–192. doi: 10.5344/ajev.2011.09054
- Hashimoto, M., Kisseleva, L., Sawa, S., Furukawa, T., Komatsu, S., and Koshiba, T. (2004). A novel rice PR10 protein, RSOsPR10, specifically induced in roots by biotic and abiotic stresses, possibly via the jasmonic acid signaling pathway. *Plant Cell Physiol.* 45, 550–559. doi: 10.1093/pcp/pch063
- Hentati, F., Tounsi, L., Djomdi, D., Pierre, G., Delattre, C., Ursu, A. V., et al. (2020). Bioactive polysaccharides from seaweeds. *Molecules* 25, 3152. doi: 10.3390/molecules25143152
- Ibrahim, M. I. A., Amer, M. S., Ibrahim, H. A. H., and Zaghloul, E. H. (2022). Considerable production of ulvan from ulva lactuca with special emphasis on its antimicrobial and anti-fouling properties. *Appl. Biochem. Biotechnol.* 194, 3097–3118. doi: 10.1007/s12010-022-03867-y
- Ihrmark, K., Bödeker, I. T. M., Cruz-Martinez, K., Friberg, H., Kubartova, A., Schenck, J., et al. (2012). New primers to amplify the fungal ITS2 region - evaluation by 454-sequencing of artificial and natural communities. *FEMS Microbiol. Ecol.* 82, 666–677. doi: 10.1111/j.1574-6941.2012.01437.x
- January, G. G., Naidoo, R. K., Kirby-McCullough, B., and Bauer, R. (2019). Assessing methodologies for fucoidan extraction from south African brown algae. *Algal Res.* 40, 101517. doi: 10.1016/j.algal.2019.101517
- Jaulneau, V., Lafitte, C., Corio-Costet, M.-F., Stadnik, M. J., Salamagne, S., Briand, X., et al. (2011). An ulva armoricana extract protects plants against three powdery mildew pathogens. *Eur. J. Plant Pathol.* 131, 393–401. doi: 10.1007/s10658-011-9816-0
- Jindo, K., Goron, T. L., Pizarro-Tobias, P., Sánchez-Monedero, M.Á., Audette, Y., Deolu-Ajayi, A. O., et al. (2022). Application of biostimulant products and biological control agents in sustainable viticulture: A review. *Front. Plant Sci.* 13. doi: 10.3389/fpls.2022.932311
- Kidgell, J. T., Magnusson, M., de Nys, R., and Glasson, C. R. K. (2019). Ulvan: A systematic review of extraction, composition and function. *Algal Res.* 39, 101422. doi: 10.1016/j.algal.2019.101422
- Kortekamp, A. (2006). Expression analysis of defence-related genes in grapevine leaves after inoculation with a host and a non-host pathogen. *Plant Physiol. Biochem.* 44, 58–67. doi: 10.1016/j.plaphy.2006.01.008
- Krzyzaniak, Y., Trouvelot, S., Negrel, J., Cluzet, S., Valls, J., Richard, T., et al. (2018). A plant extract acts both as a resistance inducer and an oomycete against grapevine downy mildew. *Front. Plant Sci.* 9, 1085. doi: 10.3389/fpls.2018.01085
- Kunkel, B. N., and Brooks, D. M. (2002). Cross talk between signaling pathways in pathogen defense. *Curr. Opin. Plant Biol.* 5, 325–331. doi: 10.1016/S1369-5266(02)00275-3
- Lacuesta, M., Saiz-Fernández, I., Podlešáková, K., Miranda-Apodaca, J., Novák, O., Doležal, K., et al. (2018). The trans and cis zeatin isomers play different roles in regulating growth inhibition induced by high nitrate concentrations in maize. *Plant Growth Regul.* 85, 199–209. doi: 10.1007/s10725-018-0383-7
- Lafarga, T., Acien-Fernández, F. G., and García-Vaquero, M. (2020). Bioactive peptides and carbohydrates from seaweed for food applications: Natural occurrence, isolation, purification, and identification. *Algal Res.* 48, 101909. doi: 10.1016/j.algal.2020.101909
- Latouche, G., Bellow, S., Poutaraud, A., Meyer, S., and Cerovic, Z. G. (2013). Influence of constitutive phenolic compounds on the response of grapevine (*Vitis vinifera* L.) leaves to infection by plasmopara viticola. *Planta* 237, 351–361. doi: 10.1007/s00425-012-1776-x
- Leubner-Metzger, G., and Meins, F. J. (1999). “Functions and regulation of plant β-1,3-glucanases (PR2),” in *Pathogenesis-related proteins in plants*. Eds. S. K. Datta and S. Muthukrishnan (Boca Raton, FL, USA: CRC Press LLC), 49–76.
- Liu, J., Moore, S., Chen, C., and Lindsey, K. (2017). Crosstalk complexities between auxin, cytokinin, and ethylene in arabidopsis root development: From experiments to systems modeling, and back again. *Mol. Plant* 10, 1480–1496. doi: 10.1016/j.molp.2017.11.002
- Liu, R., Wang, L., Zhu, J., Chen, T., Wang, Y., and Xu, Y. (2015). Histological responses to downy mildew in resistant and susceptible grapevines. *Protoplasma* 252, 259–270. doi: 10.1007/s00709-014-0677-1
- Maehre, H. K., Malde, M. K., Eilertsen, K.-E., and Elvevoll, E. O. (2014). Characterization of protein, lipid and mineral contents in common Norwegian seaweeds and evaluation of their potential as food and feed: Biochemical composition of marine macroalgae. *J. Sci. Food Agric.* 94, 3281–3290. doi: 10.1002/jsfa.6681
- Mishko, A., and Lutsky, E. (2020). The effect of *Saccharomyces cerevisiae* on antioxidant system of grape leaves infected by downy mildew. *Bio Web Conf.* 25, 6006. doi: 10.1051/bioconf/20202506006
- Monteiro, E., Gonçalves, B., Cortez, I., and Castro, I. (2022). The role of biostimulants as alleviators of biotic and abiotic stresses in grapevine: A review. *Plants* 11, 396. doi: 10.3390/plants11030396
- Nabti, E., Jha, B., and Hartmann, A. (2017). Impact of seaweeds on agricultural crop production as biofertilizer. *Int. J. Environ. Sci. Technol.* 14, 1119–1134. doi: 10.1007/s13762-016-1202-1
- Nerva, L., Pagliarini, C., Pugliese, M., Monchiero, M., Gonthier, S., Gullino, M. L., et al. (2019). Grapevine phyllosphere community analysis in response to elicitor application against powdery mildew. *Microorganisms* 7, 662. doi: 10.3390/microorganisms7120662
- Paolacci, A. R., Catarcione, G., Ederli, L., Zadra, C., Pasqualini, S., Badiani, M., et al. (2017). Jasmonate-mediated defence responses, unlike salicylate-mediated responses, are involved in the recovery of grapevine from bois noir disease. *BMC Plant Biol.* 17, 118. doi: 10.1186/s12870-017-1069-4
- Perazzolli, M., Antonielli, L., Storari, M., Puopolo, G., Pancher, M., Giovannini, O., et al. (2014). Resilience of the natural phyllosphere microbiota of the grapevine to chemical and biological pesticides. *Appl. Environ. Microbiol.* 80, 3585–3596. doi: 10.1128/AEM.00415-14
- Perazzolli, M., Nesler, A., Giovannini, O., Antonielli, L., Puopolo, G., and Pertot, I. (2020). Ecological impact of a rare sugar on grapevine phyllosphere microbial communities. *Microbiological Res.* 232, 126387. doi: 10.1016/j.micres.2019.126387

- Pérez-López, U., Miranda-Apodaca, J., Lacuesta, M., Mena-Petite, A., and Muñoz-Rueda, A. (2015). Growth and nutritional quality improvement in two differently pigmented lettuce cultivars grown under elevated CO₂ and/or salinity. *Scientia Hort.* 195, 56–66. doi: 10.1016/j.scienta.2015.08.034
- Pérez-López, U., Robredo, A., Lacuesta, M., Mena-Petite, A., and Muñoz-Rueda, A. (2012). Elevated CO₂ reduces stomatal and metabolic limitations on photosynthesis caused by salinity in hordeum vulgare. *Photosynth. Res.* 111, 269–283. doi: 10.1007/s11202-012-9721-1
- Pérez-López, U., Robredo, A., Lacuesta, M., Sgherri, C., Muñoz-Rueda, A., Navari-Izzo, F., et al. (2009). The oxidative stress caused by salinity in two barley cultivars is mitigated by elevated CO₂. *Physiologia Plantarum* 135, 29–42. doi: 10.1111/j.1399-3054.2008.01174.x
- Pinto, C., Pinho, D., Sousa, S., Pinheiro, M., Egas, C., and Gomes, A. C. (2014). Unravelling the diversity of grapevine microbiome. *PLoS One* 9, e85622. doi: 10.1371/journal.pone.0085622
- Pollard-Flamand, J., Boulé, J., Hart, M., and Úrbez-Torres, J. R. (2022). Biocontrol activity of trichoderma species isolated from grapevines in British Columbia against botryosphaeria dieback fungal pathogens. *JoF* 8, 409. doi: 10.3390/jof8040409
- Raj, T. S., Vignesh, S., Nishanthi, P., Graff, K. H., and Suji, H. A. (2018). Induction of defence enzymes activities in grape plant treated by seaweed algae against plasmopara viticola and ucinula necator causing downy and powdery mildews of grapes. *Novel Res. Microbiol. J.* 2, 122–137. doi: 10.21608/NRMJ.2018.22705
- Ren, C., Liu, Z., Wang, X., and Qin, S. (2022). The seaweed holobiont: from microecology to biotechnological applications. *Microbial Biotechnol.* 15, 738–754. doi: 10.1111/1751-7915.14014
- Repetto, O., Bertazzon, N., De Rosso, M., Miotti, L., Flamini, R., Angelini, E., et al. (2012). Low susceptibility of grapevine infected by GLRaV-3 to late plasmopara viticola infections: Towards understanding the phenomenon. *Physiol. Mol. Plant Pathol.* 79, 55–63. doi: 10.1016/j.pmpp.2012.04.001
- Ross, J. J., Weston, D. E., Davidson, S. E., and Reid, J. B. (2011). Plant hormone interactions: how complex are they? *Physiologia Plantarum* 141, 299–309. doi: 10.1111/j.1399-3054.2011.01444.x
- Sabir, A., Yazar, K., Sabir, F., Kara, Z., Yazici, M. A., and Goksu, N. (2014). Vine growth, yield, berry quality attributes and leaf nutrient content of grapevines as influenced by seaweed extract (*Ascophyllum nodosum*) and nanosize fertilizer pulverizations. *Scientia Hort.* 175, 1–8. doi: 10.1016/j.scienta.2014.05.021
- Salvi, L., Brunetti, C., Cataldo, E., Niccolai, A., Centritto, M., Ferrini, F., et al. (2019). Effects of ascophyllum nodosum extract on vitis vinifera: Consequences on plant physiology, grape quality and secondary metabolism. *Plant Physiol. Biochem.* 139, 21–32. doi: 10.1016/j.plaphy.2019.03.002
- Šamec, D., Karalija, E., Šola, I., Vujčić Bok, V., and Salopek-Sondi, B. (2021). The role of polyphenols in abiotic stress response: The influence of molecular structure. *Plants* 10, 118. doi: 10.3390/plants10010118
- Samuels, L. J., Setati, M. E., and Blancaquert, E. H. (2022). Towards a better understanding of the potential benefits of seaweed based biostimulants in vitis vinifera l. cultivars. *Plants* 11, 348. doi: 10.3390/plants11030348
- Santana, I., Félix, M., Guerrero, A., and Bengoechea, C. (2022). Processing and characterization of bioplastics from the invasive seaweed rugulopteryx okamurae. *Polymers* 14, 355. doi: 10.3390/polym14020355
- Santner, A., and Estelle, M. (2009). Recent advances and emerging trends in plant hormone signalling. *Nature* 459, 1071–1078. doi: 10.1038/nature08122
- Sels, J., Mathys, J., De Coninck, B. M. A., Cammue, B. P. A., and De Bolle, M. F. C. (2008). Plant pathogenesis-related (PR) proteins: A focus on PR peptides. *Plant Physiol. Biochem.* 46, 941–950. doi: 10.1016/j.plaphy.2008.06.011
- Sharma, P., Jha, A. B., Dubey, R. S., and Pessarakli, M. (2012). Reactive oxygen species, oxidative damage, and antioxidative defense mechanism in plants under stressful conditions. *J. Bot.* 2012, 1–26. doi: 10.1155/2012/217037
- Shomron, A., Duanis-Assaf, D., Galsurker, O., Golberg, A., and Alkan, N. (2022). Extract from the macroalgae ulva rigida induces table grapes resistance to botrytis cinerea. *Foods* 11, 723. doi: 10.3390/foods11050723
- Sipiczki, M. (2006). *Metschnikowia* strains isolated from botrytized grapes antagonize fungal and bacterial growth by iron depletion. *Appl. Environ. Microbiol.* 72, 6716–6724. doi: 10.1128/AEM.01275-06
- Sparvoli, F., Martin, C., Scienza, A., Gavazzi, G., and Tonelli, C. (1994). Cloning and molecular analysis of structural genes involved in flavonoid and stilbene biosynthesis in grape (*Vitis vinifera* L.). *Plant Mol. Biol.* 24, 743–755. doi: 10.1007/BF00029856
- Stadnik, M. J., and de Freitas, M. B. (2014). Algal polysaccharides as source of plant resistance inducers. *Trop. Plant Pathol.* 39, 111–118. doi: 10.1590/S1982-56762014000200001
- Tavares, S., Vesentini, D., Fernandes, J. C., Ferreira, R. B., Laureano, O., Ricardo-Da-Silva, J. M., et al. (2013). Vitis vinifera secondary metabolism as affected by sulfate depletion: Diagnosis through phenylpropanoid pathway genes and metabolites. *Plant Physiol. Biochem.* 66, 118–126. doi: 10.1016/j.plaphy.2013.01.022
- Torres, P. B., Nagai, A., Jara, C. E. P., Santos, J. P., Chow, F., and dos Santos, D. Y. A. C. (2021). Determination of sulfate in algal polysaccharide samples: a step-by-step protocol using microplate reader. *Ocean Coast. Res.* 69, e21021. doi: 10.1590/2675-2824069.21-010pbt
- Trotel-Aziz, P., Abou-Mansour, E., Courteaux, B., Rabenoelina, F., Clément, C., Fontaine, F., et al. (2019). Bacillus subtilis PTA-271 counteracts botryosphaeria dieback in grapevine, triggering immune responses and detoxification of fungal phytotoxins. *Front. Plant Sci.* 10. doi: 10.3389/fpls.2019.00025
- Trouvelot, S., Hâloir, M.-C., Poinssot, B., Gauthier, A., Paris, F., Guiller, C., et al. (2014). Carbohydrates in plant immunity and plant protection: roles and potential application as foliar sprays. *Front. Plant Sci.* 5. doi: 10.3389/fpls.2014.00592
- Vannozzi, A., Dry, I. B., Fasoli, M., Zenoni, S., and Lucchin, M. (2012). Genome-wide analysis of the grapevine stilbene synthase multigenic family: genomic organization and expression profiles upon biotic and abiotic stresses. *BMC Plant Biol.* 12, 130. doi: 10.1186/1471-2229-12-130
- van Loon, L. C., Rep, M., and Pieterse, C. M. (2006). Significance of inducible defense-related proteins in infected plants. *Annu. Rev. Phytopathol.* 44, 135–162. doi: 10.1146/annurev.phyto.44.070505.143425
- Vera, J., Castro, J., Gonzalez, A., and Moenne, A. (2011). Seaweed polysaccharides and derived oligosaccharides stimulate defense responses and protection against pathogens in plants. *Mar. Drugs* 9, 2514–2525. doi: 10.3390/md9122514
- Wang, Y., Cao, X., Han, Y., Han, X., Wang, Z., Xue, T., et al. (2022). Kaolin particle film protects grapevine cv. Cabernet sauvignon against downy mildew by forming particle film at the leaf surface, directly acting on sporangia and inducing the defense of the plant. *Front. Plant Sci.* 12. doi: 10.3389/fpls.2021.796545
- Yakhin, O. I., Lubyantsev, A. A., Yakhin, I. A., and Brown, P. H. (2017). Biostimulants in plant science: A global perspective. *Front. Plant Sci.* 7, 2049. doi: 10.3389/fpls.2016.02049
- Yuan, Z., Cao, Q., Zhang, K., Ata-Ul-Karim, S. T., Tian, Y., Zhu, Y., et al. (2016). Optimal leaf positions for SPAD meter measurement in rice. *Front. Plant Sci.* 7. doi: 10.3389/fpls.2016.00719



OPEN ACCESS

EDITED BY

Alessandra Ferrandino,
University of Turin, Italy

REVIEWED BY

Dongming Ma,
Guangzhou University of Chinese
Medicine, China
Lorenza Dalla Costa,
Fondazione Edmund Mach, Italy

*CORRESPONDENCE

Justin Graham Lashbrooke
✉ jglash@sun.ac.za

SPECIALTY SECTION

This article was submitted to
Plant Metabolism and Chemodiversity,
a section of the journal
Frontiers in Plant Science

RECEIVED 30 November 2022

ACCEPTED 28 February 2023

PUBLISHED 16 March 2023

CITATION

Bosman RN, Vervalle JA-M, November DL,
Burger P and Lashbrooke JG (2023)
Grapevine genome analysis demonstrates
the role of gene copy number variation in
the formation of monoterpenes.
Front. Plant Sci. 14:1112214.
doi: 10.3389/fpls.2023.1112214

COPYRIGHT

© 2023 Bosman, Vervalle, November, Burger
and Lashbrooke. This is an open-access
article distributed under the terms of the
[Creative Commons Attribution License](#)
(CC BY). The use, distribution or
reproduction in other forums is permitted,
provided the original author(s) and the
copyright owner(s) are credited and that
the original publication in this journal is
cited, in accordance with accepted
academic practice. No use, distribution or
reproduction is permitted which does not
comply with these terms.

Grapevine genome analysis demonstrates the role of gene copy number variation in the formation of monoterpenes

Robin Nicole Bosman¹, Jessica Anne-Marie Vervalle²,
Danielle Lisa November¹, Phyllis Burger³
and Justin Graham Lashbrooke^{1*}

¹South African Grape and Wine Research Institute, Stellenbosch University, Stellenbosch, South Africa,

²Laboratory of Nematology, Department of Plant Sciences, Wageningen University,

Wageningen, Netherlands, ³Department for Crop Development, Agricultural Research Council -
Infruitec-Nietvoorbij, Stellenbosch, South Africa

Volatile organic compounds such as terpenes influence the quality parameters of grapevine through their contribution to the flavour and aroma profile of berries. Biosynthesis of volatile organic compounds in grapevine is relatively complex and controlled by multiple genes, the majority of which are unknown or uncharacterised. To identify the genomic regions that associate with modulation of these compounds in grapevine berries, volatile metabolic data generated via GC-MS from a grapevine mapping population was used to identify quantitative trait loci (QTLs). Several significant QTLs were associated with terpenes, and candidate genes were proposed for sesquiterpene and monoterpene biosynthesis. For monoterpenes, loci on chromosomes 12 and 13 were shown to be associated with geraniol and cyclic monoterpene accumulation, respectively. The locus on chromosome 12 was shown to contain a geraniol synthase gene (*VvGer*), while the locus on chromosome 13 contained an α -terpineol synthase gene (*VvTer*). Molecular and genomic investigation of *VvGer* and *VvTer* revealed that these genes were found in tandemly duplicated clusters, displaying high levels of hemizygoty. Gene copy number analysis further showed that not only did *VvTer* and *VvGer* copy numbers vary within the mapping population, but also across recently sequenced *Vitis* cultivars. Significantly, *VvTer* copy number correlated with both *VvTer* gene expression and cyclic monoterpene accumulation in the mapping population. A hypothesis for a hyper-functional *VvTer* allele linked to increased gene copy number in the mapping population is presented and can potentially lead to selection of cultivars with modulated terpene profiles. The study highlights the impact of *VvTPS* gene duplication and copy number variation on terpene accumulation in grapevine.

KEYWORDS

terpenes, TPS, grapevine, gene copy number, genomics, QTL, VOC

Introduction

Terpenes are one of the largest classes of metabolites in plants, where they serve various primary and specialized roles. Volatile terpenes, such as monoterpenes and sesquiterpenes, mainly function as specialized metabolites and are involved in plant-pathogen interactions, protection of plants against herbivores, and are also produced to attract pollinators and seed-dispersing animals (Dudareva et al., 2013; Vranová et al., 2013). Together with additional volatile organic compounds (VOCs) such as short-carbon chain compounds (green leaf volatiles), C13-norisoprenoids and methoxypyrazines, they contribute to the varietal aroma of grape berries (Dunlevy et al., 2009). Indeed, monoterpenes and sesquiterpenes have been extensively studied for their contribution to the distinctive varietal aroma of aromatic cultivars such as Muscat-cultivars (monoterpene alcohols including linalool, geraniol, and α -terpineol), 'Shiraz' (the sesquiterpene rotundone), 'Riesling' and 'Gewürztraminer' (the monoterpene rose-oxide) (Dunlevy et al., 2009).

Biosynthesis of monoterpenes and sesquiterpene occurs *via* the methyl-erythritol-phosphate (MEP) and mevalonic acid (MVA) pathways, respectively. The first step in the MEP pathway is catalysed by 1-deoxy-D-xylulose-5-phosphate synthase (DXS), an enzyme which is considered to be the vital rate-limiting enzyme in plastidial terpene biosynthesis (Tholl, 2015; Bosman and Lashbrooke, 2023). Several QTL mapping and association studies in grapevine have identified a singular SNP in the active site of *VvDXS1* as a causal mutation for increased monoterpene content in Muscat cultivars (Doligez et al., 2006; Battilana et al., 2009; Emanuelli et al., 2010). A SNP at position 1822 of *VvDXS1* (G>T) in Muscat cultivars causes a non-synonymous substitution of a lysine (K) with an asparagine (N) at position 284 of the *VvDXS1* protein. Functional characterisation of *VvDXS1* showed that the non-synonymous amino acid substitution influences enzyme kinetics by increasing the catalytic efficiency of *VvDXS1*, thereby increasing the total monoterpene content of cultivars carrying this SNP (Battilana et al., 2011).

While *VvDXS1* is able to regulate total monoterpene accumulation *via* biosynthesis of the prenyldiphosphate precursors, terpene synthases (TPSs) are responsible for the formation of specific terpenes (Steele et al., 1998; Chen et al., 2011). Monoterpene synthases catalyse the coupled ionisation, isomerisation and cyclisation of geranyldiphosphate (GPP) leading to the formation of a reactive carbocation intermediate and subsequent reactions e.g. deprotonation or ring closures will form the final monoterpene product (Davis and Croteau, 2000; Degenhardt et al., 2009).

The *Vitis vinifera* reference genome, PN40024, has a greatly expanded TPS gene family, with an initial prediction of 152 loci and 69 putatively functional TPSs (Jaillon et al., 2007; Martin et al., 2010). However, the recent availability of phased diploid grapevine genomes of various cultivars (Minio et al., 2019; Zhou et al., 2019; Massonnet et al., 2020) reveals that the TPS gene family size varies greatly between cultivars (Smit et al., 2020). Furthermore, *VvTPSs* are organised in large tandemly duplicated clusters, and a great portion of genes are hemizygous (Martin et al., 2010; Jiang et al.,

2019; Smit et al., 2020). Recent research has also shown that grapevine has cultivar-specific TPS genes (Drew et al., 2016; Smit et al., 2019). Cultivar-specific TPSs arise due to small sequence variations, such as single nucleotide polymorphisms (SNPs), which cause a functional change of the enzyme. The extensive level of duplication and functional plasticity of *VvTPSs* contribute to the neofunctionalisation of these enzymes and results in the large diversity in metabolites formed by *VvTPSs* (Bosman and Lashbrooke, 2023).

This study utilises a biparental grapevine cross population established by crossing a wine cultivar and a table grape cultivar. A dense linkage map has previously been created for this mapping population (Vervalle et al., 2022) which segregates for various traits, including aromatic profile. Quantification of volatile organic compounds in this population over several seasons was performed and genomic regions associated with these compounds identified. Genomic regions containing multiple TPS genes were further interrogated, and the large variety in cultivar specific TPS copy number associated with accumulation of specific monoterpenes characterised.

Materials and methods

Plant materials and sampling

82 progenies of the mapping population ('Deckrot' x G1-7720), which is held at the Agricultural Research Council (ARC) Nietvoorbij (Stellenbosch, South Africa, 33° 54' 47.6" S, 18° 51' 54.9" E) were used for analysis. G1-7720 is a table grape selection developed by the ARC and is a cross between 'Black Rose' and 'Muscat Seedless'. Grape berries from the progenies and parents were sampled at veraison (EL-stage 35) in January 2019, and at harvest ripeness (EL-stage 38) in February 2021 and 2022. Veraison berries from each bunch were further divided into "pre-veraison" (berries that were still green and firm) and "veraison" (berries which had changed colour and softened). The skin and flesh of all berries (pre-veraison, veraison and harvest ripe) were separated. Additionally, the parent cultivars were sampled at various early developmental stages (EL-stages 19, 23, 26, 29, 31 and 33) between October-December 2020. Three biological replicates were sampled for both cultivars at each developmental stage. Flowers and berries were removed from the rachis, and the rachis was discarded. All plant material was frozen in liquid nitrogen, ground to a fine powder and stored at -80°C.

Volatile organic compound analysis

Approximately 150 mg of ground frozen berry skin tissue was weighed into a 20-mL GC vial and 2 mL tartaric acid buffer (5 g.L⁻¹ tartaric acid, 2 g.L⁻¹, 0.8 g.L⁻¹ and 4.28 M NaCl; pH 3.2), containing 5 g.L⁻¹ internal standard (3-octanol), was added to the vial. Headspace solid phase microextraction (HS-SPME) and gas chromatography mass spectrometry (GCMS) were performed according to the method described in Joubert et al. (2016).

Samples were extracted from the vial head space using a 50/30 μm grey divinylbenzene/carboxen/polydimethylsiloxane (DVB/CAR/PDMS) fiber (Supelco, USA). The GCMS analysis was carried out on an Agilent 7890B GC equipped with a 5977B MSD and a PAL RSI 85 autosampler. Chromatographic separation was achieved using a HP-5MSUI capillary column (30m x 0.25 μm x 0.25 mm). The purge flow was 30 mL.min⁻¹ (for 90 seconds). The oven parameters were as follows: initial temperature of 40°C (2 min), a linear increase to a final temperature of 250°C (at a rate of 6°C.min⁻¹), and the temperature was held at 250°C for a final 5 min. The MS detector was operated in scan mode (from 35 to 350 m/z).

Agilent MassHunter Qualitative and Quantitative software packages were used for data analysis. Volatile compounds were identified according to their elution times and masses compared to those of respective authentic standards. Compounds without available authentic standards were identified by matching their mass spectrum with the NIST (Linström and Mallard, 2001) mass spectral library, in combination with Kovatz retention indices (RIs). Relative quantification of the compounds was achieved by normalising the peak area of each compound with the peak area of the internal standard. Concentrations are expressed as μg of 3-octanol equivalents per gram fresh weight.

For α -terpineol and geraniol, quantification was achieved through external standard calibration which was done by plotting standard curves using the internal response ratio versus the standard concentration. The resultant concentrations in $\mu\text{g.L}^{-1}$ were then normalised to the berry fresh weight to obtain the concentration (in $\mu\text{g.g}^{-1}$ FW).

QTL mapping

A total of 137 progeny of the 'Deckrot' x G1-7720 mapping population have previously been genotyped with the Vitis18K SNP chip and 92 simple sequence repeat (SSR) markers (Vervalle et al., 2022). The genotyping data were used to construct parental linkage maps for 'Deckrot' and G1-7720 with JoinMap[®]5 (Van Ooijen, 2006). Both maps represented all 19 linkage groups of grapevine and contained 1910 and 2252 markers in the maternal and paternal maps respectively. The maps displayed an average inter-locus gap distance of 0.80 cM. The genetic maps were combined with the metabolomic data to perform QTL analyses in MapQTL[®]6 (Van Ooijen, 2009). QTL regions were first identified through interval mapping with the maximum likelihood mixture model algorithm. Subsequently, regions were further defined with the multiple-QTL models (MQM) mapping. Genome-wide significant LOD thresholds were determined with permutation tests of 1000 permutations each. All maps were drawn with MapChart v2.32 (Voorrips, 2002).

Genomic analysis of significant QTLs

The position of significant QTLs on the grapevine reference genome (PN40024) version 2 (Jaillon et al., 2007) was determined from the physical positions of the two neighbouring flanking

markers. Annotated genes within each QTL were retrieved from URGI (<https://urgi.versailles.inra.fr/Species/Vitis/Annotations>) and is based on the VCost v.3 structural annotation of the 12X.2 reference genome (Jaillon et al., 2007; Canaguier et al., 2017). Gene function was predicted via BLASTp analysis (<https://blast.ncbi.nlm.nih.gov/Blast.cgi>) by querying protein sequences against the UniProtKB/SwissProt database and selecting the top hit for each sequence. Candidate genes were selected based on evidence from literature and their function was further investigated through molecular phylogeny. Phylogenetic trees were created on "Geneious Tree Builder" 2022.0.1 (<https://www.geneious.com>) using the default 'Geneious Tree Builder' function which used the UPGMA method with the Jukes-Cantor distance measure algorithm and 100 bootstrapping replicates. Multiple sequence alignments were created using the default 'Geneious Alignment' setting. Candidate gene expression was compared to metabolite data using the Transcriptomics & Metabolomics integrated database (TransMetaDb) (Savoi et al., 2016; Savoi et al., 2017) available on the Vitis Visualization platform (VitViz) (<http://www.vitviz.tomsbiolab.com/>).

TaqMan SNP genotyping assay

A custom TaqMan SNP genotyping assay (ThermoFisher Scientific) was designed for the *VvDXS1* SNP and used to genotype the mapping population under investigation. Genomic DNA was extracted from grape berry skins as described in Reid et al. (2006) however the DNase treatment step was substituted with a RNase treatment to eliminate RNA. The custom assay mix consisted of 1X TaqMan[®] MasterMix (ThermoFisher Scientific), 1X Custom Assay mix which contains the custom primers and probes (Table S1), and 1 μL (10–40 ng) of genomic DNA. Primers and probes were designed using PrimerExpress (Singh and Pandey, 2015). The assay was performed in QuantStudio 3 Real-Time PCR System with the following conditions: a pre-read stage for 30 seconds at 60°C, initial denaturation at 95°C for 5 minutes, 40 cycles of denaturation (95°C for 15 seconds) and annealing/extension (60°C for 1 minute), and then a post-read stage for 30 seconds at 60°C.

Confirmation of the results from the TaqMan assay was performed for a subset (20 progeny and the parents) of the mapping population. *VvDXS1* was isolated from gDNA via polymerase chain reaction (PCR). The reaction mixture (25 μL) contained 0.2 μM of the forward (5'-GTCATAGGTGATGGAGCCA-3') and reverse (5'-ATCTTACCTGTTCTGTCTAGC-3') primers (Emanuelli et al., 2014), 1 μL DNA (approximately 50 ng) and 1X GoTaq[®]Green Master Mix (Promega, USA). PCR products were visualised on a 1% agarose gel, excised and purified using Zymoclean Gel DNA recovery kit, and subsequently sequenced via Sanger sequencing.

Analysis of gene copy number variation

Total genomic DNA was extracted from pre-veraison samples as described in Reid et al. (2006), and relative gene copy number

was determined *via* a qPCR-based method described previously (Ma and Chung, 2014; Bhattacharya et al., 2019). qPCR was performed in a QuantStudio 3 Real-Time PCR System (ThermoFisher) in a 15 μ L reaction mixture which contained 1X SYBR (Power SYBR Green, Applied Biosystems), 0.2 μ M of each primer pair, 2 μ L of genomic DNA (approximately 90 ng) and nuclease-free water. Reactions were repeated in technical triplicate for each gene-sample combination, making use of *VvActin* primers to normalise for the amount of genomic DNA assayed in each sample and either *VvGer* or *VvTer* gene specific primers for amplification of the respective gene copies (for primer sequences see Table S2). The PCR conditions were: initial denaturation step at 95°C for 3 minutes, 40 cycles (95°C for 3 seconds and 60°C for 20 seconds), and melt curve analysis from 60 to 95°C. Relative gene copy number was determined with the $2^{-\Delta\Delta C_t}$ method (Ma and Chung, 2014), making use of the QuantStudio Design and Analysis Desktop Software package (v1.5.1) from Applied Biosystems for processing relative copy number and 95% confidence intervals. All gene copy numbers are reported relative to the gene copies present in the ‘Deckrot’ cultivar.

Correlation analysis, Pearson’s correlation (R) and Spearman’s rank correlation (ρ), between expression, copy number and metabolite data was performed with XLStat (version 20213.1) add-on for Excel (Addinsoft, 2023).

Gene expression quantification

Total RNA was extracted from pre-veraison samples using the SpectrumTM Plant Total RNA Kit (Sigma-Aldrich) with the removal of genomic DNA *via* on-column DNase digestion using the On-Column DNase I Digestion Set (Sigma-Aldrich) according to the manufacturer’s instructions. 1 μ g of RNA was converted to cDNA using the GoScriptTM Reverse Transcription mix, Oligo (dT) (Promega).

The relative expression of genes was measured *via* qPCR using primers from literature or newly designed primers (Table S2) with *VvActin* used as an endogenous control. qPCR was performed as described for gene copy number variation analysis above. Gene expression data for the progeny is reported relative to the individual with the lowest expression, while gene expression data for the parents’ developmental stages are reported relative to gene expression in ‘Deckrot’ green berry stage (EL-stage 33).

Gene isolation, transformation, sequencing

Genes were isolated from cDNA samples *via* polymerase chain reaction (PCR) using primers listed in Table S2. The PCR mixture (25 μ L) contained 0.2 μ M of the forward primer and reverse primers, 5 μ L cDNA (1:10 dilution), 1X ExTaq Buffer and 1U ExTaq polymerase (Takara). The reaction was performed in an Applied BiosystemsTM MiniAmp thermal cycler (ThermoFisher Scientific) and conditions were as follows: initial denaturation at 95°C for 3 minutes, then 40 cycles (95°C for 30 seconds, 55°C for 30 seconds, 72°C for 2 minutes) and a final elongation step at 72°C for

7 minutes. PCR products were purified using Zymoclean Gel DNA Recovery Kit (Zymo Research) as per the manufacturer’s protocol.

PCR products were ligated into pGEM[®] T-Easy Vector System (Promega) overnight at 4°C. Ligated vectors were subsequently transformed into competent DH5 α *E. coli* cells *via* heat-shock. Transformed cells were plated on LB agar containing ampicillin and after overnight incubation at 37°C, colonies were screened *via* PCR using M13 primers. Plasmids were isolated from positive colonies using GenEluteTM Plasmid Miniprep Kit (Sigma-Aldrich), as per the manufacturer’s protocol. Sanger sequencing was performed by the Central Analytical Facilities at Stellenbosch University (Stellenbosch, South Africa).

Results

The parents of the cross population differ for terpene accumulation

68 different volatile compounds were identified from the GCMS analysis: six alcohols, three ketones, ten aldehydes, two esters, four C13-norisoprenoids, 18 monoterpenes and 25 sesquiterpenes (Table S3). The volatile profiles of the parent cultivars were compared (Figure 1) and show clear segregation. Overall, the table grape selection, G1-7720, which is categorised as having a muscat aroma (Vervalle et al., 2022), has a higher volatile content regardless of developmental stage. While, the terpene content of both parents is highest at veraison, G1-7720 has a significant increase in sesquiterpene content from pre-veraison to veraison berries. G1-7720 shows significantly higher terpene levels than that of ‘Deckrot’. Aldehydes and alcohols also make up a major proportion of the volatile composition of each cultivar,

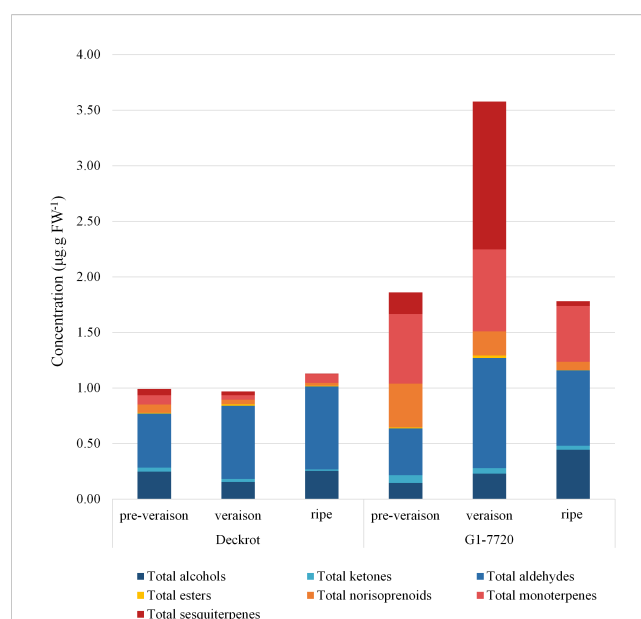


FIGURE 1
The volatile composition of the parent cultivars ‘Deckrot’ and G1-7720 during pre-veraison, veraison and harvest ripe stage.

specifically ‘Deckrot’, with hexanal, *trans*-2-hexenal and (*E*)-3-hexen-1-ol being the most significant contributors.

The distribution of the various volatile compound classes in the progeny is shown in Figure S1. Aldehydes are the most abundant compound class in the population; the average ratio of total aldehydes to total VOCs ranges between 34–47% across the various developmental stages. *Trans*-2-hexenal (an aldehyde) is the most abundant compound in the population. In fact, all six-carbon volatiles, also known as green leaf volatiles (GLVs), are among the most abundant VOCs within the population in all development stages. Sesquiterpenes are the most diverse class of compounds identified (26 compounds) in this study however they are present in low concentrations during most years, with the highest concentrations found in unripe veraison berries.

Candidate genes for were identified in several genomic regions associated with volatile organic compounds

186 Significant QTLs were identified associated with 54 compounds across the various seasons under analysis (Table S4). Consistent QTLs which were identified in at least two stages were mapped to the PN40024 v2 genome and annotated genes in each region were counted and inspected manually for their potential to regulate the associated metabolic phenotypes. QTLs associated with various monoterpenes were identified on chromosomes 5, 12, 13 and 17, while a QTL associated with the sesquiterpenes *trans*-caryophyllene and α -cubebene was identified on chromosome 19 and a QTL for total aldehydes and *trans*-2-hexenal was identified on chromosome 2 (Figure 2). Inspection of these genomic regions identified an average of 370 candidate genes in each QTL (Table 1).

A QTL on chromosome 2 associated with both total aldehydes and *trans*-2-hexenal and contained 335 genes. A Stearoyl-[acyl-carrier-protein] 9-desaturase 6 (SAD) was identified as candidate gene from this region. The *Vitis vinifera* SAD (VvSAD) was compared to other functionally characterised SAD enzymes from various species (Figure S2 and Table S5) to infer function.

Three geraniol derived compounds, namely *cis*-rose oxide, (*E*)-citral and nerol oxide associated with a QTL on chromosome 17. The enzymes involved in conversion of geraniol to *cis*-rose oxide, (*E*)-citral and nerol oxide are not described in grapevine however the reaction likely starts with the reduction of geraniol by an unknown reductase (Lin et al., 2019). To that end five short-chain dehydrogenase/reductases (VvSDR1–5) which co-localises with this QTL were selected as candidate genes. Comparison of VvSDR1–5 expression to metabolite data using TransMetaDb showed that VvSDR4 and VvSDR5 had strong positive correlation with citronellol accumulation ($R = 0.71$ and 0.70 , respectively), while VvSDR1 had a negative correlation ($R = -0.54$) with citronellol. Additionally, VvSDR3 had a negative correlation ($R = -0.62$) with nerol. Molecular phylogenetic analysis of the protein sequences of the identified VvSDRs were compared to that of other plant SDRs (Figure S3 and Table S5), and it was found that the VvSDRs cluster with three nepetalactol synthases which catalyse the conversion of 8-oxogeraniol to nepetalactol in catmint (Lichman et al., 2019).

While total sesquiterpenes did not produce any significant QTLs, the sesquiterpenes α -cubebene and *trans*-caryophyllene associated with a QTL on chromosome 19. This QTL co-localises with two predicted sesquiterpene synthases (VvTPS29 and VvTPS69), however VvTPS69 represented a partial gene and was thus not considered a candidate.

The QTLs associated with monoterpenes predominantly localised to chromosomes 5, 12 and 13. The majority of monoterpenes associated with a QTL region on chromosome 5 which co-localises with VvDXS1. Similarly, total monoterpenes and total C₁₃-norisoprenoids, localised to the same region on chromosome 5. While the C₁₃-norisoprenoid 6-Methyl-5-hepten-2-one (MHO) also showed a QTL on the same region on chromosome 5.

The acyclic monoterpenes geraniol and β -myrcene associated with an additional QTL on chromosome 12 while several cyclic monoterpenes associated with an additional QTL on chromosome 13. Genomic inspection of these QTLs found that they co-localise with clusters of terpene synthases (TPSs). When compared to the PN42004 v2 reference genome the QTL on chromosome 12 was found to co-localise with a cluster of eight TPS genes, while the QTL on chromosome 13 was found to co-localise with a TPS cluster that contains 11 terpene synthases (summarised in Table S6).

A phylogenetic tree comparing the VvTPSs in these QTL regions to functionally characterised *Vitis vinifera* TPSs is shown in Figure 3. VvTPS52 and VvTPS51 fall within a cluster with functionally characterised geraniol synthases (TPS-g), indeed VvTPS52 is the PN40024 gene model for geraniol synthase (VvGer) (Martin et al., 2010) and therefore VvTPS52/VvGer was selected as candidate gene for the QTL associated with geraniol in this mapping population. VvTPS39, VvTPS119 and VvTPS116 cluster with VvTer1 and VvTer2, α -terpineol synthases in the TPS-a clade, however, VvTPS119 and VvTPS116 represent pseudogenes (disrupted by numerous deletions, frameshifts and/or stop codons) in the PN40024 v2 genome. VvTPS39/VvTer was therefore considered the likely candidate gene underpinning the QTL region. Lastly, VvTPS29 clusters with *trans*-caryophyllene synthases (VvSHTPS27, VvMATPS27 and VvGwECar2) and a germacrene D synthase (VvGerD) in the TPS-a clade.

A SNP in VvDXS1 is associated with monoterpene accumulation

DNA sequencing of the VvDXS1 alleles revealed that while ‘Deckrot’ was homozygous (GG) for the wild-type allele, G1-7720 was heterozygous (GT) for the muscat aroma linked SNP (Doligez et al., 2006; Battilana et al., 2009; Emanuelli et al., 2010). A TaqMan assay was used to ascertain how the mapping population under investigation segregates for the G>T SNP. Results show that of the 82 progenies genotyped, 50 were heterozygous (GT) and 32 were homozygous (GG) (Table S7). Comparison of the total monoterpene content in the progeny with the occurrence of the G>T SNP found that GG-progeny displayed relatively low

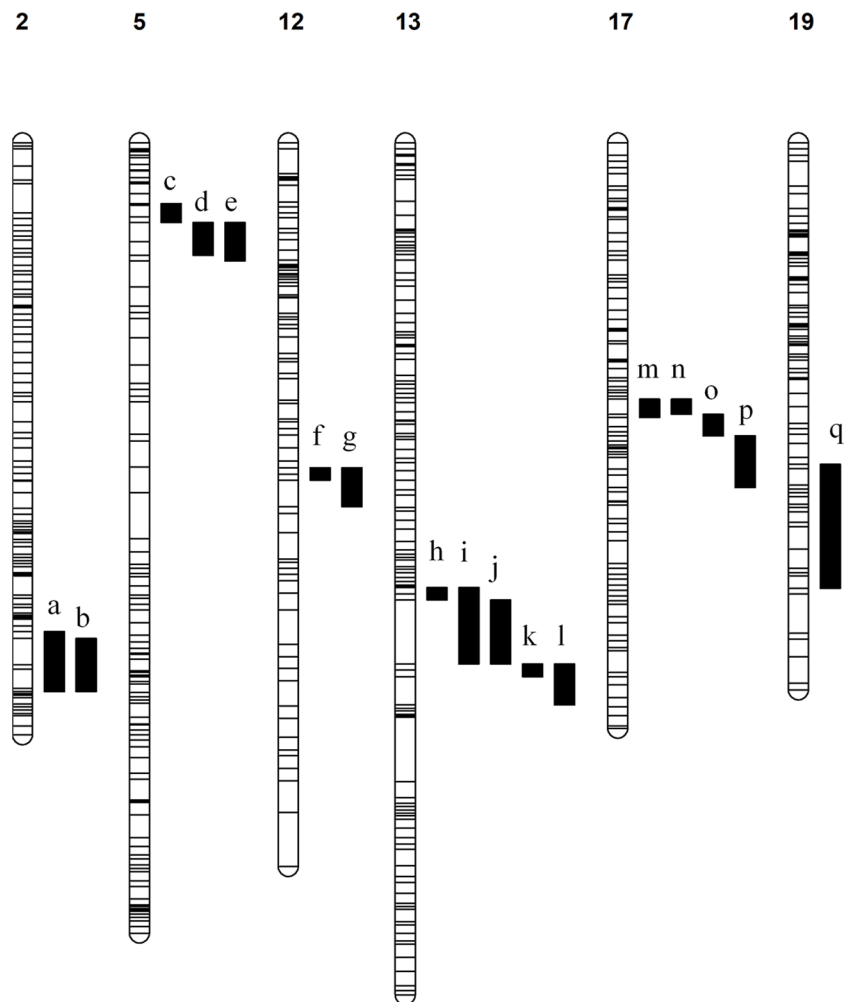


FIGURE 2

Linkage maps with associated QTLs. The chromosome number is indicated above each map and all QTLs are numbered a – q. The associated compounds for each QTL are listed. a) aldehydes total (veraison 2019) and trans-2-hexenal (veraison 2019). b) aldehydes total (2022) and trans-2-hexenal (2022). c) E-citral (veraison & 2021), β -citronellol (pre-veraison & 2022), cis-rose oxide (veraison, 2021 & 2022), geraniol (2022), limonene (2022), linalool (2022), total monoterpenes (2022), nerol oxide (veraison), p-mentha-1,5-dien-8-ol (veraison & 2021), trans- β -Ocimene (2022), α -terpinene (2022), α -terpineol (2022), α -terpinolene (2022), β -Myrcene (2022), γ -Terpinene (2022), p-Cymene (2022). d) 6-Methyl-5-hepten-2-one (pre-veraison, veraison, 2021), cis-rose oxide (pre-veraison), linalool (pre-veraison), p-Cymene (pre-veraison & veraison), p-mentha-1,5-dien-8-ol (pre-veraison), trans- β -Ocimene (pre-veraison & veraison), α -terpinene (veraison), γ -Terpinene (pre-veraison & veraison). e) β -Citronellol/Nerol (pre-veraison & 2021), C13-norisoprenoids total (veraison & 2021), geraniol (pre-veraison, veraison & 2021), limonene (pre-veraison, veraison & 2021), linalool (2021), linalool oxide (pre-veraison, veraison & 2021), monoterpenes total (pre-veraison, veraison & 2021), nerol oxide (pre-veraison & veraison), p-Cymene (2021), Terpinene-4-ol (pre-veraison, veraison & 2021), trans- β -Ocimene (2021), α -terpinene (veraison & 2021), α -Terpineol (pre-veraison, veraison & 2021), α -terpinolene (pre-veraison, veraison & 2021), β -Myrcene (pre-veraison, veraison & 2021), γ -Terpinene (2021). f) Geraniol (pre-veraison) & β -Myrcene (pre-veraison). g) Geraniol (veraison) & β -Myrcene (veraison). h) α -Terpineol (veraison) & α -terpinolene (veraison). i) Terpinene-4-ol (2021). j) 1,8-Cineole (pre-veraison & veraison), limonene (veraison), nerol oxide (veraison), p-Cymene (veraison & 2021), p-mentha-1,5-dien-8-ol (pre-veraison & veraison), Terpinene-4-ol (pre-veraison & veraison), α -terpinene (pre-veraison & veraison), γ -Terpinene (pre-veraison). k) limonene (pre-veraison), α -terpinene (2021), γ -Terpinene (veraison). l) p-Cymene (pre-veraison), p-mentha-1,5-dien-8-ol (2021), α -terpinolene (pre-veraison). m) cis-rose oxide (2021) & nerol oxide (veraison). n) nerol oxide (pre-veraison). o) cis-rose oxide (veraison). p) E-citral (2021) & cis-rose oxide (pre-veraison). q) α -Cubebene (pre-veraison & veraison) & trans-caryophyllene (pre-veraison and veraison).

monoterpene accumulation, while GT-progeny displayed relatively increased monoterpene accumulation levels, with a continuous variation in distribution (Figure 4). Orthogonal partial least squares (OPLS) analysis of the full volatile dataset across the population and *VvDXSI* genotypes show that the population clearly segregates for the SNP (Figure S4). The population segregate for the SNP across principal component 1 (PC1) which explains 27.1% of the variation.

Expression of *VvTer* shows correlation with cyclic monoterpene accumulation

VvTer and *VvGer* gene expression was quantified during the late flower and early berry development in 'Deckrot' and G1-7720 (Figure 5). *VvGer* showed the highest level of expression in young flowers for both parents, while geraniol content only peaked in the following stage. *VvTer* expression was highest after fruit-set

TABLE 1 List of candidate genes for significant QTLs associated with VOCs.

Linkage group	Compounds	12xV2 position (bp) ^a	Number of genes	Candidate gene	Accession number	Function (based on UniProt/SwissProt hit)
chr02	Total aldehydes Trans-2-hexenal	9086122 - 15054521	335	VvSAD	Vitvi02g01527	Stearoyl-[acyl-carrier-protein] 9-desaturase 6 (SAD)
chr05	Several monoterpenes ^b Total monoterpenes Geranyl acetone 6-Methyl-5-hepten-2-one Total C13-norisoprenoids	2217503 - 4373666	214	VvDXS1	Vitvi05g00372	1-deoxy-D-xylulose-5-phosphate synthase (DXS)
chr12	Geraniol and β -myrcene	7725827-9589001	225	VvTPS52/VvGer	Vitvi12g02178	Geraniol terpene synthase
chr13	Several cyclic monoterpenes ^c	18786002-21772519	201	VvTPS39/VvTer	Vitvi13g01307	α -terpineol synthase
chr17	Cis rose-oxide Nerol oxide E-citral	5844409 - 8181258	262	VvSDR1 VvSDR2 VvSDR3 VvSDR4 VvSDR5	Vitvi17g00538 Vitvi17g00537 Vitvi17g00534 Vitvi17g00535 Vitvi17g01453	Short chain dehydrogenase/reductase (SDR)
chr19	Trans-Caryophyllene α -Cubebene	8950369-20638362	984	VvTPS29	Vitvi19g00956	Germacrene D synthase

^aThese positions provide a consensus region for overlapping QTLs on the same chromosome. Table S4 shows the exact position of each compounds' associated QTL.
^b α -terpinene, p-Cymene, trans- β -Ocimene, γ -Terpinene, Linalool Oxide, α -terpinolene, Linalool, cis-Rose oxide, Terpinene-4-ol, α -Terpineol, Geraniol, Limonene, β -Citronellol/Nerol, (E)-Citral, β -myrcene.
^c α -terpinene, p-Cymene, 1,8-Cineole, γ -Terpinene, α -terpinolene, Terpinene-4-ol, α -Terpineol.

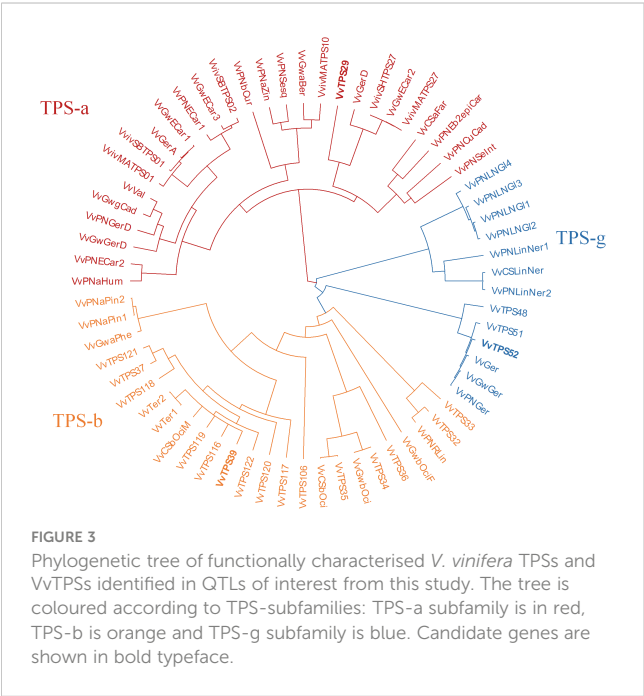
(EL-29), while α -terpineol concentration peaked earlier in the flowering stages. Both *VvTer* and *VvGer* expression, as well as α -terpineol and geraniol concentration, decrease towards later berry development and is lowest in green berries (EL-33). Furthermore, α -terpineol and geraniol concentration is significantly higher in G1-

7720 than 'Deckrot', irrespective of developmental stage or gene expression (Figure 5).

The expression of *VvTer* and *VvGer* was measured in a subset of the progeny to determine whether gene expression correlates with cyclic monoterpene or geraniol accumulation, respectively. The expression was measured in progenies with the *VvDXS1* SNP (GT) and without the *VvDXS1* SNP (GG). Linear regression analysis showed weak correlations between *VvTer* expression and cyclic monoterpene accumulation and between *VvGer* expression and geraniol accumulation (Figure S5). However, in progeny possessing the *VvDXS1* SNP, *VvTer* gene expression and cyclic monoterpene content showed relatively strong correlation ($R = 0.78$, $p < 0.0001$), indicating a positive linear relationship between *VvTer* expression and cyclic monoterpene accumulation (Figure 6).

Multiple *VvTer* and *VvGer* gene copies were isolated from 'Deckrot' and G1-7720

Multiple cDNA clones of *VvTer* and *VvGer* from both 'Deckrot' and G1-7720 were sequenced in order to identify potential sequence variants. Using single primer pairs for each gene several unique expressed *VvTer* and *VvGer* gene copies were isolated from each parent cultivar (Table 2 and Figure S6). The nucleotide sequences of all gene copies were compared to functionally characterised terpene synthases in *Vitis vinifera* via molecular phylogeny (Table S8 and Figure 7). Regardless of cultivar, all *VvTer* sequences fall within the TPS-b family cluster while *VvGer* falls within the TPS-g subfamily.



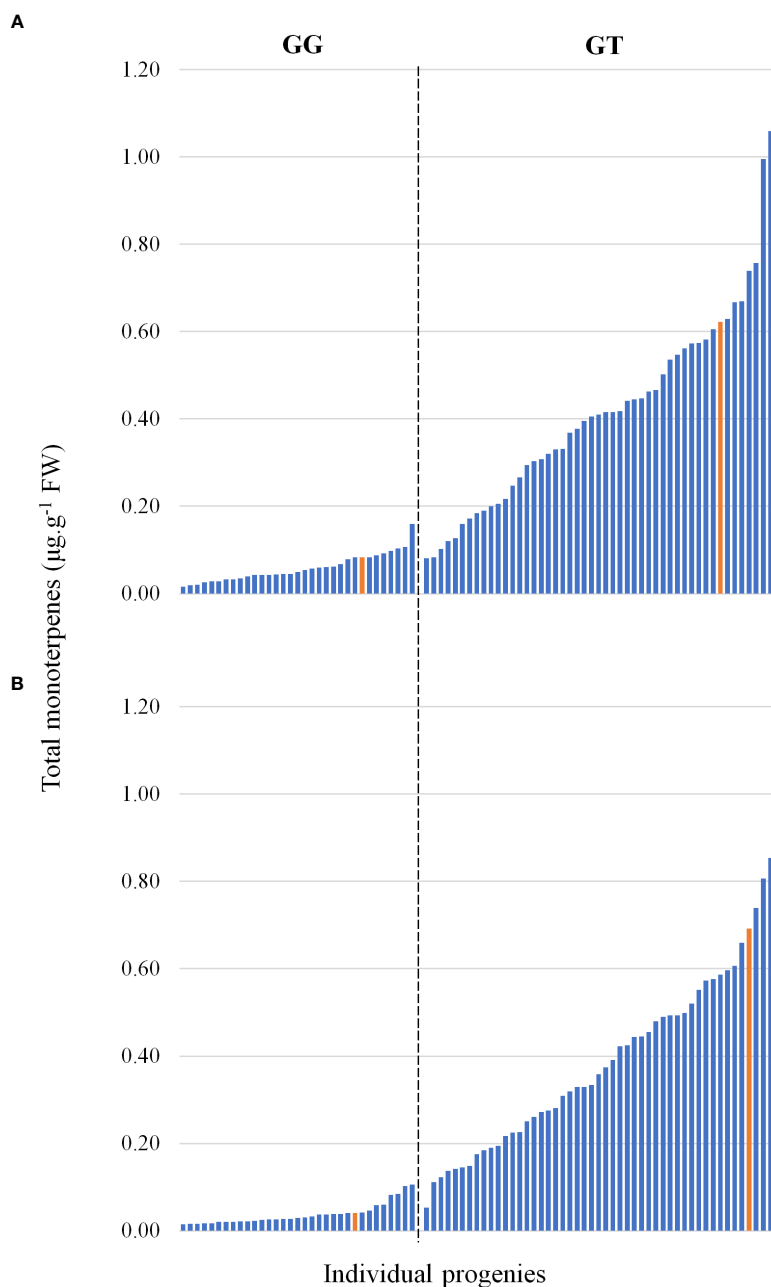


FIGURE 4

The total monoterpene content in the mapping progeny at (A) pre-veraison and (B) veraison. Each bar represents a member of the progeny, and the parents are shown in yellow. The bars are grouped into absence/presence of the *VvDXS1* SNP.

Interestingly, ‘Deckrot’ *VvTer* genes (*DRTer*) and G1-7720 *VvTer* genes (*G1Ter*) form two distinct clusters. Furthermore, *VvGer* gene copies from ‘Deckrot’ and G1-7720 share sequence similarity with functionally characterised *V. vinifera* geraniol synthases (*VvGer*, *VvGwGer* and *VvPNGer*), respectively. *DRTer* gene copies are similar to functionally characterised α -terpineol synthases (*VvTer1* and *VvTer2*), while *G1Ter* gene copies share sequence similarity with an (*E*)- β -ocimene/myrcene synthase (*VvCSbOciM*). *VvTer1*, *VvTer2* and *VvCSbOciM* are described as TPS39 genes with *VvTer1* and *VvTer2* being isolated from ‘Gewürtztraminer’, while *VvCSbOciM* was isolated from Cabernet Sauvignon (Martin and Bohlmann, 2004; Martin et al., 2010).

Copy number of *VvTer* is correlated with cyclic monoterpene content

The relative copy numbers of *VvTer* and *VvGer* were determined for 82 progenies of the mapping population, as well as the parents (Table S9). Both *VvTer* and *VvGer* copy numbers were higher in G1-7720 than in ‘Deckrot’; *VvGer* had a 10:19 ratio for ‘Deckrot’:G1-7720 while *VvTer* had a 5:12 ratio. Gene copy number in the population were expressed as relative to ‘Deckrot’ gene copies, such that *VvTer* copy number ranges between 0.7–2.8 relative copies, while *VvGer* ranges between 1 – 2.1 relative copies. Additionally, a few individuals from the progeny were outliers.

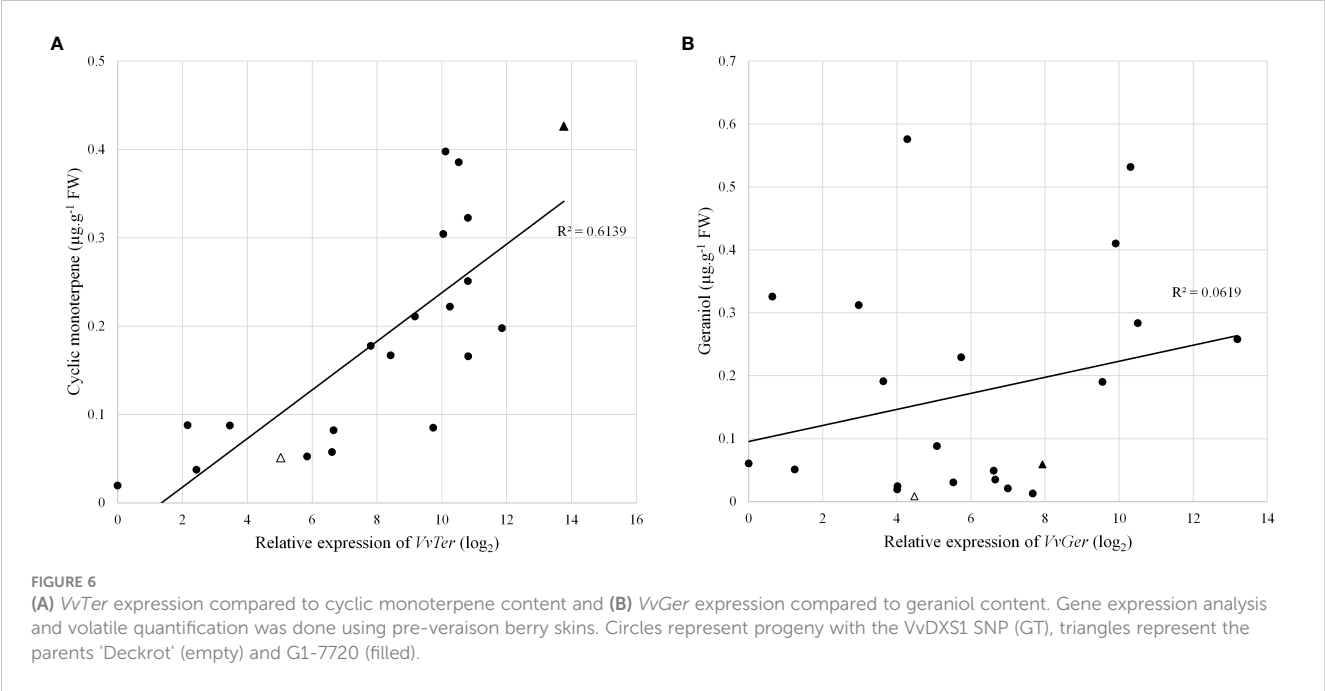
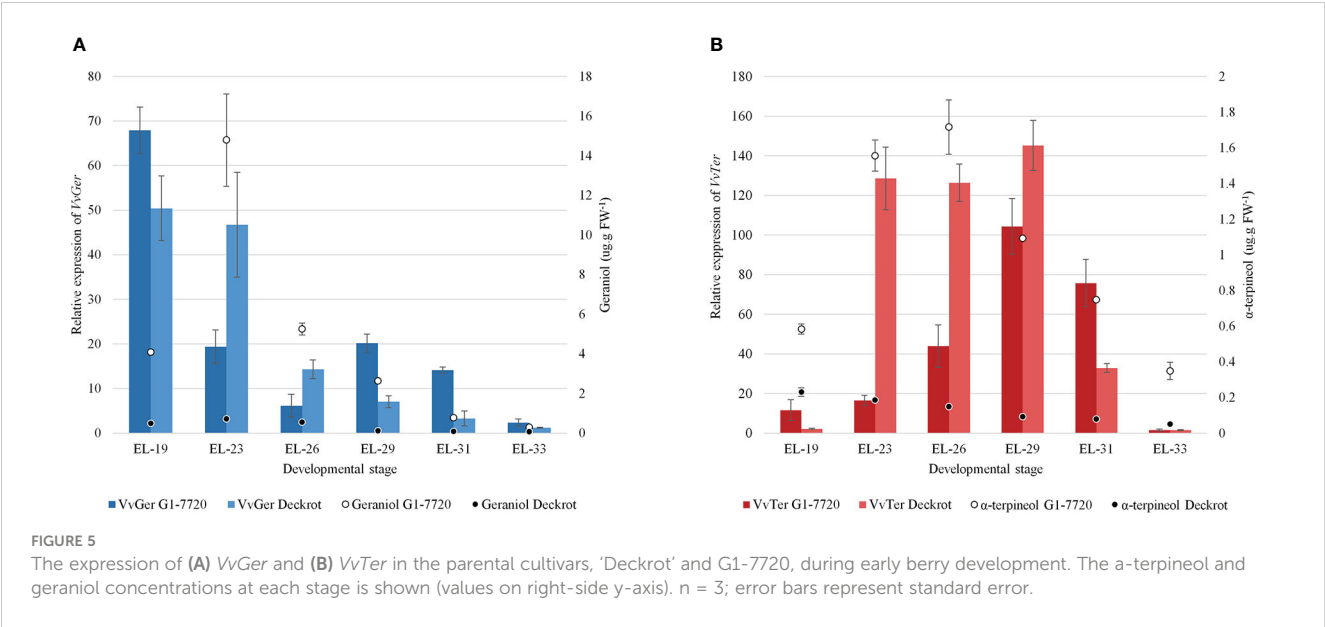
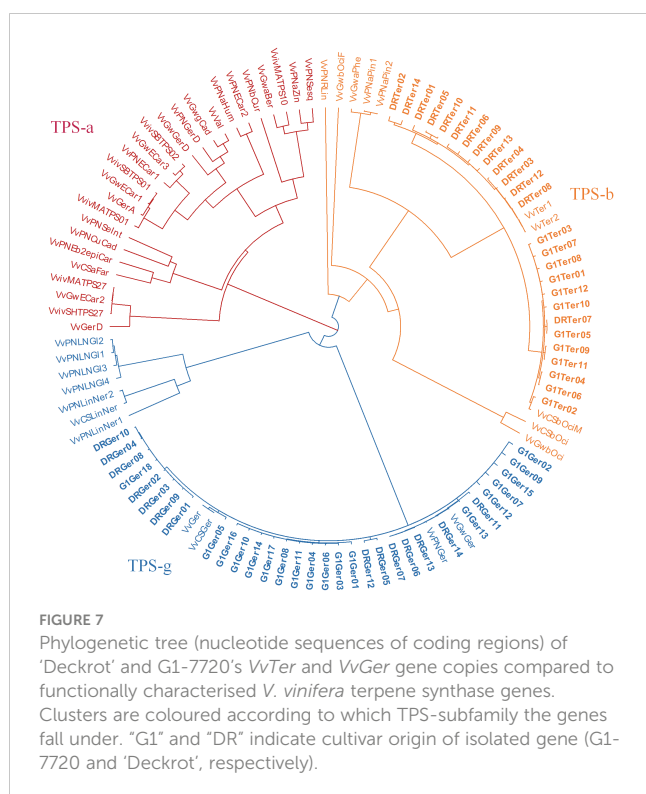


TABLE 2 The number of unique *VvTer* and *VvGer* cDNA clones that were identified for 'Deckrot' and G1-7720.

Parent cultivar	Gene of interest	cDNA clones sequenced	unique cDNA sequences	Putatively functional
'Deckrot'	<i>VvTer</i>	16	14	10
	<i>VvGer</i>	16	14	12
G1-7720	<i>VvTer</i>	14	12	9
	<i>VvGer</i>	23	18	15



VvGer had the most outliers (6 progenies) with copy numbers up to 12.8 times higher than that observed for 'Deckrot'.

Spearman's rank correlation (ρ) analysis found *VvTer* copy number possessed a strong correlation with *VvTer* expression ($\rho = 0.748$), but *VvGer* copy number and expression had weak correlation ($\rho = 0.189$). The geraniol and total cyclic monoterpene content was binned into three categories: low, moderate and high (Figure 8A). *VvGer* copy number shows no discernible pattern between geraniol content and copy number, while total cyclic monoterpene content seems to show a positive correlation with *VvTer* copy number. The correlation between gene copy number and several monoterpenes was investigated in the progeny (Figure 8B). There was no correlation between *VvGer* copy number and any monoterpenes in the progeny, regardless of the presence of the *VvDXS1* SNP. However, *VvTer* showed different degrees of correlation with cyclic monoterpenes depending on the presence of the *VvDXS1* SNP. Progeny which did not have the G>T *VvDXS1* SNP (GG) showed weak correlation ($-0.1 < \rho < 0.1$) between *VvTer* copy number and cyclic monoterpenes, while in progeny with the *VvDXS1* SNP (GT) there was a strong positive correlation ($\rho > 0.6$).

Heterozygous distribution of terpene synthases observed in a diploid *Vitis vinifera* genome

Analysis of the draft diploid genome of Cabernet Sauvignon identified 29 putative α -terpineol synthase (*VvCSTer*) loci, and nine putative geraniol synthase (*VvCSGer*) loci (Table S10). The majority of α -terpineol synthases were localised to chromosome 13 while geraniol synthases predominantly localised to chromosome 12, and

the remaining genes were unplaced (Table S10). The nucleotide coding sequences of *VvCSTer* genes had a pairwise identity of 90.8% and *VvCSGer* genes shared 98.2% pairwise identity. Furthermore, the loci appeared in clusters on the chromosomes, with adjacent genes in clusters being less than 100 kb apart (Figure 9). Haplotype 2 of chromosome 13 has three separate *VvCSTer* clusters which are approximately 1 Mb apart. The high similarity as well as proximity of these genes indicate an extensive level of tandem gene duplication, particularly for *VvCSTer* genes.

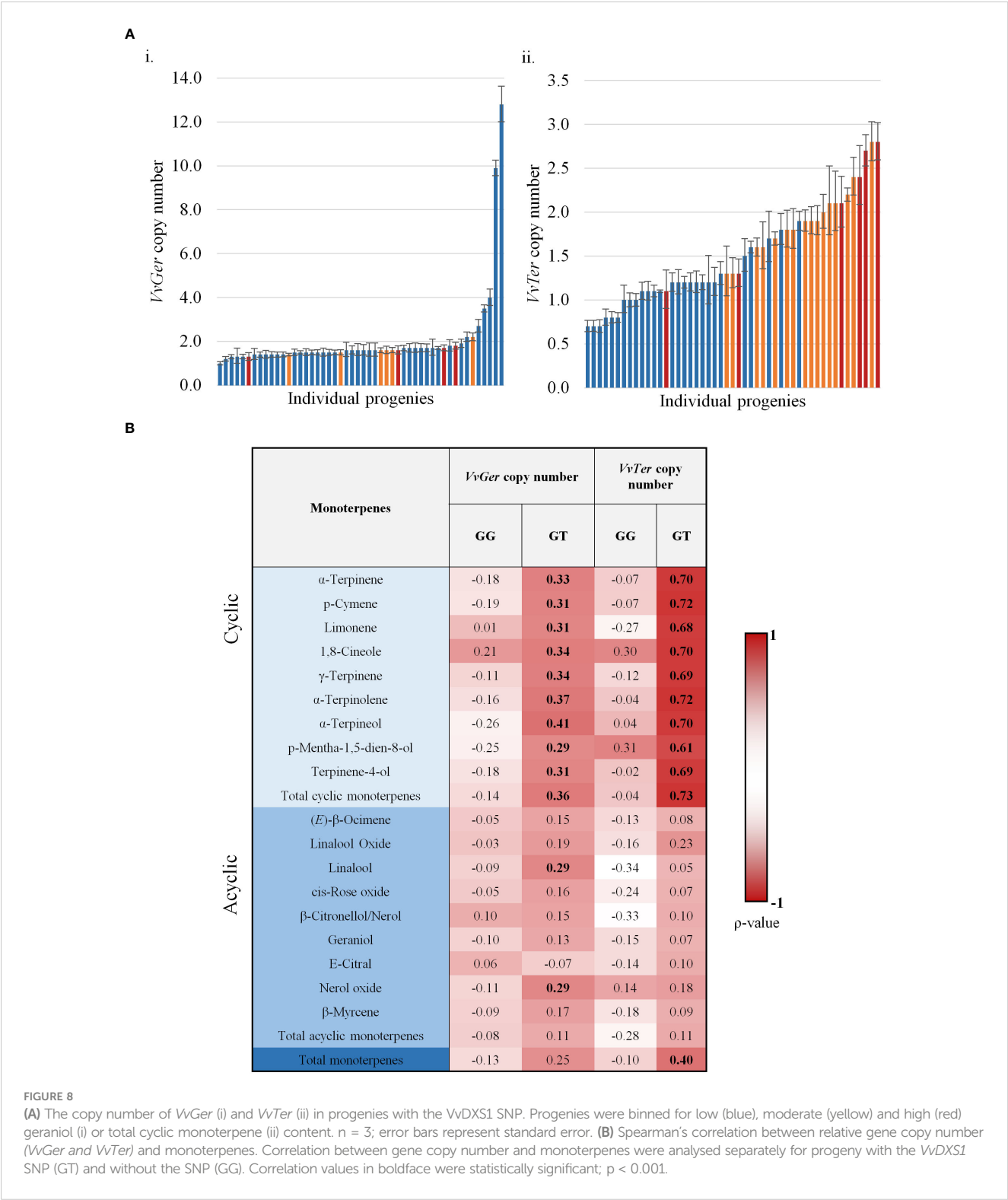
11 of the 29 predicted Cabernet Sauvignon α -terpineol synthase loci encode for putatively functional enzymes, while 4 of the 9 geraniol synthase loci encode for putatively functional enzymes. A phylogenetic tree (Figure S7) was constructed to compare the putatively functional Cabernet Sauvignon α -terpineol and geraniol synthases with functionally characterised *Vitis vinifera* terpene synthases. All putatively functional *VvCSGer* proteins fall within the TPS-g cluster while *VvCSTer* proteins fall within the TPS-b cluster.

Discussion

Elucidation of the genetics underlying the VOC profile of the mapping population

Studies analysing volatile accumulation show mixed results with regards to the accumulation pattern of different VOC classes (Ferrandino et al., 2012; Vilanova et al., 2012; Ji et al., 2021; Liu et al., 2022), and it is therefore challenging to compare the metabolite data observed here with previous studies. Importantly, however, the genetic control of VOC accumulation was evident through the observed segregation of compound accumulation in the population under study, and the subsequent associated QTLs that were identified. The significant QTL on chromosome 5 associated with total monoterpene content, houses the well described *VvDXS1* gene (Doligez et al., 2006; Battilana et al., 2009; Emanuelli et al., 2010). In the population under investigation here we show that the SNP contributing to high terpene level and a "muscat like aroma" is derived from G1-7720, the aromatic parent. Importantly this SNP was found to be a prerequisite for high monoterpene levels in the progeny, but not an absolute indicator (Figures 4, S4). This is likely due to the multigenic nature of terpene formation, further highlighted by the various other QTLs identified in this study and others (Doligez et al., 2006; Battilana et al., 2009; O'Reilly-Wapstra et al., 2011; Yu et al., 2017; Reichardt et al., 2020; Barbey et al., 2021). Importantly, accumulation of the plastid derived C13-norisoprenoids also associated with this SNP, while the cytosolic derived sesquiterpenes did not. This suggests that, at least in the case of this grapevine population, there is limited isoprenoid crosstalk from plastid to cytosol (Gutensohn et al., 2013).

While the *VvDXS1* SNP can be considered a master regulator of monoterpene accumulation, candidate genes which co-localise with QTLs for geraniol, cyclic monoterpenes and sesquiterpenes were also identified in this study. Geraniol shows a QTL on chromosome 12 which co-localised with a cluster of eight terpene synthase genes. *VvTPS52*, one of the eight *VvTPSs* in this region, was predicted to



function as a geraniol synthase (*VvGer*) and has indeed been previously functionally characterised as a geraniol synthase in various other cultivars (Martin et al., 2010). Several cyclic monoterpenes showed overlapping associated QTLs on chromosome 13. These QTLs co-localise with a cluster of terpene synthase genes containing putative α -terpineol synthases. *VvTPS39* was proposed as candidate gene for this QTL as it was the closest related gene that was not a predicted pseudogene and has been characterised as an α -terpineol synthase (*VvTer*) via *in vitro* enzyme assay in ‘Gewurztraminer’ (Martin and Bohlmann, 2004). Interestingly, the authors found that *VvTPS39* produced α -terpineol, 1,8-cineole and β -pinene as major products and various

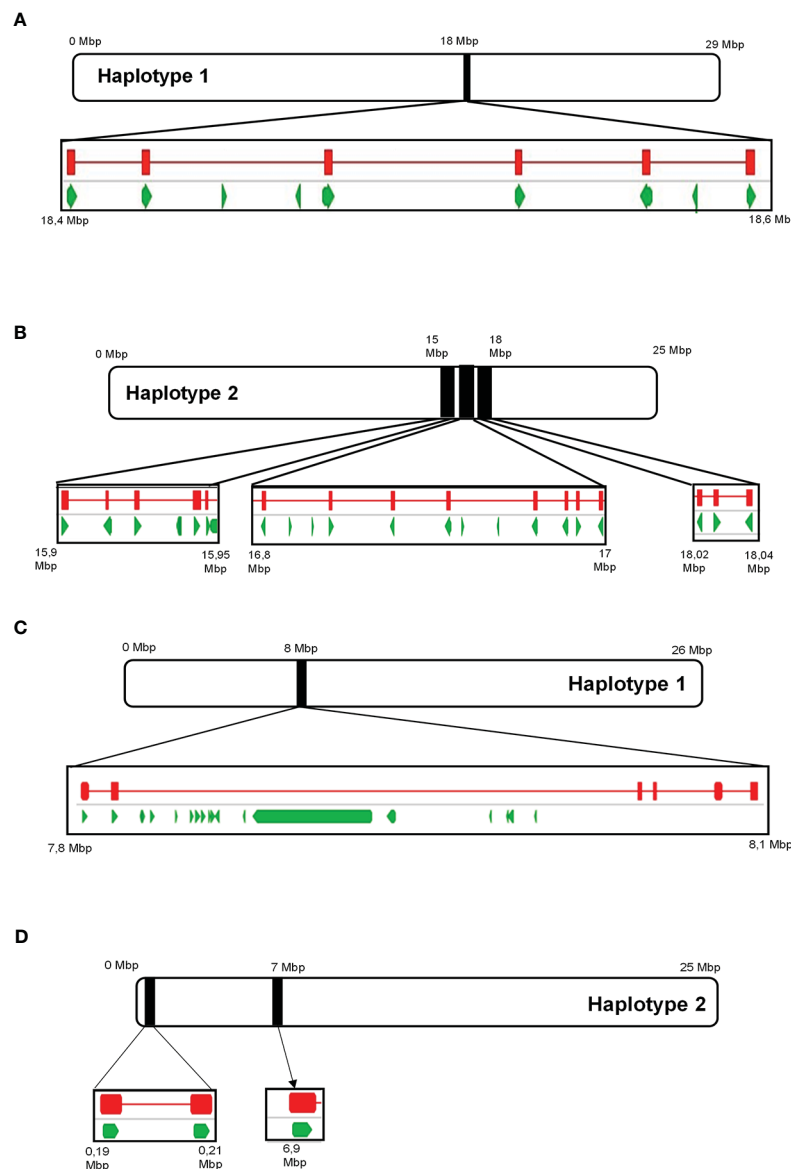


FIGURE 9

The position of predicted 'Cabernet Sauvignon' *VvTer* and *VvGer* genes on chromosome 13 (A, B) and chromosome 12 (C, D), respectively. Black blocks indicate the position of the predicted *VvTer* or *VvGer* clusters on the chromosomes, and squares underneath provide a magnified view of the region. Green arrows represent predicted genes as annotated in Massonnet et al. (2020), while red lines indicate the position of BLAST hits for *VvTer* or *VvGer*.

minor product including α -thujene, α -pinene, myrcene, sabinene, β -pinene, limonene, and terpinolene. The multi-product nature of terpene synthases may explain why this study found multiple cyclic monoterpenes mapping to the same region on chromosome 13. It is likely that *VvTer* (and possibly some of the other *VvTPS*s that clustered in the same region) produce cyclic monoterpenes in varying ratios, with α -terpineol being the major product.

The sesquiterpenes α -cubebene and trans-caryophyllene, associated with a large QTL (approximately 11.65 Mbp) on chromosome 19. *VvTPS29* was proposed as a candidate gene and this was further supported by molecular phylogenetic evidence. *VvTPS29* showed to be closely related to functionally characterised trans-caryophyllene synthases and a germacrene D synthase

(Figure 3). Additionally, an isocaryophyllene/ β -cadinene synthase (*VvShirazTPS-Y2*) which shares 100% similarity with *VvTPS29* has been characterised in 'Shiraz' (Dueholm et al., 2019).

Non-terpene VOCs were also found to associate with QTLs in this study. C6-compounds or green leaf volatiles (GLVs) were the most abundant VOCs present in the progeny at all developmental stages, as has been reported in other studies (Kalua and Boss, 2009; Vilanova et al., 2012). A QTL associated with trans-2-hexenal and total aldehydes was identified on chromosome 2 and co-localised with a Stearoyl-[acyl-carrier-protein] 9-desaturase 6 (*SAD*). *SAD* catalyses the conversion of stearoyl-ACP to oleoyl-ACP which serves as a precursor for the fatty acids α -linolenic acid and linoleic acid. α -linolenic acid and linoleic acid in turn can be

broken down to form green leaf volatiles which are synthesised via the lipoxygenase (LOX) pathway (Matsui and Engelberth, 2022). GLVs are rapidly released upon plant wounding which is thought to play a role in plant signalling and defence (Matsui, 2006; Bouwmeester et al., 2019; Matsui and Engelberth, 2022). C6-aldehydes and -alcohols contribute to the undesirable “green aroma” of wine (Dunlevy et al., 2009), and therefore understanding their metabolism may contribute to improved wine aroma.

A QTL associated with cis-rose oxide, E-citral and nerol oxide was identified in the same region on chromosome 17. A cluster of five short chain dehydrogenase/reductases which co-localised with the QTL were selected as candidate genes. All three of the compounds are derived from geraniol, however importantly geraniol did not associate with this QTL. Geraniol dehydrogenases which catalyse the formation of citral and citronellol have been identified in several plant species but not in grapevine (Iijima et al., 2006; Sato-Masumoto and Ito, 2014; Xu et al., 2017). Lin et al. (2019) summarises a proposed pathway for citronellol, nerol and cis-rose oxide in grapevine but to date none of the proposed enzymes in the pathway have been identified and characterised. Further characterisation of the *VvSDRs* identified in this QTL may therefore prove promising in elucidating the biosynthesis of these compounds.

Investigation of the *VvTer* and *VvGer* loci highlights extensive gene duplication

In an attempt to isolate the monoterpene synthase genes underlying the QTLs associated with geraniol and cyclic monoterpene accumulation it was discovered that there were more gene copies than represented in the reference genome. Furthermore, as the genes isolated represent cDNA clones, the number of gene copies shown in Table 2 is not exhaustive representation of all the possible *VvTer* and *VvGer* copies. Importantly, phylogenetic analysis of the sequenced ‘Deckrot’ and G1-7720 *VvTer* and *VvGer* gene copies found strong cultivar specific clustering, indicating this gene duplication has occurred post cultivar diversification.

Due to the somewhat surprising nature of observed *VvTPS* gene duplication in the cultivars in this study an *in silico* analysis of *VvTer* and *VvGer* in the diploid ‘Cabernet Sauvignon’ genome was performed. This analysis confirmed massive gene duplication and revealed that both genes occur in tandem duplications on chromosome 13 and chromosome 12, respectively. *VvTer* had the most extensive duplications with 29 copies on the ‘Cabernet Sauvignon’ genome. Analysis of the draft diploid genome further indicated that *VvTer* genes were unequally distributed between the two haplotypes of chromosome 13. *VvGer* genes also occurred unequally distributed on the haplotypes of chromosome 12. The distribution *VvTer* and *VvGer* loci were uneven on the two haplotypes of chromosomes 12 and 13, revealing a high level of hemizygosity. Furthermore, due to the high sequence similarity between these genes, it is difficult to predict which loci are allelic and which are hemizygous.

Further study is necessary to ascertain the function of the *VvTPS* candidate genes in this mapping population. High levels of gene duplication contribute to the diverse functions of TPSs through neofunctionalisation and sub-functionalisation (Tholl, 2015). Furthermore, the function of TPSs can be changed by small amino acid substitutions which alter the active site conformation and further contributes to the diverse functions of TPSs (Degenhardt et al., 2009; Karunanithi and Zerbe, 2019) and this has also been shown by the presence of cultivar-specific TPSs in grapevine (Martin et al., 2010; Drew et al., 2016; Smit et al., 2019) therefore it remains a challenge to predict the function of *VvTPSs* based on sequence similarity to functionally characterised genes alone.

VvTer gene copy number and expression correlate with cyclic monoterpene accumulation

The pattern of *VvGer* and *VvTer* expression was similar in both parent cultivars during berry development, but the expression patterns did not correspond with the accumulation of α -terpineol or geraniol. Previous studies have shown that *VvTPS* developmental expression patterns do not always match the accumulation patterns of their associated metabolites (Martin et al., 2012; Matarese et al., 2013; Matarese et al., 2014). Furthermore, only the volatile fractions of geraniol and α -terpineol were quantified in this study, while monoterpenes are also present in non-volatile glycosylated forms in grapevine (Dunlevy et al., 2009; Hjelmeland and Ebeler, 2015).

However, the expression of *VvTer* across the mapping population correlated with several cyclic monoterpenes, specifically in progeny containing the *VvDXS1* SNP. The high similarity between *VvTer* paralogs potentially skews qPCR data as the primers have the potential to bind to more than one *VvTer* gene locus. This fact together with the *VvTPS* gene duplication data described above led to investigation of the *VvTer* gene copy number. Importantly, the parent cultivars under investigation showed unequal *VvTer* gene copy number, with G1-7720 showing 2.4-fold greater number of copies of *VvTer* than ‘Deckrot’. Relative *VvTer* gene copy number showed a positive correlation with the accumulation of several individual cyclic monoterpenes as well as total cyclic monoterpenes. The correlation of *VvTer* gene expression with multiple monoterpenes is in agreement with the fact that this gene cluster co-localises with the QTL for cyclic monoterpenes. Furthermore, *VvTer* is potentially a multi-product forming enzyme similar to other terpene synthases (Martin et al., 2010; Karunanithi and Zerbe, 2019), and potentially forms several structurally related monoterpene compounds, such as cyclic monoterpenes.

Hypotheses for the correlation of *VvTer* copy number and cyclic monoterpene accumulation are somewhat more speculative and are detailed in the following sections. The first hypothesis is that *VvTer* copy number may cause a dosage effect, i.e. the more copies of the gene, the more transcripts produced, and the more enzyme translated. This is supported by the strong correlation between *VvTer* expression and copy number. However, dosage does not explain why some low copy number individuals have high levels of cyclic monoterpenes and vice versa (Figure 8).

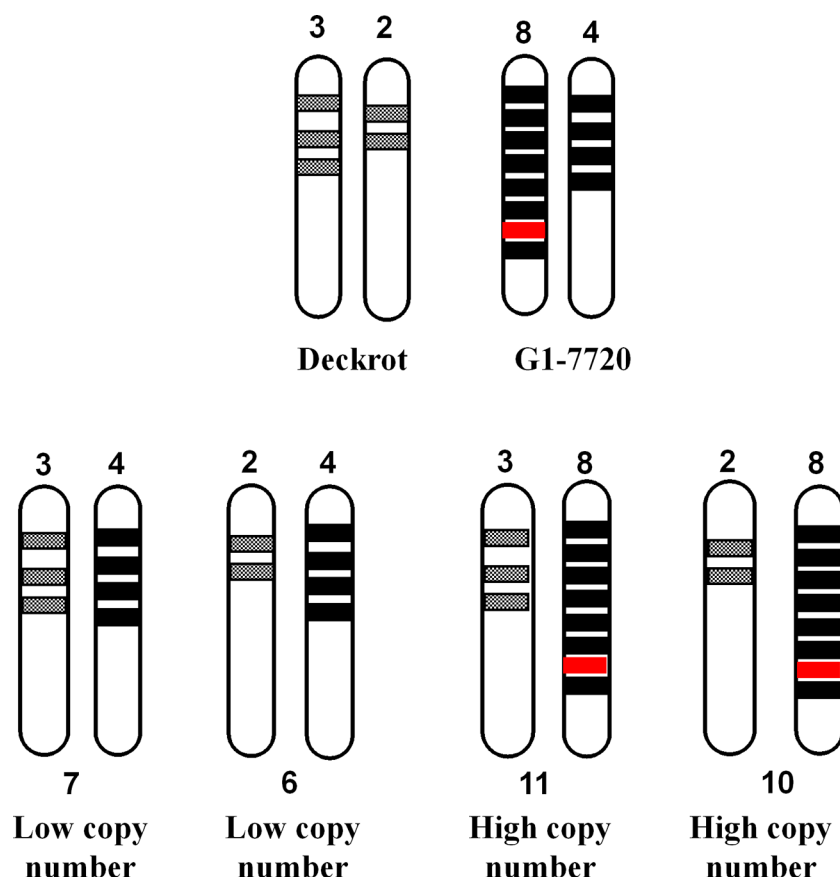


FIGURE 10

A diagram to explain the correlation between *VvTer* copy number and cyclic monoterpene accumulation. *VvTer* genes are represented by shaded blocks and the “hyper-functional” gene is shown in red. The “hyper-functional” gene falls on the parent allele with the highest copy number and is the causal factor for higher cyclic monoterpene content in this parent. The progeny from ‘Deckrot’ x G1-7720 have an equal chance having one of four possible *VvTer* copies: 6, 7, 10 or 11. Progenies with 6 or 7 copies would be considered “low copy number” individuals and would not inherit the “hyper-functional” gene resulting in lower/normal accumulation of cyclic monoterpenes. Progenies with 10 or 11 copies would be considered “high copy number individuals” and will inherit the “hyper-functional” gene resulting in higher cyclic monoterpene accumulation.

Another possible explanation is that a “hyper-functional” gene/genetic element co-localises with the high copy number allele (Figure 10). “Hyper-functional” is defined as any sequence variation which significantly improves cyclic monoterpene synthase enzyme activity, resulting in increased cyclic monoterpene biosynthesis. In Figure 10 we assume that “Deckrot” has 5 copies of *VvTer* (3 copies on allele A and 2 copies on allele B) and G1-7720 has 12 copies (8 copies on allele A and 4 copies on allele B) as this fulfils the 5:12 (‘Deckrot’:G1-7720) ratio of *VvTer* copy number in the parents. It is important to note that while the exact gene copy numbers cannot be determined, sequencing of cDNA clones suggests a relatively high *VvTer* copy number. Furthermore, the fact that the progeny typically presented a higher copy number than ‘Deckrot’, and a lower copy number than G1-7720, indicate that both alleles for G1-7720 have a higher copy number than the ‘Deckrot’ alleles.

In this hypothesis the progeny has an equal chance of inheriting one allele from each parent in four potential different combinations. If a hyper-functional gene/genetic element co-localizes with the high copy number allele, all individuals that inherited the high copy number allele will

have high cyclic monoterpene levels. Therefore, individuals with a high copy number do not have higher levels of cyclic terpenes due to additive effects but due to the co-segregation of high copy number and a “gain-of-function” gene/genetic element. The high level of hemizygosity of *VvTer* genes in the ‘Cabernet Sauvignon’ genome, as well as the large discrepancy between *VvTer* copy numbers of ‘Deckrot’ and G1-7720 (G1-7720 has 2.4 times as many *VvTer* copies as ‘Deckrot’) support this theory. While the exact distribution of *VvTer* loci in the parent cultivars are unknown, it is safe to assume that both also have high hemizygosity which results in them having either a “high copy number” or “low copy number” allele.

This hypothesis also explains why some individuals have a low copy number but high cyclic monoterpene level. If the hyper-functional element is transferred to a “low copy number” allele during a recombination event, some low copy number individuals will have high cyclic monoterpene levels. Recombination events at a specific locus are rare and would thus only affect a few individuals in the population (Choi, 2017). Furthermore, this hypothesis explains why there is no correlation between *VvGer* copy number and geraniol levels. The difference in *VvGer* copy numbers between

G1-7720 and 'Deckrot' is less prominent, therefore making differentiation between "high copy number" and "low copy number" alleles difficult. The "hyper-functional" element of *VvGer* thus co-segregates with high copy number similarly to *VvTer*, but the difference between high and low copy number is too small to make any significant distinction and no correlation is observed.

Conclusion

During berry development *VvGer* and *VvTer* gene expression patterns did not align with the accumulation patterns of geraniol and α -terpineol, respectively, indicating that terpene synthase gene expression cannot solely be used to infer gene function. Furthermore, the extensively duplicated nature of the TPS gene family complicates gene expression analysis as well as identification of sequence variants leading to enzyme activity modulation. *VvGer* and *VvTer* genes are present in tandemly duplicated gene clusters and these clusters are unequally distributed across chromosome haplotypes indicating extreme levels of hemizygosity for these genes. Furthermore, *VvTer* is highly duplicated in grapevine genomes and *VvTer* copy number correlated with cyclic monoterpene accumulation.

Extensive gene duplication is a common feature of TPS-gene families in several plant species and results in the presence of multiple highly similar gene paralogs in these genomes. While the influence of small polymorphisms, such as SNPs and indels, on TPS functions and terpene accumulation are commonly researched, very few studies investigate the influence of this gene copy number variation on terpene accumulation. The knowledge gained from this study further contributes to our understanding of terpene metabolism in grapevine and the potential impact of TPS copy number variation on grapevine terpene accumulation.

Data availability statement

The original contributions presented in the study are included in the article/**Supplementary materials**. Further inquiries can be directed to the corresponding author.

References

- Addinsoft. (2023). *XLSTAT statistical and data analysis solution*. (New York, USA). <https://www.xlstat.com/en>.
- Barbey, C. R., Hogshead, M. H., Harrison, B., Schwartz, A. E., Verma, S., Oh, Y., et al. (2021). Genetic analysis of methyl anthranilate, mesifurane, linalool, and other flavor compounds in cultivated strawberry (*Fragaria × ananassa*). *Front. Plant Sci.* 12, 615749. doi: 10.3389/fpls.2021.615749
- Battilana, J., Costantini, L., Emanuelli, F., Sevin, F., Segala, C., Moser, S., et al. (2009). The 1-deoxy-d-xylulose 5-phosphate synthase gene co-localizes with a major QTL affecting monoterpene content in grapevine. *Theor. Appl. Genet.* 118 (4), 653–669. doi: 10.1007/s00122-008-0927-8
- Battilana, J., Emanuelli, F., Gambino, G., Gribaudo, I., Gasperi, F., Boss, P. K., et al. (2011). Functional effect of grapevine 1-deoxy-D-xylulose 5-phosphate synthase substitution K284N on Muscat flavour formation. *J. Exp. Bot.* 62 (15), 5497–5508. doi: 10.1093/jxb/err231
- Bhattacharya, S., Holowka, T., Orner, E. P., and Fries, B. C. (2019). Gene duplication associated with increased fluconazole tolerance in candida auris cells of advanced generational age. *Sci. Rep.* 9 (1), 5052. doi: 10.1038/s41598-019-41513-6
- Bosman, R. N., and Lashbrooke, J. G. (2023). Grapevine mono- and sesquiterpenes: Genetics, metabolism, and ecophysiology. *Front. Plant Sci.* 14. doi: 10.3389/fpls.2023.1111392
- Bouwmeester, H., Schuurink, R. C., Bleeker, P. M., and Schiestl, F. (2019). The role of volatiles in plant communication. *Plant J.* 100 (5), 892–907. doi: 10.1111/tj.14496
- Canaguier, A., Grimplet, J., Di Gaspero, G., Scalabrini, S., Duchêne, E., Choise, N., et al. (2017). A new version of the grapevine reference genome assembly (12X.v2) and

Author contributions

RB designed and performed experiments, analyzed data, and was the primary author of the manuscript. JV performed experiments, analyzed data and co-wrote the manuscript. DN performed experiments. PB designed and performed experiments. JL conceptualized the research, designed experiments, analyzed data, and co-wrote the manuscript. All authors contributed to the article and approved the submitted version.

Funding

This work is based on the research supported by grants from the South African Table Grape Industry (SATI), Winetech and The National Research Foundation of South Africa. Grant numbers: S005411, S006681 and 129344, respectively.

Conflict of interest

The authors declare that the research was conducted in the absence of any commercial or financial relationships that could be construed as a potential conflict of interest.

Publisher's note

All claims expressed in this article are solely those of the authors and do not necessarily represent those of their affiliated organizations, or those of the publisher, the editors and the reviewers. Any product that may be evaluated in this article, or claim that may be made by its manufacturer, is not guaranteed or endorsed by the publisher.

Supplementary material

The Supplementary Material for this article can be found online at: <https://www.frontiersin.org/articles/10.3389/fpls.2023.1112214/full#supplementary-material>

of its annotation (VCost.v3). *Genomics Data* 14, 56–62. doi: 10.1016/j.jdata.2017.09.002

Chen, F., Tholl, D., Bohlmann, J., and Pichersky, E. (2011). The family of terpene synthases in plants: A mid-size family of genes for specialized metabolism that is highly diversified throughout the kingdom. *Plant J.* 66 (1), 212–229. doi: 10.1111/j.1365-3113.2011.04520.x

Choi, K. (2017). Advances towards controlling meiotic recombination for plant breeding. *Mol. Cells* 40 (11), 814. doi: 10.14348/molcells.2017.0171

Davis, E. M., and Croteau, R. (2000). Cyclization Enzymes in the Biosynthesis of Monoterpenes, Sesquiterpenes, and Diterpenes. In: F. J. Leeper and J. C. Vederas (eds) *Biosynthesis. Topics in Current Chemistry*, vol 209. Berlin, Heidelberg: Springer, 53–95. doi: 10.1007/3-540-48146-X_2

Degenhardt, J., Köllner, T. G., and Gershenzon, J. (2009). Monoterpene and sesquiterpene synthases and the origin of terpene skeletal diversity in plants. *Phytochemistry* 70 (15–16), 1621–1637. doi: 10.1016/j.phytochem.2009.07.030

Doligez, A., Audiot, E., Baumes, R., and This, P. (2006). QTLs for muscat flavor and monoterpene odorant content in grapevine (*Vitis vinifera* L.). *Mol. Breed.* 18 (2), 109–125. doi: 10.1007/s11032-006-9016-3

Drew, D. P., Andersen, T. B., Sweetman, C., Möller, B. L., Ford, C., and Simonsen, H. T. (2016). Two key polymorphisms in a newly discovered allele of the *vitis vinifera* TPS24 gene are responsible for the production of the rotundone precursor α -guaiane. *J. Exp. Bot.* 67 (3), 799–808. doi: 10.1093/jxb/erv491

Dudareva, N., Klempien, J., Muhlemann, J. K., and Kaplan, I. (2013). Biosynthesis, function and metabolic engineering of plant volatile organic compounds. *New Phytol.* 198 (1), 16–32. doi: 10.1111/nph.12145

Dueholm, B., Drew, D. P., Sweetman, C., and Simonsen, H. T. (2019). In planta and in silico characterization of five sesquiterpene synthases from *vitis vinifera* (cv. Shiraz) berries. *Planta* 249 (1), 59–70. doi: 10.1007/s00425-018-2986-7

Dunlevy, J. D., Kalua, C., Keyzers, R., and Boss, P. (2009). The Production of Flavour & Aroma Compounds in Grape Berries. In: K. A. Roubelakis-Angelakis Ed. *Grapevine Molecular Physiology & Biotechnology*. (Dordrecht: Springer). doi: 10.1007/978-90-481-2305-6

Emanuelli, F., Battilana, J., Costantini, L., Le Cunff, L., Boursiquot, J. M., This, P., et al. (2010). A candidate gene association study on muscat flavor in grapevine (*Vitis vinifera* L.). *BMC Plant Biol.* 10 (1), 1–17. doi: 10.1186/1471-2229-10-241

Emanuelli, FR, Sordo, MA, Lorenzi, SI, Battilana, JU, and Grando, M. (2014). Development of user-friendly functional molecular markers for VvDXS gene conferring muscat flavor in grapevine. *Mol. Breed.* 33 (1), 235–241. doi: 10.1007/s11032-013-9929-6

Ferrandino, A., Carlomagno, A., Baldassarre, S., and Schubert, A. (2012). Varietal and pre-fermentative volatiles during ripening of *vitis vinifera* cv nebbiolo berries from three growing areas. *Food Chem.* 135 (4), 2340–2349. doi: 10.1016/j.foodchem.2012.06.061

Gutensohn, M., Nagegowda, D. A., and Dudareva, N. (2012). Involvement of Compartmentalization in Monoterpene and Sesquiterpene Biosynthesis in Plants. In: T. Bach and M. Rohmer (eds) *Isoprenoid Synthesis in Plants and Microorganisms*. New York, NY: Springer. doi: 10.1007/978-1-4614-4063-5

Hjelmeland, A. K., and Ebeler, S. E. (2015). Glycosidically bound volatile aroma compounds in grapes and wine: A review. *Am. J. Enology Viticulture* 66 (1), 1–11. doi: 10.5344/ajev.2014.14104

Iijima, Y., Wang, G., Fridman, E., and Pichersky, E. (2006). Analysis of the enzymatic formation of citral in the glands of sweet basil. *Arch. Biochem. Biophys.* 448 (1–2), 141–149. doi: 10.1016/j.abb.2005.07.026

Jaillon, O., Aury, J. M., Noel, B., Policriti, A., Clepet, C., Casagrande, A., et al. (2007). The grapevine genome sequence suggests ancestral hexaploidization in major angiosperm phyla. *Nature* 449 (7161), 463–467. doi: 10.1038/nature06148

Ji, X. H., Wang, B. L., Wang, X. D., Wang, X. L., Liu, F. Z., and Wang, H. B. (2021). Differences of aroma development and metabolic pathway gene expression between kyoho and 87-1 grapes. *J. Integr. Agric.* 20 (6), 1525–1539. doi: 10.1016/S2095-3119(20)63481-5

Jiang, S.-Y., Jin, J., Sarojam, R., and Ramachandran, S. (2019). A comprehensive survey on the terpene synthase gene family provides new insight into its evolutionary patterns. *Genome Biol. Evol.* 11 (8), 2078–2098. doi: 10.1093/gbe/evz142

Joubert, C., Young, P. R., Eyéghé-Bickong, H. A., and Vivier, M. A. (2016). Field-grown grapevine berries use carotenoids and the associated xanthophyll cycles to acclimate to UV exposure differentially in high and low light (Shade) conditions. *Front. Plant Sci.* 7 (June2016). doi: 10.3389/fpls.2016.00786

Kalua, C. M., and Boss, P. K. (2009). Evolution of volatile compounds during the development of Cabernet Sauvignon grapes (*Vitis vinifera* L.). *J. Agric. Food Chem.* 57 (9), 3818–3830. doi: 10.1021/jf803471n

Karunanithi, P. S., and Zerbe, P. (2019). Terpene synthases as metabolic gatekeepers in the evolution of plant terpenoid chemical diversity. *Front. Plant Sci.* 10 (October). doi: 10.3389/fpls.2019.01166

Lichman, B. R., Kamileen, M. O., Titchiner, G. R., Saalbach, G., Stevenson, C. E., Lawson, D. M., et al. (2019). Uncoupled activation and cyclization in catmint reductive terpenoid biosynthesis. *Nat. Chem. Biol.* 15 (1), 71–79. doi: 10.1038/s41589-018-0185-2

Lin, J., Massonnet, M., and Cantu, D. (2019). The genetic basis of grape and wine aroma. *Horticul. Res.* 6 (1), 81. doi: 10.1038/s41438-019-0163-1

Linstrom, P. J., and Mallard, W. G. (2001). The NIST chemistry WebBook: A chemical data resource on the Internet. *J. Chem. Eng. Data* 46 (5), 1059–1063. doi: 10.1021/je000236i

Liu, X., Fan, P., Jiang, J., Gao, Y., Liu, C., Li, S., et al. (2022). Evolution of volatile compounds composition during grape berry development at the germplasm level. *Scientia Hort.* 293 (February 2021), 110669. doi: 10.1016/j.scienta.2021.110669

Ma, L., and Chung, W. K. (2014). Quantitative analysis of copy number variants based on real-time LightCycler PCR. *Curr. Protoc. Hum. Genet.* 80, 7.21.1–7.21.8. doi: 10.1002/0471142905.hg0721s80

Martin, D. M., and Bohlmann, J. (2004). Identification of *vitis vinifera* (–)- α -terpineol synthase by in silico screening of full-length cDNA ESTs and functional characterization of recombinant terpene synthase. *Phytochemistry* 65 (9), 1223–1229. doi: 10.1016/j.phytochem.2004.03.018

Martin, D. M., Fan, P., Jiang, J., Gao, Y., Liu, C., Li, S., et al. (2010). Functional annotation, genome organization and phylogeny of the grapevine (*Vitis vinifera*) terpene synthase gene family based on genome assembly, FLDNA cloning, and enzyme assays. *BMC Plant Biol.* 10 (1), 226. doi: 10.1186/1471-2229-10-226

Martin, D. M., Chiang, A., Lund, S. T., and Bohlmann, J. (2012). Biosynthesis of wine aroma: Transcript profiles of hydroxymethylbutenyl diphosphate reductase, geranyl diphosphate synthase, and linalool/nerolidol synthase parallel monoterpenol glycoside accumulation in gewürztraminer grapes. *Planta* 236 (3), 919–929. doi: 10.1007/s00425-012-1704-0

Massonnet, M., Cochetel, N., Minio, A., Vondras, A. M., Lin, J., Muyle, A., et al. (2020). The genetic basis of sex determination in grapes. *Nat. Commun.* 11 (1), 2902. doi: 10.1038/s41467-020-16700-z

Matarese, F., Cuzzola, A., Scalabrelli, G., and D'Onofrio, C. (2014). Expression of terpene synthase genes associated with the formation of volatiles in different organs of *vitis vinifera*. *Phytochemistry* 105, 12–24. doi: 10.1016/j.phytochem.2014.06.007

Matarese, F., Scalabrelli, G., and D'Onofrio, C. (2013). Analysis of the expression of terpene synthase genes in relation to aroma content in two aromatic *vitis vinifera* varieties. *Funct. Plant Biol.* 40 (6), 552–565. doi: 10.1071/FP12326

Matsui, K. (2006). Green leaf volatiles: Hydroperoxide lyase pathway of oxylipin metabolism. *Curr. Opin. Plant Biol.* 9 (3), 274–280. doi: 10.1016/j.pbi.2006.03.002

Matsui, K., and Engelberth, J. (2022). Green leaf volatiles—the forefront of plant responses against biotic attack. *Plant Cell Physiol.* 63 (10), 1378–1390. doi: 10.1093/pcp/pcac117

Minio, A., Massonnet, M., Figueroa-Balderas, R., Castro, A., and Cantu, D. (2019). Diploid genome assembly of the wine grape *carménère*. *G3 Genes|Genomes|Genet.* 9 (5), 1331–1337. doi: 10.1534/g3.119.400030

O'Reilly-Wapstra, J. M., Freeman, J. S., Davies, N. W., Vaillancourt, R. E., Fitzgerald, H., and Potts, B. M. (2011). Quantitative trait loci for foliar terpenes in a global eucalypt species. *Tree Genet. Genomes* 7 (3), 485–498. doi: 10.1007/s11295-010-0350-6

Reichardt, S., Budahn, H., Lamprecht, D., Riewe, D., Ulrich, D., Dunemann, F., et al. (2020). The carrot monoterpene synthase gene cluster on chromosome 4 harbours genes encoding flavour-associated sabinene synthases. *Horticul. Res.* 7 (1), 190. doi: 10.1038/s41438-020-00412-y

Reid, K. E., et al. (2006). An optimized grapevine RNA isolation procedure and statistical determination of reference genes for real-time RT-PCR during berry development. *BMC Plant Biol.* 6 (1), 27. doi: 10.1186/1471-2229-6-27

Sato-Masumoto, N., and Ito, M. (2014). Two types of alcohol dehydrogenase from *perilla* can form citral and perillaldehyde. *Phytochemistry* 104, 12–20. doi: 10.1016/j.phytochem.2014.04.019

Savoi, S., Wong, D. C., Arapitsas, P., Miculan, M., Bucchetti, B., Peterlunger, E., et al. (2016). Transcriptome and metabolite profiling reveals that prolonged drought modulates the phenylpropanoid and terpenoid pathway in white grapes (*Vitis vinifera* L.). *BMC Plant Biol.* 16 (1), 67. doi: 10.1186/s12870-016-0760-1

Savoi, S., Wong, D. C., Degu, A., Herrera, J. C., Bucchetti, B., Peterlunger, E., et al. (2017). Multi-omics and integrated network analyses reveal new insights into the systems relationships between metabolites, structural genes, and transcriptional regulators in developing grape berries (*Vitis vinifera* L.) exposed to water deficit. *Front. Plant Sci.* 8. doi: 10.3389/fpls.2017.01124

Singh, A., and Pandey, G. K. (2015). Primer design using primer express® for SYBR green-based quantitative PCR. In C. Basu (eds) *PCR Primer Design. Methods in Molecular Biology*, vol 1275. (New York, NY: Humana Press), 153–164. doi: 10.1007/978-1-4939-2365-6_11

Smit, S. J., Vivier, M. A., and Young, P. R. (2019). Linking terpene synthases to sesquiterpene metabolism in grapevine flowers. *Front. Plant Sci.* 10 (February). doi: 10.3389/fpls.2019.00177

Smit, S. J., Vivier, M. A., and Young, P. R. (2020). Comparative (Within species) genomics of the *vitis vinifera* L. terpene synthase family to explore the impact of genotypic variation using phased diploid genomes. *Front. Genet.* 11 (May). doi: 10.3389/fgene.2020.00421

Steele, C. L., Crock, J., Bohlmann, J., and Croteau, R. (1998). Sesquiterpene synthases from grand fir (*Abies grandis*). *J. Biol. Chem.* 273 (4), 2078–2089. doi: 10.1074/jbc.273.4.2078

Tholl, D. (2015). Biosynthesis and biological functions of terpenoids in plants. *Adv. Biochem. engineering/biotechnol.* 148 (February), 63–106. doi: 10.1007/10_2014_295

- Van Ooijen, J. W. (2006). *JoinMap*® 4 software for the calculation of genetic linkage maps in experimental populations. Kyazma BV, Wageningen, 33(10.1371).
- Van Ooijen, J. W. (2009). *MapQTL 6 - software for the mapping of quantitative trait loci in experimental populations of diploid species*. Wageningen: Kyazma BV.
- Vervalle, J. A., Costantini, L., Lorenzi, S., Pindo, M., Mora, R., Bolognesi, G., et al. (2022). A high-density integrated map for grapevine based on three mapping populations genotyped by the Vitis18K SNP chip. *Theor. Appl. Genet.*, 1–20. doi: 10.1007/s00122-022-04225-6
- Vilanova, M., Genisheva, Z., Bescansa, L., Masa, A., and Oliveira, J. M. (2012). Changes in free and bound fractions of aroma compounds of four vitis vinifera cultivars at the last ripening stages. *Phytochemistry* 74, 196–205. doi: 10.1016/j.phytochem.2011.10.004
- Voorrips, R. E. (2002). MapChart: Software for the graphical presentation of linkage maps and QTLs. *J. Heredity* 93 (1), 77–78. doi: 10.1093/jhered/93.1.77
- Vranová, E., Coman, D., and Gruissem, W. (2013). Network analysis of the MVA and MEP pathways for isoprenoid synthesis. *Annu. Rev. Plant Biol.* 64 (1), 665–700. doi: 10.1146/annurev-arplant-050312-120116
- Xu, H., Bohman, B., Wong, D. C., Rodriguez-Delgado, C., Scaffidi, A., Flematti, G. R., et al. (2017). Complex sexual deception in an orchid is achieved by Co-opting two independent biosynthetic pathways for pollinator attraction. *Curr. Biol.* 27 (13), 1867–1877.e5. doi: 10.1016/j.cub.2017.05.065
- Yu, Y., Bai, J., Chen, C., Plotto, A., Yu, Q., Baldwin, E. A., et al. (2017). Identification of QTLs controlling aroma volatiles using a “Fortune” x “Murcott” (*Citrus reticulata*) population. *BMC Genomics* 18 (1), 646. doi: 10.1186/s12864-017-4043-5
- Zhou, Y., Minio, A., Massonnet, M., Solares, E., Lv, Y., Beridze, T., et al. (2019). The population genetics of structural variants in grapevine domestication. *Nat. Plants* 5 (9), 965–979. doi: 10.1038/s41477-019-0507-8



OPEN ACCESS

EDITED BY

Claudio Bonghi,
University of Padua, Italy

REVIEWED BY

Sahap Kaan Kurtural,
University of California, Davis, United States
Claudio D'Onofrio,
University of Pisa, Italy

*CORRESPONDENCE

María Esperanza Valdés Sánchez
✉ esperanza.valdes@juntaex.es

SPECIALTY SECTION

This article was submitted to
Crop and Product Physiology,
a section of the journal
Frontiers in Plant Science

RECEIVED 21 December 2022

ACCEPTED 16 March 2023

PUBLISHED 09 May 2023

CITATION

Lavado Rodas N, Uriarte Hernández D,
Moreno Cardona D, Mancha Ramírez LA,
Prieto Losada MH and Valdés Sánchez ME
(2023) Forcing vine regrowth under
different irrigation strategies: effect on
polyphenolic composition and chromatic
characteristics of cv. Tempranillo wines
grown in a semiarid climate.
Front. Plant Sci. 14:1128174.
doi: 10.3389/fpls.2023.1128174

COPYRIGHT

© 2023 Lavado Rodas, Uriarte Hernández,
Moreno Cardona, Mancha Ramírez, Prieto
Losada and Valdés Sánchez. This is an
open-access article distributed under the
terms of the [Creative Commons Attribution
License \(CC BY\)](https://creativecommons.org/licenses/by/4.0/). The use, distribution or
reproduction in other forums is permitted,
provided the original author(s) and the
copyright owner(s) are credited and that
the original publication in this journal is
cited, in accordance with accepted
academic practice. No use, distribution or
reproduction is permitted which does not
comply with these terms.

Forcing vine regrowth under different irrigation strategies: effect on polyphenolic composition and chromatic characteristics of cv. Tempranillo wines grown in a semiarid climate

Nieves Lavado Rodas^{1,2}, David Uriarte Hernández²,
Daniel Moreno Cardona¹, Luis A. Mancha Ramírez²,
María Henar Prieto Losada² and
María Esperanza Valdés Sánchez^{1*}

¹CICYTEX-INTAEX, Technological Institute of Food and Agriculture of Extremadura, Badajoz, Spain,

²CICYTEX-FOV, Agricultural Research Institute Finca La Orden-Valdesequera, Crta. A-V,
Badajoz, Spain

One of the effects of climate change in warm areas is the asynchrony between the dates of the technological and the phenolic maturity of grapes. This is important because the quality and color stability of red wines are directly related to the content and distribution of phenolic compounds. A novel alternative that has been proposed to delay grape ripening and make it coincide with a seasonal period more favorable for the formation of phenolic compounds is crop forcing. This consists of severe green pruning after flowering, when the buds of the following year have already differentiated. In this way, the buds formed during the same season are forced to sprout, initiating a new delayed cycle. The aim of the present work is to study the effect on the phenolic composition and color of wines elaborated from vines fully irrigated (C), grown using conventional non-forcing (NF) and forcing (F) techniques (C-NF and C-F), and wines from vines subjected to regulated irrigation (RI), grown using NF and F techniques (RI-NF and RI-F). The trial was carried out in an experimental vineyard of the Tempranillo variety located in a semi-arid area (Badajoz, Spain) in the 2017–2019 seasons. The wines (four by treatment) were elaborated and stabilized according to the classic methodologies for red wine. All wines had the same alcohol content, and malolactic fermentation was not carried out in any of them. Anthocyanin profiles were analyzed by HPLC, and total polyphenolic content, anthocyanin content, catechin content, the contribution to color due to co-pigmented anthocyanins, and various chromatic parameters were also determined. Although a significant effect of year was found for almost all the parameters analyzed, a general increasing trend in F wines was found for most of

them. The anthocyanin profile of F wines was found to differ from that of C wines, especially in delphinidin, cyanidin, petunidin, and peonidin content. These results indicate that by using the forcing technique it was possible to increase the polyphenolic content by ensuring that the synthesis and accumulation of these substances occurred at more suitable temperatures.

KEYWORDS

anthocyanin, catechin, tannin, malvidin, petunidin, delphinidin, peonidin, cyanidin

1 Introduction

The climate is a determining factor of the physico-chemical characteristics of grapes and, consequently, of the wines obtained (Mira de Orduña, 2010). Air temperature, thermal oscillation, CO₂ content in the air and solar radiation all play an essential role, as they condition the processes of synthesis, transport, and accumulation of primary and secondary metabolites during grape ripening (Van Leeuwen and Destrac-Irvine, 2017; Van Leeuwen et al., 2019; Jones et al., 2022). In recent decades and in many regions, the previous balance between the above factors has been upset by the changes that have been occurring to the climate as a result of global warming and the associated temperature increases over ever lengthening periods, more severe and longer periods of drought, and increases in CO₂ and ultraviolet radiation (Sadras and Moran, 2012; Moriondo et al., 2013).

It is known that high temperatures accelerate the accumulation of total soluble solids (TSS) (Petrie and Sadras, 2008), affect the content of acids present in the berries, and modify the content and distribution in grapes of phenolic compounds (Tate, 2001; Monagas et al., 2005; Downey et al., 2006; Rienth et al., 2016; Arrizabalaga-Arriazu et al., 2020). It has also been reported that secondary metabolites in *Vitis vinifera* L. cv. Tempranillo grapes are influenced by ultraviolet radiation, affecting berry development (Del-Castillo-Alonso et al., 2021).

The degree of grape maturity at harvest time is one of the most important parameters for obtaining high-quality red wines. Under current climatic conditions, the grapes reach high TSS values and very low total acidity (TA) before achieving phenolic maturity. That is, technological maturity (adequate concentrations of sugars and acids) and phenolic maturity (determined by the optimal concentration and profile of phenolic compounds) are not simultaneously reached. These changes affect the microbiology process in winemaking progress, as well as the physico-chemical composition and organoleptic characteristics of the wine (Jones et al., 2005; Mira de Orduña, 2010; Palliotti et al., 2014), leading to the production of unbalanced wines with high alcohol content, low acidity, a modified varietal aroma, and a lack of color (Martínez De Toda et al., 2019).

Soil water availability is also a critical factor for vine performance and wine composition (Intrigliolo and Castel, 2010; Afifi et al., 2021; Lizama et al., 2021; Valdés et al., 2022). In arid and

semi-arid environments, irrigation is a major tool used to regulate the availability of soil water to vines. Due to the increase in periods of drought and the decreasing availability of water, regulated deficit irrigation (RDI) has become a widely used strategy to reduce the possible negative impact of irrigation on grapes, improving grape composition, and resulting in water savings (Pérez-Álvarez et al., 2021). Deficit irrigation consists in applying water rates to replace only part of the potential vine evapotranspiration either throughout the season or only during specific and previously established phenological periods to control growth and reproductive development and/or improve water use efficiency (Intrigliolo and Castel, 2010). In previous studies, when compared with conventional irrigation RDI techniques resulted in modification of the anthocyanin profile, increasing the anthocyanin content of the grapes and the corresponding wines and improving the sensory characteristics of cv. Tempranillo from vines grown in different semi-arid climate regions of the Iberian Peninsula (Valdés et al., 2009; Intrigliolo and Castel, 2010; Intrigliolo and Castel, 2011; Santesteban et al., 2011; Gamero et al., 2014; Torres et al., 2021). In addition, it has been found that the effect of RDI is highly dependent on the timing of the water deficit (Girona et al., 2009; Valdés et al., 2009; Intrigliolo et al., 2012; Valdés et al., 2022).

In order to maintain and/or improve the characteristics of the wines typical of each area, as well as to preserve the viability of vineyards, it is necessary to adapt them to the new climatic conditions. Such adaptation commonly involves decisions concerning vineyard topographic variables, as well as rootstock, variety, clone, training system, row orientation, and slope selection (Torres et al., 2017; Díaz-Fernández et al., 2022; Gutiérrez-Gamboa et al., 2020; Muñoz-Organero et al., 2022).

Today, short-term viticulture strategies are also being investigated which comprise the establishment of techniques capable of delaying grape ripening and, therefore, shifting harvest date to periods of more favorable temperatures. One such recently proposed technique is crop forcing which consists of severe green pruning after flowering when the buds of the following year have already differentiated. In this way, the flowering of the buds formed that same season is forced, and the whole phenological cycle is delayed, including the beginning of the ripening cycle and the harvest date. This technique was studied by Gu et al. (2012) who managed to significantly delay the harvest date significantly, while other authors have achieved similar results (Lavado et al., 2019;

Martínez De Toda et al., 2019; Martínez-Moreno et al., 2019; Kishimoto et al., 2022). While these studies showed lower yield and increased acidity and phenolic compound values as a result of the use of this technique, little is still known about the effects of crop forcing and its interaction with irrigation strategies on the acid, phenolic, and chromatic characteristics of the resulting wines. Other questions that require further research include how the effect of crop forcing changes depending on the meteorological conditions of the year in question, as well as the long-term effect of the technique.

The aim of the work presented here was to study for three consecutive years the effect of crop forcing and its interaction with a pre-veraison RDI strategy on the physico-chemical characteristics, with particular emphasis on the anthocyanin profile, of the resulting wines. An additional aim was to observe the influence of different meteorological circumstances on the effect of the techniques applied.

2 Materials and methods

2.1 Location and description of the vineyard

The study was carried out in an experimental vineyard located at Badajoz, Extremadura, Spain (38°N 51' N; 6° 40' W; 198 m) in a cv. Tempranillo vineyard (*Vitis vinifera* L.) with vines grafted on Richter 110 rootstock and trained as bilateral cordons in a vertical trellis system with a drip irrigation system of 8 L/h per vine. All vines were winter pruned to six spurs and two buds per spur. The rows are E-W oriented and row and vine spacing were 2.5 m and 1.2 m, respectively. The soil is alluvial, with a loam to sandy texture, slightly acidic, and lacking in organic matter. Soil depth is greater than 2.5 m and with low stone content.

2.2 Treatments and experimental design

The experimental design was a split-plot with four replications (Table 1). The main factor was pruning with two treatments, one with crop forcing technique (F) applied 22 days after anthesis (May 18, 2017; May 29, 2018; May 20, 2019), the other without crop forcing techniques (NF) with vines grown under conventional practices (just winter pruning). Crop forcing consisted of hedging the growing shoots to seven nodes and removing all the summer laterals, leaves, and clusters with scissors to force the bursting of the primary buds developed in the current season. As a secondary factor, two irrigation treatments were established: a treatment with no water stress (C), supplying water to maintain a pre-established midday stem water potential (SWP), and a pre-veraison deficit irrigation (RI).

TABLE 1 Summary of the treatments applied in the study.

Treatment	No crop forcing (NF)	Crop forcing (F)
Fully irrigated (C)	C-NF	C-F
Deficit irrigation (RI)	RI-NF	RI-F

Vine water requirements were calculated based on the crop evapotranspiration (ET_c) using the crop coefficient (K_c) recommended by FAO for these latitudes for the NF treatments. For the F treatments, ET_c was calculated directly with a weighing lysimeter (Picón-Toro et al., 2012) for two crop forcing vines, integrated in the study plot. Irrigation started when a threshold SWP value of -0.6 MPa was reached. Irrigation was applied five to six times per week, measuring the amount of water applied to each subplot through volumetric water meters, and maintaining irrigation until the beginning or middle of October. The experimental unit consisted of six rows per 18 vines. The 10 central vines of the four central rows were used for sampling.

2.3 Weather conditions

The area has a Mediterranean climate with a mild Atlantic influence, dry and hot summers, with high daily radiation and evaporative demand. The meteorological data was obtained from a weather station belonging to the Extremadura Irrigation Advisory Network (REDAREX for its initials in Spanish) located 100 m from the plot, with the characteristics described in Martí et al. (2015). Figure 1 shows the meteorological conditions (T max, med and min and rainfall) in the budburst to fruit set, fruit set to veraison, and veraison to harvest periods for the different treatments and the 3 years of trial.

2.4 Vine phenology

Phenology monitoring was performed weekly according to the modified E-L system (Coombe, 1995). Starting from mid-March ("cotton bud" stage), a visual inspection was made of 10 plants per plot to determine the most representative growth stage (the stage shown by at least 50% of plants) as well as the most backward and the most advanced stages in the samples. Table 2 shows the day of year of the different phenological states from budbreak to harvest in the different treatments (Lavado et al., 2023).

2.5 Water status

The SWP was measured with a pressure chamber (Soil Moisture Corp., Model 3500, Santa Barbara, CA, USA), following the procedure described by Shackel (2007), using leaves on the north side of the trellis (in the shade), close to trunk level and wrapped in aluminum foil at least 2 h before data recording. Measurements were taken weekly on one leaf per vine and in two plants per subplot. Table 3 shows the average midday SWP (MPa) throughout the different phenological stages in 2017, 2018, and 2019 (Lavado et al., 2023).

2.6 Yield parameters

All treatments were harvested manually at 23–24°Brix, a common criterion for picking red grape varieties in the study

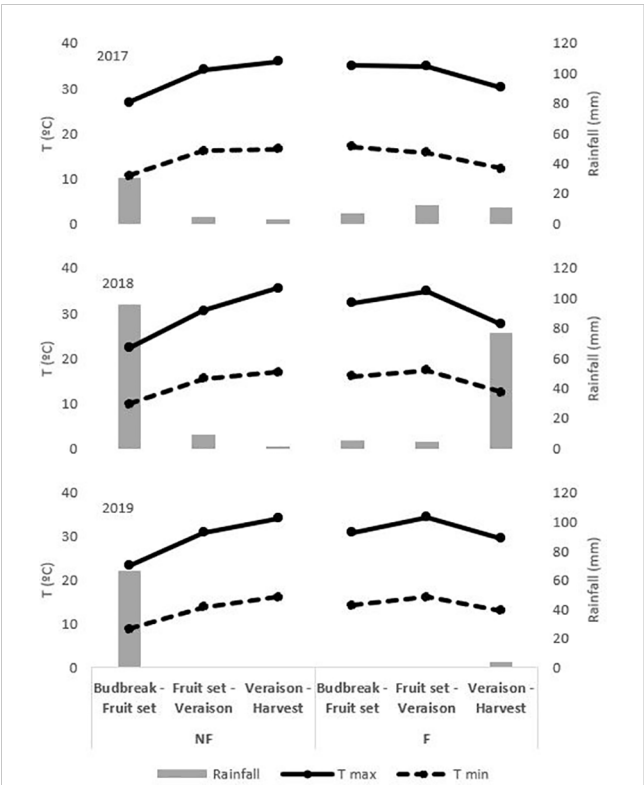


FIGURE 1 Meteorological conditions on budburst to fruit set, fruit set to veraison and veraison to harvest period on NF and F treatments in 2017, 2018 and 2019. Treatments: NF (no forcing) and F (forcing).

area. The average TSS of the berries from the four elementary plots was considered for each treatment. To determine the effects of the treatments on yield parameters and berry weight, all the clusters of 10 vines per experimental plot were weighed (40 vines per treatment) and samples of 100 g of berries per plot were weighed fresh.

2.7 Microvinifications

Each year, 16 microvinifications were carried out (4 treatments × 4 experimental blocks) according to the following experimental protocol: samples of about 60 kg were destemmed and mechanically crushed (Modelo Micra/15, Agrovín, Spain). One aliquot (100 g) of initial mash

(pulp, juice, skins and seeds) was frozen (-80°C) for the analysis of polyphenol compounds. On the other hand, 50 mL of must were taken, filtered and immediately analyzed. The mash was fermented in 50-L steel tanks at 22–24°C. Initially, sulphur dioxide (SO₂) was added at 50 mg/kg and *Saccharomyces cerevisiae* (Viniferm 3D, Agrovín, Spain) were inoculated (25 g/hL). Fermentation was monitored daily, measuring density and total phenolic index (TPI) by spectrophotometric absorbance at 280 nm (UV/visible UV-1700 spectrophotometer, Shimadzu, Shimadzu Corporation, Kyoto, Japan). During vatting, fermenting must wines were punched twice per day. The musts were racked when the increase in TPI leveled off. Once fermentation was completed, the wines were settled at 4°C, and sulphur was then added to the wine to achieve 30 mg/L of free SO₂. Finally, the wines were bottled and stored at 15°C until analysis, without initiating malolactic fermentation. Thus, 16 different wines were obtained (4 treatments × 4 blocks per treatment).

2.8 Analytical methods

2.8.1 General oenological parameters

The TSS (°Brix) of musts was determined by refractometry (RE40D, Mettler Toledo, Greifensee, Switzerland). Wine analysis was carried out 4 months after bottling. In musts and wines, analysis for pH and TA (g tartaric acid/L) was conducted following the OIV (Organisation Internationale de la Vigne et du Vin) methods (1990) in an automatic titrator (T50, Mettler Toledo, Greifensee, Switzerland) according to ECC formal methods (ECC, 1990). Tartaric acid (TAR, g/L) and malic acid (MAL, g/L) were analyzed following the Rebelein and the enzymatic reaction methods, respectively, in an autoanalyzer (Y15, Biosystems, Barcelona, Spain).

2.8.2 Nitrogen parameters

Free amino nitrogen (FAN, mg/L) and ammonium (NH₄⁺, mg/L) content were enzymatically analyzed according to ECC formal methods (ECC, 1990) using an autoanalyzer (Y15, Biosystems, Barcelona, Spain).

2.8.3 Phenolic compounds

The extraction of phenolic substances from the initial mash was carried out following a methodology based on previous works (Portu

TABLE 2 Day of the year for the different phenological stages in each treatment and day of application of crop forcing during the 2017, 2018 and 2019 seasons (Lavado et al., 2023).

Phenological stage	2017		2018		2019	
	NF	F	NF	F	NF	F
Budbreak	93	93	93	99	85	91
Crop forcing		157		168		154
Fruit set	150	201	156	214	140	200
Veraison	187	256	204	261	200	253
Harvest	234	292	241	302	240	283

Treatments: NF (no forcing) and F (forcing). Each treatment represents the two irrigation regimes as no differences were found between them.

TABLE 3 Average midday stem water potential (MPa) throughout the different phenological stages in 2017, 2018 and 2019.

Year	Phenological Stage	Treatment			
		C-NF	C-F	RI-NF	RI-F
2017	BB-CFP		−0.63		−0.62
	CFP-F	−0.49	−0.55	−0.56	−0.69
	F-FS	−0.64	−0.79	−0.72	−1.03
	FS-V	−0.61	−0.74	−1.12	−0.9
	V-H	−0.82	−0.58	−1.24	−0.71
2018	BB-CFP		−0.49		−0.51
	CFP-F	−0.41		−0.48	
	F-FS	−0.41	−0.62	−0.48	−0.78
	FS-V	−0.49	−0.61	−1.00	−0.96
	V-H	−0.61	−0.59	−0.92	−0.67
2019	BB-CFP		−0.64		−0.73
	CFP-F				
	F-FS	−0.65	−0.58	−0.77	−0.58
	FS-V	−0.70	−0.64	−1.06	−0.78
	V-H	−0.75	−0.62	−0.78	−0.77

Treatments: C-NF (no forcing and full irrigation); C-F (forcing and full irrigation); RI-NF (no forcing and deficit irrigation) and RI-F (forcing and deficit irrigation). BB, Budbreak; CFP, Crop forcing pruning; F, Flowering; FS, Fruit set; V, Veraison; H, Harvest (Lavado et al., 2023).

et al., 2016; Díaz-Fernández et al., 2022). An aliquot (1.0 g) of the frozen mash was homogenized for 30 s in a Freshboost blender (LM180110, Moulinex, Aleçon, France) with 10 mL of a hydroalcoholic solution (methanol/water/formic acid 50:48.5:1.5, v/v/v) and then the mixture was macerated (30 min, 4°C, ultrasonic bath USC-TH, VWR, Radnor, USA) and centrifuged (4°C, 10 min 5810 R, Eppendorf, Hamburg, Germany). The supernatant was separated, and the resulting pellet was reextracted up to three times. The supernatants (phenolic extracts) were combined and the final volume was annotated. In the polyphenolic extracts obtained, total polyphenol content (TPP) was determined according to Singleton and Rossi (1965), and total anthocyanin (Ant) content by the pH differential method (Lee et al., 2005) using an autoanalyzer (Y15, Biosystems, Barcelona, Spain). Ant was considered as the sum of substances quantified by HPLC. Tannin content (Tan) was determined using the spectrophotometric method following Sarneckis et al. (2006). Catechin content (Cat) was determined according to Broadhurst and Jones (1978), and co-pigmented anthocyanin (%C-Ant) using the colorimetric effects of acetaldehyde and SO₂ on different forms of anthocyanins (Boulton, 2001).

2.8.4 Wine chromatic characteristics

Color intensity (CI) was calculated as the sum of absorbance at 420, 520, 620 nm, and hue as the ratio of the absorbance at 420 nm and 520 nm. From absorbance values at 420, 520, and 620 nm, the percentages of yellow (Yellow %), red (Red %) and blue (Blue %) were determined according to the Glories method (Glories, 1984): Yellow % = 100%

[Abs 420/(Abs 420 + Abs 520 + Abs 620)]; Red % = 100% [Abs 520/(Abs 420 + Abs 520 + Abs 620)]; Blue % = 100% [Abs 620/(Abs 420 + Abs 520 + Abs 620)]. Absorbance measurements were taken using a Shimadzu spectrophotometer with data system control software (Shimadzu Corporation, Kyoto, Japan). Samples were filtered through Millipore-AP20 filters (Bedford, MA, USA) prior to color determination.

2.8.5 Anthocyanin compounds by HPLC

HPLC separation, identification and quantification of anthocyanins were performed on an Agilent 1200 LC system (Agilent Technologies, Palo Alto, CA) equipped with a degasser, quaternary pump, column oven, 1290 infinity autosampler, UV-Vis diode-array detector (DAD) and the Chemstation software package for LC 3D systems (Agilent Technologies) to control the instrument and for data acquisition and analysis. Separation was performed in a Kromasil® 100-5-C18 (250 × 4.6 mm) column (AkzoNobel, Bohus, Sweden). The analysis was carried out as described in Natividad et al. (2013) with slight modifications to improve peak resolution. For the analysis of anthocyanins, a 10 mL extract was injected directly into the HPLC and the column was maintained at 40°C. The mobile phase consisted of a gradient mixture of a solvent A (0.85% phosphoric acid solution) and solvent B (acetonitrile), with a flow rate of 1 mL·min^{−1}. The gradient was started with 100% of solvent A and adjusted for 90% of solvent A and 10% of solvent B at 10 min; 85% of solvent A and 15% of solvent B at 20 min; 80% of solvent A and 20% of solvent B at 30 min; 67% of solvent A and 33% of solvent B at 40 min; 65% of solvent A and 35% of solvent B at

45 min; and 100% of solvent B at 55 min. Absorbance at 520 nm was measured by the DAD detector for identification of anthocyanins by their elution order and by comparison to the retention times of commercially available standards (malvidin-3-glucoside, delphinidin-3-O-glucoside, cyanidin-3-O-glucoside, and peonidin-3-O-glucoside (Extrasynthese, Genay, France). The anthocyanins present in the wines were identified as the mono-glucoside forms (G) of malvidin (MvG), petunidin (PtG), delphinidin (DpG), peonidin (PnG) and cyanidin (CyG); the acetyl-glucoside forms (MvA, PtA, DpA, PnA, and CyA), and the p-coumaroyl-glucoside forms (MvC, PtC, PnC, and CyC). All measures were expressed in mg glucoside/L.

2.9 Statistical data analysis

Normality and homogeneity of variances were tested using the Shapiro-Wilk's and Bartlett's test respectively. When the normality and homogeneity of variances were verified, yield and berry weight data were analyzed by one-factor analysis of variance (ANOVA) and the Tukey test. Differences between means were considered statistically significant when $p < 0.05$. Must and wine data were subjected to multiple analyses of variance (MANOVA) to investigate the effect of "crop forcing", "irrigation" and their interaction on each parameter evaluated, selecting $p \leq 0.001$, $p \leq 0.01$, and $p \leq 0.05$ for significance of comparisons. The interaction between effects was evaluated by calculating the least-squares means (LS means) selecting $p \leq 0.001$, $p \leq 0.01$, and $p \leq 0.05$ for significance of comparisons and the Tukey test as *post hoc* test for parametric samples. When normality and homogeneity of variances were not verified, non-parametric tests were carried out and the Kruskal-Wallis test (alternative to one-way ANOVA) and multiple comparison p values (alternative to *post-hoc* pairwise comparisons) were used. Differences between means were considered statistically significant when $p < 0.05$. Multiple factor analysis (MFA) was applied. Meteorological conditions were used as supplementary

variable, with yield and acid and phenolic composition and chromatic characteristics of the resulting wines as active variables. Principal component analysis (PCA) was performed to discriminate between treatments on the basis of the values of Mv, Pt, Dp, Pn, and Cy. These last statistical tests were performed with XLSTAT-Pro statistical software package (Addinsoft, 2009, Paris, France).

3 Results

The effect of the year on agronomical parameters and all the must and wine composition parameters studied was highly significant (data not shown), suggesting that the effect of treatments, especially that caused by the irrigation regime, on these parameters was different between seasons. For this reason, the results of each harvest are analyzed separately in this work. To minimize compositional differences between treatments associated with TSS level, a common TSS between treatments and year was considered.

3.1 Yield parameters

Table 4 shows the yield (kg/vine) and berry weight (BW, g) of the control treatment (C-NF) in the 2017–2019 period. Yields were lower than 4 kg/vine in 2017 and 2018 and close to 7 kg/vine in 2019 in the control treatment (C-NF). Significantly lower values were found each year in the F compared to the NF treatments. In 2017, the yield penalty was higher in RI-F (66%) than in C-F (29%), while in 2018 and 2019 the values were similar and close to 50% and 60%, respectively. In RI-NF, the loss of yield was 42%, 18% and 38% in 2017, 2018 and 2019 with respect to C-NF. The decrease in 2017 in this treatment was higher than in C-F, in contrast to what was observed in the following years. Regarding BW, in both forcing and irrigation treatments significant decreases were observed with respect to C-NF. The following BW sequence was observed: RI-F > C-F > RI-NF.

TABLE 4 Effect of crop forcing and water status treatment on yield (kg/vine) and berry weight (g).

Parameter	Year	C-NF values	% Decrease in harvest compared to C-NF				Fxl	NF values	% Decrease in harvest compared to NF		F	C values	% Decrease in harvest compared to C		I
			C-NF	C-F	RI-NF	RI-F			NF	F			C	RI	
Yield Kg/ha	2017	3.9	0	−29	−42	−66	n.s.	3.1	0	−34	***	3.3	0	−46	***
	2018	3.7	0	−51	−18	−52	n.s.	3.4	0	−47	***	2.8	0	−13	*
	2019	7.1	0a	−58 c	−38 b	−60 c	***	5.8	0	−49	***	5.1	0	−28	***
Berry weight (g)	2017	1.8	0a	−44 c	−28 b	−56 c	*	1.6	0	−42	***	1.4	0	−25	***
	2018	1.9	0a	−37 b	−32 b	−47 b	*	1.6	0	−31	***	1.6	0	−26	***
	2019	2.3	0a	−39 b	−35 b	−48 b	**	1.9	0	−32	***	1.9	0	−27	***

Treatments: C-NF (no forcing and full irrigation); C-F (forcing and full irrigation); RI-NF (no forcing and deficit irrigation) and RI-F (forcing and deficit irrigation); F, Forcing factor; I, Irrigation factor.

Each value represents the mean of 8 samples (4 blocks, 2 replicates). Statistical analysis: Different letters indicate the existence of statistically significant differences between treatments; n.s. indicates not significant; (*) significant at 5% level; (**) significant at 1% level and (***) significant at 0.1% level.

3.2 Must composition

Table 5 shows the acid, nitrogen and phenolic composition of the initial musts and mash from the different treatments applied to the vines and the results of the MANOVAs performed to analyze the statistical significance of the effect of crop forcing (F), irrigation treatment (I), and their interaction on these parameters in 2017, 2018 and 2019. In general, no statistical significance was observed in the *FxI* interaction (only on 3 occasions). Although the statistical significance of both F and I depended on the parameter analyzed and the year considered, it should be noted that crop forcing had a more significant number of times of statistical significance (18) than irrigation treatment (10). Musts showed similar TSS values for each year and treatment. Regarding acid composition, the results shown in Table 5 do not allow general conclusions to be drawn on the effect of F on TAR because high variability between years was observed. In 2017, an *FxI* interaction was detected because F caused a significant increase (12.0%, $p < 0.05$) in the contents of the C musts (C-F vs. C-NF), while no effect was detected in RI. In 2018, all musts presented similar values. Finally, when F must was compared with NF must in 2019, similar decreases were found regardless of irrigation treatment. With respect to the crop forcing treatment, irrigation treatment did not have any effect in any year. As Table 5 shows, crop forcing increased MAL values, with higher increases in RI treatments. The increases in 2017, 2018, and 2019 were 267%, 53%, and 105% in RI-F vs. RI-NF, but 30% and 6% and 71% in CF vs. C-NF. In 2017, a significant *FxI* interaction was found because the C-NF value was much higher than the RI-NF (233% increase), while C-F had a similar value to RI-F. In 2018, C-NF and C-F were higher than RI-NF and RI-F, respectively. Finally, in 2019 similar values were found in C and RI must. As a consequence of these results, the RI-NF musts had the lowest MAL values in the three years of the trial. The variations in TAR and especially MAL values modified the TA values. Thus, in 2017 and 2019, higher TA values were observed in the F than the NF musts ($p < 0.001$ in 2017 and $p < 0.01$ in 2019). In 2018, and as a logical consequence of the values of both MAL and TAR, the C-NF and C-F musts presented similar TA values (7.0 and 7.3, respectively), but the RI-NF value (4.8) differed considerably from that of RI-F (6.0). Moreover, in all years TA of the RI musts was significantly lower than for the corresponding C musts. Because of these results, the C-F and RI-NF musts respectively had the highest and lowest TA values in the three years of the study. Finally, in the 2017 and 2018 vintages, the pH of the F musts was significantly lower than that of the NF musts, and the RI musts, especially the NF ones, showed higher pH values than the corresponding C musts. Consequently, in those vintages, the highest pH values corresponded to RI-NF musts (3.9 and 3.7 in 2017 and 2018) and the lowest to C-F musts (3.6 and 3.4 in those same years). However, in 2019, all musts presented similar pH values.

Regardless of the treatment considered, it is noteworthy that as the study progressed, a gradual decrease in the values of nitrogen compounds (both inorganic and organic) was observed. In 2017 and 2018, the NH_4^+ values of the F musts were lower than those of the NF musts. In both irrigation strategies, the decreases were

around 50%. In 2019 no differences were found. In none of the years did the use of RDI cause significant changes in the values of this parameter. Finally, the free amino nitrogen (FAN) contents of the musts were modified in a very similar way to those of NH_4^+ , and thus the mean values of this parameter of the F musts in 2017 and 2018 (144.6 and 85.4) were significantly lower than those recorded in the NF musts (65.8 and 53.1).

The Ant, Tan, and TPP results shown in Table 5 indicate that crop forcing caused, in both C and RI, a general trend to higher values, with significant increases of Ant and TPP in 2018 and 2019 and Tan in 2019 only. The changes due to irrigation strategy were less significant. In fact, compared to C, significant increases were only observed in RI in 2017 in the Ant values, and in 2018 decreases in Tan and TPP.

3.3 Wine composition

Table 6 shows the effects of treatments on the alcohol content (AD, % v/v), acid composition, phenolic composition and chromatic characteristics of the wines from 2017, 2018, and 2019. In 2017 and 2018, all wines showed similar AD values, while in 2019, contrary to expected, since the initial musts had similar TSS values, the AD of the C-F (12.8) and RI-F (13.2) wines was lower than that of the C-NF (14.0) and RI-NF (14.2) wines.

3.3.1 Acid composition

As Table 6 reflects, the statistical significance of the *FxI* interaction was only observed five times and the effect of F and I depended on the parameter analyzed and on the year in question. As in the case of musts, crop forcing was statistically significant more times (7) than the irrigation treatment (2).

A general trend to increase was found in the values of TAR and MAL in F compared to NF wines. The significance of the effect on these substances depended on the year considered and, in some cases, on the irrigation strategy. Thus, in 2018 higher values of MAL were registered in RI-F vs. RI-NF, but in 2018 C-F values were similar than C-NF. In general, TA values were higher in F than in NF wines, with the most noticeable effect on the RI wines. In this way, a significant *FxI* interaction was found in 2018 and 2019, because only the value of RI-F wines (7.5 and 7.8 in 2018 and 2019) was higher than the corresponding RI-NF (6.2 and 7.5, respectively). Finally, crop forcing decreased the pH values in 2018 only. Concerning irrigation effect, and in agreement with the trend registered in the musts, no differences were observed in TAR values of C and RI (F and NF) wines in any year, and the differences in MAL values found between C and RI musts were only slightly reflected in the wines, with only the C-NF value being significantly higher than the RI-NF value in 2018. Finally, C wines had higher TA than RI wines in 2018 and 2019, in both NF and F wines in 2018 and 2019 and in 2019 in NF wines only. In consequence, in 2018 the pH of RI wines was higher than C wines (regardless of crop forcing), but in 2019 significant increases were only registered in RI-NF vs. C-NF.

TABLE 5 Effect of crop forcing and water status on composition of cv. Tempranillo musts.

Parameter	Year	Treatment										
		C-NF	C-F	RI-NF	RI-F	<i>F_xI</i>	NF	F	<i>F</i>	C	RI	<i>I</i>
TSS (°Brix)	2017	24.8	23.7	24.0	23.2	<i>n.s.</i>	24.4	23.5	<i>n.s.</i>	24.3	23.6	<i>n.s.</i>
	2018	25.2	24.1	23.8	22.8	<i>n.s.</i>	24.5	23.5	<i>n.s.</i>	24.7	23.3	<i>n.s.</i>
	2019	22.5	23.2	23.6	23.9	<i>n.s.</i>	23.0	23.5	<i>n.s.</i>	22.8	23.7	<i>n.s.</i>
<i>Acid composition</i>												
TAR (g/L)	2017	3.9 b	4.4 a	4.1 ab	4.2 ab	*	4.0	4.3	**	4.2	4.2	<i>n.s.</i>
	2018	4.6	4.8	4.5	4.4	<i>n.s.</i>	4.5	4.6	<i>n.s.</i>	4.7	4.5	<i>n.s.</i>
	2019	5.0	4.6	5.2	4.7	<i>n.s.</i>	5.1	4.7	**	4.8	4.9	<i>n.s.</i>
MAL (g/L)	2017	2.0 b	2.6 a	0.6 c	2.2 ab	*	1.3	2.4	***	2.3	1.4	***
	2018	3.1	3.3	1.9	2.9	<i>n.s.</i>	2.5	3.1	*	3.2	2.4	**
	2019	2.1	3.6	1.8	3.7	<i>n.s.</i>	2.0	3.6	***	2.8	2.8	<i>n.s.</i>
TA (g/L)	2017	4.4	5.6	3.7	4.9	<i>n.s.</i>	4.1	5.3	***	5.0	4.3	**
	2018	7.0	7.3	4.8	6.0	<i>n.s.</i>	5.9	6.7	<i>n.s.</i>	7.1	5.4	**
	2019	6.8	7.2	5.3	7.0	<i>n.s.</i>	6.1	7.1	**	7.0	6.2	*
pH	2017	3.9	3.6	3.9	3.6	<i>n.s.</i>	3.9	3.6	***	3.7	3.7	<i>n.s.</i>
	2018	3.5	3.4	3.7	3.4	<i>n.s.</i>	3.6	3.4	**	3.4	3.5	*
	2019	3.4	3.5	3.6	3.5	<i>n.s.</i>	3.5	3.5	<i>n.s.</i>	3.4	3.5	<i>n.s.</i>
<i>Nitrogen composition</i>												
NH ₄ ⁺ (mg/L)	2017	125.0	71.8	121.8	68.0	<i>n.s.</i>	123.4	69.9	***	98.4	94.9	<i>n.s.</i>
	2018	81.8	40.9	93.8	47.7	<i>n.s.</i>	87.8	44.3	**	61.3	70.7	<i>n.s.</i>
	2019	67.7	58.2	82.0	54.5	<i>n.s.</i>	74.8	56.3	<i>n.s.</i>	62.9	68.3	<i>n.s.</i>
FAN (mg/L)	2017	148.3	68.8	141.0	62.8	<i>n.s.</i>	144.6	65.8	***	108.5	101.9	<i>n.s.</i>
	2018	70.3 b	52.8 b	100.5 a	53.3 b	*	85.4	53.1	***	61.5	76.9	*
	2019	57.7	57.0	91.0	56.4	<i>n.s.</i>	74.3	56.7	<i>n.s.</i>	57.3	73.7	<i>n.s.</i>
<i>Phenolic composition</i>												
Ant (mg/L)	2017	918.3	982.8	1212.1	1286.3	<i>n.s.</i>	1065.2	1134.5	<i>n.s.</i>	950.6	1249.2	**
	2018	916.1	1222.7	956.6	1436.9	<i>n.s.</i>	936.4	1329.8	***	1069.4	1196.8	<i>n.s.</i>
	2019	705.5	1138.8	867.0	1264.8	<i>n.s.</i>	786.2	1201.8	**	922.1	1065.9	<i>n.s.</i>
Tan (mg/L)	2017	4738.4	5041.9	4385.4	4743.4	<i>n.s.</i>	4561.9	4892.7	<i>n.s.</i>	4890.2	4564.4	<i>n.s.</i>
	2018	4932.5	6120.7	4105.2	4211.2	<i>n.s.</i>	4518.8	5166.0	<i>n.s.</i>	5526.6	4158.2	**
	2019	4436.1	5671.3	4588.6	5199.6	<i>n.s.</i>	4512.4	5435.4	**	5053.7	4894.1	<i>n.s.</i>
TPP (mg/L)	2017	4934.3	5155.2	4552.1	5106.9	<i>n.s.</i>	4743.2	5131.1	<i>n.s.</i>	5044.8	4829.5	<i>n.s.</i>
	2018	4928.5	6741.2	4235.3	5361.6	<i>n.s.</i>	4581.9	6051.4	**	5834.8	4798.4	**
	2019	3392.6	5328.1	3759.7	5030.4	<i>n.s.</i>	3576.1	5179.2	***	4360.4	4395.0	<i>n.s.</i>

Treatments: C-NF (no forcing and full irrigation); C-F (forcing and full irrigation); RI-NF (no forcing and deficit irrigation) and RI-F (forcing and deficit irrigation); F, Forcing factor; I, Irrigation factor.

Parameters: Total soluble solids (TSS), Tartaric acid (TAR), Malic acid (MAL), Total acid (TA), pH, Free amino nitrogen (FAN), Ammonium (NH₄⁺), Anthocyanins (Ant), Tannins (Tan) and Total polyphenols (TPP).

Each value represents the mean of 8 samples (4 blocks, 2 replicates). Statistical analysis: Different letters indicate the existence of statistically significant differences between treatments; *n.s.* indicates not significant; (*) significant at 5% level; (**) significant at 1% level and (***) significant at 0.1% level.

TABLE 6 Effect of crop forcing and water status on composition and chromatic characteristics of Tempranillo wines.

Parameter	Year	Treatment										
		C-NF	C-F	RI-NF	RI-F	FxI	NF	F	F	C	RI	I
AD (%)	2017	14.8	13.8	14.0	13.5	<i>n.s.</i>	14.4	13.6	<i>n.s.</i>	14.3	13.7	<i>n.s.</i>
	2018	14.9	14.1	14.3	13.3	<i>n.s.</i>	14.6	13.7	<i>n.s.</i>	14.5	13.8	<i>n.s.</i>
	2019	14.0	12.8	14.2	13.2	<i>n.s.</i>	14.1	13.0	*	13.4	13.7	<i>n.s.</i>
Acid composition												
TAR (g/L)	2017	1.8	2.4	2.2	2.6	<i>n.s.</i>	2.0	2.5	**	2.1	2.4	<i>n.s.</i>
	2018	2.2	2.2	2.3	2.5	<i>n.s.</i>	2.3	2.3	<i>n.s.</i>	2.2	2.4	<i>n.s.</i>
	2019	2.4	2.5	2.3	2.5	<i>n.s.</i>	2.3	2.5	<i>n.s.</i>	2.4	2.4	<i>n.s.</i>
MAL (g/L)	2017	2.0	2.8	1.6	2.7	<i>n.s.</i>	1.8	2.8	***	2.4	2.2	<i>n.s.</i>
	2018	3.2 a	3.1 a	2.5 b	3.1 a	*	2.9	3.1	<i>n.s.</i>	3.2	2.8	*
	2019	2.1 c	2.9 a	2.4 bc	2.7 ab	*	2.2	2.8	***	2.5	2.6	<i>n.s.</i>
TA (g/L)	2017	5.5	6.8	5.0	6.9	<i>n.s.</i>	5.2	6.9	***	6.1	6.0	<i>n.s.</i>
	2018	7.8 ab	8.2 a	6.2 c	7.5 b	*	7.0	7.8	***	8.0	6.8	***
	2019	7.5 a	7.6 a	6.0 b	7.8 a	**	6.8	7.7	**	7.6	6.9	*
pH	2017	4.1	4.0	3.9	3.9	<i>n.s.</i>	4.0	3.9	<i>n.s.</i>	4.0	3.9	<i>n.s.</i>
	2018	3.7	3.7	3.8	3.7	<i>n.s.</i>	3.8	3.7	**	3.7	3.8	*
	2019	3.5 b	3.6 ab	3.7 a	3.6 ab	*	3.6	3.6	<i>n.s.</i>	3.5	3.6	*
Phenolic composition												
Ant (mg/L)	2017	148.2	199.2	227.3	217.5	<i>n.s.</i>	187.8	208.4	<i>n.s.</i>	173.7	222.4	*
	2018	280.0	441.6	239.7	373.9	<i>n.s.</i>	259.9	407.7	**	360.8	306.8	<i>n.s.</i>
	2019	187.5 c	321.3 a	232.0 bc	288.4 ab	*	209.8	304.9	***	254.4	260.2	<i>n.s.</i>
Cat (mg/L)	2017	995.7	1752.1	715.8	1655.2	<i>n.s.</i>	855.7	1703.6	***	1373.9	1185.5	<i>n.s.</i>
	2018	1528.3	2837.3	1052.5	1888.9	<i>n.s.</i>	1290.4	2363.1	***	2182.8	1470.7	**
	2019	1810.8 b	3641.1 a	1149.5 c	3633.6 a	**	1480.2	3637.3	***	2726.0	2391.5	*
Tan (mg/L)	2017	1330.7	1995.9	951.7	1634.7	<i>n.s.</i>	1141.2	1815.3	***	1663.3	1293.2	*
	2018	2005.7	1535.6	1526.3	1624.5	<i>n.s.</i>	1766.0	1580.0	<i>n.s.</i>	1770.7	1575.4	<i>n.s.</i>
	2019	1871.3 b	2707.0 ab	990.5 c	2983.8 a	*	1430.9	2845.4	***	2289.2	1987.1	<i>n.s.</i>
TPP (mg/L)	2017	1581.9	2212.0	1546.4	2101.3	<i>n.s.</i>	1564.1	2156.6	***	1896.9	1823.8	<i>n.s.</i>
	2018	2228.6	2570.1	1783.4	2233.1	<i>n.s.</i>	2006.0	2401.6	***	2399.4	2008.2	***
	2019	1855.8	2594.5	1762.0	2581.7	<i>n.s.</i>	1808.9	2588.1	***	2225.1	2171.9	<i>n.s.</i>
Chromatic characteristics												
C-Ant (%)	2017	17.8	26.1	22.6	31.9	<i>n.s.</i>	20.2	29.0	*	22.0	27.3	<i>n.s.</i>
	2018	32.3	37.1	33.8	44.1	<i>n.s.</i>	33.1	40.6	**	34.7	38.9	*
	2019	25.9	40.2	32.3	40.5	<i>n.s.</i>	29.1	40.3	***	33.0	36.4	<i>n.s.</i>
CI	2017	3.7	5.8	4.1	6.5	<i>n.s.</i>	3.9	6.1	**	4.7	5.3	<i>n.s.</i>
	2018	13.6	14.8	13.8	15.7	<i>n.s.</i>	13.7	15.3	*	14.2	14.8	<i>n.s.</i>
	2019	8.7	12.9	9.7	14.1	<i>n.s.</i>	9.2	13.5	**	10.8	11.9	<i>n.s.</i>

(Continued)

TABLE 6 Continued

Parameter	Year	Treatment										
		C-NF	C-F	RI-NF	RI-F	<i>FxI</i>	NF	F	<i>F</i>	C	RI	<i>I</i>
Yellow (%)	2017	33.8	31.8	31.3	30.1	<i>n.s.</i>	32.5	31.0	<i>n.s.</i>	32.8	30.7	*
	2018	31.0	29.4	31.9	28.2	<i>n.s.</i>	31.4	28.8	**	30.2	30.1	<i>n.s.</i>
	2019	28.6 b	29.6 ab	30.3 a	29.4 ab	*	29.5	29.5	<i>n.s.</i>	29.1	29.9	<i>n.s.</i>
Red (%)	2017	53.8	57.0	57.4	59.2	<i>n.s.</i>	55.6	58.1	<i>n.s.</i>	55.4	58.3	*
	2018	56.8	61.2	54.4	62.3	<i>n.s.</i>	55.6	61.8	***	59.0	58.3	<i>n.s.</i>
	2019	62.2 a	59.9 ab	58.3 b	60.0 ab	**	60.2	60.0	<i>n.s.</i>	61.0	59.2	**
Blue (%)	2017	12.4	11.2	11.3	10.7	<i>n.s.</i>	11.9	10.9	<i>n.s.</i>	11.8	11.0	<i>n.s.</i>
	2018	12.2	9.4	13.7	9.5	<i>n.s.</i>	13.0	9.4	***	10.8	11.6	<i>n.s.</i>
	2019	9.2 b	10.5 ab	11.3 a	10.5 a	**	10.3	10.5	<i>n.s.</i>	9.9	10.9	**
Hue	2017	3.1	2.8	2.7	2.6	<i>n.s.</i>	2.9	2.7	<i>n.s.</i>	3.0	2.6	*
	2018	5.5	4.8	5.9	4.5	<i>n.s.</i>	5.7	4.7	**	5.1	5.2	<i>n.s.</i>
	2019	4.6 b	4.9 ab	5.2 a	4.9 ab	*	4.9	4.9	<i>n.s.</i>	4.8	5.1	*

Treatments: C-NF (no forcing and full irrigation); C-F (forcing and full irrigation); RI-NF (no forcing and deficit irrigation) and RI-F (forcing and deficit irrigation); F, Forcing factor; I, Irrigation factor.

Parameters: Alcoholic degree (AD); Tartaric acid (TAR); Malic acid (MAL); Total acid (TA); pH; Anthocyanins (Ant); Catechins (Cat); Tannins (Tan); Total polyphenolics (TPP); Percentage of color due to anthocyanins (C-Ant); Color intensity (CI); % Absorbance 420 nm (Yellow%); % Absorbance 520 nm (Red%); % Absorbance 620 nm (Blue%) and Color tonality (Hue).

Each value represents the mean of 8 samples (4 blocks, 2 replicates). Statistical analysis: Different letters indicate the existence of statistically significant differences between treatments; *n.s.* indicates not significant; (*) significant at 5% level; (**) significant at 1% level and (***) significant at 0.1% level.

3.3.2 Phenolic composition and chromatic characteristics

As a general trend, no interactions were found in terms of wine phenolic composition, chromatic characteristics or anthocyanin profile between the two techniques applied to the vines (Tables 6, 7). The effect of crop forcing and irrigation can therefore be examined, in most cases, separately. As observed in the initial mash, a general trend to higher values of phenolic substances was found in the F compared to the NF wines (Table 6), and significant increases were registered in the values of F wines compared to NF wines in all phenolic substances analyzed each year with the exception of Ant in 2017 and Tan in 2018. It can thus be concluded that crop forcing had a clear and consistent effect over the years and improved the phenolic content of the wines. However, the effect of *I* was less significant (significant differences were found five times only) and less consistent because the statistical significance depended on the year considered and the crop forcing applied. Thus, compared to C-NF and C-F, anthocyanin values in RI-NF and RI-F were higher in 2017 (53% and 9%), lower in 2018 (14.4% and 15.3%), while a significant *FxI* interaction was registered in 2019. In contrast to the effect found in F, a general trend to lower catechins ($p < 0.01$ in 2018, $p < 0.05$ in 2019) and tannins ($p > 0.05$ in 2017) was recorded in the RI compared to the C wines.

These changes in the values of phenolic compounds of the wines had an impact on their chromatic characteristics. According to the results shown in Table 6, F wines had higher C-Ant values (%) than NF wines in the 3 years of the study, and this trend was observed when RI were compared with C wines. Moreover, the CI values registered in the F and RI wines were higher than in the NF and C wines. It should be noticed that only F had a significant effect.

Therefore, the C-Ant (%) and CI values followed the order RI-F > C-F > RI-NF > C-NF. No significant changes were observed in color composition (calculated as % 420, % 520, and % 620). Differences were found in the values of these percentages between C-NF and RI-NF wines in the 2019 vintage only. Finally, the Hue values of the RI wines tended to be lower than those found in the C wines, with significantly different values in the 2017 and 2019 vintage.

3.3.3 Anthocyanin profile of Tempranillo wines

The amounts of the different anthocyanin substances (mg/L) found in the wines from the different treatments in 2017–2019 years are indicated in Table 7. As previously described, the anthocyanins present in wines were identified as the mono-glucoside forms (G) and acetyl-glucoside forms (A) of delphinidin (Dp), cyanidin (Cy), petunidin (Pt), peonidin (Pn), and malvidin (Mv) and the p-coumaroyl-glucoside forms (C) of Mv, Pt, Pn, and Cy. Regardless of year, mono-glucosides were always higher than acetyl-glycosides and acetyl-glycosides higher than acetates, with Mv derivatives the most abundant in all samples. The major compound was MvG in all samples analyzed, with amounts (mg/L) ranging from 88.3, (C-NF, 2017), to 202.5 (C-F, 2018), while the lowest values corresponded to PtA (0.3 in C-NF, 2017), and CyA (0.3 in C-NF, 2018 and 1.3 in RI-NF, 2019). With respect to anthocyanidin derivatives, each year in the NF wines and in 2017 in the F wines the sequence was $\Sigma Mv > \Sigma Pt > \Sigma Dp > \Sigma Pn > \Sigma Cy$, and in the F wines in 2018 and 2019 it was $\Sigma Mv > \Sigma Dp > \Sigma Pt > \Sigma Pn > \Sigma Cy$. Since, no significant interactions were found when the effects of crop forcing and irrigation systems were investigated on individual anthocyanin compounds, the effects of crop forcing and irrigation were also analyzed separately (Table 7). The significance of the effect of F on individual

TABLE 7 Effect of crop forcing and water status on the anthocyanin profile of Tempranillo wines.

Compound	Year	Treatment										
		C-NF	C-F	RI-NF	RI-F	<i>F</i> */ <i>I</i>	NF	F	<i>F</i>	C	RI	<i>I</i>
MvG	2017	88.3	115.9	129.9	124.4	n.s.	109.1	120.2	n.s.	102.1	122.9	*
	2018	141.0	202.5	144.1	178.8	n.s.	142.6	190.7	**	171.7	173.3	n.s.
	2019	88.9 b	150.9 a	118.0 ab	137.8 a	*	103.5	144.3	***	119.9	134.4	n.s.
PtG	2017	13.8	24.3	21.1	27.8	n.s.	17.5	26.1	**	19.0	22.7	n.s.
	2018	32.9	61.9	24.0	53.4	n.s.	28.5	57.6	***	47.4	42.9	n.s.
	2019	16.0 b	40.6 a	23.2 b	37.3 a	*	19.6	39.0	***	28.3	31.9	n.s.
DpG	2017	9.1	21.7	14.0	24.9	n.s.	11.5	23.3	**	15.4	17.8	n.s.
	2018	31.6	77.2	17.0	65.9	n.s.	24.3	71.6	***	54.4	47.1	n.s.
	2019	18.0	52.7	18.7	46.7	n.s.	18.4	49.7	***	35.4	35.7	n.s.
PnG	2017	3.4	8.0	3.4	6.9	n.s.	3.4	7.4	***	5.7	5.7	n.s.
	2018	23.1	36.6	8.4	22.0	n.s.	15.7	29.3	***	29.8	22.5	***
	2019	4.2	13.1	3.4	10.8	n.s.	3.8	12.0	***	8.7	8.3	n.s.
CyG	2017	0.6 c	1.8 a	0.8 c	1.5 b	**	0.7	1.7	**	1.2	1.3	n.s.
	2018	5.1	11.5	1.5	5.7	n.s.	3.3	8.6	***	8.3	6.5	**
	2019	2.3	6.5	2.2	5.5	n.s.	2.2	6.0	***	4.4	4.4	n.s.
ΣG	2017	115.2	171.7	169.2	185.6	n.s.	142.2	178.7	*	143.5	170.5	*
	2018	233.7	389.6	195	325.8	n.s.	214.3	357.7	***	311.7	292.3	n.s.
	2019	129.4 b	263.8 a	165.5 b	238.0 a	*	147.4	250.9	***	196.6	214.7	n.s.
MvA	2017	2.9	2.9	5.8	4.1	n.s.	4.3	3.5	n.s.	2.9	4.3	**
	2018	3.4	5.5	3.0	4.8	n.s.	3.2	5.1	**	4.4	4.2	n.s.
	2019	4.8	6.3	5.9	4.6	n.s.	5.3	5.5	n.s.	5.6	6.1	n.s.
PtA	2017	0.3 c	1.3 b	2.2 a	1.6 b	***	1.3	1.5	n.s.	0.8	1.8	***
	2018	2.4	3.2	2.3	3.0	n.s.	2.4	3.1	**	2.8	2.8	n.s.
	2019	2.4	3.8	3.4	3.3	n.s.	2.9	3.5	n.s.	3.1	3.6	n.s.
DpA	2017	1.2	1.3	2.0	1.7	n.s.	1.6	1.5	n.s.	1.3	1.6	**
	2018	1.9	3.2	1.5	3.2	n.s.	1.7	3.2	***	2.5	2.3	n.s.
	2019	2.3	4.8	3.3	5.1	n.s.	2.8	4.9	*	3.5	4.0	n.s.
PnA	2017	0.4 b	0.5 b	0.7 a	0.6 ab	**	0.5	0.5	n.s.	0.4	0.6	**
	2018	1.4	1.5	1.4	1.1	n.s.	1.4	1.3	n.s.	1.4	1.4	n.s.
	2019	2.3	1.6	2.8	1.6	n.s.	2.5	1.6	n.s.	1.9	2.2	n.s.
CyA	2017	0.8	0.8	0.9	0.8	n.s.	0.8	0.8	n.s.	0.8	0.9	n.s.
	2018	0.3	0.6	0.3	0.6	n.s.	0.3	0.6	*	0.5	0.5	n.s.
	2019	1.3	2.9	1.2	3.3	n.s.	1.2	3.1	***	2.1	2.0	n.s.

(Continued)

TABLE 7 Continued

Compound	Year	Treatment										
		C-NF	C-F	RI-NF	RI-F	<i>F</i> */ <i>I</i>	NF	F	<i>F</i>	C	RI	<i>I</i>
ΣA	2017	5.5 b	6.8 b	11.7 a	8.8 ab	*	8.6	7.8	n.s.	6.1	9.2	**
	2018	9.5	14.0	8.5	12.8	n.s.	9.0	13.4	**	11.7	11.2	n.s.
	2019	13.0	19.4	16.6	17.9	n.s.	14.8	18.6	n.s.	16.2	18	n.s.

Treatments: C-NF (no forcing and full irrigation); C-F (forcing and full irrigation); RI-NF (no forcing and deficit irrigation) and RI-F (forcing and deficit irrigation). Each value represents the mean of 8 samples (4 blocks, 2 replicates)

Parameters: Malvidin-3-glucoside (MvG); Petunidin-3-glucoside (PtG); Delphinidin-3-glucoside (DpG); Peonidin-3-glucoside (PnG); Cyanidin-3-glucoside (CyG); Total monoglucoside forms (ΣG); Malvidin-3-glucoside acetate (MvA); Petunidin-3-glucoside acetate (PtA); Delphinidin-3-glucoside acetate (DpA); Peonidin-3-glucoside acetate (PnA); Cyanidin-3-glucoside acetate (CyA); Total acetyl-glucoside forms (ΣA); Malvidin-3-glucoside coumarate (MvC); Petunidin-3-glucoside coumarate (PtC); Peonidin-3-glucoside coumarate (PnC); Cyanidin-3-glucoside coumarate (CyC); Total coumaroyl-glucoside forms (ΣC); Total malvidin derivatives (ΣMv); Total petunidin derivatives (ΣPt); Total delphinidin derivatives (ΣDp); Total peonidin derivatives (ΣPn); Total cyanidin derivatives (ΣCy).

Statistical analysis: Different letters indicate the existence of statistically significant differences between treatments; n.s. indicates not significant; (*) significant at 5% level; (**) significant at 1% level and (***) significant at 0.1% level.

anthocyanin compounds varied depending on the year, with statistical significance observed seven times in 2017, 11 in 2018, and 10 in 2019. Also, each year significantly higher values of the mono-glucoside forms were found in the F compared to the NF wines, with the exception of MvG in 2017, and therefore higher values of ΣG were found in F compared to NF wines in all study years. Although, in general, the values of acetyl-glucoside forms were higher in F than in NF, ΣA was only significant in 2018. Finally, an opposite trend was observed in the coumaroyl-glucoside forms, with significant decreases in ΣC found when F wines were compared with NF wines. Additionally, the values of ΣMv, ΣPt, ΣDp, ΣPn, and ΣCy were higher in F than in NF wines each year, with the exception of ΣMv and ΣPt in 2017. It should also be noted that the magnitude of the increase (in %) in ΣDp and ΣPt compounds was higher than in the other compounds. Finally, it is also of interest to note that, in general, although the interaction had no statistical significance, the increases were higher in C than in RI wines in 2017 and 2019, while in 2018 the opposite trend was registered. Thus, in 2017 and 2019 the increases found in Dp were 123% and 153% in CF wines compared to C-NF, and 67.3% and 109.1% in RI-F compared to RI-NF wines. However, in 2018 Dp increases were 112.8% and 237.8% in RI-F vs. RI-NF and C-F vs. C-NF. The effect of irrigation strategy depended on the year, the compound, and the crop forcing treatment, with a significant effect in seven individual anthocyanin compounds in 2017, three in 2018, and none in 2019. In 2017, higher values were found in RI than C wines, with higher increases (in %) in NF than F wines being the general trend. Significant increases were found in every anthocyanin form and in every derivate. The highest increases were found in the values of PtA (633.3%), MvA (100%), PtC (91.9%), and PtG (52.9%) of the RI-NF wines compared to the C-NF wines. In 2018, as a general trend, lower values were found in RI compared to C, with decreases (in %) slightly higher in NF wines, although the decreases were only significant in CyG, PnG, and PnC. Finally, in 2019, the irrigation treatment did not cause changes in the values of any anthocyanin substance present in either NF or F wines. The effect of irrigation depended on the crop forcing treatment, with a trend to increased values of ΣMv, ΣPt, and ΣDp observed in RI-NF compared to C-NF. However, the opposite trend was detected when C-F and RI-F were compared. In consequence,

in 2017, the highest values of ΣMv were found in RI-NF (170.7), of ΣPt (33.5) and Dp (26.6) in RI-F, and of Pn and Cy in C-F. The following year, 2018, the maximum values of all anthocyanidin groups were registered in C-F. Finally, in 2019, the maximum values of Mv, Pt, Dp, Pn, and Cy corresponded to the C-F treatment, with very close values registered in RI-F. The minimum values of all the anthocyanidin derivatives were registered in NF treatments; more specifically, in C-NF in 2017, Mv in C-NF, and the rest in RI-NF in 2018, and Mv, Pt, and Dp in C-NF and Pn and Cy in RI-NF in 2019.

3.4 Classification of wines; classification parameters

Multiple factor analysis (MFA) is a useful statistical method to analyze the similarities and discrepancies between a set of observations explained by data tables of different parameter sets and can also be used to explore the correlation between these parameter sets (Escofier et al., 1994). In this study, MFA was performed on the data matrices of the yield (Yield and BW), acid (TAR, MAL, TA and pH), phenolic (TPP, Ant, Cat and Tan), and chromatic (%C-Ant, CI, and Hue) group parameters. In addition, meteorological parameters (maximum temperature and SWP) were used as supplementary (non-active) variables to further explore the influence of both temperature and SWP on the composition of grapes and wines. The MFA allowed, on the one hand, exploring the differences and similarities between the different wines due to the treatment applied to the vines and, on the other hand, to know which set of variables can be used as markers of the wines from the different treatments.

Figures 2A–C show the results of the MFA carried out on the results of the wines from the 2017, 2018, and 2019 vintages, respectively. In all years, a good variance explanation was achieved (98.5%, 89.3%, and 98.5% in 2017, 2018, and 2019, respectively). In all years, the wines were distributed along the horizontal axis F1 (which explained 71.7%, 57.2%, and 66.2% of the total variance) and were grouped according to wines from forced (F) or non-forced (NF) vines. On the other hand, the vertical axis F2, which explained 26.8%, 32.1%, and 32.4% of the total variance, separated the samples according to irrigation treatment. In 2017, NF and F samples were located on the positive and negative side of

F1, respectively. According to variable contributions (%) showed in Table 8, this axis was defined by the yield (25.0%), acid (27.1%), phenolic (20.8%), and chromatic (27.0%) group parameters. Thus, all groups of variables contributed to a similar extent to differentiate the F from the NF samples. Almost all of the individual variables were related to higher values in F wines, with the exception of Hue, pH, yield, and BW, compared to NF wines. However, F2 was mainly associated with phenolic (43.5%) and acid (35.6%) groups of variables. Thus, the F2 axis allows distinguishing the C samples from the RI samples. The latter, located on the negative side of F2, were defined mainly by higher Ant values. In 2018, the distribution of samples on the plane defined by F1 and F2 was similar to that of the previous year. F1 grouped the samples by crop forcing and F2 by irrigation strategy. As Table 8 reflects, in 2018, the yield (24.7%), phenolic (27.8%), and chromatic (31.6%) parameters group contributed with similar values to F1, but the acid parameters group with 16.0% only. Thus, F samples were located on the negative side of F1 and NF on the positive side (Figure 2B). The latter were associated to higher BW, Tan, yield, Hue, and pH. As in 2017, C and RI samples were located on the positive and negative side, respectively, of the F2 axis. RI samples were mainly defined by higher TAR and pH values. Finally, as Table 8 shows, in 2019, all groups of variables contributed to the same extent to F1. This axis grouped NF (C and RI) wines on the negative side. These samples were defined by higher yield and BW. It should be noted that F2 differentiated RI-NF and C-NF by pH and Hue values (higher in RI-NF), and, also in 2019, RI-F and C-F were closely located on the F2 axis. Therefore, in all years of the trial, F (C and RI) wines, elaborated from vines with lower yield and smaller berries than NF, were distinguished by higher amounts of MAL, TAR, TA, TPP, Ant, Cat, CI, and % C-Ant than NF wines. In addition, RI-F wines were characterized by the maximum values of TAR and TA and C-F wines by the maximum value of polyphenolic substances. On the other hand, in 2017 and 2019, RI (F and NF) wines, from RI with lower production and smaller berries than C vines, and higher SWP were characterized by lower pH and Hue values than C wines.

PCA was performed with the values of ΣMv , ΣDp , ΣPt , ΣPn , and ΣCy of each year to determine general trends in the different wines. Figures 3A–C shows the distribution of samples in 2017, 2018, and 2019, respectively. PC-a, PC-b and PC-c accounted for more than 95% of the total variance. F1 axe covered 75% in 2017 and about 90% in the following years. From these figures, it is clear that, with the exception of RI-NF in 2017, the wines can be grouped in NF and F. These last samples were related with higher values of all derivate compounds with the exception of ΣMv in 2017.

4 Discussion

The dates of the most relevant phenological stages were modified in the forced treatments compared to the non-forced vines (Table 2). This implied that temperatures were also different during the ripening period (veraison to harvest), with cooler maximum and minimum temperatures in the forced treatments (Figure 1). This lower evapotranspirative demand during berry ripening in forced vines was also reflected in the vine water status for which, regardless

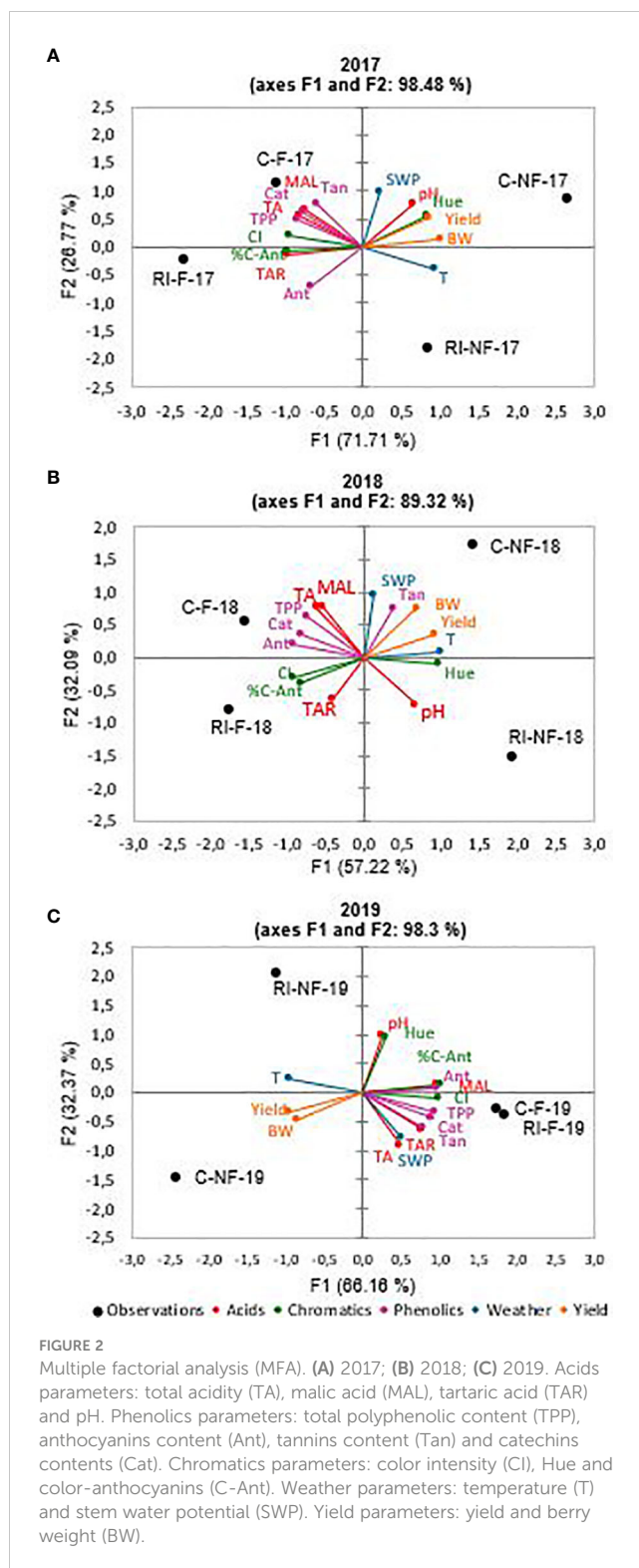


FIGURE 2

Multiple factorial analysis (MFA). (A) 2017; (B) 2018; (C) 2019. Acids parameters: total acidity (TA), malic acid (MAL), tartaric acid (TAR) and pH. Phenolics parameters: total polyphenolic content (TPP), anthocyanins content (Ant), tannins content (Tan) and catechins contents (Cat). Chromatics parameters: color intensity (CI), Hue and color-anthocyanins (C-Ant). Weather parameters: temperature (T) and stem water potential (SWP). Yield parameters: yield and berry weight (BW).

of the irrigation strategy applied, water stress during ripening (from veraison to harvest) was milder than in the non-forced treatments, with SWP values ranging between -0.58 MPa and -0.62 MPa and between -0.67 MPa and -0.77 MPa in C-F and RI-F, respectively. In this trial, coinciding with that reported by Gu et al. (2012) in cv. Cabernet Sauvignon and by Martinez De Toda et al. (2019) in cv. Tempranillo, the application of forcing, regardless of the irrigation

TABLE 8 Variable contributions (%) to multiple factorial analysis (MFA).

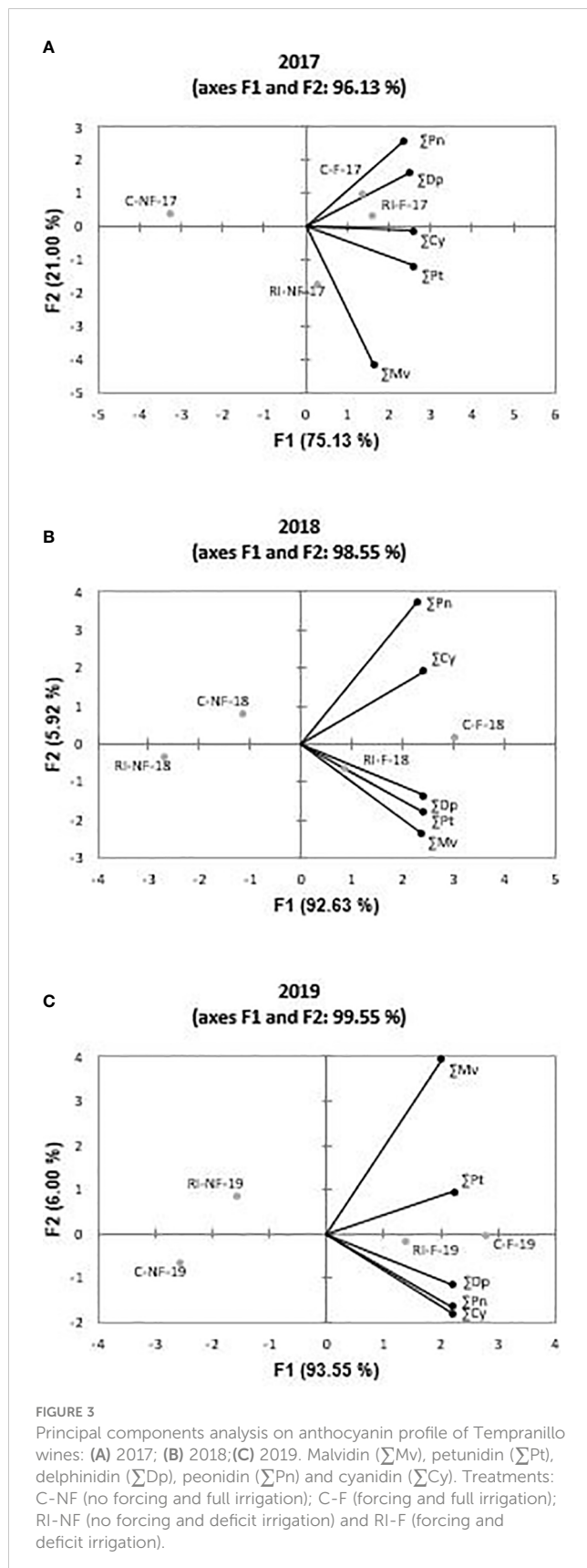
Parameter	Year					
	2017		2018		2019	
	F1 axe	F2 axe	F1 axe	F2 axe	F1 axe	F2 axe
TAR	9.9	0.6	2.1	8.8	6.9	9.7
MAL	5.9	11.4	3.6	13.4	10.8	0.4
TA	6.9	8.3	4.9	13.1	2.5	18.7
pH	4.4	15.3	5.4	10.8	0.7	22.4
Acids parameters	27.1	35.6	16.0	46.2	20.9	51.1
TPP	7.1	6.1	6.9	8.6	7.2	1.8
Ant	4.2	12.4	10.8	0.9	7.6	0.1
Cat	6.0	9.5	8.3	3.0	6.5	3.3
Tan	3.5	15.4	1.7	13.1	5.0	6.3
Phenolics parameters	20.8	43.5	27.8	25.6	26.2	11.4
%C-Ant	10.0	0.2	8.8	3.5	13.7	0.5
CI	9.9	1.1	10.7	2.2	13.5	0.3
Hue	7.1	8.8	12.1	0.2	1.2	26.2
Chromatics parameters	27.0	10.1	31.6	5.9	28.4	27.0
Yield	10.5	10.3	16.1	4.2	13.3	3.5
BW	14.5	0.6	8.6	18.1	11.2	6.9
Yield parameters	25.0	10.8	24.7	22.4	24.5	10.5

Acids parameters: Total Acidity (TA), Malic acid (MAL), Tartaric acid (TAR) and pH. Phenolics parameters: Total polyphenolic content (TPP), Anthocyanin content (Ant), Tannin content (Tan) and Catechin contents (Cat). Chromatics parameters: Color intensity (CI), Hue and Color-Anthocyanins (C-Ant). Weather parameters: Temperature (T) and Stem water potential (SWP). Yield parameters: Yield and Berry weight (BW).

strategy, caused a delay in the harvest date and decreases in BW and yield. The factors responsible for the production penalty are the number and weight of berries in the forced treatments. The displacement of the phenological cycle due to crop forcing places the new flowering and berry growth between July and August, coinciding with a period of higher temperatures (Figure 1). According to Kliever and Antcliff (1970), both the lower fruit set rate and the decreases in berry weight could be attributable to increases in temperature during flowering and fruit set and in the ambient light regime in the microclimate around the clusters. This could influence the berry sink capacity (i.e. the ability to attract photoassimilates) in F berries compared to NF berries. The yield decrease in RI treatments compared to C treatments may have been due to the worse water status of the RI vines, both in the pre-veraison period with a mild level of stress and in the post-veraison period with a more severe level as shown by the SWP values recorded during the 2017–2019 seasons (Table 3) (Grimes and Williams, 1990; Intrigliolo and Castel, 2010; Santesteban et al., 2011; Intrigliolo et al., 2012; Pérez-Álvarez et al., 2021). The intensity of this effect may vary with variety (Mirás-Avalos and Intrigliolo, 2017), but in cv. Tempranillo, previous work carried out in this same vineyard reported a significant decrease in final berry size and yield at harvest when pre-veraison water stress was applied (Valdés et al., 2009; Uriarte et al., 2015; Mancha et al., 2021). In this regard, it should be

considered that the degree of pre-veraison water stress that can be naturally induced depends on the soil water available at flowering, which in turn depends on previous rainfall levels and the water used by the vine during the spring (Lopes et al., 2011). Again, the change in phenology due to forcing shifted the pre-veraison period later in the season, when soil water content had possibly already decreased significantly. This allowed lower SWP to be reached in the forcing vines during pre-veraison throughout the three study seasons (Table 3) and, consequently, contributed to the yield penalty and lower berry weight observed in the forcing treatments (C-F and RI-F).

Acidity is not only important for flavor balance and the organoleptic properties of wine, but also contribute to wine stability (Van Leeuwen and Darriet, 2016). Malic and tartaric acids are the most common organic acids in grapevine fruit and they are the determinants of the TA of berries and wines. Normally, both acids reach their highest concentrations near veraison. In the second phase of growth, termed ripening, metabolite concentrations increase or decrease depending on net biosynthesis or metabolization and growth dilution, both mechanisms being genotype-dependent (Dai et al., 2011; Keller et al., 2016). It is believed that, once synthesized, tartaric acid remains stable and that the content does not vary in terms of quantity per fruit during ripening (Terrier et al., 2001; Rösti et al.,



2018). Malic acid, however, is metabolized and used as an energy source during the process (Rienth et al., 2016). Therefore, tartaric acid concentration decreased in the samples of must and wines

from the more irrigated treatments which resulted in the highest berry weight (C-NF). It is known this acid is less affected than malic acid by environmental conditions (Ruffner, 1982), and thus its concentration was probably more determined by the dilution effect in must as well as by increased precipitation of bitartrate potassium salts (Iland and Coombe, 1988). In our case, the lower temperatures during the ripening period of the F berries impeded the combustion of this acid in NF samples. Torres et al. (2017) reported that in cv. Tempranillo the extent of alteration in primary metabolism due to temperature was higher than in secondary metabolism, which was mainly affected by deficit irrigation. The effect of water stress during the herbaceous period of berry development on acidity has been reported for cv. Tempranillo and other varieties (Salón et al., 2005; Girona et al., 2009; Intrigliolo and Castel, 2010). Must and wines from F were more acid mainly because of the much larger concentration of malic acid than in the NF samples, especially in RI treatments. This organic acid was the main contributor to changes of acidity (García Romero et al., 1993). In this work, in general, the highest TA values were found in C-F samples (must and corresponding wines). These results are a consequence of one hand, of the increase in the synthesis of malic and tartaric acid due to higher assimilation rates (Esteban et al., 1999; De Souza et al., 2005; Salón et al., 2005). On the other hand, the lower malic acid respiration rate decreased by the lower temperatures reached by the clusters less exposed to sunlight as a result of the increase in leaf area in C irrigation practices due to higher vegetative growth (Spayd et al., 2002; De Souza et al., 2005). Our findings are in agreement with those of previous works that independently analyzed the effect of forcing (Martinez De Toda et al., 2019) and reduced deficit irrigation (Uriarte et al., 2016) on cv. Tempranillo. In this regard, it should be noted that the present study is the first to report that the better climatic conditions and temperatures during the ripening of RI-F samples mitigated the decrease caused by the RI strategy in NF wines, with TA values of RI-F wines always close to those found in C-F wines. Since malic is a weaker acid than tartaric (i.e. malic acid has higher pKa and dissociates incompletely), unfortunately, the effect of crop forcing on wine pH was only slight. These results reduce the success of the crop forcing technique because one of the main problems, particularly pronounced in Tempranillo wines, of current oenology is the high pH of wines.

Temperature, water status drought, and light intensity are factors of influence in the synthesis, accumulation, and concentration at harvest of phenolic substances of grapes and, in consequence, of the wines that are elaborated (Arrizabalaga et al., 2018; Del-Castillo-Alonso et al., 2021; Pérez-Álvarez et al., 2021; Valdés et al., 2022). Since, in this work, crop forcing and irrigation modified the temperature (Figure 1) and water status during the vegetative period (Table 3) and the yield and berry weight to different extents according to year and treatment (Table 4), the initial C-F, RI-F, and RI-NF meshes displayed different phenolic content than C-NF and, in consequence, the content of polyphenolic families and the chromatic characteristics of the wines were also modified. The increase in anthocyanin content in F samples (initial meshes and in the respective wines) could be associated with the lower temperatures registered during the ripening cycle of these treatments than in the NF samples

(Figure 1). It is known that as summer temperature rises to atypical values, the anthocyanin biosynthetic genes are downregulated, reducing berry skin anthocyanin biosynthesis (Conde et al., 2016). Arrizabalaga et al. (2018) showed in different Tempranillo clones that elevated temperature reduced anthocyanin concentration. They reported that, with the same °Brix, the anthocyanin concentration was lower at 28°C/18°C than 24°C/14°C, indicating a decoupling effect of elevated temperature during berry ripening explained by changes in the relative rate of response of anthocyanin and sugar build up, rather than delayed onset of anthocyanin accumulation. These authors also referenced the inhibition of mRNA transcription of the anthocyanin biosynthetic genes, as well as chemical and/or enzymatic degradation of the anthocyanins by the high temperatures reported in previous works (Mori et al., 2007). Furthermore, temperature may also reduce the anthocyanin content, affecting its subcellular transport through the down-regulation of several transmembrane transporter-encoding genes involved in the import of anthocyanins in the vacuole (Carbonell Bejerano and Martínez Zapater, 2013). With respect to NF and C, in both F and I samples the increase in anthocyanins is also associated with a berry-size concentrating effect associated with a decrease in BW and lower vine vigor (Cortell et al., 2007; Pérez-Álvarez et al., 2021; Aris et al., 2022; Valdés et al., 2022). Additionally, in the RI effect, the up-regulation of the biosynthetic pathway caused by water stress should be considered (Castellarin et al., 2007). It is known that the release of anthocyanin and tannin compounds from berry skins into the wine is affected by several viticulture and oenological practices (Guidoni & Hunter, 2012). In this work, since in terms of Ant, the wines reflect the trend observed in the initial mash, our results suggest that the extractability of anthocyanin from the grapes was scarcely modified by the treatments. However, in the case of tannins, in 2017 while no significant differences were found in the tannin content of the initial mash due to forcing and irrigation, they were found in the wines. In 2018, lower values ($p < 0.05$) were found in the RI must but not in RI wines compared to their respective C samples. These results need to be confirmed in future research.

Since acylated and coumarate derivatives are considered to be among the most stable compounds (Ortega-Regules et al., 2006), and Cy, Dp, and Pt derivatives are more sensitive to enzymatic oxidation (except for laccase) and non-enzymatic oxidation (catalyzed by copper or iron ions) to produce o-diquinones, or even o-diphenol dimers than Mv and Pn (Jackson, 2008), the anthocyanin profile determines the color and stability of wines. It is therefore essential to examine the effect of the techniques applied on the anthocyanin profile of the wines produced. While the extent of the change depended on the derivative considered, crop forcing modified the anthocyanin profile of the wines elaborated. Regardless of irrigation strategy, the highest increases were registered in Dp anthocyanidin. In this regard, Tarara et al. (2008) reported that lower temperatures were associated with increases in Dp, Cy, Pt, and Pn derivatives, but found no influence on concentrations of Mv derivatives. This behavior was only found in our study in 2017 because Σ Mv increased in 2018 and 2019. Otherwise, Mv and Pn compounds are more resistant to

oxidation, than Cy, Dp, and Pt. When the HS/LS (high sensitivity/low sensitivity) ratio was calculated as $\Sigma(\text{Cy} + \text{Dp} + \text{Pt})/\Sigma(\text{Mv} + \text{Pn})$, the mean values reached 0.68 in C-NF, 0.85 in C-F, 0.55 in RI-NF, and 0.83 in RI-F. The order RI-NF < C-NF < RI-F < C-F was observed in all years. Thus, F wines were more sensitive to oxidation than NF wines and, for a given crop forcing treatment, RI wines more than their respective C wines. The different wine profiles are a consequence of the changes found in the anthocyanin profiles of the grapes (results not shown) and the different rates and amounts of individual anthocyanin extraction from skins into wine and their transformation during fermentation (Guidoni and Hunter, 2012).

Along with anthocyanins, catechins and tannins can strongly impact the quality of red wines *via* their contributions to wine bitterness and astringency (Cheynier et al., 1997; Vidal et al., 2003; Kennedy et al., 2006). Our results are in agreement with those of other studies that showed a reduced response of tannins to irrigation treatments (Ollé et al., 2011). The increase of these compounds in F wines (C and RI) may be attributable to high temperatures impairing tannin synthesis of the berries and also the degree of galloylation at the transcriptomic levels, as described by Rienth et al. (2016). According to Bonada et al. (2015), temperature could affect tannin extractability from seed or skin indirectly by uncoupling berry seed and skin development and modifying the number of seeds or skin mass per berry. In this last regard, F grapes had a higher percentage of seeds in the fresh berry weight than NF grapes (4.6 and 4.0, respectively, as global interannual mean).

With respect to C-NF, these changes may modify the phenolic profile evolution of the wines elaborated and their color stability and their consequent chromatic characteristics. Since F and RI treatments caused a loss of yield it would be interesting to elaborate blend wines.

Many studies have used statistical techniques to find correlations between phenolic compounds and color parameters during the maturation and ageing processes of red wine (Gamero et al., 2018). In one interesting work Monagas et al. (2006) showed that chromatic attributes of red wines could be predicted by their phenolic profile using polynomial regression techniques. The substances which provided the best fitting model in that study were the anthocyanin compounds. In addition, when Gamero et al. (2014) investigated the correlations between the phenolic composition and the chromatic characteristics of Tempranillo wines, they found that CI was high and positively correlated with the presence of G, C, Dp, Mv, and Pt. In consequence CI was higher in F than in NF wines. Crop forcing modified the maximum temperature during the vegetative period. This parameter, considered as supplementary variable in MFA, was significant and strongly correlated to F1 axis. The irrigation strategies modified the SWP parameter correlated with F2 axis. Since F1 axis explained 71.7%, 57.2%, and 66.2% of the variation, and the location of samples was similar all years, it implies that the temperature during the vegetative period had a strong effect and a consistent response. Our results are in agreement with previous research in that Torres et al. (2017) reported a good separation of grape samples grown at different temperatures mainly based on differences in TAR. When Arrizabalaga et al. (2018) employed a PCA on plants grown at 24°C/14°C and 28°C/18°C, the first two principal components explained

about 75% of the total variability and clearly separated samples according to the temperature regime. F2 axe explained a lower percentage of the variance of F1. Therefore, the impact of irrigation strategy was lower and varied with the year considered. It is noticed that while the contribution of the each parameter group to F1axe was similar in the 3 years under study the contributions to F2 axe depended on the year considered, with NF samples more affected by the irrigation strategy than F samples. When Bonada et al. (2015) subjected to PCA the chemical and sensory profiles of Shiraz grape wines produced from vines exposed and not exposed to hydric and thermal stress, they found that F1 axe explained ~53% of the variation and was a function of the temperature treatment, with the remaining 37% explained by F2 and F3 axes, which were related to the water treatment. According to these authors, those differences suggest a comparatively higher impact of temperature than water on grape and wine composition. Thus, it can be concluded that, in line with Arrizabalaga et al. (2018), the extent of alteration in primary metabolism due to temperature was higher than in secondary metabolism, which was mainly affected by deficit irrigation. Finally, it has been noted that berry weight did not constitute a determining factor in wine composition. In this sense, these results support the findings of Walker et al. (2005) and Matthews & Nuzzo (2007) who argued that the viticultural practices used to control yield in a vineyard are more important than the yield values per se in determining the quality of the resulting grapes and wines, and that the environmental conditions determining berry size are more important than the size per se in determining the quality of the grapes and resulting wines.

5 Conclusions

The impact of climate change factors requires the use of direct short-term methods that involve changing environmental factors. This research provides evidence of changes in the composition of Tempranillo cv. wines in response to temperature and water status of vines during the vegetative period. The significance and extent of the temperature impact was higher and more consistent than that of water status. Wines from forced vines (elaborated with berries grown at lower temperature) had, in general, higher values of total acidity, malic acid, anthocyanins, catechins, and total polyphenols. In addition, color intensity and co-pigmented anthocyanin contents were higher in these wines. However, wines from forced vines were more sensitive to oxidation than wines from non-forced vines. Moreover, the significance and extent of the response to crop forcing was more consistent than irrigation across the different vintages. Thus, these results indicate that adaptation to climate change in south Mediterranean Europe might be plausible with the application of crop forcing. However, due to the decrease in yield, wines from crop forcing could be used as “good modifiers” of wines from vines grown with conventional techniques to improve their acid and phenolic composition as well their chromatic characteristics.

Data availability statement

The raw data supporting the conclusions of this article will be made available by the authors, without undue reservation.

Author contributions

Conceptualization, NL, DM, and MEV; Data curation, NL, MP, DM, and MEV; Formal analysis, NL, MP, DM, LM, DU, and MEV; Funding acquisition, MP; Investigation, NL, MP, DM, LM, DU, and MEV; Methodology, NL, MP, DM, LM, DU, and MEV; Project administration, MP; Resources, MP, DU, and MV; Software, NL and MEV; Supervision, NL and MEV; Validation, NL and MEV; Writing, original draft, NL and MEV; Writing, review and editing, NL and MEV. All authors contributed to the article and approved the submitted version.

Funding

This research was supported by funds from INIA Project RTA-2015-00089-C02-01, the ERDF, Junta de Extremadura, AGA001 (GR21196), AGROS2022 and IB20082. NL was supported by FPI-INIA CPD2016-0081.

Acknowledgments

The authors would like to thank Nuria Balas and Balbina Palacios for their technical support. Special thanks also go to Jordi Marsal for his contribution to the design of this project.

Conflict of interest

The authors declare that the research was conducted in the absence of any commercial or financial relationships that could be construed as a potential conflict of interest.

Publisher's note

All claims expressed in this article are solely those of the authors and do not necessarily represent those of their affiliated organizations, or those of the publisher, the editors and the reviewers. Any product that may be evaluated in this article, or claim that may be made by its manufacturer, is not guaranteed or endorsed by the publisher.

References

- Afi, M., Obenland, D., and El-kereamy, A. (2021). The complexity of modulating anthocyanin biosynthesis pathway by deficit irrigation in table grapes. *Front. Plants Sci.* 12. doi: 10.3389/fpls.2021.713277
- Aris, G., Cuneo, I. F., Pastenes, C., and Cáceres-Mella, A. (2022). Anthocyanin composition in cabernet sauvignon grape skins: effect of regulated deficit irrigation in a warm climate. *Horticulturae* 8 (9), 1–13. doi: 10.3390/horticulturae8090796
- Arrizabalaga, M., Morales, F., Oyarzun, M., Delrot, S., Gomès, E., Irigoyen, J. J., et al. (2018). Tempranillo clones differ in the response of berry sugar and anthocyanin accumulation to elevated temperature. *Plant Sci.* 267, 74–83. doi: 10.1016/j.plantsci.2017.11.009
- Arrizabalaga-Arriazu, M., Gomès, E., Morales, F., Irigoyen, J. J., Pascual, I., and Hilbert, G. (2020). High temperature and elevated carbon dioxide modify berry composition of different clones of grapevine (*Vitis vinifera* L.) cv. Tempranillo. *Front. Plant Sci.* 11. doi: 10.3389/fpls.2020.603687
- Bonada, M., Jeffery, D. W., Petrie, P. R., Moran, M. A., and Sadras, V. O. (2015). Impact of elevated temperature and water deficit on the chemical and sensory profiles of barossa Shiraz grapes and wines. *Aust. J. Grape Wine Res.* 21 (2), 240–253. doi: 10.1111/ajgw.12142
- Boulton, R. B. (2001). The copigmentation of anthocyanins and its role in the color of red wine: Comments on a critical review. *Am. J. Enol. Vitic.* 52 (2), 67–87.
- Broadhurst, R. B., and Jones, W. T. (1978). Analysis of condensed tannins using acidified vanillin. *J. Sci. Food Agric.* 29 (9), 788–794. doi: 10.1002/jsfa.2740290908
- Carbonell Bejerano, P., and Martínez Zapater, J. (2013). Estructura y composición de la uva y su contribución al vino. *Sebbm* 176, 5–8.
- Castellarin, S. D., Pfeiffer, A., Sivilotti, P., Degan, M., Peterlunger, E., and Di Gasparo, G. (2007). Transcriptional regulation of anthocyanin biosynthesis in ripening fruits of grapevine under seasonal water deficit. *Plant Cell Environ.* 30 (11), 1381–1399. doi: 10.1111/j.1365-3040.2007.01716.x
- Cheyrier, V., Prieur, C., Guyot, S., Rigaud, J., and Moutounet, M. (1997). The structures of tannins in grapes and wines and their interactions with proteins. *ACS Symposium Ser.* 661, 81–93. doi: 10.1021/bk-1997-0661.ch008
- Conde, A., Breia, R., Moutinho-Pereira, J., Grimplet, J., and Gerós, H. (2016). “Metabolic rearrangements in grapevine response to salt stress” in *Grapevine in a changing environment: a molecular and ecophysiological perspective*. Eds. H. Gerós, M. M. Chaves, H. M. Gil and S. Delrot (Chichester, UK: Wiley), 279–298.
- Coombe, D. G. (1995). Adoption of a system for identifying grapevine growth stages. *Aust. J. Grape Wine Res.* 1, 100–110.
- Cortell, J. M., Halbleib, M., Gallagher, A. V., Righetti, T. L., and Kennedy, J. A. (2007). Influence of vine vigor on grape (*Vitis vinifera* L. cv. Pinot Noir) anthocyanins. 1 Anthocyanin concentration and composition in fruit. *J. Agric. Food Chem.* 55 (16), 6575–6584. doi: 10.1021/jf070195v
- Dai, Z. W., Ollat, N., Gomès, E., Decroocq, S., Tandonnet, J. P., Bordenave, L., et al. (2011). Ecophysiological, genetic, and molecular causes of variation in grape berry weight and composition: A review. *Am. J. Enol. Vitic.* 62 (4), 413–425. doi: 10.5344/ajev.2011.10116
- Del-Castillo-Alonso, M. Á., Monforte, L., Tomás-Las-Heras, R., Ranieri, A., Castagna, A., Martínez-Abaigar, J., et al. (2021). Secondary metabolites and related genes in *Vitis vinifera* L. cv. Tempranillo grapes as influenced by ultraviolet radiation and berry development. *Physiologia Plantarum* 173 (3), 709–724. doi: 10.1111/ppl.13483
- De Souza, C. R., Maroco, J. P., Dos Santos, T. P., Rodrigues, M. L., Lopes, C. M., Pereira, J. S., et al. (2005). Grape berry metabolism in field-grown grapevines exposed to different irrigation strategies. *Vitis - J. Grapevine Res.* 44 (3), 103–109.
- Díaz-Fernández, Á., Díaz-Losada, E., Moreno, D., and Esperanza Valdés Sánchez, M. (2022). Anthocyanin profile of Galician endangered varieties. A tool for varietal selection. *Food Res. Int.* 154. doi: 10.1016/j.foodres.2022.110983
- Downey, M. O., Dokoozlian, N. K., and Krstic, M. P. (2006). Cultural practice and environmental impacts on the flavonoid composition of grapes and wine: A review of recent research. *Am. J. Enol. Vitic.* 57 (3), 257–268.
- ECC (1990). Commission regulation no. 2676/90. concerning the establishment of common analytical methods in the sector of wine. *Off. J. Eur. Communities L272* (3), 1–192.
- Esteban, M. A., Villanueva, M. J., and Lissarrague, J. R. (1999). Effect of irrigation on changes in berry composition of Tempranillo during maturation. Sugars, organic acids, and mineral elements. *Am. J. Enol. Vitic.* 50, 418–434.
- Gamero, E., Espinosa, F., Moreno, D., Uriarte, D., Prieto, M. H., Garrido, I., et al. (2018). Convenience of applying of viticulture technique as a function of the water status of the vine-stock. *Grapes Wines - Adv. Production Processing Anal. Valorization*. doi: 10.5772/intechopen.72799
- Gamero, E., Moreno, D., Vilanova, M., Uriarte, D., Prieto, M. H., and Valdés, M. E. (2014). Effect of bunch thinning and water stress on chemical and sensory characteristics of Tempranillo wines. *Aust. J. Grape Wine Res.* 20 (3), 394–400. doi: 10.1111/ajgw.12088
- García Romero, E., Sánchez Muñoz, G., Martín Álvarez, P. J., and Cabezedo Ibáñez, M. D. (1993). Determination of organic acids in grape musts, wines and vinegars by high-performance liquid chromatography. *J. Chromatogr. A* 655 (1), 111–117. doi: 10.1016/0021-9673(93)87018-H
- Girona, J., Marsal, J., Mata, M., Del Campo, J., and Basile, B. (2009). Phenological sensitivity of berry growth and composition of Tempranillo grapevines (*Vitis vinifera* L.) to water stress. *Aust. J. Grape Wine Res.* 15 (3), 268–277. doi: 10.1111/j.1755-0238.2009.00059.x
- Glories, Y. (1984). La couleur des vins rouges. Ire partie : les équilibres des anthocyanes et des tanins. *OENO One* 18 (3), 195. doi: 10.20870/oeno-one.1984.18.3.1751
- Grimes, D. W., and Williams, L. E. (1990). Irrigation effects on plant water relations and productivity of thompson seedless grapevines. *Crop Sci.* 30 (2), 255. doi: 10.2135/cropsci1990.0011183x003000020003x
- Gu, S., Jacobs, S. D., McCarthy, B. S., and Gohil, H. L. (2012). Forcing vine regrowth and shifting fruit ripening in a warm region to enhance fruit quality in “Cabernet Sauvignon” grapevine (*Vitis vinifera* L.). *J. Hortic. Sci. Biotechnol.* 87 (4), 287–292. doi: 10.1080/14620316.2012.11512866
- Guidoni, S., and Hunter, J. J. (2012). Anthocyanin profile in berry skins and fermenting must/wine, as affected by grape ripeness level of *Vitis vinifera* cv. Shiraz/R99. *Eur. Food Res. Technol.* 235 (3), 397–408. doi: 10.1007/s00217-012-1744-5
- Gutiérrez Gamboa, G., Zheng, W., and Martínez de Toda, F. (2020). Strategies in the vineyard establishment to face global warming in viticulture: A mini review. *J. Sci. Food Agric.* doi: 10.10102/jsfa.10813
- Iland, P. G., and Coombe, B. G. (1988). Malate, tartrate, potassium, and sodium in flesh and skin of Shiraz grapes during ripening: Concentration and compartmentation. *Am. J. Enol. Vitic.* 39, 71–76.
- Intrigliolo, D. S., and Castel, J. R. (2010). Response of grapevine cv. “Tempranillo” to timing and amount of irrigation: water relations, vine growth, yield and berry and wine composition. *Irrigation Sci.* 28 (2), 113–125. doi: 10.1007/s00271-009-0164-1
- Intrigliolo, D. S., and Castel, J. R. (2011). Interactive effects of deficit irrigation and shoot and cluster thinning on grapevine cv. Tempranillo. Water relations, vine performance and berry and wine composition. *Irrigation Sci.* 29 (6), 443–454. doi: 10.1007/s00271-010-0252-2
- Intrigliolo, D. S., Pérez, D., Risco, D., Yeves, A., and Castel, J. R. (2012). Yield components and grape composition responses to seasonal water deficits in Tempranillo grapevines. *Irrigation Sci.* 30 (5), 339–349. doi: 10.1007/s00271-012-0354-0
- Jackson, R. (2008). *Wine: Science, Principles and Applications* (San Diego, CA: Academic Press).
- Jones, G. V., Duchêne, E., Tomasi, D., Yuste, J., Braslavská, O., Schultz, H., et al. (2005). Changes in European winegrape phenology and relationships with climate. *XIV Int. GESCO Viticulture Congress* 44, 54–61.
- Jones, G. V., Edwards, E. J., Bonada, M., Sadras, V. O., Krstic, M. P., and Herderich, M. J. (2022). Climate change and its consequences for viticulture. *Managing Wine Qual.* 727–778. doi: 10.1016/B978-0-08-102067-8.00015-4
- Keller, M., Romero, P., Gohil, H., Smithyman, R. P., Riley, W. R., Casassa, L. F., et al. (2016). Deficit irrigation alters grapevine growth, physiology, and fruit microclimate. *Am. J. Enol. Vitic.* 67 (4), 426–435. doi: 10.5344/ajev.2016.16032
- Kennedy, J. A., Saucier, C., and Glories, Y. (2006). Grape and wine phenolics: History and perspective. *Am. J. Enol. Vitic.* 57 (3), 239–248. doi: 10.5344/ajev.2006.57.3.239
- Kishimoto, M., Yamamoto, T., and Kobayashi, Y. (2022). Of lateral or secondary induced shoot use on number of bunches and fruit quality in forcing cultivation by current shoot cutting and flower cluster removal to shift grape ripening to a cooler season. *Hortic. J.* 91 (2), 169–175. doi: 10.2503/hortj.UTD-314
- Kliwer, W. M., and Antcliff, A. J. (1970). Influence of defoliation, leaf darkening, and cluster shading on the growth and composition of sultana grapes. *Am. J. Enol. Vitic.* 21, 26–36.
- Lavado, N., Uriarte, D., Mancha, L. A., Moreno, D., Valdés, M. E., and Prieto, M. H. (2023). Evaluation of the carry-over effect of the “crop-forcing” technique and water deficit in grapevine “Tempranillo”. *Agronomy* 13 (2), 395.
- Lavado, N., Uriarte, D., Mancha, L. A., Moreno, D., Valdés, E., and Prieto, M. H. (2019). Effect of forcing vine regrowth on “Tempranillo” (*Vitis vinifera* L.) berry development and quality in extremadura. *Vitis - J. Grapevine Res.* 58, 135–142. doi: 10.5073/vitis.2019.58.special-issue.135-142
- Lee, J., Durst, R. W., and Wrolstad, R. E. (2005). Determination of total monomeric anthocyanin pigment content of fruit juices, beverages, natural colorants, and wines by the pH differential method: Collaborative study. *J. AOAC Int.* 88 (5), 1269–1278. doi: 10.1093/jaoac/88.5.1269
- Lizama, V., Perez-Álvarez, E. P., Intrigliolo, D. S., Chirivella, C., Álvarez, I., and García-Esparza, M. J. (2021). Effects of the irrigation regimes on grapevine cv. Bobal in a Mediterranean climate: II. Wine, skins, seeds, and grape aromatic composition. *Agric. Water Manage.* 256, 107078.
- Lopes, C. M., Santos, T. P., Monteiro, A., Rodrigues, M. L., Costa, J. M., and Chaves, M. M. (2011). Combining cover cropping with deficit irrigation in a Mediterranean low vigor vineyard. *Scientia Hort.* 129 (4), 603–612. doi: 10.1016/j.scienta.2011.04.033
- Mancha, L. A., Uriarte, D., Valdés, E., Moreno, D., and Prieto, M. D. H. (2021). Effects of regulated deficit irrigation and early cluster thinning on production and quality parameters in a vineyard cv. Tempranillo under semi-arid conditions in southwestern Spain. *Agronomy* 11 (1). doi: 10.3390/agronomy11010034

- Martí, P., González-Altozano, P., López-Urrea, R., Mancha, L. A., and Shiri, J. (2015). Modeling reference evapotranspiration with calculated targets: assessment and implications. *Agric. Water Manage.* 149, 81–90. doi: 10.1016/j.agwat.2014.10.028
- Martínez De Toda, F., García, J., and Balda, P. (2019). Preliminary results on forcing vine regrowth to delay ripening to a cooler period. *Vitis - J. Grapevine Res.* 58 (1), 17–22. doi: 10.5073/vitis.2019.58.17-22
- Martínez-Moreno, A., Sanz, F., Yeves, A., Gil-Muñoz, R., Martínez, V., Intrigliolo, D. S., et al. (2019). Forcing bud growth by double-pruning as a technique to improve grape composition of *Vitis vinifera* L. cv. Tempranillo in a semi-arid Mediterranean climate. *Scientia Hort.* 256, 108614. doi: 10.1016/j.scienta.2019.108614
- Matthews, M. A., and Nuzzo, V. (2007). Berry size and yield paradigms on grapes and wines quality. *Acta Hort.* 754, 423–436. doi: 10.17660/ActaHortic.2007.754.56
- Mira de Orduña, R. (2010). Climate change associated effects on grape and wine quality and production. *Food Res. Int.* 43 (7), 1844–1855. doi: 10.1016/j.foodres.2010.05.001
- Mirás-Avalos, J. M., and Intrigliolo, D. S. (2017). Grape composition under abiotic constraints: Water stress and salinity. *Front. Plant Sci.* 8. doi: 10.3389/fpls.2017.00851
- Monagas, M., Bartolomé, B., and Gómez-Cordovés, C. (2005). Updated knowledge about the presence of phenolic compounds in wine. *Crit. Rev. Food Sci. Nutr.* 45 (2), 85–118. doi: 10.1080/10408690490911710
- Monagas, M., Martín-Álvarez, P. J., Bartolomé, B., and Gómez-Cordovés, C. (2006). Statistical interpretation of the color parameters of red wines in function of their phenolic composition during aging in bottle. *Eur. Food Res. Technol.* 222 (5–6), 702–709. doi: 10.1007/s00217-005-0037-7
- Mori, K., Goto-Yamamoto, N., Kitayama, M., and Hashizume, K. (2007). Loss of anthocyanins in red-wine grape under high temperature. *J. Exp. Bot.* 58 (8), 1935–1945. doi: 10.1093/jxb/erm055
- Moriondo, M., Jones, G. V., Bois, B., Dibari, C., Ferrise, R., Trombi, G., et al. (2013). Projected shifts of wine regions in response to climate change. *Climatic Change* 119 (3–4), 825–839. doi: 10.1007/s10584-013-0739-y
- Muñoz-Organero, G., Espinosa, F. E., Cabello, F., Zamorano, J. P., Urbanos, M. A., Puertas, B., et al. (2022). Phenological study of 53 Spanish minority grape varieties to search for adaptation of viticulture to climate change conditions. *Horticulturae* 8 (11), 984. doi: 10.3390/horticulturae8110984
- Natividade, M. M. P., Corrêa, L. C., Souza, S. V. C., Pereira, G. E., and Lima, L. C. de O. (2013). Simultaneous analysis of 25 phenolic compounds in grape juice for HPLC: Method validation and characterization of São Francisco valley samples. *Microchemical J.* 110, 665–674. doi: 10.1016/j.microc.2013.08.010
- Ollé, D., Guiraud, J. L., Souquet, J. M., Terrier, N., Ageorges, A., Cheynier, V., et al. (2011). Effect of pre- and post-veraison water deficit on proanthocyanidin and anthocyanin accumulation during Shiraz berry development. *Aust. J. Grape Wine Res.* 17 (1), 90–100. doi: 10.1111/j.1755-0238.2010.00121.x
- Ortega-Regules, A., Romero-Cascales, I., Ros-García, J. M., López-Roca, J. M., and Gómez-Plaza, E. (2006). A first approach towards the relationship between grape skin cell-wall composition and anthocyanin extractability. *Analytica Chimica Acta* 563 (1–2 SPEC. ISS.), 26–32. doi: 10.1016/j.aca.2005.12.024
- Pallioti, A., Tombesi, S., Silvestroni, O., Lanari, V., Gatti, M., and Poni, S. (2014). Changes in vineyard establishment and canopy management urged by earlier climate-related grape ripening: A review. *Scientia Hort.* 178, 43–54. doi: 10.1016/j.scienta.2014.07.039
- Pérez-Álvarez, E. P., Intrigliolo, D. S., Almajano, M. P., Rubio-Bretón, P., and Garde-Cerdán, T. (2021). Effects of water deficit irrigation on phenolic composition and antioxidant activity of monastrell grapes under semiarid conditions. *Antioxidants* 10 (8). doi: 10.3390/antiox10081301
- Petrie, P. R., and Sadras, V. O. (2008). Advancement of grapevine maturity in Australia between 1993 and 2006: Putative causes, magnitude of trends and viticultural consequences. *Aust. J. Grape Wine Res.* 14 (1), 33–45. doi: 10.1111/j.1755-0238.2008.00005.x
- Picón-Toro, J., González-Dugo, V., Uriarte, D., Mancha, L., and Testi, L. (2012). Effects of canopy size and water stress over the crop coefficient of a “Tempranillo” vineyard in south-western Spain. *Irrigation Sci.* 30, 419–432. doi: 10.1007/s00271-012-0351-3
- Portu, J., López, R., Baroja, E., Santamaría, P., and Garde-Cerdán, T. (2016). Improvement of grape and wine phenolic content by foliar application to grapevine of three different elicitors: Methyl jasmonate, chitosan, and yeast extract. *Food Chem.* 201, 213–221. doi: 10.1016/j.foodchem.2016.01.086
- Rienth, M., Torregrosa, L., Sarah, G., Ardisson, M., Brillouet, J. M., and Romieu, C. (2016). Temperature desynchronizes sugar and organic acid metabolism in ripening grapevine fruits and remodels their transcriptome. *BMC Plant Biol.* 16 (1), 1–24. doi: 10.1186/s12870-016-0850-0
- Rösti, J., Schumann, M., Cleroux, M., Lorenzini, F., Zufferey, V., and Rienth, M. (2018). Effect of drying on tartaric acid and malic acid in Shiraz and Merlot berries. *Aust. J. Grape Wine Res.* 24 (4), 421–429. doi: 10.1111/ajgw.12344
- Ruffner, H. P. (1982). Metabolism of tartaric and malic acids in *Vitis*: A review - part B. *Vitis* 21, 346–358.
- Sadras, V. O., and Moran, M. A. (2012). Elevated temperature decouples anthocyanins and sugars in berries of Shiraz and Cabernet Franc. *Aust. J. Grape Wine Res.* 18 (2), 115–122. doi: 10.1111/j.1755-0238.2012.00180.x
- Salón, J. L., Chirivella, C., and Castel, J. R. (2005). Response of cv. Bobal to timing of deficit irrigation in Requena, Spain: Water relations, yield, and wine quality. *Am. J. Enol. Vitic.* 56 (1), 1–8. doi: 10.5344/ajev.2005.56.1.1
- Santesteban, L. G., Miranda, C., and Royo, J. B. (2011). Regulated deficit irrigation effects on growth, yield, grape quality and individual anthocyanin composition in *Vitis vinifera* L. cv. “Tempranillo”. *Agric. Water Manage.* 98 (7), 1171–1179. doi: 10.1016/j.agwat.2011.02.011
- Sarneckis, C. J., Damberg, R. G., Jones, P., Mercurio, M., Herderich, M. J., and Smith, P. A. (2006). Teens, food choice, and health: how can a multi-method research methodology enhance the study of teen food choice and health messaging? *Aust. J. Grape Wine Res.* 12 (1), 39–49.
- Shackel, K. A. (2007). Water relations of woody perennial plant species. *J. Int. Des. Sci. la Vigne du Vin* 41, 121–129. doi: 10.20870/oeno-one.2007.41.3.847
- Singleton, V. L., and Rossi, J. A. (1965). Colorimetry of total phenolics with phosphomolybdic-phosphotungstic acid reagents. *Am. J. Enol. Vitic.* 16, 144–158.
- Spayd, S. E., Tarara, J. M., Mee, D. L., and Ferguson, J. C. (2002). Separation of sunlight and temperature effects on the composition of *Vitis vinifera* cv. Merlot berries. *Am. J. Enol. Vitic.* 53 (3), 171–182.
- Tarara, J., Lee, J., and Spayd, S. (2008). Berry temperature and solar radiation alter acylation, proportion, and concentration of anthocyanin in “Merlot” grapes. *Am. J. Enol. Vitic.* 59 (3), 235–247.
- Tate, A. B. (2001). Global warming’s impact on wine. *Int. J. Phytoremediation* 21 (1), 95–109. doi: 10.1080/09571260120095012
- Terrier, N., Sauvage, F., Ageorges, A., and Romieu, C. (2001). Changes in acidity and in proton transport at the tonoplast of grape berries during development. *Planta* 213, 20–28.
- Torres, N., Hilbert, G., Luquin, J., Goicoechea, N., and Antolín, M. C. (2017). Flavonoid and amino acid profiling on *Vitis vinifera* L. cv Tempranillo subjected to deficit irrigation under elevated temperatures. *J. Food Composition Anal.* 62, 51–62. doi: 10.1016/j.jfca.2017.05.001
- Torres, N., Yu, R., Martínez-Lüscher, J., Kostaki, E., and Kurtural, S. K. (2021). Effects of irrigation at different fractions of crop evapotranspiration on water productivity and flavonoid composition of Cabernet Sauvignon grapevine. *Front. Plants Sci.* 12. doi: 10.3389/fpls.2021.712622
- Uriarte, D., Intrigliolo, D. S., Mancha, L. A., Picón-Toro, J., Valdes, E., and Prieto, M. H. (2015). Interactive effects of irrigation and crop level on Tempranillo vines in a semiarid climate. *Am. J. Enol. Vitic.* 66 (2), 101–111. doi: 10.5344/ajev.2014.14036
- Uriarte, D., Intrigliolo, D. S., Mancha, L. A., Valdés, E., Gamero, E., and Prieto, M. H. (2016). Combined effects of irrigation regimes and crop load on “Tempranillo” grape composition. *Agric. Water Manage.* 165. doi: 10.1016/j.agwat.2015.11.016
- Valdés, M. E., Moreno, D., Gamero, E., Uriarte, D., Prieto, M. D. H., Manzano, R., et al. (2009). Effects of cluster thinning and irrigation amount on water relations, growth, yield and fruit and wine composition of Tempranillo grapes in extremadura (Spain). *J. Int. Des. Sci. la Vigne Du Vin* 43 (2), 67–76. doi: 10.20870/oeno-one.2009.43.2.799
- Valdés, M. E., Talaverano, M. I., Moreno, D., Uriarte, D., Mancha, L., and Vilanova, M. (2022). Improving the phenolic content of Tempranillo grapes by sustainable strategies in the vineyard. *Plants* 11 (11). doi: 10.3390/plants11111393
- Van Leeuwen, C., and Darriet, P. (2016). The impact of climate change on viticulture and wine quality. *J. Wine Economics* 11 (1), 150–167. doi: 10.1017/jwe.2015.21
- Van Leeuwen, C., and Destrac-Irvine, A. (2017). Modified grape composition under climate change conditions requires adaptations in the vineyard. *Oeno One* 51 (2), 147–154. doi: 10.20870/oeno-one.2016.0.0.1647
- Van Leeuwen, C., Destrac-Irvine, A., Dubernet, M., Duchêne, E., Gowdy, M., Marguerit, E., et al. (2019). An update on the impact of climate change in viticulture and potential adaptations. *Agronomy* 9 (9), 1–20. doi: 10.3390/agronomy9090514
- Vidal, S., Francis, L., Guyot, S., Marnet, N., Kwiatkowski, M., Gawel, R., et al. (2003). The mouth-feel properties of grape and apple proanthocyanidins in a wine-like medium. *J. Sci. Food Agric.* 83 (6), 564–573. doi: 10.1002/jsfa.1394
- Walker, R. R., Blackmore, D. H., Clingeleffer, P. R., Kerridge, G. H., Rühl, E. H., and Nicholas, P. R. (2005). Shiraz Berry size in relation to seed number and implications for juice and wine composition. *Aust. J. Grape Wine Res.* 11 (1), 2–8. doi: 10.1111/j.1755-0238.2005.tb00273.x



OPEN ACCESS

EDITED BY

Alessandra Ferrandino,
University of Turin, Italy

REVIEWED BY

Silvia Guidoni,
University of Turin, Italy
Daniela Farinelli,
University of Perugia, Italy
Maurizio Petrozziello,
Council for Agricultural and Economics
Research (CREA), Italy

*CORRESPONDENCE

Isabella Ghiglieri
✉ isabella.ghiglieri@unibs.it

†PRESENT ADDRESS

Isabella Ghiglieri,
Department of Civil, Environmental,
Architectural Engineering and Mathematics,
Agrofood Research Hub, University of
Brescia, Brescia, Italy

†These authors have contributed
equally to this work and share
first authorship

RECEIVED 16 December 2022

ACCEPTED 17 April 2023

PUBLISHED 17 May 2023

CITATION

Ghiglieri I, Carlin S, Cola G, Vrhovsek U,
Valenti L, Garcia-Aloy M and Mattivi F
(2023) Impact of meteorological
conditions, canopy shading and leaf
removal on yield, must quality, and
norisoprenoid compounds content in
Franciacorta sparkling wine.
Front. Plant Sci. 14:1125560.
doi: 10.3389/fpls.2023.1125560

COPYRIGHT

© 2023 Ghiglieri, Carlin, Cola, Vrhovsek,
Valenti, Garcia-Aloy and Mattivi. This is an
open-access article distributed under the
terms of the [Creative Commons Attribution
License \(CC BY\)](#). The use, distribution or
reproduction in other forums is permitted,
provided the original author(s) and the
copyright owner(s) are credited and that
the original publication in this journal is
cited, in accordance with accepted
academic practice. No use, distribution or
reproduction is permitted which does not
comply with these terms.

Impact of meteorological conditions, canopy shading and leaf removal on yield, must quality, and norisoprenoid compounds content in Franciacorta sparkling wine

Isabella Ghiglieri^{1*†}, Silvia Carlin^{2†}, Gabriele Cola¹,
Urska Vrhovsek², Leonardo Valenti¹, Mar Garcia-Aloy²
and Fulvio Mattivi²

¹Department of Agricultural and Environmental Sciences - Production, Landscape, Agroenergy,
University of Milan, Milan, Italy, ²Metabolomic Unit, Food Quality and Nutrition Department, Research
and Innovation Center, Edmund Mach Foundation, S. Michele all'Adige, Italy

Climate change is a major concern in agriculture; in grapevine production, climate change can affect yield and wine quality as they depend on the complex interactions between weather, plant material, and viticultural techniques. Wine characteristics are strongly influenced by microclimate of the canopy affecting primary and secondary metabolites of the grapevine. Air temperature and water availability can influence sugar and acid concentration in grapes and relative wines, and their content of volatile compounds such as norisoprenoids. This becomes relevant in sparkling wine production where grapes are generally harvested at a relatively low pH, high acidity, and low sugar content and where the norisoprenoids significantly contributes to the final aroma of the wine. The effect of climate change on grapevine and wine, therefore, calls for the implementation of on-field adaptation strategies. Among them canopy management through leaf removal and shading have been largely investigated in the wine growing sector. The present study, conducted over 4 years (2010-2013) aims at investigating how leaf removal and artificial shading strategies affect grape maturation, must quality and the production of norisoprenoids, analyzed using an untargeted approach, in sparkling wine. Specifically, this paper investigates the effect of meteorological conditions (i.e., water availability and temperatures) and the effect of leaf removal and shading on *Vitis vinifera* L. cv. Chardonnay and Pinot noir, which are suitable to produce sparkling wine in the DOCG Franciacorta wine growing area (Lombardy, Italy). The effect of leaf removal and shading practices on norisoprenoids has been the focus of the study. No defoliation and artificial shading treatments play an important role in the preservation of the acidity in warm seasons and this suggests calibrating defoliation activities in relation to the meteorological trend without standardized procedures. This is particularly relevant in the case of sparkling wine, where the acidity is essential to determine wine quality. The

enhanced norisoprenoid aromas obtained with a total defoliation represent a further element to direct defoliation and shading strategies. The obtained results increase knowledge about the effect of different defoliation and artificial shading applications in relation to meteorological condition supporting the management decision-making in the Franciacorta wine growing area.

KEYWORDS

vine (*Vitis vinifera* L.), leaf removal, grapevine shading, must quality, yield, sparkling wine, aroma compounds, norisoprenoid

1 Introduction

Climate change means any changes in weather patterns caused by natural events and human activities during a certain period (IPCC, 2007). The temperature increase that has characterized Europe and Italy since the end of the 1980s has relevant consequences on the quantity and quality of crops, representing a major concern in agriculture (Mariani et al., 2012; Suter et al., 2021). In grape-growing for wine production, climate change can significantly affect yield and, indirectly, wine quality (Fraga et al., 2012), as they depend on the complex interactions between weather variables, plant material, and viticultural techniques (Nesbitt et al., 2016; van Leeuwen et al., 2019; Mirás-Avalos and Araujo, 2021). Air temperature, water availability, and sunlight are the most relevant factors that, influencing grape and must quality, indirectly affect wine quality. Grapes and musts characteristics are, indeed, strongly influenced by climatic conditions as changes in the microclimate of the canopy have an impact on the primary and secondary metabolites of the grapevine.

Water availability and water stress lead to different effects depending on the grapevine developmental stage, cultivar and wine target (Deloire et al., 2004; Santos et al., 2020; Mirás-Avalos and Araujo, 2021). During post-veraison excessive humidity tends to promote sugar dilution (Reynolds and Naylor, 1994), delaying the harvesting time (Tonietto, 1999) and avoiding an excessive accumulation of total soluble solids (Intrigliolo et al., 2016). In general, the water status correlates positively with berry size, total acidity, and malic acid concentration (Mirás-Avalos and Intrigliolo, 2017).

Many studies focused on the effect of temperature increases on grapevine and wine quality (Biasi et al., 2019; Santos et al., 2020). The mean air temperatures during the growing season are directly related to the length of the growing season for each variety (Jones et al., 2005); the different stages of development generally take place earlier and the time between veraison and ripening is shorter (Schultz, 2000; Jones et al., 2005). Excessively hot weather during the veraison-maturity period can significantly influence sugar accumulation (Greer, 2013), reducing the level of acidity in grapevines and, consequently, in wines (Pons et al., 2017). This becomes relevant in grapevines suitable to produce sparkling wines. In sparkling wines production grapevines are in fact generally harvested at a relatively low pH, higher titratable acidity, and

lower soluble sugar content than those for table wine production (Alfonzo et al., 2020). The synthesis of these compounds tends to increase during the herbaceous phase of the berry, while their degradation is enhanced after veraison and during the final stages of ripening. Carotenoids are the precursors of the norisoprenoids, volatile compounds. Norisoprenoids can be generated by the direct degradation of carotenoids such as β -carotene and neoxanthin, and can be stored as glycoconjugates, which can then release their volatile aglycones during wine fermentation or ageing; hydrolysis is often slow and depends on various factors, such as storage duration, temperature, and pH (Winterhalter and Schreier, 1994; Deluc et al., 2009; Song et al., 2012). The olfactory perception thresholds of these compounds are very low and, therefore, they have a high sensorial impact on the wine aroma (Mendes-Pinto, 2009). The most important C13 norisoprenoids are: TDN, vitispirane, actinidols, β -damascenone, β -ionone, and E-1-(2,3,6-trimethylphenyl) buta-1,3diene (TBP-1).

Although the concentration of norisoprenoids in grapes depends on many factors, such as variety and stage of ripeness, the environmental conditions, have a fundamental role in influencing their synthesis. This is confirmed by the behavior of norisoprenoid β -damascenone that decreases in white wines in conditions of exposure to light and higher temperature (Marais et al., 1992; Kwasniewski et al., 2010).

The effect of climate change on grapes, musts and, consequently, on wine quality, therefore, calls for the implementation of on-field adaptation strategies. Among these, the management of the canopy through leaf removal and shading have been largely investigated in the wine growing sector (Downey et al., 2006; Caravia et al., 2016; Ghiglieri et al., 2020; Martínez-Lüscher et al., 2020). The influence of these agronomic practices on canopy microclimate has been widely studied (Crippen and Morrison, 1986; Jackson and Lombard, 1993; Downey et al., 2006; Ghiglieri et al., 2020). The direct solar radiation on grape caused by leaf removal and the consequent increase in berry temperature during maturation, influence berry ripening and metabolism, promoting sugar contents accumulation (Riou et al., 1994), reducing titratable acidity, and increasing malic acid degradation (Lakso and Kiewer, 1975; Conde et al., 2006; de Oliveira et al., 2019). Moreover, excessive sunlight inhibits the development of flavor and aroma components (Jones et al., 2005). Much has been written about how canopy management practices affect the content

in norisoprenoids, especially TDN and vitispirane (Marais et al., 1992; Chen et al., 2017; Asproudi et al., 2018; Wang et al., 2018). Some authors (Kwasniewski et al., 2010) have indeed demonstrated that the timing of leaf removal can alter the carotenoid profile, as well as TDN and vitispirane precursors in mature Riesling grapes: if the leaves were removed one month after the berry set, they observed elevated total amounts in both must and wine. With regard to grapevine shading, although previous studies reported that artificial shading protects grapes from sunlight exposure but leads to an increase of air temperature in the fruit zone (Chorti et al., 2010), other researches carried out in Franciacorta wine growing area demonstrated that this agronomical practice also allows to decrease inner berry temperature (Ghiglierio et al., 2020). This effect of artificial on canopy microclimate makes this practice a good adaptation strategy to climate change. Many authors (Reynolds et al., 1986; Smart et al., 1990; Dokoozlian and Kliewer, 1996; Filippetti et al., 2015; Martin et al., 2016) have in fact demonstrated the effect of shading on delaying ripening and preserving acidity, in terms of both titratable acidity and malate concentration. The response of pH and potassium to artificial shading is less clear: some authors demonstrated a positive effect of shading on pH and potassium (Smart et al., 1985; Scafidi et al., 2013; Toda and Balda, 2014), while more recent studies reported that this treatment does not significantly affect these parameters (Filippetti et al., 2015).

The present 4-year (from 2010 to 2013) study aims to investigate how leaf removal and artificial shading strategies affect grape maturation, must quality and the production of norisoprenoids in sparkling wine. Wine volatiles compounds were analyzed using an untargeted approach aimed at a holistic view rather than restricted only to a list of target compounds (Cozzolino, 2016). Specifically, the paper investigates the effect of meteorological conditions (i.e., water availability and temperatures) on grapevine production and must quality. Moreover, the practice of application of different canopy shading levels on *Vitis vinifera* L. cv. Chardonnay and Pinot noir is studied to understand their effect on grapevine production and must quality as well as the on the aroma of sparkling wine in the DOCG Franciacorta wine growing area (Lombardy, Italy). Understanding the response of musts and wine quality to leaf removal and shading, in relation to the meteorological variability of each year, is useful to direct agronomical management in tackling the issue of climate change (e.g., early ripening, acidity degradation, wine aroma profile variation) that is affecting sparkling wine quality in particular. The leaf removal and shading practices on norisoprenoids compounds shall also be examined. The concentrations of these aromatic compounds tend to increase during wine aging, especially in sparkling wines, and can reach the level above the threshold of the characteristic aroma of aged wine which is sometimes detrimental for the wine quality. Since there aren't, to our knowledge, studies that had been conducted on the modulation of norisoprenoids in relation to canopy management in finished sparkling wine, this work could be useful to understand the effect of these treatments in the final product.

2 Materials and methods

2.1 Experimental setting

This study was carried out in the winegrowing area of Franciacorta DOCG, a famous Italian sparkling wine production area located in the Lombardy Region. The experiment was repeated for four consecutive years (from 2010 to 2013) in a vineyard (45.572850° Lat, 9.967622° Lon) belonging to Azienda Agricola Castello Bonomi Tenute in Franciacorta. This company is located in the southern part of the Franciacorta region (Supplementary Figure 1).

The soil of experimental vineyard is grass-covered and characterized by a loamy texture, high total organic carbon content and CEC (Cation Exchange Capacity). The vineyard, with row orientation from north to south, was planted in 2004 with two international *Vitis vinifera* L. cultivars, Chardonnay (clone ENTAV-INRA® 96) and Pinot noir (clone 292), both grafted onto Kober 5BB rootstock. Both cultivars are cordon trained.

The experimental plan included five different treatments: a control test without defoliation and shading (ND), a test where about six basal leaves, equal to about 35% of total leaf area, were removed, east and west side (TD), and three different systems adopting shading nets applied along the bunch zone; two of the shaded treatments were defoliated as for TD and covered with one layer of shading net (TD1) or two layers of shading net (TD2), while a third treatment was covered by only one layer of shading net, but not defoliated (ND1L).

The treatments were replicated on both the Chardonnay and Pinot noir cultivars. All treatments were set in two replicates represented by two rows of the vineyard for each cultivar. Each treatment was extended for 25 vines for each of the two replicates. All treatments took place at about 20% veraison, corresponding to July 19th, July 14th, July 19th, July 29th, respectively, in 2010, 2011, 2012 and 2013. Both manual leaf removal and shading net application were carried out along the bunch zone; shading was realized through a UVstabilized polyethylene net of approximately 95 g m⁻² (shading net OF50N supplied by Retes srl). The transmittance of global solar radiation of the single layer and double layer nets was preliminarily tested in order to evaluate the percentage of global solar radiation passing through the nets. A reduction by 50% and 70% was detected for single- and double-layer shading nets, respectively.

2.2 Meteorological data and agrometeorological indices

During the four years, weather conditions were monitored by means of the weather station of Rovato (BS) of the Agrometeorological Network of the Province of Brescia, which is located at a distance of 5 km from the experimental vineyard.

To provide a more precise description of the thermal conditions in the experimental vineyard a four-channel data logger (Onset

HOBO U12) equipped with an air temperature sensor (thermistor Onset HOBO S-THC), protected by a solar shield was placed in the vineyard.

Precipitation data recorded by the Rovato weather station and temperature data from the vineyard thermometer were used to characterize the general meteorological features of the four years of investigation and to calculate thermal indices, the grapevine water balance and the derived water stress indices, as described further below.

2.2.1 Water stress

In order to provide a description of the relationship between plant growth and water resources, a single-layer reservoir model with a daily time step was created (Cola et al., 2014), considering a reference soil reservoir of 120 mm. The daily reference evapotranspiration (ET₀) was calculated by means of the Hargreaves-Samani method and the daily maximum evapotranspiration of grapevine (ET_M) was obtained by means of a dynamic crop multiplicative coefficient (K_c), as a function of the phenological stage of the plant, modelled on the base of air temperature-based course (Mariani et al., 2013). The daily real grapevine evapotranspiration (ETR) was obtained by means of the water limiting factor (WLFR) response curve, that relates the soil water content with the plant stress. When the soil water level is between the field capacity and the easily available water limit, the plant does not face stress, WLFR is equal to 1 and ETR=ET_M. Otherwise, when the water content moves above the field capacity up to saturation or when it moves from the easily available water limit down to the wilting point, WLFR linearly decreases toward 0. As a consequence, the stress increases and ETR decreases.

In this work, the seasonal water stress (WSTR) was obtained cumulating the daily values of 1-WLFR, so that a day without water stress weights 0 and a day with maximum water stress weights 1. Additionally, the cumulated evapotranspiration deficit (Δ ET) was obtained, on the base of the daily difference [mm] between ET_M and ETR throughout the season.

2.2.2 Thermal regime

In order to describe the air thermal condition during fruit development and ripening, thermal resources and limitations were obtained on the basis of the air temperature, applying the Normal Heat Hours (NHH) response curve (Mariani et al., 2012; Mariani et al., 2013; Cola et al., 2020). This method tries to overcome the overestimation of high temperature in terms of plant development that characterizes the classic growing degree-days approach of the Winkler Index (Amerine and Winkler, 1944) in which a very warm day is translated into a high value of the index, meaning a strong positive contribution to plant growth when high air temperature values are detrimental for the plant development.

Indices were calculated considering meteorological conditions along the berry development period (i.e., from berry set stage to harvest) and specifically: from June 1st to August 26th for 2010; from May 20th to August 1st 2011; from May 29th to August 8th 2012; from June 6th to August 22nd 2013.

NHH indicates the total hourly thermal resources useful for berry maturation from fruit set to physiological maturity (Cola et al., 2017; Cola et al., 2020) and represent thermal resources. Low Heat Hours (LHH) represents the stress caused by hourly temperatures below the optimal level and High Heat Hours (HHH) is the stress caused by hourly temperatures above the optimal level.

More in detail, air temperature is weighed on the base of four parameters, namely, low cardinal - LC, low optimal cardinal - LOC, upper optimal cardinal - UOC and upper cardinal UC, respectively:

- * When the hourly air temperature is below LC: LHH=1, NHH=0, HHH=0, meaning that the whole hour was spent by the plant under stressing conditions caused by low temperatures.
- * When the hourly air temperature is above UC: LHH=0, NHH=0, HHH=1 meaning that the whole hour was spent by the plant under stressing conditions caused by high temperatures.
- * When the hourly air temperature sits between LOC and UOC: LHH=0, NHH=1, HHH=0 meaning that the whole hour was spent by the plant under restful conditions and the development was non limited.
- * Between LC and LOC the low temperature stress decreases linearly moving from LC to LOC, so that LHH moves from 1 to 0 and NHH from 0 to 1 (always with LHH+NHH=1 and HHH=0).
- * Between UOC and UC the high temperature stress increases linearly moving from UOC to UC so that NHH moves from 1 to 0 and HHH from 0 to 1 (always with NHH+HHH=1 and LHH=0).

The parametrization of the four parameters (LC=12°C, LOC=24°C, UOC=26°C, UC=33°C) proved to perform very well in describing the development of several cultivars (Cabernet-Sauvignon, Chardonnay, Barbera and Georgian cultivars Mtsvane Kakhuri, Rkatsiteli, Ojaleshi and Saperavi) (Mariani et al., 2013; Cola et al., 2014; Cola et al., 2017).

In this work, NHH, LHH and HHH were cumulated from fruit-set to harvest to describe the thermal course of the season. Phenological stages of each plot were determined on the base of weekly phenological monitoring.

Additionally, the stress caused by heat waves (33STR) was obtained by counting the number of days between fruit set and physiological maturity with a maximum temperature above 33°C (Cola et al., 2020).

2.3 Yield components and the composition of must

With the aim to compare musts and wine composition at a standard potential alcohol degree, for both cultivars and all treatments, the harvesting time was established on the basis of the

strategy adopted by the wine company for the specific year and ranging from 10 to 10.7% of potential alcohol.

The evolution of ripening for both Chardonnay and Pinot noir was monitored weekly (maintaining an interval of 7–5 days between each sampling), in order to identify the relevant harvesting time for each treatment.

Experimental harvesting was organized by selecting 5 grapevines from the two 25 vine replicates for each treatment, for a total of 10 vines per treatment (ND, TD, TD1, TD2 and ND1L). For each grapevine, the average bunch weight (ABW) was calculated counting the number of bunches and weighing the entire grapevine production. A sample of three bunches was collected from each grapevine to check must quality. These samples were then crushed and the total soluble solids concentration (TSS), pH, titratable acidity (TA) and malic acid (MA) concentration were analyzed in the resulting musts. These measurements were determined using a traditional handheld refractometer for soluble solids concentration, a Crison compact titrator analyser for both pH and TA, and the enzymatic method (Hyperlab wine analyser) to determine MA concentration.

2.4 Wine production

About 100 kg of grapes were harvested for each cultivar and treatment upon reaching the standard potential alcohol. Grapes were harvested in small boxes weighing maximum 15 kg, and stocked in a cold room at about 10°C. Microvinifications was then initiated according to a standardized protocol. The wine-making protocol was organized in different steps described in [Supplementary Figure 2](#).

The wine so obtained was stocked in 15 l demijohns and periodically monitored for free sulfur content, using the WineScanTM SO₂ (FOSS) instrument, to avoid undesired malic fermentation. After about five months the wine was stabilized by adding 10 ml hl⁻¹ silica sol and 1 ml hl⁻¹ gelatin. The wine was then bottled using 0.75 l bottles (for a total of 18 bottles); nine bottles were then stocked and 0.3 g l⁻¹ of yeast and 22 g l⁻¹ of sugar were added to the other nine bottles to induce refermentation, thus allowing to produce a final sparkling wine. After this last step, all bottles were stocked and manually disgorged, after a manual remuage to remove the residue of yeasts without any further addition. Disgorgement was performed for all wine samples at the time of the volatile aroma compounds analysis in 2016 and 3 different bottles for each treatment were used as replicates.

2.5 Analysis of volatile aroma compounds by GC×GC-TOF-MS

All the analyses were carried out following the method described in our previous works ([Carlin et al., 2016](#); [Carlin et al., 2022](#)). In order to monitor instrument stability, pooled quality controls (QC) consisting of equal proportion of each sample were placed at the beginning of the run (n=5) and thereafter every 10th sample as a common practice in metabolomics studies ([Arapitsas et al., 2016](#)). For

each sample, 2 ml of wine with 50 µl of internal standard solution (2-octanol in ethanol at a concentration of 1 mg l⁻¹) was mixed with 1 g NaCl in a 20 ml headspace vial. A Gerstel MultiPurpose Sampler autosampler (Gerstel GmbH & Co. KG Mülheim an der Ruhr Germany) with an agitator and SPME fiber 2 cm (50/30 DVB/CAR/PDMS), from Supelco Merk KGaA (Darmstadt, Germany), was used to extract the volatiles from the sample vial headspace. The sample was pre-incubated for 5 min at 35°C. Adsorption lasted 20 min, at the same temperature. Then, desorption took place in the injector in splitless mode (4 min) at 250°C. The fiber was then reconditioned for 10 min at 250°C. The GC×GC system was the Agilent 7890 A (Agilent Technologies, Santa Clara, CA). Injections were performed in splitless mode. Equipped columns were the VF-Wax column (100% polyethylene glycol; 30 m × 0.25 mm × 0.25 µm, Agilent J&W Scientific Inc., Folsom, CA) as the 1st dimension and Rxi-17Sil MS 1.50 m × 0.15 mm × 0.15 µm, Restek Bellefonte, USA) as the 2nd dimension. The GC system was equipped with a secondary column oven and non-moving quadjet dual-stage thermal modulator. The injector/transfer line was maintained at 250°C. Oven temperature program conditions were as follows: initial temperature of 40°C for 4 min, programmed at 6°C min⁻¹ at 250°C, where it remained for 5 min. The secondary oven was kept at 5°C above the primary oven throughout the chromatographic run. The modulator was offset by +15°C in relation to the secondary oven; the modulation time was 7 s and 1.4 s of hot pulse duration. Helium (99.9995% purity) was used as carrier gas at a constant flow of 1.2 ml min⁻¹. The MS signal was obtained with a Pegasus IV time-of-flight mass spectrometer (Leco Corporation, St. Joseph, MI) with electron ionization at 70 eV and the ion source temperature at 230°C, detector voltage of 1317 V, mass range of m/z 35–450 and acquisition rate of 200 spectra s⁻¹.

For GC×GC-MS data, LECO ChromaTOF Version 4.22 software was used for all acquisition control, data processing and Fisher ratio calculations. Automated peak detection and spectral deconvolution with a baseline offset of 0.8 and signal-to-noise of 100 were used during data treatment. Before proceeding with the data analysis a quality control of the data sets, checking the distribution of the QC injections was carried out ([Arapitsas et al., 2016](#)). The identification of the wine volatile compounds was achieved by comparing the mass spectrometric information for each chromatographic peak with NIST 2.0, Wiley 8 and the FFNSC 2 mass spectral library (Chromaleont, Messina, Italy), with a library similarity match factor of 750 and comparing also the experimental linear temperature retention index (LTPRI) with retention indices reported in the literature for 1D-GC (VCF Volatile Compounds in Food 16.1 database). Retention data for a series of n-alkanes (C10–C30), under the same experimental conditions employed for chromatographic analysis of wine volatiles, were used for experimental LTPRI calculation. The content of norisoprenoids were expressed as peak areas.

2.6 Statistical analysis

In the statistical analysis, Chardonnay and Pinot noir were kept separated in relation to the different composition of their grapes and

their different sensory characterization in wines (Herrero et al., 2016).

The effect of the year was initially investigated for variables related to ABW and musts quality through an analysis of variance (ANOVA) and Siegel-Tukey's *post-hoc* test using the SPSS software (Statistical Package for Social Science) (IBM Corp, 2021).

The relationships between year and agrometeorological indices and AWB and must quality were also investigated through a principal component analysis (PCA) on autoscaled data (i.e., mean-centered and divided by the standard deviation of each variable), through R software (R Core Team, 2022). In the PCA analysis for each cultivar, five points for each year, corresponding to the average value of the single treatment in a specific year, were considered. This approach was used because one single value of agrometeorological indices was available for each year without having the possibility to differentiate between treatments.

Additional ANOVA and Siegel-Tukey's *post-hoc* test were performed to determine the influence of the treatment on variables related to ABW and musts quality (TSS, TA, MA, pH). In this analysis, both the cultivars and the four years were considered separately. The decision to process the different years separately was determined by the meteorological differences in the individual years and the effect on the AWB and must quality revealed by the results obtained from the analysis of the relationship between year and these variables.

Considering the limited number of biological replicates used for the untargeted volatile compounds analyses (i.e., 3 replicates for each cultivar, treatment, and year) a different approach was outlined. In this case, it was checked whether there were any statistically significant differences associated with each treatment compared to the untreated thesis (ND) by means of a linear model on log-scaled data using R software (R Core Team, 2022).

3 Results

3.1 Meteorological characterization

Table 1 shows the monthly variation of temperature and precipitation by season, respectively, while the agrometeorological indices are shown in Table 2.

The year 2010 was characterized by optimal water conditions. The scarce precipitation of the winter period (Jan-Mar) was preceded by good precipitations in the 2009 Oct-Dec period and followed by abundant spring precipitations. From a thermal point of view, 2010 showed lower maximum temperatures during spring than 2011 and 2012, resulting in the highest NHH value in the series. However, the indices for this year were strongly affected by a longer interval between fruit set and harvest, than in the other three years. Low temperature stress (LHH) was the second highest over the four years and high temperature stress (HHH) was the highest. The 33°C limit was exceeded for 65 days during the season.

The year 2011 was still characterized by very low water stress, thanks to the refilling of the water reservoir during winter and the good distribution of precipitation over the months. As compared to other years, low temperatures caused a high level of NHH (second highest), the highest value of low temperature stress (LHH) and the lowest value of high temperature stress (HHH), confirmed by only 2 days with maximum temperatures above 33°C.

The year 2012 was characterized by the highest water stress value over the four years (as shown by WSTR and ΔET values), mainly due to the limited precipitation during June, July and August that led to a long period of a limited water soil content. From a thermal point of view, the year 2012 featured the lowest levels in terms of NHH accumulation (though very close to 2013),

TABLE 1 Monthly average and standard deviation of maximum and minimum temperature and monthly total precipitation for the seasons 2010–2013.

Month	Air Temperature [°C]								Monthly Precipitation [mm]			
	Minimum				Maximum							
	2010	2011	2012	2013	2010	2011	2012	2013	2010	2011	2012	2013
Jan	-1.3 (2.2)	-0.6 (2.2)	-1.4 (2.7)	0.4 (1.7)	4.9 (2.8)	6.1 (2.3)	8.8 (3.8)	7.3 (3.8)	32	29	26	59
Feb	0.9 (3.1)	1.7 (2.7)	-2.8 (4.8)	-0.1 (2.0)	8.9 (3.2)	11.4 (3.0)	7.3 (6.8)	7.6 (3.1)	93	62	12	61
Mar	3.7 (4.4)	5.2 (3.5)	6.8 (2.6)	3.8 (2.3)	13.5 (4.8)	14.7 (4.2)	19.3 (3.9)	11.3 (3.6)	49	46	11	137
Apr	8.1 (3.2)	10.1 (2.0)	7.9 (2.6)	9.4 (3.3)	19.9 (4.2)	23.0 (3.3)	17.8 (3.7)	18.5 (5.0)	71	13	146	96
May	12.2 (2.1)	12.9 (3.1)	12.1 (3.0)	10.9 (2.3)	23.1 (3.9)	26.5 (3.2)	24.5 (4.0)	22.1 (3.3)	165	44	128	180
Jun	16.8 (2.9)	16.0 (1.5)	17.4 (2.8)	15.5 (3.2)	28.7 (3.7)	26.9 (2.9)	30.0 (3.8)	28.7 (3.9)	94	122	33	53
Jul	19.2 (2.8)	16.7 (2.5)	18.6 (1.9)	19.2 (1.9)	32.0 (2.6)	28.7 (2.2)	32.2 (1.9)	32.1 (1.9)	91	79	39	50
Aug	16.7 (2.8)	18.2 (2.3)	19.7 (2.4)	17.5 (2.3)	29.2 (3.2)	31.0 (2.3)	33.5 (3.2)	30.9 (3.2)	154	93	35	109
Sep	13.1 (2.4)	16.4 (2.4)	14.4 (2.6)	14.3 (2.5)	24.8 (3.0)	28.3 (2.4)	25.9 (3.1)	26.1 (3.2)	105	143	125	23
Oct	8.1 (3.3)	8.5 (3.9)	10.5 (3.5)	11.8 (2.4)	17.5 (3.4)	20.2 (5.5)	19.9 (4.5)	19.0 (2.3)	128	60	146	91
Nov	6.0 (3.9)	4.6 (4.6)	6.8 (2.5)	5.6 (4.5)	12.6 (3.6)	13.9 (2.9)	14.3 (2.5)	13.4 (4.2)	178	63	140	111
Dec	-1.7 (3.7)	1.6 (3.0)	-0.9 (2.5)	1.4 (3.0)	5.3 (3.5)	9.4 (2.3)	7.2 (3.6)	10.9 (2.7)	151	32	68	62

TABLE 2 Environmental indices for the characterization of the four seasons.

	WSTR	ΔET	NHH	LHH	HHH	33STR
2010	3.50	4.30	1276	412	324	65
2011	2.86	8.62	1151	468	140	2
2012	24.83	79.18	1020	288	315	93
2013	18.95	52.91	1075	315	321	99

and LHH and the highest level in HHH (thermal excess, with 93 days of maximum temperature above 33°C).

The year 2013 was very similar to 2012, with a certain amount of water stress (second highest in both indices), the second lowest in NHH and LHH, and the second highest in HHH and the first in the number of days with a maximum temperature above 33°C (99 days).

Considering the thermal behavior in the four seasons in relative terms, in 2010 the percentages of NHH, LHH and HHH versus their total (NHH+LHH+HHH) were 63.85, 18.23 and 17.92 respectively. 2012 and 2013 showed a similar behavior with 62.85, 17.78, 19.38 and 62.81, 18.41, 18.77 respectively. The year 2011, with 65.41, 26.62, 7.97 showed a strongly different repartition, again emphasizing its unique environmental conditions.

3.2 Year effect

3.2.1 Average bunch weight

The ABW varies over the years equally for both cultivars (Figure 1). The year 2012 showed a significantly lower value of ABW than that of the other years. The year 2013 showed an intermediate response, while 2011 and 2010 recorded higher values.

3.2.2 Harvesting time

The four years were characterized by different harvesting times due to varying ripening rates. The year 2010 was characterized by a delayed maturation. Harvesting times ranged from 24/08 to 2/09 for

the cv. Chardonnay, and from 26/08 to 6/09 for Pinot noir. The delay in ripening was further confirmed by the lower average sugar content reached at harvesting time (i.e., 18°Brix). The years 2011 and 2012 had the earliest vintages, while year 2013 can be considered in between, having recorded harvesting times from 28/08 to 2/09 for Chardonnay and from 20/08 to 24/08 for Pinot noir.

3.2.3 Must characterization

The results obtained in must characterization (Figure 2) underlined a similar response concerning TSS when comparing Chardonnay and Pinot noir, while some differences were observed in terms of acidity and pH.

TSS was higher in 2012, while 2010 recorded the lowest value; in the case of Pinot noir no significant differences were recorded between 2012 and 2011.

The year 2012 also showed a high TA value for both cultivars, as in 2011 for Chardonnay and in 2013 for Pinot noir. The year 2010 recorded the lowest TA value for Pinot noir, while no significant differences were recorded compared to the 2013 value for Chardonnay.

Results related to MA were similar to TA: for Pinot noir, the year 2012 differed significantly from 2010, recording the highest and the lowest values, respectively; in the case of Chardonnay the highest value was recorded in 2011 and the lowest value in 2013. pH values were high in 2010 for both cultivars, as in 2012 for Chardonnay. Pinot noir showed no differences over 2011, 2012 and 2013 for this variable, while Chardonnay showed the lowest value in the case of 2013.

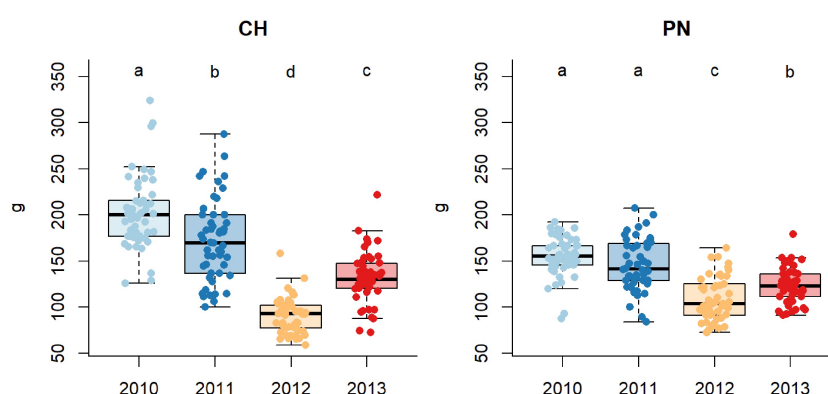


FIGURE 1

Boxplots showing average bunch weight (ABW in grams) over the 4 different vintages for Chardonnay (CH) and Pinot noir (PN): different letters indicate that values are significantly different at $p < 0.05$ obtained by one-way ANOVA and Siegel-Tukey's *post-hoc* test.

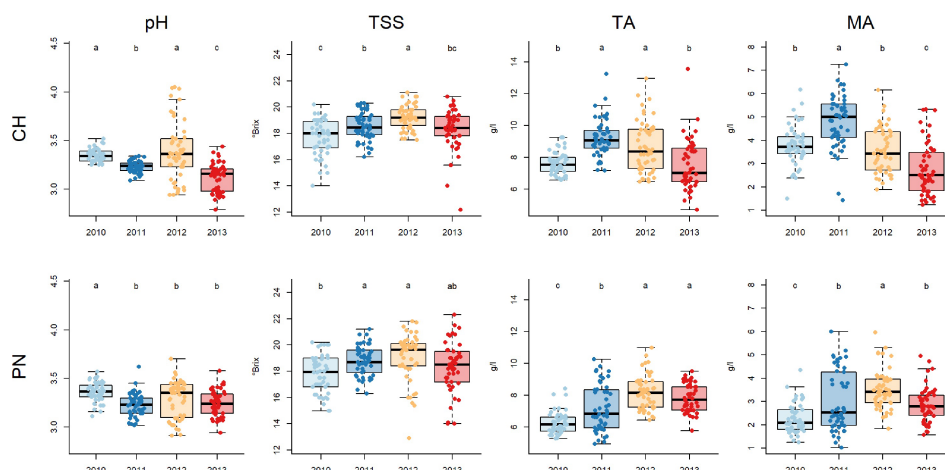


FIGURE 2

Boxplots showing data of total soluble solids concentration (TSS), titratable acidity (TA), malic acid (MA) and pH over the 4 different vintages for Chardonnay (CH) and Pinot noir (PN): different letters indicate that values are significantly different at $p < 0.05$ obtained by one-way ANOVA and Siegel-Tukey's post-hoc test.

3.2.4 Years general responses

The biplots obtained from PCA analysis allowed to visualize the distributions of the data collected for Chardonnay and Pinot noir during the four-year 2010–2013 period (Figure 3). The pattern in the sample distribution highlighted a differentiation, especially between the years 2010, 2011 and 2012–2013. In both PCAs, the first two dimensions explained around 75% of variance. Vectors made it possible to display the inner relationship between years and variables (i.e., meteorological variables and ABW and must quality). Supporting the results described in the previous Section 3.1, the years 2012 and 2013 were associated, for both cultivar, to stress caused by water scarcity, higher evapotranspiration (ΔET) and temperatures (HHH and 33STR), while 2011 was associated with lower temperatures (LHH). The pattern in the distribution of years

concerning vectors related to average bunch weight (ABW) and musts quality variables (pH, TSS, TA, MA) confirms the findings previously reported in Sections 3.2.1 and 3.2.3.

3.3 Treatment effect

3.3.1 Average bunch weight

The results obtained for Chardonnay ABW by comparing treatments showed no homogeneous response over the years (Figure 4). In general, no significant differences were found between treatments. A significant difference emerged in 2011 between the less shaded (i.e., TD and TD1) and high shaded (i.e., ND1L, and TD2) treatments. Pinot noir recorded a generally

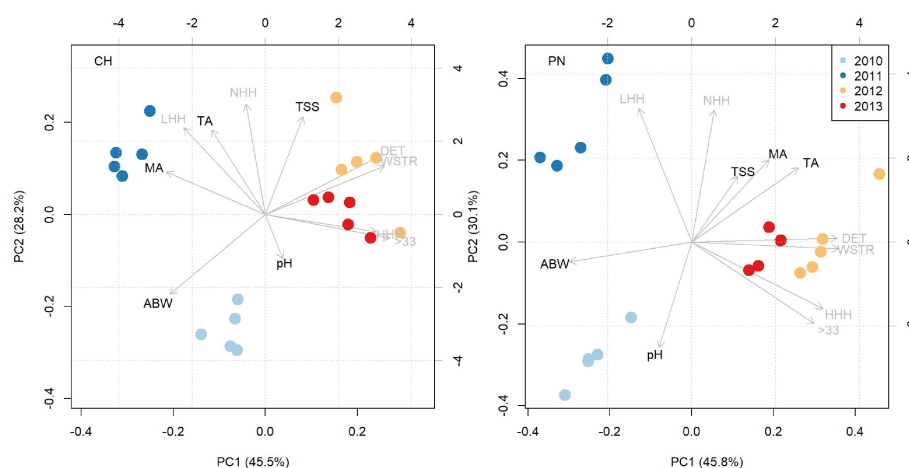


FIGURE 3

Biplot showing the distribution of data along of the two first principal component dimensions for Chardonnay (CH) and Pinot noir (PN). Stress caused by heat waves (33STR), High Heat Hours (HHH), daily evapotranspiration deficit (ΔET), seasonal water stress (WSTR), Normal Heat Hours (NHH), Low Heat Hours (LHH), average bunch weight (ABW), total soluble solids concentration (TSS), titratable acidity (TA), malic acid (MA), pH are shown as vectors. Data from a single year is identified by different colored dots. Each dot represents the average value of the single treatment in a specific year.

negative effect of defoliation without shading (TD) on ABW in 2012 and 2013 (Figure 4). The years 2010 and 2011 showed a different response, reporting an intermediate value for TD. Other treatments related to defoliation and shading (TD1 and TD2) showed the opposite response in 2010 and 2011, resulting in a higher ABW in 2010 compared to no defoliated treatment (ND and ND1L) and a lower ABW in 2011 compared to ND and ND1L.

3.3.2 Must characterization

3.3.2.1 Chardonnay

Concerning sugar concentration (TSS), no significant differences were highlighted in 2013, while differences among treatments emerged in the other years (Figure 5). Specifically, the ND1L generally recorded high TSS values compared to other treatments. This can be observed by comparing ND1L and ND in 2010, ND1L and all other treatments in 2011 and comparing ND1L and TD2 in 2012. Titratable acidity (TA) and malic acid showed, in general, the same response (Figure 5). Not defoliated treatments (ND and ND1L) tended to preserve the acidity better than defoliated treatments (TD, TD1 and TD2). This can be seen in all the years considered, except in 2011, when no significant differences were found. The efficiency of the not defoliation and shading effect on acidity preservation is more evident in 2012 and 2013; in these years, the not defoliated and shaded treatment (ND1L) recorded the highest level of both titratable acidity and malic acid concentration. Significant differences can be observed in 2010, 2012 and 2013 for pH, even though the response was generally not uniform between years (Figure 5). In 2012 and 2013 the highest values recorded concerned TD2, while in 2010 the highest values can be associated to TD1.

3.3.2.2 Pinot noir

Figure 6 shows the results obtained for Pinot noir musts characterization. Sugar concentration (TSS) showed no significant differences among treatments with the exception of year 2011. In

this year, the defoliated treatment recorded a higher sugar concentration than ND1L. Regarding titratable acidity (TA) and malic acid concentration (MA), the treatments revealed similar trends in 2010 and 2011. Considering these two years, the totally defoliated (TD) and defoliated and shaded (TD1 and TD2) treatments recorded the lowest values in both titratable acidity and malic acid concentration, with the exception of the results obtained for TD1, which in 2010 were similar to those obtained for the not defoliated treatments (ND and ND1L). Significant differences were highlighted only in the case of titratable acidity in 2012 and in the case of malic acid concentration in 2013; in these cases, ND1L and TD recorded the highest values. pH didn't show significant differences in 2010. As described in the case of Chardonnay, the trend observed for pH was not homogeneous over the years.

3.3.3 Effect on sparkling wine norisoprenoids

As indicated in the Section 2.6 statistical analyses performed on norisoprenoids abundances were restricted to check whether, within a specific cultivar and year, there were statistically significant differences associated to each treatment compared to reference treatment, i.e. the not defoliated thesis (ND). In order to display the data, a matrix plot was performed (Figure 7) by indicating with colored cells the statistically significant comparisons, using a red color when the treatment mean value was statistically higher than the mean value of the reference treatment, or a blue color in the opposite case (grey cells indicate those cases of no statistical significance).

3.3.3.1 Chardonnay

In the 2010 vintage, TDN, vitispirane, ethoxy actinidol 1 and the unknown norisoprenoid were present in greater quantities in the total defoliated treatment (TD), the unknown norisoprenoid was also greater in the TD2 treatment, while the lowest contents were observed in ND1L treatment. Vitispirane was high also in

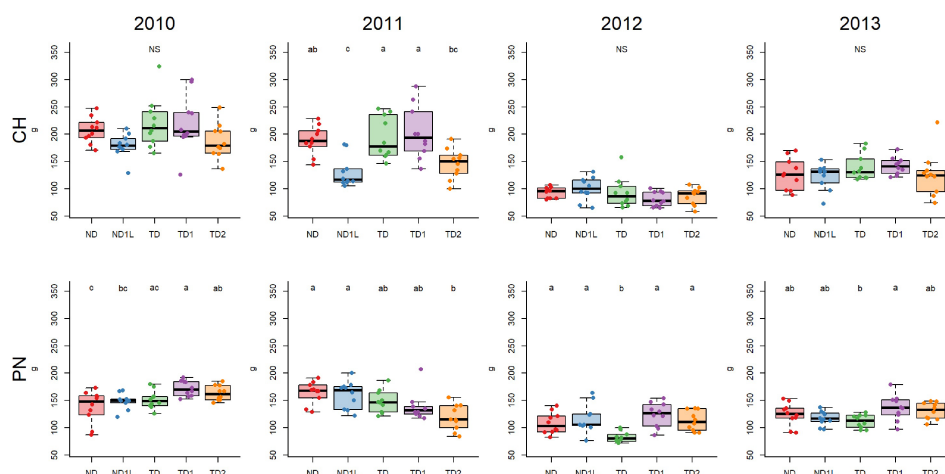


FIGURE 4

Boxplots showing average bunch weight (ABW in grams) for each treatment considering 4 years, for Chardonnay (CH) and Pinot noir (PN): different letters indicate that values are significantly different at $p < 0.05$; NS indicates no significant differences among treatments at $p < 0.05$ obtained by one-way ANOVA and Siegel-Tukey's *post-hoc* test.

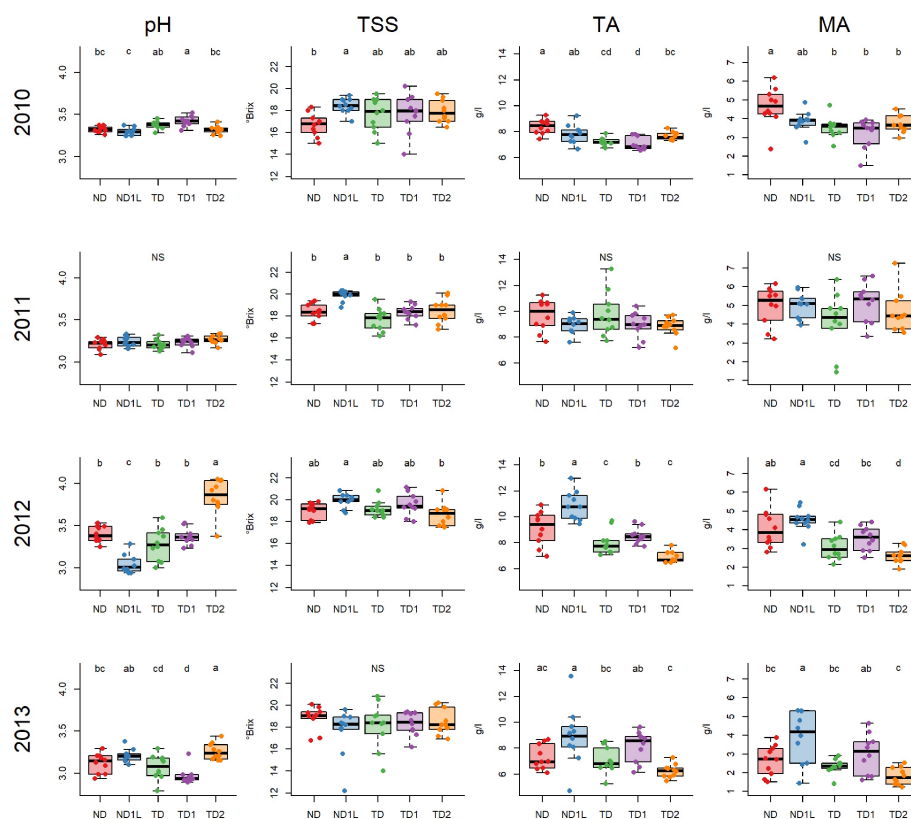


FIGURE 5

Boxplots showing total soluble solids concentration (TSS), titratable acidity (TA), malic acid (MA) and pH for each treatment considering 4 years, 2010, 2011, 2012, 2013, for Chardonnay: different letters indicate that values are significantly different at $p < 0.05$; NS indicates no significant differences among treatments at $p < 0.05$ obtained by one-way ANOVA and Siegel Tukey's *post-hoc* test. Each column is referred to one variable (each variable is reported in the upper part of the graph); each row is referred to one year (each year is reported in the left part of the graph).

defoliated and shaded (TD1 and TD2) treatments. In 2011, it was observed that all the norisoprenoids considered were higher in TD and some others, such as ethoxy actinidol 1 also increased in the TD1 and TD2 treatments. The ND1L treatment showed lower contents for ethoxy actinidol 1, vitispirane and TDN. In 2012, a greater quantity was observed in TD for the unknown norisoprenoid, ethoxy actinidol 1 and vitispirane; ethoxy actinidol 1 was also more abundant in the TD1 treatment. In 2013, only vitispirane was higher in TD, and ethoxy actinidol 1 for TD1 treatment, while ethoxy actinidol 1 was present in less quantities in the ND1L treatment. Chardonnay wine seems to be highly influenced by the agronomic interventions on the canopy, indeed, it is clear that for the main norisoprenoids the total defoliated treatment (TD) was often higher followed by the artificial shading and defoliated treatments. The boxplots of norisoprenoids for each year and treatment are included in the supplementary material (Supplementary Figure 3).

3.3.3.2 Pinot noir

Conversely, Pinot Noir wine seems to be less influenced by the treatments (Figure 7), although showing similar trends to that seen for Chardonnay, in all the years surveyed ethoxy actinidol 1 was prevailing in the defoliated treatment. In 2010 all compounds except TPB-1 were prevailing in the TD2 treatment while in 2011 only TDN was highest in

this treatment. In 2012 vitispirane was the highest in TD treatment while ethoxy actinidol 1 and the unknown norisoprenoid were the lowest in ND1L treatment. In the 2010 and 2013 vintages, safranal, ethoxy actinidol 1 and the unknown norisoprenoids were the highest in the TD1 treatment. In 2013 also the unknown norisoprenoid were highest in the TD treatment as well. The boxplots of norisoprenoids for each year and treatment are reported in the supplementary material (Supplementary Figure 4).

4 Discussion

4.1 Effect of meteorological conditions

The results obtained in this study highlight the influence of temperature and water availability on grapevine yield, musts quality and on the composition of aromas in wine. This confirms the results obtained by other authors that underlined the effect of meteorological conditions on grape and wine quality (Mariani et al., 2009). The average weight of the bunches was higher when water needs were satisfied; 2010 and 2011 were, indeed, characterised by lower water stress indices (WSTR and ΔET) and the highest values of ABW. The grapevine yield positive response to higher water availability was confirmed by other authors (Ramos

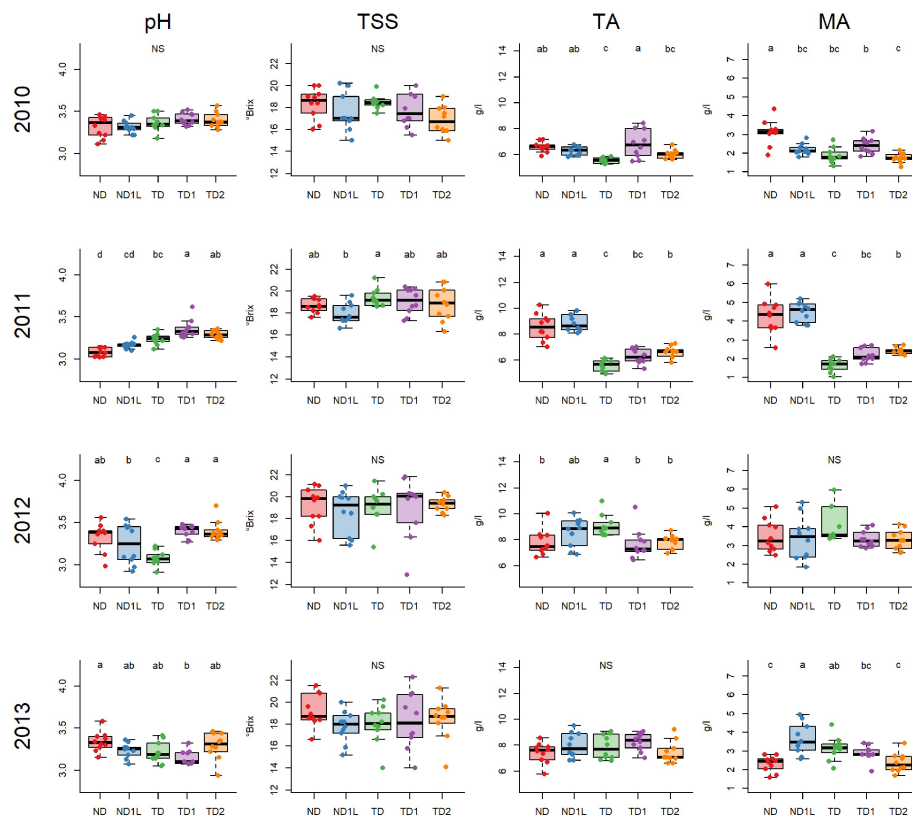


FIGURE 6

Boxplots showing mean and unit variance of total soluble solids concentration (TSS), titratable acidity (TA), malic acid (MA) and pH for each treatment considering 4 years, 2010, 2011, 2012, 2013, for Pinot noir: different letters indicate that values are significantly different at $p < 0.05$; NS indicates no significant differences among treatments at $p < 0.05$ obtained by one-way ANOVA and Siegel-Tukey's *post-hoc* test. Each column is referred to one variable (each variable is reported in the upper part of the graph); each row is referred to one year (each year is reported in the left part of the graph).

and Mulligan, 2005; Ramos and Martínez-Casasnovas, 2006; Intrigliolo et al., 2016; Pérez-Álvarez et al., 2021; Ohana-Levi et al., 2022). On the other hand, water scarcity in 2012 led to a reduction of the bunch weight, causing in turn the typical phenomena of sugar and acidity concentration (Intrigliolo et al., 2016; Pérez-Álvarez et al., 2021) and pH level increase (Reynolds and Naylor, 1994).

Previous studies reported how the ripening of grapes for sparkling wine production was positively influenced by a cool climate (Jones et al., 2014). The optimum temperature for the accumulation of malic acid during grape ripening was estimated to be around 20°C (Lakso and Kliewer, 1975), while the negative correlation between high temperatures and MA content after véraison was reported by many studies (Rienth et al., 2016; Blank et al., 2019). Preserving malic acid degradation made it possible to contrast the decrease of the acidic level in must (Volschenk et al., 2006), which is a desirable condition for sparkling wine production (Jones et al., 2014). In the present study, the positive effect of cooler temperatures on must quality was revealed in 2011, when high values of indicators of suboptimal temperature and optimal temperature were recorded. This led in 2011 to an early ripening (1 August – 12 August), while preserving the must sugar-acid balance, and a low pH. On the contrary in 2010, where similar

values for meteorological indicators were reported, the reference sugar level was reached later (24 August – 6 September), leading to lower acidic levels, and higher pH levels. Moreover, the year 2010 reported the highest total amount of cumulated precipitation between berry set and harvest. The low level of titratable acidity and the high value of pH in musts can therefore be related to the effect of dilution of acidic components (Keller, 2006) and the increase of K absorption (Marais et al., 1992) caused by water absorption. The negative effect of high temperatures on the must acidic content was evident in 2013, when a value of the stress caused by heat waves (33STR) was recorded. This was particularly evident in the case of malic acid in Chardonnay musts that showed low values during this vintage. Many previous studies reported the increase of malic acid degradation kinetics when high temperatures were recorded (Michelini et al., 2021).

4.2 The effect of leaf removal and artificial shading

Leaf removal and artificial shading effects were differentiated by year and cultivar. In general, years characterized by satisfying water availability and cooler temperatures (i.e., 2010 and 2011)



FIGURE 7

Matrix plot colored cells showing the statistically significant comparison of some norisoprenoids using a red color when mean value of treatment was statistically higher than the mean value of the reference treatment (ND) or a blue color in the opposite case over the 4 years (2010, 2011, 2012, 2013) for Chardonnay and Pinot noir. NS means not significant, NA means not available data.

emphasized the difference in ripening delay between the non-artificial shaded and the artificial shaded treatments. This is in agreement with previous papers that reported how shading makes it possible to slow down grape maturation (Caravia et al., 2016; Ghiglieno et al., 2020). The effect of no defoliation and artificial shading on acidity preservation was more evident in years characterized by high temperatures and high-water stress (i.e., 2012 and 2013). This can be related to the positive relationships between malic acid degradation and high temperature and water scarcity (Blank et al., 2019) that suggest the need for shading during warm and dry vintages. In the case of ABW and pH there was no unique response.

The analysis of the main norisoprenoids showed how the canopy treatments greatly affect their quantity (boxplots in Supplementary Figures 3, 4). A general increasing effect of total defoliation can be highlighted, especially concerning Chardonnay. Even though Oliveira et al. (2004) reported that carotenoid contents were consistently higher in grapes in the shade than in those exposed to direct sunlight, the positive effect of exposure on norisoprenoids was underlined by many previous studies (Marais et al., 1991; Marais et al., 1992; Asproudi et al., 2016; Asproudi et al., 2020). The results obtained in the present study, in terms of TDN content in wines, showed that this aromatic compound, even if not always in a statistically significant way, was produced in larger quantities in TD while the shaded theses TD1 and TD2 contained less TDN; this behavior was clearly visible in Chardonnay and in

two vintages of Pinot noir, and would suggest that it is the light that most influences the biosynthesis of this compound. TDN with a very low olfactory threshold ($2 \mu\text{g l}^{-1}$), can sometimes represent a problem, especially in sparkling wines intended for a long period of aging, because it increases over time. It has been seen that the olfactory threshold of TDN in sparkling wine is slightly higher and goes from $2.1 \mu\text{g l}^{-1}$ in still Riesling to $4.0 \mu\text{g l}^{-1}$ in sparkling Riesling (Ziegler et al., 2019); however, this is a compound to pay attention to when deciding on agronomic practices. Several glycosylated precursors have also been reported to originate these compounds during fermentation and wine ageing, through acid-catalysed reactions, and these reactions are certainly promoted in a wine with a low pH, such as sparkling wine (Schneider et al., 2001; Janusz et al., 2003).

The content in vitispirane was always much higher in TD theses and also in this case, although in Pinot noir there was no statistical proof, the defoliated and shaded theses presented a lower content of this compound. The olfactory descriptor of vitispirane is “camphor” or “eucalyptus”. Some studies (Silva Ferreira and Guedes de Pinho, 2004) showed that in aged wines the presence of vitispirane can reach the threshold of perception ($800 \mu\text{g l}^{-1}$) and, consequently, that it participates in the aroma of wine. As with the TDN, pH and temperature are the two factors that have the greatest influence on its formation over time.

(E)-1-(2,3,6-trimethylphenyl) buta-1,3-diene (TPB-1) was tendentially higher in the TD and less present in the shady theses

TD1-TD2; this compound, like TDN at high concentrations, could lead to an unpleasant chemical note at higher content (40 ng l⁻¹ sensory threshold) (Janusz et al., 2003). The behavior of actinidols and their ethoxy forms was very similar to that seen previously with a higher content in TD, a little lower in the shaded theses and even lower in the not defoliated ones. For this compound the situation was very clear in both Chardonnay and Pinot Noir. Actinidols have an odor that has been described as camphoraceous or as woody and resinous, but their contribution to wine aroma is considered limited at best, as their concentrations are usually much lower than their detection threshold. Perhaps the corresponding ethyl ethers that have been found with the GC-O technique by Schneider et al. (2001), with fruity, citric and eucalyptus notes offer a greater contribution to the aroma.

Another compound that has been increasingly found in TD treatments and less in the other not defoliated and shaded ones was safranal. This compound is responsible for the characteristic smell of saffron and can in some cases exceed the olfactory threshold and be considered too intense, leading to possible depreciation in sparkling wine. It is known that the principal monoterpene glycoside precursor of safranal in saffron is picrocrocin (Zougagh et al., 2006). We don't know if picrocrocin is a precursor also in wine or if safranal is formed starting from some other precursor or by the rearrangement of some other molecules, but previous studies reported that the content in this compound tends to increase over time, especially at low pH and if the temperature during the storage of the wine is high. Very similar trends in both Chardonnay and Pinot noir, with high levels in the TD thesis and less content in other thesis, were also observed for an unidentified norisoprenoid. On the other hand, we did not observe any clear treatment effects for β -damascenone.

5 Conclusions

The results obtained in the present study showed the importance of canopy management, in terms of defoliation and shading, on must and wine quality. This increases our knowledge about the effect of different defoliation and artificial shading application in relation to meteorological condition, supporting the management decision-making in the Franciacorta wine-growing area. The results obtained with no defoliation and artificial shading in the preservation of the acidic composition in warmer vintages suggest that defoliation activities should be calibrated in relation to the meteorological trends, without standardized procedures. This is particularly relevant in the case of sparkling wine production, where the acidic composition is essential to determine wine quality. The enhanced values of some norisoprenoids obtained with the total defoliation treatment represent a further element to direct defoliation and shading strategies. The very low sensory thresholds of some norisoprenoids place them among the important compounds for the final characteristics of the wine. Moreover, the concentrations of these aromatic compounds tend to increase during ageing, especially in sparkling wines, and can reach levels above the threshold, thus developing the characteristic aroma of aged wine, which is sometimes a detrimental wine quality. For example, TDN and TPB-1 found in wine, have a pleasant aroma

at low concentrations, but they can reduce the quality of the wine at high concentrations, and it is assumed that other compounds such as safranal, if present at high concentrations, may also be undesirable. However, further studies are needed to establish the olfactory threshold of this compounds in the wine, and which are their precursors in the sparkling wine base before refermentation.

Data availability statement

The raw data supporting the conclusions of this article will be made available by the authors, without undue reservation.

Author contributions

IG, SC, GC, LV and FM contributed to the conception and design of the study. IG, SC, GC and UV performed the experiments and analyzed the data. IG, SC, GC and MG-A organized the databases. IG, SC and MG-A performed the statistical analysis. IG, SC and GC wrote the first draft of the manuscript. IG, SC and MG-A prepared figures and tables UV, LV and FM reviewed the drafts of the manuscript. All authors contributed to the article and approved the submitted version.

Acknowledgments

Our thanks go to Castello Bonomi Tenute in Franciacorta, which hosted the experimental tests and the 'Consorzio per la tutela del Franciacorta', which promoted and inspired a collaboration between the universities and the wine sector. Our heartfelt thanks also go to Pietro Franceschi for his helpful discussion.

Conflict of interest

The authors declare that the research was conducted in the absence of any commercial or financial relationships that could be construed as a potential conflict of interest.

Publisher's note

All claims expressed in this article are solely those of the authors and do not necessarily represent those of their affiliated organizations, or those of the publisher, the editors and the reviewers. Any product that may be evaluated in this article, or claim that may be made by its manufacturer, is not guaranteed or endorsed by the publisher.

Supplementary material

The Supplementary Material for this article can be found online at: <https://www.frontiersin.org/articles/10.3389/fpls.2023.1125560/full#supplementary-material>

References

- Alfonzo, A., Francesca, N., Mercurio, V., Prestianni, R., Settanni, L., Spanò, G., et al. (2020). Use of grape racemes from grillo cultivar to increase the acidity level of sparkling base wines produced with different *saccharomyces cerevisiae* strains. *Yeast* 37, 475–486. doi: 10.1002/yea.3505
- Amerine, M., and Winkler, A. (1944). Composition and quality of musts and wines of California grapes. *Hilgardia* 15, 493–675. doi: 10.3733/hilg.v15n06p493
- Arapitsas, P., Ugliano, M., Perenzoni, D., Angeli, A., Pangrazzi, P., and Mattivi, F. (2016). Wine metabolomics reveals new sulfonated products in bottled white wines, promoted by small amounts of oxygen. *J. Chromatogr. A* 1429, 155–165. doi: 10.1016/j.chroma.2015.12.010
- Asproudi, A., Ferrandino, A., Bonello, F., Vaudano, E., Pollon, M., and Petrozziello, M. (2018). Key norisoprenoid compounds in wines from early-harvested grapes in view of climate change. *Food Chem.* 268, 143–152. doi: 10.1016/j.foodchem.2018.06.069
- Asproudi, A., Petrozziello, M., Cavalletto, S., Ferrandino, A., Mania, E., and Guidoni, S. (2020). Bunch microclimate affects carotenoids evolution in cv. nebbiolo (V. vinifera L.). *Appl. Sci.* 10, 3846. doi: 10.3390/app10113846
- Asproudi, A., Petrozziello, M., Cavalletto, S., and Guidoni, S. (2016). Grape aroma precursors on phenology and quality traits of vitis vinifera L.: the contribution of local knowledge. *Plants* 8, 121. doi: 10.3390/plants8050121
- Blank, M., Hofmann, M., and Stoll, M. (2019). Seasonal differences in vitis vinifera L. cv. pinot noir fruit and wine quality in relation to climate. *OENO One* 53, 189–203. doi: 10.20870/oeno-one.2019.53.2.2427
- Caravia, L., Collins, C., Petrie, P., and Tyerman, S. (2016). Application of shade treatments during Shiraz berry ripening to reduce the impact of high temperature. *Aust. J. Grape Wine Res.* 22, 422–437. doi: 10.1111/ajgw.12248
- Carlin, S., Mattivi, F., Durantini, V., and Panagiotis, A. (2022). Flint glass bottles cause white wine aroma identity degradation. *PNAS* 119 (29), e2121940119. doi: 10.1073/pnas.2121940119
- Carlin, S., Vrhovsek, U., Franceschi, P., Lotti, C., Bontempo, L., Camin, F., et al. (2016). Regional features of northern Italian sparkling wines, identified using solid-phase micro extraction and comprehensive two-dimensional gas chromatography coupled with time-of-flight mass spectrometry. *Food Chem.* 208, 68–80. doi: 10.1016/j.foodchem.2016.03.112
- Chen, W.-K., Yu, K.-J., Liu, B., Lan, Y.-B., Sun, R.-Z., Li, Q., et al. (2017). Comparison of transcriptional expression patterns of carotenoid metabolism in 'Cabernet sauvignon' grapes from two regions with distinct climate. *J. Plant Physiol.* 213, 75–86. doi: 10.1016/j.jplph.2017.03.001
- Chorti, E., Guidoni, S., Ferrandino, A., and Novello, V. (2010). Effect of different cluster sunlight exposure levels on ripening and anthocyanin accumulation in nebbiolo grapes. *Am. J. Enol. Vitic.* 61, 23–30. doi: 10.5344/ajev.2010.61.1.23
- Cola, G., Failla, O., Maghradze, D., Megrelidze, L., and Mariani, L. (2017). Grapevine phenology and climate change in Georgia. *Int. J. Biometeorol.* 61, 761–773. doi: 10.1007/s00484-016-1241-9
- Cola, G., Mariani, L., Maghradze, D., and Failla, O. (2020). Changes in thermal resources and limitations for Georgian viticulture. *Aust. J. Grape Wine Res.* 26, 29–40. doi: 10.1111/ajgw.12412
- Cola, G., Mariani, L., Salinari, F., Civardi, S., Bernizzoni, F., Gatti, M., et al. (2014). Description and testing of a weather-based model for predicting phenology, canopy development and source-sink balance in vitis vinifera L. cv. barbera. *Agric. For. Meteorol.* 184, 117–136. doi: 10.1016/j.agrformet.2013.09.008
- Conde, C., Silva, P., Fontes, N., Dias, A., Tavares, R., Sousa, M., et al. (2006). Biochemical changes throughout grape berry development and fruit and wine quality. *Food* 1, 5–6.
- Cozzolino, D. (2016). Metabolomics in grape and wine: definition, current status and future prospects. *Food Anal. Methods* 9, 2986–2997. doi: 10.1007/s12161-016-0502-x
- Crippen, D., and Morrison, J. (1986). The effects of sun exposure on the compositional development of Cabernet-sauvignon berries. *Am. J. Enol. Vitic.* 37, 235–242. doi: 10.5344/ajev.1986.37.4.235
- Deloire, A., Carbonneau, A., Wang, Z., and Ojeda, H. (2004). Vine and water: a short review. *OENO One* 38, 1–13. doi: 10.20870/oeno-one.2004.38.1.932
- Deluc, L. G., Quilici, D. R., Decendit, A., Grimplet, J., Wheatley, M. D., Schlauch, K. A., et al. (2009). Water deficit alters differentially metabolic pathways affecting important flavor and quality traits in grape berries of Cabernet sauvignon and Chardonnay. *BMC Genomics* 10, 212. doi: 10.1186/1471-2164-10-212
- de Oliveira, J. B., Egipto, R., Laureano, O., de Castro, R., Pereira, G. E., and Ricardo-da-Silva, J. M. (2019). Climate effects on physicochemical composition of syrah grapes at low and high altitude sites from tropical grown regions of Brazil. *Food Res. Int.* 121, 870–879. doi: 10.1016/j.foodres.2019.01.011
- Dokoozlian, N., and Kliewer, W. (1996). Influence of light on grape berry growth and composition varies during fruit development. *J. Am. Soc. Hortic. Sci.* 121 (5), 869–874. doi: 10.21273/jashs.121.5.869
- Downey, M. O., Dokoozlian, N. K., and Krstic, M. P. (2006). Cultural practice and environmental impacts on the flavonoid composition of grapes and wine: a review of recent research. *Am. J. Enol. Vitic.* 57, 257–268. doi: 10.5344/ajev.2006.57.3.257
- Filippetti, I., Movahed, N., Allegro, G., Valentini, G., Pastore, C., Colucci, E., et al. (2015). Effect of post-veraison source limitation on the accumulation of sugar, anthocyanins and seed tannins in vitis vinifera cv. sangiovese berries. *Aust. J. Grape Wine Res.* 21, 90–100. doi: 10.1111/ajgw.12115
- Fraga, H., Malheiro, A. C., Moutinho-Pereira, J., and Santos, J. A. (2012). An overview of climate change impacts on European viticulture. *Food Energy Secur.* 1, 94–110. doi: 10.1002/fes3.14
- Ghiglieno, I., Mattivi, F., Cola, G., Trionfini, D., Perenzoni, D., Simonetto, A., et al. (2020). The effects of leaf removal and artificial shading on the composition of Chardonnay and pinot noir grapes. *OENO One* 54, 761–777. doi: 10.20870/oeno-one.2020.54.4.2556
- Greer, D. H. (2013). The impact of high temperatures on vitis vinifera cv. semillon grapevine performance and berry ripening. *Front. Plant Sci.* 4. doi: 10.3389/fpls.2013.00491
- Herrero, P., Sáenz-Navajas, P., Culleré, L., Ferreira, V., Chatin, A., Chaperon, V., et al. (2016). Chemosensory characterization of Chardonnay and pinot noir base wines of champagne: two very different varieties for a common product. *Food Chem.* 207, 239–250. doi: 10.1016/j.foodchem.2016.03.068
- IBM Corp (2021). *IBM SPSS Statistics for windows, version 28.0* (Armonk, NY: IBM Corp).
- Intrigliolo, D. S., Lizama, V., García-Esparza, M. J., Abrisqueta, I., and Álvarez, I. (2016). Effects of post-veraison irrigation regime on Cabernet sauvignon grapevines in Valencia, Spain: yield and grape composition. *Agric. Water Manag.* 170, 110–119. doi: 10.1016/j.agwat.2015.10.020
- IPCC (2007). "Climate change 2007: the physical science basis," in *Contribution of working group I to the fourth assessment report of the intergovernmental panel on climate change*. Eds. S. Solomon, D. Qin, M. Manning, Z. Chen, M. Marquis, K. B. Averyt, M. Tignor and H. L. Miller (Cambridge: Cambridge University Press).
- Jackson, D., and Lombard, P. (1993). Environmental and management practices affecting grape composition and wine quality - a review. *Am. J. Enol. Vitic.* 44, 409–430. doi: 10.5344/ajev.1993.44.4.409
- Janusz, A., Capone, D. L., Puglisi, C. J., Perkins, M. V., Else, G. M., and Sefton, M. A. (2003). (E)-1-(2,3,6-Trimethylphenyl) buta-1,3-Diene: a potent grape-derived odorant in wine. *J. Agric. Food Chem.* 51 (26), 7759–7763. doi: 10.1021/jf0347113
- Jones, G. V., Duchêne, E., Tomasi, D., Yuste, J., Braslavsky, O., Schultz, H., et al. (2005). Changes in European winegrape phenology and relationships with climate. *XIV Int. GESCO Vitic. Congr. Geisenh. Ger.* 23–27 August 2005, 54–61.
- Jones, J. E., Kerslake, F. L., Close, D. C., and Damberg, R. G. (2014). Viticulture for sparkling wine production: a review. *Am. J. Enol. Vitic.* 65, 407–416. doi: 10.5344/ajev.2014.13099
- Keller, M. (2006). Ripening grape berries remain hydraulically connected to the shoot. *J. Exp. Bot.* 57, 2577–2587. doi: 10.1093/jxb/erl020
- Kwasniewski, M. T., Vanden Heuvel, J. E., Pan, B. S., and Sacks, G. L. (2010). Timing of cluster light environment manipulation during grape development affects C13 norisoprenoid and carotenoid concentrations in Riesling. *J. Agric. Food Chem.* 58, 6841–6849. doi: 10.1021/jf904555p
- Lakso, A. N., and Kliewer, W. M. (1975). The influence of temperature on malic acid metabolism in grape berries: i. enzyme responses. *Plant Physiol.* 56, 370–372. doi: 10.1104/pp.56.3.370
- Marais, J., Wyk, C., and Rapp, A. (1991). Carotenoid levels in maturing grapes as affected by climatic regions, sunlight and shade. *South Afr. J. Enol. Vitic.* 12, 64–69. doi: 10.21548/12-2-2209
- Marais, J., Wyk, C. J., and Rapp, A. (1992). Effect of sunlight and shade on norisoprenoid levels in maturing weisser Riesling and chenin blanc grapes and weisser Riesling wines. *South Afr. J. Enol. Vitic.* 13, 23–32. doi: 10.21548/13-1-2191
- Mariani, L., Alilla, R., Cola, G., Monte, G. D., Epifani, C., Puppi, G., et al. (2013). IPHEN—a real-time network for phenological monitoring and modelling in Italy. *Int. J. Biometeorol.* 57, 881–893. doi: 10.1007/s00484-012-0615-x
- Mariani, L., Parisi, S. G., Cola, G., and Failla, O. (2012). Climate change in Europe and effects on thermal resources for crops. *Int. J. Biometeorol.* 56, 1123–1134. doi: 10.1007/s00484-012-0528-8
- Mariani, L., Parisi, S., Failla, O., Cola, G., Zoia, G., and Bonardi, L. (2009). Tiran (1624–1930): a long time series of harvest dates for grapevine. *Italain J. Agrometeorology* 1, 7–16.
- Martin, D., Grose, C., Fedrizzi, B., Stuart, L., Albright, A., and McLachlan, A. (2016). Grape cluster microclimate influences the aroma composition of sauvignon blanc wine. *Food Chem.* 210, 640–647. doi: 10.1016/j.foodchem.2016.05.010
- Martinez-Lüscher, J., Chen, C. C. L., Brillante, L., and Kurtural, S. K. (2020). Mitigating heat wave and exposure damage to "Cabernet sauvignon" wine grape with partial shading under two irrigation amounts. *Front. Plant Sci.* 11. doi: 10.3389/fpls.2020.579192

- Mendes-Pinto, M. M. (2009). Carotenoid breakdown products the-norisoprenoids—in wine aroma. *Arch. Biochem. Biophys.* 483, 236–245. doi: 10.1016/j.abb.2009.01.008
- Michelini, S., Tomada, S., Kadison, A. E., Pichler, F., Hinz, F., Zeffart, M., et al. (2021). Modeling malic acid dynamics to ensure quality, aroma and freshness of pinot blanc wines in south tyrol (Italy). *OENO One* 55, 159–179. doi: 10.20870/oeno-one.2021.55.2.4570
- Mirás-Avalos, J. M., and Araujo, E. S. (2021). Optimization of vineyard water management: challenges, strategies, and perspectives. *Water* 13, 746. doi: 10.3390/w13060746
- Mirás-Avalos, J. M., and Intrigliolo, D. S. (2017). Grape composition under abiotic constraints: water stress and salinity. *Front. Plant Sci.* 8. doi: 10.3389/fpls.2017.00851
- Nesbitt, A., Kemp, B., Steele, C., Lovett, A., and Dorling, S. (2016). Impact of recent climate change and weather variability on the viability of UK viticulture - combining weather and climate records with producers' perspectives. *Aust. J. Grape Wine Res.* 22, 324–335. doi: 10.1111/ajgw.12215
- Ohana-Levi, N., Mintz, D. F., Hagag, N., Stern, Y., Munitz, S., Friedman-Levi, Y., et al. (2022). Grapevine responses to site-specific spatiotemporal factors in a Mediterranean climate. *Agric. Water Manage.* 259, 107226. doi: 10.1016/j.agwat.2021.107226
- Oliveira, C., Ferreira, A. C., Costa, P., Guerra, J., and Guedes de Pinho, P. (2004). Effect of some viticultural parameters on the grape carotenoid profile. *J. Agric. Food Chem.* 52, 4178–4184. doi: 10.1021/jf0498766
- Pérez-Álvarez, E. P., Intrigliolo Molina, D. S., Vivaldi, G. A., García-Esparza, M. J., Lizama, V., and Álvarez, I. (2021). Effects of the irrigation regimes on grapevine cv. bobal in a Mediterranean climate: i. water relations, vine performance and grape composition. *Agric. Water Manage.* 248, 106772. doi: 10.1016/j.agwat.2021.106772
- Pons, A., Allamy, L., Schüttler, A., Rauhut, D., Thibon, C., and Darriet, P. (2017). What is the expected impact of climate change on wine aroma compounds and their precursors in grape? *OENO One* 51, 141–146. doi: 10.20870/oeno-one.2017.51.2.1868
- Ramos, M. C., and Martínez-Casasnovas, J. A. (2006). Trends in precipitation concentration and extremes in the Mediterranean penedès-anoia region, Ne Spain. *Clim. Change* 74, 457–474. doi: 10.1007/s10584-006-3458-9
- Ramos, M. C., and Mulligan, M. (2005). Spatial modelling of the impact of climate variability on the annual soil moisture regime in a mechanized Mediterranean vineyard. *J. Hydrol.* 306, 287–301. doi: 10.1016/j.jhydrol.2004.09.013
- R Core Team (2022). *R: a language and environment for statistical computing* (Vienna, Austria: R Foundation for Statistical Computing). Available at: <https://www.R-project.org/>.
- Reynolds, A. G., and Naylor, A. P. (1994). 'Pinot noir' and 'Riesling' grapevines respond to water stress duration and soil water-holding capacity. *HortScience* 29, 1505–1510. doi: 10.21273/HORTSCI.29.12.1505
- Reynolds, A., Pool, R., and Mattick, R. (1986). Influence of cluster exposure on fruit composition and wine quality of seyval blanc grapes. *Vitis* 25, 85–95.
- Rienth, M., Torregrosa, L., Sarah, G., Ardisson, M., Brillouet, J.-M., and Romieu, C. (2016). Temperature desynchronizes sugar and organic acid metabolism in ripening grapevine fruits and remodels their transcriptome. *BMC Plant Biol.* 16, 164. doi: 10.1186/s12870-016-0850-0
- Riou, C., Pieri, P., and Clech, B. L. (1994). Consommation d'eau de la vigne en conditions hydriques non limitantes. formulation simplifiée de la transpiration. *VITIS - J. Grapevine Res.* 33, 109–109. doi: 10.5073/vitis.1994.33.109-115
- Santos, J. A., Fraga, H., Malheiro, A. C., Moutinho-Pereira, J., Dinis, L.-T., Correia, C., et al. (2020). A review of the potential climate change impacts and adaptation options for European viticulture. *Appl. Sci.* 10, 3092. doi: 10.3390/app10093092
- Scafidi, P., Pisciotto, A., Patti, D., Tamborra, P., Di Lorenzo, R., and Barbagallo, M. G. (2013). Effect of artificial shading on the tannin accumulation and aromatic composition of the grillo cultivar (*Vitis vinifera* L.). *BMC Plant Biol.* 13, 175. doi: 10.1186/1471-2229-13-175
- Schneider, R., Razungles, A., Augier, C., and Baumes, R. (2001). Monoterpenic and norisoprenoid glycoconjugates of vitis vinifera L. cv. melon b. as precursors of odorants in muscadet wines. *J. Chromatogr. A* 936, 145–157. doi: 10.1016/S0021-9673(01)01150-5
- Schultz, H. (2000). Climate change and viticulture: a European perspective on climatology, carbon dioxide and UV-b effects. *Aust. J. Grape Wine Res.* 6, 2–12. doi: 10.1111/j.1755-0238.2000.tb00156.x
- Silva Ferreira, A. C., and Guedes de Pinho, P. (2004). Norisoprenoids profile during port wine ageing—influence of some technological parameters. *Anal. Chim. Acta* 513, 169–176. doi: 10.1016/j.aca.2003.12.027
- Smart, R. E., Dick, J. K., Gravett, I. M., and Fisher, B. M. (1990). Canopy management to improve grape yield and wine quality - principles and practices. *South Afr. J. Enol. Vitic.* 11, 3–17. doi: 10.21548/11-1-2232
- Smart, R. E., Robinson, J. B., Due, G. R., and Brien, C. J. (1985). Canopy microclimate modification for the cultivar Shiraz II. effects on must and wine composition. *Vitis - J. Grapevine Res.* 24, 119–128. doi: 10.5073/vitis.1985.24
- Song, J., Shellie, K. C., Wang, H., and Qian, M. C. (2012). Influence of deficit irrigation and kaolin particle film on grape composition and volatile compounds in merlot grape (*Vitis vinifera* L.). *Food Chem.* 134, 841–850. doi: 10.1016/j.foodchem.2012.02.193
- Suter, B., Destrac Irvine, A., Gowdy, M., Dai, Z., and van Leeuwen, C. (2021). Adapting wine grape ripening to global change requires a multi-trait approach. *Front. Plant Sci.* 12. doi: 10.3389/fpls.2021.624867
- Toda, M. D., and Balda, P. (2014). Reducing the pH of wine by increasing grape sunlight exposure: a method to mitigate the effects of climate warming. *Vitis - J. Grapevine Res.* 53, 17–20. doi: 10.5073/vitis.2014.53
- Tonietto, J. (1999). *Les Macroclimats viticoles mondiaux et l'influence du mésoclimat sur la typicité de la syrah et du Muscat de hambourg dans le sud de la France: méthodologie de caractérisation* (Montpellier: PhD dissertation, Ecole Nationale Supérieure Agronomique).
- van Leeuwen, C., Destrac-Irvine, A., Dubernet, M., Duchêne, E., Gowdy, M., Marguerit, E., et al. (2019). An update on the impact of climate change in viticulture and potential adaptations. *Agronomy* 9, 514. doi: 10.3390/agronomy9090514
- Volschenk, H., Vuuren, H., and Viljoen-Bloom, M. (2006). Malic acid in wine: origin, function and metabolism during vinification. *South Afr. J. Enol. Vitic.* 27, 123–136. doi: 10.21548/27-2-1613
- Wang, Y., He, L., Pan, Q., Duan, C., and Wang, J. (2018). Effects of basal defoliation on wine aromas: a meta-analysis. *Molecules* 23, 779. doi: 10.3390/molecules23040779
- Winterhalter, P., and Schreier, P. (1994). C13-norisoprenoid glycosides in plant tissues: an overview on their occurrence, composition and role as flavour precursors. *Flavour Fragr. J.* 9, 281–287. doi: 10.1002/ffj.2730090602
- Ziegler, M., Gök, R., Bechtloff, P., Winterhalter, P., Schmarr, H.-G., and Fischer, U. (2019). Impact of matrix variables and expertise of panelists on sensory thresholds of 1,1,6-trimethyl-1,2-dihydronaphthalene known as petrol off-flavor compound in Riesling wines. *Food Qual. Prefer.* 78, 103735. doi: 10.1016/j.foodqual.2019.103735
- Zougagh, M., Rios, A., and Valcárcel, M. (2006). Determination of total safranal by *in situ* acid hydrolysis in supercritical fluid media: application to the quality control of commercial saffron. *Anal. Chim. Acta* 578, 117–121. doi: 10.1016/j.aca.2006.06.064



OPEN ACCESS

EDITED BY

Stefan Martens,
Fondazione Edmund Mach, Italy

REVIEWED BY

Justin Graham Lashbrooke,
Stellenbosch University, South Africa
Sergio Tombesi,
Catholic University of the Sacred Heart,
Italy

*CORRESPONDENCE

Alessandra Ferrandino

✉ alessandra.ferrandino@unito.it

RECEIVED 15 December 2022

ACCEPTED 26 May 2023

PUBLISHED 19 June 2023

CITATION

Ferrandino A, Pagliarani C and
Pérez-Álvarez EP (2023) Secondary
metabolites in grapevine: crosstalk of
transcriptional, metabolic and hormonal
signals controlling stress defence
responses in berries and vegetative organs.
Front. Plant Sci. 14:1124298.
doi: 10.3389/fpls.2023.1124298

COPYRIGHT

© 2023 Ferrandino, Pagliarani and Pérez-Álvarez. This is an open-access article distributed under the terms of the [Creative Commons Attribution License \(CC BY\)](#). The use, distribution or reproduction in other forums is permitted, provided the original author(s) and the copyright owner(s) are credited and that the original publication in this journal is cited, in accordance with accepted academic practice. No use, distribution or reproduction is permitted which does not comply with these terms.

Secondary metabolites in grapevine: crosstalk of transcriptional, metabolic and hormonal signals controlling stress defence responses in berries and vegetative organs

Alessandra Ferrandino^{1*}, Chiara Pagliarani²
and Eva Pilar Pérez-Álvarez³

¹Department of Agricultural, Forest and Food Sciences (DISAFA), University of Torino, Grugliasco, Italy,

²National Research Council, Institute for Sustainable Plant Protection (CNR-IPSP), Torino, Italy, ³Grupo VIENAP. Finca La Grajera, Instituto de Ciencias de la Vid y del Vino (ICVV), Logroño, La Rioja, Spain

Abiotic stresses, such as temperature, heat waves, water limitation, solar radiation and the increase in atmospheric CO₂ concentration, significantly influence the accumulation of secondary metabolites in grapevine berries at different developmental stages, and in vegetative organs. Transcriptional reprogramming, miRNAs, epigenetic marks and hormonal crosstalk regulate the secondary metabolism of berries, mainly the accumulation of phenylpropanoids and of volatile organic compounds (VOCs). Currently, the biological mechanisms that control the plastic response of grapevine cultivars to environmental stress or that occur during berry ripening have been extensively studied in many viticultural areas, in different cultivars and in vines grown under various agronomic managements. A novel frontier in the study of these mechanisms is the involvement of miRNAs whose target transcripts encode enzymes of the flavonoid biosynthetic pathway. Some miRNA-mediated regulatory cascades, post-transcriptionally control key MYB transcription factors, showing, for example, a role in influencing the anthocyanin accumulation in response to UV-B light during berry ripening. DNA methylation profiles partially affect the berry transcriptome plasticity of different grapevine cultivars, contributing to the modulation of berry qualitative traits. Numerous hormones (such as abscisic and jasmonic acids, strigolactones, gibberellins, auxins, cytokinins and ethylene) are involved in triggering the vine response to abiotic and biotic stress factors. Through specific signaling cascades, hormones mediate the accumulation of antioxidants that contribute to the

quality of the berry and that intervene in the grapevine defense processes, highlighting that the grapevine response to stressors can be similar in different grapevine organs. The expression of genes responsible for hormone biosynthesis is largely modulated by stress conditions, thus resulting in the numerous interactions between grapevine and the surrounding environment.

KEYWORDS

secondary metabolism, *Vitis vinifera* L., interaction with pathogens and environment, transcriptional and post-transcriptional regulation, epigenetic

1 Introduction

Climate change-associated stresses, such as frequent drought events and heat waves during the growing season, have been seriously impacting the viticultural sector worldwide (Horton et al., 2016; Wolkovich et al., 2018). Unexpected long, hot, and dry periods during summer cause intensification of some pest and pathogen spread (Corredor-Moreno and Saunders, 2020), with dramatic effect on potential vine yield and quality. In the last few years, incidence of some fungal/oomycete-associated diseases significantly increased due to climate alterations (Gullino et al., 2018). The analysis of the impact of these phenomena led some climate-based predictive models to project a decline in the suitability of traditional wine growing regions (Hannah et al., 2013). Such predictions, however, do not consider potential buffering effects due to the high intraspecific genetic variability in grapevine and to grapevine phenotypic plasticity. The ability of grapevine varieties and clones to respond to changing conditions by shaping their phenotype (Sultan, 2010; Dal Santo et al., 2018) could indeed limit the forecasted decline of viticultural areas (Wolkovich et al., 2018; Morales-Castilla et al., 2020). Additionally, mitigating the effects of climate change also relies on the adoption of specific agricultural practices like optimizing rootstock choice. Through such practices, the grapevine's capability to recover from water stress can be exploited with retention if not improvement of the berries' qualitative traits (Patono et al., 2022). Global warming negative effects on grapevine phenology could be limited by exploiting the great intraspecific variability of wine grapes that exists at the cultivar/clone level and that deeply influences the genotype physiological responses to environmental cues like drought (Bota et al., 2016; van Leeuwen et al., 2019). Moreover, the use of late-ripening and drought-resistant cultivars and/or grafting onto drought-tolerant rootstocks represent cost-effective and environmentally friendly strategies for improving vine resilience to water deficit and high temperatures, thereby ensuring the production of high-quality wines. The development of cutting-edge agronomic practices for enhancing grapevine tolerance to stress is therefore a strict requirement that inevitably calls for an in-depth knowledge of the biological mechanisms controlling the vine metabolic responses to climate change effects (e.g.

accumulation of defence- and quality-associated secondary metabolites). A comprehensive understanding of the genetic regulation of grape berry secondary metabolism in response to altered climatic conditions is indeed crucial to identifying the drivers of fruit quality. The challenge to filling the knowledge gaps on such themes is deeply felt among both the scientific community and viticulturists, as demonstrated by the increasing number of studies addressing the analysis of berry secondary metabolic composition in different grapevine genotypes exposed to abiotic stresses. The main achievements in this research field have been outlined in recent reviews. Gouot et al. (2019) provide a closer look into the impact of increasing temperatures on grape flavonoid metabolism, and Rienth et al. (2021a) discuss the influence of the main abiotic stresses (high temperature, drought, excessive UV-B radiation, high CO₂ concentrations) on shifts in the amounts and partitioning of berry secondary metabolites.

Besides their well-known contribution to berry ripening, secondary metabolites are important players in plant defence. Nevertheless, their role in biotic stress response has been studied only recently in *Vitis* spp. The analysis of grapevine responses to pathogen attacks in relation to the modulation of secondary metabolic pathways involves both berries and vegetative tissues. In fact, leaves, stems, wood, and roots are the organs where many diseases spread, such as powdery and downy mildews, wood diseases, viruses, and bacteria. Based on this context, the present review will discuss the effect of the main abiotic and biotic stresses on secondary metabolic processes occurring in berries and vegetative organs by detailing how the accumulation of individual classes of compounds is mediated by molecular signalling cascades such as those triggered by short RNAs (sRNAs), epigenetic modifications and hormonal crosstalk. The impact that the genotype × environment interaction exerts in orchestrating plant defence-signalling cascades will also be considered. Finally, attention will be given to highlight those secondary metabolic changes that underlie tolerance/resistance mechanisms to environmental cues, particularly to some grapevine pathogens (i.e. *Botrytis cinerea*, Grapevine Trunk Diseases and phytoplasmas). From the short to medium-term perspective, the identification of the biological processes at the basis of grapevine resilience to stress should indeed provide precious information for optimising sustainable disease protection practices in viticulture.

2 Molecular and hormonal crosstalk modulating the grape berry secondary metabolism in response to abiotic stress

To disclose the complexity of stress-dependent molecular players either driving or inhibiting the accumulation of secondary metabolites, it is pivotal to understand how these metabolic pathways are under genetic control. Notably, in the last years, research in this field has been boosted owing to the great advances made in high-throughput sequencing techniques, coupled with the availability of the reference grapevine genome (Jaillon et al., 2007) and the release of the genome sequences of several *Vitis vinifera* cultivars and rootstocks (<http://www.grapegenomics.com/>; Minio and Cantu, 2022). Recently, Rienth et al. (2021a) provided an in-depth overview on the changes in the expression of key genes regulating the biosynthesis and mobilisation of grapevine secondary metabolites in response to different abiotic stresses. To avoid overlapping with this recent review, in this section we focus on the molecular and hormonal crosstalk beneath secondary metabolism in grapevine berries. We detail: i) post-transcriptional and epigenetic regulation; ii) hormonal cross talk regulation; and iii) genotype \times environment interaction effects on berry secondary metabolite composition.

2.1 Stress-induced post-transcriptional and epigenetic changes regulating berry secondary metabolism

In the last decade, several studies attempted to dissect the whole transcriptional reprogramming associated with modification of secondary metabolism in response to stress. Unlike other crop species (Jogawat et al., 2021), post-transcriptional regulatory mechanisms linked to those responses, such as those mediated by small RNAs (sRNAs), have been rarely considered in grapevine.

sRNAs represent tiny signalling molecules that modulate a *plethora* of plant growth and developmental processes by transcriptionally and post-transcriptionally regulating their target genes. Emerging experimental evidence has proven that the synergic interplay among sRNAs and hormone signalling pathways is crucial for driving plant responses to multiple environmental changes (Li et al., 2020). Of note, sRNAs, and mainly microRNAs (miRNAs), respond to, or exhibit overlapping regulatory activities with those of phytohormones (Curaba et al., 2014). As a result, miRNAs are often referred to as RNA hormones. Intriguingly, hormones and sRNAs can move cell-to-cell or systemically within the plant vascular tissues, thereby controlling their targets over long distance (Pagliarani and Gambino, 2019). Pinto et al. (2016) analysed the distribution of small RNAs in the berries of Cabernet Sauvignon and Sangiovese, in order to compare the changes occurring in response to three different environments. The study disclosed key relationships between the differential expression of specific miRNAs and some genes involved in secondary metabolism, leading to the identification of two novel

miRNAs whose target transcripts encoded enzymes of the flavonoid biosynthetic branch. It also emerged that environmental and vineyard-management conditions did affect the transcription of miRNA-producing gene *loci*, although, patterns of miRNA accumulation were predominantly influenced by the cultivar genotype and by the specific berry developmental stage. A close overview on the effect of abiotic stress factors on the modulation of small RNAs regulating secondary metabolism in grape berries has recently been provided by Sunitha et al. (2019). In a study of Cabernet Sauvignon vines grown both under greenhouse and field conditions, the researchers analysed the impact of UV-B radiation on the abundance of miRNAs and of phased small-interfering-RNA (phasi-RNAs)-producing *loci* during the fruit development and berry ripening periods. They identified novel and conserved miRNA-mediated regulatory cascades (including the autoregulatory loop involving miR828-TAS4) that by post-transcriptionally controlling key MYB transcription factors, shape the accumulation of anthocyanins in response to UV-B light during berry ripening (Sunitha et al., 2019).

Another intriguing and still little investigated research matter is represented by the analysis of epigenetic marks underpinning the modulation of berry secondary metabolic pathways in response to environmental stressors. Although important breakthroughs in the understanding of epigenetic phenomena controlling the plant adaptation to drought and temperature stress have been made in many economically important crops (Varotto et al., 2020), very little information is available in grapevine (Fortes and Gallusci, 2017). A mechanistic link between epigenetic modifications and accumulation of specific berry secondary metabolites has not been provided so far. Nevertheless, it was shown that changes in DNA methylation profiles could partially affect the berry transcriptome plasticity of different grapevine cultivars (Dal Santo et al., 2018), and in turn contribute to the modulation of fruit and wine quality traits related to terroir (Xi et al., 2017). Further investigation on the role of stress-responsive sRNAs and epigenetic modifications in the control of berry secondary metabolic pathways will also be valuable to gain more information on the activation of specific defence processes. For instance, a still to be deepened subject in grapevine is the study of the synergy between sRNA/epigenetic-based regulatory networks and other overlapping signalling routes, such as those dependent on hormones and those dependent on the accumulation of defence and quality-associated molecules.

2.2 Hormonal cross talk regulating the berry secondary metabolism upon stress

Transcriptional reprogramming events can thoroughly modify hormone metabolism and signalling. Moreover, molecular players and hormone crosstalk pathways synergically work to reach a tight control on secondary metabolism during berry development (Kuhn et al., 2014). Notably, hormone amounts do vary according to the vine stress response (Ferrandino and Lovisolo, 2014) and to the specific berry developmental stage (Kuhn et al., 2014). The progressive hormone accumulation in the berry serves as a trigger for the synthesis of secondary metabolites, such as the case of the

ABA-mediated activation of the anthocyanin biosynthesis at véraison (Castellarin et al., 2016). Available literature also clearly attested the predominant role that diverse hormone signalling cascades exert on the regulation of berry secondary metabolism upon stress conditions (Fortes et al., 2015). Even though many papers described the effects exerted by temperature, heat flash, light intensity, and quality on grapevine secondary metabolism, much less is known about the hormonal crosstalk behind these events. A recent study by Min Liu and co-workers (2020) revealed that grapevine response to heat stress and heat acclimation treatments drives an intense transcriptional reprogramming involving the overexpression of 25 heat-shock proteins, 11 antioxidases and 31 transcription factors. Notably, those transcriptional modifications occur in parallel with changes in the sugar-ABA signalling cross talk. Particularly, it was observed that following acclimation to heat stress, grapevine genes encoding sucrose phosphate synthases, sucrose synthases and invertases were transcriptionally inhibited, thereby leading to an overall decrease in the cell sucrose amounts. Such condition represented the trigger for the activation of the ABA signaling pathway and the downstream induction of stress-responsive genes (Min Liu et al., 2020). This picture of molecular and biochemical interactive networks suggests a shift in the growth-defence trade off balance, which may divert the vine energy metabolism to establish stress defence reactions associated with thermotolerance. A stress-induced shift from primary to secondary metabolic reactions is also a hallmark of grapevine response to high light exposure. Light quality and intensity (high light in particular) conditions were indeed shown to favour the accumulation of antioxidant molecules and secondary metabolites in grape berries at the expense of carbohydrate metabolism. Such events were found to occur through extensive modifications of grapevine transcriptome, which mainly rely on the upregulation of defence related genes, including those involved in the production of anthocyanins, flavonols and carotenoids (du Plessis et al., 2017). Additionally, the overexpression of the 9-cis-epoxycarotenoid dioxygenase encoding gene (*VvNCED*) directly linked to ABA biosynthesis suggested an increase in ABA concentration and a consequent activation of the ABA signalling pathways that may, in turn, promote grapevine adaptation to high light intensity. It is thus clear that, among all phytohormones, ABA plays the major role in the control of berry phenology and stress perception (Kuhn et al., 2014; Pilati et al., 2017). Moreover, it has long been demonstrated in different cultivars that exogenous ABA application can mediate the accumulation of phenolic components in the berries (Quiroga et al., 2012; Xi et al., 2013; Luan et al., 2014) by activating transcription of key genes involved in the flavonoid pathway, such as phenylalanine ammonia lyase, chalcone synthase, glutathione S-transferase and MyB-related transcription factors (Koyama et al., 2010). Additionally, exogenous ABA treatment of berries is an effective strategy for managing the uncoupling of technological and phenolic fruit ripening in wine grape varieties due to the imbalance between sugars and anthocyanin concentrations upon challenging environmental conditions (Wang et al., 2021). Application of exogenous ABA in the presence of abiotic factors such as UV-B light and water deficit was shown not only to promote the biosynthesis and accumulation of anthocyanins, but also to

increase the amounts of piceid and *trans*-resveratrol in the berry skin of cv Malbec. The latter result was mainly observed when ABA application was performed in concomitance with elevated UV-B radiation. Unlike phenylpropanoids, volatile aromatic components were poorly affected by the imposed ABA treatments (Alonso et al., 2021).

Further research efforts have been made to unlock the complexity of interconnected networks of hormones that shape the grapevine metabolism in response to the environment. For instance, it was proposed that other carotenoid-derived hormones, like strigolactones (SLs), could interact with ABA regulatory pathways, particularly with the ABA-mediated anthocyanin accumulation in the berries at véraison (Ferrero et al., 2018). Grape berries co-treated with ABA and the synthetic strigolactone analogue GR24 experienced a delay in anthocyanin accumulation at véraison, which is supported by the down-regulation of the anthocyanin-related genes *VvMybA1* and *VvUFGT*. The ABA-GR24 co-treatment also negatively affected ABA concentration in the berry. Interestingly, this condition was not achieved by inhibiting the transcription of ABA biosynthetic genes (i.e. *VvNCED*), but rather it depended on the activation of the hormone catabolic pathway (e.g. ABA-8'-hydroxylases) and on perturbation of the ABA cellular/apoplastic delivery (Ferrero et al., 2018). These findings may thus call for a role of SLs within the interactive network of molecular players that regulate ABA accumulation and signalling.

Moreover, increasing evidence shows that another crucial crosstalk in the regulation of the plant's response to abiotic stress is established between ABA and jasmonate (JA) signalling pathways (Yang et al., 2019). Like ABA, the plant's response to JA elicits different defence processes, including detoxification of reactive oxygen species and increase of osmoprotectant concentrations at the cellular level. In different crop species it was demonstrated that the two hormones operate in a synergistic way by reciprocally activating the molecular effectors involved in their biosynthetic and signalling routes (Kim et al., 2021). For instance, the first step of the ABA-JA crosstalk involves the dynamic interaction between the ABA-induced PYRABACTIN RESISTANCE1-Like protein (PYL) and the JA-based JAZ-MYC2 module, responsible for the signalling cascade that coordinates the balance between the activation of either plant growth or defence mechanisms (Yang et al., 2019). Consistently, experiments conducted on *V. vinifera* cv Summer Black vines attested that endogenous levels of both ABA and JA strongly increased in stressed leaves. Such metabolic changes occurred concomitantly with a steep upregulation of many transcripts encoding the defence-associated proteins that typically participate in plant immunity, such as heat shock proteins, MAP kinases, and WRKY transcription factors. In parallel, molecular effectors of the ABA and JA signalling pathways, like phosphatase 2C, calmodulin (CAL), calcineurin B like proteins (CBL), and jasmonate ZIM-domain proteins (JAZ) were also overexpressed (Haider et al., 2017). It must be noted that some of the observed transcriptional changes, such as the increase in CAL and CBL mRNAs, also indicated an overlapping with other stress-responsive signals, particularly the Ca^{2+} -based ones, thus adding a further level of complexity into the molecular regulatory networks that control the plant's response to abiotic stress.

Auxin-mediated molecular signals, on the other hand, are antagonistic to those induced by ABA. The analysis of the crosstalk between auxin and ABA highlighted a tight coordination occurring among the two hormonal pathways and sugars (sucrose) that is crucial for priming berry development. For instance, while ABA and sucrose treatments on the cultivar Fujiminori berries triggered fruit ripening processes, the application of IAA (indolacetic acid) delayed them, negatively affecting sugar and anthocyanin accumulation, fruit firmness, cell wall metabolism, and aroma spread. Such differences among the imposed treatments were underpinned at the transcriptome level by a strong transcriptional reprogramming of the main genes associated with berry ripening and flavonoid biosynthesis, like pectin esterases, polygalacturonases, pectate lyases, flavanone 3'-hydroxylases (*F3'H*), *CHS*, and *UFGT* (Jia et al., 2017). Analyses performed in Cabernet Sauvignon grapes following treatments with ABA and synthetic auxin further confirmed the effect of the ABA-auxin interaction on the regulation of anthocyanin and norisoprenoid biosynthesis, at both the metabolite and transcriptional levels (He et al., 2020; He et al., 2021). A tight interaction among hormone regulatory routes is also at the basis of the regulation of mono- and sesquiterpene biosynthesis in grapevine. Despite the accumulation of these molecules during the berry ripening and in response to stress cues was established to primarily depend on jasmonates (jasmonic acid, JA and methyl-jasmonate, MeJA) (Yang et al., 2019), a crosstalk between these and other ripening and stress-associated hormones, such as ABA, ethylene, and auxin, does also occur (Wang et al., 2022). Finally, treatments with exogenous ABA and gibberellins (GA3) were shown to differently affect the production and partitioning of antioxidants (proline and anthocyanins) and defence compounds (terpenes) in leaves, berries, and roots of cv Malbec plants (Murcia et al., 2017). These findings suggested that the interaction between ABA and gibberellin-dependent routes could promote the establishment of priming phenomena in the treated vines, prompting them to better cope with environmental stresses.

2.3 Grapevine adaptability to environmental stress: phenotypic plasticity and its effect on berry secondary metabolism

Vitis cultivars are adapted to grow in different mesoclimates (Morales-Castilla et al., 2020), making grapevine an interesting model species to study the genetic and molecular bases that underlie phenotypic plasticity (Dal Santo et al., 2013; Dal Santo et al., 2016; Dal Santo et al., 2018) in response to multiple environmental cues. The analysis of genotype-based transcriptional modifications influenced by the G × E interplay is crucial to understand the different regulation of metabolic pathways during berry ripening (Dal Santo et al., 2013; Massonnet et al., 2017). Existing literature takes into account the responses i) of the same cultivar to different growing areas (Cramer et al., 2014; Anesi et al., 2015; Dal Santo et al., 2016), ii) of several cultivars within the same growing area (Degu et al., 2014; Massonnet et al., 2017); and iii) of

different genotypes cultivated across different viticultural sites and climate conditions (Ghan et al., 2015; Dal Santo et al., 2018). Anesi et al. (2015) analysed the whole transcriptome and metabolome of berries from a single Corvina clone grown in seven different vineyards during a 3-year trial period. The authors attested that some berry transcriptional and metabolic changes, like those resulting in the accumulation of flavonoids, anthocyanins, stilbenes and sesquiterpenes were significantly shaped by the *terroir* and this effect was maintained over several vintages. Conversely, the biosynthesis of other metabolic components, such as hydroxycinnamic acid derivatives and flavan-3-ols/procyanidins showed the least level of plastic response to environment (Anesi et al., 2015). Among the studies addressing the response of different cultivars to the same growing area, the one by Degu and coworkers (2014) was the first to combine data from targeted metabolomics and transcriptome sequencing with the goal to dissect changes occurring during ripening in the berry skin of Shiraz and Cabernet Sauvignon grown in the same semiarid environment. Notably, the outcomes of the study were maximised by the fact that two red-grape varieties used displayed opposite physiological behaviours to water deficit. The authors reported that along with ripening and water deficit progression, the regulation of berry development in Shiraz was based on a better coordination between primary and secondary metabolic signals with respect to Cabernet Sauvignon, and this resulted in a higher transcription of genes of the phenylpropanoid pathway. Such genotype-dependent features also led to increased production of stress-responsive secondary metabolites in Shiraz berries that, since véraison, showed higher amounts of piceid and of coumaroyl derivatives of anthocyanin than Cabernet Sauvignon. Those data, together with the exclusive upregulation of 19 hormone-related genes involved in abscisic acid (ABA) metabolism, suggested that physiological and metabolic responses to drought conditions were enhanced in Shiraz (Degu et al., 2014). Dal Santo and collaborators (2018) characterised plastic changes occurring across two vintages in the berry transcriptome and genome methylation landscapes of Cabernet Sauvignon and Sangiovese cultivated in three different geographical areas. From this comprehensive survey, it emerged that the G × E interaction exerts a key role in the modulation of genotype specific berry quality traits, such as those linked to the production of flavonoid and volatile organic compounds (VOCs). The importance of the genotype contribution in the regulation of berry secondary metabolism was further addressed by Gambino et al. (2021), who outlined the transcriptional changes occurring over ripening in berries of the red-grapes Nebbiolo and Barbera. Besides transcriptional modifications leading to distinct anthocyanin profiles typical of the considered varieties, the study highlighted, in Nebbiolo, a unique reprogramming of transcripts involved in the biosynthesis of defensive secondary metabolites (stilbene synthases), which, being activated regardless of pathogen or stress factor presence, suggested a more active basal defence metabolism in this cultivar. Studies of grapevine plastic metabolic responses to environmental conditions should also consider effects due to grapevine intra-varietal variability. Indeed, beside cultivar-based responses, clone-mediated signals can also affect the composition of berry secondary metabolites. The influence of

clonal variability on secondary metabolism had been investigated at the analytical level, in different cultivars including Barbera, Cabernet Franc and Merlot (Ferrandino and Guidoni, 2010; van Leeuwen et al., 2013; Pantelić et al., 2016). On the contrary, clone \times environment ($C \times E$)-dependent changes underlying fruit quality were poorly studied at the molecular level. Research efforts in this direction were made by analysing in two vintages berry transcriptomic and metabolic data collected during ripening from three Nebbiolo clones grown in different vineyards (Pagliarini et al., 2019). Transcripts associated with sugar and hormone signalling cascades, that control anthocyanin and flavonoid biosynthesis downstream, were affected by the berry developmental stage. Conversely, genes linked to anthocyanin transport were expressed depending on the $C \times E$ interaction and according to changes in the berries' anthocyanin partitioning. The study also indicated a strong effect of the vineyard sanitary status on the regulation of secondary metabolic pathways, leading to the production of antimicrobial compounds, such as phytoalexins (Pagliarini et al., 2019).

In terms of practical impact, overall information collected from $G \times E$ studies offers a valuable theoretical basis to orient the adoption of suited agronomic practices considering growing site and specific cultivar or clone. In parallel, it also provides scientific support for developing *ad hoc* breeding programs for selecting genotypes with improved tolerance to environmental threats.

3 Transcriptional reprogramming, hormonal crosstalk and specific molecule accumulation during pathogen pressure

Knowledge of the effects of the main biotic stresses on berry secondary metabolism has recently been revised in relation to fungal and viral pathogens (Rienth et al., 2021b). In the present review, we considered the effects of *Botrytis cinerea*, GTDs, and phytoplasma on grapevine secondary metabolism, focusing on the hormonal crosstalk involved in these three grapevine defence response patho-systems.

3.1 Botrytis cinerea (Bc)

Bc induces a substantial reprogramming of hormonal metabolism during grape berry ripening (Figure 1). A recent study reported a dramatic increase in ABA (up to 140-fold) and dihydrophaseic acid (DPA) in Noble Rot (NR)-infected berries (cv Furmint), but not in grey mold-infected Marselan berries (Pogány et al., 2022). ABA is a versatile player in the resistance against *Bc*. While on one hand this hormone contributes to *Botrytis* susceptibility in tomato leaves (Audenaert et al., 2002), on the other hand, and to a larger extent, it activates the transcription of MYB genes (AbuQamar et al., 2009; Blanco-Ulate et al., 2015), which in turn drive the biosynthesis of stilbenes, proanthocyanidins and anthocyanins, even in a white berry cultivar, such as Sémillon (Blanco-Ulate et al., 2015). In addition, Noble Rot (NR) (but not

grey mold) induced different expressions of genes related to auxin and salicylic acid (up-regulated) and of one gene related to cytokinin (down-regulated). Two jasmonate *O*-methyltransferase isoforms were markedly induced both in the NR \times Furmint interaction and in bunch rot inoculated Marselan berries (Pogány et al., 2022). In this study, NR development triggered the transcription of genes involved in the initial steps of the phenylpropanoid pathway, such as several isoforms of PAL and trans-cinnamate 4-monooxygenases (CYP). Their activation enabled the formation of key phenolic compounds, such as cinnamic acid and *p*-coumaric acid, which are the initial bricks of polyphenol biosynthesis. Remarkably, the activation of those genes was not limited to *Bc* in the NR form, as it is also shown to be a common transcriptional signature of grape berry cells elicited by *Bc* infection (Kelloniemi et al., 2015; Agudelo-Romero et al., 2013). Stilbene synthase (*STS*) isoforms were uniformly upregulated in both NR and bunch rot (BR) berries. Oppositely, the expression of two chalcone synthase-encoding genes (*CHS*) varied between NR and BR. Indeed, NR triggers a downregulation of *CHS*, which could justify the limited amounts of flavonols found in Sémillon berries affected by NR (Blanco-Ulate et al., 2015), whereas BR upregulated expression of these genes (Pogány et al., 2022).

At the leaf level (Figure 2), the resistance mechanisms induced by *Bc* require the hormonal crosstalk of abscisic acid (ABA), salicylic acid (SA), ethylene (ETH), brassinosteroids (BRs) and jasmonic acid (JA) (Jia et al., 2022). Many genes are involved in the leaf's resistance to *Bc*; they encode for pathogenesis-related proteins (*PRs*), disease resistance proteins (*RPS*), calcium-binding proteins (*CMLs*), *WRKY* transcription factors, brassinosteroid insensitive 1 (*BAK1*) factor, ethylene-responsive transcription factor (*ERF*), and chitinase 5. These genes were expressed differently in young and adult leaves. Furthermore, numerous infection-related metabolic biomarkers were identified, including glutathione and proline, which accumulated particularly in the young leaves, thereby suggesting a defensive activation based on leaf age (Pogány et al., 2022).

The activation of *ERF* transcripts following *Bc* infection was also demonstrated (Wang et al., 2018; Wang et al., 2020; Jia et al., 2022; Pogány et al., 2022; Zhu et al., 2022). In *Vitis amurens*, *ERF20* (*VaERF20*) was induced by inoculation with *Bc*, both in leaves collected from the resistant Shuangyou cultivar (*V. amurens*) and in those from the susceptible *V. vinifera* cv Red Globe. Accordingly, *Arabidopsis thaliana* mutants over-expressing (OE) *VaERF20* displayed enhanced resistance to *Bc* and a decrease in the concentration of pathogen-induced reactive oxygen species (ROS). These findings point to a specific response of tolerant genotypes to necrotrophic pathogens (Mengiste, 2012; Wang et al., 2018). Both salicylic acid (SA) and jasmonic acid/ethylene (JA/ET), responsive-defence genes were up-regulated in *VaERF20*-OE *Arabidopsis* plants inoculated with *Bc*. Pattern-Triggered Immunity (PTI) responses associated with increased expression of *PTI* genes, callose accumulation and stomatal closure were boosted in the transgenic lines with respect to wild-type controls. These data prove that *VaERF20* is involved in various signal transduction cascades and acts as an inducer of the plant immune response. In *Vitis amurens*, *ERF16* (*VaERF16*), expressed during *Bc* infection

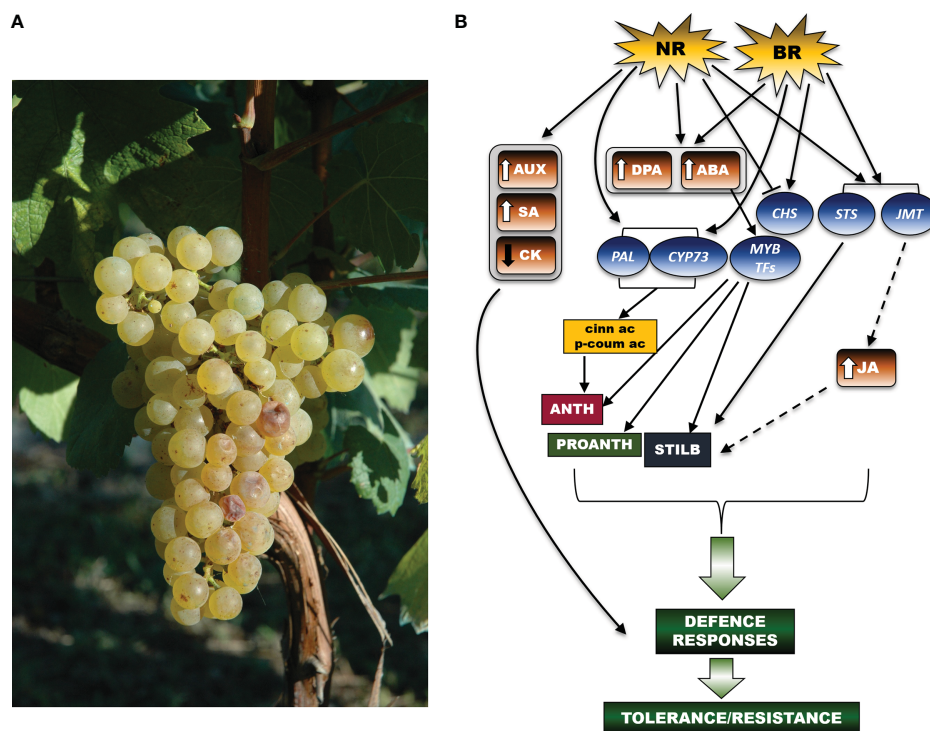


FIGURE 1

A schematic representation of the networks of hormonal and molecular signals regulating the secondary metabolism in the grapevine berry in response to *Botrytis cinerea*. **(A)** A grape bunch of *Vitis vinifera* cv Chardonnay showing very initial symptoms of *Botrytis cinerea* infection (credits: A. Ferrandino). **(B)** At the berry level, both NR (Noble Rot) and BR (Bunch Rot) infection induce an increase in DPA (dihydrophaseic acid) and ABA (abscisic acid) concentrations. ABA accumulation in turn activates the transcription of *MYB* genes regulating the biosynthesis of stilbenes, proanthocyanidins (PROANTH) and anthocyanins (ANTH). Response to NR also involves the upregulation of genes linked to auxin (AUX) and salicylic acid (SA) metabolism, and, in parallel the downregulation of the cytokinin (CK) metabolism. Following both NR and BR infection, the observed upregulation of jasmonate *O*-methyltransferase (*JMT*) transcripts suggests that jasmonate (JA)-mediated signals (stilbene = STILB biosynthesis) are also established. Furthermore, upon NR and BR development, genes of the phenylpropanoid pathway (*PAL*, phenylalanine ammonium lyase; *CYP73*, trans-cinnamate 4-monooxygenases) are turned on, downstream leading to the production of cinnamic acid (cinn ac) and p-coumaric acid (p-coum ac), which are intermediate bricks of the phenylpropanoid pathway. While *STS* isoforms are highly expressed in both NR and BR-infected berries, transcription of chalcone synthase (*CHS*) genes is differently regulated between NR (downregulation) and BR (upregulation). The set of displayed signals all converge to initiate defence mechanisms in turn leading to tolerance or resistance responses to the pathogen (as underlined by the curly green bracket). In the figure scheme, the arrows connecting the different signal effectors highlight activation of a specific molecular or metabolic pathway, whereas the blunt arrow points to inhibition of the downstream target(s). The dashed arrows display those signalling cascades that have been suggested but still need further experimental confirmation. The arrows beside the hormone acronyms refer to increase (↑) or decrease (↓) of accumulation. The thick green arrows point to the establishment of plant defence processes resulting from the activation of the upstream signalling pathway(s). Brown boxes refer to phytohormones, blue balloons indicate genes, while the rectangular refer to metabolites.

and in response to ET and methyl jasmonate (MeJA) treatments, is also significantly up-regulated in berries (cv Shuang You; Zhu et al., 2022). Such results confirm a previous study reporting that *ERF16* was overexpressed in grapevine leaves inoculated with *Bc* (Zhu et al., 2019), thereby suggesting that *VaERF16* positively affects the plant's immunity system against this pathogen. Although *Bc* is classified as a necrotrophic fungus, besides the JA/ET hormonal crosstalk, SA-mediated signalling (generally associated with biotrophic responses) also regulates the *Bc* × *Vitis* spp. interaction (Wang et al., 2020, *Bc* × *Vitis quinquangularis*). Zhu and co-workers (2022) confirmed the involvement of the SA-based regulatory network in the *Vitis amurensis*-*Bc* pathosystem, indicating that in leaves, *ERF* genes contribute to the immune responses through both SA and JA/ET signalling pathways. Moreover, *ERF16* was suggested to regulate plant immune responses by interaction with other genes. In particular, *ERF16* interacts with *VaMYB306*, a homologue of

AtMYB30, which is a positive regulator of the hypersensitive cell death programme in response to pathogen attack (Vailleau et al., 2002). Seventy-two hours after the *Bc* inoculum, the transcription of *VaMYB306* was induced up to 6-fold in the leaves of *V. amurensis* 'Shuang You' in comparison with the non-inoculated controls. Accordingly, the leaves from *VaMYB306*-OE plants showed enhanced resistance against the pathogen whereas those from *VaMYB306*-silencing lines experienced an increased susceptibility. Moreover, both MeJA and ET enhanced *VaMYB306* transcription. This suggests that *VaMYB306* could promote resistance to *Bc* in a JA/ET signalling-dependent manner. Another important, recent finding elucidating the complex grapevine response to *Bc*, concerns the combined effect exerted by *VaERF16* and *VaMYB306*: together, they increased by 3.5-fold the promoter activity of *VaPDF1.2*, a key defence gene functioning downstream of the JA and ET signalling pathways (Zhu et al., 2022).

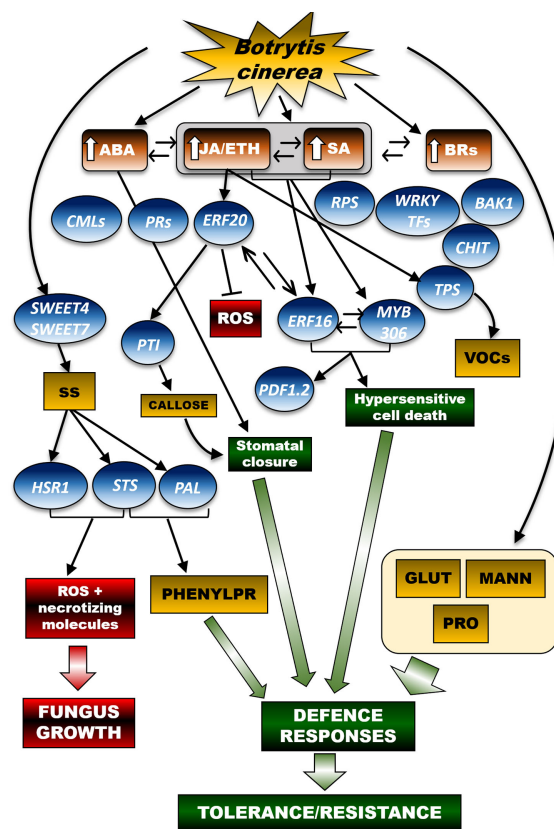


FIGURE 2

A schematic representation to display the networks of hormonal and molecular signals controlling defence secondary metabolic pathways in the grapevine leaf in response to *Botrytis cinerea* (*Bc*). In young and adult grapevine leaves, tolerance/resistance responses to *Bc* involve the crosstalk of different hormonal pathways, namely ABA (abscisic acid), JA/ETH (jasmonic acid/ethylene), SA (salicylic acid) BRs (brassinosteroids), in turn leading to activation of key molecular effectors of the plant defence system, such as PRs (pathogenesis-related proteins), RPS (disease resistance protein), CMLs (calcium-binding proteins), WRKY transcription factors, BAK1 factor (brassinosteroid insensitive 1 factor), ERF (ethylene responsive factor), and CHIT (chitinases). Infection-mediated metabolic biomarkers also include GLUT (glutathione) and osmoprotectants, such as MANN (mannitol) and PRO (proline). In parallel, defence mechanisms to *Bc* involve the activation of the sugar transporters SWEET4 and SWEET7 (Sugars Will Eventually be Exported Transporter 4 and 7), in turn enabling a leaf-specific increase in soluble sugar (SS) concentration. On one hand, SS accumulation turns on the transcription of STS (stilbene-synthase) and HSR1 (hypersensitivity related protein 1 genes). The sugar signal triggers PAL-based biosynthetic pathways leading to the accumulation of key defence secondary metabolites (stilbenes). Upon *Bc* infection, JA/ETH and SA-responsive molecular cascades trigger the ERF20-mediated transcription of PTI genes, thereby facilitating plant immunity processes and inhibition of ROS (reactive oxygen species). Crosstalk between the JA/ETH and SA-based pathways enables ERF16 and MYB306, whose coordinated activity stimulates key immunity-related molecular effectors, such as the PDF1.2 factor (plant defensin factor 1.2), and hypersensitive cell death programs able to counteract the pathogen spread. Based on the infection timing, JA/ETH-responsive signals also promote the expression of TPS, thereby leading to the production of defence VOCs (volatile organic compounds). In the figure scheme, the arrows connecting the different signal effectors highlight activation of a specific molecular or metabolic pathway, whereas the blunt arrow points to inhibition of the downstream target(s). Crosstalk of hormonal or molecular signals is instead displayed by double arrows. The arrow beside the hormone acronyms refers to increase (↑) of that hormone accumulation. The thick green arrows point to the establishment of metabolic processes resulting from the activation of the upstream signalling pathway(s), namely defence responses of the plant (green boxes) or fungus growth-related processes (red boxes). Brown boxes refer to phytohormones, blue balloons indicate genes and yellow rectangles refer to metabolites. SS, soluble sugars; VOCs, volatile organic compounds; ROS, reactive oxygen species; GLUT, glutathione; MANN, mannitol; PRO, proline; PHENYLPR, phenylpropanoids.

Based on the trigger effect exerted by JA on the accumulation of VOCs, including terpenoids, the influence of *Bc* infection on VOCs has been investigated by many authors. Recently, this subject has been thoroughly reviewed in grapevine (Lazazzara et al., 2021). In berries of Muller-Thurgau and Garganega artificially infected with *Bc*, a strong transcriptional activity of genes related to jasmonic acid and ethylene production was found (Lovato et al., 2019). These events were mainly directed to trigger the phenylpropanoid pathway, including the stilbenoid branch, as terpene synthase genes were highly expressed exclusively at the earliest stages of *Bc* infection. At later stages, a decrease in the expression of terpene

synthase (TPS) genes was observed, indeed reducing the accumulation of terpenoids, in turn, and most likely enhancing the plant's susceptibility to the pathogen. A recent study on tomato plants has demonstrated that methyl-jasmonate-knockout-mutants plants showed a much lower TPS expression than wild-type controls, in turn resulting in a higher susceptibility to *Bc* (Cao et al., 2022). It was previously demonstrated that the timing of *Bc* infection could influence the regulation of TPS expression (Mendes et al., 2014). TPS transcripts were overexpressed early, following the fungal infection, and afterwards they were progressively downregulated. This information suggests that the *Vitis vinifera* ×

Bc interaction does not exclusively influence the higher or lower expression of *TPS*, but that these effects may co-exist, and a major role in defining their occurrence seems to be played by the moment at which the interaction is studied. A recent metabolomic analysis further revealed significant differences in the initial metabolic profiles of berries from two Greek *Vitis vinifera* varieties, Limnio and Roditis, which display high and limited tolerances to the pathogen, respectively. In response to the inoculation, the abundance of several osmoprotectants increased in the resistant Limnio cultivar, namely proline and mannitol, and some phenylpropanoids and metabolites associated with lignin biosynthesis (Tziros et al., 2022). Sugar transporter genes (*SWEET*s genes, Sugars Will Eventually be Exported Transporter) are also involved in the grapevine response to necrotrophic pathogens. In detail, *SWEET4* was upregulated in response to *Bc* infection in the leaves of *Vitis vinifera* line 40024, 72 and 96 hours after pathogen inoculation, together with two other isoforms (*VvSWEET2* and *VvSWEET7*), which were moderately induced (Chong et al., 2014). The *SWEET4* upregulation occurred concomitantly with a tissue-specific increase in sugar concentration. This probably facilitated the fungus's nutrition and is associated with increased expression of *VvSTS* and *VvHSR*, higher accumulation of ROS, and higher accumulation of necrotizing molecules (Chong et al., 2014). Additionally, *SWEET7* expression was induced upon *Bc* (and *Erysiphe necator*) infection, probably to support the pathogen nutrition and to promote the grapevine response to the pathogen via production of defensive secondary metabolites (Breia et al., 2021). Accordingly, the local *SWEET*-mediated increase in sugar concentration could serve as a trigger for the observed activation of the phenylpropanoid pathway. Such strict relationship between sugar accumulation and phenylpropanoid pathway activation was long-time demonstrated in berries (Pirie and Mullins, 1976). It is therefore conceivable that the up-regulation of *SWEET* genes can not only support the pathogen growth, but it can also boost the grapevine's defence metabolism through the activation of the PAL-mediated-downstream pathways. In the *Bc* (as NR) × grapevine interaction, carbohydrate-related enzymes were activated, particularly at the onset of NR development, during the transition from the phase I to II of berry growth. In line with what was observed for *TPS*, these findings reveal that the main structural changes in the plant's defence metabolism occur early in the NR process (Hegyi et al., 2022).

3.2 Grapevine trunk diseases

The five main diseases recently referred to as GTDs are: *Botryosphaeria* dieback, *Eutypa* dieback, the esca disease complex, *Phomopsis* dieback and *Black foot* (Bertsch et al., 2013). However, other fungal genera and species, especially *Ascomycota* and *Basidiomycota*, have been found in association with GTDs, and it has also been demonstrated that the specific fungal association depends on climatic and geographical factors. *Ascomycota* *Eutypa lata* is the main causal agent of *Eutypa* dieback, and *Phaeomoniella chlamydospora*, *Phaeoacremonium minimum* and *Fomitiporia mediterranea* are the main causal agents of one or more of the

syndromes associated with the esca complex. These fungal species are certainly the most widely diffused, though several other pathogenic fungi have been isolated from esca symptomatic plants (Mugnai et al., 1999; Surico, 2009; Del Frari et al., 2021). GTDs main symptoms include wood discoloration, necrosis and foliar symptoms. Strong manifestation of these symptoms induces profound alteration of the grapevine physiology, leading to shoot death, yield reduction, and the death of canes, spurs and even the vine. A progressive weakness of the viticultural agro-ecosystem can be ascribed to GTDs *per se* and to their interactions with vines in increasingly arid conditions. Another factor that significantly influences the GTD × grapevine interaction is the grapevine's age. The GTD-associated fungal population inhabiting adult vines includes esca, *Botryosphaeria*, and *Eutypa*. Conversely, the main GTDs in young leaves are the Black foot disease, Petri disease or diebacks due to *Botryosphaeriaceae*, *Verticillium* or *Fusarium* as recently reviewed by Claverie and co-workers (2020). These authors proposed three conceptual models of the framework grapevine × GTDs × environment. The first describes the possible timing of events leading to leaf symptoms. Accordingly, foliar symptoms appear at the end of three steps (infection, colonization and symptom appearance) that can last from few months to several years, or can occur several times per year and on different parts of the plant, ultimately leading to yield reduction, berry quality loss, and wood destruction. The second model considers the grapevine × pathogen interaction and explains that the vine's need to establish a defence response should be considered as a further sink for carbon demand. This sink becomes a competitor of shoot growth, floral induction, berry set, and berry ripening, thereby unbalancing the physiological status of the whole vine and seriously endangering the plant's survival, sometimes leading to apoplexy. The third model provides a complex and holistic interpretation that adds to the grapevine × fungi relationship the microbiota and the environment. Since viticulturists design the vineyard establishment, including rootstock choice and agronomic and protection practices, they must be aware that their choices can also impact GTD spread, and in turn impact grapevine physiology.

The contribution of this review is mainly based upon the second and the third models. In a vineyard historically affected by Esca disease, beside the main Esca-associated fungi *P. chlamydospora* and *Fomitiporia* sp., five further genera (*Debaryomyces*, *Trematosphaeria*, *Biatrispora*, *Lopadostoma*, and *Malassezia*) were found in adult (19 years old) grapevines of Cabernet Sauvignon vines (Del Frari et al., 2019). Collectively, the authors identified 289 taxa, revealing the greatest fungal richness until now. However, 80% of these taxa displayed very low abundances (< than 0.1%) and high variability in their composition depending on factors such as plant age, agricultural practice, and environmental conditions. No positive, neutral or negative roles have been ascribed to them. Nevertheless, in the ongoing climate change scenario, one can speculate that these or other new taxa could emerge in the next years, and either become detrimental for viticulture or remain neutral (Corredor-Moreno and Saunders, 2020). Oppositely, they could acquire a positive role, if they are able to limit the development of more pathogenic taxa. The type of fungal species associated with the Esca disease in wood depends on the analysed

organ (Del Frari et al., 2019) and on the *Vitis* species. Artificial inoculations of *Fomitiporia punctata* in Kober 5BB (*V. berlandieri* × *Vitis riparia*) led to low re-isolation percentages of this pathogen (8% of inoculated plants; Sparapano et al., 2000). Del Frari and co-workers (2019) did not find *Fomitiporia* sp. in the graft union point of 140 Ru (*V. berlandieri* × *V. rupestris*), albeit *Fomitiporia* sp. was well represented in all permanent wood of Cabernet Sauvignon. Such findings confirm the hypothesis that the *Vitis* genotype can profoundly influence the disease development. Interactions of the mycobiome with *Vitis* genotype, plant age, organs, and environment, clearly demonstrate that studies on singular interactions between grapevine with one or a few wood pathogens are limitative with respect to reality in a viticultural context. However, the biological understanding of the interplay that comes from these kinds of studies is fundamental to interpreting present and future grapevine/wood disease interactions on a broader scale, as well as at a productive level.

Modifications of plant metabolism occurring early during the disease development have been detailed, demonstrating that alterations become greater as soon as visible symptoms appear on the leaf (Valtaud et al., 2009). Mainly, an increase in leaf sugar concentration was observed together with *PAL* transcript activation and consequent polyphenolic accumulation in leaves. Changes in tannin content (increase) and glutathione concentration (decrease) in apparently healthy-looking leaves located on infected shoots were described at the beginning of the season. Furthermore, changes in glutathione *S*-transferase (*GST*) gene expression in the leaves of Ugni blanc collected from healthy and diseased grapevines in field conditions were assessed. At early stages of infection prior to the appearance of visible leaf symptoms, *GST* activity, amounts of *GSTU1*- and *GSTF2*-encoding genes and abundance of the *GSTU1* and *GSTF2* proteins were the highest. Afterwards, they progressively decreased during the season, as soon as visible leaf symptoms emerged (Valtaud et al., 2009). Moreover, in another study conducted on adult (>20 years old) Chardonnay grapevines grafted onto the 41B rootstock (*V. vinifera* × *V. berlandieri*) and affected by the leaf stripe form of Esca, an early induction of *GST1* expression was noticed in pre-symptomatic leaves, suggesting that early and transient activation of *GST1* could help the vine to detoxify fungal toxins (Magnin-Robert et al., 2011). In that study, an inverse regulation of photosynthesis- and defence-related genes was also observed. Similarly, a gradual, transient increase in *PAL*, *LOX* and *PR6* expression occurred in pre-symptomatic leaves in parallel to a decrease in the vine's assimilation rates. Unexpectedly, the expression of those defence-related genes was inhibited in the green area of fully symptomatic leaves and no alteration was observed in the chlorotic area. These results suggest that grapevine may perceive some signals and react by triggering defence pathways before the appearance of foliar symptoms. This highlights the grapevine's ability to activate its defence system promptly; however it is also evidence of reduced capability to promote strong defence reactions once the leaves become symptomatic. Previous studies demonstrated that the activation of *PAL* and *STS* genes involved in the biosynthesis of stilbenoids result in high amounts of resveratrol both in woody tissues (Amalfitano et al., 2000; Martin et al., 2009) and in leaves and berries of esca-

affected vines (Calzarano et al., 2008). The *GST* pathway activation could be an early grapevine response to Esca disease, intended to distribute the pathogen-induced signals throughout the vine vascular system (Valtaud et al., 2009; Magnin-Robert et al., 2016). Amounts of fungal metabolites, plant metabolites (stilbenes) and hormones (ABA), and plant transcripts involved in pathogenesis and water stress response (e.g. *PRs*, *HSPs*, *SOD*, *GSTs*, *TIPs*, *NCED*), changed in apoplectic and pre-apoplectic grapevine tissues. Moreover, carbohydrate, aminoacid and phenylpropanoid related-gene expression varied with grapevine age. For instance, young apoplectic grapevines had higher phenol concentrations in wood than esca-diseased plants, while asymptomatic wood of diseased plants showed higher stilbene concentration (Magnin-Robert et al., 2016). This knowledge, together with previous information on phenylpropanoid activation after different pathogen attacks may call for a shift toward either *CHS* or *STS* activation in grapevine tissue following biotic stress events. A recent paper (Khattab et al., 2021) proved that some lines of *V. vinifera sylvestris*, the ancestor of the cultivated *V. vinifera*, with different levels of susceptibility to *Neofusicoccum parvum* (associated with *Botryosphaeriaceae*-related dieback), accumulated higher amounts of stilbenoids, resveratrol and trimeric viniferins. The authors proposed that a stress signal, including a JA-mediated signal, triggered the activation of *PAL*, *STS* and *JAZ* in all genotypes, regardless of their level of susceptibility. Furthermore, while susceptible lines accumulated piceid (the glucosidic form of resveratrol, probably less efficient in limiting pathogens, due to its lower antioxidant activity), the resistant lines produced high amounts of non-glycosylated resveratrol and viniferins.

Time can influence the grapevine × GTD interaction: a time-dependent response of grapevine varieties to *P. chlamydospora* was found in a model study of cuttings of three grapevine cultivars, Merlot and Carignan - considered moderately susceptible - and Cabernet Sauvignon - considered highly susceptible - were let absorbing a culture filtrate of the fungus. Very early, the least susceptible varieties showed an overexpression of *PR*-proteins, *PAL* and *STS* genes, together with a higher concentration of stilbenoids, respect to highly susceptible Cabernet Sauvignon (Lambert et al., 2013). Overexpression of *PAL* and *STS* was also found in Cabernet Sauvignon cuttings inoculated with *P. chlamydospora* alone, with *Phaeoacremonium aleophilum* alone, or with the two pathogens together (Pierron et al., 2016). These authors noticed that other genes were also overexpressed, namely *PR10.3*, *TL*, *TLb*, *Vv17.3*, *STS8*, *CWinv*, *PIN*, *CAM*, *LOX*, and that all of them (with the exception of *LOX* and *CAM*) were up-regulated in response to the wounding caused during the pathogen inoculation. However, although this baseline noise was detected, it was clearly found that gene overexpression still differs based on perception of mycelium. Moreover, 48 hours after inoculation, the induction of *PAL* and *STS8* differed depending on the pathogen, revealing a higher over expression in the interaction of grapevine with *P. aleophilum* rather than with *P. chlamydospora* (Pierron et al., 2016).

Further important breakthroughs into the understanding of GTD × grapevine interaction were provided by Fischer and co-workers (2016). In the totally controlled conditions of the co-culture of *Vitis vinifera* L. calli (cv Gamay Fréaux) with

P. aleophilum and *P. chlamydospora*, changes were observed in the fungus metabolism. Transcriptome reprogramming events were differently induced by the two fungi: *P. chlamydospora* triggered an increase in the expression of oxidoreductases, plant cell-wall degrading enzymes and detoxifying enzymes, whereas *P. aleophilum* activated only some genes encoding oxidoreductase, as well as heat shock and chaperon-like proteins, and enzymes involved in primary metabolism. Although the two fungi occupied the same ecological niche within the grapevine trunk, by predominantly developing within the xylem vessels and surrounding cell walls, they displayed different metabolic expressions (Fischer et al., 2016). However, regardless of the fungal species, the number of fungal genes differentially modulated during the grapevine's callus formation was extremely low, probably because the plant cells did not cause extreme stress on the fungi and did not solicit very aggressive measures by the fungi. These findings are consistent with the observation that *P. aleophilum* and *P. chlamydospora* can be found in apparently healthy plants, that the outbreak of the disease may take several years to occur, and that young vineyards rarely show Esca symptoms.

In a study concerning the tripartite interactions among greenhouse-grown cv Cabernet Sauvignon at the state of 7-8 expanded leaves, *P. chlamydospora*, and the biocontrol-oomycete *Pythium oligandrum*, both the grapevine's and the fungus's metabolisms were affected. The biocontrol oomycete *Pythium oligandrum* shaped the expression of specific grapevine defence-related genes, and the *P. chlamydospora* + *P. oligandrum* association promoted JA/ET signalling pathways, particularly at early infection stages (Yacoub et al., 2020). Previous studies on *P. chlamydospora* demonstrated its pectinolytic capacity (Marchi et al., 2001), suggesting that the fungus can degrade pectin-rich pit membranes as well as deposits of gel/tylose that are secreted in vessels by the host in response to infection. Accordingly, histopathological studies confirm that *P. chlamydospora* mainly resides in the vasculature (Valtaud et al., 2009; Fleurat-Lessard et al., 2010) and can also spread within those vessels occluded by tyloses and gels, thanks to its pectinolytic activity. The grapevine's need to synthesize occluding material to limit the fungus progression might reduce the energy resources otherwise used to establish active chemical defence responses, particularly in peri-vascular tissues. Therefore, for cultivars with xylem vessels of small diameter, like Merlot, vessel occlusion strategies could be quicker and easier, and consume less energy to restrict the spread of mycotoxins throughout the sap. On the contrary, in cultivars with wider vessels (e.g. Cabernet Sauvignon) those reactions could be less efficient in hindering the fungus's spread. In addition, in small vessel-cultivars, the ease of occluding the vasculature could favour the physical compartmentalization of fungi (Pouzoulet et al., 2014; Pouzoulet et al., 2020a). A recent study showed that in the nursery, three different grafting techniques adopted on three different *V. vinifera* varieties onto the same rootstock (Kober 5BB) allowed diverse levels of callus formation and vascularization of the grafting point (Battiston et al., 2022). Such results confirm the influence of the genotype on wood formation and response to pathogens. However, these authors did not find a strict relationship between vessel

diameter/density and the potential susceptibility of the vine to GTDs. Ramsing and co-workers (2021) correlated 25 *Vitis* spp. rootstocks with DNA concentration of *P. chlamydospora* and *P. minimum*, demonstrating that some of them, such as *V. berlandieri* Resseguier 1 and Castel 6736 (*V. riparia* × *V. rupestris*), harboured significantly lower pathogen DNA concentrations in association with significantly narrower vessel diameters. Based on the rootstock genotype, the authors reported narrower vessel diameters for *V. berlandieri* × *V. vinifera*, *V. riparia*, *V. riparia* × *V. rupestris* and *V. rupestris*. The threshold for the identification of grapevine susceptibility to *P. chlamydospora* and *P. minimum* was associated with the pathogen DNA load. For instance, significantly higher *P. chlamydospora* DNA concentrations were detected for vessel diameters ranging from 55 to 64 µm and vessel area of 0.2–0.24 mm². Conversely, a higher *P. minimum* titre was found for a xylem density of above 66 vessels/mm² (Ramsing et al., 2021). Foglia and collaborators (2022) studied the vessel diameter of 24 red-berry varieties and 27 white-berry varieties, all grafted on Kober 5BB (*V. berlandieri* × *V. riparia*), and showed that *V. vinifera* varieties display a wide variability in vessel diameters, ranging from 70–80 µm to around 160 µm. Interestingly, authors found an on-average higher vessel diameter in the white varieties respect to the red ones. However, they did not identify any clear correlation between vessel diameter and cultivar susceptibility to GTDs.

We were not able to find specific information about Kober 5BB vessel diameter, however we could for SO4, another hybrid of *V. berlandieri* × *V. riparia*. In 2016 Santarosa and co-workers classified this genotype as a vigorous rootstock (Santarosa et al., 2016). Ramsing et al. (2021) confirmed these features, also showing high vessel density and high level of vascularization.

Since European viticulture is mostly grafted, it is important to merge this fundamental information. Different *Vitis* species display different vessel diameters, which confer to the rootstock-scion combination different vessel embolization tendency: wider the vessel, higher the hydraulic conductivity, higher the vigour induced to the scion, but higher the tendency to embolize under drought. Moreover, grapevine vessel diameters depend on the water availability of the season, as morphological traits of the vascular system, such diameters, are known to present developmental plasticity that responds to environmental factors during the plant growth (Lovisolo and Schubert, 1998; Munitz et al., 2018; Pouzoulet et al., 2020b). Besides the hydraulic aspects tied to vessel dimensions and density, the higher/lower regulation of water transport under perivascular cell metabolic control in both root and shoot (Lovisolo et al., 2008a; Perrone et al., 2012; Chitarra et al., 2014) could be pivotal to understanding the GTD relationship with embolism repair strategies in grapevine. For instance, it can be hypothesized that *V. berlandieri* × *V. rupestris* rootstocks, which embolize less than *V. berlandieri* × *V. riparia* rootstocks, and also display a more efficient way to recover from drought embolisms (Lovisolo et al., 2008a), could be less susceptible to GTDs in field conditions. In turn, this feature could be linked to the mainly ABA-mediated metabolic control of water transport within the vasculature and vessel-associated cells (VACs). Cycles of drought events followed by fast recovery are progressively becoming more frequent in many viticultural areas worldwide (Patono et al., 2022) due to the pressure

of climate change. Such conditions can increase xylem sap ABA concentration (Lovisolo et al., 2008b; Morabito et al., 2021) and ABA delivery from root to shoot. Since ABA signalling triggers the activation of *PAL* genes, we can suggest that the root-to-shoot ABA transport could regulate the accumulation of polyphenols in VACs, thereby acting as defence response to GTDs. This would therefore mirror what happens in leaves and fruits during fruit ripening, in line with what has been thoroughly investigated in grapevine × abiotic stress interactions (reviewed in Ferrandino and Lovisolo, 2014).

Such an intricate network of players adds to the changing vineyard environment and highlights the complexity of the study of the biological response of grapevine to GTDs; consequently, it also explains why successful protection practices addressed to control GTDs are still to be developed.

3.3 Phytoplasma infection

Phytoplasmas represent a group of phloem-limited wall-less microorganisms similar to bacteria, and taxonomically ascribed to the class of *Mollicutes*, which cause serious losses in productivity of many crops worldwide (Bendix and Lewis, 2018). In European viticulture, phytoplasma-associated diseases are commonly referred to as grapevine yellows; the most economically impacting are Flavescence dorée (FD) and Bois Noir (BN). Although FD outbreak occurred more recently than BN, vineyard damages due to its rapid spread were, and still are, heavier, especially in some countries like France and Italy. Symptoms associated with FD and BN infections are often indistinguishable visually; both typically display leaf yellowing or reddening depending on the grape cultivar, leaf downward curling, drying of inflorescences and bunches, fruit abortion, shortening of internodes, and lack of shoot lignification. Although no resistance to the two diseases has been detected yet, an increasing number of studies have reported different tolerance degrees according to specific cultivars (Eveillard et al., 2016) as well as cases of spontaneous symptom remission in field-grown vines (Morone et al., 2007; Santi et al., 2013; Landi et al., 2019). Additionally, it clearly appears that such physiological responses are often correlated with the accumulation of specific defensive secondary metabolites.

Mounting experimental evidence has demonstrated that among the first metabolic effects of FD and BN infection, there is a serious alteration in primary metabolic pathways and in the transport of hexose sugars, which relies, at the molecular level, on a wide transcriptional reprogramming of the functional gene categories linked to carbohydrate, photosynthesis, and energy metabolism (Hren et al., 2009; Prezelj et al., 2016; Pacifico et al., 2019; Pagliarani et al., 2020). These responses reflect the impaired physiological functions of infected vines, which display a reduction in the rates of assimilation, stomatal conductance and chlorophyll content (Vitali et al., 2013). Changes in photosynthate translocation inevitably cause a block of sugar export that, by strongly reducing phloem loading, causes the source-to-sink switch of leaves: a plant defence response also reported in

presence of other leaf pathogens, such as fungi and viruses (Hayes et al., 2010; Chitarra et al., 2018). In parallel, this intense modification in sugar transport interferes and changes the secondary metabolite build-up; indeed, it is well established that mobilized sugars enter the shikimate pathway and the subsequent secondary metabolic reactions, particularly those tied to the phenylpropanoid biosynthesis (Ehness et al., 1997; Rolland et al., 2002). In fact, a common hallmark of phytoplasma infection is the conspicuous accumulation of flavonoid molecules in the leaves, particularly of anthocyanins, due to the sugar-mediated transcriptional activation of many flavonoid biosynthetic genes. Therefore, it has been proposed that the strong mobilization of sugars and antioxidant compounds can represent a biological strategy for counteracting pathogen spread and protecting plant tissues from further oxidative damage (Margaria et al., 2014).

Over the last years, knowledge of secondary metabolic modifications triggered by phytoplasma infection has been significantly advanced. This has highlighted interesting differences occurring in the profiling of specific classes of secondary metabolites that were put in correlation with genotype susceptibility, as well as with recovery mechanisms. In 2014, Margaria and co-workers, provided the first integrated metabolic and transcriptomic survey concerning the analysis of different compounds of the flavonoid biosynthetic pathway in FD-infected, recovered, and healthy leaves of the red-grapes Nebbiolo and Barbera, which are respectively reported to display low and high susceptibility to FD (Roggia et al., 2014). Although an increase in total anthocyanins did occur in both varieties following infection, anthocyanin concentrations were much higher in Barbera than in FD-infected-Nebbiolo samples, in accordance with the overall more intense reddening of the leaves of this cultivar. Nevertheless, infected Nebbiolo leaves showed an increase in quercetin glycosides with respect to kaempferol-derivatives, and a higher constitutive and FD-induced accumulation of low-molecular weight proanthocyanidins. These data, corroborated with different expression of key related genes and coupled with the observation that healthy and recovered Nebbiolo leaves were characterized by a higher basal content of proanthocyanidins than Barbera, led the researchers to hypothesize that those metabolic signatures could underpin the low susceptibility of Nebbiolo to the disease (Margaria et al., 2014). A thorough modulation of the phenylpropanoid biosynthetic pathway also typically occurs in vines affected by BN. Experiments recently performed by Negro et al. (2020) evidenced that BN-infected leaves of the red-grape Sangiovese accumulated high levels of total phenolics and flavonoids, concomitantly with a reduction in lignin concentration; they suggested this aspect was most likely a consequence of the diversion of the common precursors (hydroxycinnamic acids) towards the flavonoid pathway. The authors' findings also revealed that increased levels of total anthocyanins in BN-positive samples were exclusively due to the predominant synthesis of cyanidin 3-O-glucoside, whereas BN-negative leaves accumulated the highest concentrations of quercetin.

It is, however, important to remember that some of the above-described responses are strongly dependent on the cultivar

genotype; moreover, they could change based on the phytoplasma type and even on the specific phytoplasma strain (e.g. FDp C or D). For instance, in a study conducted on the highly FD susceptible cultivar Modra frankinja, Prezlj and co-workers (2016) found that compounds downstream of the proanthocyanidin branch, like epicatechin and catechin, accumulated greatly in infected samples. This is in line with what was found in infected Barbera vines (high susceptibility) studied in Margaria et al. (2014).

Intriguingly, besides depending on genotype and sanitary status, the overall quantity and partitioning of secondary metabolites could differ based on the portion of analysed leaf tissue, as demonstrated in infected, recovered and healthy plants of Nebbiolo and Barbera by comparing levels and profiles of target metabolites in whole leaves, leaf blades and leaf mid veins (Ferrandino et al., 2019). Although flavonols were constitutively more expressed in whole leaves of Barbera than of Nebbiolo, the separate analysis of leaf blades and veins revealed that FD-infected Nebbiolo samples had higher flavonol contents, particularly quercetin glycoside. The authors also found that hydroxycinnamate (HCTA) concentrations followed different genotype-dependent accumulation patterns, indeed their concentration was higher in entire leaves of Barbera than Nebbiolo, regardless of the sanitary status. Conversely, in Nebbiolo, increases in HCTA amounts were detected only in association with the phytoplasma presence and only when leaf veins and blades were analysed separately, also disclosing a higher percent-incidence of the caffeic acid ester. Similar accumulation patterns were also shown for flavan-3-ols, for which higher synthesis of the dimeric proanthocyanidin B1 was observed in Nebbiolo, together with a higher constitutive and FD-induced concentration of astilbin (dihydroquercetin-rhamnoside; Kedrina-Okutan et al., 2018) in veins. Such peculiar changes at the level of single phenylpropanoid molecules may contribute to enhancing the antioxidant capacity of Nebbiolo, thus making this cultivar more efficient at limiting the phytoplasma spread than Barbera (Ferrandino et al., 2019).

Similar considerations on the involvement of individual molecules in phytoplasma pathogenesis and genotype-mediated defence responses come from the analysis of stilbenoids. However, it has been emerging only recently that increases in some groups of these compounds could also elicit disease tolerance and/or recovery mechanisms to phytoplasma diseases. Pagliarani et al. (2020) reported the highest concentrations of total stilbenoids in FD leaf vein-enriched samples of cv Barbera, but they observed the presence of specific stilbenoids, such as viniferin, exclusively in the samples taken from recovered vines and consistently with the overexpression of many stilbene synthase-encoding genes.

Distinct biological functions of single stilbenoid categories in relation to a specific sanitary condition (i.e. infected or recovered) were also suggested in the presence of BN. For instance, Negro et al. (2020) found higher amounts of resveratrol in BN positive samples. Therefore, changes in the polyphenol profiles can mark the different susceptibility degree of grapevine genotypes to phytoplasma. Further information gained on additional genotypes with intermediate levels of susceptibility to FD or BN will be precious for elucidating to what extent the phenylpropanoid pathway can contribute to establishing

specific defence responses in different *V. vinifera* cultivated varieties. Additionally, the survey carried out by Paolacci and co-workers (2017) proved that the production of distinct phenols, stilbenoids in particular, in association with either infection or recovery is achieved through deep perturbations in hormone signalling cascades, respectively involving salicylic (SA) and jasmonic (JA) acids. Such tight relationship between phytoplasma infection/recovery and hormone-based regulation of stilbene metabolism is an intriguing research matter (Dermastia, 2019) that has recently been further investigated by considering diversification of such signals depending on genotype-phytoplasma interaction and on the phenological phase (Dermastia et al., 2021). For instance, cv Zweigelt infected with '*Candidatus Phytoplasma solani*' showed high induction of three transcripts of several genes that encoded for S-adenosyl-L-methionine:salicylic acid carboxyl methyltransferase, which catalyses the formation of the volatile ester methyl salicylate from salicylic acid, showing a peak in the early growing season, concomitant with the overexpression of genes encoding PR proteins. This allowed the identification of a salicylic-acid-dependent, systemic-acquired, resistance signalling. In addition, some genes of the auxin-responsive *GH3* gene family were up-regulated in the infected grapevines of cv Zweigelt. *Candidatus Phytoplasma solani* and FD induced the differential expression of several genes involved in jasmonate biosynthesis, generally showing opposite behaviour in the expression of lipoxygenases, so that the JA role in phytoplasma x grapevine interaction has still to be elucidated. Fifty-nine of the genes associated with ethylene metabolism were affected by *Candidatus Phytoplasma solani* infection of cv Zweigelt, with marked difference during the vegetative season: four genes were up-regulated more than 3-fold early in the season, whereas two genes of the ethylene signalling network were down-regulated later in the growing season. A similar trend was noticed for gibberellin 3-oxidase1 and for a proline-rich protein, which displayed more than 3-fold increase of expression early in the growing season, whereas an overall decrease in gibberellin oxidase gene expression was observed later. Finally, a strong down-regulation of two members of the brassinosteroid biosynthetic branch, both involved in sterol production, was observed in the late growing (Dermastia et al., 2021).

Unlike phenylpropanoids, phytoplasma-mediated changes charged to isoprenoid metabolic pathways have been much less investigated. Recently, novel insights into this subject have been reported by Teixeira et al. (2020) in vines of the Portuguese cultivar 'Loureiro' affected by FD. Following an integrated approach of targeted metabolomics and candidate gene expression analysis, the authors showed that FD infection significantly inhibited all the isoprenoid core metabolic pathways in infected leaves by strongly repressing the key genes associated with chlorophyll, carotenoid, quinone and tocopherol metabolism. Notably, it also emerged that despite the accumulation of many carotenoids, leaf ABA levels increased following FD infection. This is an interesting finding, which deserves further investigation, as it was not accompanied in that survey by upregulation of related biosynthetic genes. Additionally because other authors have reported ABA increases but in association with the recovery, instead of infected sanitary condition (Pagliarani et al., 2020).

4 Concluding remarks and perspectives

All investigations above-described well underline the great complexity of the molecular dynamics governing the build-up of grapevine secondary metabolites in response to altered climate scenario, biotic stress, and genotypes.

Despite the available information, further research efforts should be made to gain a complete picture of the interconnection of primary and secondary metabolic pathways that regulate genotype-specific quality traits at the berry level, particularly those depending on hormonal and sRNA networks. For instance, many open questions remain in the elucidation of epigenetic marks that prime grapevine adaptability to environmental stresses. A deeper knowledge of all those subjects would be undoubtedly helpful for improving viticultural practices and also developing sustainable breeding approaches. In the ongoing scenario of climate change, the main goal for grape growers is to adapt available vineyard management strategies to increasingly challenging conditions, based on the support provided by the research and technical communities. Clone and rootstock choices represent indeed a precious resource for helping in the mitigation of environmental stress effects, both abiotic and biotic. One must be able to mitigate the effects of climate alterations by boosting the grapevine's defence system while preserving fruit quality traits, and to do this, novel, sustainable viticultural practices are needed in the short term (as recently reviewed by [Gutiérrez-Gamboa et al., 2021](#)).

Additionally, although modern genome editing techniques could offer promising cutting-edge tools for improving cultivar resilience and productivity ([Bailey-Serres et al., 2019](#)), the use of such technologies in viticulture is still prohibited in the EU. In addition, the commercialisation of resistant grapevine hybrids is limited and still under discussion, with issues raised related to the preservation of geographical identity of grape cultivars and consumer's appreciation ([Pedneault and Provost, 2016](#)). The commercialisation of new varieties released by breeders is slow because of the long juvenile period of grapevines and of the need of field experiments ([Brault et al., 2022](#)). Therefore, the possibility to adopt and adapt viticultural practices able to mitigate the numerous issues arisen by climate change represents the most valuable strategy on the short-term period.

However, a further emerging strategy to face the negative effects of climate alterations and spread of diseases and pests relies on the exploitation of existing grapevine biodiversity. An effective and timely response to the current global and rapidly changing challenges will indeed be feasible only if the variability of grapevine genetic resources is as large as possible. Rediscovering

and re-evaluating minor but important local varieties can offer interesting applications in terms of sustainable breeding approaches in viticulture. Those are indeed varieties naturally adapted to the conditions of the areas where they had been domesticated, and that can produce wines with unique qualitative and sensory characteristics, able to mirror the character, typicity and success of the wines that historically attract the consumers. A deeper knowledge of the physiological processes underlying the tolerance of these minor, autochthonous grapevine genotypes to abiotic and biotic stresses will be valuable for increasing the resilience of the whole viticultural system ([Wolkovich et al., 2018](#)). Such an approach is therefore particularly promising as it could offer a practical solution for adapting the 'tomorrow' viticulture to future environmental conditions ([Antolín et al., 2022](#)).

Author contributions

AF and CP contributed to the conception of the review. AF, CP and EP-A wrote the first draft of the manuscript. AF and CP wrote and over-viewed the final version. All authors contributed to the article and approved the submitted version.

Acknowledgments

The authors would gratefully acknowledge Prof. Claudio Lovisolo for the helpful discussion and John Joseph Albert Culmone for critical reading and help with English editing of the manuscript.

Conflict of interest

The authors declare that the research was conducted in the absence of any commercial or financial relationships that could be construed as a potential conflict of interest.

Publisher's note

All claims expressed in this article are solely those of the authors and do not necessarily represent those of their affiliated organizations, or those of the publisher, the editors and the reviewers. Any product that may be evaluated in this article, or claim that may be made by its manufacturer, is not guaranteed or endorsed by the publisher.

References

- AbuQamar, S., Luo, H., Laluk, K., Mickelbart, M. V., and Mengiste, T. (2009). Crosstalk between biotic and abiotic stress responses in tomato is mediated by the AIM1 transcription factor. *Plant J.* 58, 347–360. doi: 10.1111/j.1365-3113.2008.03783.x
- Agudelo-Romero, P., Erban, A., Sousa, L., Pais, M. S., Kopka, J., and Fortes, A. M. (2013). Search for transcriptional and metabolic markers of grape pre-ripening and ripening and insights into specific aroma development in three Portuguese cultivars. *PLoS One* 8 (4), e60422. doi: 10.1371/journal.pone.0060422
- Alonso, R., Berli, F. J., Fontana, A., Piccoli, P., and Bottini, R. (2021). Absciscic acid's role in the modulation of compounds that contribute to wine quality. *Plants* 10, 938. doi: 10.3390/plants10050938
- Amalfitano, C., Evidente, A., Surico, G., Tegli, S., Bertelli, E., and Mugnai, L. (2000). Phenols and stilbene polyphenols in the wood of esca-diseased grapevines. *Phytopathol. Mediterr.* 39, 178–183.
- Anesi, A., Stocchero, M., Dal Santo, S., Commisso, M., Zenoni, S., Ceoldo, S., et al. (2015). Towards a scientific interpretation of the terroir concept, plasticity of the grape berry metabolome. *BMC Plant Biol.* 15, 191. doi: 10.1186/s12870-015-0584-4
- Antolín, M. C., Salinas, E., Fernández, A., Gogorcena, Y., Pascual, I., Irigoyen, J. J., et al. (2022). Prospecting the resilience of several Spanish ancient varieties of red grape under climate change scenarios. *Plants* 11, 2929. doi: 10.3390/plants11212929
- Audenaert, K., De Meyer, G. B., and Höfte, M. M. (2002). Absciscic acid determines basal susceptibility of tomato to botrytis cinerea and suppresses salicylic acid-dependent signalling mechanisms. *Plant Physiol.* 128, 491–501. doi: 10.1104/pp.010605
- Bailey-Serres, J., Parker, J. E., Ainsworth, E. A., Oldroyd, G. E. D., and Schroeder, J. I. (2019). Genetic strategies for improving crop yields. *Nature* 75, 109–118. doi: 10.1038/s41586-019-1679-0
- Battiston, E., Falsini, S., Giovannelli, A., Schiff, S., Tani, C., Panaiia, R., et al. (2022). Xylem anatomy and hydraulic traits in *Vitis* grafted cuttings in view of their impact on the young grapevine decline. *Front. Plant Sci.* 13. doi: 10.3389/fpls.2022.1006835
- Bendix, C., and Lewis, J. D. (2018). The enemy within: phloem-limited pathogens. *Mol. Plant Pathol.* 19 (1), 238–254. doi: 10.1111/mp.12526
- Bertsch, C., Ramirez-Suero, M., Magnin-Robert, M., Larignon, P., Chong, J., Abou-Mansour, E., et al. (2013). Grapevine trunk diseases: complex and still poorly understood. *Plant Pathol.* 62, 243–265. doi: 10.1111/j.1365-3059.2012.02674.x
- Blanco-Ulate, B., Amrine, K. C. H., Collins, T. S., Rivero, R. M., Vicente, A. R., Morales-Cruz, A., et al. (2015). Developmental and metabolic plasticity of white-skinned grape berries in response to *Botrytis cinerea* during noble rot. *Plant Phys.* 169, 2422–2443. doi: 10.1104/pp.15.00852
- Bota, J., Tomas, M., Flexas, J., Medrano, H., and Escalona, J. M. (2016). Differences among grapevine cultivars in their stomatal behavior and water use efficiency under progressive water stress. *Agric. Water Manage.* 164, 91–99. doi: 10.1016/j.agwat.2015.07.016
- Brault, C., Lazerges, J., Doligez, A., Thomas, M., Ecartot, M., Roumet, P., et al. (2022). Interest of phenomic prediction as an alternative to genomic prediction in grapevine. *Plant Methods* 18, 108. doi: 10.1186/s13007-022-00940-9
- Breia, R., Conde, A., Badim, H., Fortes, A. M., Geros, H., and Granell, A. (2021). Plant SWEETS: from sugar transport to plant–pathogen interaction and more unexpected physiological roles. *Plant Phys.* 186, 836–852. doi: 10.1093/plphys/kiab127
- Calzarano, F., D'Agostino, V., and Del Carlo, M. (2008). Trans-resveratrol extraction from grapevine: application to berries and leaves from vines affected by esca proper. *Anal. Lett.* 41, 649–661. doi: 10.1080/00032710801910585
- Cao, Y., Liu, L., Ma, K., Wang, W., Lv, H., Gao, M., et al. (2022). The jasmonate-induced bHLH gene SJLH functions in terpene biosynthesis and resistance to insects and fungus. *J. Integr. Plant Biol.* 64, 1102–1115. doi: 10.1111/jipb.13248
- Castellarin, S. D., Gambetta, G. A., Wada, H., Krasnow, M. N., Cramer, G. R., Peterlunger, E., et al. (2016). Characterization of major ripening events during softening in grape, turgor, sugar accumulation, absciscic acid metabolism, colour development, and their relationship with growth. *J. Exp. Bot.* 67, 709–722. doi: 10.1093/jxb/erv483
- Chitarra, W., Balestrini, R., Vitali, M., Pagliarini, C., Perrone, I., Schubert, A., et al. (2014). Gene expression in vessel-associated cells upon xylem embolism repair in *Vitis vinifera* l. petioles. *Planta* 239, 887–899. doi: 10.1007/s00425-013-2017-7
- Chitarra, W., Cuozzo, D., Ferrandino, A., Secchi, F., Palmano, S., Perrone, I., et al. (2018). Dissecting interplays between *Vitis vinifera* l. and grapevine virus b (GVB) under field conditions. *Mol. Plant Pathol.* 12, 2651–2666. doi: 10.1111/mp.12735
- Chong, J., Piron, M. C., Meyer, S., Merdinoglu, D., Bertsch, C., and Mestre Source, P. (2014). The SWEET family of sugar transporters in grapevine: VvSWEET4 is involved in the interaction with *Botrytis cinerea*. *J. Exp. Bot.* 65 (22), 6589–6601. doi: 10.1093/jxb/ere033
- Claverie, M., Notaro, M., Fontaine, F., and Wéry, H. (2020). Current knowledge on grapevine trunk diseases with complex etiology: a systemic approach. *Phytopathol. Mediterr.* 59 (1), 29–53. doi: 10.14601/Phyto-11150
- Corredor-Moreno, P., and Saunders, E. (2020). Expecting the unexpected: factors influencing the emergence of fungal and oomycete plant pathogens. *New Phytol.* 225, 118–1252. doi: 10.1111/nph.16007
- Cramer, G. R., Ghan, R., Schlauch, K. A., Tillett, R. L., Heymann, H., Ferrarini, A., et al. (2014). Transcriptomic analysis of the late stages of grapevine *Vitis vinifera* cv. Cabernet sauvignon berry ripening reveals significant induction of ethylene signaling and flavor pathways in the skin. *BMC Plant Biol.* 14, 370. doi: 10.1186/s12870-014-0370-8
- Curaba, J., Singh, M. B., and Bhalla, P. L. (2014). miRNAs in the crosstalk between phytohormone signalling pathways. *J. Exp. Bot.* 65 (6), 1425–1438. doi: 10.1093/jxb/eru002
- Dal Santo, S., Fasoli, M., Negri, S., D'Inca, E., Vicenzi, N., Guzzo, F., et al. (2016). Plasticity of the berry ripening program in a white grape variety. *Front. Plant Sci.* 7. doi: 10.3389/fpls.2016.00970
- Dal Santo, S., Tornielli, G. B., Zenoni, S., Fasoli, M., Farina, L., Anesi, A., et al. (2013). The plasticity of the grapevine berry transcriptome. *Genome Biol.* 14, R54. doi: 10.1186/gb-2013-14-6-r54
- Dal Santo, S., Zenoni, S., Sandri, M., De Lorenzis, G., Magris, G., De Paoli, E., et al. (2018). Grapevine field experiments reveal the contribution of genotype, the influence of environment and the effect of their interaction GxE on the berry transcriptome. *Plant J.* 93, 1143–1159. doi: 10.1111/tj.13834
- Degu, A., Hochberg, U., Sikron, N., Venturini, L., Buson, G., Ghan, R., et al. (2014). Metabolite and transcript profiling of berry skin during fruit development elucidates differential regulation between Cabernet sauvignon and Shiraz cultivars at branching points in the polyphenol pathway. *BMC Plant Biol.* 14, 188. doi: 10.1186/s12870-014-0188-4
- Del Frari, G., Calzarano, F., and Ferreira, R. B. (2021). Understanding the control strategies effective against the esca leaf stripe symptom: the edge hypothesis. *Phytopathol. Mediterr.* 61 (1), 153–164. doi: 10.36253/phyto-13295
- Del Frari, G., Gobbi, A., Aggerbeck, M. R., Oliveira, H., Hansen, L. H., and Ferreira, R. B. (2019). Characterization of the wood mycobiome of *Vitis vinifera* in a vineyard affected by esca: spatial distribution of fungal communities and their putative relation with leaf symptoms. *Front. Plant Sci.* 10. doi: 10.3389/fpls.2019.00910
- Dermastia, M. (2019). Plant hormones in phytoplasma infected plants. *Front. Plant Sci.* 10. doi: 10.3389/fpls.2019.00477
- Dermastia, M., Škrlić, B., Strah, R., Anžić, B., Tomaž, Š., Kriznik, M., et al. (2021). Differential response of grapevine to infection with 'Candidatus phytoplasma solani' in early and late growing season through complex regulation of mRNA and small RNA transcriptomes. *Int. J. Mol. Sci.* 22, 3531. doi: 10.3390/ijms22073531
- du Plessis, K., Young, P. R., Eyéghé-Bickong, H. A., and Vivier, M. A. (2017). The transcriptional responses and metabolic consequences of acclimation to elevated light exposure in grapevine berries. *Front. Plant Sci.* 8. doi: 10.3389/fpls.2017.01261
- Ehness, R., Ecker, M., Godt, D. E., and Roitsch, T. (1997). Glucose and stress independently regulate source and sink metabolism and defence mechanisms via signal transduction pathways involving protein phosphorylation. *Plant Cell* 9, 1825–1841. doi: 10.1105/tpc.9.10.1825
- Eveillard, S., Jollard, C., Labrousseau, F., Khalil, D., Perrin, M., Desqué, D., et al. (2016). Contrasting susceptibilities to flavescence dorée in *Vitis vinifera*, rootstocks and wild vitis species. *Front. Plant Sci.* 7. doi: 10.3389/fpls.2016.01762
- Ferrandino, A., and Guidoni, S. (2010). Anthocyanins, flavonols and hydroxycinnamates, an attempt to use them to discriminate *Vitis vinifera* l. cv 'Barbera' clones. *Eur. Food Res. Technol.* 230, 417–427. doi: 10.1007/s00217-009-1180-3
- Ferrandino, A., and Lovisolo, C. (2014). Abiotic stress effects on grapevine *Vitis vinifera* l., focus on absciscic acid-mediated consequences on secondary metabolism and berry quality. *Environ. Exp. Bot.* 103, 138–147. doi: 10.1016/j.envexpbot.2013.10.012
- Ferrandino, A., Pagliarini, C., Kedrina-Okutan, O., Icardi, S., Bove, M., Lovisolo, C., et al. (2019). Non-anthocyanin polyphenols in healthy and flavescence dorée infected barbera and nebbiolo leaves. *Bio Web Conferences* 13, 3003. doi: 10.1051/bioconf/20191303003
- Ferrero, M., Pagliarini, C., Novák, O., Ferrandino, A., Cardinale, F., Visentin, I., et al. (2018). Exogenous strigolactone interacts with absciscic acid-mediated accumulation of anthocyanins in grapevine berries. *J. Exp. Bot.* 69 (9), 2391–2401. doi: 10.1093/jxb/ery033
- Fischer, J., Company, S., Pierron, R. J. G., Gorfer, M., Jacques, A., Thines, E., et al. (2016). Differing alterations of two esca associated fungi, *Phaeoacremonium aleophilum* and *Phaeoaniella chlamydospora* on transcriptomic level, to Co-cultured *Vitis vinifera* l. calli. *PLoS One* 11 (9), e0163344. doi: 10.1371/journal.pone.0163344
- Fleurat-Lessard, P., Luini, E., Berjeaud, J. M., and Roblin, G. (2010). Diagnosis of grapevine esca disease by immunological detection of *Phaeoaniella chlamydospora*. *Aust. J. Grape Wine Res.* 16, 455–463. doi: 10.1111/j.1755-0238.2010.00106.x
- Foglia, R., Landi, L., and Romanazzi, G. (2022). Analyses of xylem vessel size on grapevine cultivars and relationship with incidence of esca disease, a threat to grape quality. *Appl. Sci.* 12, 1177. doi: 10.3390/app12031177
- Fortes, A. M., and Gallusci, P. (2017). Plant stress responses and phenotypic plasticity in the epigenomics era, perspectives on the grapevine scenario, a model for perennial crop plants. *Front. Plant Sci.* 8. doi: 10.3389/fpls.2017.00082

- Fortes, A. M., Teixeira, R. T., and Agudelo-Romero, P. (2015). Complex interplay of hormonal signals during grape berry ripening. *Molecules* 20 (5), 9326–9343. doi: 10.3390/molecules20059326
- Gambino, G., Boccardi, P., Pagliarini, C., Perrone, I., Cuzzo, D., Mannini, F., et al. (2021). Secondary metabolism and defence responses are differently regulated in two grapevine cultivars during ripening. *Int. J. Mol. Sci.* 22, 3045. doi: 10.3390/ijms22063045
- Ghan, R., Van Sluyter, S. C., Hochberg, U., Degu, A., Hopper, D. W., Tillet, R. L., et al. (2015). Five omic technologies are concordant in differentiating the biochemical characteristics of the berries of five grapevine *Vitis vinifera* l. cultivars. *BMC Genomics* 16, 946. doi: 10.1186/s12864-015-2115-y
- Gouot, J. C., Smith, J. P., Holzapfel, B. P., Walker, A. R., and Barril, C. (2019). Grape berry flavonoids: a review of their biochemical responses to high and extreme high temperatures. *J. Exp. Bot.* 70 (2), 397–423. doi: 10.1093/jxb/ery392
- Gullino, M. L., Pugliese, M., Gilardi, G., and Garibaldi, A. (2018). Effect of increased CO₂ and temperature on plant diseases: a critical appraisal of results obtained in studies carried out under controlled environment facilities. *J. Plant Pathol.* 100, 371–389. doi: 10.1007/s42161-018-0125-8
- Gutiérrez-Gamboa, G., Zheng, W., and Martínez de Toda, F. (2021). Current viticultural techniques to mitigate the effects of global warming on grape and wine quality: a comprehensive review. *Food Res. Int.* 139, 109946. doi: 10.1016/j.foodres.2020.109946
- Haider, M. S., Kurjogi, M. M., Khalil-Ur-Rehman, M., Fiaz, M., Pervaiz, T., Jiu, S., et al. (2017). Grapevine immune signaling network in response to drought stress as revealed by transcriptomic analysis. *Plant Physiol. Biochem.* 121, 187–195. doi: 10.1016/j.plaphy.2017.10.026
- Hannah, L., Roehrdanz, P. R., Ikegami, M., Shepard, A. V., Shaw, M. R., Tabor, G., et al. (2013). Climate change, wine, and conservation. *PNAS* 110 (17), 6907–6912. doi: 10.1073/pnas.1210127110
- Hayes, A., Feechan, A., and Dry, I. B. (2010). Involvement of abscisic acid in the coordinated regulation of a stress-inducible hexose transporter (VvHT5) and a cell wall invertase in grapevine in response to biotrophic fungal infection. *Plant Physiol.* 153, 211–221. doi: 10.1104/pp.110.154765
- He, L., Meng, N., Castellari, S. D., Wang, Y., Sun, Q., Li, X.-Y., et al. (2021). Combined metabolite and transcriptome profiling reveals the norisoprenoid responses in grape berries to abscisic acid and synthetic auxin. *Int. J. Mol. Sci.* 22, 1420. doi: 10.3390/ijms22031420
- He, L., Ren, Z.-Y., Wang, Y., Fu, Y. Q., Li, Y., Meng, N., et al. (2020). Ripening time interval induced by abscisic acid and synthetic auxin affecting transcriptome and flavor compounds in Cabernet sauvignon grape berry. *Plants* 9, 630. doi: 10.3390/plants9050630
- Hegyí, Á. L., Otto, M., Geml, J., Hegyi-Kaló, J., Kun, J., Gyenesi, A., et al. (2022). Metatranscriptomic analyses reveal the functional role of botrytis cinerea in biochemical and textural changes during noble rot of grapevines. *J. Fungi* 8, 378. doi: 10.3390/jof8040378
- Horton, R. M., Mankin, J. S., Lesk, C., Coffel, E., and Raymond, C. (2016). A review of recent advances in research on extreme heat events. *Curr. Clim. Change Rep.* 2, 242–259. doi: 10.1007/s40641-016-0042-x
- Hren, M., Nikolić, P., Rotter, A., Blejcek, A., Terrier, N., Ravnika, M., et al. (2009). 'Bois noir' phytoplasma induces significant reprogramming of the leaf transcriptome in the field grown grapevine. *BMC Genomics* 10 (1), 460. doi: 10.1186/1471-2164-10-460
- Jaillon, O., Aury, J. M., Noel, B., Policriti, A., Clepet, C., Casagrande, A., et al. (2007). The grapevine genome sequence suggests ancestral hexaploidization in major angiosperm phyla. *Nature* 449, 463–467. doi: 10.1038/nature06148
- Jia, H., Li, T., Haider, M. S., Sadeghnezhad, E., Pang, Q., Han, J., et al. (2022). Comparative transcriptomic and metabolomic profiling of grapevine leaves (cv. kyoho) upon infestation of grasshopper and *Botrytis cinerea*. *Plant Mol. Biol. Rep.* 40, 539–555. doi: 10.1007/s11105-022-01336-8
- Jia, H., Xie, Z., Wang, C., Shangguang, L., Qian, N., Cui, M., et al. (2017). Absciscic acid, sucrose, and auxin coordinately regulate berry ripening process of the fujiminori grape. *Funct. Integr. Genomics* 17 (4), 441–457. doi: 10.1007/s10142-017-0546-z
- Jogawat, A., Yadav, B., Chhaya, L., Lakra, N., Singh, A. K., and Narayan, O. P. (2021). Crosstalk between phytohormones and secondary metabolites in the drought stress tolerance of crop plants: a review. *Physiol. Plant* 172 (2), 1106–1132. doi: 10.1111/ppl.13328
- Kedrina-Okutan, O., Novello, V., Hoffmann, T., Hadersdorfer, J., Occhipinti, A., Schwab, W., et al. (2018). Constitutive polyphenols in blades and veins of grapevine (*Vitis vinifera* L.) healthy leaves. *J. Agric. Food Chem.* 66, 10977–10990. doi: 10.1021/jf072162l
- Kelloniemi, J., Trouvelot, S., Héloir, M. C., Simoin, A., Dalmis, B., Frettinger, P., et al. (2015). Analysis of the molecular dialogue between Gray mold (*Botrytis cinerea*) and grapevine (*Vitis vinifera*) reveals a clear shift in defence mechanisms during berry ripening. *Mol. Plant Microb. Int.* 28 (11), 1167–1180. doi: 10.1094/MPMI-02-15-0039-R
- Khattab, I. M., Sahi, V. P., Baltenweck, R., Maia-Grondard, A., Huguency, P., Bieler, E., et al. (2021). Ancestral chemotypes of cultivated grapevine with resistance to *Botryosphaeria*-related dieback allocate metabolism towards bioactive stilbenes. *New Phytol.* 229, 1133–1146. doi: 10.1111/nph.16919
- Kim, H., Seomun, S., Yoon, Y., and Jang, G. (2021). Jasmonic acid in plant abiotic stress tolerance and interaction with abscisic acid. *Agronomy* 11, 1886. doi: 10.3390/agronomy11091886
- Koyama, K., Sadamatsu, K., and Goto-Yamamoto, N. (2010). Absciscic acid stimulated ripening and gene expression in berry skins of the Cabernet sauvignon grape. *Funct. Integr. Genomics* 10 (3), 367–381. doi: 10.1007/s10142-009-0145-8
- Kuhn, N., Guan, L., Dai, Z. W., Wu, B. H., Lauvergeat, V., Gomès, E., et al. (2014). Berry ripening, recently heard through the grapevine. *J. Exp. Bot.* 65, 4543–4559. doi: 10.1093/jxb/ert395
- Lambert, C., Khiook, I. L. K., Lucas, S., Télé-Micoulet, N., Mérellon, J.-M., and Cluzet, S. (2013). A faster and a stronger defence response: one of the key elements in grapevine explaining its lower level of susceptibility to esca? *Phytopathol.* 103, 1028–1034. doi: 10.1094/PHYTO-11-12-0305-R
- Landi, L., Murolo, S., and Romanazzi, G. (2019). Detection of 'Candidatus phytoplasma solani' in roots from Bois noir symptomatic and recovered grapevines. *Sci. Rep.* 9, 2013. doi: 10.1038/s41598-018-38135-9
- Lazazzara, V., Avesani, S., Robatscher, P., Oberhuber, M., Pertot, I., Schuhmacher, R., et al. (2021). Biogenic volatile organic compounds in the grapevine response to pathogens, beneficial microorganisms, resistance inducers, and abiotic factors. *J. Exp. Bot.* 73 (2), 529–554. doi: 10.1093/jxb/erab367
- Li, T., Gonzalez, N., Inzé, D., and Dubois, M. (2020). Emerging connections between small RNAs and phytohormones. *Trends Plant Sci.* 25 (9), 912–929. doi: 10.1016/j.tplants.2020.04.004
- Lovato, A., Zenoni, S., Tornielli, G. B., Colombo, T., Vandelle, E., and Polverari, A. (2019). Specific molecular interactions between vitis vinifera and botrytis cinerea are required for noble rot development in grape berries. *Postharvest Biol. Technol.* 156, 110924. doi: 10.1016/j.postharvbio.2019.05.025
- Lovisolo, C., Perrone, I., Hartung, W., and Schubert, A. (2008b). An abscisic acid-related reduced transpiration promotes gradual embolism repair when grapevines are rehydrated after drought. *New Phytol.* 180 (3), 642–651. doi: 10.1111/j.1469-8137.2008.02592.x
- Lovisolo, C., and Schubert, A. (1998). Effects of water stress on vessel size and xylem hydraulic conductivity in *Vitis vinifera* L. *J. Exp. Bot.* 49 (321), 693–700. doi: 10.1093/jexbot/49.321.693
- Lovisolo, C., Tramontini, S., Flexas, J., and Schubert, A. (2008a). Mercurial inhibition of root hydraulic conductance in vitis spp. rootstocks under water stress. *Environ. Exp. Bot.* 63, 178–182. doi: 10.1016/j.envexpbot.2007.11.005
- Luan, L. Y., Zhang, Z. W., Xi, Z. M., Huo, S. S., and Ma, L. N. (2014). Comparing the effects of exogenous abscisic acid on the phenolic composition of van 73 and Cabernet sauvignon (*Vitis vinifera* L.) wines. *Eur. Food Res. Technol.* 239, 203–213. doi: 10.1007/s00127-014-2206-z
- Magnin-Robert, M., Letousey, P., Spagnolo, A., Rabenoelina, F., Jacquens, L., Mercier, L., et al. (2011). Leaf stripe form of esca induces alteration of photosynthesis and defence reactions in presymptomatic leaves. *Funct. Plant Biol.* 38 (11), 856–866. doi: 10.1071/FP11083
- Magnin-Robert, M., Spagnolo, A., Boulanger, A., Joyeux, C., Clément, C., Abou-Mansour, E., et al. (2016). Changes in plant metabolism and accumulation of fungal metabolites in response to esca proper and apoplexy expression in the whole grapevine. *Phytopathol.* 106, 541–553. doi: 10.1094/PHYTO-09-15-0207-R
- Marchi, G., Roberti, S., D'Ovidio, R., and Mugnai, L. (2001). Pectic enzymes production by *Phaeoaniella chlamydospora*. *Phytopathol. Mediterr.* 40, S407–S416. doi: 10.14601/Phytopathol_Mediterr-1632
- Margaria, P., Ferrandino, A., Caciagli, P., Kedrina, O., Schubert, A., and Palmano, S. (2014). Metabolic and transcript analysis of the flavonoid pathway in diseased and recovered nebbiolo and barbera grapevines (*Vitis vinifera* L.) following infection by flavescence dorée phytoplasma. *Plant Cell Environ.* 37 (9), 2183–2200. doi: 10.1111/pce.12332
- Martin, N., Vesentini, D., Rego, C., Monteiro, S., Oliveira, H., and Boavida Gerreira, R. (2009). *Phaeoaniella chlamydospora* infection induces changes in phenolic compounds content in *Vitis vinifera*. *Phytopathol. Mediterr.* 48, 101–108.
- Massonnet, M., Fasoli, M., Tornielli, G. B., Altieri, M., Sandri, M., Zuccolotto, P., et al. (2017). Ripening transcriptomic program in red and white grapevine varieties correlates with berry skin anthocyanin accumulation. *Plant Physiol.* 174, 2376–2396. doi: 10.1104/pp.17.00311
- Mendes, M. D., Figueiredo, C. A., Oliveira, M. M., and Trindade, H. (2014). Influence of culture media and fungal extracts on essential oils composition and on terpene synthase gene expression in thymus caespitius. *Plant Cell Tissue Organ Cult.* 118, 457–469. doi: 10.1007/s11240-014-0498-0
- Mengiste, T. (2012). Plant immunity to necrotrophs. *Annu. Rev. Phytopathol.* 50, 267–294. doi: 10.1146/annurev-phyto-081211-172955
- Minio, A., and Cantu, D. (2022). Grapegenomics.com: a web portal with genomic data and analysis tools for wild and cultivated grapevines. *Zenodo*. doi: 10.5281/zenodo.7027886
- Min Liu, M., Jua, Y., Mina, Z., Fanga, Y., and Menga, J. (2020). Transcriptome analysis of grape leaves reveals insights into response to heat acclimation. *Scientia Hort.* 272, 109554. doi: 10.1016/j.scienta.2020.109554
- Morabito, C., Orozco, J., Tonel, G., Cavalletto, S., Meloni, G. R., Schubert, A., et al. (2021). Do the ends justify the means? impact of drought progression rate on stress response and recovery in *Vitis vinifera*. *Physiologia Plantarum* 174, e13590. doi: 10.1111/ppl.13590

- Morales-Castilla, I., García de Cortázar-Atauri, I., Cook, B. I., Lacombe, T., Parker, A. K., van Leeuwen, C., et al. (2020). Diversity buffers winegrowing regions from climate change losses. *Proc. Natl. Acad. Sci. U.S.A.* 117 (6), 2864–2869. doi: 10.1073/pnas.1906731117
- Morone, C., Boveri, M., Giosuè, S., Gotta, P., Rossi, V., Scapin, I., et al. (2007). Epidemiology of *Flavescence dorée* in vineyards in northwestern Italy. *Phytopathology* 97, 1422–1427. doi: 10.1094/PHYTO-97-11-1422
- Mugnai, L., Graniti, A., and Surico, G. (1999). Esca (Black measles) and brown wood-streaking: two old and elusive diseases of grapevines. *Plant Dis.* 83 (5), 404–418. doi: 10.1094/PDIS.1999.83.5.404
- Munitz, S., Netzer, Y., Shtein, I., and Schwartz, A. (2018). Water availability dynamics have long-term effects on mature stem structure in *Vitis vinifera*. *Am. J. Bot.* 105, 1443–1452. doi: 10.1002/ajb2.1148
- Murcia, G., Fontana, A., Pontin, M., Baraldi, R., Bertazza, G., and Piccoli, P. N. (2017). ABA and GA3 regulate the synthesis of primary and secondary metabolites related to alleviation from biotic and abiotic stresses in grapevine. *Phytochem* 135, 34–52. doi: 10.1016/j.phytochem.2016
- Negro, C., Sabella, E., Nicoli, F., Pierro, R., Materazzi, A., Panattoni, A., et al. (2020). Biochemical changes in leaves of *Vitis vinifera* cv. sangiovese infected by Bois noir phytoplasma. *Pathogens* 9, 269. doi: 10.3390/pathogens9040269
- Pacifico, D., Margaria, P., Galletto, L., Legovich, M., Abbà, S., Veratti, F., et al. (2019). Differential gene expression in two grapevine cultivars recovered from “Flavescence dorée”. *Microbiol. Res.* 220, 72–82. doi: 10.1016/j.micres.2018.12.005
- Pagliarani, C., Boccacci, P., Chitarra, W., Cosentino, E., Sandri, M., Perrone, I., et al. (2019). Distinct metabolic signals underlie clone by environment interplay in “Nebbiolo” grapes over ripening. *Front. Plant Sci.* 10. doi: 10.3389/fpls.2019.01575
- Pagliarani, C., and Gambino, G. (2019). Small RNA mobility: spread of RNA silencing effectors and its effect on developmental processes and stress adaptation in plants. *Int. J. Mol. Sci.* 20 (17), 4306. doi: 10.3390/ijms20174306
- Pagliarani, C., Gambino, G., Ferrandino, A., Chitarra, W., Vrhovsek, U., Cantu, D., et al. (2020). Molecular memory of flavescence dorée phytoplasma in recovering grapevines. *Hortic. Res.* 7, 126. doi: 10.1038/s41438-020-00348-3
- Pantelić, M., Dabić Zagorac, D., Natić, M., Gašić, U., Jović, S., Vujović, D., et al. (2016). Impact of clonal variability on phenolics and radical scavenging activity of grapes and wines, a study on the recently developed merlot and Cabernet franc clones *Vitis vinifera* L. *PLoS One* 11, e0163823. doi: 10.1371/journal.pone.0163823
- Paolacci, A. R., Catarcione, G., Ederli, L., Zadra, C., Pasqualini, S., Badiani, M., et al. (2017). Jasmonate-mediated defence responses, unlike salicylate-mediated responses, are involved in the recovery of grapevine from bois noir disease. *BMC Plant Biol.* 17, 118. doi: 10.1186/s12870-017-1069-4
- Patono, D. L., Said-Pulicino, D., Elói Alcatraz, L., Firbus, A., Ivaldi, G., and Chitarra, W. (2022). Photosynthetic recovery in drought-rehydrated grapevines is associated with high demand from the sinks, maximizing the fruit-oriented performance. *Plant J.* 112, 1098–1111. doi: 10.1111/tjp.16000
- Pedneault, K., and Provost, C. (2016). Fungus resistant grape varieties as a suitable alternative for organic wine production: benefits, limits, and challenges. *Sci. Hortic.* 208, 57–77. doi: 10.1016/j.scienta.2016.03.0160304-4238
- Perrone, I., Pagliarani, C., Lovisolo, C., Chitarra, W., Roman, F., and Schubert, A. (2012). Recovery from water stress affects grape leaf petiole transcriptome. *Planta* 235, 1383–1396. doi: 10.1007/s00425-011-1581-y
- Pierron, R. J. G., Pouzoulet, J., Couderc, C., Judic, E., Company, S., and Jacques, A. (2016). Variations in early response of grapevine wood depending on wound and inoculation combinations with *Phaeoacremonium aleophilum* and *Phaeoacremonium chlamydospora*. *Front. Plant Sci.* 7. doi: 10.3389/fpls.2016.00268
- Pilati, S., Bagagli, G., Sonogo, P., Moretto, M., Brazzale, D., Castorina, G., et al. (2017). Abscissic acid is a major regulator of grape berry ripening onset: new insights into ABA signaling network. *Front. Plant Sci.* 8. doi: 10.3389/fpls.2017.01093
- Pinto, D. L., Brancadoro, L., Dal Santo, S., De Lorenzis, G., Pezzotti, M., Meyers, B. C., et al. (2016). The influence of genotype and environment on small RNA profiles in grapevine berry. *Front. Plant Sci.* 7. doi: 10.3389/fpls.2016.01459
- Pirie, A., and Mullins, M. G. (1976). Changes in anthocyanin and phenolics content of grapevine leaf and fruit tissues treated with sucrose, nitrate, and abscissic acid. *Plant Physiol.* 58, 468–472. doi: 10.1104/pp.58.4.468
- Pogány, M., Dankó, T., Hegyi-Kaló, J., Kámán-Tóth, E., Szám, D. R., Hamow, K. A., et al. (2022). Redox and hormonal changes in the transcriptome of grape (*Vitis vinifera*) berries during natural noble rot development. *Plants* 11, 864. doi: 10.3390/plants11070864
- Pouzoulet, J., Pivovarov, A. L., Santiago, L. S., and Rolshausen, P. E. (2014). Can vessel dimension explain tolerance toward fungal vascular wilt diseases in woody plants? lessons from Dutch elm disease and esca disease in grapevine. *Front. Plant Sci.* 5. doi: 10.3389/fpls.2014.00253
- Pouzoulet, J., Pivovarov, A. L., Scudiero, E., De Guzman, M. E., Rolshausen, P. E., and Santiago, L. S. (2020b). Contrasting adaptation of xylem to dehydration in two *Vitis vinifera* L. sub-species. *Vitis* 59, 53–61. doi: 10.5073/vitis.2020.59.53-61
- Pouzoulet, J., Rolshausen, P., Charbois, R., Chen, J., Guillaumie, S., Ollat, N., et al. (2020a). Behind the curtain of the compartmentalization process: exploring how xylem vessel diameter impacts vascular pathogen resistance. *Plant Cell Environ.* 43, 2782–2796. doi: 10.1111/pce.13848
- Prezelj, N., Covington, E., Roitsch, T., Gruden, K., Fagner, L., Weckwerth, W., et al. (2016). Metabolic consequences of infection of grapevine (*Vitis vinifera* L.) cv. “Modra frankinja” with flavescence dorée phytoplasma. *Front. Plant Sci.* 7. doi: 10.3389/fpls.2016.00711
- Quiroga, A. M., Deis, L., Cavagnaro, J. B., Bottini, R., and Silva, M. F. (2012). Water stress and abscissic acid exogenous supply produce differential enhancements in the concentration of selected phenolic compounds in Cabernet sauvignon. *J. Berry Res.* 2, 33–44. doi: 10.3233/JBR-2011-026
- Ramsing, C. K., Gramaje, D., Mocholi, S., Agustí, J., Cabello Sáenz de Santa María, F., Armengol, J., et al. (2021). Relationship between the xylem anatomy of grapevine rootstocks and their susceptibility to *Phaeoacremonium minimum* and *Phaeoacremonium chlamydospora*. *Front. Plant Sci.* 12. doi: 10.3389/fpls.2021.726461
- Rienth, M., Vigneron, N., Darriet, P., Sweetman, C., Burbidge, C., Bonghi, C., et al. (2021a). Grape berry secondary metabolites and their modulation by abiotic factors in a climate change scenario—a review. *Front. Plant Sci.* 12. doi: 10.3389/fpls.2021.643258
- Rienth, M., Vigneron, N., Walker, R. P., Castellarin, S. D., Sweetman, C., Burbidge, C. A., et al. (2021b). Modification of grapevine berry composition induced by main viral and fungal pathogens in a climate change scenario. *Front. Plant Sci.* 12. doi: 10.3389/fpls.2021.717223
- Roggia, C., Caciagli, P., Galetto, L., Pacifico, D., Veratti, F., Bosco, D., et al. (2014). Flavescence dorée phytoplasma titre in field-infected barbera and nebbiolo grapevines. *Plant Pathol.* 63, 31–41. doi: 10.1111/ppa.12068
- Rolland, F., Moore, B., and Sheen, J. (2002). Sugar sensing and signaling in plants. *Plant Cell* 14, 185–205. doi: 10.1146/annurev.arplant.57.032905.105441
- Santarosa, E., Dutra de Souza, P. V., de Araujo Mariath, J. E., and Lourosa, G. V. (2016). Physiological interaction between rootstock-scion: effects on xylem vessels in Cabernet sauvignon and merlot grapevines. *Am. J. Enol. Vitic.* 67, 65–76. doi: 10.5344/ajev.2015.15003
- Santi, S., De Marco, F., Polizzotto, R., Grisan, S., and Musetti, R. (2013). Recovery from stolbur disease in grapevine involves changes in sugar transport and metabolism. *Front. Plant Sci.* 4. doi: 10.3389/fpls.2013.00171
- Sparapano, L., Bruno, G., Ciccarone, C., and Graniti, A. (2000). Infection of grapevines by some fungi associated with esca. II. interaction among *Phaeoacremonium chlamydosporum*, *P. aleophilum* and *Fomitiporia punctata*. *Phytopathol. Mediterr.* 39, 53–58.
- Sultan, S. E. (2010). Phenotypic plasticity for plant development, function and life history. *Trends Plant Sci.* 5, 537–542. doi: 10.1016/S1360-1385(00)01797-0
- Sunitha, S., Loyola, R., Alcalde, J. A., Arce-Johnson, P., Matus, J. T., and Rock, C. D. (2019). The role of UV-B light on small RNA activity during grapevine berry development. *G3 (Bethesda)* 9 (3), 769–787. doi: 10.1534/g3.118.200805
- Surico, G. (2009). Towards a redefinition of the diseases within the esca complex of grapevine. *Phytopathol. Mediterr.* 48, 5–10. doi: 10.14601/Phytopathol_Mediterr-2870
- Teixeira, A., Martins, V., Frusciant, S., Cruz, T., Noronha, H., Diretto, G., et al. (2020). Flavescence dorée derived leaf yellowing in grapevine (*Vitis vinifera* L.) is associated to a general repression of isoprenoid biosynthetic pathways. *Front. Plant Sci.* 11. doi: 10.3389/fpls.2020.00896
- Tziros, T. G., Ainalidou, A., Samaras, A., Kollaros, M., Karamanolis, K., Menkissoglou-Spirodi, U., et al. (2022). Differences in defence-related gene expression and metabolite accumulation reveal insights into the resistance of Greek grape wine cultivars to *Botrytis* bunch rot. *Oenone* 56 (2), 111–115. doi: 10.20870/oenone.2022.56.2.5451
- Vaillau, F., Daniel, X., Tronchet, M., Montillet, J. L., Triantaphyllide, C., and Roby, D. (2002). A R2R3-MYB gene, AtMYB30, acts as a positive regulator of the hypersensitive cell death program in plants in response to pathogen attack. *PNAS* 99 (15), 10179–10184. doi: 10.1073/pnas.152047199
- Valtaud, C., Foyer, C. H., Fleurat-Lessard, P., and Bourbouloux, A. (2009). Systemic effects on leaf glutathione metabolism and defence protein expression caused by esca infection in grapevines. *Funct. Plant Biol.* 36, 260–279. doi: 10.1021/jf050863h
- van Leeuwen, C., Destrac-Irvine, A., Dubernet, M., Duchêne, E., Gowdy, M., Marguerit, E., et al. (2019). An update on the impact of climate change in viticulture and potential adaptations. *Agronomy* 9, 514. doi: 10.3390/agronomy9090514
- van Leeuwen, C., Roby, J.-P., Alonso-Villaverde, V., and Gindro, K. (2013). Impact of clonal variability in *Vitis vinifera* ‘Cabernet franc’ on grape composition, wine quality, leaf blade stilbene content, and downy mildew resistance. *J. Agric. Food Chem.* 61, 19–24. doi: 10.1021/jf304687c
- Varotto, S., Tani, E., Abraham, E., Krugman, T., Kapazoglou, A., Melzer, R., et al. (2020). Epigenetics: possible applications in climate-smart crop breeding. *J. Exp. Bot.* 71 (17), 5223–5236. doi: 10.1093/jxb/eraa188
- Vitali, M., Chitarra, W., Galetto, L., Bosco, D., Marzachi, C., Gullino, M. L., et al. (2013). Flavescence dorée phytoplasma deregulates stomatal control of photosynthesis in *Vitis vinifera*. *Ann. Appl. Biol.* 162, 335–346. doi: 10.1111/aab.12025
- Wang, L., Brouard, E., Hilbert, G., Renaud, C., Petit, J.-P., Edwards, P., et al. (2021). Differential response of the accumulation of primary and secondary metabolites to leaf-to-fruit ratio and exogenous abscissic acid. *Aust. J. Grape Wine Res.* 27, 527–539. doi: 10.1111/ajgw.12509
- Wang, L., Liu, W., and Wang, Y. (2020). Heterologous expression of Chinese wild grapevine VqERFs in *Arabidopsis thaliana* enhance resistance to *Pseudomonas syringae*

- pv. tomato DC3000 and to *Botrytis cinerea*. *Plant Sci.* 293, 110421. doi: 10.1016/j.plantsci.2020.110421
- Wang, J., VanderWeide, J., Yan, Y., Tindjau, R., Pico, J., Deluc, L., et al. (2022). Impact of hormone applications on ripening-related metabolites in gewürztraminer grapes (*Vitis vinifera* L.): the key role of jasmonates in terpene modulation. *Food Chem.* 388, 132948. doi: 10.1016/j.foodchem.2022.132948
- Wang, M., Zhu, Y., Han, R., Yin, W., Guo, C., Li, Z., et al. (2018). Expression of *Vitis amurensis* VaERF20 in *Arabidopsis thaliana* improves resistance to *Botrytis cinerea* and *Pseudomonas syringae* pv. tomato DC3000. *Int. J. Mol. Sci.* 19, 696. doi: 10.3390/ijms19030696
- Wolkovich, E. M., García de Cortázar-Atauri, I., Morales-Castilla, I., Nicholas, K. A., and Lacombe, T. (2018). From pinot to xinomavro in the world's future wine-growing regions. *Nat. Clim. Change* 8, 29–37. doi: 10.1038/s41558-017-0016-6
- Xi, H., Konate, M., Sai, N., Tesfamichael, K. G., Cavagnaro, T., Gilliam, M., et al. (2017). Global DNA methylation patterns can play a role in defining terroir in grapevine *Vitis vinifera* cv. Shiraz. *Front. Plant Sci.* 8, 1860. doi: 10.3389/fpls.2017.01860
- Xi, Z.-M., Meng, J.-F., Huo, S.-S., Luan, L.-Y., Ma, L.-N., and Zhang, Z.-W. (2013). Exogenously applied abscisic acid to Yan73 (*V. vinifera*) grapes enhances phenolic content and antioxidant capacity of its wine. *Int. J. Food Sci. Nutr.* 64, 444–451. doi: 10.3109/09637486.2012.746291
- Yacoub, A., Magnin, N., Gerbore, J., Haidar, R., Bruez, E., Company, S., et al. (2020). The biocontrol root-oomycete, *Pythium oligandrum*, triggers grapevine resistance and shifts in the transcriptome of the trunk pathogenic fungus, *Phaeoemoniella chlamydospora*. *Int. J. Mol. Sci.* 21, 6876. doi: 10.3390/ijms21186876
- Yang, J., Duan, G., Li, C., Liu, L., Han, G., Zhang, Y., et al. (2019). The crosstalks between jasmonic acid and other plant hormone signaling highlight the involvement of jasmonic acid as a core component in plant response to biotic and abiotic stresses. *Front. Plant Sci.* 10. doi: 10.3389/fpls.2019.01349
- Zhu, Y., Li, Y., Zhang, S., Zhang, X., Yao, J., Luo, Q., et al. (2019). Genome-wide identification and expression analysis reveal the potential function of ethylene responsive factor gene family in response to *Botrytis cinerea* infection and ovule development in grapes (*Vitis vinifera* L.). *Plant Biol.* 21, 571–584. doi: 10.1111/plb.12943
- Zhu, Y., Zhang, X., Zhang, Q., Chai, S., Yin, W., Gao, M., et al. (2022). The transcription factors VaERF16 and VaMYB306 interact to enhance resistance of grapevine to botrytis cinerea infection. *Mol. Plant Pathol.* 23, 1415–1432. doi: 10.1111/mpp.13223



OPEN ACCESS

EDITED BY

Eva Pilar Pérez-Álvarez,
Spanish National Research Council
(CSIC), Spain

REVIEWED BY

Luigi Bavaresco,
Catholic University of the Sacred
Heart, Italy
Osvaldo Failla,
University of Milan, Italy

*CORRESPONDENCE

Andriani Asproudi

✉ andriani.asproudi@crea.gov.it

RECEIVED 03 March 2023

ACCEPTED 14 July 2023

PUBLISHED 04 August 2023

CITATION

Asproudi A, Bonello F, Ragkousi V,
Gianotti S and Petrozziello M (2023) Aroma
precursors of Grignolino grapes (*Vitis
vinifera* L.) and their modulation by vintage
in a climate change scenario.
Front. Plant Sci. 14:1179111.
doi: 10.3389/fpls.2023.1179111

COPYRIGHT

© 2023 Asproudi, Bonello, Ragkousi, Gianotti
and Petrozziello. This is an open-access
article distributed under the terms of the
[Creative Commons Attribution License](#)
(CC BY). The use, distribution or
reproduction in other forums is permitted,
provided the original author(s) and the
copyright owner(s) are credited and that
the original publication in this journal is
cited, in accordance with accepted
academic practice. No use, distribution or
reproduction is permitted which does not
comply with these terms.

Aroma precursors of Grignolino grapes (*Vitis vinifera* L.) and their modulation by vintage in a climate change scenario

Andriani Asproudi^{1*}, Federica Bonello¹, Vasiliki Ragkousi¹,
Silvia Gianotti^{2,3} and Maurizio Petrozziello¹

¹Research centre for Viticulture and Enology, Council for Agricultural Research and Economics (CREA), Asti, Italy, ²Associazione Monferace, Alessandria, Italy, ³Wine Consulting Mario Ronco, Asti, Italy

Current climatic conditions may cause significant changes in grapevine phenology and maturity dynamics linked often with changes to ecoclimatic indicators. The influence exerted by different meteorological conditions during four consecutive years on the aromatic potential of Grignolino grapes was investigated for the first time. The samples were collected from three vineyards characterized by different microclimatic conditions mainly related to the vineyard exposure and by a different age of the plants. Important differences as far as temperature and rainfall patterns are concerned during ripening were observed among the 4 years. Grape responses to abiotic stress, with particular emphasis on aromatic precursors, were evaluated using gas chromatography coupled to mass spectrometry. The results highlighted significant differences among the vintages for each vineyard in terms of the berry weight and the aromatic precursor concentration. For the grapes of the younger-vine vineyard, the content of aroma compounds showed a different variability among the vintages if compared to the old-vine vineyards. Optimal conditions in terms of temperature and rainfall during the green phase followed by a warm and dry post-veraison period until harvest favored all classes of compounds especially terpenoids mainly in the grapes of the old vines. High-temperature (>30°C) and low-rainfall pattern before veraison led to high benzenoid contents and increased differences among vineyards such as berry weight, whereas cooler conditions favored the terpenoid levels in grapes from southeast-oriented vineyards. In a hilly environment, lack of rainfall and high temperature that lately characterize the second part of berry development seem to favor the grape quality of Grignolino, a cultivar of medium-late ripening, by limiting the differences on bunch ripening, allowing a greater accumulation of secondary metabolites but maintaining at the same time an optimum balance sugar/acidity.

KEYWORDS

C₁₃-norisoprenoids, Benzenoids, Terpenoids, Grignolino, seasonal stress conditions, Hilly viticulture, old vineyards

1 Introduction

Most wine-producing regions around the world suffer from the effects of climate change. In the temperate zones, large fluctuations of the main climatic parameters are observed over the years, and above all, a gradual and irreversible tendency towards an increase in average seasonal temperatures and a significant decrease in rainfall associated to a different distribution during the grape ripening period. Grapevine cultivation for winemaking is highly dependent on climate fluctuations that exert profound effects on vine phenology and grape composition. Global climate change directly modifies mainly abiotic factors such as temperature and both water availability and distribution during the grapevine growth cycle (Jackson and Lombard, 1993; Fraga et al., 2018; Rienth et al., 2021). Additionally, climate change can cause shifts in phenological stages, resulting in alterations to the optimal photoperiod. This, in turn, affects the rate of photosynthesis and the phenological stages of the grapevine, ultimately influencing grape composition.

The increase in average and extreme temperatures of summer months, as a major consequence of climate change, as well as changes of rainfall patterns during the ripening phase, leads not only to a higher concentration of sugar and a general change of the acidic profile of grapes, but also to the modification of secondary metabolite profiles (De Orduna, 2010; Van Leeuwen and Darriet, 2016; Asproudi et al., 2018). Therefore, in several viticulture areas, ripening occurs when both color and aroma profile can be adversely affected (Mori et al., 2007; Asproudi et al., 2016), which, in wine, is translated to a loss of typicity and terroir expression (van Leeuwen et al., 2020). Owing to climate change, a mismatch is also noted between the different parameters of technological, phenolic, and aromatic quality as they are regulated by different biosynthetic pathways and therefore are influenced differently.

Sunlight radiation has been suggested to promote grape ripeness, modulating the metabolic profile of berries, and activating the synthesis and accumulation of diverse compounds in the skin of berries, including sugars, organic acids, amino acids, and phenylpropanoids (Carbonell-Bejerano et al., 2014), although it was difficult to separate the combined effect with temperature.

High sun irradiation and high temperatures after veraison are reported to be factors that greatly affect the ripening of grapes (Bergqvist et al., 2001) and can lead to an anticipation of the ripening period earlier during the warmest part of the season. Conversely, mild temperatures during spring and ripening and late rainfall events during veraison might cause a delay in the ripening process, generating grapes with low pH, high total acidity, and high varietal aroma potential, as previously mentioned (Webb et al., 2012).

Several other parameters such as the age and the exposure of vines as well the altitude of vineyards may affect the response of plants to climate change. Younger vines, for instance, seem to be more sensitive to water stress conditions, due to less developed root systems, whereas vine age may also affect phenology and gas exchange parameters (Riffle et al., 2021). Young vines have been reported to show lower photosynthesis (Zufferey and Maigre, 2007),

stomatal conductance, and transpiration compared to old vines. As a consequence, a slower berry formation but quicker berry ripening may be noted, and optimal technological ripening parameters are reached earlier than in old vines (Bou Nader et al., 2019).

The effects of high sun radiation and temperatures on secondary metabolism control have been characterized for phenolics, mostly in artificial growing conditions, while little is known with respect to aromas; a decrease in the skin/pulp ratio, with possible effect on the aromatic potential, was mentioned (Pérez-Álvarez et al., 2021). The concept of grape and wine quality is inextricably linked to secondary metabolites. The color, aroma, and flavor of the wine, as well as their stability over time, depend strictly on the concentration of these compounds present in the grapes and their transformation during the winemaking process. These transformations are well known and can include oxidation, reduction, enzymatic reactions, and chemical reactions between compounds, such as esterification, hydrolysis, and polymerization. These changes can significantly impact the sensory profile and overall quality of the final wine product. Conversely, a relatively limited number of studies have dealt with the effect of climate and microclimate factors on the volatile composition of grapes and on aroma precursors, although much of the perceived quality of a wine by the consumer depends closely on the contribution to aroma of these molecules.

Some studies evidence the probable effect of sunlight conditions on some aroma compounds (e.g., terpenes, alcohols, and aldehydes) since they seem implicated in the protection of grapes against photooxidation (He et al., 2020). Moreover, recent research indicated that microclimate conditions, which varied according to the vintage, may affect the timing of the peak concentration of norisoprenoid precursors and their final content in Nebbiolo berries whereas high temperature during the last stages of grape ripening evidently led to a decrease of the total norisoprenoids (Asproudi et al., 2016). Previous research on other cultivars instead, implicating modified light condition in the fruit zone (leaf management), showed an increase of norisoprenoids in the grapes of Riesling, Pinot, noir, and other cultivars (Feng et al., 2015; Yuan et al., 2015; Alem et al., 2019).

Most volatile benzenoids are generated from phenylalanine through the shikimate acid pathway and it has been demonstrated that environmental stresses can activate this pathway and further promote the accumulation of secondary metabolites (Zhang et al., 2012).

Certainly, climate fluctuations among seasons may lead to relevant quality differences between wines produced from grapes of the same cultivar (Crespo et al., 2018). A cultivar maintains typical characteristics if cultivated in different regions, but the aromatic potential of grapes and wine strongly depends on meteorological factors such as rain level and temperature fluctuations during the berry development and the ripening period (Crespo et al., 2018). Thus, in the context of significant changes in climate and increased stress conditions, further studies should analyze the specific consequences of these multifactorial phenomena on the aromatic and flavor components of wines and their aging potential (Drappier et al., 2016; Wu et al., 2019).

Lately, winemakers are looking for vineyards that face north, as well as those at higher elevations, while southwest-facing vineyards have been seen to be optimum in case of stress, light, and temperature conditions (Hannah et al., 2013). For centuries, some of the world's greatest vineyards in the Northern Hemisphere were planted on hillsides, with suitable soils, facing south or southeast, where they would receive the most sun and warmth, allowing grapes to fully ripen (Santos et al., 2020). The same formula governed the placement of Grignolino vineyards since this cv often displays non-uniform ripening and berries in the same bunch are often of very different color, due to the uneven ripening.

Grignolino is an Italian autochthonous cultivar of high interest for the local (North Italy) and international wine market. Despite being a native cultivar closely linked to its original territory (Piedmont), it is also grown in other Italian regions as well as in California and the United States outside of Italy (Robinson et al., 2013). This grape has probably been cultivated in the Monferrato hills, since the XIII century (Mainardi, 2003) and nowadays represents the historical and oenological identity of the Monferrato in Piedmont. This territory, included in the World Heritage List designated by UNESCO, is famous for its strong vocation to produce high-quality wines from several autochthonous grape varieties.

More specifically, this region, is a rainfed hilly vine-growing area in Piedmont in which current climatic conditions caused significant changes in grapevine phenology and maturity dynamics, depending on the variety. Recent research, indeed, investigated the influence of increasing temperature and Huglin index in anticipating the harvest period, particularly the harvest beginning, mentioning that it was highly significant for all the considered varieties and vineyards in the Monferrato area (Bagagiolo et al., 2021).

Grignolino grapes, the subject of this study, are obtained from vines cultivated, according to the guidelines for the production of "Monferrato" wine, in the Aleramic Monferrato region, which is bounded by the Po and Tanaro rivers in the heart of Piedmont. The vineyards are exclusively hilly with optimal sun exposure to ensure proper grape ripening. The soils must be calcareous-silt-clayey, in various combinations, with the possibility of naturally occurring sandy sediment. No vine forcing is permitted; only emergency irrigation is allowed (Monferrato a Grignolino of Excellence, 2023). These wines require many years to reach a balance between the aromatic complexity and pronounced astringency and acidity. From an aromatic point of view, Grignolino is a cultivar with a neutral character characterized by significant concentrations of glycosylated aroma compounds, particularly terpenols, norisoprenoids, and benzenoids, which may release their potentially odoriferous free aglycons during winemaking or storage, contributing to define the final complex and distinctive aroma of the wine. Some recent research highlighted that aroma glycoside conjugates can also influence taste properties of the wine, such as the aromatic persistence (Parker et al., 2017; Liang et al., 2022). The concentration of grapes in aromatic precursors may thus significantly influence the fragrance of long-aged wines. Furthermore, the amount and type of glycosylated aromas present in a wine are influenced by multiple factors, including the weather

conditions during berry development and ripening (Ferreira and Lopez, 2019; Caffrey and Ebeler, 2021). It is therefore essential to evaluate the impact of climate change on grape aroma precursors in order to adapt new strategies aimed to maintain high-quality productions.

This research study willed to add new knowledge about this important Italian variety to face the challenge of climate crisis, and to comprehend when, how, and which meteorological variables may affect the various chemical classes of compounds that determine the wine aroma. To assess the influence of different meteorological conditions among years on the aroma potential of Grignolino grapes, solid-phase extraction (SPE) and subsequent enzymatic hydrolysis were the analytical strategies used, respectively, to isolate and release the glycosylated grape compounds prior to their determination *via* gas chromatography-mass spectrometry (GC-MS).

2 Materials and methods

2.1 Vineyard sites and grape technological composition

Data presented in this article concern four consecutive years, over the 2019, 2020, 2021, and 2022 growing seasons. Grape samples of Grignolino cv were collected in three different vineyards, located near Vignale Monferrato (45°0'45" N, 8°23'51" E, Piedmont, Italy), one with a medium vine age of 20 years (young) and two with 50-year-old vines (old). Plants were grafted onto 1103 Paulsen, the training system used is Guyot, with an elevation of approximately 300 m a.s.l. and a plant density from 4,500 to 5,000 plants/hectare all planted in a hilly area. The three vineyards were characterized by different microclimatic conditions mainly related to different aspects and vine ages: one old-vine vineyard was southeast oriented (Old SE), whereas the second old-vine and the younger-vine vineyards were southwest oriented (Old SW and Young SW). During this study, no emergency irrigation was carried out.

Three blocks for each vineyard were identified as representative and used as biological replicates. The sampling of Grignolino grapes was carried out for four consecutive years at ripening. The harvesting time was established according to the strategy adopted by each wine company for the specific year. Approximately 15 clusters for each biological replicate were harvested manually. For each replicate, 500 berries were collected with their pedicels randomly from different sides of the bunches, both shady and sunlit, to prepare grape extracts for aroma and phenolic compound measurements. The analysis of the main physicochemical parameters, namely, berry weight, titratable acidity (TA), and total soluble solids (TSS), were also carried out at ripening (Compendium of international methods of wine and must analysis-OIV, 2020).

Extraction of the polyphenolic fraction from the grapes was performed according to previous works (Di Stefano and Cravero, 1991). Total polyphenol content (TPI, total polyphenol index) was determined using the Folin-Ciocalteu method, whereas the

determination of anthocyanins (TAI, total anthocyanin index) was carried out spectrophotometrically as described by Di Stefano and co-workers with some revision (Di Stefano and Guidoni, 1989; Asproudi et al., 2018).

2.2 Climate and meteorological assessments

The meteorological data, measured in 2019, 2020, 2021 and 2022, were provided by a weather station near the vineyards (Vignale Monferrato) equipped with a thermohydrometer and a rain gauge (Table 1). The station is managed by the Meteo hydrographic Monitoring Network of Arpa Piemonte (Piedmont Environmental Protection Agency). The average values of the period 2009–2018 were obtained from data collected from the same weather station. The mean of maximum temperatures (Tmax mean), the mean of minimum temperatures (Tmin mean), the average of the monthly maximum temperature values, the number of days with temperatures higher than 35°C ($T > 35^{\circ}\text{C}$), the total rainfall, and the number of rainy days with rainfall of more than 1 mm ($\text{RD} \geq 1$) are shown in Table 1.

Cumulative growing degree days (GDD) were computed as the sum of the average daily temperature above a base temperature of 10°C (Amerine and Winkler, 1944). GDD were calculated from the 1 April to 30 October.

Furthermore, to better characterize each season, two periods were considered and the sum of rain, GDD, $T > 35^{\circ}\text{C}$, and T in the range between 25 and 35°C were assessed during the first pre-veraison period (April–August) and after veraison until harvest (August–September).

2.3 Extraction and determination of aroma precursors from grapes

2.3.1 Extraction of bounded aroma compounds from grapes

A total of 100 berries of Grignolino, previously weighted and stripped of seeds, were homogenized (Di Stefano et al., 1998). The suspension was then centrifuged (4000g for 15 min) and the supernatant was transferred to a 300-ml volumetric flask, washed, and brought up to volume with tartaric acid buffer ($\text{pH} = 3.0$, 0.04 M). Three replicates of all samples were analyzed. The isolation of grape heterosides was performed as previously reported for a grape and wine matrix (Mateo et al., 1997; Asproudi et al., 2016; Asproudi et al., 2018) after appropriate modifications for better extraction of target compounds from Grignolino grape extracts. Briefly, 250 ml of extract was passed through a 5-g C18 End Capped cartridge (Biotage AB, Uppsala, Sweden) previously activated with methanol and distilled water in sequence. After washing (water and dichloromethane), the glycosides were recovered with 25 ml of methanol (Sigma Aldrich Co., St. Louis, MO, USA). C18 sorbents were indicated to be more suitable for selective extraction of less polar precursors such as terpenic and norisoprenoid precursors. Furthermore, the same standardized procedure was applied for all samples to obtain reliable comparison results between vineyards and vintages (Jesús Ibarz et al., 2006; Liu et al., 2017).

2.3.2 Hydrolysis of glycosides by exogenous enzyme

The hydrolysis of glycosides by exogenous enzyme was carried as previously reported (Mateo et al., 1997; Asproudi et al., 2016; Asproudi et al., 2018). Briefly, the methanolic phase underwent

TABLE 1 Meteorological characterization of the four seasons (the values are calculated both for the entire year “a” and for the grapevine vegetative period: April–October “b”).

a) January to December	Tmax	Tmin	Tmax-M	Total rainfall	GDD 10°	Days T>30°C	Rainy days
Years	°C	°C	°C	mm	°C	number	number
2019	20.9	11.8	27.1	773	–	56	72
2020	20.6	11.5	26.5	629	–	45	68
2021	20.6	11.0	26.6	507	-	45	53
2022	22.2	12.6	28.7	349	-	76	37
Averages 2009–2018	20.9	11.4	27.5	673	-	53	66
b) April to October	Tmax	Tmin	Tmax-M	Total rainfall	GDD 10°	Days T>30°C	Rainy days
Years	°C	°C	°C	mm	°C	number	number
2019	24.6	14.7	30.5	443	2,069	56	42
2020	24.8	14.4	29.0	509	2,046	45	45
2021	24.5	14.1	29.9	329	2,005	45	26
2022	25.4	14.7	32.3	216	2,407	76	24
Averages 2009–2018	25.1	14.4	30.7	388	2,102	53	37

Data reported were recorded by the Vignale Monferrato meteorological station after reprocessing based on measures collected by the Arpa Piemonte Meteor Hydrographic Monitoring Network. Tmax: average daily maximum air temperature (°C); Tmin: average daily minimum air temperature (°C); Tmax-M average monthly maximum air temperature; Total rainfall: annual total precipitation (mm); GDD 10°: Growing Degree Days using a lower threshold of 10°C; days T>30°C: number of days with maximum temperatures above 30°C; Rainy days: Days with precipitation over 1 mm. Bold values denote statistically significant differences against average values calculated between 2009 and 2018 (one-sample z-test/two-tailed test; $p < 0.05$).

evaporation until dryness was achieved, employing a rotary evaporator under reduced pressure keeping bath temperature and rotation speed of the flask constant and equal for all samples. Subsequently, the residue was dissolved in 5 ml of citrate-phosphate buffer, adjusted to a pH of 5.0. Then, the enzymatic hydrolysis was carried out with Pectinol (Genencor, Palo Alto, CA, USA) with glycosidase side activity at 40°C for 24 h, to obtain free aglycon compounds. After hydrolysis, 0.25 ml of 2-octanol (50 mg/L), used as internal standard, was added and the extract passed through a 1-g C18-RP cartridge previously activated to isolate the aglycons. After a water wash and drying step, the aglycons were eluted with dichloromethane and collected in a 25-ml Erlenmeyer flask. The organic layer was dried using anhydrous Na₂SO₄, transferred into a distillation flask, and reduced to a small volume (approximately 200 µl) at room temperature. The sample was stored at −20°C until the analysis by GC–MS.

2.3.3 Gas chromatography–mass spectrometry determinations

GC–MS analysis was carried out by an Agilent 7890A gas chromatograph, equipped with an Agilent 5975C Mass Selective Detector (Agilent Technologies, Palo Alto, CA, USA). The samples (2 µl of dichloromethane extract) were manually injected into the injector at 250°C in split less mode. The separation was achieved using a Zebron ZB-WAX, Column 60 m × 0.25 mm × 0.25 µm (Phenomenex, Torrance, CA, USA). The oven temperature was held at 45°C for 2 min, then raised to 60°C at a rate of 30°C/min, from 60 to 230°C at a rate of 2°C/min, and held at 230°C for 20 min. Helium was the carrier gas and the column flow was maintained at 1.2 ml min^{−1}. The transfer line was set at 230°C. The ionization voltage was 70 eV, the quadrupole was set at 230°C, and the source was set at 250°C. The acquisition of mass spectra for the analysis of compounds was carried out in total ion current mode (TIC) and a 29–300 m/z range was recorded. To identify the volatile compounds, mass spectra and retention indices of authentic standards were compared to those of the analytes. In cases where an authentic standard was not available, recorded spectra and LRI values were compared to the NIST14 and WILEY275 databases, as well as the gas chromatographic retention indices reported in the literature (see [Supplementary Table 1](#)). The quantification was performed by comparing the areas of the chromatographic peaks to that of the internal standard (IS), 2-octanol, and the compound concentrations were calculated as equivalents of 2-octanol, which was used as the IS. Particular attention was given to the composition of the grapes in terpenoid, C₁₃-norisoprenoid, and benzenoid compounds. The results were expressed both as µg/kg of berries, as frequently reported in the literature, and as µg/100 berries to prevent the influence of the different berry size on the result interpretation.

2.4.5 Statistical analysis

All statistical analyses were carried out using XLSTAT-Pro (Data Analysis and Statistical Solution for Microsoft Excel, Addinsoft, Paris, France 2017). To generally examine the effects of the vintage (year) and vineyard as well vineyard and vintage

interaction (Vineyard *Year) on berry physical, chemical, polyphenolic, and aromatic composition, data were subjected to three two-way ANOVAs and differences among means were assessed according to the least significant difference from Tukey's test with a confidence interval of 95% ($p < 0.05$). To obtain more information, the relationship between meteorological parameters, vineyards, and vintages, with the chemical classes of the volatile hydrolytically released compounds quantified in Grignolino grape berries, was assessed with a two-principal component analysis (PCA) multivariate approach using XLSTAT software.

3 Results and discussion

3.1 Meteorological assessment

The four considered vintages presented some peculiarities from a meteorological point of view. Season 2019, as shown in [Figure 1A](#) was characterized by maximum temperatures similar to the average values monitored over the previous decade ([Table 1](#)), whereas the days with temperatures above 30°C were slightly higher than those of the reference period taken into consideration. In the Vignale area, the 2019 annual rainfall was more abundant compared to the subsequent years but did not show a statistically significant difference when compared to the previous 10 years. The early spring period that coincides with the green phase of the berry development was characterized by frequent rain events and average temperatures that rarely exceeded 20°C followed by a hot (>30°C) and dry pre-veraison period. Concurrently to the veraison, a strong rainfall was registered, whereas after that, an equal distribution of light rainfall until harvest was observed.

2020 was the cooler year if compared to the others ([Figure 1B](#)), with maximum temperatures lower than the mean values registered in the decade 2009–2018 that rarely exceeded 30°C. Even if the annual total rainfall was similar to the reference period, rainfall was much more concentrated from April to October, that is, in the period of berry development and ripening, especially in two phases before veraison and close to harvest.

On the other hand, the 2021 ([Figure 1C](#)) season was characterized by maximum temperatures, referring to the April–October period, lower than those of the decade 2009–2018; number of rainy days and total rainfall were significantly lower too. A regular distribution of rainfall during the green phase and until veraison can be noticed followed by a warm and dry post-veraison period until harvest.

For 2022 vintage ([Figure 1D](#)) instead, a series of extreme conditions occurred in terms of both temperature and rainfall. Monthly Tmax, heat accumulation (GDD), and particularly the number of days with maximum temperatures above 30°C (76 days) were significantly above the average values registered for the previous decade, while often temperature exceeds 35°C during the veraison time. Conversely, values of rainy days and especially total rainfall were decidedly lower during ripening with respect to the previous years of study and the reference decade, which denotes scarce water availability more specifically in the green phase of berry

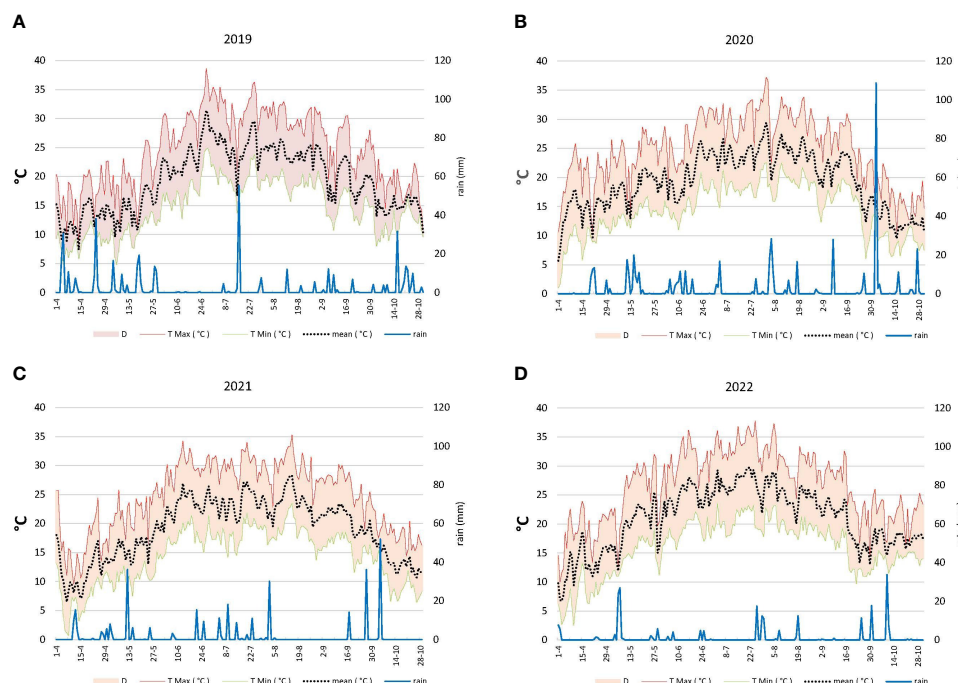


FIGURE 1

(A) Meteorological pattern during 2019. T: temperature; D: differences between T max and T min. (B) Meteorological pattern during 2020. T: temperature; D: differences between T max and T min. (C) Meteorological pattern during 2021. T: temperature; D: differences between T max and T min. (D) Meteorological pattern during 2022. T: temperature; D: differences between T max and T min.

development. Meteorological conditions observed for 2022 brought an anticipation of approximately 10 days of both veraison (25/30 July) and ripening (5/10 September).

3.2 Grape technological parameters

Grignolino grapes showed an adequate and uniform bunch ripening in the 4 years of study. The age and exposure of the vineyards did not appear to have an impact on the timing of phenological phases, such as veraison and maturity, that occurred

in the same period in all vineyards for each year. Grapes harvested over the 4 years of study in the three vineyards reached technological maturity and were harvested during the third week of September for the first 3 years, whereas for 2022, a 10-day advance shift of the harvest was registered. For 2019 and especially for 2022 vintage, mean berry weight was significantly lower at harvest with respect to the two vintages 2020 and 2021 (Table 2). Moreover, the data regarding the berry composition and main polyphenolic parameters showed that the average values among years were similar as regards TA and pH, with slightly higher °Brix values for the 2022 season and lower polyphenolic levels in 2020.

TABLE 2 Principal chemical and physical analysis on Grignolino berries harvested in vintages 2019, 2020, 2021, and 2022.

	Year (Y)				Vineyards (V)			ANOVA		
	2019	2020	2021	2022	Old SE	Old SW	Young SW	sig. Y	sig. V	sig. Y*V
Berry weight (g)	1.34 b	1.80 a	1.74 a	1.18 c	1.70 a	1.43 b	1.41 b	***	***	**
TSS (° Brix)	25.1 b	24.0 b	24.5 b	26.3 a	25.8 a	24.3 b	25.0 ab	**	*	ns
TA (g/L)	6.9	6.5	6.9	6.4	6.8	6.7	6.5	ns	ns	ns
pH	3.25	3.30	3.18	3.25	3.24	3.25	3.24	ns	ns	ns
TPI (mg/berry)	2.9 a	2.4 b	2.6 a	1.7 c	2.7 a	2.2 b	2.2 b	***	***	***
TPI (mg/kg)	1.690 a	1.317 b	1.529 a	1.478 a	1.697 a	1.548 b	1.566 b	**	**	***
TAI (mg/berry)	0.6 a	0.4 b	0.6 a	0.4 b	0.6 a	0.5 b	0.4 c	***	***	***
TAI (mg/kg)	425 a	225 b	351 a	364 a	356 a	350 a	317 b	***	***	**

TSS, total soluble solids; TA, titratable acidity; TPI, total polyphenol index measured in berry skins as mg/kg and mg/berry; TAI, total anthocyanin index measured in berry skins as mg/kg and mg/berry. Data were subjected to the analysis of variance (ANOVA) and post-hoc Tukey test. ANOVA significance, ns (not significant): p -value > 0.05 , $0.01 \leq p$ -value < 0.05 , $0.001 \leq p$ -value < 0.01 , $***p$ -value < 0.001 . Different letters indicate different least square means.

On average, vineyard Old SE had significantly higher contents in TAI and TPI when results are expressed per berry, and also had considerably higher berry weight while Young SW berries tend to present the lowest values as regards technological parameters.

3.3 Aroma precursors of Grignolino berries

The main hydrolytically released compounds detected in the berries of Grignolino can be arranged into four groups, namely, terpenoids, C₁₃-norisoprenoids, benzenoids, and C₆ aldehydes and alcohols (see [Supplementary Table 1](#)), in amounts consistent with the non-aromatic character of this cv. The most representative compounds among terpenoids were geraniol, p-ment-1-ene-7,8-diol, and geranic acid; among C₁₃-norisoprenoids, 3-oxo- α -ionol, 3-OH- β -damascone, and 3-hydroxy-7,8-dihydro- β -ionol; and among benzenoids, benzyl alcohol and phenylethyl alcohol. The primary C₆ aldehydes and alcohols identified were 1-hexanol (see [Supplementary Tables 2, 3](#)).

The first results of ANOVA carried out on the average total values of the aroma compounds, to globally examine the effects of the vintage (year) and vineyards, are shown in [Table 3](#). From this first analysis, we detected that both season and vineyard exerted a significant influence on most of the variables (classes of aroma precursors) studied. The composition of the grapes collected from the different vineyards over the 4 years indeed showed significant differences among years for almost all classes of precursors. Considering the average content values measured in the grapes of the three vineyards for each year of study, we can note higher contents of C₁₃-norisoprenoids, benzenoids, and C₆ aldehydes and alcohols for 2022 when results are expressed as μg per kg of berries and significantly higher values of terpenoids and C₁₃-norisoprenoids per berry for 2021. In 2021, the terpenoid amounts were mainly significantly higher than in the other years. 2020 presents the lowest content of precursors especially in terpenoids and benzenoids. Benzenoids, instead, were the most represented compounds in the berries of Grignolino for 2019 and

2022, whereas terpenoids and benzenoids were the most represented compounds for 2021 vintage.

As far as the differences among the vineyards are concerned, a significantly higher average content over the years for Old SE was observed for almost all chemical families of compounds. Lower average amounts for terpenoids and benzenoids over the years were noted for the Young SW vineyard.

Analysis of variance was carried out to globally examine the effects of the vintage (year) on single compounds, highlighting significant differences among the years for the most important compounds, especially when the results were expressed as $\mu\text{g}/100$ berries; 2021 registered the higher amounts of the representative compounds mentioned before, except for the 3-oxo- α -ionol among norisoprenoids and for the C₆ aldehydes and alcohols ([Supplementary Table 2](#)). In the vintage year 2020, the lowest amounts for almost all compounds were reported. Similar considerations can be made when the results are expressed as $\mu\text{g}/\text{kg}$ of berries.

As regards the differences among vineyards, the concentrations of the predominant compounds of benzenoids and terpenoids were significantly higher in the Old SE grapes merely when the results were expressed as $\mu\text{g}/100$ berries, whereas no significant differences were noted for 3-oxo- α -ionol and 3-hydroxy-7,8-dihydro- β -ionol (see [Supplementary Tables 2, 3](#)).

3.4 Aroma precursor trends in the vineyards

ANOVA results reported in [Table 4](#) show the mean differences between the vineyards calculated separately for each season. Variability was mostly associated with compounds such as terpenoids and especially benzenoids. Examining the differences between the vineyards in 2019, it can be noted that vineyard Old SE tends to show greater contents for all chemical classes of compounds, but statistically significant differences are highlighted only for benzenoid compounds.

TABLE 3 Average values of each chemical aroma family measured in the three vineyards (Old SW, Old SE, and Young SE) for each vintage year (2019, 2020, 2021, and 2022).

		Year (Y)				Vineyards (V)			ANOVA		
		2019	2020	2021	2022	Old SW	Old SE	Young SW	sig. Y	sig. V	sig. (Y*V)
Terpenoids	$\mu\text{g}/100$ berries	63 b	53 b	112 a	70 b	69 b	105 a	49 c	***	***	ns
	$\mu\text{g}/\text{kg}$ of berries	464 b	319 c	634 a	585 ab	496 b	607 a	398 b	***	**	ns
C ₁₃ -Norisoprenoids	$\mu\text{g}/100$ berries	27 b	32 b	50 a	40 ab	33 b	49 a	29 b	**	**	ns
	$\mu\text{g}/\text{kg}$ of berries	197 b	193 b	284 ab	344 a	239 a	284 a	240 a	**	ns	ns
Benzenoids	$\mu\text{g}/100$ berries	85 b	54 c	118 a	128 a	99 b	128 a	62 c	***	***	**
	$\mu\text{g}/\text{kg}$ of berries	607 b	330 c	663 b	1,090 a	708 a	768 a	541 b	***	**	***
C ₆ aldehydes and alcohols	$\mu\text{g}/100$ berries	12	15	15	16	14 b	18 a	11 b	ns	**	*
	$\mu\text{g}/\text{kg}$ of berries	86 b	88 b	79 b	142 a	99 a	106 a	91 a	**	ns	ns

Data were subjected to the analysis of variance (ANOVA) and post-hoc Tukey test. Means followed by a different letter are significantly different. ANOVA significance, ns (not significant); p-value > 0.05, *0.01 ≤ p-value < 0.05, **0.001 ≤ p-value < 0.01, ***p-value < 0.001.

TABLE 4 Average values of each aroma chemical group, berry weight, and sugar content in degrees Brix (°Brix) measured in the grapes of the three vineyards (O. SW: Old SW, O. SE: Old SE, and Y. SE: Young SW) for each year (2019, 2020, 2021, and 2022).

Year		2019				2020				2021				2022			
Vineyard		O. SW	O. SE	Y. SW	Sig.	O. SW	O. SE	Y. SW	Sig.	O. SW	O. SE	Y. SW	Sig.	O. SW	O. SE	Y. SW	Sig.
Terpenoids	µg/100 berries	56	99	34	ns	50	63	46	ns	109	162	63.7	ns	65 b	96 a	54 b	*
	µg/kg	474	656	261	ns	321	355	281	ns	653	779	468	ns	569 b	673 a	574 b	***
C₁₃-Norisoprenoids	µg/100 berries	25	40	16	ns	36	33	26	ns	41	69	39	ns	36	57	33	ns
	µg/kg	206	262	123	ns	231	188	161	ns	248	330	273	ns	317	402	380	ns
Benzenoids	µg/100 berries	50 b	149 a	54 b	***	56	57	50	ns	168 a	148 a	38.4 b	**	128	161	102	ns
	µg/kg	422 b	988 a	409 b	**	359	324	306	ns	1,009 a	710 a	270 b	**	1,123	1,132	1,117	ns
C₆ aldehydes and alcohols	µg/100 berries	11	13	10	ns	12	18	14	ns	15 b	24 a	5 c	**	18	20	14	ns
	µg/kg	96	88	75	ns	79	100	86	ns	88 a	116 a	32 b	**	163	148	151	ns
Berry weight	g	1.2 b	1.5 a	1.3 b	*	1.6	1.9	1.9	ns	1.7	1.8	1.7	ns	1.1 b	1.5 a	0.9 c	***
Total soluble solids	°Brix	26	25	25	ns	23 b	25 a	24 a	*	25	25	24	ns	27 a	27 a	25 b	**

Data were subjected to the analysis of variance (ANOVA) and post-hoc Tukey test. Means followed by a different letter are significantly different. ANOVA significance, ns (not significant); p-value > 0.05, *0.01 ≤ p-value < 0.05, **0.001 ≤ p-value < 0.01, ***p-value < 0.001.

In 2020 vintage, no statistically significant differences were observed among vineyards but generally the old vineyards had higher contents of aroma precursors than the young one.

As in the previous vintage 2019, also in 2021, vineyard Old SE tends to show higher values for all chemical classes of compounds. Statistically significant differences are observed only regarding the concentrations of C₆ aldehydes and alcohols and benzenoids. Generally, a higher concentration of terpenoids and benzenoids in the grapes of old-vine vineyards was noted with respect to Young SW grapes who showed the lowest values for all precursors and significantly lowest contents of benzenoids.

Finally, in 2022, grape berries of all the studied vineyards are characterized by high contents of benzenoids while Old SE grapes tend to contain higher amounts of all the groups of compounds as observed for the previous years but are significantly richer in terpenoids as well (per 100 berries and per kg of berries).

3.5 Vintage effect on aroma precursors

The mean differences for aroma precursors among the vintages, calculated for each vineyard, are highlighted in [Figures 2–4](#). Meteorological conditions during 2021 favored the accumulation of significant amounts of terpenoids and benzenoids in the berries of the examined vineyards for the old ones, especially when results are expressed per berry. 2021 vintage tended to favor C₁₃-norisoprenoids amounts too, but not in a significant way.

Significantly higher values of C₁₃-norisoprenoids were noticed in 2022 only for the Young SW vineyard when results are expressed per kg of berries. Benzenoids were the main compounds that accumulated in Grignolino berries especially during 2022. As far as vintage 2020 is concerned, the lowest concentrations for all classes of aroma precursors were reported especially for Old SE with respect to the previous years.

Although similar considerations can be made for old-vine vineyards, the effect of vintage instead was different for the young-vine vineyard (Young SW) which showed significantly higher amounts of almost all classes of precursors in 2022 when results were expressed in µg per kg due to the excessive low berry weight. The worst vintage year especially for terpenol and C₁₃-norisoprenoid accumulation was 2019 for this vineyard.

3.6 PCA results

Variables related to the grape characteristics (berry weight and °Brix) and to aroma precursors (µg/100 berries) have been subjected to PCA in relation to the meteorological parameters. The PCA model explained an adequate level of variance. Climatic factors that characterized each year such as the days of optimal and maximum temperatures, GDD, and rain distribution before (BVe) and after veraison (AVe) were considered and indicated as 25–35°C BVe and AVe, >35° BVe and AVe, GDD BVe and AVe, and rainfall BVe and AVe in [Figure 5](#).



FIGURE 2

Terpenoids contents in Grignolino berries ($\mu\text{g}/100$ berries and $\mu\text{g}/\text{kg}$ of berries) measured in each vintage year (2019, 2020, 2021, 2022) for the three vineyards (Old SW, Old SE, Young SE). Data were subjected to the analysis of variance (ANOVA) and post hoc Turkey test. Different letters indicate contents significantly different among the years for $P < 0.05$, n.s.: not significant.

Results (Figure 5) showed the projection of the year vintages and vineyards in the space defined by the meteorological parameters related to the first stage of berry development (from April until veraison) and to the second part of ripening (from veraison until harvest) together with berry weight, °Brix, and the concentration of the four groups of aroma precursors of the grapes at harvest, expressed as $\mu\text{g}/100$ berries (Figure 5). The two components (PC1 and PC2) explained 85.43% of the total variance. The first component (48.86% of total variance) is positively correlated with sugar content, benzenoid amounts, the GDD, and temperature ranges measured after veraison, and negatively correlated with the berry weight and the total days of rainfall calculated before veraison. The second component (36.57% of total variance) correlates positively with C_{13} -norisoprenoids and terpenoids among aroma variables and the range 25–35°C before veraison but negatively with the rain after veraison. PCA results showed that each season was linked to a distinct group.

More specifically, PCA clearly emphasizes the positive relation between the amounts of C_{13} -norisoprenoids and terpenoids in grapes and the total days of optimal temperature in the early

stage of berry development (25–35°C BVe) and links season 2021 to these variables. Furthermore, a positive correlation of °Brix, the amounts in benzenoids, GDD, and hot days after veraison with 2022 is noted. The negative correlation of most compounds with rainfall both before and after veraison is evidenced mainly for terpenoids and C_{13} -norisoprenoids, and the projection of seasons 2019 and 2020 follows the same pattern. Optimal conditions like those during 2021 seem to emphasize the differences among vineyards that otherwise are flattened as observed for instance for vintage 2020 (Table 4).

4 Discussion

The observations of this multi-year research study have permitted us to draw some important conclusions. Grapes harvested over the 4 years of study in the three vineyards reached similar physical and chemical parameters at maturity, showing instead differences for °Brix in 2022 and polyphenolic content in 2020. The meteorological pattern observed for each vintage

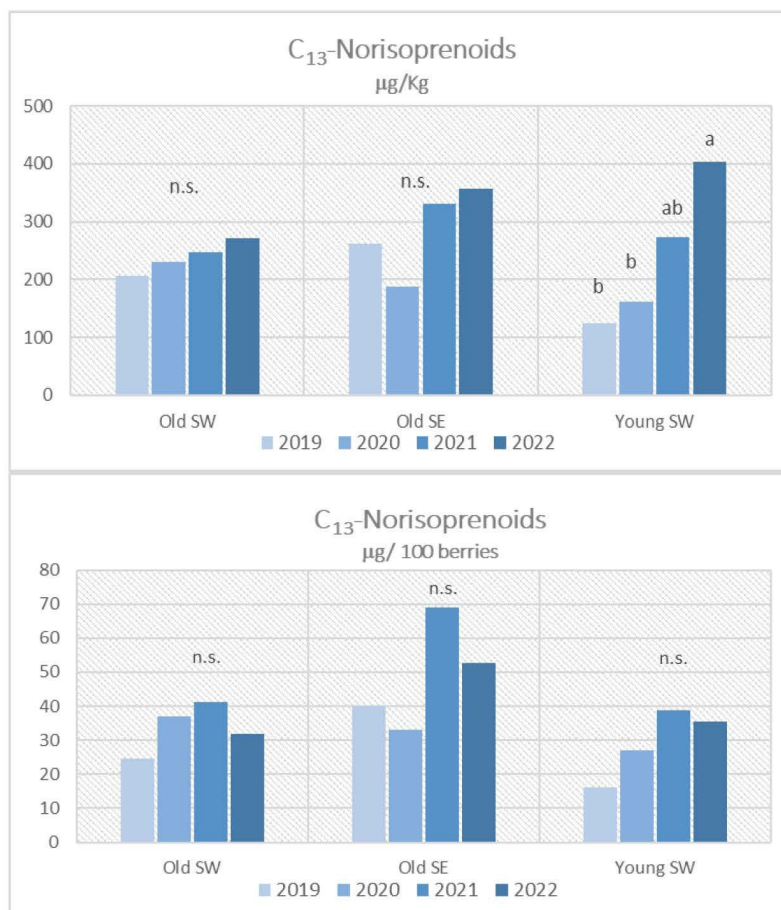


FIGURE 3

C₁₃-norisoprenoid contents in Grignolino grape berries (µg/100 berries and µg/kg of berries) measured in each vintage year (2019, 2020, 2021, 2022) for the three vineyards (Old SW, Old SE, Young SE). Data were subjected to the analysis of variance (ANOVA) and *post hoc* Turkey test. Different letters indicate contents significantly different among the years for $P < 0.05$. n.s.: not significant.

influenced the size and the composition of the berries. The hot ($>30^{\circ}\text{C}$) and dry pre-veraison period (June) observed in 2019 has probably penalized the berry weight at harvest. Despite the increased skin-to-pulp ratio in 2019, terpenol and norisoprenoid amounts were lower especially for the Young SW grapes probably due to a high rainfall just before veraison that alternated with high temperature ($>35^{\circ}\text{C}$) (Figure 1A) and to the low GDD in the post-veraison stage. According to some literature, the most important terpenes seem to be negatively correlated with high precipitations before veraison (Rienth et al., 2021). Furthermore, most water-involved studies on grape aroma compounds show very heterogeneous results, depending on the type of aroma compounds considered and certainly on the water retention capacity of the soil. However, the reported effects of water availability on aroma compounds are less evident than for phenolic compounds (Alem et al., 2019).

The low concentrations for all classes of aroma precursors reported in 2020 can be attributed to the abundant rainfall close to harvest time that affected their contents in the berry. Rainfall concentrated in the period of berry development and ripening, especially before veraison and close to harvest, has also flattened the

differences among vineyards. It is remarkable that 2020 presents the lowest content of precursors especially in terpenoids and benzenoids even if the same average weight of berry was registered at harvest as for the year 2021.

Mild spring temperature conditions and a regular distribution of rainfall during the green phase as well as a warm ($25\text{--}35^{\circ}\text{C}$) but not hot and dry post-veraison period until harvest that characterized 2021 vintage favored the accumulation of all classes of aroma precursors but especially terpenoids in the berries of old vineyards.

The meteorological conditions that occurred during 2022 affected vine behavior by anticipating the timing of the phenological phases; veraison and harvest dates occurred earlier than in the previous years. GDD and hot days after veraison also characterized this season, highlighting a positive correlation with the higher °Brix and the amounts in benzenoids. Intense conditions occurred in terms of high temperature in combination with probably less water due to the lack of rainfall in the pre-veraison stage, also attributed to, as in 2019, a significantly lower berry weight especially for the grapes produced by the young vines, which also accumulated less sugar. According to previous research, water

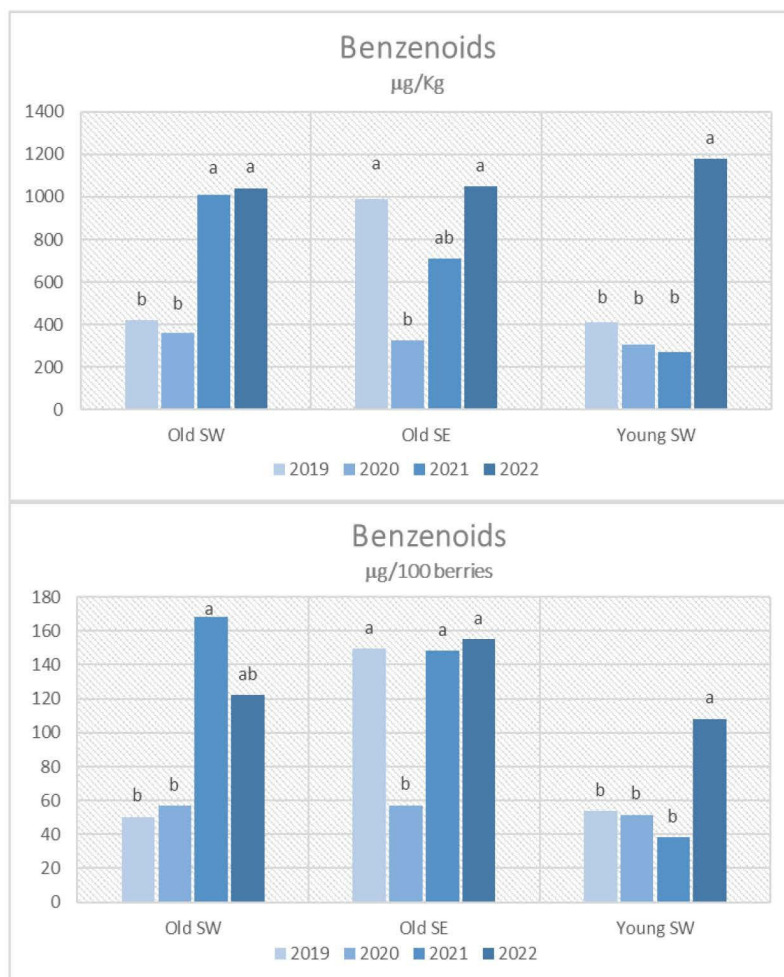


FIGURE 4

Benzenoids contents in Grignolino berries (µg/100 berries and µg/kg of berries) measured in each vintage year (2019, 2020, 2021, 2022) for the three vineyards (Old SW, Old SE, Young SE). Data were subjected to the analysis of variance (ANOVA) and post hoc Turkey test. Different letters indicate contents significantly different among the years for $P < 0.05$. n.s.: not significant.

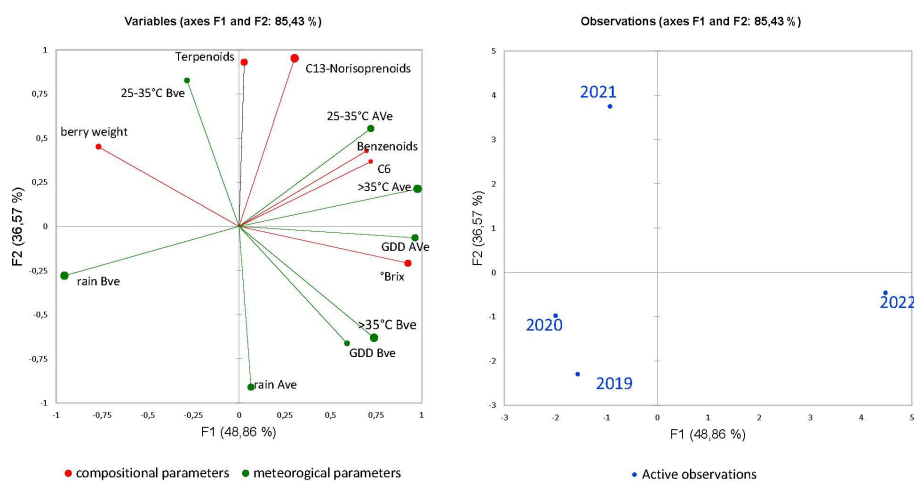


FIGURE 5

PCA of, °Brix, berry weight and meteorological conditions (BVe: before veraison and Ave: after veraison), in correlation with the classes of the aroma precursors expressed as µg /100 berries and the projection of the vintage years.

deficit stress during the green growth phase has the highest impact on final berry volume (He et al., 2020; Rienth et al., 2021). Furthermore, high amounts of benzenoids were reported in the grapes of all vineyards, especially in the Young SW grapes, where higher amounts were found with respect to the previous years. According to literature, water deficit can cause a reduction of berry volume and an increase of the skin-to-pulp ratio, leading to a higher concentration of these compounds synthesized in the skin cells. Environmental stresses, indeed, can activate the shikimate acid pathway and further promote the accumulation of secondary metabolites such as benzenoids that share with flavonoids the same substrate phenylalanine (Zhang et al., 2012).

As regards the differences noted among the vineyards, optimal conditions seem to emphasize the differences among vineyards as highlighted by the PCA (Figure 5B). The younger-vine vineyard showed a different compositional variability among the vintages, mainly as regards the effect of the vintage on the berry weight, which tends to show lower concentrations in aroma precursors. The grapes produced from the old southeastern vineyard instead showed higher amounts for almost all chemical classes and in each season. Under dry-hot conditions like those verified during 2022, grape cluster exposure to sunlight tends to raise both solar radiation and daytime temperature on grapes, and gives rise to the phenomenon of degradation of aroma compounds (Scafidi et al., 2013; Asproudi et al., 2016). Considering that, in the Northern Hemisphere, south- and west-facing areas are warmer, characterized by the harsh afternoon sun, such conditions, more than the eastern one, can stress vines during ripening in warm climates. Old SE grapes presented significantly higher amounts of terpenoids in 2022, showing that the cooler and fresh seasonal conditions during ripening may protect the precursors that accumulated in the grapes during the earlier stages of ripening (Young et al., 2016).

This research study highlighted that the current climate change conditions in a hilly environment may positively affect the quality of Grignolino grapes both by limiting the differences on bunch ripening and by promoting the accumulation of secondary metabolites, especially in the older vineyards. Furthermore, new knowledge was added on how specific meteorological conditions such as rainfall and temperature patterns and their timing during berry development and ripening may impact grape aroma precursors, to adapt new strategies aimed at maintaining high-quality production.

Data availability statement

The original contributions presented in the study are included in the article/Supplementary Material. Further inquiries can be directed to the corresponding author.

Author contributions

AA and MP devised the main body, structure, and research content of the manuscript. AA, FB, and VR provided laboratory and instrumental analyses. SG provided assistance as regards experimental plan, sample collection, and vineyard information. All authors reviewed the manuscript. All authors contributed to the article and approved the submitted version.

Funding

The “SESAMO” project, which forms the basis of this article, was funded by the Fondazione CRT – Cassa di Risparmio di Torino (RF = 2019.2337) and carried out by the CREA Research Centre for Viticulture and Enology between 2019 and 2022.

Acknowledgments

The authors express their gratitude to the Monferace association for their unwavering and invaluable support in the implementation of the “SESAMO” project. In particular, they wish to extend their thanks to the producers who generously provided the grapes for the experiment, as well as to enologist Mario Ronco for his expert technical assistance.

Conflict of interest

The authors declare that the research was conducted in the absence of any commercial or financial relationships that could be construed as a potential conflict of interest.

Publisher's note

All claims expressed in this article are solely those of the authors and do not necessarily represent those of their affiliated organizations, or those of the publisher, the editors and the reviewers. Any product that may be evaluated in this article, or claim that may be made by its manufacturer, is not guaranteed or endorsed by the publisher.

Supplementary material

The Supplementary Material for this article can be found online at: <https://www.frontiersin.org/articles/10.3389/fpls.2023.1179111/full#supplementary-material>

References

- Alem, H., Rigou, P., Schneider, R., Ojeda, H., and Torregrosa, L. (2019). Impact of agronomic practices on grape aroma composition: a review. *J. Sci. Food Agric.* 99, 975–985. doi: 10.1002/jsfa.9327
- Amerine, M. A., and Winkler, A. J. (1944). Composition and quality of musts and wines of California grapes. *Hilg* 15, 493–675. doi: 10.3733/hilg.v15n06p493
- Asproudi, A., Ferrandino, A., Bonello, F., Vaudano, E., Pollon, M., and Petrozziello, M. (2018). Key norisoprenoid compounds in wines from early-harvested grapes in view of climate change. *Food Chem.* 268, 143–152. doi: 10.1016/j.foodchem.2018.06.069
- Asproudi, A., Petrozziello, M., Cavalletto, S., and Guidoni, S. (2016). Grape aroma precursors in cv. Nebbiolo as affected by vine microclimate. *Food Chem.* 211, 947–956. doi: 10.1016/j.foodchem.2016.05.070
- Bagagiolo, G., Rabino, D., Biddoccu, M., Nigrelli, G., Berro, D. C., Mercalli, L., et al. (2021). Effects of inter-annual climate variability on grape harvest timing in Rainfed Hilly Vineyards of Piedmont (NW Italy). *Ital. J. Agrometeorol.* (1), 37–49. doi: 10.36253/ijam-1083
- Bergqvist, J., Dokoozlian, N., and Ebisuda, N. (2001). Sunlight exposure and temperature effects on berry growth and composition of cabernet sauvignon and grenache in the central San Joaquin Valley of California. *Am. J. Enol. Vitic.* 52, 1–7. doi: 10.5344/ajev.2001.52.1.1
- Bou Nader, K., Stoll, M., Rauhut, D., Patz, C.-D., Jung, R., Loehnertz, O., et al. (2019). Impact of grapevine age on water status and productivity of *Vitis vinifera* L. cv. Riesling. *Eur. J. Agron.* 104, 1–12. doi: 10.1016/j.eja.2018.12.009
- Caffrey, A., and Ebeler, S. E. (2021). The occurrence of glycosylated aroma precursors in *Vitis vinifera* fruit and humulus lupulus hop cones and their roles in wine and beer volatile aroma production. *Foods* 10, 935. doi: 10.3390/foods10050935
- Carbonell-Bejerano, P., Diago, M.-P., Martínez-Abaigar, J., Martínez-Zapater, J. M., Tardáguila, J., and Núñez-Olivera, E. (2014). Solar ultraviolet radiation is necessary to enhance grapevine fruit ripening transcriptional and phenolic responses. *BMC Plant Biol.* 14, 183. doi: 10.1186/1471-2229-14-183
- Compendium of international methods of wine and must analysis-OIV (2020) (Rue de Monceau 75008 Paris, France) 35.
- Crespo, J., Rigou, P., Romero, V., García, M., Arroyo, T., and Cabellos, J. M. (2018). Effect of seasonal climate fluctuations on the evolution of glycoconjugates during the ripening period of grapevine cv. Muscat à petits grains blancs berries. *J. Sci. Food Agric.* 98, 1803–1812. doi: 10.1002/jsfa.8656
- De Orduna, R. M. (2010). Climate change associated effects on grape and wine quality and production. *Food Res. Int.* 43, 1844–1855. doi: 10.1016/j.foodres.2010.05.001
- Di Stefano, R., Bottero, S., Pigella, R., Borsia, D., Bezze, G., and Corino, L. (1998). Precursori d'aroma glicosilati presenti nelle uve di alcune cultivar a frutto colorato. *Enotecnica* 34, 63–76.
- Di Stefano, R., and Cravero, M. C. (1991). Metodi per lo studio dei polifenoli dell'uva. *Riv. Vitic. Enol.* 44, 37–45.
- Di Stefano, R., and Guidoni, S. (1989). La determinazione dei polifenoli totali nei mosti e nei vini. *Vignevini* 16, 47–52.
- Drappier, J., Zhu, J., Thibon, C., Darriet, P., Delrot, S., Pieri, P., et al. (2016). Sensitivity of berries ripening to higher temperature - Grape and wine aromatic compounds. Available at: <https://hal.inrae.fr/hal-02744237> (Accessed January 31, 2023). p.
- Feng, H., Yuan, F., Skinkis, P. A., and Qian, M. C. (2015). Influence of cluster zone leaf removal on Pinot noir grape chemical and volatile composition. *Food Chem.* 173, 414–423. doi: 10.1016/j.foodchem.2014.09.149
- Ferreira, V., and Lopez, R. (2019). The actual and potential aroma of winemaking grapes. *Biomolecules* 9, 818. doi: 10.3390/biom9120818
- Fraga, H., García de Cortázar Atauri, I., and Santos, J. A. (2018). Viticultural irrigation demands under climate change scenarios in Portugal. *Agric. Water Manage.* 196, 66–74. doi: 10.1016/j.agwat.2017.10.023
- Hannah, L., Roehrdanz, P. R., Ikegami, M., Shepard, A. V., Shaw, M. R., Tabor, G., et al. (2013). Climate change, wine, and conservation. *Proc. Natl. Acad. Sci.* 110, 6907–6912. doi: 10.1073/pnas.1210127110
- He, L., Xu, X.-Q., Wang, Y., Chen, W.-K., Sun, R.-Z., Cheng, G., et al. (2020). Modulation of volatile compound metabolome and transcriptome in grape berries exposed to sunlight under dry-hot climate. *BMC Plant Biol.* 20, 59. doi: 10.1186/s12870-020-2268-y
- Jackson, D. I., and Lombard, P. B. (1993). Environmental and management practices affecting grape composition and wine quality - A review. *Am. J. Enol. Vitic.* 44, 409–430. doi: 10.5344/ajev.1993.44.4.409
- Jesús Ibarz, M., Ferreira, V., Hernández-Orte, P., Loscos, N., and Cacho, J. (2006). Optimization and evaluation of a procedure for the gas chromatographic-mass spectrometric analysis of the aromas generated by fast acid hydrolysis of flavor precursors extracted from grapes. *J. Chromatogr. A* 1116, 217–229. doi: 10.1016/j.chroma.2006.03.020
- Liang, Z., Fang, Z., Pai, A., Luo, J., Gan, R., Gao, Y., et al. (2022). Glycosidically bound aroma precursors in fruits: A comprehensive review. *Crit. Rev. Food Sci. Nutr.* 62, 215–243. doi: 10.1080/10408398.2020.1813684
- Liu, J., Zhu, X.-L., Ullah, N., and Tao, Y.-S. (2017). Aroma glycosides in grapes and wine. *J. Food Sci.* 82, 248–259. doi: 10.1111/1750-3841.13598
- Mainardi, G. (2003). Il Grignolino: un Piemontese raffinato e di classe. *OICCE TIMES - Rivista di enologia tecnica qualità e territorio. IV* 10, 12.
- Mateo, J. J., Gentilini, N., Huerta, T., Jime'nez, M., and Di Stefano, R. (1997). Fractionation of glycoside precursors of aroma in grapes and wine. *J. Chromatogr. A* 778, 219–224. doi: 10.1016/S0021-9673(97)00566-9
- Monferace a Grignolino of Excellence. (2023). *Monferace*. Available at: <https://monferace.it/en/> (Accessed February 9, 2023).
- Mori, K., Goto-Yamamoto, N., Kitayama, M., and Hashizume, K. (2007). Loss of anthocyanins in red-wine grape under high temperature. *J. Exp. Bot.* 58, 1935–1945. doi: 10.1093/jxb/erm055
- Parker, M., Capone, D. L., Francis, I. L., and Herderich, M. J. (2017). Aroma precursors in grapes and wine: Flavor release during wine production and consumption. *J. Agric. Food Chem.* 66, 2281–2286. doi: 10.1021/acs.jafc.6b05255
- Pérez-Álvarez, E. P., Intrigliolo Molina, D. S., Vivaldi, G. A., García-Esparza, M. J., Lizama, V., and Álvarez, I. (2021). Effects of the irrigation regimes on grapevine cv. Bobal in a Mediterranean climate: I. Water relations, vine performance and grape composition. *Agric. Water Manage.* 248, 106772. doi: 10.1016/j.agwat.2021.106772
- Rienth, M., Vigneron, N., Darriet, P., Sweetman, C., Burbidge, C., Bonghi, C., et al. (2021). Grape berry secondary metabolites and their modulation by abiotic factors in a climate change scenario—a review. *Front. Plant Sci.* 12, 262. doi: 10.3389/fpls.2021.643258
- Riffle, V., Palmer, N., Casassa, L. F., and Dodson Peterson, J. C. (2021). The Effect of Grapevine Age (*Vitis vinifera* L. cv. Zinfandel) on Phenology and Gas Exchange Parameters over Consecutive Growing Seasons. *Plants* 10, 311. doi: 10.3390/plants10020311
- Robinson, J., Harding, J., and Vouillamoz, J. (2013). *Wine grapes: a complete guide to 1,368 vine varieties, including their origins and flavours* (Penguin UK: Penguin Books Ltd).
- Santos, J. A., Fraga, H., Malheiro, A. C., Moutinho-Pereira, J., Dinis, L.-T., Correia, C., et al. (2020). A review of the potential climate change impacts and adaptation options for European viticulture. *Appl. Sci.* 10, 3092. doi: 10.3390/app10093092
- Scafidi, P., Pisciotto, A., Patti, D., Tamborra, P., Di Lorenzo, R., and Barbagallo, M. G. (2013). Effect of artificial shading on the tannin accumulation and aromatic composition of the Grillo cultivar (*Vitis vinifera* L.). *BMC Plant Biol.* 13, 175. doi: 10.1186/1471-2229-13-175
- van Leeuwen, C., Barbe, J.-C., Darriet, P., Geffroy, O., Gomès, E., Guillaumie, S., et al. (2020). Recent advancements in understanding the terroir effect on aromas in grapes and wines. *OENO One* 54, 985. doi: 10.20870/oeno-one.2020.54.4.3983
- Van Leeuwen, C., and Darriet, P. (2016). The impact of climate change on viticulture and wine quality. *J. Wine Economics* 11, 150–167. doi: 10.1017/jwe.2015.21
- Webb, L. B., Whetton, P. H., Bhend, J., Darbyshire, R., Briggs, P. R., and Barlow, E. W. R. (2012). Earlier wine-grape ripening driven by climatic warming and drying and management practices. *Nat. Clim Change* 2, 259–264. doi: 10.1038/nclimate1417
- Wu, J., Drappier, J., Hilbert, G., Guillaumie, S., Dai, Z., Geny, L., et al. (2019). The effects of a moderate grape temperature increase on berry secondary metabolites: This article is published in cooperation with the 21th GIESCO International Meeting, June 23-28 2019, Thessaloniki, Greece. Guests editors : Stefanos Koundouras and Laurent Torregrosa. *OENO One* 53 (2), 321–333. doi: 10.20870/oeno-one.2019.53.2.2434
- Young, P. R., Eyeghe-Bickong, H. A., du Plessis, K., Alexandersson, E., Jacobson, D. A., Coetzee, Z., et al. (2016). Grapevine plasticity in response to an altered microclimate: sauvignon blanc modulates specific metabolites in response to increased berry exposure. *Plant Physiol.* 170, 1235–1254. doi: 10.1104/pp.15.01775
- Yuan, F., Feng, H., and Qian, M. C. (2015). "C13-norisoprenoids in grape and wine affected by different canopy management," in *Advances in Wine Research ACS Symposium Series* (Washington, DC: American Chemical Society; Chemical Society), 147–160. doi: 10.1021/bk-2015-1203.ch010
- Zhang, Z.-Z., Li, X.-X., Chu, Y.-N., Zhang, M.-X., Wen, Y.-Q., Duan, C.-Q., et al. (2012). Three types of ultraviolet irradiation differentially promote expression of shikimate pathway genes and production of anthocyanins in grape berries. *Plant Physiol. Biochem.* 57, 74–83. doi: 10.1016/j.plaphy.2012.05.005
- Zufferey, V., and Maigre, D. (2007). Age de la vigne. I. Influence sur le comportement physiologique des souches. *Rev. suisse viticulture arboriculture horticulture* 39, 257–261.

Frontiers in Plant Science

Cultivates the science of plant biology and its applications

The most cited plant science journal, which advances our understanding of plant biology for sustainable food security, functional ecosystems and human health.

Discover the latest Research Topics

[See more →](#)

Frontiers

Avenue du Tribunal-Fédéral 34
1005 Lausanne, Switzerland
frontiersin.org

Contact us

+41 (0)21 510 17 00
frontiersin.org/about/contact

